ATTACHMENT D

Research Description and Findings

to

Self-Consolidating Concrete for Precast, Prestressed Concrete Bridge Elements

Final Report for NCHRP Project 18-12

Prepared by:

Kamal Henri Khayat, University of Sherbrooke, Sherbrooke, Quebec, Canada
Denis Mitchell, McGill University, Montreal, Quebec, Canada

May 2008

ACKNOWLEDGEMENT OF SPONSORSHIP

This work was sponsored by the American Association of State Highway and Transportation Officials, in cooperation with the Federal Highway Administration, and was conducted in the National Cooperative Highway Research Program, which is administered by the Transportation Research Board of the National Academies.

DISCLAIMER

This is an uncorrected draft as submitted by the research agency. The opinions and conclusions expressed or implied in the report are those of the research agency. They are not necessarily those of the Transportation Research Board, the National Academies, or the program sponsors.

TABLE OF CONTENTS

LIST OF FIGURES ..... **D-v**

LIST OF TABLES ..... **D-vii**

D.1 INTRODUCTION, LITERATURE REVIEW, AND RESEARCH APPROACH **D-1**

D.1.1 Background **D-1**
D.1.2 Literature Review **D-2**
D.1.2.1 Workability characteristics and test methods *D-3*
D.1.2.2 Material constituents and mix design *D-4*
D.1.2.3 Production and placement characteristics *D-6*
D.1.2.4 Mechanical properties *D-7*
D.1.2.5 Visco-elastic properties *D-8*
D.1.2.6 Durability characteristics *D-9*
D.1.3 Research Approach **D-9**
D.1.3.1 Parametric study *D-9*
D.1.3.2 Factorial design approach *D-12*
D.1.3.3 Test methods used in experimental factorial design *D-17*
D.1.4 Material Characteristics **D-18**
D.1.4.1 Binder *D-18*
D.1.4.2 Aggregate *D-18*
D.1.4.3 Chemical admixtures *D-19*

D.2 TEST METHODS AND WORKABILITY PERFORMANCE-BASED SPECIFICATIONS **D-20**

D.2.1 Test Methods to Assess Workability of SCC **D-20**
D.2.2 Repeatability of Workability Properties **D-20**
D.2.2.1 Single-operator repeatability *D-21*
D.2.2.2 Multi-operator repeatability *D-22*
D.2.2.3 Recommended test methods to evaluate workability *D-23*
D.2.3 Relationships Between Various Workability Responses **D-24**
D.2.3.1 Passing ability vs. filling capacity *D-24*
D.2.3.2 Combined test methods to evaluate filling capacity *D-25*
D.2.3.3 Evaluation of static stability *D-27*
D.2.3.4 Relationship between workability characteristics and rheological parameters *D-30*
D.2.4 Recommended Test Methods and Workability Performance-Based Specifications **D-33**

D.3 EFFECT OF MIXTURE CONSTITUENTS AND COMPOSITION ON WORKABILITY AND MECHANICAL PROPERTIES OF SCC **D-35**

D.3.1 Evaluation Scheme **D-35**
D.3.2 Effect of Binder Type on SCC Performance **D-37**

D.3.3 Effect of Maximum Coarse Aggregate Size and Type on SCC Performance D-38
D.3.4 Effect of *w/cm* and Air Entrainment on SCC Performance D-39
D.3.5 Effect of Fluidity Level on SCC Performance D-40
D.3.6 Effect of Viscosity-Modifying Admixture on SCC Performance D-41
D.3.7 Guidelines for Material Selection D-42

D.4 FACTORIAL DESIGN TO MODEL FRESH AND HARDENED PROPERTIES OF SCC USED IN PRECAST PRESTRESSED APPLICATIONS D-43

D.4.1 Statistical Models for Fresh Concrete Properties D-44
D.4.1.1 Established statistical models D-44
D.4.1.2 Validation of established models for fresh properties D-47
D.4.2 Formwork Pressure D-48
D.4.3 Temperature Rise under Semi-Adiabatic Conditions D-49
D.4.4 Statistical Models for Mechanical Properties D-51
D.4.4.1 Established statistical models D-51
D.4.4.2 Validation of statistical models for mechanical properties D-54
D.4.5 Statistical Models for Visco-Elastic Properties D-55
D.4.6 Guidelines for Proportioning SCC for Precast, Prestressed Girder Construction D-61

D.5 VALIDATION OF CODE PROVISIONS FOR MECHANICAL AND VISCO-ELASTIC PROPERTIES D-65

D.5.1 Mechanical Properties D-65
D.5.1.1 Compressive strength D-65
D.5.1.2 Modulus of elasticity D-68
D.5.1.3 Flexural strength D-71
D.5.2 Visco-Elastic Properties D-73
D.5.2.1 Drying shrinkage D-73
D.5.2.2 Creep in compression D-77
D.5.3 Recommendations for Prediction of Mechanical and Visco-Elastic Properties of SCC Used for Precast, Prestressed Girders D-79

D.6 STRUCTURAL PERFORMANCE D-82

D.6.1 Bond Strength of Prestressing Strands D-82
D.6.1.1 Bond strength and in-situ compressive strength determination D-84
D.6.1.2 Pull-out bond strength and modification factor D-87
D.6.1.3 Effect of stability on homogeneity of in-place compressive and bond strength D-88
D.6.1.4 Recommendations to ensure homogenous in-situ properties D-91
D.6.2 Structural Performance of Full-Scale AASHTO-Type Girders D-92
D.6.2.1 Testing program and details of AASHTO-Type II girders D-92
D.6.2.2 Instrumentation D-95
D.6.2.3 Pretensioning operation D-95
D.6.2.4 Casting and steam curing of AASHTO girders D-95

D.6.2.5 Pretensioning release *D-96*
D.6.2.6 Concrete material properties *D-99*
D.6.2.7 Reinforcing steel and prestressing steel properties *D-102*
D.6.2.8 Test setup and procedure *D-102*
D.6.3 Flexural Behavior D-103
D.6.3.1 Camber measurements *D-103*
D.6.3.2 Overall response in flexure *D-104*
D.6.4 Shear Behavior D-105
D.6.5 Conclusions D-107

D.7 CONCLUSIONS D-109
D.7.1 Test Methods and Material Requirements D-109
D.7.2 Material Constituents and Mix Design D-110
D.7.3 Validation of Code Provisions to Estimate Mechanical and Visco-elastic Properties D-113
D.7.4 Homogeneity of In-Situ Strength and Bond to Reinforcement D-114
D.7.5 Structure Performance of AASHTO-Type II Girders D-114

APPENDIX A D-116
LITERATURE REVIEW OF FACTORS AFFECTING PERFORMANCE OF SCC USED IN PRECAST, PRESTRESSED APPLICATIONS
APPENDIX B D-264
TEST METHODS TO ASSESS WORKABILITY OF SCC
APPENDIX C D-277
VARIATIONS OF TEMPERATURES OF CHAMBER AND CONCRETE DURING STEAM CURING
APPENDIX D D-283
DECAY IN FORMWORK PRESSURE DETERMINED ON 3.6-FT (1.1-M) HIGH COLUMNS (CASTING RATE 4 – 5 M/HR)
APPENDIX E D-289
MATERIALS CHARACTERISTICS OF CEMENT, SUPPLEMENTARY CEMENTITIOUS MATERIALS, SAND, AND COARSE AGGREGATE
APPENDIX F D-294
MIXTURE PROPORTIONING OF MIXTURES NO. 1 TO 22 EVALUATED IN FACTORIAL DESIGN
APPENDIX G D-299
FRESH PROPERTIES OF MIXTURES NO. 1 TO 22 EVALUATED IN FACTORIAL DESIGN

APPENDIX H **D-304**

BINGHAM FLOW CURVES AND RHEOLOGICAL PARAMETERS OF 22 SCC MIXTURES INVESTIGATED IN FACTORIAL DESIGN

APPENDIX I **D-310**

BREAKDOWN AREA CURVES OF 22 SCC MIXTURES INVESTIGATED IN FACTORIAL DESIGN

APPENDIX J **D-316**

MECHANICAL PROPERTIES OF MIXTURES NO. 1 TO 22 EVALUATED IN FACTORIAL DESIGN

APPENDIX K **D-326**

STATISTICAL MODELS FOR FRESH AND MECHANICAL PROPERTIES

APPENDIX L **D-328**

COMPARISONS OF MEASURED AND PREDICTED DRYING SHRINKAGE STRAINS

APPENDIX M **D-333**

COMPARISONS OF MEASURED AND PREDICTED CREEP STRAINS

APPENDIX N **D-338**

PULL-OUT LOAD VERSUS FREE-END SLIP RESPONSES DETERMINED ON WALL ELEMENTS NO. 1 TO 6

APPENDIX O **D-340**

IN-PLACE COMPRESSIVE STRENGTH OF WALL ELEMENTS CAST WITH DIFFERENT SCC WITH DIFFERENT STABILITY LEVELS

APPENDIX P **D-342**

STRUCTURAL PERFORMANCE OF FULL-SCALE AASHTO-TYPE GIRDERS

LIST OF FIGURES

Fig. D.1 – Steam curing regime D-12
Fig. D.2 – Relationship between filling capacity and J-Ring flow measured at 10 minutes D-25
Fig. D.3 – Relationship between filling capacity and difference between slump and J-Ring flow values measured at 10 minutes D-25
Fig. D.4 – Variations of filling capacity with L-box blocking ratio..... D-26
Fig. D.5 – "Workability box" for filling capacity as a function of L-box blocking ratio and slump flow D-26
Fig. D.6 – Lower limits of slump flow and difference between slump and J-Ring flow values of SCC made with crushed aggregate to secure minimum filling capacity of 80%..... D-27
Fig. D.7 – Relationship between rate of settlement and maximum settlement..... D-28
Fig. D.8 – Variation in column segregation index with rate of surface settlement..... D-29
Fig. D.9 – Relationship between column segregation index (C.O.V.) and percent of static of segregation (S) D-30
Fig. D.10 – Relationship between plastic viscosity and L-box blocking ratio D-32
Fig. D.11 – Variations of the rate of surface settlement determined after 30 minutes of testing and initial plastic viscosity for SCC made with different coarse aggregates..... D-32
Fig. D.12 – Variations of the segregation index and plastic viscosity determined at 10 minutes..... ..... D-33
Fig. D.13 − SCC mixtures used to validate the derived models D-47
Fig. D.14 − Comparison between predicted and measured workability responses: (slump flow – J-Ring flow) and plastic viscosity..... D-48
Fig. D.15 − Comparison between temperature variations under semi-adiabatic conditions D-50
Fig. D.16 – Development of compressive strength of 20 SCC and two HPC mixtures D-51
Fig. D.17 – Comparison between predicted and measured mechanical properties: 18-hour and 56-day compressive strength..... D-55
Fig. D.18 – Variations of creep strain for SCC and HPC mixtures..... D-56
Fig. D.19 – Variations of autogenous shrinkage for SCC and HPC mixtures D-58
Fig. D.20 – Variations of drying shrinkage for SCC and HPC mixtures D-59
Fig. D.21 – Comparison of measured and predicted compressive strength (plotted data include 18-hour, 7-, 28-, and 56-day compressive strength results)..... D-66
Fig. D.22 – Comparison of measured and predicted compressive strength data for modified models (plotted data include 18-hour, 7-, 28-, and 56-day compressive strength results) D-68
Fig. D.23 – Comparison of measured and predicted moduli of elasticity D-69
Fig. D.24 – Comparison of measured and predicted elasticity moduli from modified models D-70
Fig. D.25 – Comparison of measured and predicted flexural strengths..... D-72
Fig. D.26 – Measured vs. predicted flexural strengths from modified models..... D-72
Fig. D.27 – Comparison of measured and predicted drying shrinkage values D-76
Fig. D.28 – Comparison of measured and predicted drying shrinkage from modified models D-77
Fig. D.29 – Comparison of measured and predicted creep values..... D-78
Fig. D.30 – Comparison of measured and predicted creep values from modified models..... D-79
Fig. D.31 – Detail dimensions of experimental wall elements (mm, 1 in. = 25.4 mm)..... D-84
Fig. D.32 – Pull-out testing arrangement..... D-85
Fig. D.33 – Pull-out response of strands embedded at different heights (mixture 4, wall 1) ... D-85
Fig. D.34 − Distribution of in-place compressive strength at 56 days determined from core

samples along experimental wall elements D-86
Fig. D.35 − Variation in relative core compressive strength with height compared to reference cylinders D-86
Fig. D.36 − Variations in in-place compressive strength with height (strength ratio relative to bottom layer) D-87
Fig. D.37 − Variation in bond strength of prestressing strands along wall height D-87
Fig. D.38 − Variation of modification factor of prestressing strands along wall height D-88
Fig. D.39 − Relationship between surface settlement results determined on PVC columns and wall elements D-89
Fig. D.40 − Relationship between mean relative in-place compressive strength (core to reference cylinders) and maximum surface settlement (PVC settlement test) D-89
Fig. D.41 − Image analysis of cast core sample D-90
Fig. D.42 − Relationship between modification factor and stability of SCC D-91
Fig. D.43 – Details of precast, prestressed AASHTO-Type II girders D-93
Fig. D.44 – Details of non-prestressed reinforcement D-94
Fig. D.45 – Locations of strain gages and vibrating wire gages D-95
Fig. D.46 – Temperature history of chamber and concrete girder during steam curing D-96
Fig. D.47 – Measurement of transfer length D-98
Fig. D.48 – Variations of autogenous shrinkage with time for SCC and HPC D-101
Fig. D.49 – Variations of drying shrinkage with time for SCC and HPC D-101
Fig. D.50 – Test setup and locations of LVDTs D-102
Fig. D.51 – Specimen H8 before testing D-103
Fig. D.52 – Variation of camber with time D-103
Fig. D.53 – Moment versus central deflection responses of the girders D-104
Fig. D.54 – Comparison of shear versus deflection responses for the four specimens (deflection measured at the loading point) D-105
Fig. D.55 – Girders just before and just after failure D-106

LIST OF TABLES

Table D.1 – Parametric experimental program D-10
Table D.2 – Experimental program of parametric investigation (43 mixtures) D-11
Table D.3 − Curing conditions used in parametric and factorial design investigations..... D-12
Table D.4 – Details of experimental program used in factorial design..... D-14
Table D.5 – Testing program used in factorial design D-15
Table D.6 – Test methods relevant for fabrication of precast, prestressed bridge elements D-20
Table D.7 – Single-operator repeatability of workability test results of SCC with 27.5 ± 0.4 in. (700 ± 10 mm) slump flow D-21
Table D.8 – Single-operator repeatability of workability test results of SCC with 25.0 ± 0.4 in. (635 ± 10 mm) slump flow D-22
Table D.9 – Multi-operator repeatability of workability test results of SCC with 27.5 ± 0.4 in. (700 ± 10 mm) slump flow D-23
Table D.10 – Multi-operator repeatability of workability test results of SCC with 25.0 ± 0.4 in. (635 ± 10 mm) slump flow D-23
Table D.11 – Summary of relative errors for recommended workability test methods D-24
Table D.12 – Rheological parameters determined at 10 minutes D-31
Table D.13 – Combined test methods and recommended workability values for medium and high densely reinforcements D-34
Table D.14 – Evaluation method to compare effect of material constituents and mix design parameters on workability and mechanical properties of SCC..... D-35
Table D.15 – Relative performance of SCC mixtures for precast, prestressed applications D-36
Table D.16 – Evaluation method to rank the relative influence material constituents and mixture parameters on workability and mechanical properties of SCC..... D-37
Table D.17 – Effect of binder type on SCC performance D-38
Table D.18 – Effect of aggregate size and type on SCC performance..... D-39
Table D.19 – Effect of w/cm and air entrainment on SCC performance D-40
Table D.20 – Effect of fluidity level on SCC performance..... D-41
Table D.21 – Effect of fluidity level on SCC performance..... D-42
Table D.22 − Recommendations for mixture proportioning for SCC used in precast, prestressed applications D-42
Table D.23 – Absolute and coded values of modeled parameters D-43
Table D.24 − Mean values and relative errors of central points (90% confidence limit) D-44
Table D.25 − Derived statistical models for fresh concrete [slump flow = 26.8 ± 0.8 in. (680 ± 20 mm)]..... D-45
Table D.26 − Mixture proportioning used to validate the derived statistical models D-47
Table D.27 – Initial form pressure and time to pressure cancellation of SCC and HPC D-49
Table D.28 − Derived statistical models for mechanical properties D-54
Table D.29 − Mean values and relative errors of central points (90% confidence limit) D-54
Table D.30 − Derived statistical models for visco-elastic properties D-60
Table D.31 – Relative significance of modeled SCC parameters D-62
Table D.32 – Recommendations for proportioning SCC for precast prestressed applications (based on statistical models) D-63
Table D.33 – ACI 209 and CEB-FIP MC90 compressive strength prediction equations D-65
Table D.34 – Suggested modifications to model codes to predict compressive strength of SCC 67

Table D.35 – AASHTO 2007, CEB-FIP MC90, and ACI models for elastic modulus D-69
Table D.36 – Model for modulus of elasticity and relevant changes to model coefficients D-70
Table D.37 – Modified flexural strength prediction model D-71
Table D.38 – Summary of various models for drying shrinkage D-74
Table D.39 – Summary of various models for creep D-75
Table D.40 – Summary of suggested coefficients for models used to predict mechanical and visco-elastic properties of SCC used in precast, prestressed applications D-80
Table D.41 – Recommended mechanical and visco-elastic prediction models for SCC used in precast, prestressed girder constructions D-81
Table D.42 – SCC and HPC mixtures for strand bond testing D-82
Table D.43 – Mixture proportioning and fresh properties of tested concretes D-83
Table D.44 – Recommendations to secure homogenous in-situ properties of SCC D-91
Table D.45 – Average values of strand set D-97
Table D.46 – Summary of 95% AMS transfer lengths D-98
Table D.47 – Mixture proportioning of SCC and HPC for girders D-99
Table D.48 – Fresh properties of SCC and HPC mixes used for girders D-100
Table D.49 – Comparison of flexural responses of four specimens D-104
Table D.50 – Comparison of shear responses of four specimens D-107
Table D.51 − Performance-based specifications and workability test methods D-109
Table D.52 – Relative significance of modeled SCC parameters D-110
Table D.53 – Recommendations for proportioning SCC for precast prestressed applications D-111

D.1 INTRODUCTION, LITERATURE REVIEW, AND RESEARCH APPROACH

D.1.1 Background

Use of SCC in the construction of precast bridge members, bridge substructures, and in the repair of bridges has been limited in the United States. Properly designed SCC is expected to provide similar properties as the conventional counterparts except for the high workability. However changes in mix design and fluidity of SCC can result in SCC with hardened properties and performance that are different from that commonly expected from conventional concrete.

Proper selection of material constituents is necessary for workability and overall performance of the concrete. Unlike conventional vibrated concrete, successful design of SCC implies that some factors require greater attention than conventional concrete, including the type of nominal size of coarse aggregate, aggregate packing, binder composition and content, and water-cementitious materials ratio (*w/cm*).

A number of test methods have been used to characterize SCC workability, including filling ability, passing ability, and segregation resistance. No single test method has been found to fully characterize all the relevant workability aspects of SCC. The establishment of proven combination of test methods can provide adequate quality control for field applications.

Material properties that can significantly influence the design, constructability, and performance of precast, prestressed bridge elements made with SCC need to be thoroughly investigated. Knowledge of compressive strength, elastic modulus, and flexural strength of concrete is important to estimate camber of prestressed members at the release of the prestressing load, as well as to determine elastic deflections caused by dead and live loads, axial shortening and elongation, as well as prestress losses. Literature review showed that SCC can exhibit up to 20% reduction in modulus of elasticity compared to high-performance concrete (HPC) of normal consistency given the lower coarse aggregate volume of SCC. However, under air-drying conditions, the modulus of elasticity of SCC can be higher than that of normal concrete at long term. Limited published data are available on relationships between flexural strength and compressive strength of SCC, hence the various code models need to be validated when using SCC.

Typically, SCC has higher binder content and lower coarse aggregate volume and nominal size. These factors could increase the risk of thermal, autogenous and drying shrinkage, as well as creep leading to loss of prestress and high deflections and elastic shortening. According to the literature survey, there seems to be some discrepancy regarding the visco-elastic properties of SCC. Several factors can explain this discrepancy, in particular mix design (*w/cm*), type and content of coarse aggregates, type of chemical admixture, and testing exposure. It is reported that the creep potential of SCC appears to be slightly higher than that of conventional concrete made with the same raw materials and 28-day compressive strength. Depending on the selected binder, *w/cm*, and ambient temperature at the precasting plant, the use of new generation polycarboxylate ether-based high-range water reducing admixture (HRWRA) may eliminate the need to use radiant heat or steam curing to secure high early-age strength development.

SCC used in precast, prestressed applications is typically proportioned with low *w/cm* of 0.32 to 0.36. Low *w/cm* coupled with high binder content can lead to greater degree of autogenous shrinkage. Autogenous shrinkage increases with the fineness of cement, supplementary cementitious materials, and fillers in use. Therefore, in addition to drying shrinkage, the increased volume of ultra-fines in SCC can lead to higher autogenous shrinkage and thermal contraction that have to be managed in the mix design and detailing of the prestressed element.

Experimental shrinkage strains for SCC were found to be larger than those estimated by various prediction models for drying shrinkage. Similarly, comparison of experimental creep data to creep-prediction models did not yield accurate results. Work is therefore required to compare creep and shrinkage data of SCC mixtures made with representative mix designs and material constituents available in the United States to AASHTO shrinkage and creep prediction models and propose relevant modifications if necessary.

The resistance of SCC to bleeding, segregation, and surface settlement (i.e., static stability) is a key material property to ensure homogeneous development of the microstructure, and hence uniform distribution of mechanical properties and transport properties of concrete structures. The lack of static stability of SCC can lead to non-uniformity distribution of bond strength between the concrete and reinforcement along the height of cast elements. Some studies indicate that bond strength of the reinforcement to SCC can be lower than that of conventional concrete. Other studies, however, indicate that for a given compressive strength, reinforced concrete members made with SCC can develop higher bond than in the case of normal concrete. Therefore, it is essential to evaluate the effect of SCC composition and workability on the distribution of bond strength between SCC and prestressing strands to derive proper bond modification factors for SCC.

The structural design concerns regarding the use of SCC for constructing prestressed girders include the likely lower modulus of elasticity and greater shrinkage of SCC leading to possibly larger prestress losses. Furthermore, the use of either a smaller maximum size aggregate or lower volume of coarse aggregate could lead to reduced shear resistance of the SCC. Full-scale testing of AASHTO girders is required to compare the structural response of SCC to HPC of conventional fluidity. The structural response includes transfer lengths, cambers, flexural cracking, shear cracking, and shear strengths.

The large body of information generated in this and other investigations is exploited to propose changes to AASHTO LRFD bridge design and construction specifications. Such information is also used to compile guidelines for the use of SCC in bridge elements. These guidelines along with the proposed changes to AASHTO LRFD bridge specifications can provide highway agencies with the information necessary for considering the use of SCC mixtures that are expected to expedite construction and yield economic and other benefits associated with SCC (surface finish, reduction in labor cost, etc.).

D.1.2 Literature Review

An extensive literature review was carried out to validate factors affecting the performance of SCC used in precast, prestressed structural applications. Workability characteristics, test methods, requirements for constituent materials and mix design guidelines, production and placement characteristics, factors affecting mechanical properties and structural performance, factors

affecting visco-elastic properties, and durability characteristics of SCC were considered in the literature review. The most significant factors affecting the performance of SCC used in precast, prestressed applications are provided at the end of each section of the literature review, and are briefly summarized below. The literature review document is given in its entirety in CD format in Appendix A.

D.1.2.1 Workability characteristics and test methods

SCC should exhibit high filling ability, proper passing ability, and adequate segregation resistance to adequately flow into place and encapsulate the prestressing strands and reinforcing bars without segregation or blockage. The SCC should exhibit adequate retention for a given period of time (typically 30 minutes for SCC prepared at precast plants) to enable transport and casting without the need to readjust the mixture. The concrete should exhibit proper dynamic stability to maintain homogeneous suspension of the mixture constituents during transport and placement. It should also exhibit high resistance to segregation, bleeding, and surface settlement after casting until the onset of hardening, i.e. proper static stability. The latter characteristic is especially important to maintain uniform properties of the hardened concrete. The finished element should also have uniform surface quality and superior surface finish. In selecting the fresh characteristics of the SCC, the section intricacy, depth, minimum thickness, and length; the reinforcement density; as well as the selected placement method should be taken into consideration to ensure proper performance.

The most promising test methods that are relevant for the fabrication of precast, prestressed concrete bridge elements are shown below. However, limited information regarding the repeatability and relative error of these methods and the influence of the operator on the testing accuracy are available.

	Test methods for mix design	Test methods for quality control at plant
Filling ability	Slump flow (ASTM C1611) T-50$_{cm}$ slump flow	Slump flow (ASTM C1611) T-50$_{cm}$ slump flow
Passing ability	L-box J-Ring (ASTM C1621) V-funnel	L-box J-Ring (ASTM C1621)
Filling capacity	Caisson test (filling vessel)	
Segregation resistance	Visual stability index (VSI) Surface settlement and rate of settlement Column segregation (ASTM C1610)	Visual stability index (VSI) Rate of settlement after 30 minutes Column segregation (ASTM C1610)

The VSI test provides visual assessment of the homogeneity of the SCC. However, a mixture with rating of 0 or 1 determined shortly before casting of a structural element does not guarantee proper resistance to segregation during the plastic state. It is recommended to complement the VSI test with a quantitative test, such as the column segregation or surface settlement test. The former is rather long as it involves the determination of the relative coarse aggregate content at four sections along a concrete column. For field use, this may be substituted by determining the relative coarse aggregate content at the top and bottom sections only, as suggested in ASTM C1610 standard test method. The waiting time of 15 minutes before removing the concrete from

various sections for wet sieving may also be reduced providing that the concrete is subjected to some controlled vibration in the form of shock. The surface settlement test is rather long for use as a quality control test in the field. Instead, the rate of settlement after 30 minutes can be determined; such value has been shown to correspond well to the maximum surface settlement.

Deformability and stability can be related to the rheological parameters of the concrete, yield stress and plastic viscosity. The slump flow and T-50 values can be related to yield stress and plastic viscosity, respectively. The speed of spread of SCC through the V-funnel, U-box, and L-box can be related to plastic viscosity. Some of the workability characteristics, such as segregation index of the column segregation test, are shown to depend on both the yield stress and plastic viscosity. Better understanding of the rheological parameters that control the workability of SCC is important in developing mix design approaches and interpreting quality control test methods.

SCC made with polycarboxylate-based HRWRA can exhibit, in some cases, increase in air volume during mixing and agitation. Such increase in air content does not necessary lead to better air-void system, in the absence of air-entraining admixture. Therefore, the stability of the air must be well determined and controlled in developing the concrete mixture and in quality control during production, especially in regions where air-entrainment is required for frost durability.

D.1.2.2 Material constituents and mix design

Material characteristics and mix design of SCC have marked effect on production, placement, and performance of SCC. Compared to conventional vibrated concrete, there are a number of factors that should be taken into consideration to a greater degree when designing SCC. This includes the type and shape of coarse aggregate, combined gradation of sand and coarse aggregate, content of cement and supplementary cementitious materials, paste volume, and *w/cm*. In the selection of material constituents and mixture proportioning for precast, prestressed applications, it is essential that the concrete achieves the targeted properties in terms of early-strength development. In addition, to achieve required workability and surface finish characteristics, the concrete should be proportioned to develop the required early-age strength, design strength, as well as durability requirements.

Type I Portland cement is generally used in applications where special properties, such as early-strength or sulphate attack, are not required. Type III cement is used to accelerate strength gain, thus allowing earlier prestressing and demolding to ensure optimal re-use of forms. The use of Type III cement, or finely ground Type I cement, can reduce or eliminate the need for steam curing or radiant heat curing.

Deformability and stability characteristics of the concrete depend on the SCC mix design, which is affected by the type and properties of the cement and supplementary cementitious materials in use. For example, for a given *w/cm*, Type III cement requires higher water and HRWRA demand than Type I/II cement to achieve a given consistency. Furthermore, the loss of fluidity in the case of SCC made with Type III cement than that with Type I/II.

The content of C_3A in the cement and Blaine fineness of the cement and supplementary cementitious materials affect water demand, fluidity retention, as well as setting and hardening characteristics. For a given water content, the increase in cement fineness increases greater water and HRWRA demand. Given the workability, strength, and durability requirements, the fineness

of cement should be limited to avoid sharp loss in workability during production of prestressed concrete members.

The use of supplementary cementitious materials is widely accepted in the precast, prestressed industry. For example, Washington State DOT allows the use of fly ash, but limits the replacement of fly ash in Type IP (MS) to 25% by mass of the cementitious materials. New York State DOT specifications [2002] stipulate that the contents of fly ash, silica fume, and blast-furnace slag should not exceed 22%, 10%, 22%, by mass, respectively, of the total binder for Types IP, SF, and SM blended cements.

The total content of cementitious materials used in SCC is relatively high compared to conventional concrete, and can range between 715 to 1000 lb/yd^3 (424 to 593 kg/m^3). The binder content and its composition have direct influence on water and HRWRA demand, fluidity retention, finishing characteristics of fresh concrete, temperature rise, setting, early age strength, and the performance of the hardened concrete.

Properly graded aggregates are required to reduce the risk of bleeding and segregation as well as the inter-particle friction needed to lower water demand. The shape and content of coarse aggregate have marked effect on flow ability, filling capacity, and static stability of SCC. Rounded aggregates improve flow characteristics of SCC, given the lower internal friction among aggregate particles. Therefore, SCC made with rounded aggregate requires lower HRWRA dosage than that with crushed aggregate. The maximum size of aggregate (MSA) should be selected based on the minimum clear spacing between the reinforcing steel and prestressing stands, clear cover to the reinforcement, and geometry of the elements to be cast. The reduction in MSA is required to enhance deformability and to reduce segregation and blockage during placement. The decrease in coarse aggregate content, reduction of MSA, and increase in the content of powder material can also enhance the resistance to segregation and surface settlement.

Chemical admixtures are used in precast, prestressed concrete to reduce water content, improve deformability and stability, provide air entrainment, accelerate strength development, enhance workability retention, and retard setting time. The performance of these admixtures depends on other mixture parameters, including *w/cm*, binder characteristics, and presence of other admixtures. Of particular interest to precast, prestressed applications is the use of polycarboxylate-based HRWRA; such HRWRA can lead to high reduction water demand without extended set retardation, which could reduce or eliminate heat curing.

SCC used in precast, prestressed applications is typically proportioned with low *w/cm* to secure strength development. The relatively low free water content in such concrete increase the plastic viscosity of the SCC and reduces the need for incorporating a VMA to control segregation. VMA is typically used in SCC proportioned with low to moderate binder content, for example, less than 715 lb/yd^3 (425 kg/m^3), or mixtures with *w/cm* values greater than 0.40. Still, the incorporation of VMA in SCC designated for precast applications can lead to more robust and consistent production of SCC. This is especially true for SCC with relatively low powder content and non-optimum grain-size distribution, especially in the case where the moisture control of aggregate is not adequate. Mixtures made with VMA tend to be more tolerant to small changes in moisture content and fineness modulus of the sand, dosage of HRWRA, and temperature of the fresh concrete.

The use of polycarboxylate-based HRWRA may lead to the entrapment of large volume of coarse air bubbles. This is related to the type and content of the de-foamer in use and the mixing and agitation energy of the concrete after the addition of HRWRA. Concrete subjected to prolonged mixing or agitation after the introduction of HRWRA could exhibit some increase in air content, without necessary refinement in the size of air bubbles. Investigations carried out with naphthalene-based HRWRA indicate that the stability of air volume can be enhanced in SCC mixtures proportioned with a relatively low *w/cm* (i.e. high binder contents) or those made with VMA. However, beyond a certain viscosity level, the stability of fine air bubbles during agitation could be hindered. The use of AEA is required, through at low dosage, to ensure proper air-void system whenever the concrete is designated for frost durability. In order to ensure stable air volume in the fresh concrete, the SCC should be viscous to retain the air bubbles in uniform suspension.

D.1.2.3 Production and placement characteristics

The constructability of SCC depends on the reliability of material quality control, mixing process, transportation, casting, finishing, and curing.

Greater care and precision are required for the production of SCC than conventional concrete, thus increasing the need for inspection and quality control. Strict quality control should be used with respect to aggregate gradation, moisture content, and fineness modulus of the sand. It is essential to maintain uniform quality of all constituent materials in the production of SCC. A lower tolerance for batching errors is required for SCC, necessitating more frequent calibration of batching equipments to limit the potential for fluctuations in the batched proportions. A batching sequence should be established that promotes optimal concrete production.

The type and condition of the mixer have an impact on mixing efficiency. Special considerations are given to mixer condition before mixing SCC to avoid concrete contamination by water or admixtures used in previous batches. Generally, the mixing time for SCC needs to be longer than that for conventional concrete to achieve a homogenous and well-dispersed mass. The mixing method should be adequately established on the basis of field experience or testing. Suitable mixing sequence should be optimized and adhered to strictly to produce uniform quality concrete. The batch size should be determined in consideration of the type of SCC, efficiency of the mixer, batch volume, and production rate.

Delivery and placement of SCC must be completed within the workability-retention time of the concrete. Adequate inspection of workability is important when casting SCC. At the completion of placement, the concrete should still satisfy the stipulated deformability, passing ability, and stability requirements.

The method of transport and discharge should be taken into consideration in finalizing the workability characteristics of the SCC. The required workability of SCC should be compatible with the rate at which the concrete is discharged, the total volume of concrete being discharged, and whether or not the placement process is continuous or discontinuous.

The casting rate of SCC should be established adequately according to the geometry of members, reinforcement conditions, and mixture proportions on the basis of test results and field experience. It is recommended to cast precast, prestressed beams in one continuous operation to avoid lift lines. The flow distance of the SCC should be limited to 20 ft (6 m) in densely reinforced beam elements to maintain uniform in-situ properties of the hardened concrete. Free-

fall distance of SCC in the formwork should be controlled to avoid segregation, surface pores, and honeycombs and should be limited to 6.6 ft (2 m) for casting of wall and beam elements.

The necessity of having a quality surface finish can be dictated by the characteristics of the SCC mixture itself, and by the skill and timing of the finisher during placement. The form release agent, casting rate, deformability of the SCC, powder content, and incorporation of VMA play an important role on the quality and outcome of the finished surface. Improved surface appearance is generally obtained with SCC that has high slump flow consistency; care must be taken to eliminate bleeding and ensure adequate segregation resistance. SCC surfaces should be roughly leveled to the specified dimensions, and the finishing should then be applied at an appropriate time before the concrete stiffens. Care must be exercised in thixotropic mixtures where "stickiness" can increase rapidly after placement.

SCC tends to dry faster than conventional concrete because there is little or no bleed water at the surface. This is especially the case when casting in hot, sunny, or windy conditions. Initial curing should be commenced as soon as practicable after placement and finishing operations are completed in order to minimize plastic shrinkage. If the surface of the concrete begins to dry before the selected curing method can be applied, the surface of the concrete shall be kept moist by a fog spray. Care must be taken to avoid surface damage.

D.1.2.4 Mechanical properties

Changes in mix design and workability of SCC can influence hardened properties and performance that can diverge from what is commonly expected from conventional concrete. The design of most precast, prestressed concrete members is based on 28-day compressive strength, which is typically 5000 to 6000 psi (34.5 to 41.4 MPa). However, mixtures for precast, prestressed girder elements should be proportioned to achieve the specified release strength of 4000 psi (27.6 MPa) within 18 hours after casting, as specified in AASHTO LRFD Bridge Design Specifications 1998. However, the high early-strength requirement and the typically low *w/cm* used in some SCC to enhance stability of SCC could lead to 28-day compressive strength greater than 8000 psi (55.2 MPa).

Knowledge of the elastic modulus of concrete is important to estimate camber of prestressed members at the release of the prestressing load, as well as to determine elastic deflections caused by dead and live loads, axial shortening and elongation, and prestress losses. The modulus of elasticity of the parent rock and the relative volume of the aggregate in the concrete mixture has significant influence on the modulus of elasticity of the concrete. In addition to the total aggregate volume, adjustments of the sand-to-aggregate ratio (S/A) can influence the elastic modulus of the SCC. Spread of up to 20% could be obtained compared to the modulus of elasticity of high-performance concrete of normal consistency given the lower coarse aggregate volume of SCC. However, under air-drying conditions, the elastic modulus of SCC can be higher than that of conventional concrete in long term. These results can be attributed to the lower loss of water that may occur in the case of SCC.

Because of the relatively low *w/cm* typically used in proportioning SCC and the incorporation of supplementary cementitious materials, SCC could develop higher flexural strength and flexural-to-compressive ratio than conventional slump concrete. Limited published data are available on relationships between flexural strength and compressive strength of SCC, and the various code models need to be validated for SCC.

The stability of SCC is a key property in ensuring uniform mechanical properties and adequate performance of precast, prestressed bridge girders. Properly designed SCC mixtures can exhibit uniform distribution of in-situ compressive strength. Stability of SCC can be enhanced by using low *w/cm*, reducing the MSA, or incorporating a VMA.

Bond strength and its uniformity along the height of cast girders can be influenced by flow properties of the SCC, grading of the aggregate, and content of fines. Some studies have found that bond strength of the reinforcement to SCC can be lower than that of normal concrete. Other studies, however, have shown that for a given compressive strength, reinforced concrete members made with SCC can develop higher bond than in the case of normal concrete. Tests carried out using full-scale girders revealed that the strand transfer length obtained on experimental girders cast with SCC is about 30% longer than the limit recommended by AASHTO. Full-scale tests revealed that immediately after prestress release (18 hours), girders cast with SCC are shown to exhibit similar initial camber and comparable strand slip-end as those of girders cast with normal concrete. SCC can develop similar top-bar effect as that of conventional concrete when it is proportioned with sufficient static stability.

The shear strength of the concrete affects the structural performance of precast, prestressed girders. Given the relatively high compressive strength of SCC used in precast structural applications and the fact that the interfacial transition zone with the aggregate is intact, cracked surfaces can involve a greater degree of intergranular crack propagation. This can then reduce aggregate interlock crack-friction capacity of members made with SCC.

D.1.2.5 Visco-elastic properties

The most relevant material characteristics that can affect creep and shrinkage of concrete are: volume fraction and rigidity of the aggregate, cement type, the type and content of supplementary cementitious materials, paste volume, water content, type of chemical admixtures, and compressive strength of the matrix, which is related to air content. Decrease in relative humidity, increase in ambient temperature, oscillation of ambient conditions, early exposure to drying and loading, reduction in element size, use of irregular shape and sizes of structural elements, as well as the location of these elements in the structure (loading level) are also important factors that affect creep and shrinkage.

According to the literature review, there seems to be some discrepancy regarding the visco-elastic properties of SCC. Several factors can explain this discrepancy, in particular the mix design (*w/cm* or *w/b*), type and content of coarse aggregates, type of chemical admixture, and testing exposure. The discrepancy also lies in the type of comparison used in the experimental program. Some studies have compared the visco-elastic properties of SCC proportioned differently from normal vibrated concrete, while others have compared the performance of SCC and conventional concrete of similar mix design and compressive strength levels.

Creep behavior is related to the compressive strength of the matrix, coarse aggregate type, and relative content of the aggregate. It is reported that the creep potential of SCC appears to be slightly higher than that of conventional concrete made with the same raw materials and having the same 28-day compressive strength.

Relatively low *w/cm* coupled with high content of binder in SCC can lead to greater degree of autogenous shrinkage than conventional concrete. Autogenous shrinkage can also increase with

the fineness of the binder and fillers in use. Higher autogenous shrinkage has to be managed in the mix design process and in the structural detaining of the prestressed element.

Compared to existing prediction models, studies have shown that the scatter between measured and predicted shrinkage values is greater in the case of SCC than that for conventional concrete. Experimental shrinkage strains for SCC were reported to be larger than those estimated by various prediction models for drying shrinkage. Similarly, comparison of experimental creep data to major creep-prediction models did not result in accurate results, thus justifying the need for investigating creep and shrinkage of SCC designated for precast, prestressed applications.

D.1.2.6 Durability characteristics

Critical factors contributing to the durability of concrete structures include: w/cm, cement content, consolidation of fresh concrete, curing, cover over the reinforcement, and reactivity of aggregate-cement combinations. Similarly, the main factors that control the permeation properties of concrete are the relative volume of the paste, the pore structure of the bulk matrix, and the interfacial zone between the cement paste and aggregate particles. Precast, prestressed concrete bridge beams produced with conventional, vibrated concrete usually have good performance in aggressive environments.

The incorporation of high powder content and HRWRA in SCC can lead to changes in the pore structure of the cement paste compared to conventional concrete. On the other hand, the high fluidity of such concrete can result in greater potential of bleeding and segregation and lead to weak interfacial zone between the cement paste and the aggregate. However, when properly designed and cast, SCC can lead to more homogeneous microstructure and denser interfacial zone with reinforcement and coarse aggregate particles. The type of supplementary cementitious materials and fillers and their levels of substitution, as well as type of chemical admixture in use must be selected to avoid any adverse effect on impermeability and electrical resistance of the concrete.

A denser microstructure can decrease diffusion of chloride ions and other harmful substances, increase frost resistance, and improve service life of the structure. Densification of the cement matrix and increase in concrete cover in well-cured and uncracked concrete can reduce the risk of corrosion. At similar compressive strength, SCC can develop significantly lower permeability coefficient, water sorptivity, and water absorption compared to conventional vibrated concrete.

Bridge structures constructed in environments prone to freezing and thawing necessitate air-entrainment when 20 or more cycles of freezing and thawing per year are expected at the project location. Despite these conditions, some states do not require air entrainment in prestressed concrete beams. One of the reasons lies in the fact that the bridge deck shelters the beams, thus reducing the rate of saturation of the concrete and exposure to any deicing salt applied on the bridge deck.

D.1.3 Research Approach

D.1.3.1 Parametric study

A parametric study was undertaken to evaluate the influence of binder type, *w/cm*, and coarse aggregate type and nominal size on workability and compressive strength development of SCC designated for the construction of precast, prestressed AASHTO girders. As presented in Table D.1, 24 non-air entrained SCC mixtures (No. 1 to 24) were prepared to evaluate workability,

rheology, stability, and strength development characteristics. The mixtures were prepared using either crushed aggregate or gravel with three maximum size aggregate (MSA) of ¾, ½, and 3/8 in. (19, 12.5, and 9.5 mm), *w/cm* of 0.33 and 0.38, and three binder compositions: Type I/II cement as well as Type III cement with either 30% slag or 20% Class F fly ash replacement. Three air-entrained SCC (No. 25 to 27) with low *w/cm* were also investigated.

Table D.1 – Parametric experimental program

Type	Mixture No.	Aggregate type and MSA				Type and content of binder			*w/cm*	
		Crushed ¾ in. (19 mm)	Crushed 3/8 in. (9.5 mm)	Crushed ½ in. (12.5 mm)	Gravel ½ in. (12.5 mm)	Type I/II 809 pcy (480 kg/m^3)	Type III + 30% Slag 775 pcy (460 kg/m^3)	Type III + 20% fly ash 775 pcy (460 kg/m^3)	0.33	0.38
Non air-entrained concrete	1	x				x			x	
	2	x					x		x	
	3	x						x	x	
	4	x				x				x
	5	x					x			x
	6	x						x		x
	7		x			x			x	
	8		x				x		x	
	9		x					x	x	
	10		x			x				x
	11		x				x			x
	12		x					x		x
	13			x		x			x	
	14			x			x		x	
	15			x				x	x	
	16			x		x				x
	17			x			x			x
	18			x				x		x
	19				x	x			x	
	20				x		x		x	
	21				x			x	x	
	22				x	x				x
	23				x		x			x
	24				x			x		x
Air-entrained concrete	25-27	• Air entrainment of 4%-7% and slump flow of 26.0-27.5 in. (660-700 mm) • *w/cm* of 0.33, Type III+20% Class F fly ash, crushed aggregate with MSA of ½ in. (12.5 mm)								
Non air-entrained concrete	28-30	• Low filling ability, slump flow of 23.5-25.0 in. (600-635 mm) • *w/cm* of 0.33, Type III+30% slag, crushed aggregate with MSA of ¾ in. (19 mm)								
	31-33	• High filling ability, slump flow of 28.0-30.0 in. (710-760 mm) • *w/cm* of 0.38, Type III+30% slag, crushed aggregate with MSA of ¾ in. (19 mm)								
	34-43	• Two levels of slump flow consistency for evaluation of repeatability: 25.0 and 27.5 in. (635 and 700 mm) • *w/cm* of 0.38, Type I/II, crushed aggregate with MSA of ½ in. (12.5 mm)								

Sand-to-total aggregate ratio (S/A) is fixed at 0.50, by volume

Three SCC mixtures (No. 28 to 30), similar to mixtures No. 1 to 3, having relatively low slump flow of 23.5 to 25.0 in. (600 to 635 mm) and three other mixtures (No. 31 to 33) similar to mixtures No. 4 to 6 with high slump flow values of 28.0 to 30.0 in. (710 to 760 mm) were prepared. These mixtures (No. 28 to 33) were used to evaluate the effect of fluidity level on passing ability, filling capacity, static stability, and compressive strength development of SCC. The first 33 concrete mixtures in Table D.1 were tested for workability characteristics, compressive strength, and modulus of elasticity, as indicated in Table D.2. Full description of the test methods that were used to evaluate the workability of SCC is provided in Appendix B.

Ten SCC mixtures (No. 34 to 43) having mixture proportioning similar to concrete No. 16 were also used to evaluate the repeatability of the selected workability test methods, which is important to establish the repeatability and reproducibility of each test method.

Table D.2 – Experimental program of parametric investigation (43 mixtures)

SCC behavior	Property	Test Method	Test age	Number of samples per mixture	Comments
Rheology	Yield stress and plastic viscosity	Modified Tattersall MK III rheometer	10 & 40 min	N.A.*	
Filling ability	Slump flow and T-50	AASHTO T 119 ASTM C 1611	10 & 40 min	N.A.	
Passing ability	J-Ring	ASTM C 1621	10 & 40 min	N.A.	
	L-box and V-funnel flow	-	10 & 40 min	N.A.	
Filling capacity	Caisson filling capacity	-	10 & 40 min	N.A.	
Stability	Surface settlement	-	Over the first 24 hours	1	
	Column segregation	ASTM C 1610	10 min	1	
	Visual stability index	ASTM C 1611		N.A.	
	Stability of air**	AASHTO T 152	Over 40 min	N.A.	
Mechanical properties	Compressive strength	AASHTO T 22	18 hours	3 air-cured 3 steam-cured	*Air curing* at 50% ± 4% RH and 73 ± 4°F (23 ± 2°C) *Moist curing* at 100% RH and 73 ± 4°F (23 ± 2°C) *Only steam curing* for 16 hours (Fig. D.1)
			28 days	3 moist-cured	
			56 days	3 moist-cured	
	Modulus of elasticity	ASTM C 469	18 hours	2 steam-cured	

* N.A.: Not applicable
** Agitation of concrete between 10 and 40 minutes at 6 rpm

Several 4×8 in. (100×200 mm) concrete cylinders were sampled within 10 minutes after cement and water contact to evaluate compressive strength and modulus of elasticity. The cylinders were cast in one lift without any mechanical consolidation. The cylinders used in the parametric and factorial design investigations were cured under three curing conditions, as summarized in Table D.3. The targeted steam curing regime is shown in Fig. D.1. In some cases, the curing regime was modified to achieve the targeted release compressive strength of 5,000 psi (34.5 MPa) at 18 hours.

Table D.3 − Curing conditions used in parametric and factorial design investigations

Curing methods	Stages	Details
Steam-cured	I	Ambient temperature for 2 hours after water-cement contact
	II	Temperature raised for 2 hours
	III	Concrete temperature maintained for 10 hours
	IV	Temperature decreases over 2 hours to ambient temperature
	V	Air-curing until age of testing at 18 hours
Moist-cured	I	18 hours in molds with wet burlap at 73 ± 4°F (23 ± 2°C)
	II	Moist-cured at 73 ± 4°F (23 ± 2°C) until testing age
Air-cured	I	18 hours in molds with wet burlap at 73 ± 4°F (23 ± 2°C)
	II	Air-dried at 73 ± 4°F (23 ± 2°C) until testing age

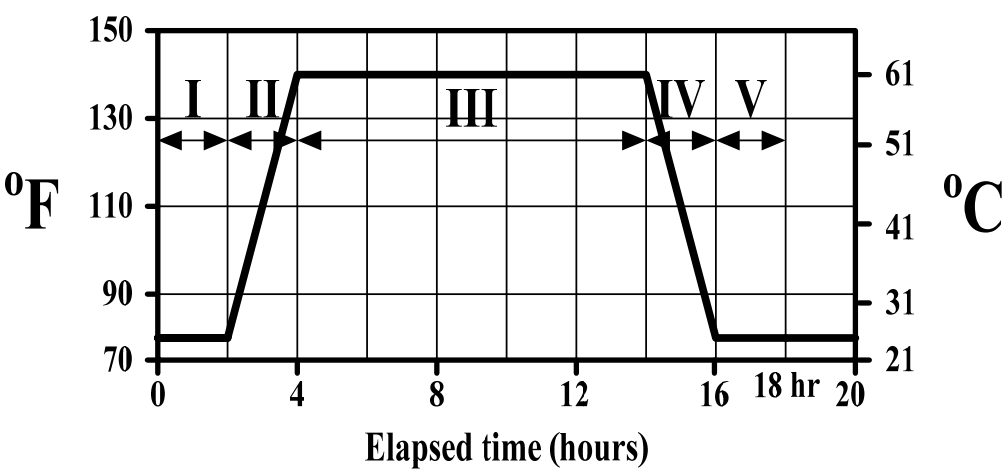

Fig. D.1 – Steam curing regime

D.1.3.2 Factorial design approach

As presented in Table D.4, an experimental factorial design was undertaken to evaluate the influence of mixture proportioning and constituent material characteristics on a number of properties that are critical to the performance of precast, prestressed concrete girders. The effect of primary material characteristics and mix design parameters on workability and key

engineering properties of SCC was evaluated. Based on the literature review and parametric study, four mixture proportioning and one mixture ingredient were considered in the experimental design. The factors included the binder content, binder type, *w/cm*, sand-to-total aggregate ratio (S/A), and dosage of thickening-type viscosity-modifying admixture (VMA). In total, 16 SCC mixtures were developed to establish a factorial design with five main factors. Four of the five parameters used in the factorial design were quantitative in nature, while the fifth one (binder type) was qualitative. Each factor was considered at two levels, as follows:

- binder content: 742 and 843 lb/yd^3 (440 and 500 kg/m^3);
- *w/cm*: 0.34 and 0.40;
- dosage of VMA: 0 and moderate dosage;
- binder type: Type I/II and Type III cement with 20% Class F fly ash;
- sand-to-total aggregate ratio: 0.46 and 0.54, by volume.

The ranges of these variables are selected to cover wide scope of material ingredients and mix designs used in precast plants in the United States. The choices of w/cm and binder type were based on the results of the parametric study. A low *w/cm* was chosen for superior mechanical performance, while the higher *w/cm* limit was selected to reduce HRWRA demand. Type III binder with 20% of Class F fly ash was chosen given the better overall performance of the SCC in terms of workability and compressive strength development compared to similar concrete made with Type III binder and 30% slag.

The coarse aggregate employed for the factorial design was crushed aggregate with MSA of ½ in. (12.5 mm). This aggregate was shown to offer better performances in terms of workability and strength development than gravel of similar MSA or crushed aggregate with 3/8 or ¾ in. (9.5 or 19 mm). Three replicate central points were prepared to estimate the experimental errors for the modeled responses.

The main responses evaluated in the factorial design included rheology, retention of slump flow for 30 minutes, passing ability, filling capacity, static stability, formwork pressure, setting time, compressive and flexural strengths and elastic modulus developments, autogenous and drying shrinkage, and creep. The air-void system and frost durability were evaluated for selected mixtures, as indicated Table D.5.

Table D.4 – Details of experimental program used in factorial design

Type			Mix No.	Coded values					Absolute values				
				Binder	*w/cm*	VMA*	Binder type	S/A**	Binder lb/yd^3 (kg/m^3)	*w/cm*	VMA	Binder type	S/A
Non air-entrained concrete	SCC (26-27.6 in.(660-700 mm slump flow)	Fractional factorial points	1	-1	-1	-1	-1	1	742 (440)	0.34	0	I/II	0.54
			2	-1	-1	-1	1	-1	742 (440)	0.34	0	III***	0.46
			3	-1	-1	1	-1	-1	742 (440)	0.34	moderate	I/II	0.46
			4	-1	-1	1	1	1	742 (440)	0.34	moderate	III	0.54
			5	-1	1	-1	-1	-1	742 (440)	0.40	0	I/II	0.46
			6	-1	1	-1	1	1	742 (440)	0.40	0	III	0.54
			7	-1	1	1	-1	1	742 (440)	0.40	moderate	I/II	0.54
			8	-1	1	1	1	-1	742 (440)	0.40	moderate	III	0.46
			9	1	-1	-1	-1	-1	843 (500)	0.34	0	I/II	0.46
			10	1	-1	-1	1	1	843 (500)	0.34	0	III	0.54
			11	1	-1	1	-1	1	843 (500)	0.34	moderate	I/II	0.54
			12	1	-1	1	1	-1	843 (500)	0.34	moderate	III	0.46
			13	1	1	-1	-1	1	843 (500)	0.40	0	I/II	0.54
			14	1	1	-1	1	-1	843 (500)	0.40	0	III	0.46
			15	1	1	1	-1	-1	843 (500)	0.40	moderate	I/II	0.46
			16	1	1	1	1	1	843 (500)	0.40	moderate	III	0.54
		Central points		0	0	0	0	0	792 (470)	0.37	moderate	I/II-III	0.50
				0	0	0	0	0	792 (470)	0.37	moderate	I/II-III	0.50
				0	0	0	0	0	792 (470)	0.37	moderate	I/II-III	0.50
	HPC		17	• *w/cm* = 0.34, Type I/II cement, ½ in. (12.5 mm) crushed aggregate • Normal consistency mixtures with 6-in. (150-mm) slump									
			18	• *w/cm* = 0.38, Type III + 20% Class F fly ash, ½ in. (12.5 mm) crushed aggregate • Normal consistency mixtures with 6-in. (150-mm) slump									
Air-entrained concrete	SCC		19-22	• Air-entrainment of 4% to 7% and slump flow of 26-27.6 in. (660-700 mm) • Selection of four SCC mixtures based on performance of *Non air-entrained concrete*									

* Thickening-type VMA
** Crushed aggregate with MSA of ½ in. (12.5 mm) and natural sand
*** Type III cement + 20% Class F fly ash

Table D.5 – Testing program used in factorial design

SCC behavior	Property	Test method	Test age	Number of samples per mixture	Comments
Rheology	Yield stress, plastic viscosity, thixotropy	Modified Tattersall MK III rheometer	10 & 40 min	N.A.	
Filling ability	Slump flow, T-50	AASHTO T 119 ASTM C 1611	10 & 40 min	N.A.	
Passing ability & filling capacity	J-Ring	ASTM C 1621	10 & 40 min	N.A.	
	L-box, caisson filling capacity	-			
Stability	Surface settlement	-	Over the first 24 hrs	1	
	Column segregation	ASTM C 1610		1	
	Visual stability index	ASTM C 1611		N.A.	
	Stability of air*	AASHTO T 152	Over 40 min	N.A.	
Mechanical properties	Compressive strength	AASHTO T 22	18 hours	3 air-cured 3 steam-cured	*Air curing* - 50% ± 4% RH, 73 ± 4°F (23 ± 2°C) *Moist curing* - 100% RH, 73 ± 4°F (23 ± 2°C) *Steam curing* for 16 hours (Fig. D.1)
			7 days	3 moist-cured	
			28 days	3 moist-cured	
			56 days	3 moist-cured	
	Modulus of elasticity	ASTM C 469	18 hours	2 air-cured 2 steam-cured	
			28 days	2 moist-cured	
			56 days	2 moist-cured	
	Flexural strength	AASHTO T 97	7 days	3 moist-cured	*Moist curing* - 100% RH, 73 ± 4°F (23 ± 2°C)
			28 days	3 moist-cured	
			56 days	3 moist-cured	

* Agitation of concrete between 10 and 40 min at 6 rpm

Table D.5 (cont'd) – Testing program in experimental design

SCC behavior	Property	Test Method	Test age	Number of samples per mixture	Comments
Hydration kinetics	Temperature rise (semi-adiabatic conditions)		Over the first 24 hrs	1	
	Setting time	AASHTO T 197		1	
Form pressure characteristics	Initial formwork pressure		2 to 4 hours	1	Rate of rise of 13.1 to 16.4 ft/hr (4 to 5 m/hr)
	Variation of pressure with time		First 24 hours	1	
Visco-elastic properties	Autogenous shrinkage	Embedded vibrating wire gages	Over 10 to14 days	2	Sealed prisms after removal from molds at release time
	Drying shrinkage	AASHTO T 160	Over 11 months	3	Same curing regime used for release strength
	Creep	ASTM C 512	Over 11 months	3	Loading at release time
Frost durability	Air-void parameters	ASTM C 457	Starting at 56 days	1	
	Freezing and thawing resistance	AASHTO T 161, Method A	Starting at 56 days	2	
Bond strength	Pull-out load-end slip response		56 days	5 SCC & 1 HPC mixtures	*Air curing* at 50% ± 4% RH and 73 ± 4°F (23 ± 2°C)

The initial slump flow of the 16 fractional factorial and three central SCC mixtures was set at 26.0 to 27.5 in. (660 to 700 mm). The targeted release compressive strength after 18 hours of steam curing and 56-day compressive strength were 5,000 psi (34.5 MPa) and 8,000 to 10,000 psi (55 to 69 MPa), respectively. The compressive strength was determined on 4 × 8 in. (100 × 200 mm) cylinders. For 56-day compressive strength, the specimens were stored at 100% relative humidity and 73 ± 4°F (23 ± 2°C) until the time of testing. The variations of temperatures in the

chamber and in reference cylinders measuring 4 × 8 in. (100 × 200 mm) during the steam curing are provided in Appendix C.

In addition to the 16 SCC mixtures, two HPC mixtures of normal consistency were evaluated. Four SCC mixtures were prepared to evaluate the effect of air-entrainment (4% to 7%) on fresh properties, fluidity retention, strength development, flexural strength, elastic modulus, air-void spacing factor, and frost durability of SCC.

D.1.3.3 Test methods used in experimental factorial design

In addition to common test methods used to evaluate workability of SCC and standard methods to determine mechanical properties presented in Table D.5 and in Appendix B, a number of special tests were used to investigate SCC performance. These tests are described below.

Formwork pressure

The initial maximum pressure exerted by SCC and HPC was evaluated by casting concrete in rigid poly-vinyl chloride (PVC) column measuring 3.6 ft (1.1 m) in height and 7.9 in. (200 mm) in diameter. SCC is cast at a rate of 13 to 16 ft/hr (4 to 5 m/hr). Drop in lateral pressure was monitored until pressure cancellation (results are presented in Attachment D). Pressure sensors were installed at 2, 10, and 18 in. (50, 250, and 450 mm) from the bottom of the pressure decay tube. The sensors were set flush with the inner surface of the PVC column; the drilled holes through the PVC tubing were sealed to avoid leakage. The pressure sensors had a capacity of 25 psi (170 kPa), can operate over a temperature range of -58 to 212 ^{o}F (-50 to 100 ^{o}C), and were calibrated using a mechanical calibration instrument prior to use.

Temperature rise

Temperature rise was measured in 6 × 12 in. (150 × 300 mm) concrete cylinder that was inserted at the center of styrofoam box measuring 3.3 × 3.3 × 3.3 ft (1 × 1 × 1 m). Three thermo-couples were installed inside the concrete cylinders, one in the centre of the cylinder, one in the middle height of the inner side of cylinder, and one in the top of the inner side of the cylinder, to determine of temperature rise under semi-adiabatic conditions.

Autogenous shrinkage

Autogenous shrinkage was measured on prisms 3 × 3 × 11.8 in. (75 × 75 × 285 mm). The prisms were sealed immediately after removal from the molds at 18 hours of age and kept at 73 ± 4°F (23 ± 2°C) until the end of testing. Autogenous shrinkage was monitored using embedded vibrating wire strain gages until stabilization which occurred after approximately three weeks of age. The autogenous shrinkage was obtained by subtracting the total shrinkage from thermal deformation. A linear thermal expansion coefficient of 6.4 µin./in./ºF (11.5 µm/m/ºC) was used for adjusting vibrating wire gages readings. The thermal expansion coefficient of the concrete was determined from the slope of the total deformation-temperature curve of concrete prisms subjected to control temperature changes. Two prisms were initially immersed in water at approximate temperature of 122°F (50°C). Once the temperature of the samples is stabilized, the water is allowed to cool down to approximately 68°F (20°C). The resulting deformations are used to estimate the coefficient of thermal expansion/contraction of the concrete.

Drying shrinkage and creep

Six 6 × 12 in. (150 × 300 mm) test specimens were cast to monitor creep and drying shrinkage. The specimens were steam cured until the age of 16 hours and were then demolded. The ends of creep cylinders were ground and external studs were installed for deformation measurements. A digital-type extensometer was used to determine drying shrinkage and creep. Creep and shrinkage testing started at the age of 18 hours. The applied creep loading corresponded to 40% of the 18-hour compressive strength of the steam-cured concrete cylinders. Creep and shrinkage specimens were kept in a temperature-controlled room at 73 ± 4°F (23 ± 2°C) and 50% ± 4% relative humidity. Initial elastic deformations were measured directly after loading; creep and drying shrinkage deformations were monitored for 11 months; the long-term deformations were all stabilized at that time.

Pull-out bond strength

Pull-out testing of prestressing strands was conducted for five SCC mixtures and one conventional concrete mixture. The SCC mixtures were proportioned with different viscosity and static stability levels. Tests were conducted to determine the maximum pull-out load versus the end slip response of strands that were horizontally embedded in experimental wall elements. In total, 16 Grade 270, 0.6 in. (15.2 mm) diameter low-relaxation prestressing strands were embedded at four heights in the wall elements. The wall elements measured 60.6 H × 84.6 L × 7.9 W in. (1,540 H × 2,150 L × 200 W mm). Rigid plastic sheathing was tightly attached to the outer end of each strand near the loaded end as bond breaker to reduce secondary confining stresses along the bonded region.

The formwork was removed one day after concrete casting. The concrete wall elements were then maintained under wet curing until 7 days of age before air-drying. Pull-out tests were conducted at 56 days of age. The pull-out load was applied gradually and recorded using a load cell; the net slip was measured using a linear voltage differential transducer (LVDT) connected to the unloaded end of the strand.

D.1.4 Material Characteristics

D.1.4.1 Binder

The specific gravities of the Type I/II, Type III, Class F fly ash, and blast-furnace slag that were employed in this investigation are 3.14, 3.15, 2.53, and 2.95, respectively. The Blaine fineness values are 390, 530, 410, and 400 m^2/kg, respectively. The Type III cement was combined with either 30% blast-furnace slag or 20% Class F fly ash, by mass of total cementitious materials. More information on the physical and chemical characteristics of the binder materials can be found in Appendix E.

D.1.4.2 Aggregate

Three types of crushed aggregates corresponding to MSA of ¾ in. (19 mm), 3/8 in. (9.5 mm), ½ in. (12.5 mm) and a gravel with MSA of ½ in. (12.5 mm) were selected. The aggregates conform to AASHTO T 27 specifications. Natural sand conforming to AASHTO T 27 was used for all concrete mixtures. The particle-size distributions of the aggregate combinations are within the AASHTO recommended limits, as presented in Appendix E.

D.1.4.3 Chemical admixtures

Polycarboxylate ether-based HRWRA complying with AASHTO M 194, Type F was used. Such HRWRA is widely used in the precast industry in the United States. An air-entraining admixture (AEA) (AASHTO M 154) was incorporated to obtain an initial air content of 4% to 7% in selected SCC mixtures. An organic, thickening-type VMA representative of products commonly used in the precast industry in North America was used for the factorial design program.

D.2 TEST METHODS AND WORKABILITY PERFORMANCE-BASED SPECIFICATIONS

D.2.1 Test Methods to Assess Workability of SCC

Workability of SCC is described in terms of filling ability, passing ability, and stability. **Filling ability** (also referred to as deformability or unconfined flowability) describes the ability of the concrete to undergo changes in shape and flow around obstacles to completely encapsulate the reinforcement and fill the formwork under its own weight without any mechanical consolidation. **Passing ability** refers to the ability of the concrete to pass among various obstacles and narrow spacing in the formwork without blockage, in the absence of mechanical vibration. **Filling capacity** is the ability of the concrete to completely fill intricate formwork or formwork containing closely spaced obstacles, such as reinforcement. SCC can achieve high filling capacity if it has high levels of filling ability and passing ability to spread into a predetermined section, fill the form by the action of gravity alone, and achieve complete filling of the section without segregation or blockage. **Stability** describes the ability of the concrete to maintain a homogeneous distribution of its various constituents. There are two types of stability characteristics: dynamic and static stability. **Dynamic stability** describes the resistance of the concrete to the separation of the constituents during transport, placement, and spread into the formwork. **Static stability** refers to the resistance of the concrete to bleeding, segregation, and surface settlement after casting until the beginning of setting.

Various test methods have been used to assess workability of SCC. In general, these methods include the components required for evaluating simultaneously deformability, passing ability, and stability. The most promising test methods that are relevant for the fabrication of precast, prestressed concrete bridge elements are presented in Table D.6. Details of these test methods are provided in Appendix B.

Table D.6 – Test methods relevant for fabrication of precast, prestressed bridge elements

	Test methods
Filling ability	Slump flow T-50$_{cm}$ (or T-20$_{in.}$) slump flow
Passing ability	L-box J-Ring V-funnel
Filling capacity	Caisson filling vessel test
Segregation resistance	Visual stability index (VSI) Surface settlement Column segregation

D.2.2 Repeatability of Workability Properties

SCC mixture No. 16 (Table D.1) was used to evaluate the repeatability of various workability test methods that can be used to evaluate the filling ability, passing ability, and filling capacity of

SCC. The dosage of HRWRA was adjusted to secure initial slump flow consistency levels of 25.0 in. (635 mm) and 27.5 in. (700 mm). This was done to determine the repeatability of the various test methods at relatively medium and high fluidity levels. For each consistency level, the concrete was batched five times (mixtures No. 34 to 43 in Table D.1). Each test was repeated five times by the same operator to establish single-operator precision values. Furthermore, for selected mixtures, each of the workability tests was conducted by five different operators to assess multi-operator precision values that could occur during testing.

D.2.2.1 Single-operator repeatability

Tables D.7 and D.8 present the results of the repeatability of the responses carried out on multiple concrete batches to determine single-operator errors for mixtures made with relatively high and moderate slump flow values, respectively. In general, test methods involving the removal of the slump cone or a trap door to determine the rate of concrete flow resulted in higher error values. The L-box, V-funnel, and T-50 flow times had high relative errors of 54%, 33%, and 27%, respectively, compared to l1%, 6%, and 13% obtained for the slump flow, J-Ring flow, and L-box blocking ratio (h_2/h_1) test values, respectively.

SCC mixtures with the higher slump flow of 27.5 in. (700 mm) exhibited higher relative errors for the L-box and V-funnel flow times compared to similar mixtures with 25.0 in. (635 mm) slump flow, as shown in Tables D.7 and D.8.

Based on the repeatability test results carried out by a single operator, the slump flow, J-Ring flow, L-box blocking ratio (h_2/h_1), and filling capacity tests can result in lower errors than the L-box, V-funnel, and T-50 flow times.

Table D.7 – Single-operator repeatability of workability test results of SCC with 27.5 ± 0.4 in. (700 ± 10 mm) slump flow

	Mean	Standard deviation	C.O.V., %	Relative error with 90% confidence level, %
Slump flow, in. (mm)	27.9 (707)	0.179 (4.47)	0.6	1.4
T-50 flow time, sec	1.8	0.223	12.6	26.8
J-Ring flow, in. (mm)	27.0 (686)	0.792 (19.81)	2.9	6.2
V-funnel flow, sec	5.7	0.896	15.7	33.5
L-box flow time, sec	1.7	0.431	25.4	54.1
L-box blocking ratio (h_2/h_1)	0.8	0.049	5.9	12.6
Filling capacity, %	98	0.517	0.5	1.1

Table D.8 – Single-operator repeatability of workability test results of SCC with 25.0 ± 0.4 in. (635 ± 10 mm) slump flow

	Mean	Standard deviation	C.O.V., %	Relative error with 90% confidence level, %
Slump flow, in. (mm)	25.2 (640)	0.400 (10.0)	1.6	3.3
T-50 flow time, sec	2.10	0.155	7.4	15.7
J-Ring flow, in. (mm)	24.2 (616)	0.684 (17.1)	2.8	5.9
V-funnel flow, sec	8.19	0.328	4.0	8.5
L-box flow time, sec	1.97	0.154	7.9	16.7
L-box blocking ratio (h_2/h_1)	0.73	0.042	5.7	12.1
Filling capacity, %	94.3	1.149	1.2	2.6

D.2.2.2 Multi-operator repeatability

Test responses obtained with a single concrete mixture using multi operators are summarized in Tables D.9 and D.10. As in the case of the single-operator precision, higher relative errors were obtained for the L-box flow time, V-funnel flow time, and T-50 tests at both slump flow consistency levels. These relative errors were 29%, 40%, and 15%, respectively, in the case of SCC with high slump flow consistency (Table D.9) and 25%, 40%, and 39%, respectively, for SCC with moderate slump flow consistency (Table D.10). The relative errors varied between 1% and 16% for the other test methods.

The L-box flow time, V-funnel flow time, and T-50 test values had relatively high variability for both slump flow consistency levels. The coefficient of variation (C.O.V.) values were 14%, 19%, and 7%, respectively, for the SCC with slump flow of 27.5 ± 0.4 in. (700 ± 10 mm). The C.O.V. values were 19%, 12%, and 18%, respectively, for these test methods for SCC with slump flow of 25.0 ± 0.4 in. (635 ± 10 mm) compared to 0.6% to 7.5% for the other workability test values presented in Tables D.9 and D.10. Therefore, the slump flow, J-Ring flow, L-box blocking ratio (h_2/h_1), and filling capacity tests are shown to provide greater precision and lower relative error than the other workability tests.

Table D.9 – Multi-operator repeatability of workability test results of SCC with 27.5 ± 0.4 in. (700 ± 10 mm) slump flow

Test method	Mean	Standard deviation	C.O.V., %	Relative error with 90% confidence level, %
Slump flow, in. (mm)	27.8 (706)	0.167 (4.18)	0.6	1.3
T-50 flow time, sec	2.3	0.166	7.1	15.1
J-Ring flow, in. (mm)	26.0 (660)	1.030 (25.74)	4.0	8.4
V-funnel flow, sec	6.7	1.282	19.0	40.5
L-box flow time, sec	1.3	0.174	13.6	29.0
L-box blocking ratio (h_2/h_1)	0.78	0.058	7.5	16.0
Filling capacity, %	97	1.148	1.2	2.5

Table D.10 – Multi-operator repeatability of workability test results of SCC with 25.0 ± 0.4 in. (635 ± 10 mm) slump flow

Test method	Mean	Standard deviation	C.O.V., %	Relative error with 90% confidence level, %
Slump flow, in. (mm)	26.1 (663)	0.390 (9.75)	1.5	3.1
T-50 flow time, sec	2.4	0.440	18.1	38.6
J-Ring flow, in. (mm)	24.9 (632)	0.228 (5.70)	0.9	1.9
V-funnel flow, sec	9.0	1.050	11.7	25.0
L-box flow time, sec	2.0	0.371	18.8	40.0
L-box blocking ratio (h_2/h_1)	0.7	0.034	4.9	10.5
Filling capacity, %	94	0.800	0.9	1.8

D.2.2.3 Recommended test methods to evaluate workability

Based on the repeatability evaluation, the slump flow, J-Ring flow, L-box blocking ratio, and filling capacity test methods that yielded relatively low errors are recommended to evaluate the filling ability, passing ability, and filling capacity of SCC. The relative errors of these mixtures are summarized in Table D.11.

Table D.11 – Summary of relative errors for recommended workability test methods

Single-operator error (90% confidence limit)				
	Slump flow 27.5 ± 0.4 in. (700 ± 10 mm)		Slump flow 27.0 ± 0.4 in. (630 ± 10 mm)	
	Absolute error	Relative error, %	Absolute error	Relative error, %
Slump flow, in. (mm)	0.38 (9.5)	1.4	0.85 (21.3)	3.3
J-Ring flow, in. (mm)	1.69 (42.2)	6.2	1.46 (36.5)	5.9
L-box blocking ratio (h_2/h_1)	0.10	12.6	0.09	12.1
Filling capacity (%)	1.1	1.1	2.5	2.6
Multi-operator error (90% confidence limit)				
Slump flow, in. (mm)	0.36 (8.9)	1.3	0.83 (20.8)	3.1
J-Ring flow, in. (mm)	2.2 (54.9)	8.4	0.49 (12.2)	1.9
L-box blocking ratio (h_2/h_1)	0.12	16.0	0.07	10.5
Filling capacity (%)	2.4	2.5	1.7	1.8

D.2.3 Relationships Between Various Workability Responses

The workability responses obtained in the parametric investigation are used to compare the various test responses for SCC and highlight advantages and limitations of these test methods.

D.2.3.1 Passing ability vs. filling capacity

The L-box, J-Ring, and V-funnel tests were primarily employed to evaluate the narrow-opening passing ability of SCC. On the other hand, the testing of the filling capacity was employed to simultaneously evaluate the narrow-opening passing ability and filling ability of the SCC.

In order to obtain a caisson filling capacity values greater or equal to 80%, which is considered to be adequate for complete filling congested or restricted sections, the concrete should have a high level of passing ability with J-Ring flow value greater than 23.0 in. (580 mm). This limit should be increased to 23.5 in. (595 mm) for mixtures made with crushed coarse aggregate of ¾ in. (19 mm), as indicated in Fig. D.2.

Similarly, the difference between slump and J-Ring flow values can be correlated with the filling capacity values, as presented in Fig. D.3. Such spread should be lower than 3 in. (75 mm). As shown in Fig. D.4, SCC with L-box blocking ratio (h_2/h_1) greater than 0.5 can develop filling capacity greater than 80%. This limit should be increased to 0.55 for SCC made with crushed coarse aggregate of ¾ in. (19 mm).

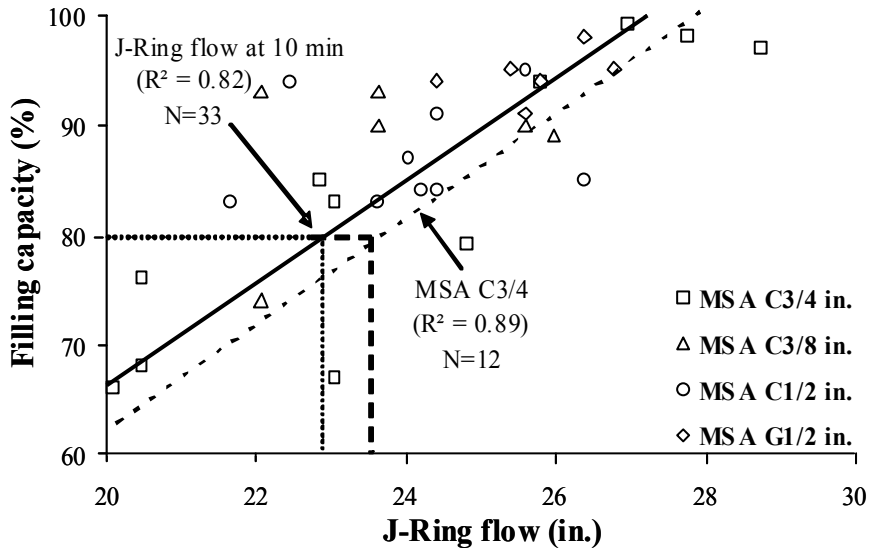

Fig. D.2 – Relationship between filling capacity and J-Ring flow measured at 10 minutes

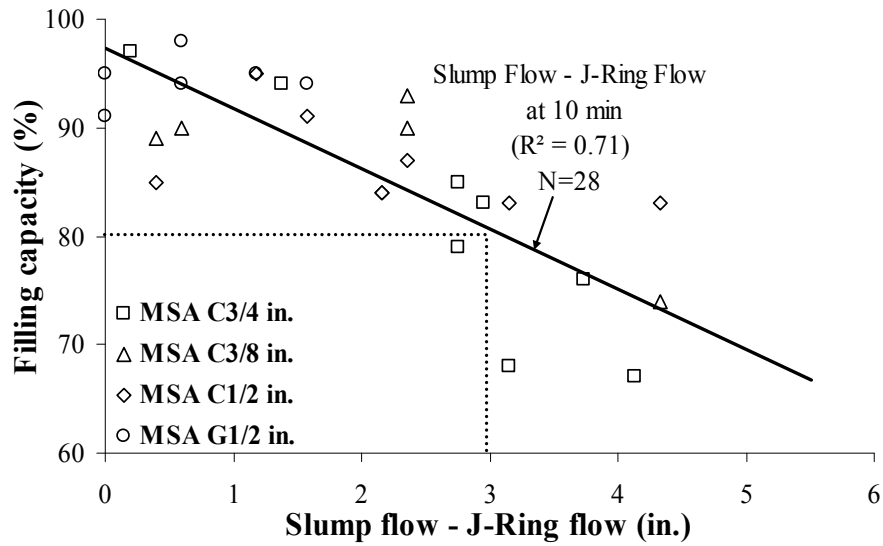

Fig. D.3 – Relationship between filling capacity and difference between slump and J-Ring flow values measured at 10 minutes

D.2.3.2 Combined test methods to evaluate filling capacity

In general, test methods used to evaluate workability of SCC provide one workability index, which is not sufficient to adequately describe the flow behavior of SCC. Therefore, proper combinations of various test methods can be employed to facilitate the assessment of workability of SCC. The establishment of proven combination of test methods that are adequate for field application can reduce time and labor as well as the number of tests required for quality control.

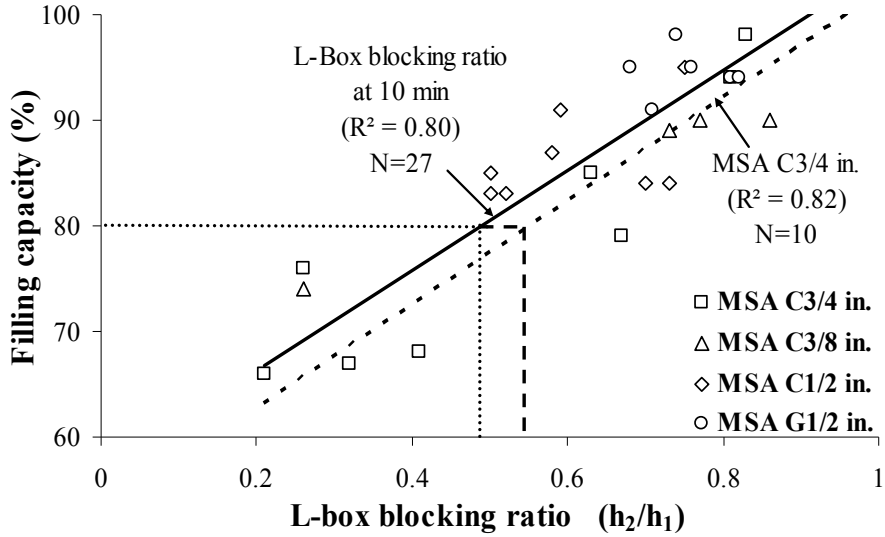

Fig. D.4 – Variations of filling capacity with L-box blocking ratio

The passing ability can be used in combination with slump flow to estimate the filling capacity of SCC. This is illustrated in Fig. D.5 where the filling capacity is expressed in terms of slump flow and h_2/h_1 and then in Fig. D.6 in terms of difference between slump and J-Ring flow. The region where SCC develops 80% minimum filling capacity ("workability box") is highlighted.

For the SCC mixture tested in the parametric experimental plan, mixtures with filling capacities greater or equal to 80% correspond to those with minimum slump flow and h_2/h_1 values of 25 in. (635 mm) and 0.5, respectively. A number of SCC mixtures in Fig. D.6 that had slump flow values greater than 26 in. (660 mm) and spreads in slump and J-Ring flow values over the recommended limit of 3 in. (75 mm), yet they yielded filling capacities greater than 80%. These mixtures were proportioned with ½ in. (12.5 mm) MSA.

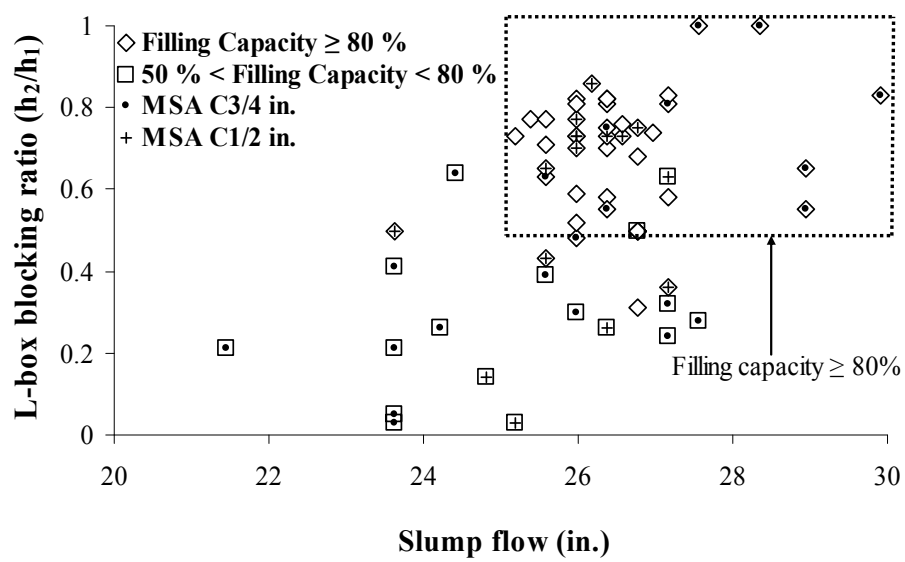

Fig. D.5 – "Workability box" for filling capacity as a function of L-box blocking ratio and slump flow

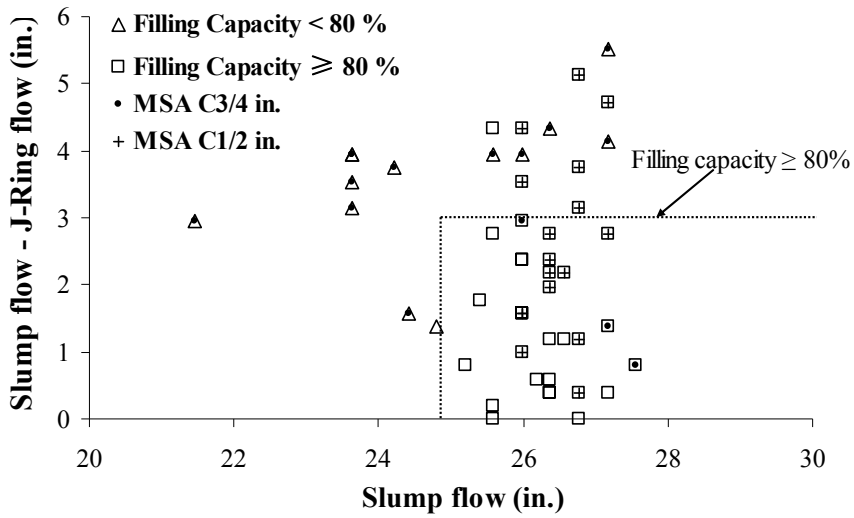

Fig. D.6 – Lower limits of slump flow and difference between slump and J-Ring flow values of SCC made with crushed aggregate to secure minimum filling capacity of 80%

The workability test results from the parametric study were used to derive multi-regression equations relating the filling capacity of SCC with slump flow and passing ability test results. Most of the evaluated mixtures had initial slump flow values of 26.0 to 27.5 in. (660 to 700 mm). The relationships obtained with the L-box and J-Ring results can be expressed as follows:

Filling capacity (%) = – 9.64 + 3.03 slump flow (in.) + 28.25 h_2/h_1 ($R^2 = 0.82$) (1)

Filling capacity (%) = – 33.53 + 1.3 slump flow (in.) + 3.52 J-Ring flow (in.) ($R^2 = 0.83$) (2)

The filling capacity can also be expressed as a function of the difference between slump flow and J-Ring flow diameters, as follows:

Filling capacity (%) = – 0.59 + 3.62 slump flow (in.)

– 3.56 {Slump flow (in.) – J-Ring flow (in.)} ($R^2 = 0.80$) (3)

The filling capacity can be expressed as a function of L-box blocking ratio (h_2/h_1) and J-Ring flow diameter, as follows:

Filling capacity (%) = 17.45 + 2.37 J-Ring flow (in.) + 19.8 h_2/h_1 ($R^2 = 0.85$) (4)

The above multiple regression equations (Eq. 1 to 4) are valid for stable mixtures with slump flow consistency of 23.5 to 30.0 in. (600 to 760 mm) prepared with crushed coarse aggregate of ¾ in. (19 mm), 3/8 in. (9.5 mm), and ½ in. (12.5 mm) MSA and gravel with ½ in. (12.5 mm) MSA.

D.2.3.3 Evaluation of static stability

Based on in-situ compressive strength and pull-out bond strength results obtained from this project, SCC mixtures having maximum surface settlement of 0.5% are found to have more homogenous in-situ properties than those of vibrated HPC mixtures. This includes an upper limit of 1.4 as a modification factor for bond to prestressing strands. The surface settlement test involves the determination of the capacity of the concrete to undergo a settlement due to

segregation and consolidation of the plastic concrete. Consolidation can occur due to movement of entrapped or entrained air or bleed water to the top surface. Surface settlement can take place in the absent of segregation, which implies separation between coarse aggregate and mortar.

In addition to determining the maximum surface settlement, the initial rate of settlement (expressed as relative settlement per hour) can be calculated as follows:

$$\text{Settlement rate (\% per hour)} = \{S_t(\%) - S_{t-5}(\%)\} / \{5 \text{ (minutes)} / 60 \text{ (minutes)}\} \quad (5)$$

where, S_t is settlement value at a given time (minute) t, S_{t-5} is the settlement value at time of t minus 5 minutes. Settlement rates determined at 15, 30, and 60 minutes after the beginning of surface settlement testing are correlated to the maximum settlement values in Fig. D.7. The 30-minute rate of settlement, which is calculated as the spread in settlement values between 25 and 30 minutes divided by 5 minutes, can be used to speed up surface settlement testing. A settlement rate of 0.27% per hour after 30 minutes is shown to correspond to the upper limit of 0.5% maximum settlement. The test period can even be reduced to 15 minutes, as in the case of the column segregation test (ASTM C 1610). In this case, a settlement rate of 0.32% per hour after 15 minutes can correspond to the upper limit of 0.5% maximum settlement.

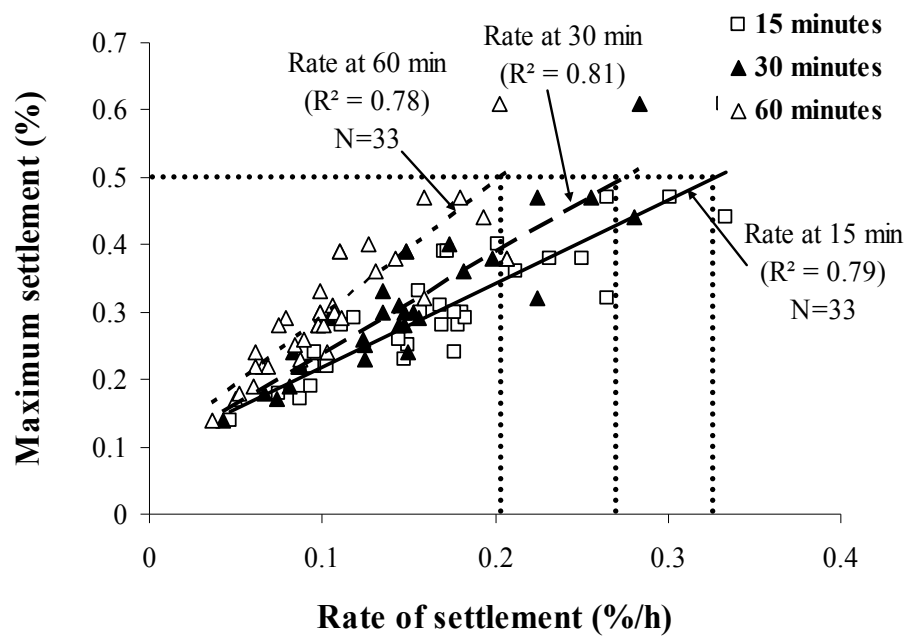

Fig. D.7 – Relationship between rate of settlement and maximum settlement

The rates of settlement at 30 minutes are compared in Fig. D.8 to the segregation index[D1] determined from the column segregation test. The latter test involves casting the concrete in an experimental column to determine the distribution of coarse aggregate along the column after 15 minutes of rest. For the column segregation test, the relative coarse aggregate portions in four sections along the experimental column are determined to calculate the C.O.V. (or the

[D1] Assaad, J., Khayat, K.H., and Daczko, J, "Evaluation of Static Stability of Self-Consolidating Concretes." *ACI Materials Journal*, Vol. 101, No. 3 (2004) pp. 207-215.

segregation index). This is in contrast with the evaluation of coarse aggregate contents from the top and bottom sections of the column, as per ASTM C 1610. These two values are used to determine the resistance to segregation, as follows:

$$Percent\ static\ segregation\,(\%) = 2 \times \left(\frac{CA_B - CA_T}{CA_B + CA_T} \right) \times 100$$

(6)

where, CA_T and CA_B refer to the mass of coarse aggregate at the top and bottom sections, respectively.

Regardless of the rate of settlement, no significant spread was found in the column segregation index (C.O.V.) for the SCC mixtures proportioned with ½ or 3/8 in. (12.5 or 9.5 mm) MSA. It is important to note that the majority of SCC mixtures tested were highly stable with surface settlements lower than 0.5%, rates of settlement at 30 minutes lower than 0.27%/hr, and column segregation indices lower than 5%.

The segregation index of SCC made with ¾ in. (19 mm) MSA is shown to increase with the increase in the rate of settlement. Given the correlations shown in Fig. D.8, stable SCC proportioned with ¾ in. (19 mm) MSA should have rates of settlement lower than 0.12%/hr in order to secure a segregation index lower than 5%.

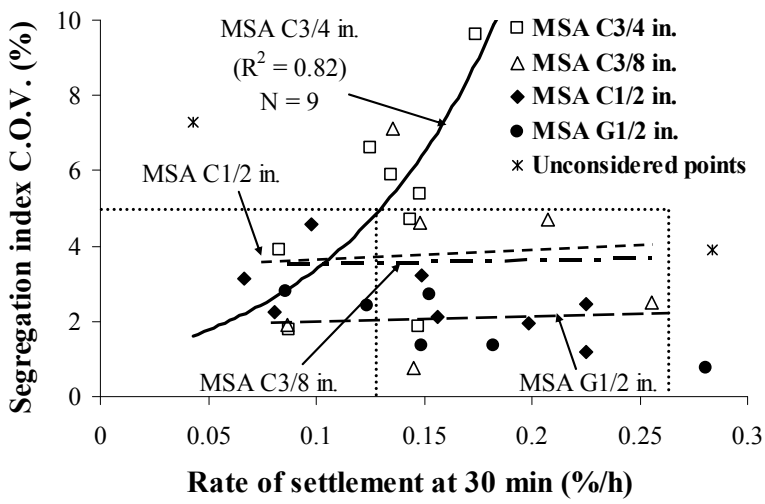

Fig. D.8 – Variation in column segregation index with rate of surface settlement

The MSA and type of coarse aggregate have therefore considerable influence on the column segregation index. For a given rate of settlement, SCC proportioned with gravel with ½ in. (12.5 mm) MSA exhibited lower segregation index (i.e. more stable) compared to similar concrete made with crushed aggregate of the same MSA. Similarly, for a given settlement rate, SCC made with ½ or 3/8 in. (12.5 or 9.5 mm) MSA had lower segregation index compared to those prepared with ¾ in. (19 mm) MSA.

As illustrated in Fig. D.9, good correlation coefficient ($R^2 = 0.76$) can be established between the segregation index (determined from four sections along the segregation column) and the percent static segregation (S) (determined only from the top and bottom sections of the segregation

column), regardless of the MSA in use. On the average, stable SCC should have percent static segregation lower than 15 to maintain a maximum segregation index of 5%.

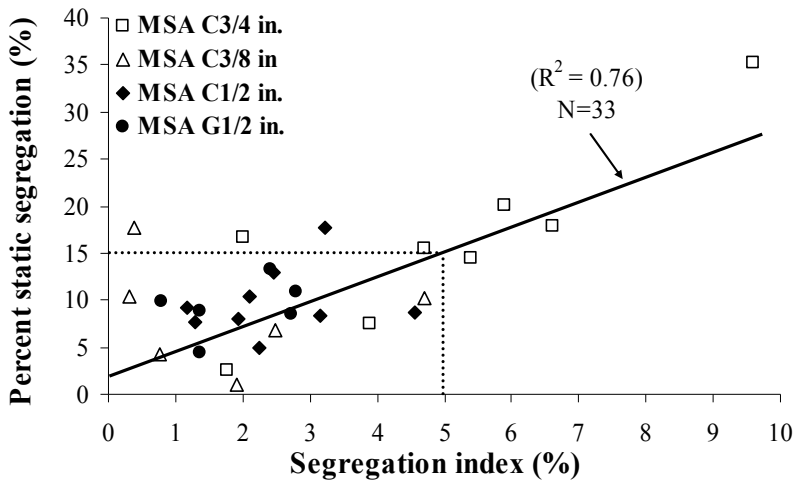

Fig. D.9 – Relationship between column segregation index (C.O.V.) and percent of static of segregation (S)

D.2.3.4 Relationship between workability characteristics and rheological parameters

Rheological measurements

The rheological measurement of the 33 SCC mixtures investigated in parametric study was performed using a modified Tattersall two-point workability rheometer (MK III model). Full description of the test methods is provided in Appendix B.

Determination of rheological parameters of SCC mixtures

The Bingham model can be expressed as a function of the shear rate (γ); $\tau = \tau_0 + \mu_p \gamma$ with τ_0 and μ_p corresponding to the yield stress and plastic viscosity, respectively. The rheological parameters determined for mixtures evaluated in the parametric experimental program at 10 minutes of age are presented in Table D.12. The yield stress values ranged between 10 and 130 Pa for SCC with slump flow values of 25.0 to 27.0 in. (635 to 690 mm). The plastic viscosity values ranged between 0.0109 and 0.1015 psi.s (75 and 700 Pa.s), with the majority of plastic viscosity results being within the 0.015 and 0.073 psi.s (100 and 500 Pa.s) range.

Correlations between rheological parameters and workability test results

The rheological parameters for the SCC mixtures were compared to the various workability test results to identify combinations of rheological parameters necessary to provide adequate filling ability, filling capacity, and stability of SCC for successful casting of precast, prestressed beams. Relatively high degree of scattering was observed for either relationship, which could be due to differences in mixture proportioning and MSA that affect the flow velocity of the SCC.

Among the various workability responses, the L-box blocking ratio (h_2/h_1) determined from the L-box test exhibited good correlation with the plastic viscosity providing that the comparison is performed for each aggregate separately. As presented in Fig. D.10, the h_2/h_1 ratio decreases with the increase in plastic viscosity. Viscous concrete can then hinder the flow and lead to low L-box

blocking ratio. Depending on the aggregate characteristics, the plastic viscosity should be limited to 0.029 psi.s (200 Pa.s) in order to secure a minimum blocking ratio of 0.5 to 0.7. The lower limit 200 Pa.s can be increased to 0.0326 psi.s (225 Pa.s) for SCC made with coarse aggregate of ½ in. (12.5 mm) MSA.

Table D.12 – Rheological parameters determined at 10 minutes

	Mixture No.	Rheological parameters			Mixture No.	Rheological parameters		
		τ_0 (Pa)	μ_p (Pa.s)*	R^2		τ_0 (Pa)	μ_p (Pa.s)	R^2
Non air-entrained concrete	1	83	238	0.99	13	10	326	0.99
	2	99	248	0.99	14	133	238	0.98
	3	64	273	0.99	15	12	502	0.99
	4	93	160	0.97	16	66	150	0.99
	5	90	141	0.99	17	62	154	0.99
	6	63	158	0.99	18	63	139	0.99
	7	31	336	0.99	19	14	275	0.99
	8	17	384	0.97	20	8	361	0.99
	9	9	415	0.99	21	22	341	0.99
	10	68	131	0.99	22	129	75	0.99
	11	52	156	0.99	23	58	99	0.99
	12	26	181	0.99	24	58	116	0.99
Air-entrained SCC (4%-7%)	25	27	422	0.99				
	26	14	399	0.99				
	27	21	586	0.99				
Low filling ability	28	18	703	0.99				
	29	87	407	0.99				
	30	23	320	0.99				
High filling ability	31	67	83	0.98				
	32	68	72	0.98				
	33	65	63	0.99				

* 1 Pa = 1.45×10^{-4} psi

For the investigated SCC mixtures that had high slump flow values, no relationship can be established between time-dependant test methods (T-50, V-funnel flow time, L-box flow time) and yield stress. Similar conclusions can be drawn by comparing the yield stress to other test methods, such as the difference between slump and J-Ring flow, L-box blocking ratio, and surface settlement.

As shown in Fig. D.11, the rate of settlement determined after 30 minutes can be correlated to the initial plastic viscosity. According to Hwang et al. (2006)[D2], SCC can be considered to have high level of static stability when the maximum surface settlement is 0.5% and the rate of settlement after 30 minutes is limited to 0.16%/hr. This latter limit can be achieved when the SCC has a minimum initial plastic viscosity of 0.0217 psi.s (150 Pa.s).

[D2] Hwang, S.-D., Khayat, K.H., and O. Bonneau, "Performance-Based Specifications of Self-Consolidating Concrete Used in Structural Applications." *ACI Materials Journal*, Vol. 103, No. 2 (2006) pp. 121-129.

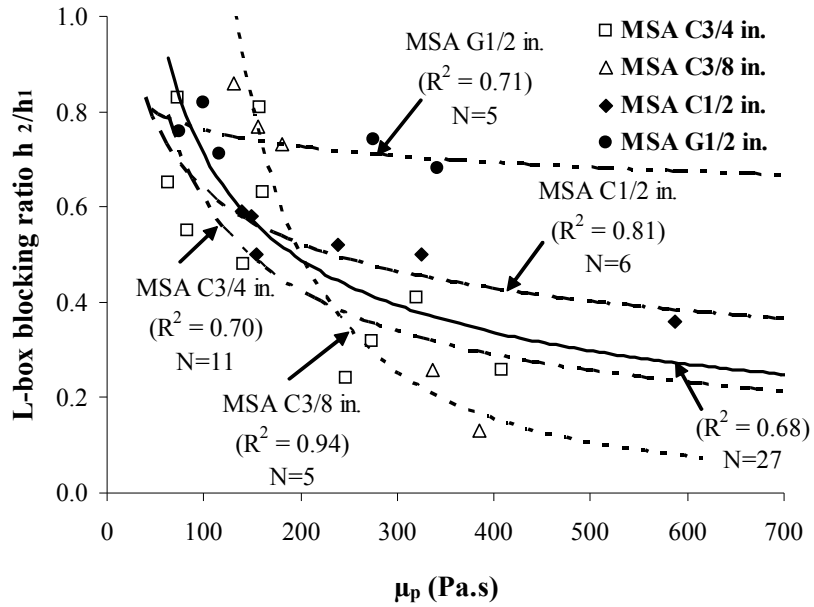

Fig. D.10 – Relationship between plastic viscosity and L-box blocking ratio

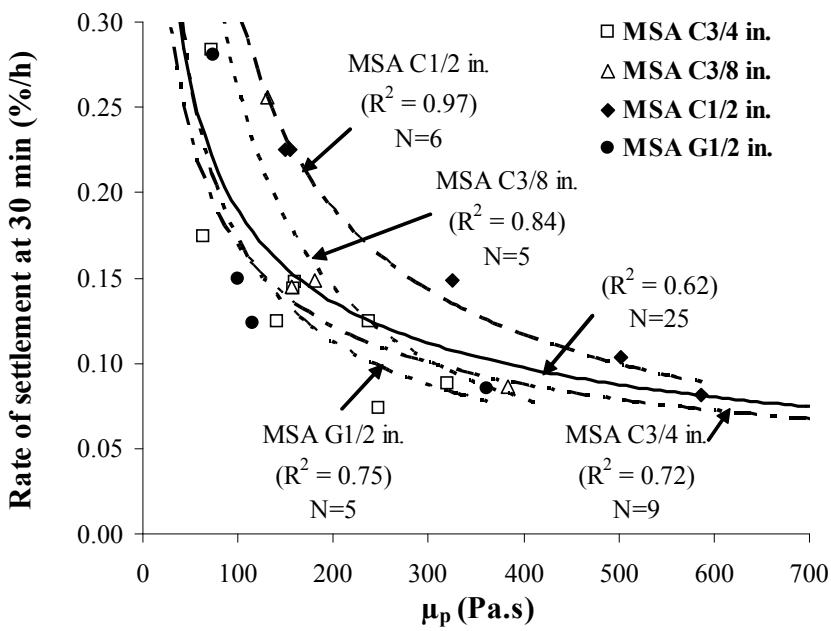

Fig. D.11 – Variations of the rate of surface settlement determined after 30 minutes of testing and initial plastic viscosity for SCC made with different coarse aggregates

The segregation index results determined from the column segregation test are compared to the plastic viscosity results determined at 10 minutes in Fig. D.12. An increase in plastic viscosity can lead to lower segregation coefficient. For a given level of viscosity, SCC made with the larger MSA can undergo greater risk of segregation. For a given upper limit of segregation

coefficient (for example 4%), SCC made with crushed aggregate with MSA of 3/8 in. (9.5 mm) or crushed aggregate or rounded gravel with MSA of ½ in. (12.5 mm) should have a minimum plastic viscosity of 0.0217 psi.s (150 Pa.s). This limit should be increased to 0.029 psi.s (200 Pa.s) for SCC made with crushed coarse aggregate of ¾ in. (19 mm) MSA.

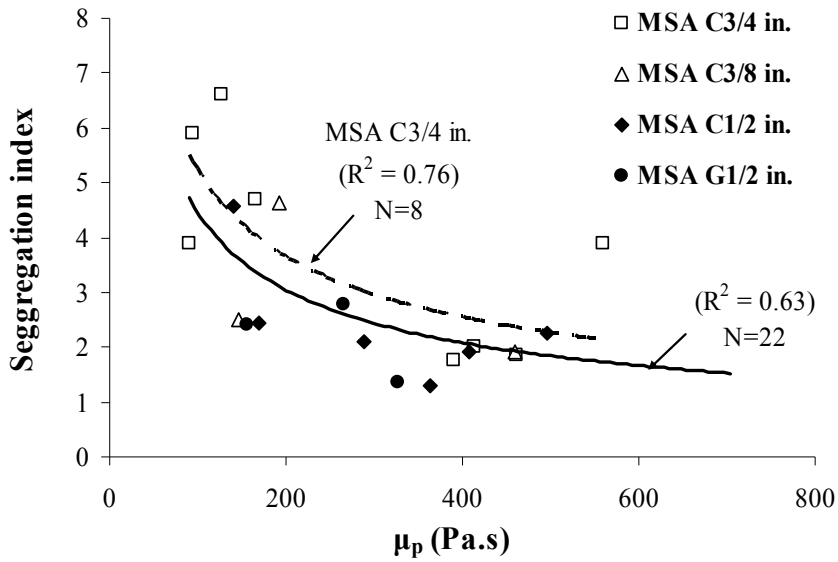

Fig. D.12 – Variations of the segregation index and plastic viscosity determined at 10 minutes

D.2.4 Recommended Test Methods and Workability Performance-Based Specifications

The use of proven combinations of test methods in precast, prestressed applications is necessary to reduce time and effort required for quality control of SCC at the precasting plant. A mean caisson filling capacity value of 80% (75% to 90%) is considered as a lower limit for casting of precast, prestressed applications. A lower limit of 70% can be tolerated for relatively simple elements. The L-box blocking ratio (h_2/h_1) index, J-Ring flow, or the difference between slump flow and J-Ring flow can be combined with the slump flow to evaluate the filling capacity of SCC. The recommend combined tests to estimate the filling capacity of SCC are:

Combined test methods I: Slump flow and L-box blocking ratio (h_2/h_1)

Combined test methods II: Slump flow and J-Ring flow

Table D.13 presents a set of performance specifications of SCC that can be used in precast, prestressed applications. Such specifications correspond to SCC with slump flow of 25 to 30 in. (635 to 760 mm) and, depending on the passing ability test in use, or h_2/h_1 greater than 0.5, or J-Ring flow of 22.5 to 27.0 in. (570 to 685 mm), and a spread in slump and J-Ring flow values lower than 3 in. (75 mm).

As indicated in Table D.13, regardless of the MSA, stable SCC should develop a column segregation index (C.O.V.) and degree of segregation (S) lower than 5% and 15%, respectively. The recommended limits for surface settlement depend on the MSA. SCC proportioned with ¾ in. (19 mm) and ½ or 3/8 in. (12.5 or 9.5 mm) MSA should have maximum rates of settlement at 30 minutes of 0.12%/hr and 0.27%/hr, respectively.

SCC mixtures investigated in this study developed yield stress values varying between 10 and 130 Pa. In the case of plastic viscosity, it is recommended that SCC made with crushed aggregate have a plastic viscosity of 0.0145 and 0.0326 psi.s (100 to 225 Pa.s) to ensure adequate passing ability and static stability. This range can range from 0.0145 and 0.058 psi.s (100 to 400 Pa.s) for SCC made with gravel having ½ in. (12.5 mm) MSA. The lower limit of 0.0145 psi.s (100 Pa.s) is required for static stability; maximum rate of settlement at 30 minutes of 0.27%/hr and a maximum column segregation index (C.O.V.) of 5%, regardless of the aggregate type (Table D.13). The upper limit of plastic viscosity of 0.0362 and 0.058 psi.s (250 and 400 Pa.s) is necessary for SCC with slump flow consistency of 26.0 to 27.5 in. (660 to 700 mm) to achieve adequate passing ability (minimum L-box blocking ratio of 0.5).

Based on the results of in-situ properties of SCC with different viscosity levels, plastic viscosity greater than 0.073 psi.s (500 Pa.s) should be avoided to eliminate inadequate consolidation which can affect the homogeneity of in-situ hardened properties of cast concrete elements.

Table D.13 – Combined test methods and recommended workability values for medium and high densely reinforcements

	Combined test methods-I	Combined test methods-II
Filling ability	Slump flow: 25-30 in. (635-760 mm)*	
Passing ability	L-box blocking ratio (h_2/h_1) ≥ 0.5	J-Ring flow: 22.5-27.0 in. (570-685 mm) Slump flow – J-Ring flow ≤ 3 in. (75 mm)
	Plant and laboratory use	Plant use
Filling capacity	Caisson filling capacity ≥ 80% (laboratory use) Combined test methods (I or II)	
Static stability	I. Segregation resistance - Column segregation index (C.O.V.) ≤ 5% - Percent static segregation (S) ≤ 15 II. Rate of surface settlement at 30 min - MSA of 3/8 and ½ in. (9.5 and 12.5 mm) ≤ 0.27 (%/hr) (Max. settlement of 0.5%) - MSA of ¾ in. (19 mm) ≤ 0.12 (%/hr) (Max. settlement of 0.3%)	
Rheological parameters to ensure proper workability**	Plastic viscosity (μ_p) - 0.0145 - 0.0326 psi.s (100 - 225 Pa.s) for SCC made with crushed aggregate - 0.0145 – 0.0580 psi.s (100 - 400 Pa.s) for SCC made with gravel	

* static and dynamic stability requirements must be met

** higher viscosity of 0.033 to 0.073 psi.s (250 to 500 Pa.s) maybe needed to ensure homogeneous in-situ properties and bond to prestressing strands in deep sections, as those discussed in Chapter 7 for AASHTO Type II beams

D.3 EFFECT OF MIXTURE CONSTITUENTS AND COMPOSITION ON WORKABILITY AND MECHANICAL PROPERTIES OF SCC

D.3.1 Evaluation Scheme

For concrete investigated in the parametric testing program, the relative effects of mixture constituents and mix design on concrete properties are compared. These properties include HRWRA demand, workability (slump flow retention over 30 minutes, passing ability, filling capacity, static stability), and mechanical properties (18-hour air-cured and steam-cured compressive strengths, 18-hour steam-cured modulus of elasticity, and 56-day compressive strength). The evaluation of the relative effect of mixture constituents and mix design parameters is carried out by comparing the relative performance of each parameter on the overall workability and mechanical properties. These properties are assigned weighting factors to reflect their relative importance on SCC performance (Table D.14). For example, the filling capacity and static stability are assigned a weighing factor of 2 to increase their relevant importance compared to other fresh properties that have weighing factors of 1.

Table D.14 – Evaluation method to compare effect of material constituents and mix design parameters on workability and mechanical properties of SCC

Property (i)	SCC behavior	Weighing factor (WF)	Score obtained
1	HRWRA demand	× 1	(+, + +, or + + +)* × 1
2	Slump flow retention over 30 min	× 1	(+, + +, or + + +) × 1
3	Passing ability	× 1	(+, + +, or + + +) × 1
4	Filling capacity	× 2	(+, + +, or + + +) × 2
5	Static stability	× 2	(+, + +, or + + +) × 2
Total fresh properties			$\sum_{i=1}^{5}(+,++,\ or+++)_i \times (WF)_i$
6	18-hour compressive strength, steam-cured	× 3	(+, + +, or + + +) × 3
7	18-hour compressive strength, air-cured	× 1	(+, + +, or + + +) × 1
8	56-day compressive strength, moist-cured	× 2	(+, + +, or + + +) × 2
9	18-hour elastic modulus, steam-cured	× 2	(+, + +, or + + +) × 2
Total hardened properties			$\sum_{i=6}^{9}(+,++,or+++)_i \times (WF)_i$
Global performance			$\sum_{i=1}^{9}(+,++,or+++)_i \times (WF)_i$
Ranking (comparative)			**I, II, III, or IV**

* Score obtained here is based on relative performance levels presented in Table D.15.

The relative performance of the various workability and mechanical property responses are ranked at three levels, as follows:

- +++ high performance (3 points)
- ++ medium performance (2 points)
- + low performance (1 point)

These rankings are based on the relative performance specifications presented in Table D.15. For example, low, medium, and high performance levels for fluidity retention would correspond to losses of slump flow between 10 and 40 minutes greater than 2.5 in. (62.5 mm), 1 to 2.5 in. (25 to 62.5 mm), and less than 1 in. (25 mm), respectively. Some of the recommended performance limits are based on correlations between various workability characteristics given in Section D.2.3.

Table D.15 – Relative performance of SCC mixtures for precast, prestressed applications

		Relative performance level		
		Low	Medium	High
Filling ability	Slump flow	23.5 - 25 in. (600 - 640 mm)	25 - 27.5 in. (640 - 700 mm)	27.5 - 29 in. (700 - 735 mm)
Fluidity retention	Slump flow at 10 min – slump flow at 40 min	≥ 2.5 in. (62.5 mm)	1 - 2.5 in. (25 - 62.5 mm)	≤ 1 in. (25 mm)
Passing ability	L-box blocking ratio (h_2/h_1)	0.5 - 0.6	0.6 - 0.7	≥ 0.7
	Slump flow – J-Ring flow	3 - 4 in. (100 mm)	2 - 3 in. (50 - 100 mm)	≤ 2 in. (50 mm)
Filling capacity	Caisson filling capacity	70% - 75%	75% - 90%	≥ 90%
Air stability	Air volume at 10 min – air volume at 40 min	≥ 1.5%	0.5% - 1.5%	≤ 0.5%
Static stability	Max. surface settlement	≥ 0.5%	0.3% - 0.5%	≤ 0.3%
	Column segregation index	≥ 5%	2% - 5%	≤ 2%
Compressive strength	18-hour compressive strength (air-cured)*	≤ 2,000 psi (13.8 MPa)	2,000 - 3,000 psi (13.8 - 20.7 MPa)	≥ 3,000 psi (20.7 MPa)
	18-hour compressive strength (steam-cured)	≤ 4,500 psi (31 MPa)	4,500 - 5,500 psi (31 - 38 MPa)	≥ 5,500 psi (38 MPa)
	56-day compressive strength (moist-cured)	≤ 8,000 psi (55 MPa)	8,000 - 10,000 psi (55 - 69 MPa)	≥ 10,000 psi (69 MPa)
Modulus of elasticity	18-hour modulus of elasticity (steam-cured)	≤ 4,000 ksi (27.6 GPa)	4,000 - 5,000 ksi (27.6 - 34.5 GPa)	≥ 5,000 ksi (34.5 GPa)

* 16 hours in molds covered under wet burlap

The total scores of the fresh and hardened properties for each material constituent and mix design parameter are determined to obtain a global evaluation of each parameter. For each parameter category, the material constituent and mix design parameter that received the highest total scores is ranked as "I", which represents the best performance of the material in terms of fresh and

hardened properties. On the other hand, a ranking of "IV" is given to the material constituent and mix design parameter that yielded the lowest global performance. Table D.16 summarizes the evaluation method used for these rankings.

Table D.16 – Evaluation method to rank the relative influence material constituents and mixture parameters on workability and mechanical properties of SCC

Ranking	Percentage of global performance score relative to maximum score in each material constituent and mixture parameter category
I	100%
II	93% – 99%
III	85% – 92%
IV	< 85%

D.3.2 Effect of Binder Type on SCC Performance

The binder content and composition were shown to have direct influence on HRWRA demand, fluidity retention, temperature rise, early-age strength development, and mechanical properties at 28 and 56 days. Among the three binder types that were used in the parametric study, mixtures made with Type III cement and 20% Class F fly ash exhibited better workability compared to similar mixtures prepared with Type I/II cement or Type III cement and 30% slag. SCC made with Type III cement and 20% fly ash had a total score of 18 compared to 16 and 15 for SCC with Type I/II and Type III cement and 30% slag, respectively. As illustrated in Table D.17, SCC containing 20% Class F fly ash developed high fluidity retention, high passing ability, high filling capacity, as well as high level of static stability. SCC proportioned with Type III cement and 30% slag exhibited relatively low passing, difference between slump flow and J-Ring flow diameters larger than 4 in. (100 mm).

Regardless of the binder type, the evaluate mixtures developed similar compressive strengths after 18 hours of steam curing and 56 days of moist curing. The concrete with Type III cement and 20% Class F fly ash had the highest total score for mechanical properties, which is mostly due to its highest 56-day compressive strength.

Based on this evaluation, Type III cement and 20% Class F fly ash was selected for the experimental evaluation that was performed to model the performance of SCC for precast and prestressed girder elements.

Table D.17 – Effect of binder type on SCC performance

SCC Behavior	Binder type		
	Type I/II	Type III + 30%Slag	Type III + 20%FA
HRWRA demand (×1)	+++	++	++
Slump flow retention (×1)	+	++	+++
Passing ability (×1)	++	+	+++
Filling capacity (×2)	+++	++	++
Static stability (×2)	++	+++	+++
Total fresh properties	**16**	**15**	**18**
18-hour compressive strength steam-cured (×3)	++	++	++
18-hour compressive strength air-cured (×1)	+++	++	++
56-day compressive strength (×2)	++	++	+++
18-hour modulus of elasticity (×2)	++	++	++
Total hardened properties	**17**	**16**	**18**
Global performance	**33**	**31**	**36**
Ranking*	**II**	**III**	**I**

* refer to Table D.15 for ranking

D.3.3 Effect of Maximum Coarse Aggregate Size and Type on SCC Performance

The size and type of coarse aggregate were shown to have marked effect on the passing ability, filling capacity, and static stability of SCC, as presented in Table D.18. The MSA should be selected given the minimum clear spacing between the reinforcement and the clear cover over the reinforcement, as well as the geometry of the cast element. The reduction in MSA can enhance stability.

From a workability point of view, SCC made with crushed aggregate of 3/8 in. (9.5 mm) MSA exhibited greater passing ability, difference between slump flow and J-Ring flow diameters lower than 2 in. (50 mm), and higher filling capacity, caisson filling capacity higher than 90%. Mixtures made with crushed aggregate of 3/8 in. (9.5 mm) MSA had a total score of 16, compared to 14 and 10 for those with crushed aggregate of ½ in. and ¾ in. (12.5 and 19 mm) MSA, respectively. In particular, mixtures containing ¾ in. (19 mm) MSA exhibited relatively low level of filling capacity (caisson filling capacity less than 70%) and relatively low resistance to segregation (column segregation index higher than 5%). The SCC prepared with 3/8 in. (9.5 mm) MSA exhibited surface settlement and column segregation index values similar to those of made with larger MSA.

As in the case of workability characteristics, mixtures made with crushed aggregate of 3/8 in. (9.5 mm) MSA developed similar or even higher compressive strength after 18 hours of steam curing and 56 days of moist curing than those with ½ or ¾ in. (12.5 and 19 mm) MSA. In terms of global performance, SCC made with crushed aggregate of ½ in. or 3/8 (12.5 or 9.5 mm) exhibited the highest performance, as indicated in Table D.18.

Table D.18 – Effect of aggregate size and type on SCC performance

SCC Behavior	Aggregate size and type			
	MSA C¾ in. (19 mm)	MSA C3/8 in. (9.5 mm)	MSA C½ in. (12.5 mm)	MSA G½ in. (12.5 mm)
HRWRA demand (×1)	+++	+	++	++
Slump flow retention (×1)	NS	NS	NS	NS
Passing ability (×1)	+	+++	++	+++
Filling capacity (×2)	+	+++	++	+++
Static stability (×2)	++	+++	+++	+++
Total fresh properties	**10**	**16**	**14**	**17**
18-hour compressive strength steam-cured (×3)	++	++	+++	++
18-hour compressive strength air-cured (×1)	+++	++	++	++
56-day compressive strength (×2)	++	+++	+++	+
18-hour modulus of elasticity (×2)	+++	++	++	++
Total hardened properties	**19**	**18**	**21**	**14**
Global Performance	**29**	**34**	**35**	**31**
Ranking	**IV**	**I**	**I**	**III**

* refer to Table D.15 for ranking

SCC proportioned with gravel developed superior passing ability and filling capacity than similar concrete made with crushed aggregate of the same MSA [½ in. (12.5 mm)]. The former SCC had high level of passing ability (h_2/h_1 greater than 0.7 and difference between slump flow and J-Ring flow diameters less than 2 in. (50 mm)) and high filling capacity (caisson filling capacity greater than 90%). Both SCC types exhibited similar segregation resistance (medium level: column segregation index of 2% to 5%). Unlike the workability response, mixtures made with gravel developed lower compressive strength and modulus of elasticity than similar concrete prepared with crushed aggregate of the same MSA. In terms of global performance of hardened concrete, mixtures made with crushed aggregate offered better performance than those made with gravel (overall score of 35 versus 31).

D.3.4 Effect of *w/cm* and Air Entrainment on SCC Performance

As presented in Table D.19, SCC mixtures made with 0.38 *w/cm* had better workability characteristics than those with 0.33 *w/cm* (score of 19 versus 16). The former concrete exhibited superior fluidity retention, passing ability, and filling capacity than SCC prepared with 0.33 *w/cm*. On the other hand, SCC proportioned with 0.33 *w/cm* developed greater static stability and higher 18-hour and 56-day compressive strengths under steam-cured and moist-cured conditions, respectively. On the other and, the air-cured SCC made with 0.33 *w/cm* exhibited relatively lower 18-hour compressive strength than the latter concrete under the same curing regime. This is due to the relatively higher dosage of HRWRA required to achieve the target initial slump

flow. No significant difference was found in the modulus of elasticity determined at 18 hours between the 0.33 and 0.38 *w/cm* mixtures.

SCC with 0.38 *w/cm* can be used to secure a minimum release compressive strength of 5,000 psi (34.5 MPa) and ultimate compressive strength of 8,000 psi (55 MPa). Such concrete can be used for casting highly reinforced and restricted concrete sections given its excellent passing ability and filling capacity. However, higher release and design compressive strengths may necessitate the use of lower *w/cm*.

Given the lower viscosity and greater paste content, air-entrained SCC exhibited superior passing ability, and filling capacity compared to concrete without air entrainment. However, such concrete developed lower static stability and lower compressive strength and modulus of elasticity, both under steam-cured and moist-cured conditions, compared to similar SCC without air entrainment.

Table D.19 – Effect of *w/cm* and air entrainment on SCC performance

SCC Behavior	*w/cm*		Air entrainment	
	0.33	0.38	without AEA	with AEA
HRWRA demand (×1)	++	+++	NS	NS
Slump flow retention (×1)	++	+++	NS	NS
Passing ability (×1)	++	+++	++	+++
Filling capacity (×2)	++	+++	++	+++
Static stability (×2)	+++	++	+++	++
Total fresh properties	**16**	**19**	**12**	**13**
18-hour compressive strength steam-cured (×3)	+++	++	+++	++
18-hour compressive strength air-cured (×1)	++	+++	++	+++
56-day compressive strength (×2)	+++	++	+++	++
18-hour modulus of elasticity (×2)	+++	+++	+++	++
Total hardened properties	**23**	**19**	**23**	**17**
Global performance	**39**	**38**	**35**	**30**
Ranking	**I**	**I**	**I**	**III**

D.3.5 Effect of Fluidity Level on SCC Performance

Workability responses and mechanical properties of SCC designed for relatively high, medium, and low slump flow values of 27.5 to 29 in. (700 to 735 mm), 25 to 27.5 in. (640 to 700 mm), and 23.5 to 25 in. (600 to 640 mm), respectively, are compared in Table D.20. SCC mixtures with low and medium slump flow values exhibited similar levels of passing ability (medium), filling capacity (medium), and resistance to surface settlement (high). Mixtures with high fluidity (slump flow) exhibited high passing ability and filling capacity, but relatively medium to low

resistance to static stability. Due to the lower static stability, SCC with high level of slump flow had lower overall workability score (12) than those with medium level of fluidity (13). As expected, SCC with high fluidity developed lower compressive strengths at 18 hours of steam curing and 56 days of moist curing and lower 18-hour modulus of elasticity than concrete with low slump flow. In general, SCC mixtures with medium fluidity level are recommended for casting highly reinforced precast, prestressed girders.

Table D.20 – Effect of fluidity level on SCC performance

SCC Behavior	Fluidity level		
	Low	Medium	High
HRWRA demand (×1)	NA	NA	NA
Slump flow retention (×1)	+++	+++	+
Passing ability (×1)	+	++	+++
Filling capacity (×2)	+	++	+++
Static stability (×2)	+++	++	+
Total fresh properties	**12**	**13**	**12**
18-hour compressive strength steam-cured (×3)	+++	+++	++
18-hour compressive strength air-cured (×1)	+++	+++	++
56-day compressive strength (×2)	+++	+++	++
18-hour modulus of elasticity (×2)	+++	+++	++
Total hardened properties	**24**	**24**	**16**
Global performance	**36**	**37**	**28**
Ranking	**II**	**I**	**IV**

D.3.6 Effect of Viscosity-Modifying Admixture on SCC Performance

For a given slump flow, SCC designed with low to moderate dosage of thickening-type VMA required 5% to 15% greater HRWRA demand. The higher dosage of HRWRA improves slump flow retention. On the other hand, the increase in HRWRA reduces early age mechanical properties. The incorporation of thickening-type VMA is shown to have considerable effect on static stability. In general, SCC designed with high *w/cm*, and low HRWRA demand exhibited greater static stability when the thickening-type VMA was incorporated. Consequently, SCC containing thickening-type VMA had higher workability score (11) than those made without VMA (9). SCC containing thickening-type VMA had lower early-age mechanical properties (score of 24 vs. 18), as presented in Table D.21.

In general, the use of low to moderate dosage of VMA is not required for SCC mixtures that are already stable (proper aggregate gradation, low *w/cm*, and high binder content). On the other hand, SCC made with relatively high *w/cm* and/or low binder content should incorporate VMA to secure stability and better homogeneity of in-situ properties, including bond to reinforcement.

D.3.7 Guidelines for Material Selection

Based on the results, guidelines for selecting material constituents, mixture proportioning, and fluidity levels to assure the best global performance of SCC for precast, prestressed girder construction are recommended in Table D.22. SCC proportioned with 0.33 *w/cm*, crushed aggregate with ½ in. (12.5 mm) MSA, and Type III cement with 20% Class F fly ash can develop the best over global performance. In the case of SCC made with higher *w/cm* of 0.40, the introduction of VMA is recommended to enhance stability and robustness.

Table D.21 – Effect of fluidity level on SCC performance

SCC Behavior	VMA	
	No VMA	Low to moderate dosage of VMA
HRWRA demand (×1)	+++	++
Slump flow retention (×1)	++	+++
Passing ability (×1)	NS	NS
Filling capacity (×2)	NS	NS
Static stability (×2)	++	+++
Total fresh properties	**9**	**11**
18-hour compressive strength steam-cured (×3)	+++	++
18-hour compressive strength air-cured (×1)	+++	++
56-day compressive strength (×2)	+++	+++
18-hour modulus of elasticity (×2)	+++	++
Total hardened properties	**24**	**18**
Global performance	**33**	**29**
Ranking	**I**	**II**

Table D.22 − Recommendations for mixture proportioning for SCC used in precast, prestressed applications

	MSA and aggregate type	*w/cm*	Binder type	Fluidity level	VMA
Fresh properties	MSA G½ in. (12.5 mm)	0.38	Type III + 20% FA	Medium	If further stability and robustness are required
Mechanical properties	MSA C½ in. (12.5 mm)	0.33	Type III + 20% FA	Low and Medium	
Global performance	MSA C½ in. (12.5 mm)	0.33	Type III + 20% FA	Medium	

D.4 FACTORIAL DESIGN TO MODEL FRESH AND HARDENED PROPERTIES OF SCC USED IN PRECAST PRESTRESSED APPLICATIONS

A factorial design was carried out to model the effect of mixture parameters and material properties on workability, mechanical, and visco-elastic properties of SCC. The modeled mixture parameters included the binder content (BC), binder type (BT), *w/cm*, dosage of thickening-type VMA, and S/A. In total, 16 mixtures were used in the factorial design, as summarized in Table D.4. The factorial design enables the evaluation of the five selected parameters with each evaluated at two distinct levels of -1 and +1 (minimum and maximum levels). Detail descriptions of factorial design are elaborated in reference below[D3]. Absolute and coded values of the modeled parameters are presented in Table D.23. Complete listing of the mixture proportioning and resulting fresh properties, rheological and thixotropic (structural breakdown) properties, and mechanical properties are presented in Appendices F, G, H, I, and J, respectively.

Table D.23 – Absolute and coded values of modeled parameters

Coded / Absolute	- 1	+ 1
Binder content (BC), lb/yd³ (kg/m³)	742 (440)	843 (500)
Binder type (BT)	Type I/II	Type III + 20% FA
w/cm	0.34	0.40
VMA content, fl oz/cwt (L/100 kg CM)	0	1.5 (0.1)
Sand-to-aggregate ratio (S/A)	0.46	0.54

The coded values are calculated as the difference between the absolute values and values corresponding to the central points divided by the difference between the absolute values corresponding to the 0 and 1 coded points, as shown below:

Coded BC = (absolute BC – 793) / 50

Coded *w/cm* = (absolute *w/cm* – 0.37) / 0.03

Coded VMA = (absolute VMA – 0.75) / 0.75

Coded S/A = (absolute S/A – 0.50) / 0.04

[D3] Khayat, H. K., Ghezal, A., and Hadriche. M.S., "Factorial Design Models for Proportioning Self-Consolidating Concrete." *Materials and Structures*, Vol. 32 (1999) pp. 679-686.

Statistical models were established using multi-regression analysis. The estimate for each factor refers to the contribution of that factor to the modeled response. Student's tests were carried out to evaluate the significance of model factors and their second-order interaction on a given response. For each modeled response, the single-operator relative error corresponding to 90% confidence limit was used to perform significance evaluation. Probability values less than 0.1 are considered as significant evidence that the factor has significant influence on the modeled response. Single-operator relative errors were determined using mixtures corresponding to the central point of the experimental domain. Mean value for each response and calculated relative errors corresponding to 90% confidence limits are summarized in Table D.24.

Table D.24 − Mean values and relative errors of central points (90% confidence limit)

	Mean	Relative error
Slump flow, in. (mm)	27.1 (688)	0.6
J-Ring flow, in. (mm)	25.5 (648)	0.7
Slump flow – J-Ring flow, in. (mm)	1.6 (40.6)	15.7
L-box blocking ratio (h_2/h_1)	0.80	7.0
Filling capacity , %	91.2	1.6
Surface settlement, %	0.50	13.0
Column segregation index, C.O.V. (%)	2.70	18.0
Plastic viscosity, psi.s (Pa.s)	0.0371 (256)	0.0012 (8.2)

D.4.1 Statistical Models for Fresh Concrete Properties

D.4.1.1 Established statistical models

The derived models that yielded high correlation coefficients (R^2) are summarized in Table D.25. All factors are expressed in terms of coded values. The R^2 values of the proposed models ranged between 0.84 and 0.99. A negative estimate signifies that an increase in the modeled parameter can lead to a reduction in the measured response. For example, in the case of HRWRA model, an increase in binder content can decrease the HRWRA demand. It is important to note that the setting time was modeled but resulted in relatively low R^2 values and is excluded from the discussion.

The binder type and binder content are found to have the most significant effect on workability. The *w/cm* also showed a significant effect on workability. For example, the slump flow loss is affected, in order of significance, by the binder type (-0.84), binder content (-0.57), and *w/cm* (0.42). On the other hand, the S/A factor had significant effect on the J-Ring flow and plastic viscosity. The thickening-type VMA content exhibited considerable effect on the column segregation index but did not have significant influence on surface settlement. This can be attributed to the relatively low dosage of thickening-type VMA as well as to the fact that the investigated mixtures had high static stability levels. The incorporation of a low dosage of VMA in the factorial design investigation and the selection of a thickening-type VMA aimed mainly at enhancing the robustness of the SCC, as the mixtures were already stable.

Second-order interactions were obtained for some of the modeled responses. For example, in the case of the caisson filling capacity, a second-order interaction between BT and *w/cm* was obtained and had a relative significance on the order of the main effect of BC.

Table D.25 − Derived statistical models for fresh concrete [slump flow = 26.8 ± 0.8 in. (680 ± 20 mm)]

	Modeled response	Derived equations	R^2
	[HRWRA demand]$^{0.5*}$ (fl oz/cwt)	4.76 – 1.06 *w/cm* – 0.33 BC + 0.33 BT + 0.11 VMA + 0.13 (*w/cm* · BT)	0.97
Filling ability	Slump flow loss (in.)**	0.16 – 0.84 BT – 0.57 BC + 0.42 *w/cm* + 0.16 S/A – 0.54 (BT · S/A) + 0.49 (BC· *w/cm*) – 0.42 (BC · BT)	0.84
Passing ability	[L-box blocking ratio]$^{1.4}$ (h_2/h_1)	0.69 + 0.13 *w/cm* + 0.12 BC – 0.13 (BC · *w/cm*)	0.93
	[J-Ring flow]^3 (in.)	16,329 + 1,344 *w/cm* + 1,324 BC + 814 BT – 729 S/A – 465 VMA – 1,140 (BC · BT) – 1,136 (BC · *w/cm*) + 824 (BT · S/A) – 650 (*w/cm* · BT) – 465 (*w/cm* · S/A) + 351 (VMA · S/A) – 291 (BC · S/A)	0.99
Filling capacity	Caisson filling capacity (%)	92 + 4.38 BC + 3.75 *w/cm* + 3.63 BT – 3.63 (BT · *w/cm*) – 2.63 (*w/cm* · BT) – 2.50 (BC · BT)	0.92
	Slump flow – J-Ring flow (in.)	1.42 – 0.70 BC – 0.63 BT – 0.55 *w/cm* + 0.26 S/A + 0.63 (BC · *w/cm*) + 0.50 (BC · BT) + 0.40 (*w/cm* · BT) – 0.26 (BT · S/A)	0.94
Stability	[Surface settlement]$^{0.5}$ (%)	0.677 + 0.037 *w/cm* + 0.036 BC – 0.024 BT	0.86
	Column segregation (C.O.V.)	3.25 – 0.30 BC – 0.61 (BC · BT) + 0.44 (BT · S/A) + 0.42 (*w/cm* · BT) – 0.39 (BC · VMA) – 0.36 VMA + 0.30 (*w/cm* · S/A)	0.89
Rheology and formwork pressure	Plastic viscosity (Pa.s)*	298 – 133.4 *w/cm* – 105.3 BC + 53.7 S/A + 49.7 (BT · *w/cm*) – 27.6 (*w/cm* · S/A)	0.93
	Thixotropy (A_b), J/m^3.sec	586 – 323.4 *w/cm* – 181.8 BC + 71.1 (BC · *w/cm*)	0.95
	Initial form pressure at 3.3 ft (1 m), K_0	0.90 + 0.027 BC + 0.027 *w/cm* – 0.014 S/A – 0.023 (BC · *w/cm*) – 0.013 (BT · *w/cm*) + 0.11 (S/A · *w/cm*)	0.96

* 1 Pa = 1.45 × 10^{-4} psi

The *w/cm* is found to exhibit the most significant effect on plastic viscosity. The binder content and S/A showed significant effect on plastic viscosity. The second order interaction of *w/cm* and BT also had considerable influence on plastic viscosity.

As in the case of plastic viscosity, the breakdown area (A_b) determined to evaluate thixotropy of concrete can decrease with the increase in BC and *w/cm*. The increase in BC and *w/cm* results in higher initial relative form pressure (K_0). On the other hand, K_o deceases with the increase in S/A. The order of importance of mixture parameters on A_b are *w/cm* and BC, as shown in the derived model of Table D.25. Similarly, both the *w/cm* and BC have the most significant effect on K_0. This is followed by the S/A and various coupled parameters.

The derived models for the filling capacity and difference between slump flow and J-Ring flow responses are affected mainly by the BC, *w/cm*, and BT. For example, the caisson filling capacity can be improved by increasing the BC and *w/cm*. It can also be improved by using Type III cement with 20% of fly ash instead of Type I/II cement (i.e. increasing the coded value from -1 to +1). The increase of these parameters (BC, *w/cm*, and BT) also resulted in a decrease in the difference between slump flow and J-Ring flow (higher passing ability).

The thickening-type VMA, *w/cm*, and BC parameters had the most significantly effect on static stability. For example, the use of thickening-type VMA and increase in BC can improve the column segregation stability index. The surface settlement response decreases with the reduction of *w/cm* and BC. Second-order interactions, such as BC · BT and BC · VMA also had important influence on the column segregation stability index.

Based on the derived models for workability, the flowing findings can be stated:

- The HRWRA demand decreases with the increase in *w/cm* and binder content. The use of Type III cement and 20% Class F fly ash necessitates higher HRWRA demand than in the case of SCC prepared with Type I/II cement.
- Better slump flow retention can be obtained with SCC made with low *w/cm* given the higher HRWRA demand to achieve 26.0 to 27.5 in. (660 to 700 mm) slump flow.
- Passing ability [L-box blocking ratio (h_2/h_1) and J-Ring flow] and filling capacity can improve with the increase in binder content and *w/cm*.
- Surface settlement of SCC increases with the binder content and *w/cm*.
- The use of thickening-type VMA at low level can enhance static stability (lower column segregation index) than that of concrete made without any VMA.
- Plastic viscosity decreases with the increase in binder content and *w/cm* but increases slightly with the increase in S/A.
- SCC made with Type III cement and 20% Class F fly ash can exhibit better slump flow retention, higher passing ability, and higher filling capacity than that with Type I/II cement.
- Thixotropy or structural build-up at rest of the SCC decreases with the increase in binder content and w/cm. Higher thixotropy can be detrimental to surface finish and advantageous to formwork pressure.
- Initial relative form pressure (K_0) at 3.3 ft (1 m) in height cast at 13.1 – 16.4 ft/hr (4 – 5 m/hr) varies between 0.80 and 0.97 of hydrostatic pressure. K_0 increases with the increase in binder content and *w/cm* but decreases with the increase in S/A.

D.4.1.2 Validation of established models for fresh properties

Eight mixtures along with three central points were selected and prepared to evaluate the accuracy of the derived models. As can be seen in Fig. D.13, the mixtures were selected to cover a wide range of mixture proportioning within the modeled regions. The mixture proportioning of the SCC used to validate the derived models is presented in Table D.26. Fresh properties of these mixtures are summarized in Table G.1 of Appendix G.

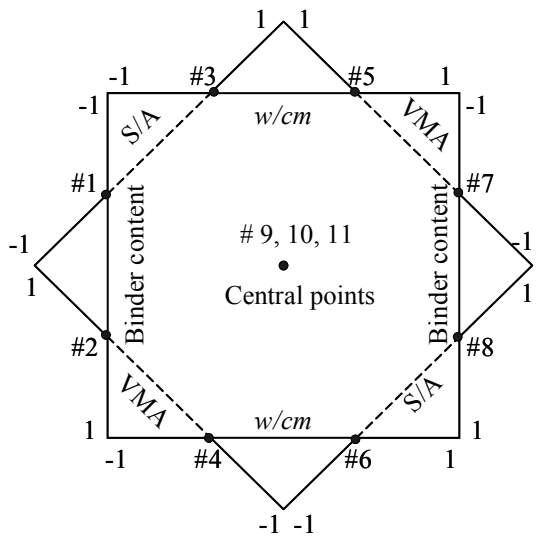

Fig. D.13 − SCC mixtures used to validate the derived models

Table D.26 − Mixture proportioning used to validate the derived statistical models

Mix no.	Coded values					Absolute values				
	Binder	*w/cm*	VMA	Binder type	S/A	Binder lb/yd³ (kg/m³)	*w/cm*	VMA (fl oz/cwt)	Binder type	S/A (%)
1	-1/3	-1	1	-1	-1/3	776 (460)	0.34	1.55	I/II	0.486
2	1/3	-1	1/3	1	-1	809 (480)	0.34	0.52	III	0.46
3	-1	-1/3	1	-1	1/3	742 (440)	0.36	1.04	I/II	0.513
4	1	-1/3	-1/3	1	-1	843 (500)	0.36	0.52	III	0.46
5	-1	1/3	1/3	-1	1	742 (440)	0.38	1.04	I/II	0.54
6	1	1/3	-1	1	-1/3	843 (500)	0.38	0	III	0.486
7	-1/3	1	-1/3	-1	1	776 (460)	0.40	0.52	I/II	0.54
8	1/3	1	-1	1	1/3	809 (480)	0.40	0	III	0.513
Central points										
9	0	0	0	0	0	792 (470)	0.37	0.78	I/II-III	0.50
10	0	0	0	0	0	792 (470)	0.37	0.78	I/II-III	0.50
11	0	0	0	0	0	792 (470)	0.37	0.78	I/II-III	0.50

Comparisons of predicted to measured values for the difference between slump flow and J-Ring flow and plastic viscosity are illustrated in Fig. D.14. Points above the 1:1 diagonal line indicate that the statistical model overestimates the measured response. The majority of the predicted (slump flow – J-Ring flow) and plastic viscosity values are within the repeatability limit of ± 0.25 in. (± 6.4 cm) and ± 0.003 psi.s (± 21 Pa.s), respectively. These limits constitute experimental errors for the (slump flow – J-Ring flow) and plastic viscosity measurements determined from the single-operator repeatability tests. On average, the predicted-to-measured ratios of (slump flow – J-Ring flow) and plastic viscosity values were 1.1 and 1.02, respectively, showing accurate prediction of the measured responses within the modeled region. Validation of statistical models for the remaining workability characteristics are elaborated in Appendix K.

The validation investigation showed that the derived models offer adequate prediction of workability responses within the experimental domain of the modeled mixture parameters. It is important to note that the absolute values of the predicted values are expected to change with changes in raw material characteristics. However, the relative contributions of the various parameters are expected to be the same, thus facilitating the mix design protocol.

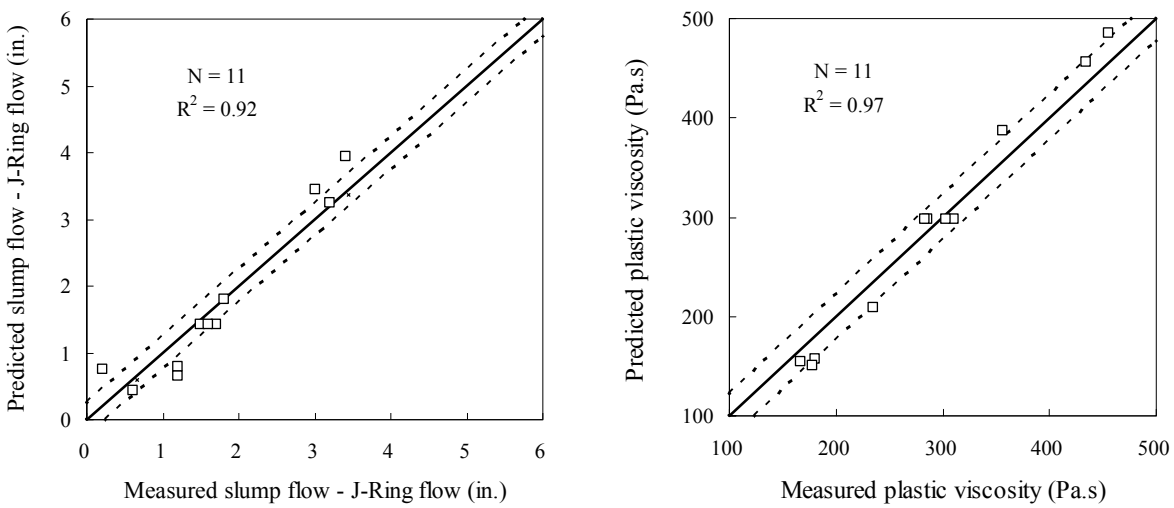

Fig. D.14 − Comparison between predicted and measured workability responses: (slump flow – J-Ring flow) and plastic viscosity

D.4.2 Formwork Pressure

As shown in Table D.27, the initial relative form pressure (K_0) values of 20 SCC mixtures varied from 0.79 to 0.97. The K_0 values of two HPC mixtures were 0.88 and 0.93. After 60 minutes, the relative pressure ranged between 0.52 and 0.91. Time to pressure cancellation for the SCC mixtures ranged between 365 and 1300 minutes. These values were 410 and 440 minutes for the two HPC mixtures. The actual variation in form pressure determined at various heights of the 20 SCC and two HPC mixtures are given in Appendix D.

Table D.27 – Initial form pressure and time to pressure cancellation of SCC and HPC

	Mixture No.	$K_0 = P_{max}/P_{hyd}$ @ bottom sensor (3.5 ft (1.08 m) concrete head)	K_{60} after 60 min	Time to pressure cancellation @ bottom sensor (3.5 ft (1.08 m) concrete head), min
SCC without AEA	1	0.79	0.66	1120
	2	0.87	0.85	1300
	3	0.84	0.73	1083
	4	0.80	0.65	1254
	5	0.93	0.57	579
	6	0.90	0.75	698
	7	0.96	0.75	366
	8	0.91	0.66	723
	9	0.93	0.59	1080
	10	0.92	0.72	827
	11	0.89	0.76	858
	12	0.96	0.82	722
	13	0.93	0.61	397
	14	0.94	0.52	571
	15	0.97	0.90	600
	16	0.92	0.69	783
HPC	17	0.88	0.79	411
	18	0.93	0.91	440
SCC with AEA	19	0.87	0.64	1132
	20	0.79	0.61	630
	21	0.88	0.69	985
	22	0.87	0.63	400

D.4.3 Temperature Rise under Semi-Adiabatic Conditions

The variations in temperature of concrete cylinders measuring 6 × 12 in. (150 × 300 mm) stored under semi-adiabatic conditions are presented in Fig. D.15. Peak temperatures of 20 SCC mixtures varied from 125 to 145°F (52 to 63°C). These values were 136 and 139°F (58 and 60°C) for the two HPC mixtures. SCC mixtures No. 13, 14, and 15 exhibited shorter time to attain peak temperature. This can be due to the higher *w/cm*. For a given *w/cm* of 0.40, SCC No. 16 made with Type III cement and 20% Class F fly ash exhibited lower peak temperature and longer time to reach peak than the other mixtures prepared with Type I/II cement. As expected, for a given *w/cm*, the use of thickening-type VMA slightly delays the hydration reaction, thus extending time to attain peak temperature

Temperature history of two HPC and four air-entrained SCC mixtures are also presented in Fig. D.15. HPC No. 17 proportioned with the lower w/cm of 0.34 and Type I/II cement had lower peak temperature and longer time to attain peak temperature than mixture No. 18 made with 0.38 w/cm and Type III cement with 20% Class F fly ash. This can be attributed to approximately 60% higher HRWRA dosage. HPC mixtures exhibited shorter time to attain peak temperature than SCC proportioned with higher HRWRA dosage.

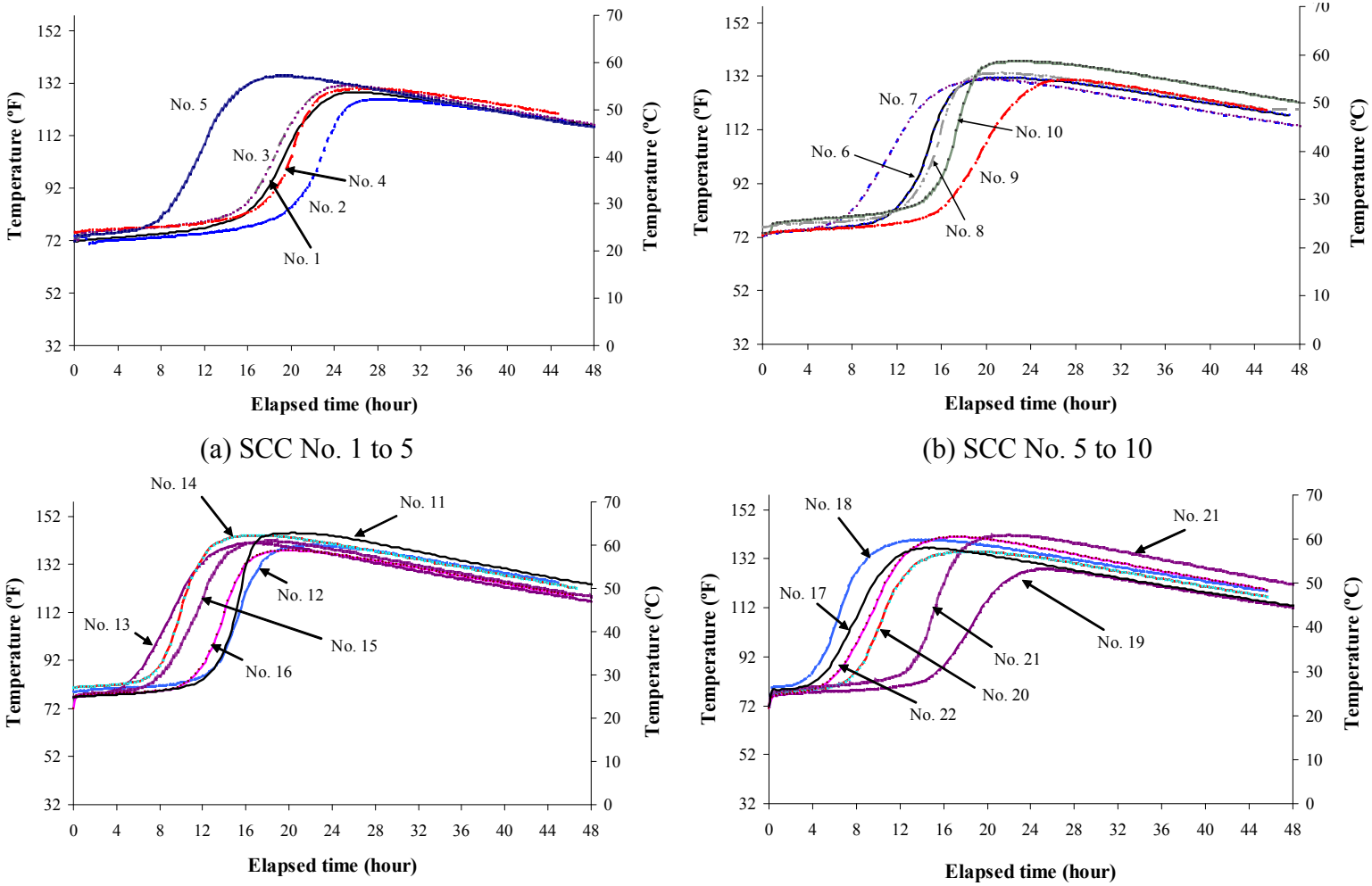

(a) SCC No. 1 to 5

(b) SCC No. 5 to 10

(c) SCC No. 11 to 16

(d) SCC No. 19 to 22 and HPC No. 17 and 18

Fig. D.15 − Comparison between temperature variations under semi-adiabatic conditions

D.4.4 Statistical Models for Mechanical Properties

D.4.4.1 Established statistical models

Gains in compressive strength between 18 hours (air curing) and 56 days (moist curing) for the 16 SCC mixtures used to establish statistical models to predict compressive strength gain as well as the two HPC mixtures are presented in Fig. D.16. SCC mixtures proportioned with 0.34 *w/cm* (No. 1 to 4 and No. 9 to 12) exhibited higher 28-day compressive strength of 8,520 to 10,190 psi (58.7 to 70.3 MPa) compared to between 6,900 to 8,170 psi (47.6 to 56.3 MPa) for those made with 0.40 *w/cm*. In general, the 7-day compressive strength was higher than approximately 80% of the 28-day result. The 7-to-28 day strength ratio of SCC made with Type I/II cement and 0.34 *w/cm* was higher than that of SCC prepared with Type III cement and 20% Class F fly ash and 0.40 *w/cm*. Similar compressive strength gain and values were obtained for SCC and HPC of similar mixture compositions. For a given mixture composition, air-entrained mixtures had lower compressive strengths than those made without any AEA.

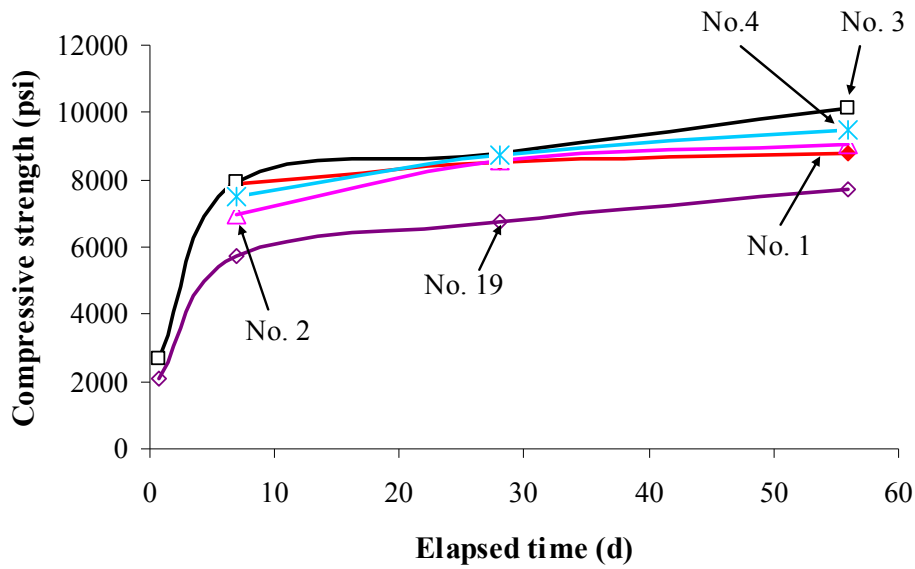

(a) *w/cm* = 0.34: SCC No. 1 to 4 and No. 19

Fig. D.16 – Development of compressive strength of 20 SCC and two HPC mixtures

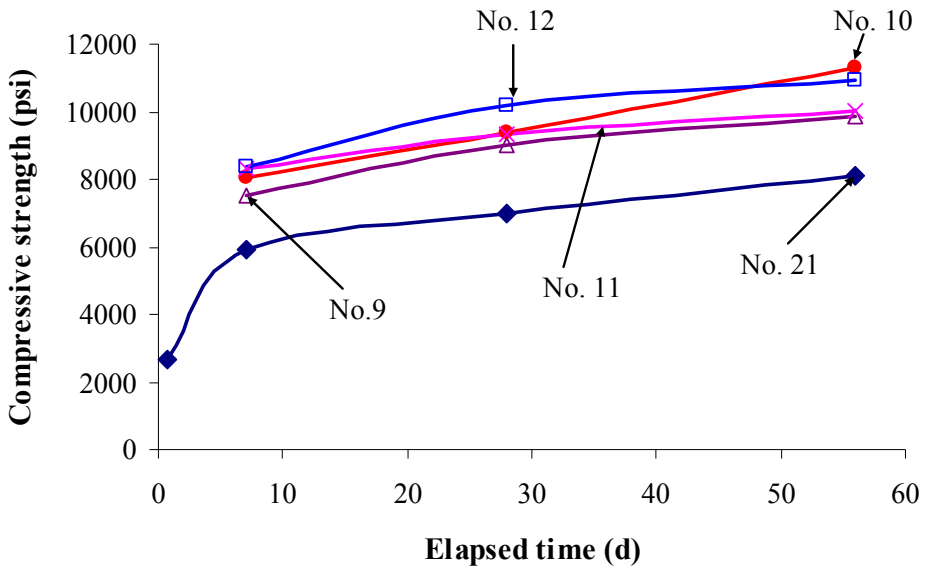

(b) *w/cm* = 0.34: SCC No. 9 to 12 and No. 21

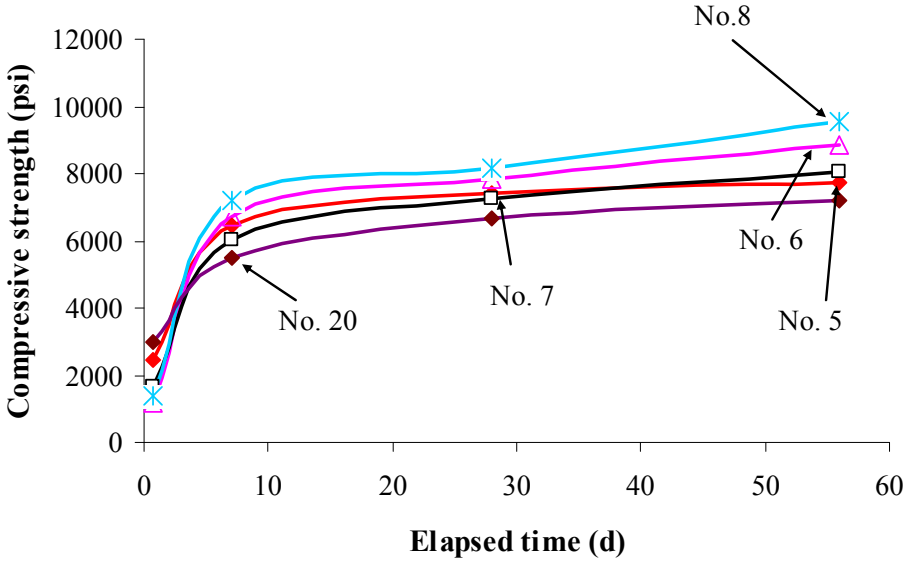

(c) *w/cm* = 0.40: SCC No. 5 to 8 and No. 20

Fig. D.16 (cont'd) – Development of compressive strength of 20 SCC and two HPC mixtures

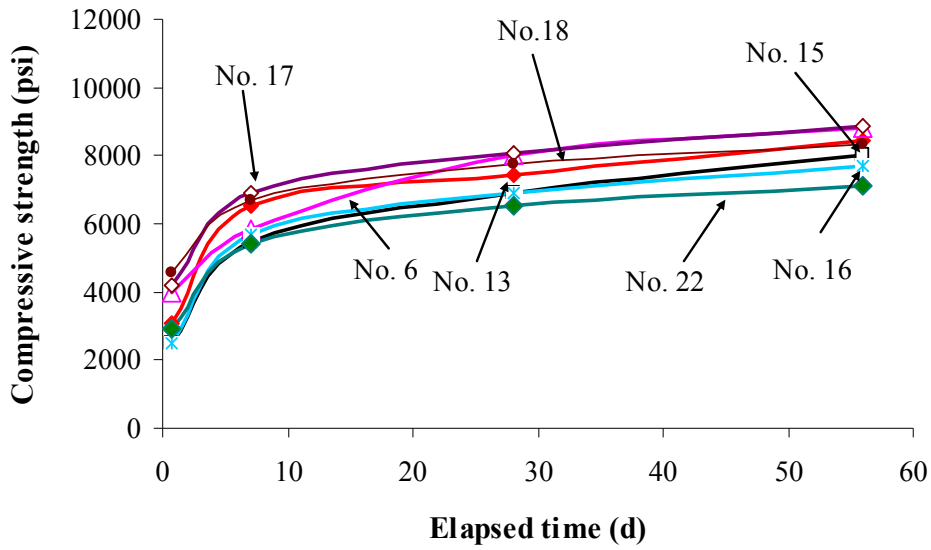

(d) *w/cm* = 0.40: SCC No. 13 to 16 and No. 22 and HPC mixtures

Fig. D.16 (cont'd) – Development of compressive strength of 20 SCC and two HPC mixtures

Parameter estimates of the statistical models derived to estimate compressive strength, modulus of elasticity (MOE), and flexural strength are summarized in Table D.28. As expected, the *w/cm* has the greatest influence on these properties. The content and type of binder had considerable effect on mechanical properties. The MOE and flexural strength responses are shown to be significantly affected by S/A. In most cases, the use of thickening-type VMA did not have significant effect on mechanical properties.

Based on the derived models for mechanical properties, the main findings can be summarized as follows:

- Mechanical properties, including compressive strength, modulus of elasticity, and flexural strength, increase with the decrease in *w/cm*.
- Increase in binder content can lead to higher 56-day compressive strength but lower 18-hour MOE and 7-day flexural strength.
- The increase in S/A has negative effect on MOE at 18 hours (steam curing) and 56 days (moist curing). On the other hand, the increase in S/A leads to higher flexural strength.
- SCC made with Type III cement and 20% Class F fly ash can exhibit higher compressive strength and MOE at 56 days but lower mechanical properties at 18 hours; this is mainly due to delayed setting resulting from greater HRWRA demand compared to concrete prepared with Type I/II cement.

Table D.28 − Derived statistical models for mechanical properties

Property	Age	Derived equations	R^2
Compressive strength, psi	18 hours	4,752 – 293 *w/cm* – 111 BT – 81 VMA + 153 (*w/cm* · BT) – 128 (VMA · S/A) – 97 (*w/cm* · VMA)	0.96
	56 days	9,176 – 773 *w/cm* + 290 BT + 220 BC – 368 (BC · *w/cm*)	0.87
Modulus of elasticity, ksi	18 hours	4,419 – 268 *w/cm* – 103 BT – 86 S/A – 78 BC – 158 (BC · *w/cm*) – 96 (BT · S/A)	0.89
	56 days	5,554 – 311 *w/cm* – 166 S/A + 69 BT + 79 (BC · BT)	0.87
Flexural strength, psi	7 days	1,036 + 123 S/A – 90 BC – 58 *w/cm* – 126 (BC · *w/cm*)	0.76
	56 days	1,128 – 110 *w/cm* + 48 S/A + 35 (BC · BT)	0.83

D.4.4.2 Validation of statistical models for mechanical properties

Eight SCC mixtures proportioned in the range of the factorial design were used to validate the statistical models for mechanical properties. Three central points were also used to evaluate the error in 90% confidence limit; the estimated relative errors corresponding to 90% confidence limit are shown in Table D.29.

Table D.29 − Mean values and relative errors of central points (90% confidence limit)

	Mean	Relative error, 90% confidence limit (%)
18-hour compressive strength, psi (MPa)	4,905 (33.8)	2.0
56-day compressive strength, psi (MPa)	9,135 (63.0)	2.9
18-hour modulus of elasticity, ksi (GPa)	4,490 (31.0)	2.5
56-day modulus of elasticity, ksi (GPa)	5,605 (38.6)	2.2
7-day flexural strength, psi (MPa)	1,095 (7.55)	4.4
56-day flexural strength, psi (MPa)	1,145 (7.89)	3.5

Based on the relative error estimates, comparisons of predicted-to-measured values for mechanical properties are illustrated in Fig. D.17. Again, data points above the solid diagonal 1:1 line indicate that the statistical model overestimates the real values, while those below the line indicate an underestimation of the actual values. Most of the data are located within the error limits, thus demonstrating the ability of the derived models to estimate the 18-hour compressive strength. The mean of predicted-to-measured values for the 18-hour compressive strength was 1.0.

The evaluated SCC mixtures exhibited 56-day compressive strength ranging from 8,000 to 11,000 psi. The mean predicted-to-measured ratio of the 56-day compressive strength was 1.01 with R^2 of 0.92. Similar results for the remaining mechanical properties are presented in Appendix K.

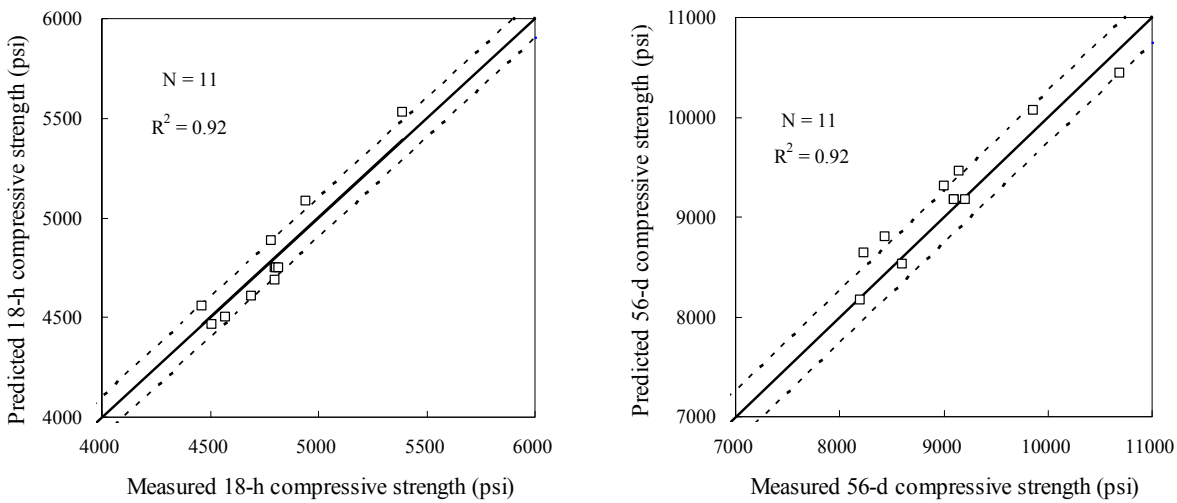

Fig. D.17 – Comparison between predicted and measured mechanical properties: 18-hour and 56-day compressive strength

D.4.5 Statistical Models for Visco-Elastic Properties

The variations of creep, autogenous shrinkage, and drying shrinkage results of the 16 SCC mixtures used to establish the statistical models to predict visco-elastic properties as well as the data for the two HPC mixtures are presented in Figs. D.18, D.19, and D.20, respectively.

The investigated mixtures in the factorial design exhibited wide range of creep strains ranging between 1025 and 1485 µstrain at 300 days. Creep values of the HPC No. 17 and 18 mixtures were 1035 and 1250 µstrain, which are slightly lower than the mean creep values of SCC mixtures. This is mainly due to the lower paste volume and higher coarse aggregate content compared to the SCC. SCC exhibited 10% to 20% higher creep after 300 days than HPC made with similar *w/cm*.

As presented in Fig. D.18, for a given *w/cm* of 0.34, mixtures made with higher binder content of 843 lb/yd^3 (500 kg/m^3) had higher creep than similar SCC prepared with 742 lb/yd^3 (440 kg/m^3). SCC mixtures No. 9, 10, 11, and 12 proportioned with 0.34 *w/cm* and binder content of 843 lb/yd^3 (500 kg/m^3) exhibited 1145 to 1370 µstrain creep after 300 days of loading. The creep of SCC No. 1, 2, 3, and 4 made with the same *w/cm* and binder content of 742 lb/yd^3 (440 kg/m^3) were 1175, 1180, 1150, and 1305 µstrain, respectively. The influence of binder content was more dominant in the case of SCC proportioned with higher *w/cm* of 0.40. For a given binder type, mixtures with 843 lb/yd^3 (500 kg/m^3) exhibited 8% to 20% higher creep than SCC prepared binder content of 742 lb/yd^3 (440 kg/m^3).

The binder type had also significant influence on creep. SCC made with Type III cement and 20% fly ash exhibited higher creep compared to similar mixtures proportioned with Type I/II cement, regardless of the binder content, *w/cm*, S/A, and use of thickening-type VMA. For a

given binder content of 742 lb/yd^3 (440 kg/m^3), SCC mixtures made with Type III cement and 20% fly ash had creep of 1180 to 1305 µstrain after 300 days. Similar results were found for SCC proportioned with binder content of 843 lb/yd^3 (500 kg/m^3). The *w/cm* was not shown to have considerable effect on creep. This can be attributed to the fact that other mixture parameters, including binder content, binder type, and S/A, have more predominant influence on creep.

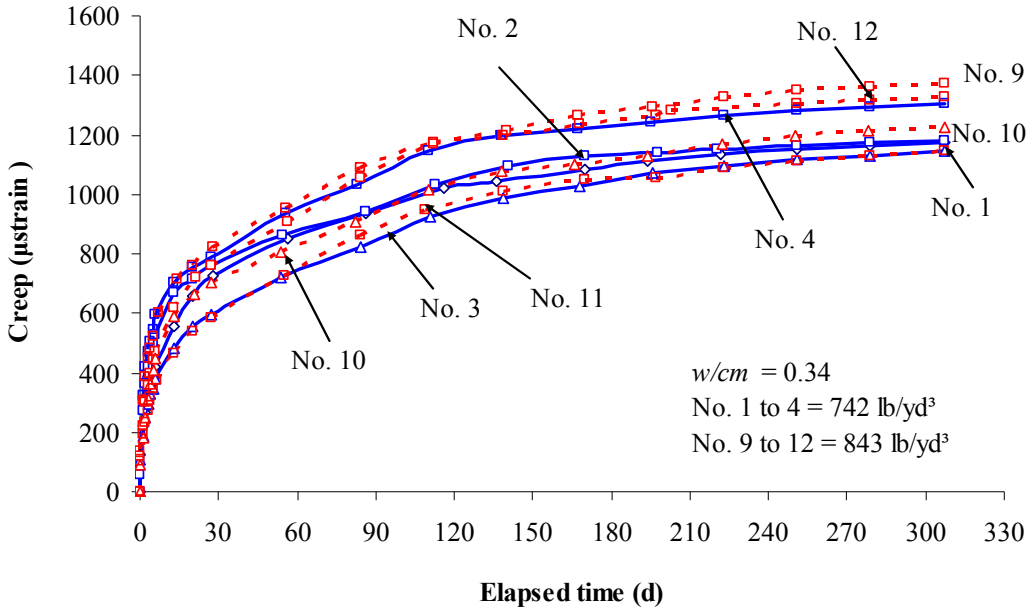

(a) SCC No. 1 to 4 and No. 9 to 12 made with *w/cm* = 0.34

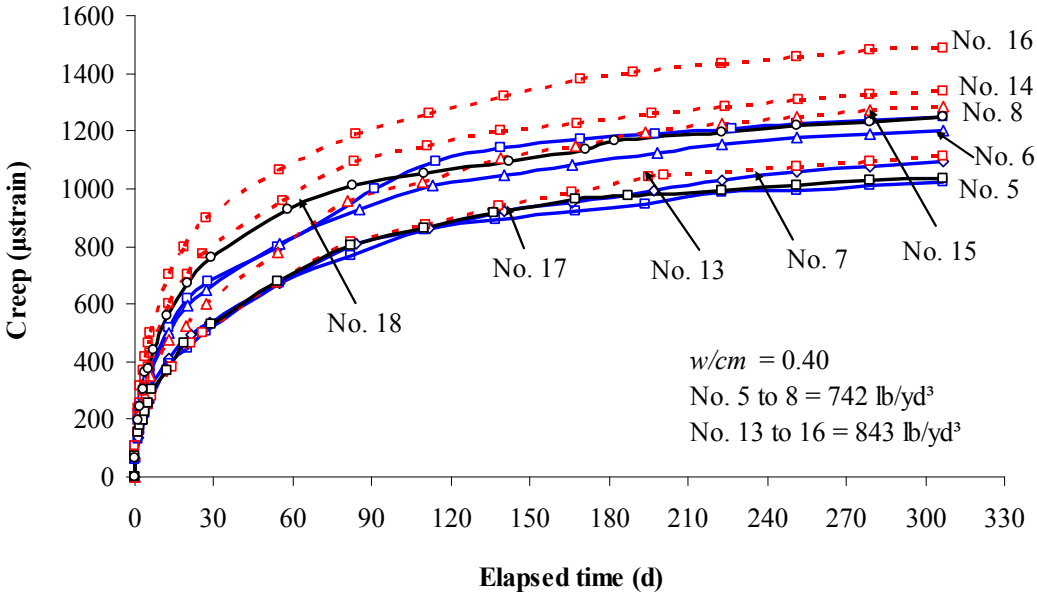

(b) SCC No. 5 to 8 and No. 13 to 16 made with *w/cm* = 0.40 and HPC mixtures (No. 17 and 18)

Fig. D.18 – Variations of creep strain for SCC and HPC mixtures

The investigated mixtures exhibited wide range of autogenous shrinkage that derived with mixture proportioning and materials in use. The autogenous shrinkage after 56 days ranged from 100 to 350 μstrain. Autogenous shrinkage of mixtures No. 1 to 4 and No. 5 to 8 made with binder content of 742 lb/yd^3 (440 kg/m^3) are presented in Fig. D. 19. SCC made with *w/cm* of 0.34 exhibited higher autogenous shrinkage of 115 to 330 μstrain compared to between 95 and 275 μstrain for SCC No. 5 to 8 that were proportioned with 0.40 *w/cm*. Similarly, mixtures No. 9 to 12 made with *w/cm* of 0.34 and binder content of 843 lb/yd^3 (500 kg/m^3) exhibited higher autogenous shrinkage compared to SCC No. 13 to 16 made with *w/cm* of 0.40 and the same binder content, as illustrated in Fig. D.19.

The binder type had considerable influence on autogenous shrinkage. SCC made with Type III cement and 20% fly ash exhibited higher autogenous shrinkage compared to similar mixtures made with Type I/II cement, regardless of the binder content, *w/cm*, S/A, and use of VMA. For a given binder content of 742 lb/yd^3 (440 kg/m^3), SCC mixtures No. 2, 4, 6, and 8 made with Type III cement and 20% fly ash had autogenous shrinkage values of 330, 280, 210, and 275 μstrain after 56 days of measurement, respectively, compared to 115, 135, 95, and 100 μstrain for SCC No. 1, 3, 5, and 7 that were prepared with Type I/II cement.

Drying shrinkage of the16 SCC and two HPC mixtures after 300 days ranged from 495 to 975 μstrain. As in the case of creep, drying shrinkage started after 18 hours of steam curing. SCC exhibited 5% to 30% higher drying shrinkage compared to HPC made with the similar *w/cm* at the age of 300 days. Figure D.20 (a) shows the variations of drying shrinkage with time for mixtures No. 1 to 4 and 9 to 12 that were proportioned with *w/cm* of 0.34 and different binder contents. Drying shrinkage of mixtures No. 5 to 8 and No. 13 to 16 made with *w/cm* of 0.40 are presented in Fig. D.20 (b). For a given *w/cm* of 0.34, mixtures No. 9 to 12 made with higher binder content of 843 lb/yd^3 (500 kg/m^3) exhibited higher drying shrinkage ranging between 635 and 975 μstrain after 300 days of drying compared to 535 to 830 μstrain for similar SCC prepared with 742 lb/yd^3 (440 kg/m^3) of binder. For a given *w/cm* and binder content, mixtures made with 0.46 S/A exhibited lower drying shrinkage compared to those prepared with 0.54 S/A, regardless of the use of VMA.

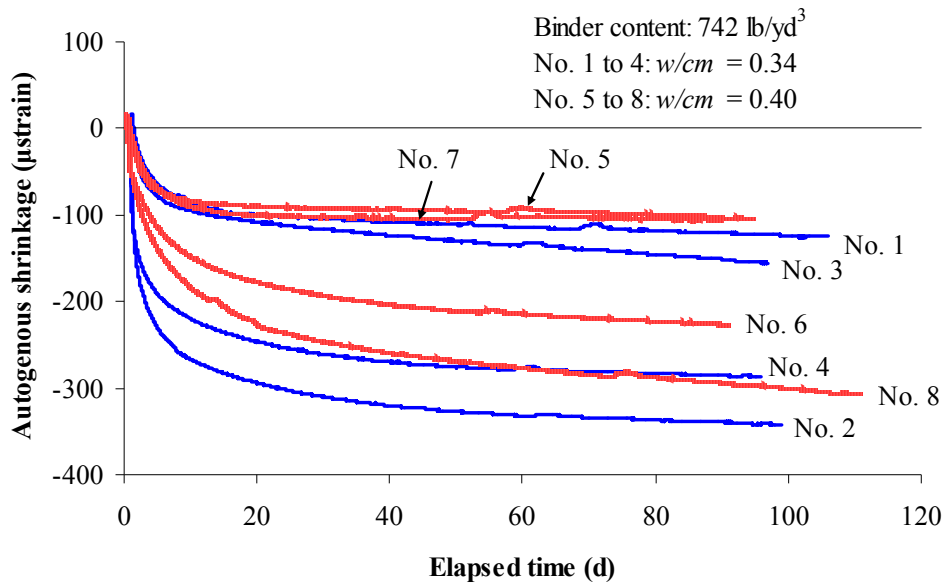

(a) SCC made with binder content of 742 lb/yd^3 (440 kg/m^3) and different *w/cm*

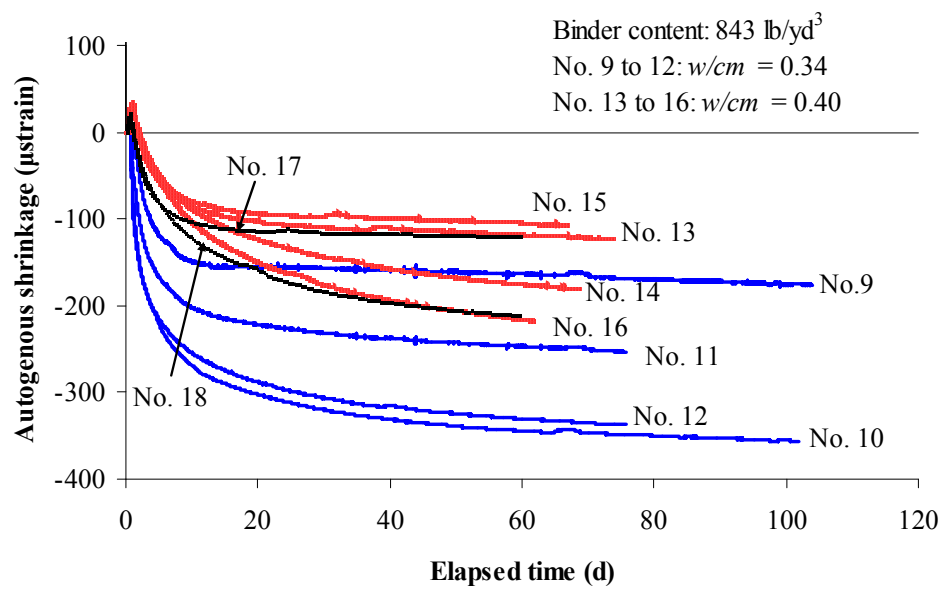

(b) SCC made with binder content of 843 lb/yd^3 (500 kg/m^3) and HPC No. 17 and No. 18

Fig. D.19 – Variations of autogenous shrinkage for SCC and HPC mixtures

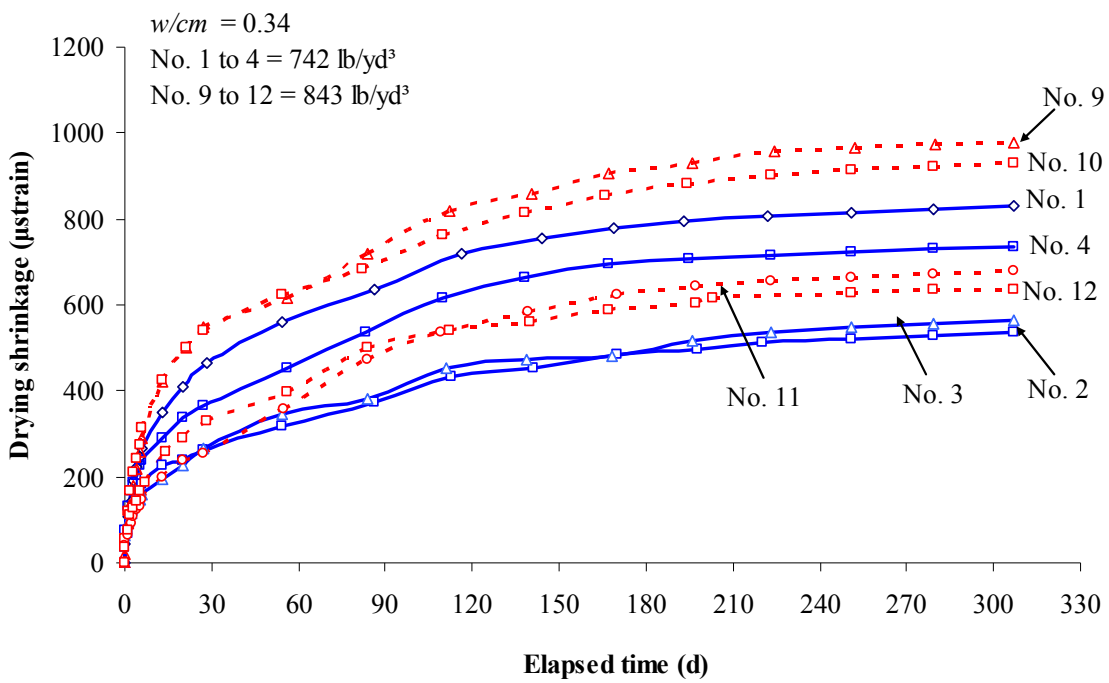

(a) SCC No. 1 to 4 and No. 9 to 12 made with *w/cm* = 0.34

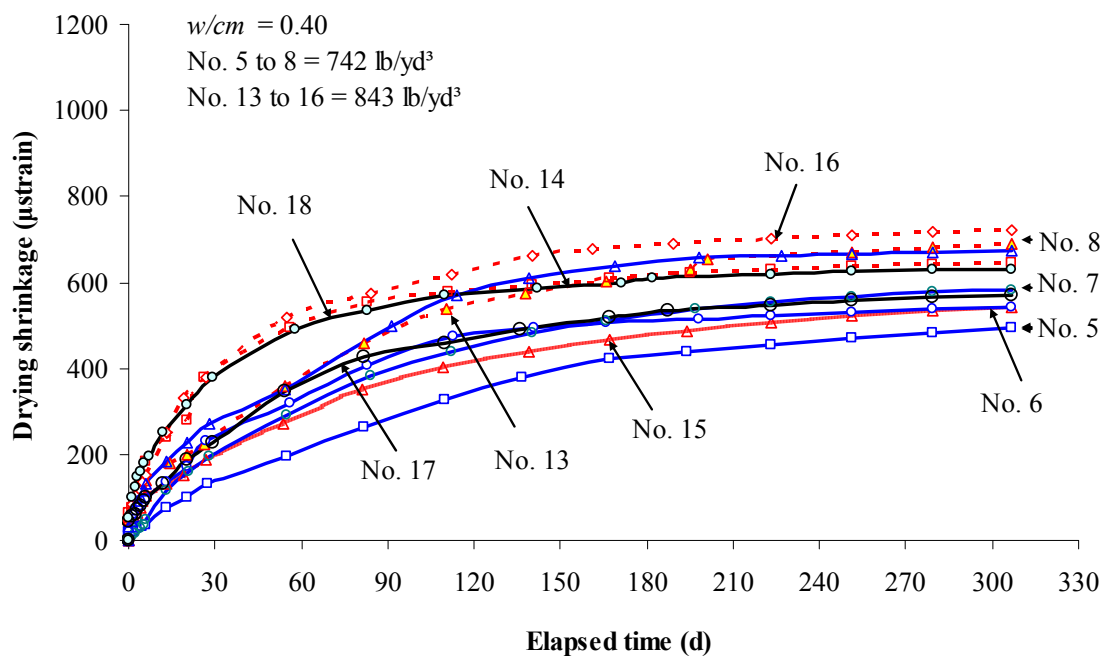

(b) SCC No. 5 to 8 and No. 13 to 16 made with *w/cm* = 0.40 and HPC mixtures (No. 17 and 18)

Fig. D.20 – Variations of drying shrinkage for SCC and HPC mixtures

Based on the statistical models derived from factorial design, the *w/cm* had the most significant influence on autogenous shrinkage, drying shrinkage, and creep. The binder type had also significant influence on autogenous shrinkage. On the other hand, the binder content had significant effect on drying shrinkage and creep responses. The derived models are summarized in Table D.30.

Table D.30 − Derived statistical models for visco-elastic properties

Property	Age	Derived equations	R^2
Autogenous shrinkage, µstrain	7 days	134 – 42.4 *w/cm* + 37.4 BT – 21.6 (BC · *w/cm*) – 20.1 (*w/cm* · BT) –15.9 (BC · BT)	0.96
	56 days	201 + 67.1 BT – 40.6 *w/cm* – 18.8 (BC · *w/cm*) + 17.8 (BC · S/A)	0.93
Drying shrinkage, µstrain	28 days	308 – 71.1 *w/cm* + 35 BC + 48.4 (*w/cm* · VMA) + 30.8 (VMA · BT)	0.78
	112 days	554 – 58.1 *w/cm* + 48.4 BC + 37.4 S/A + 46.2 (*w/cm* · VMA) + 41.9 (*w/cm* · BT) − 40.6 (BC · VMA) + 30.8 (VMA · BT)	0.96
Creep, µstrain	28 days	680 + 79.3 BT − 37.5 *w/cm* + 30.6 (VMA · BT) + 28.8 (*w/cm* · BT)	0.75
	112 days	1,036 + 73.6 BT + 38.8 BC + 40.7 (VMA · BT) + 34.9 (*w/cm* · BT) − 32.9 (BC · S/A)	0.89

The *w/cm* exhibited significant influence on most visco-elastic properties. Higher water content leads to higher drying shrinkage. The content and type of binder were shown to have considerable effect on shrinkage and creep. In most cases, S/A and thickening-type VMA had minor effect, combined with other model parameters on the measured responses. The main findings from the models derived for visco-elastic properties are given below:

- Autogenous shrinkage decreases with the increase in *w/cm* from 0.34 to 0.40.
- The increase in binder content increases drying shrinkage and creep.
- Theoretically, for a given binder content, drying shrinkage increases with increase in *w/cm*; however, the derived statistical models shown an opposite trend because drying shrinkage includes also autogenous shrinkage that decreases with the increase in *w/cm*.
- SCC made with higher S/A can exhibit higher long-term drying shrinkage.
- SCC made with Type III cement and 20% Class F fly ash can develop higher autogenous shrinkage and creep in compression compared to concrete prepared with Type I/II cement.
- The binder type does not have significant effect on drying shrinkage.

D.4.6 Guidelines for Proportioning SCC for Precast, Prestressed Girder Construction

Based on the results derived from the factorial design, the relative influence of the five investigated parameters on modeled properties of SCC are summarized in Table D.31. The binder content and *w/cm* were shown to have significant influence on the majority of workability responses, including plastic viscosity, thixotropy, and form pressure. The binder type had significant effect on slump flow retention, difference between slump flow and J-Ring flow, and caisson filling capacity. The S/A parameter was shown to exhibit moderate impact on slump flow retention, J-Ring flow, plastic viscosity, and form pressure. The thickening-type VMA content exhibited high level of effect on column segregation index, but did not influence surface settlement, given its low dosage and low w/cm of the tested mixtures.

The *w/cm* exhibited the highest effect on mechanical properties. The binder content and type were shown to have considerable effect on mechanical properties. The modulus of elasticity and flexural strength are affected by the S/A ratio. The thickening-type VMA content did not show significant effect on mechanical properties, except in the case of 18-hour compressive strength ($f_c^{'}$).

As expected, the *w/cm* was found to have the highest effect on autogenous and drying shrinkage but only moderate impact on creep. The binder type had significant effect on autogenous shrinkage and creep. The drying shrinkage varied mainly with the binder content. In most cases, the S/A and thickening-type VMA had minor effect on visco-elastic properties.

Recommendations for the proportioning of SCC are summarized in Table D.32. SCC made with 0.40 *w/cm* exhibited superior passing ability and filling capacity as well as lower creep and shrinkage compared to SCC with 0.34 *w/cm*. On the other hand, the latter concrete developed greater fluidity retention, static stability, compressive strength, and elastic modulus. SCC with 0.40 *w/cm* can be used to secure a minimum release compressive strength of 5,000 psi (34.5 MPa) when steam-cured. Such concrete can develop minimum ultimate compressive strength of 8,000 psi (55 MPa). SCC made with 0.34 *w/cm* can be used for casting bridge elements with 56-day compressive strength of 10,000 psi (69 MPa). However, special care should be taken in selecting the binder type and content to limit autogenous shrinkage and creep.

Table D.31 – Relative significance of modeled SCC parameters

	Binder content			*w/cm*			VMA content			Binder type			S/A		
	Low	Medium	High	Low	Medium	High	Low	Medium	High	Low	Medium	High	Low	Medium	High
HRWRA demand		■				■	■				■		■		
Slump flow retention			■			■	■					■		■	
J-Ring			■			■		■			■			■	
Slump flow – J-Ring flow			■			■	■					■		■	
L-box blocking ratio (h_2/h_1)			■			■	■			■			■		
Caisson filling capacity			■			■	■					■	■		
Maximum surface settlement			■			■	■				■		■		
Column segregation index			■	■					■	■			■		
Plastic viscosity			■			■	■			■				■	
Thixotropy (A_b)			■			■	■			■			■		
Form pressure			■			■	■			■				■	
18-hour f_c'	■					■		■			■		■		
56-day f_c'		■				■	■				■		■		
18-hour MOE		■				■	■				■			■	
56-day MOE	■					■	■				■				■
7-day flexural strength		■			■		■			■					■
56-day flexural strength	■					■	■			■				■	
Autogenous shrinkage at 7 days	■					■	■					■	■		
Autogenous shrinkage at 56 days	■					■	■					■	■		
Drying shrinkage after 28 days of exposure		■				■	■			■			■		
Drying shrinkage after 112 days of exposure			■			■	■				■			■	
Creep after 28 days of loading	■				■		■					■	■		
Creep after 112 days of loading		■		■			■					■	■		

* Darkened areas indicate high degree of influence for the modeled mixture parameter.

As indicated in Table D.32, the binder type has direct influence on workability and key engineering properties. In general, mixtures made with Type III cement and 20% Class F fly ash

exhibited better fluidity retention and higher passing ability, filling capacity, and high resistance to surface settlement compared to those prepared with Type I/II cement. The former SCC also developed higher 56-day compressive strength and modulus of elasticity compared to concrete made with Type I/II cement. SCC proportioned with Type I/II cement developed lower shrinkage and creep.

Mixtures proportioned with higher binder of 843 lb/yd^3 (500 kg/m^3) exhibited better fluidity retention and higher passing ability compared to those with binder content of 742 lb/yd^3 (440 kg/m^3). No clear trend can be found regarding the effect of binder content on mechanical properties. SCC with the lower binder content developed lower drying shrinkage and creep deformations.

The use of 0.46 S/A can led to better fluidity retention, greater passing ability, and lower drying shrinkage. Except for enhancing static stability, the thickening-type VMA content did not have any significant effect on workability, mechanical properties, and visco-elastic properties.

Table D.32 – Recommendations for proportioning SCC for precast prestressed applications (based on statistical models)

	w/cm		Binder type		Binder content		S/A		VMA	
	0.34	0.40	I/II	III + 20% fly ash	742 lb/yd^3 (440 kg/m^3)	843 lb/yd^3 (500 kg/m^3)	0.46	0.54	0	Moderate
Filling ability retention	■			■		■	■			
Passing ability		■		■		■	■			
Filling capacity		■		■		■				
Static stability	■			■						■
18-hour $f_c^{'}$	■		■							
56-day $f_c^{'}$	■			■		■				
18-hour MOE	■		■		■		■			
56-day MOE	■			■			■			
Flexural strength	■				■			■		
Autogenous shrinkage		■	■							
Drying shrinkage		■	■		■		■			
Creep	■		■		■					

* Darkened areas indicate better performance for each property

Based on the results and statistical models derived from the factorial design, the following combinations of mixture parameters are recommended for the mixture proportioning of SCC designated for precast and prestressed applications:

- Select a *w/cm* to secure the targeted stability, mechanical properties, visco-elastic properties, and durability. Typical *w/cm* for precast, prestressed applications can range between 0.34 and 0.40.
- Use Type III cement and 20% Class F fly ash with relatively low binder content (such as 440 kg/m^3 vs. 500 kg/m^3) to limit shrinkage and creep.
- Use of low S/A (0.46 vs. 0.54) to ensure adequate workability.
- Use of thickening-type VMA in SCC with moderate and relatively high *w/cm* and low binder content to enhance robustness of the fresh concrete and the uniformity of in-situ properties.

D.5 VALIDATION OF CODE PROVISIONS FOR MECHANICAL AND VISCO-ELASTIC PROPERTIES

D.5.1 Mechanical Properties

D.5.1.1 Compressive strength

In this investigation, the target release compressive strength was set to 5,000 psi (34.5 MPa) at 18 hours. The target 56-day compressive strength was 8,000 to 10,000 psi (55 to 69 MPa), which was determined using 4 × 8 in. (100 × 200 mm) cylinders cured at 100% relative humidity and 73 ± 4°F (23 ± 2°C).

Compressive strength values used to establish the statistical models in the factorial design are compared to predicted values deduced from ACI 209 and CEB-FIP MC90 code provisions. These code equations are presented in Table D.33.

Table D.33 – ACI 209 and CEB-FIP MC90 compressive strength prediction equations

ACI 209

$$\left(f_c^{'}\right)_t = \frac{t}{A+Bt}\left(f_c^{'}\right)_{28d}$$

where,

$(f_c^{'})_t$ = compressive strength of concrete at a given time t (in psi);

$(f_c^{'})_{28d}$ = 28-day compressive strength of concrete; t = age of concrete (in days);

A and B are material constants for cementitious materials type and curing method.

Typical values for A and B [PCI Bridge Manual, 1997]

Source	Curing	Cement type	A	B
ACI 209	Moist	I	4.00	0.85
ACI 209	Moist	III	2.30	0.92
ACI 209	Steam	I	1.00	0.95
ACI 209	Steam	III	0.70	0.98
Current Practice PCI Bridge Manual 1997	Heat (steam or radiant)	III	0.28	0.99

CEB-FIP MC90

$$f_{cm}(t) = \exp\left[s\left(1-\left(\frac{28}{t/t_1}\right)^{1/2}\right)\right] f_{cm}$$

where,

$f_{cm}(t)$ = mean compressive strength at t days (in psi);

f_{cm} = mean 28-day compressive strength;

s = coefficient depending on cement type (0.20 for high early-strength cement, 0.25 for normal-hardening cement, and 0.38 for slow-hardening cement)

t_1 = 1 day.

Figure D.21 compares the measured compressive strength values to those and predicted by the ACI 209-90 and the CEB-FIP MC90 models. The slope (A of the y = A*x equation) of the y vs. x values (i.e. predicted vs. measured strengths) reflects the degree of accuracy of the prediction model to the measured data. The R^2 values that are given in the figure indicate the degree of scatting of the predicted-to-measured strength data to the y = A*x values. The higher R^2 value in the CEB-FIP MC90 model (0.95) reflects less scattering to the mean line (y = 0.96 x) than the ACI 209 model.

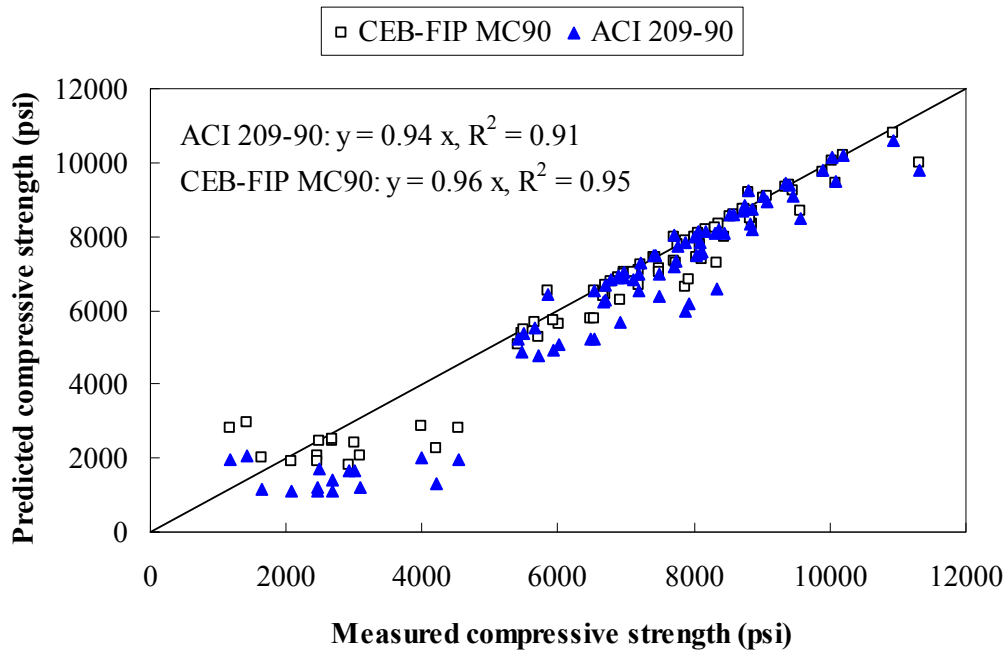

Fig. D.21 – Comparison of measured and predicted compressive strength (plotted data include 18-hour, 7-, 28-, and 56-day compressive strength results)

As shown in Table D.34, some modifications to the material constants used in the prediction models of compressive strength gain are suggested to secure a better degree of prediction of the compressive strength of the 22 SCC mixtures evaluated in the factorial design at different ages. In the case of ACI 209 model, the material constants A and B are set at 1.52 and 0.92 for the concrete made with Type I/II cement instead of 4.00 and 0.85, respectively, for moist-cured concrete made with Type I cement. Similarly, the cement type coefficient (*s*) for the CEB-FIP MC90 model was set at 0.19 for Type I/II cement instead of 0.25. These modified material constants resulted in better fitting of the predicted-to-measured compressive strengths, as indicated from the R^2 values in Table D.34. The modified models are used in Fig. D.22 to compare the predicted-to-measured strength data, which yielded mean predicted-to-measured strength ratios of 0.97. The R^2 of the modified ACI 209 model are increased to 0.95 and 0.90 when the 22 mixtures evaluated in the factorial design were taken into consideration. Better correlations were obtained when the air-entrained mixtures were excluded; the R^2 values increased to 0.97 and 0.95 from 0.94 and 0.92. Similarly, the CEB-FIP MC90 model with the modified cement coefficient (*s*) provided higher R^2 values of 0.95 and 0.92 when using Type I/II and Type III cement, respectively.

Table D.34 – Suggested modifications to model codes to predict compressive strength of SCC

	Original models	Suggested changes in model coefficients
ACI 209-90	$\left(f_c^{'}\right)_t = \frac{t}{A+Bt}\left(f_c^{'}\right)_{28d}$	
	<u>*16 non-AEA SCC + 4 AEA SCC + 2 HPC*</u>: Type I cement (moist-cured): A = 4.0; B = 0.85; R^2 = 0.92 Type III cement (moist-cured): A = 2.3; B = 0.92; R^2 = 0.89 <u>*16 non air-entrained SCC*</u>: Type I cement (moist-cured): A = 4.0; B = 0.85; R^2 = 0.94 Type III cement (moist-cured): A = 2.3; B = 0.92; R^2 = 0.92	<u>*16 non AEA SCC + 4 AEA SCC +2 HPC*</u>: Type I/II cement (moist-cured): A = 1.52; B = 0.92; R^2 = 0.95 Type III + 20% FA (moist-cured): A = 1.64; B = 0.91; R^2 = 0.90 <u>*16 non air-entrained SCC:*</u> Type I/II cement (moist-cured) A = 1.70; B = 0.90; R^2 = 0.97 Type III + 20% FA (moist-cured): A = 2.15; B = 0.89; R^2 = 0.95
CEB-FIB MC 90	$f_{cm}(t) = \exp\left[s\left(1-\left(\frac{28}{t/t_1}\right)^{1/2}\right)\right] f_{cm}$	

	<u>*16 non AEA SCC + 4 AEA SCC + 2 HPC*</u>:
	s = 0.25 normal hardening cement;
	R^2 = 0.90
	
	s = 0.20 high early strength cement;
	R^2 = 0.92
	
	<u>*16 non air-entrained SCC:*</u>
	s = 0.25 normal hardening cement;
	R^2 = 0.92
	
	s = 0.20 high early strength cement;
	R^2 = 0.93
		<u>*16 non AEA SCC + 4 AEA SCC + 2 HPC*</u>:
		s = 0.19 Type I/II cement;
		R^2 = 0.95
		
		s = 0.20 Type III + 20% FA;
		R^2 = 0.92
		
		<u>*16 non air-entrained SCC:*</u>
		s = 0.20 Type I/II cement;
		R^2 = 0.95
		
		s = 0.23 Type III + 20% FA;
		R^2 = 0.93

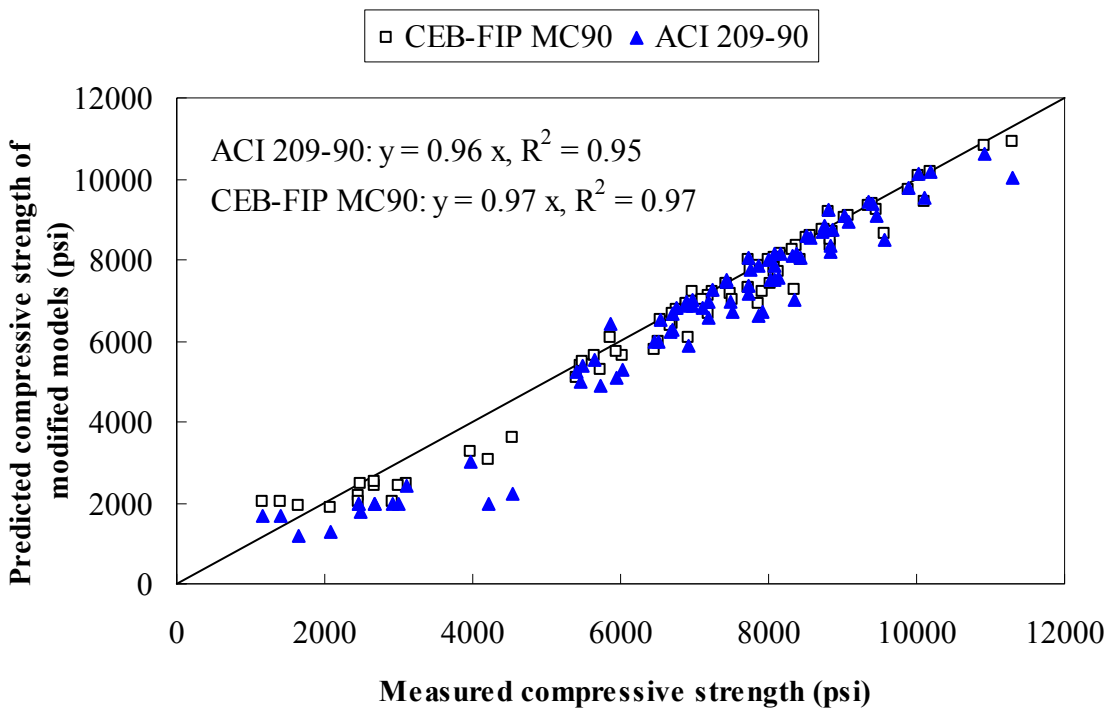

Fig. D.22 – Comparison of measured and predicted compressive strength data for modified models (plotted data include 18-hour, 7-, 28-, and 56-day compressive strength results)

D.5.1.2 Modulus of elasticity

The AASHTO 2007, CEB-FIP MC 90, ACI 363-92, and ACI 318-99 models for evaluating the modulus of elasticity of conventional concrete are summarized in Table D.35. Elastic moduli are compared in Fig. D.23 to values predicted by these models. The AASHTO 2007 code is shown to achieve better correlation between the predicted and measured values. The CEB-FIP 90 model overestimates the elastic modulus, while the ACI 363-92 and ACI 318-99 models underestimate the elastic modulus for concrete with compressive strength greater than 4,350 psi (30 MPa). The R^2 values for the AASHTO 2007, CEB-FIP MC90, ACI 363-92, and ACI 318-99 models are 0.93, 0.68, 0.78, and 0.90, respectively. It is important to note that these R^2 values of the measured elastic moduli and the regression lines of the various prediction models are different that those indicated in Fig. D.23. The latter R^2 values represent the degree of scattering of the measured values to the mean predicted-to-measured ratios (A value in y = A*x). These R^2 values are 0.95, 0.90, 0.90, and 0.90 for the AASHTO 2007, CEB-FIP MC90, ACI 363-92, and ACI 318-99 prediction models, respectively.

Based on the elastic moduli determined from the factorial design, changes to the coefficients of the various prediction models are suggested to secure better fitting of the measured data. As illustrated in Fig. D.24, the modified models exhibited better correlations, with R^2 values higher than 0.90. The AASHTO 2007 model led to good estimate of the elastic modulus for SCC mixtures (R^2 of 0.93). This model considers the unit weight of the fresh concrete. The AASHTO 2007 model may be slightly modified to increase R^2 value to 0.97. The modified models are given in Table D.36.

Table D.35 – AASHTO 2007, CEB-FIP MC90, and ACI models for elastic modulus

AASHTO LRFD Specifications 2007 $E_c = K_1 \gamma_c^{1.5} 0.043 \sqrt{f_c^{'}}$ for unit weight of 2,427 to 4,214 lb/yd^3 (1,440 and 2,500 kg/m³) and specified compressive strength of up to 15,230 psi (105 MPa) where, E_c = elastic modulus of concrete (GPa); K_1 = aggregate source correction factor (to be taken as 1.0 unless determined by physical test); γ_c = unit weight of concrete (kg/m³); $f_c^{'}$ = specified compressive strength of concrete (MPa).
CEB-FIP MC90 $E_c = 10(f_c^{'} + 8)^{1/3}$ (E_c in GPa and $f_c^{'}$ in MPa)
ACI ACI 363-92: $E_c = 3.32\sqrt{f_c^{'}} + 6.9$ for compressive strength up to 12,000 psi (83 MPa) ACI 318-99: $E_c = 4.73\sqrt{f_c^{'}}$

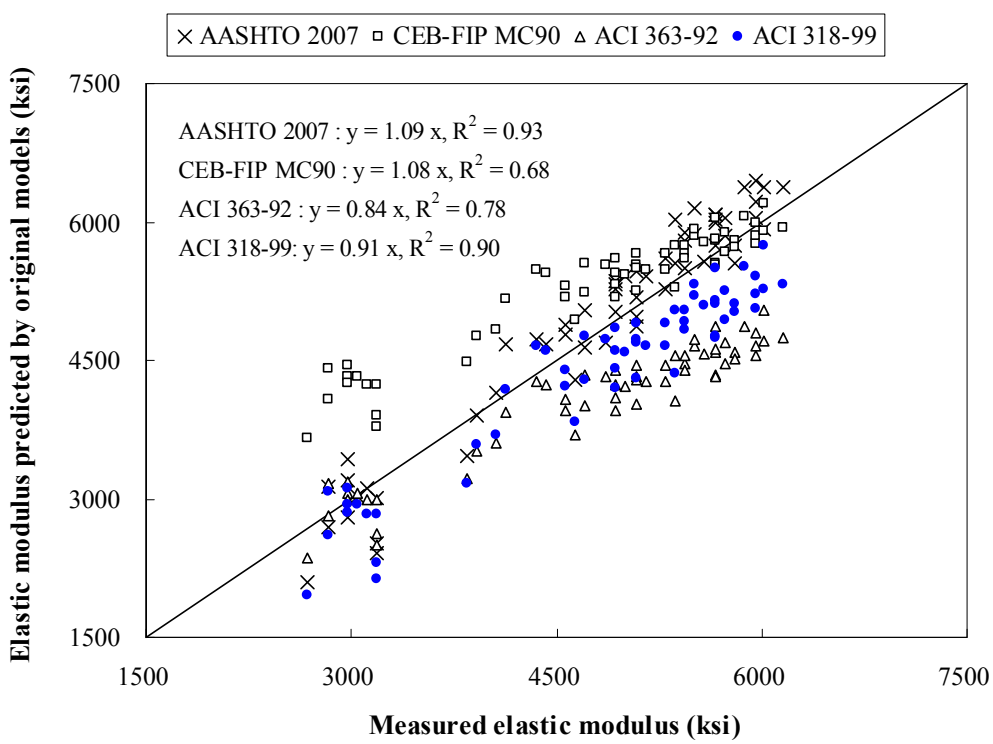

Fig. D.23 – Comparison of measured and predicted moduli of elasticity

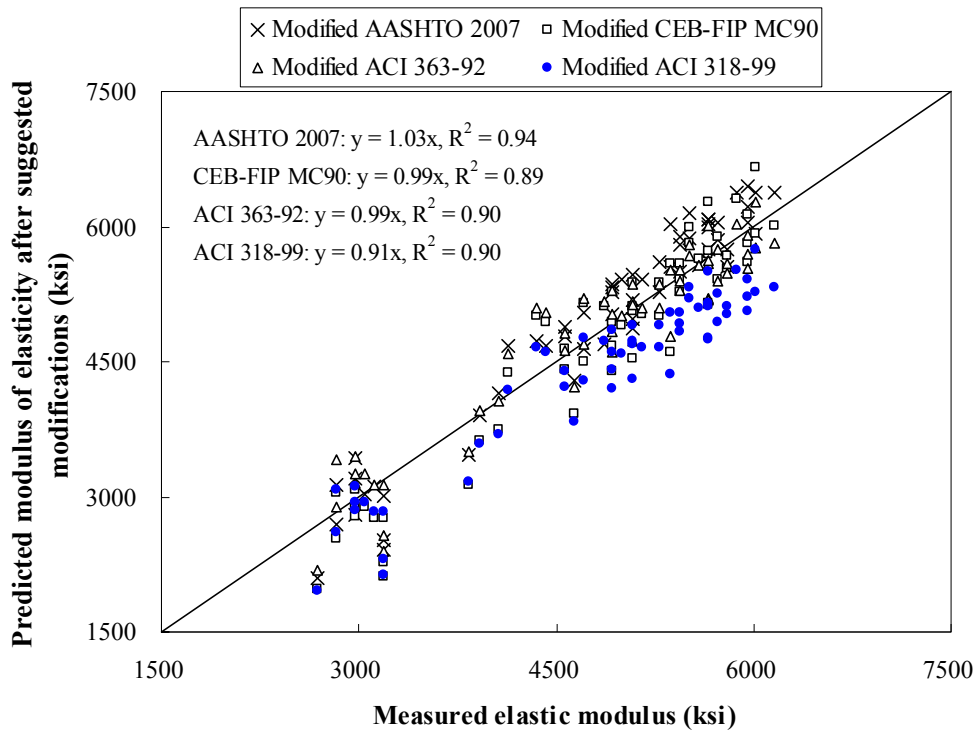

Fig. D.24 – Comparison of measured and predicted elasticity moduli from modified models

Table D.36 – Model for modulus of elasticity and relevant changes to model coefficients

References	Original model equations	Suggested changes in model coefficients
AASHTO 2007	$E_c = K_1 \gamma_c^{1.5} 0.043\sqrt{f_c^{'}}$ ($R^2 = 0.95$)	$E_c = K_1 \gamma_c^{1.5} 0.045\sqrt{f_c^{'}}$ ($R^2 = 0.97$)
CEB-FIP MC 90	$E_c = 10(f_c^{'} + 8)^{1/3}$ ($R^2 = 0.90$)	$E_c = 1.6(f_c^{'} + 8)^{0.77}$ ($R^2 = 0.92$)
ACI 363-92	$E_c = 3.32\sqrt{f_c^{'}} + 6.9$ ($R^2 = 0.90$)	$E_c = 5.08\sqrt{f_c^{'}} + 0.64$ ($R^2 = 0.92$)
ACI 318-99	$E_c = 4.73\sqrt{f_c^{'}}$ ($R^2 = 0.90$)	$E_c = 5.18\sqrt{f_c^{'}}$ ($R^2 = 0.92$)

As shown in Fig. D.24, the R^2 values representing the degree of scattering to the mean line of predicted-to-measured ratio increased to 0.94, 0.89, 0.90, and 0.90 for the AASHTO 2007, CEB-FIP MC90, ACI 363-92, and ACI 318-99 models, respectively. Similarly, the use of modified model coefficients provided mean of predicted-to-measured data (A value in y = A*x) closer to 1, thus reflecting the improved accuracy of the prediction to measured data. The A values after the suggested modifications were 1.03, 0.99, 0.99, and 0.91 for the AASHTO 2007, CEB-FIP MC90, ACI 363-92, and ACI 318-99 models, respectively, compared to 1.09, 1.08, 0.84, and 0.91 of the original models (Fig. D.23).

D.5.1.3 Flexural strength

The AASHTO 2007 and ACI 363-84 models and that suggested by Khayat et al. (1995)[D4] for flexural strength are summarized in Table D.37. As presented in Fig. D.25, the AASHTO 2007 and ACI 363-84 models overestimated the flexural strength results of SCC for mixtures having compressive strengths lower than 6,530 psi (45 MPa). Thereafter, the two models yielded better estimate of the measured values. On the other hand, the model proposed by Khayat et al. (1995) provided better prediction of flexural strength for concrete with compressive strength lower than 6,530 psi (45 MPa). Still, the prediction models for flexural strength exhibited larger scattering compared to those for compressive strength and modulus of elasticity.

Relevant changes to the constants of the three models were made to provide better fit of the measured data. The results are the modified models are plotted in Fig. D.26. The modified model coefficients provided mean predicted-to-measured data (A value in y = A*x) closer to 1. The suggested changes in the prediction models are summarized in Table D.37. The A values before the suggested modifications for the AASHTO 2007, ACI 363, and Khayat et al. models were 1.03, 0.98, and 0.87. These values became 0.98 once the modifications were incorporated in the models. The R^2 values of the three models were slightly increased from 0.67 to 0.70 in the initial models to 0.72 to 0.75 for the modified models.

The modified AASHTO 2007 for SCC offered similar degree of prediction of flexural strength as the other two models.

Table D.37 – Modified flexural strength prediction models

	Original model equations	Suggested changes in model coefficients
AASHTO 2007	For normal density concrete and specified concrete strength up to 15,230 psi (105 MPa)	
	$f_r = 0.97\sqrt{f_c^{'}}$ (R^2 = 0.67)	$f_r = 0.93\sqrt{f_c^{'}}$ (R^2 = 0.72)
ACI 363-84	($f_c^{'}$ in MPa)	
	$f_r = 0.94\sqrt{f_c^{'}}$ (R^2 = 0.68)	$f_r = 0.93\sqrt{f_c^{'}}$ (R^2 = 0.72)
Khayat, Bickley, and Hooton (1995)	or compressive strength between 6,525 to15,955 psi (45 to 110 MPa)	
	$f_r = 0.23 + 0.12 f_c^{'} - 2.18\times10^{-4} (f_c^{'})^2$ (R^2 = 0.70)	$f_r = -3.2 + 0.26 f_c^{'} - 1.43\times10^{-3} (f_c^{'})$ (R^2 = 0.75)

[D4] Khayat, K.H., Bickley, J.A., and Hooton, R.D., "High-Strength Concrete Properties Derived from Compressive Strength Values." *Cement, Concrete and Aggregates*, Vol. 17, No. 2 (1995) pp. 121-129.

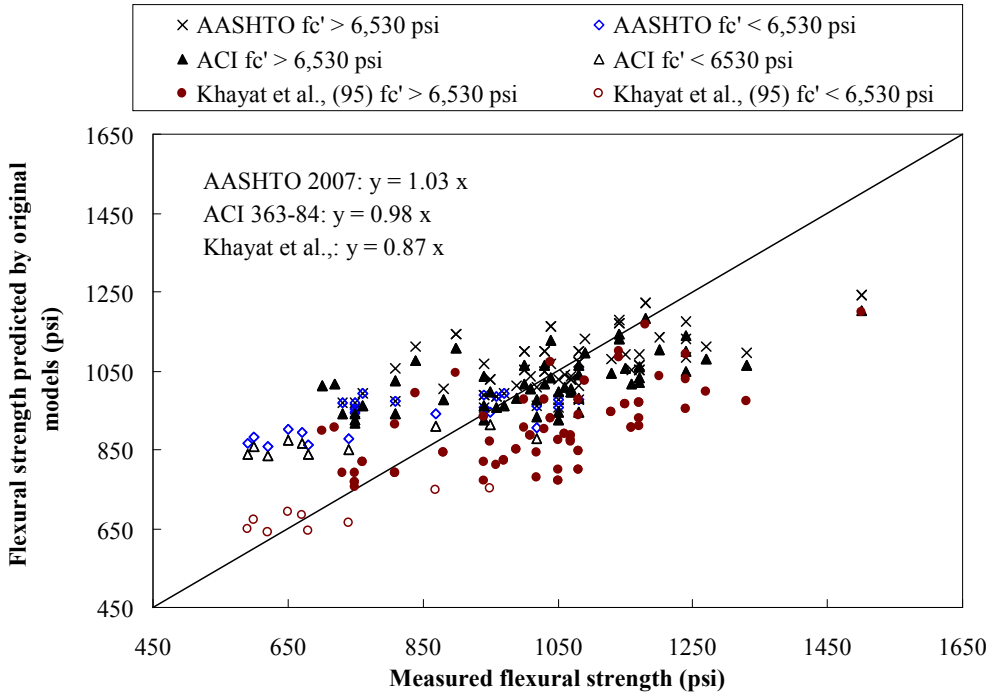

Fig. D.25 – Comparison of measured and predicted flexural strengths

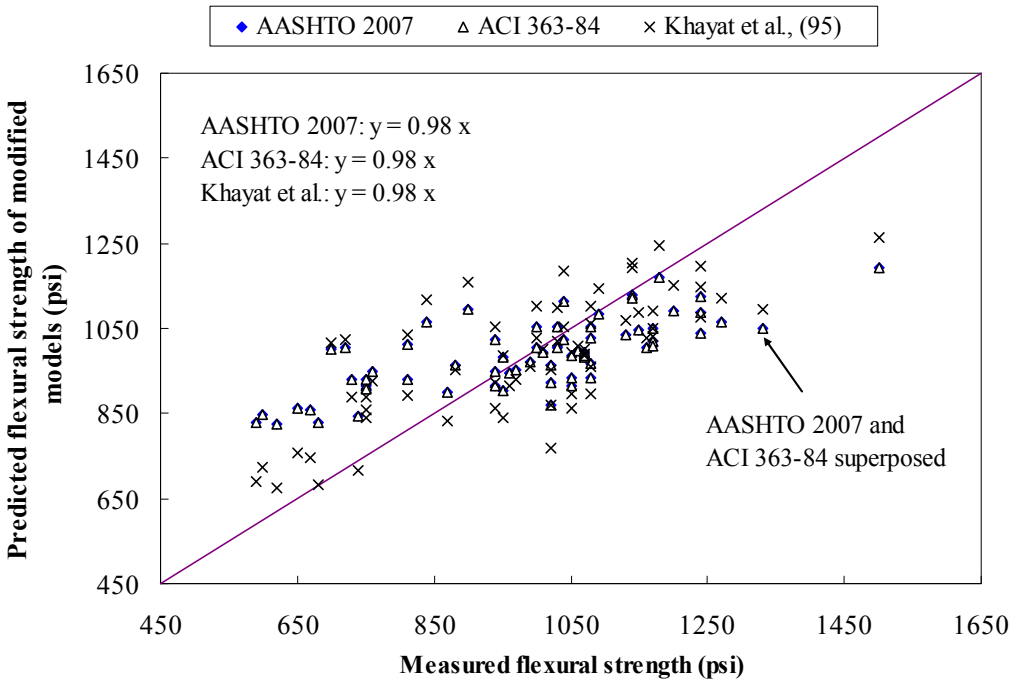

Fig. D.26 – Measured vs. predicted flexural strengths from modified models

D.5.2 Visco-Elastic Properties

Creep and shrinkage strains measured in the experimental factorial design are compared to values predicted by the AASHTO 2007, AASHTO 2004, ACI 209, CEB-FIP 1990, and GL 2000 (Gardner and Lockman, 2001)[D5] models. The models are summarized in Tables D.38 and D.39. The ACI 209 model is applicable to normal-weight and lightweight concrete tested at 40% relative humidity for moist- and steam-cured concrete made with Type I and III cements. The CEB-FIP model is applicable ordinary concrete with 28-day strength of 1,740 to 11,600 psi (12 to 80 MPa) and 40% to 100% relative humidity. The GL 2000 model can be used for concrete proportioned with 0.40 to 0.60 *w/cm* with compressive strength of up to 10,150 psi (70 MPa).

D.5.2.1 Drying shrinkage

Drying shrinkage values of 16 tested SCC and two HPC mixtures are compared in Appendix L to predicted shrinkage strains for the various code provisions. Drying shrinkage data between 1 and 252 days are compared in Fig. D.27 to values predicted by the various models. The AASHTO 2007 model underestimates shrinkage and results in larger scattering compared to the AASHTO 2004 model. The 2004 model provided better prediction of shrinkage with R^2 of 0.75 compared to 0.71 for the 2007 model. The AASHTO 2004 model had a mean predicted-to-measured shrinkage of 0.87 compared to 0.69 for the 2007 model. The AASHTO 2007, ACI 209, and GL 2000 models underestimated shrinkage above 600 μstrain. As in the case of the CEB-FIP 90 model, the GL 2000 model uses input parameters for Types I, II, and III cements. The GL 2000 and ACI 209 models had adequate prediction ranging between 200 and 500 μstrain. For the ACI 209 model, ultimate shrinkage values at approximately 11 months were used; the model can be used for concrete made with Types I and III cements.

The CEB-FIP 90 model is shown to provide the best fit of measured data for SCC with maximum shrinkage of 600 μstrain after 9 months. The mean predicted-to-measured shrinkage ratio at 9 months was 0.90 compared to 0.69 to 0.87 for the other models. This can be due to the fact that the CEB-FIP 90 model takes into consideration the cement type that was changed for the tested mixtures (Type I/II cement and Type III cement with 20% fly ash). A coefficient for cement type (A) is introduced for the AASHTO 2004 model to provide better prediction for the drying shrinkage. The coefficient is taken as the mean of eight coefficients derived for SCC made with Type I/II cement and eight others for SCC made with Type III cement + 20% FA. For each mixture, a cement coefficient was derived to best fit the drying shrinkage data for that particular mixture with time versus predicted shrinkage values for the AASHTO 2004 model modified with a cement coefficient value. The R^2 values for the 16 mixtures ranged from 0.87 to 0.99. Finally, cement coefficients of 0.918 and 1.065 are suggested for SCC made with Type I/II cement and Type III + 20% FA, respectively. The modified AASHTO 2004 model can lead to a mean value of predicted-to-measured shrinkage of 0.94 with low scattering of the data from the 1:1 equality line (R^2 = 0.89). This model, along with the CEB-FIP 90 model, can be used to predict drying shrinkage of SCC used for precast, prestressed applications (Fig. D.28).

[D5] Gardner, N.J., "Comparison of Prediction Provisions for Drying Shrinkage and Creep of Normal-Strength Concretes." *Can. Jr. Civ. Eng.,* Vol. 31 (2004) pp. 767-775.

Table D.38 – Summary of various models for drying shrinkage

	Prediction models
AASHTO 2007	$\varepsilon_{sh} = -k_{vs}k_{hs}k_f k_{td} 0.48\times10^{-3}$ in which: k_{hs} = (2.00-0.14H); $k_{vs} = 1.45 - 0.13(V/S) \geq 1.0$; $k_f = \frac{35}{7+f_{ci}^{'}}$; $k_{td} = \left(\frac{t}{61-0.58f_{ci}^{'}+t}\right)$ where, k_{hs} = humidity factor; H = relative humidity (%); k_{vs} = volume-to-surface ratio factor; k_f = concrete strength factor; k_{td} = time development factor; t = maturity of concrete (day); t_i = age of concrete at drying (day); V/S = volume-to-surface ratio; $f_{ci}^{'}$ = specified compressive strength of concrete at time of prestressing.
AASHTO 2004	$\varepsilon_{sh} = -k_s k_h \left(\frac{t}{55+t}\right)\times0.56\times10^{-3}$ (steam-cured), $k_s = \left[\frac{\frac{t}{26e^{0.0142(V/S)}+t}}{\frac{t}{45+t}}\right]\left[\frac{1064-3.70(V/S)}{923}\right]$ where, t = drying time (day); k_s = size factor; k_h = humidity factor.
ACI 209R-92	$\varepsilon_{sh}(t,t_{sh,0}) = \frac{(t-t_{sh,0})}{35+(t-t_{sh,0})}\varepsilon_{sh\infty}$ (moist-cured), $\varepsilon_{sh}(t,t_{sh,0}) = \frac{(t-t_{sh,0})}{55+(t-t_{sh,0})}\varepsilon_{sh\infty}$ (steam-cured) where, $\varepsilon_{sh}(t,t_{sh,0})$ = shrinkage strain (mm/mm); t = time (day); t_{sh0} = time at initiation of drying (day); $\varepsilon_{sh\infty}$ = ultimate shrinkage strain (mm/mm).
CEB-FIP 90	$\varepsilon_{cso} = \varepsilon_s(f_{cm})(\beta_{RH})\sqrt{\frac{(t-t_c)}{\left(350\left(\frac{2A_c}{100\mu}\right)^2+(t-t_c)\right)}}$ $\varepsilon_s(f_{cm}) = [160+10\beta_{sc}(9-0.1f_{cm})]\times10^{-6}$; $\beta_{RH} = -1.55\beta_{ARH}$; $\beta_{ARH} = 1-(RH/100)^3$ where, ε_{cso} = drying shrinkage (mm/mm); ε_s = drying shrinkage obtained from RH-shrinkage chart; β_{sc} = cement type factor; β_{RH} = relative humidity factor; f_{cm} = mean 28-day compressive strength (MPa), A_c = cross-sectional area (mm^2), μ = perimeter (mm), t_c = age of drying commenced (day), t = age of concrete (day).
GL 2000	$\varepsilon_{sh} = \varepsilon_{shu}\beta(h)\beta(t)$ $\varepsilon_{shu} = 1000k\left(\frac{30}{f_{cm28}^{'}}\right)^{1/2}\times10^{-6}$; $\beta(h) = 1-1.18h^4$; $\beta(t) = \left(\frac{(t-t_c)}{t-t_c+0.12(V/S)^2}\right)^{0.5}$ where: ε_{sh} = shrinkage strain (mm/mm); ε_{shu} = ultimate shrinkage strain (mm/mm); $\beta(h)$ = correction term for humidity; $\beta(t)$ = correction term for time; h = humidity; t = age of concrete (day); t_c = age of drying initiation (day); k = cement type factor, 1, 0.75, and 1.15 for Type I, II, and III cement, respectively.

Table D.39 – Summary of various models for creep

	Prediction models
AASHTO 2007	$\psi(t,t_i)=1.9k_{vs}k_{hc}k_f k_{td}t_i^{-0.118}$ in which: $k_{vs}=1.45-0.0051(V/S)\geq 0.0$; $k_{hc}=1.56-0.008H$; $k_f=\frac{35}{7+f_{ci}^{'}}$; $k_{td}=\left(\frac{t}{61-0.58f_{ci}^{'}+t}\right)$ where, k_{hc} = humidity factor; H = relative humidity (%); k_{vs} = volume-to-surface ratio factor; k_f = concrete strength factor; k_{td} = time development factor; t = maturity of concrete (day); t_i = age of concrete at loading (day); V/S = volume-to-surface ratio (mm); $f_{ci}^{'}$ = specified compressive strength of concrete at the time of prestressing.
AASHTO 2004	$\psi(t,t_i)=3.5k_c k_f\left(1.58-\frac{H}{120}\right)t_i^{-0.118}\frac{(t-t_i)^{0.6}}{10.0+(t-t_i)^{0.6}}$, in which: $k_f=\frac{62}{42+f_c^{'}}$ where, k_c = volume-to-surface factor; k_f = concrete strength factor; $f_{ci}^{'}$ = specified compressive strength at 28 days (MPa).
ACI 209R-92	$\nu_t=\frac{t^{0.60}}{10+t^{0.60}}\nu_u$, in which: $\nu_u=2.35\gamma_c$ (average value) where, ν_u = ultimate creep coefficient (day); γ_c = correction factors; ν_t = creep coefficient; t = time after loading (day).
CEB-FIP 90	$\phi(t,t_0)=\phi_0\beta_c(t-t_o)$, in which: $\phi_0=\phi_{RH}\beta(f_{cm})\beta(t_0)$; $\phi_{RH}=1+\frac{1-RH/RH_0}{0.46(h/h_0)^{1/3}}$; $RH_0=100\%$; $h=2A_c/u$; $h_0=100$; $\beta(f_{cm})=\frac{5.3}{(f_{cm}/f_{cm0})^{0.5}}$; $\beta(t_0)=\frac{1}{0.1+(t_0/t_1)^{0.2}}$; $\beta_c(t-t_0)=\left[\frac{(t-t_0)/t_1}{\beta_H+(t-t_0)/t_1}\right]^{0.3}$; $\beta_H=150\left[1+\left(1.2\frac{RH}{RH_0}\right)^{18}\right]\frac{h}{h_0}+250\leq 1500$; $t_1=1$; $f_{cm0}=10$ where, f_{cm} = mean compressive strength (MPa); RH = relatively humidity (%); Ac = section cross area (mm^2); u = section perimeter (mm); t = age of concrete (day); t_0 = age of concrete at loading (day).
GL 2000	$\phi_{28}=\Phi(t_c)\left[2\left(\frac{(t-t_0)^{0.3}}{(t-t_0)^{0.3}+14}\right)\left(\frac{7}{t_0}\right)^{0.5}\left(\frac{t-t_0}{t-t_0+7}\right)^{0.5}+2.5(1-1.086h^2)\left(\frac{t-t_0}{t-t_0+0.12(V/S)^2}\right)^{0.5}\right]$ where, $\Phi(t_c)$ = correction for drying before loading, if $t_0=t_c$, $\Phi(t_c)$ = 1; t_0 = age of the load applied (day).

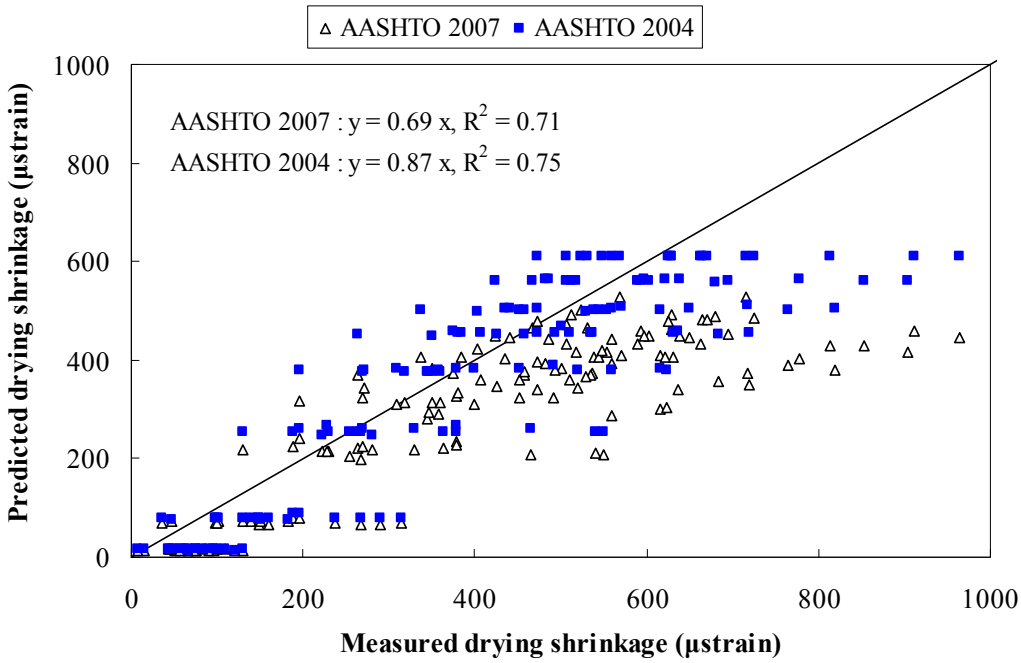

(a) AASHTO 2007 and 2004 models

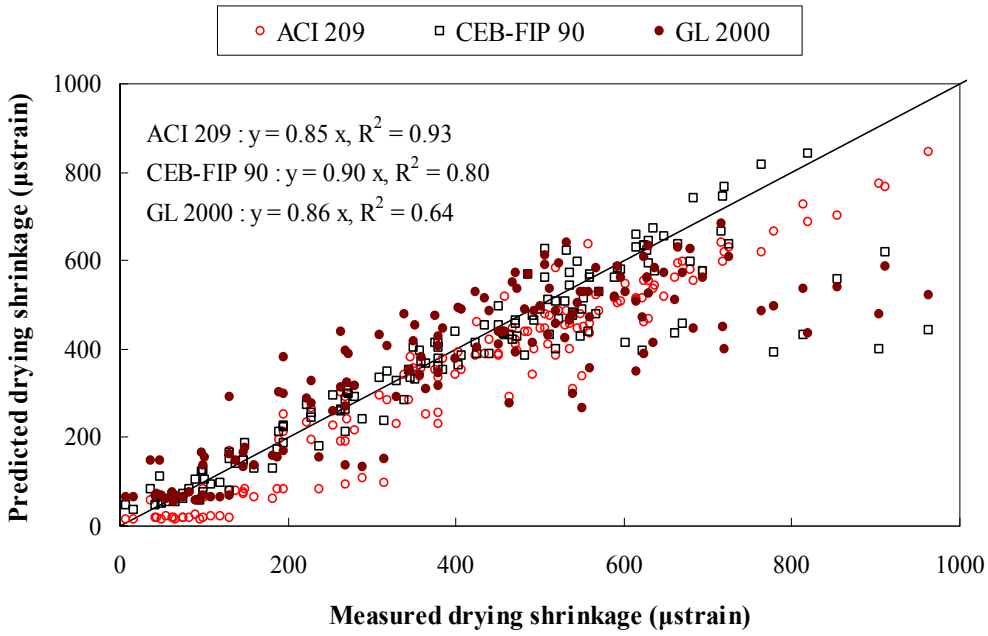

(b) ACI 209, CEB-FIP 90, and GL 2000 models

Fig. D.27 – Comparison of measured and predicted drying shrinkage values

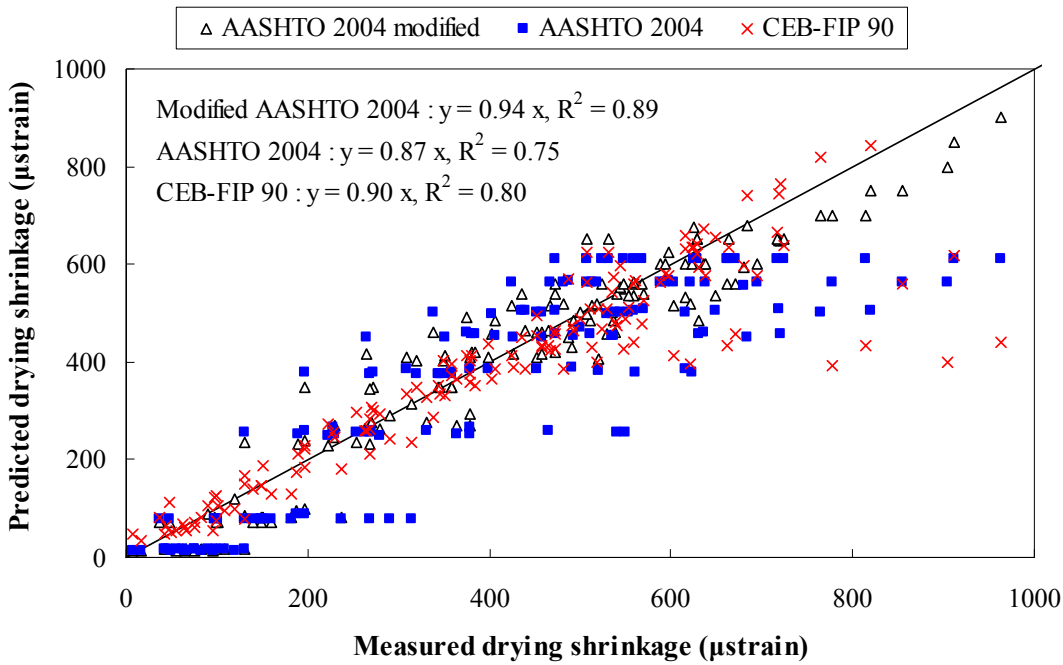

Fig. D.28 – Comparison of measured and predicted drying shrinkage from modified models

D.5.2.2 Creep in compression

Creep in compression data for the 16 tested SCC and two HPC mixtures are compared to creep strains predicted from various models in Appendix M. In general, the ACI 209, AASHTO 2004, and AASHTO 2007 models underestimated creep at most loading ages. As presented in Fig. D.29, the GL 2000 model overestimated the creep strains measured. It is interesting to note that the GL 2000 model provides good estimation for the creep when seven or 28 days of ages before loading are applied as standard creep testing. On the other hand, the use of 0.75 day (18 hours) loading age in the GL 2000 model significantly increases the basic creep, thus leading to large increase in total creep strain. This can be attributed to the fact that the maturity of concrete increased by steam curing or accelerated curing is not taken into consideration in the GL 2000 model. As shown in Fig. D.29, both AASHTO creep models underestimate the actual creep with mean predicted-to-measured ratios of 0.76 and 0.73 for the AASHTO 2007 and 2004 models, respectively. Both models had some scattering of the predicted-to-measured results with R^2 of approximately 0.86.

The CEB-FIP 90 model provided closer prediction of the measured data than the AASHTO 2004, AASHTO 2007, and ACI 209, though greater scattering (R^2 of 0.76); the CEB-FIP 90 model exhibited mean predicted-to-measured ratios of 0.99 (Fig. D.29).

A cement type factor (A) is introduced to enhance the degree of creep prediction of the AASHTO 2007 model. This coefficient is taken as the mean of eight coefficients derived for SCC made with Type I/II cement and eight others for SCC made with Type III cement with 20% of fly ash. For each mixture, a cement coefficient was derived to best fit the creep data for that particular mixture versus predicted creep values from the AASHTO 2007 model modified with a given cement coefficient. The R^2 values for the 16 tested mixtures ranged from 0.92 to 0.99.

In general, the CEB-FIP 90 creep prediction model can provide adequate prediction of the creep data. Creep strains predicted from the modified AASHTO 2007 model are compared to measured data in Fig. D.30 with mean predicted-to-measured ratio of 0.96 and relatively low scattering of the data (R^2 of 0.90).

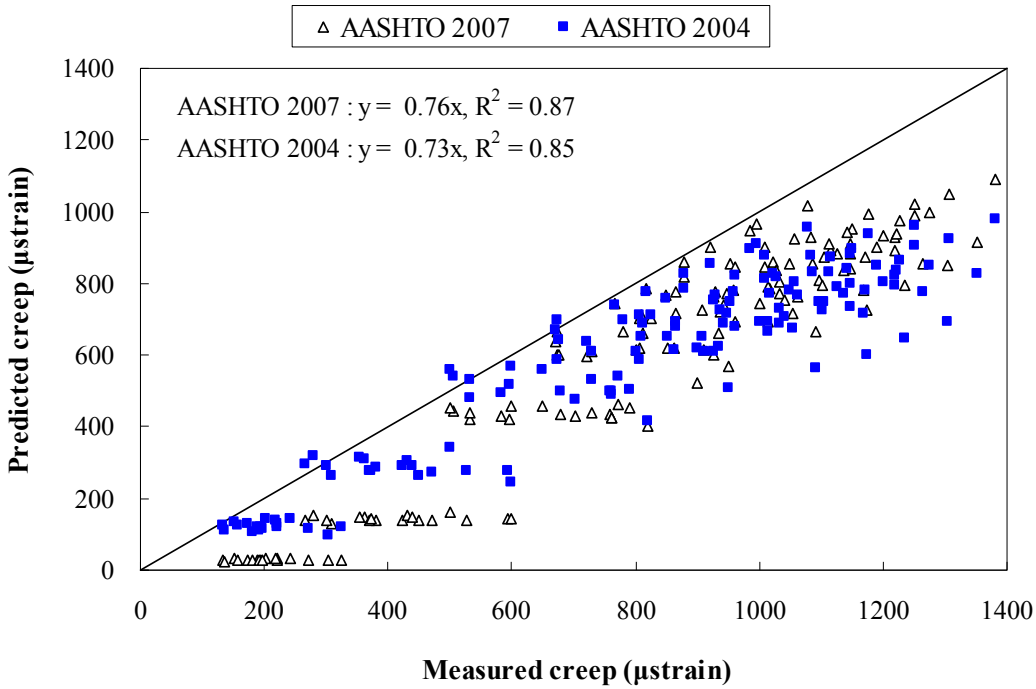

(a) AASHTO 2004 and 2007 models

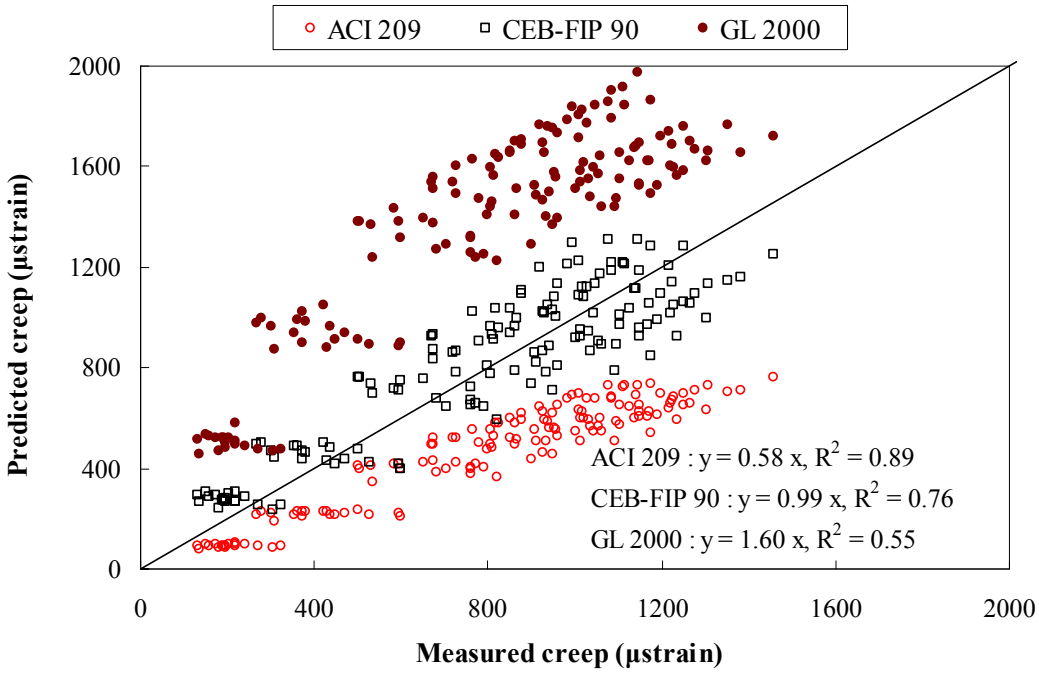

(b) ACI 209, CEB-FIP 90, and GL 2000 models

Fig. D.29 – Comparison of measured and predicted creep values

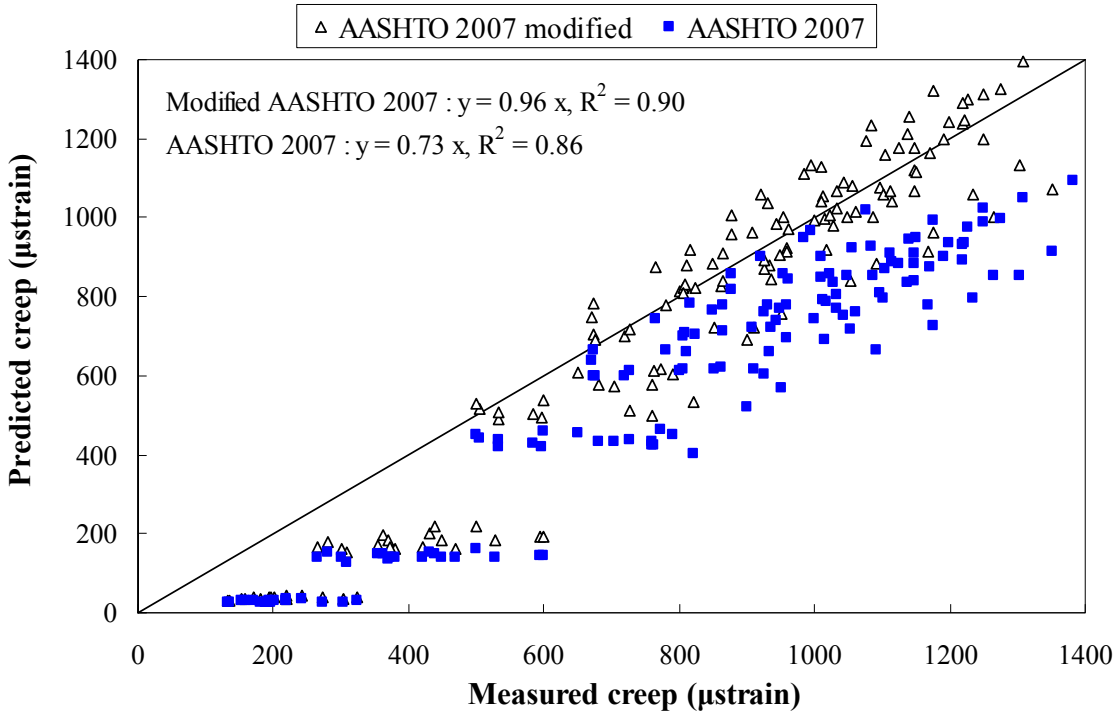

Fig. D.30 – Comparison of measured and predicted creep values from modified models

D.5.3 Recommendations for Prediction of Mechanical and Visco-Elastic Properties of SCC Used for Precast, Prestressed Girders

Material coefficients of existing prediction models were modified to provide better prediction of mechanical and visco-elastic properties of SCC. These modifications are summarized in Table D.40. Recommended prediction models for compressive strength, elastic modulus, flexural strength, creep in compression, and drying shrinkage are summarized in Table D.41.

Table D.40 – Summary of suggested coefficients for models used to predict mechanical and visco-elastic properties of SCC used in precast, prestressed applications

		Original model equation	Suggested model coefficients
Compressive strength	ACI 209-90	$\left(f_c^{'}\right)_t = \frac{t}{A+Bt}\left(f_c^{'}\right)_{28d}$	Type I/II cement (moist-cured): A = 1.70; B = 0.90 Type III + 20% FA (moist-cured): A = 2.15; B = 0.89
	CEB-FIB MC 90	$f_{cm}(t) = \exp\left[s\left(1-\left(\frac{28}{t/t_1}\right)^{1/2}\right)\right]f_{cm}$	s = 0.20 for Type I/II cement s = 0.23 for Type III + 20% FA
Modulus of elasticity	AASHTO 2007	$E_c = K_1\gamma_c^{1.5}0.043\sqrt{f_c^{'}}$	$E_c = K_1\gamma_c^{1.5}0.045\sqrt{f_c^{'}}$
	CEB-FIP MC 90	$E_c = 10(f_c^{'}+8)^{1/3}$	$E_c = 1.6(f_c^{'}+8)^{0.77}$
	ACI 363-92	$E_c = 3.32\sqrt{f_c^{'}}+6.9$	$E_c = 5.08\sqrt{f_c^{'}}+0.64$
	ACI 318-99	$E_c = 4.73\sqrt{f_c^{'}}$	$E_c = 5.18\sqrt{f_c^{'}}$
Flexural strength	AASHTO 2007	$f_r = 0.97\sqrt{f_c^{'}}$	$f_r = 0.93\sqrt{f_c^{'}}$
	ACI 363-84	$f_r = 0.94\sqrt{f_c^{'}}$	$f_r = 0.93\sqrt{f_c^{'}}$
	Khayat et al. (1995)	$f_r = 0.23+0.12f_c^{'}-2.18\times10^{-4}(f_c^{'})^2$	$f_r = -3.2+0.26f_c^{'}-1.43\times10^{-3}(f_c^{'})^2$
Drying shrinkage	AASHTO 2004	$\varepsilon_{sh} = -k_s k_h\left(\frac{t}{55+t}\right)\times0.56\times10^{-3}\times A$	Type I/II cement: A = 0.918 Type III + 20% FA: A = 1.065
Creep in compression	AASHTO 2007	$\psi\left(t,t_i\right) = 1.9k_{vs}k_{hc}k_f k_{td}t_i^{-0.118}\times A$	Type I/II cement: A = 1.186 Type III + 20% FA: A = 1.346

Table D.41 – Recommended mechanical and visco-elastic prediction models for SCC used in precast, prestressed girder constructions

Mechanical properties	Compressive strength	ACI 209 and CEB-FIP MC90 models with suggested modifications for binder composition
	Modulus of elasticity	Current AASHTO 2007
	Flexural strength	Current AASHTO 2007
Visco-elastic properties	Drying shrinkage	Modified AASHTO 2004 with suggested modifications for binder composition or Current CEB-FIP 90 (optional)
	Creep	Modified AASHTO 2007 with suggested modifications for binder composition

D.6 STRUCTURAL PERFORMANCE

The effect of SCC workability on the uniformity of bond strength between prestressing strands and concrete used for casting six wall elements as well as the distribution of compressive strength obtained from cores along these elements are discussed. The structural performance of four AASHTO-Type II girders cast with SCC and HPC of similar strengths is also presented.

D.6.1 Bond Strength of Prestressing Strands

Six wall elements measuring 60.6 × 84.6 × 7.9 in. (1,540 × 2150 × 200 mm) were cast using a reference HPC of normal consistency and five SCC mixtures of different static stability levels (Table D.42). The concrete was prepared in 0.52-yd^3 (400-L) batches using an open pan mixer. The mixture proportioning and fresh properties of the concretes are presented in Table D.43. The SCC mixtures had slump flow values of 26.7 ± 0.7 in. (680 ± 15 mm) and minimum caisson filling capacity of 80%. They also had different viscosity levels with resulting maximum surface settlement values of 0.30% to 0.62%. This surface settlement of the HPC was 0.23%.

Testing consisted of determining the maximum pull-out load vs. the end slip response of strands that are horizontally embedded in experimental wall elements. In total, 16 Grade 270 low-relaxation prestressing strands of 0.6 in. (15.2 mm) diameter were embedded at four heights in the wall elements. Rigid plastic sheathing was attached to the outer end of each strand near the loaded end as bond breaker to reduce secondary confining stresses along the bonded region.

Table D.42 – SCC and HPC mixtures for strand bond testing

	Wall	Mix	Codification	Description
SCC	1	4	34-742-III20%FA-S/A54-VMA	Highly viscous SCC (risk of not securing adequate self-consolidation) Plastic viscosity = 0.135 psi.s (930 Pa.s) Maximum settlement = 0.44%
	2	15	40-843-I/II-S/A46-VMA	Low viscosity SCC (segregation potential) Plastic viscosity = 0.010 psi.s (70 Pa.s) Maximum settlement = 0.59%
	3	7	40-742-I/II-S/A54-VMA	Medium viscosity SCC Plastic viscosity = 0.031 psi.s (215 Pa.s) Maximum settlement = 0.62%
	4	12	34-843-III20%FA-S/A46-VMA	Medium viscosity SCC Plastic viscosity = 0.033 psi.s (255 Pa.s) Maximum settlement = 0.43%
	5	2	34-742-III20%FA-S/A46	Viscosity SCC (highly stable) Plastic viscosity = 0.070 psi.s (480 Pa.s) Maximum settlement = 0.3%
HPC	6	17	34-I/II (HPC1)	Stable HPC of conventional slump Plastic viscosity = 0.051 psi.s (350 Pa.s) Maximum settlement = 0.29%

Table D.43 – Mixture proportioning and fresh properties of tested concretes

	Wall No. 1	Wall No. 2	Wall No. 3	Wall No. 4	Wall No. 5	Wall No. 6
Codification	34-742-III20%FA-S/A54-VMA	40-843-I/II-S/A46-VMA	40-742-I/II-S/A54-VMA	34-843-III20%FA-S/A46-VMA	34-742-III20%FA-S/A46	34-I/II
Cement, lb/yd^3 (kg/m^3)	Type III	Type I/II	Type I/II	Type III	Type III	Type I/II
	594 (352)	843 (500)	742 (440)	674 (400)	594 (352)	792 (470)
HRWRA demand, fl oz/cwt (L/100 kg CM)	51.6 (3.35)	9.2 (0.60)	15.4 (1.00)	30.7 (2.00)	46.1 (3.00)	7.7 (0.50)
VMA dosage, fl oz/cwt (L/100 kg CM)	1.55 (0.1)	1.55 (0.1)	1.55 (0.1)	1.55 (0.1)	0	0
Class F fly ash, lb/yd^3 (kg/m^3)	148 (88)	0	0	168 (100)	148 (88)	0
Water, lb/yd^3 (kg/m^3)	235 (139)	331 (196)	292 (172)	272 (161)	235 (139)	270 (160)
w/cm	0.34	0.40	0.40	0.34	0.34	0.34
Sand, lb/yd^3 (kg/m^3)	1658 (984)	1285 (762)	1609 (955)	1330 (789)	1415 (839)	1249 (741)
Coarse aggregate, lb/yd^3 (kg/m^3)	1412 (838)	1507 (894)	1372 (814)	1563 (927)	1661 (985)	1770 (1050)
Sand/total aggregate, by volume	0.54	0.46	0.54	0.46	0.46	0.41
Slump flow, in. (mm)	26.2 (665)	27.4 (695)	26.4 (670)	26.0 (660)	26.0 (660)	4.6 (145) *
T-50 mm, sec	6.8	1.5	1.8	2.9	5.5	-
Visual stability index	0.5	1	1	0.5	0.5	0
Air content, %	2.4	2.3	1.9	2.0	1.1	2.7
Unit weight, lb/ft^3 (kg/m^3)	144.7 (2343)	147.0 (2352)	147.8 (2365)	147.4 (2360)	150.5 (2409)	151.7 (2429)
Temperature, ^{o}F (^{o}C)	73.4 (23)	75.2 (24)	73.4 (23)	75.9 (24.4)	74.3 (23.5)	77.0 (25)
J-Ring, in. (mm)	24.8 (630)	25.2 (640)	23.7 (605)	24.8 (630)	23.8 (605)	-
Filling capacity, %	92	93	89	91	82	-
Maximum surface settlement, %	0.44	0.59	0.62	0.43	0.30	0.29
Yield stress, Pa	5	30	35	25	10	575
Plastic viscosity, Pa.s**	930	70	215	255	480	350

* Slump

** 1 Pa = 1.45×10^{-4} psi

D.6.1.1 Bond strength and in-situ compressive strength determination

The wall elements were divided into two parts, each cast with different concrete. The strands were positioned at four different heights. Details of the wall sections and positioning of the prestressing strands are shown in Fig. D.31. The formwork was removed one day after concrete casting. The concrete wall elements were then maintained under wet curing until 7 days of age before air-drying until the age of 56 days when pull-out testing was carried out. The wall elements were gently tilted onto an elevated and horizontal platform to facilitate testing. A hydraulic jack with 135-kN capacity was used for loading. As presented in Fig. D.32, the hydraulic jack was attached to the prestressing strands, and a reaction cylinder was positioned against the concrete. The pull-out load was applied gradually and recorded using a load cell. The net slip was measured using an LVDT connected to the unloaded end of the strand (Fig. D.32). After debonding, the prestressing strands were extracted to determine exact anchorage length necessary for calculation of bond stress. Mean pull-out load and free-end slip responses of four strand replicates tested at four heights for Wall No. 1 that was cast with SCC No. 4 are presented in Fig. D.33. Similar data for the remaining wall elements are given in Appendix N.

Three core samples measuring 3.75 in. (95 mm) in diameter and 8 in. (200 mm) in height were taken at heights corresponding to those of the embedded strands. In-place compressive strength of core samples were compared to those of reference cylinders cured at the same conditions as the wall elements. In-place compressive strength results are presented in Fig. D.34. Walls No. 1, 4, and 5 exhibited higher in-place compressive strengths compared to Walls No. 2, 3, and 6. Wall No. 4 showed uniform distribution of strength. Walls No. 1, 4, and 5 developed higher in-place compressive strength than Wall No. 6. This is mainly due to the difference in binder type in use (Type III and 20% fly ash compared to Type I/II cement). More details of in-place core compressive strength results are provided in Appendix O.

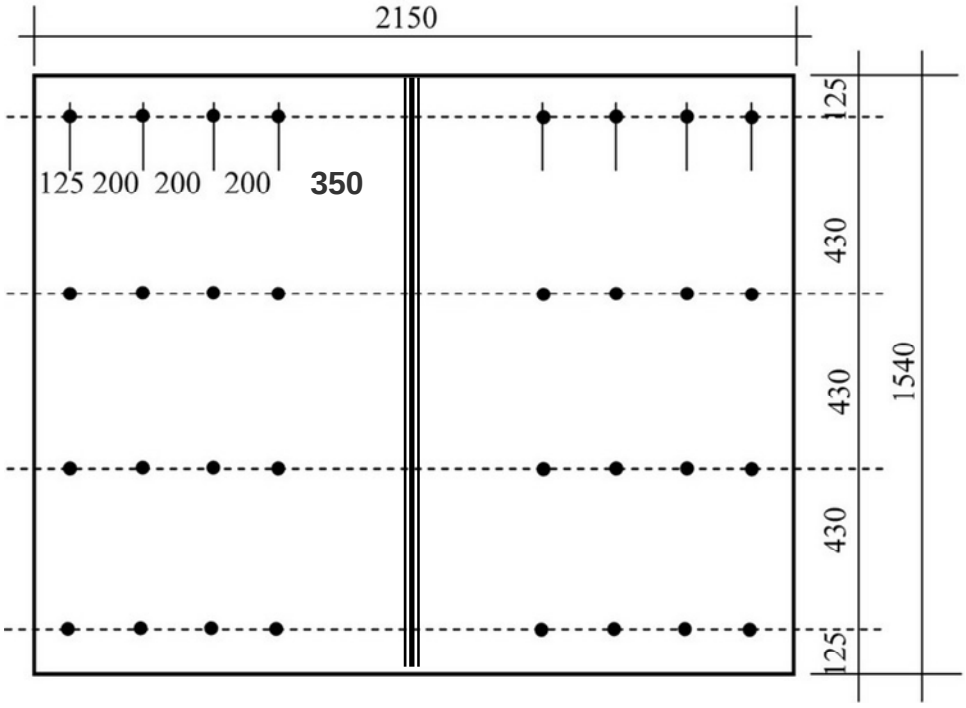

Fig. D.31 – Detail dimensions of experimental wall elements, mm (100 mm = 3.94 in.)

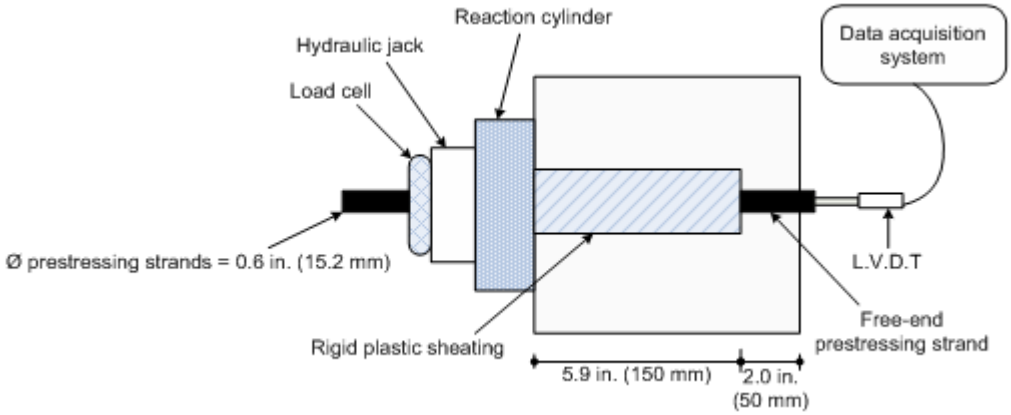

(a) Schematic of arrangement

(b) Monitoring of free-end slip of prestressing strand

Fig. D.32 – Pull-out testing arrangement

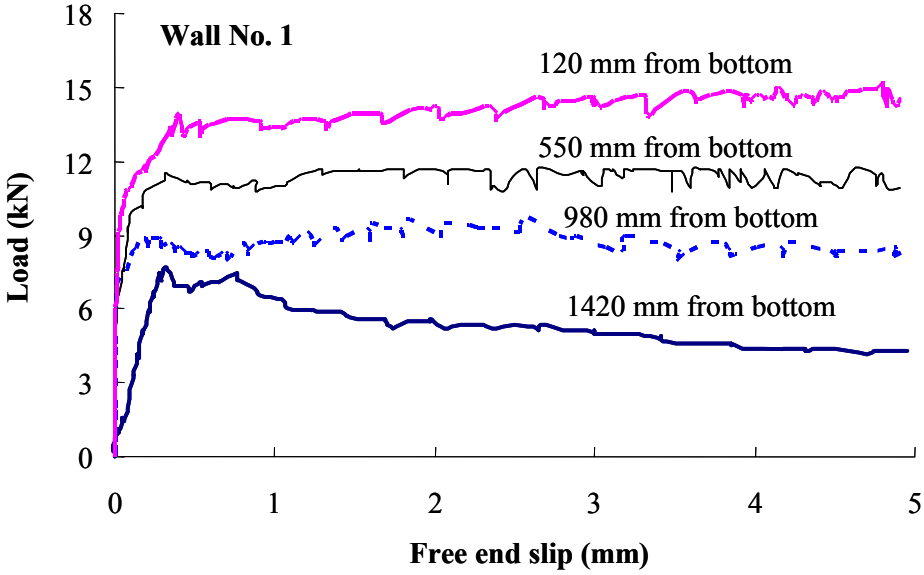

Fig. D.33 – Pull-out response of strands embedded at different heights (mixture 4, wall 1)

Compressive strengths of core samples are compared to those determined from companion cylinders in Fig. D.35. As expected, Walls No. 4, 5, and 6 cast with stable mixtures (mixture No. 12, 2, and 17) exhibited more homogenous in-place compressive strength compared to Wall No. 1, 2, and 3. On average, the relative in-place compressive strength was about 90% of the values obtained with the control cylinders. This is typical for core samples tested in compression in a perpendicular direction to the casting position. Walls No. 1 to 3 had in-place strength ratios lower than 90% at the top of the walls given the lower stability levels of these mixtures.

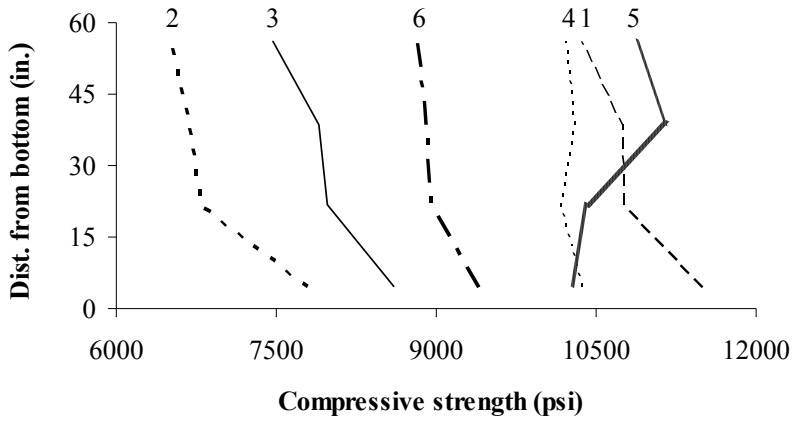

Fig. D.34 − Distribution of in-place compressive strength at 56 days determined from core samples along experimental wall elements

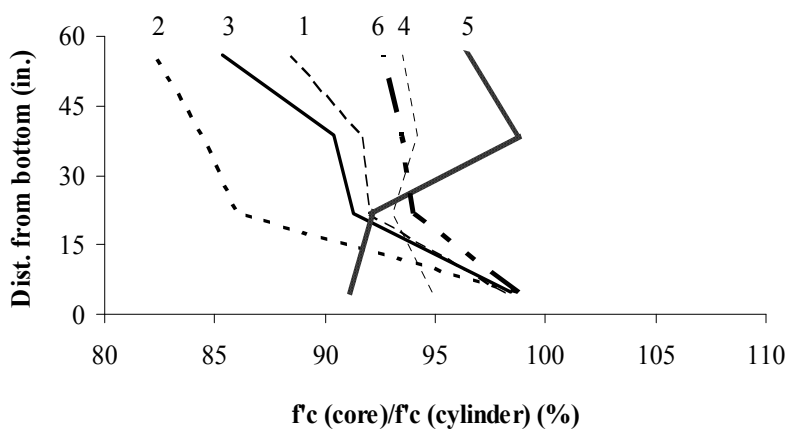

Fig. D.35 − Variation in relative core compressive strength with height compared to reference cylinders

Core strength values normalized to strengths of cores taken near the bottom of the wall elements are plotted in Fig. D.36. Wall elements 1, 2, and 3 constructed with relatively unstable mixtures had in-place compressive strengths of 90% ± 5% relative to strength values of core samples taken near the bottom. On the other hand, these values were 100% ± 6% for Wall elements 4, 5, and 6 made with stable SCC and HPC with normal slump.

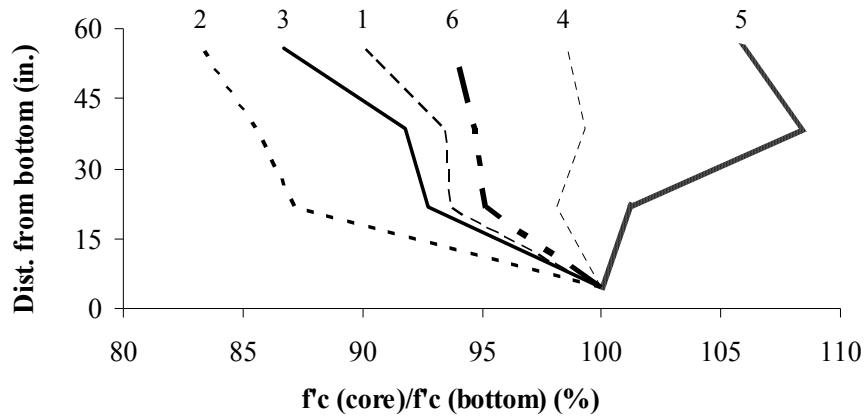

Fig. D.36 − Variations in in-place compressive strength with height (strength ratio relative to bottom layer)

D.6.1.2 Pull-out bond strength and modification factor

Bond strength results of prestressing strands determined at 56 days are summarized in Appendix N. The pull-out load at free-end slip of 1 mm is used to calculate bond strength in the post elastic cracked region. Variations of bond strength are presented in Fig. D.37. Walls No. 4 and 5 cast with stable SCC mixtures (No. 12 and 2) exhibited more homogenous pull-out bond strengths along the height compared to walls cast with unstable SCC (No. 15 and 7). Walls No. 4 and 5 exhibited even better homogeneity in bond than observed for Wall No. 6 cast with HPC.

It is interesting to note that Wall No. 1 cast with SCC No. 4 exhibited relatively large spread in pull-out bond strength along the height. This can be attributed to the high plastic viscosity of the SCC (0.135 psi.s (930 Pa.s)), which seems to hinder self-consolidation, as discussed below. Among the six tested wall elements, Wall 4 cast with SCC No. 12 had more homogenous in-situ bond strength than the other walls. SCC No. 12 developed medium plastic viscosity of 0.037 psi.s (255 Pa.s) and a maximum surface settlement of 0.43%.

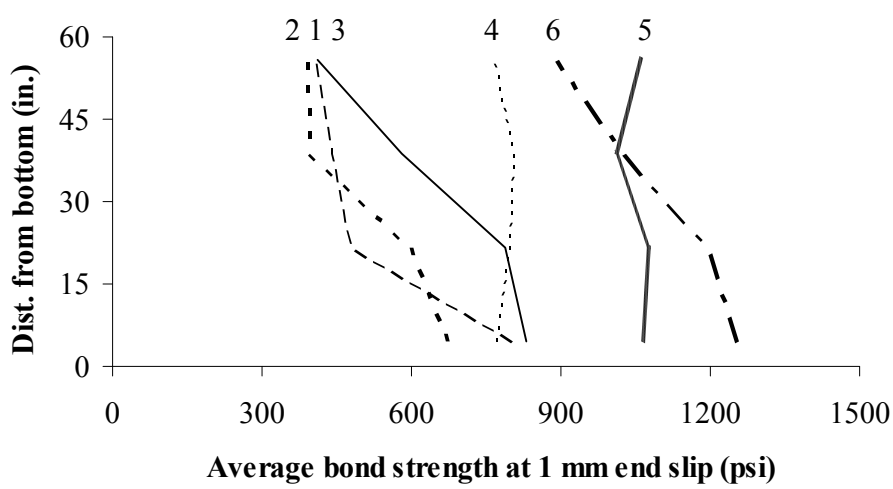

Fig. D.37 − Variation in bond strength of prestressing strands along wall height

Variations of the modification factors of bond strength between the concrete and prestressing strands are illustrated in Fig. D.38. Bond strength values are normalized by the square root of compressive strength determined from core samples at the corresponding strand heights. Normalized bond strengths are compared to those from the bottom layer. In general, Walls No. 4, 5, and 6 cast with stable SCC and HPC exhibited lower modification factor of 1, 1, and 1.36, respectively, compared to 1.57 and 1.88 for Walls No. 2 and 3 cast with unstable mixtures, respectively. Wall No. 1 cast with SCC No. 4 exhibited relatively large spread in modification factor values along the height. Again, this can be attributed to the lack of consolidation leading to undesirable bond between concrete and prestressing strand. It is interesting to note that Walls No. 4 and 5 cast with SCC No. 12 and 2, respectively, exhibited lower modification factors than Wall No. 6 made with HPC mixture. Wall 6 had higher modification factor of 1.36 compared to 1.0 to 1.1 along height for Wall 4 and 5 cast with stable SCC mixtures. This reflects the highly stable nature of these SCC mixtures of moderate viscosity levels that enabled full adequate self-consolidation and reduction in surface settlement.

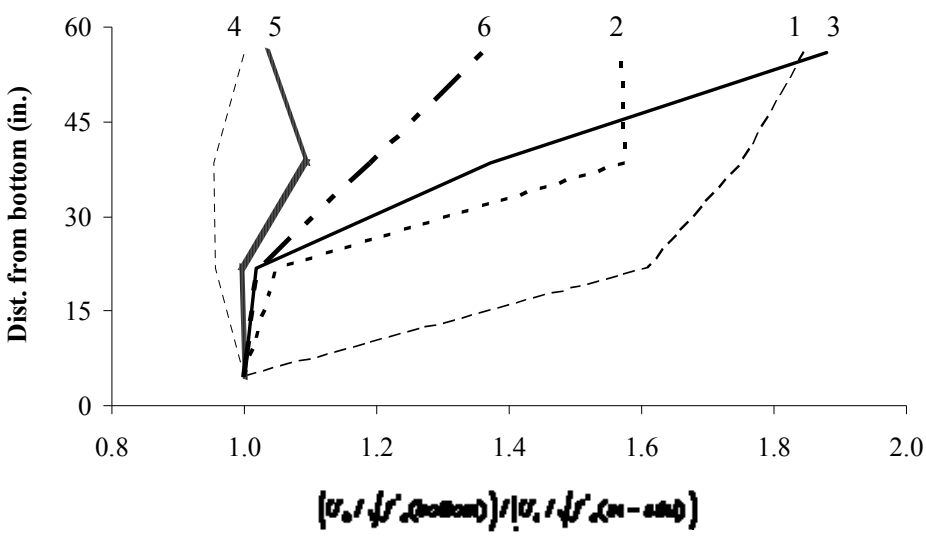

Fig. D.38 − Variation of modification factor of prestressing strands along wall height

D.6.1.3 Effect of stability on homogeneity of in-place compressive and bond strength

Relationship between static stability and in-place compressive strength

As a static stability index, surface settlement of concrete was determined using the test method described in Appendix B (PVC columns with 200 mm diameter filled with 660 mm of concrete). The surface settlement was also determined at the top of the wall elements measuring 60.6 × 84.6 × 7.9 in. (1,540 × 2150 × 200 mm). Test results showed that the maximum surface settlements determined on the wall elements were about four times lower than those obtained on the PVC column testing (Fig. D.39). Yet, the two relative settlement values can still be well correlated.

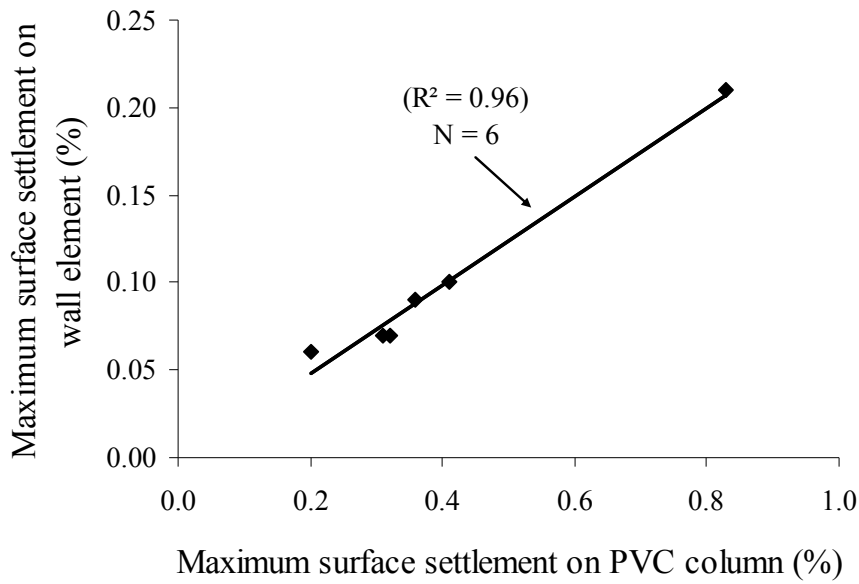

Fig. D.39 − Relationship between surface settlement results determined on PVC columns and wall elements

The surface settlement is shown to have considerable influence on in-place compressive strength relative to the reference cylinders. As presented in Fig. D.40, the mean relative in-place compressive strength increased with the decrease in maximum settlement (R^2 = 0.91). It can be concluded that concrete with maximum surface settlement of 0.5% can develop relative in-place compressive strength ratio (core/cylinder) higher than 0.92. It is important to note that the five tested SCC mixtures had VSI values of 0.5 to 1.0 at the time of casting, yet their performance in terms of in-situ properties were quite different. The actual in-situ performance was better reflected by the static stability values determined from surface settlement testing.

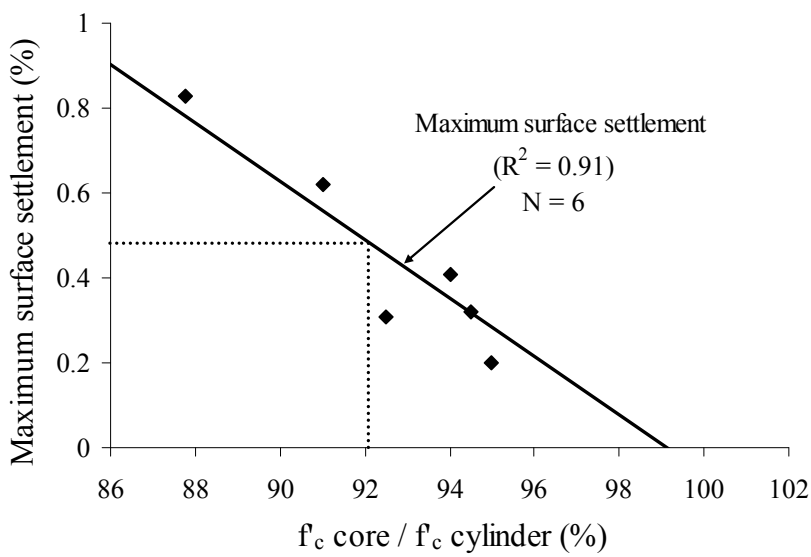

Fig. D.40 − Relationship between mean relative in-place compressive strength (core to reference cylinders) and maximum surface settlement (PVC settlement test)

Image analysis to quantify segregation

Image analysis carried out on the hardened concrete was used to evaluate segregation resistance along of cast wall elements. Four core samples measuring 3.75 × 8 in. (95 × 200 mm) were extracted longitudinally at four heights of each wall element, corresponding to the heights of the prestressing strands. Image analysis software (ImageJ), developed by the National Institute of Health in the USA, was used to determine the area of coarse aggregate particles with minimum size greater than 0.2 in. (5 mm). The software was used to transfer a color image to grey-scale using on RGB converter (Fig. D.41 (b)) and then to a binary (black-white) scale using grey-level threshold (Fig. D.41 (c)). The data were used to calculate a segregation index (Is), as follows:

Is = standard deviation of aggregate distribution × (1 – mean of relative aggregate content)

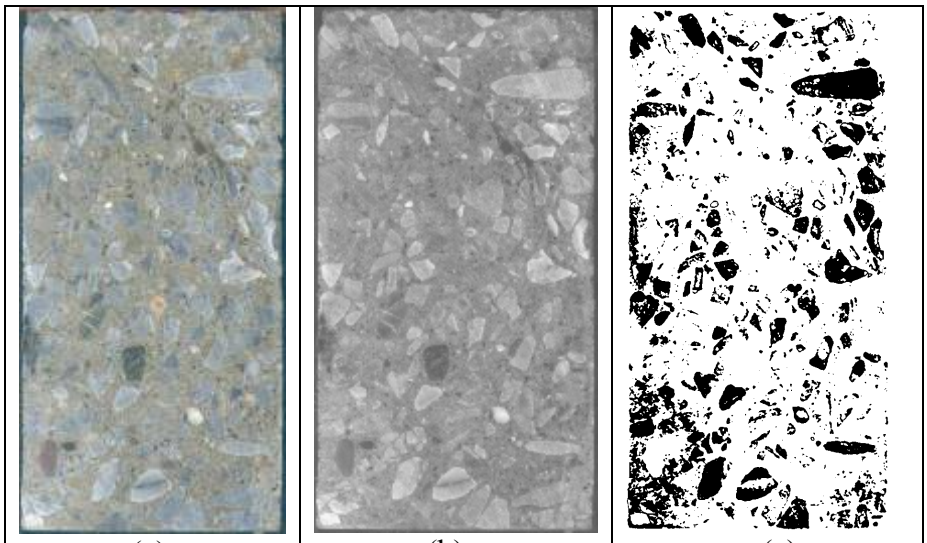

(a) (b) (c)

((a) original picture, (b) grey scale, (c) after threshold)

Fig. D.41 − Image analysis of cast core sample

As presented in Fig. D.42, the modification factor of bond strength between concrete and prestressing strands can be correlated to the maximum surface settlement and segregation index (Is); the R^2 values of these correlations were 0.67 and 0.81, respectively. Given the high viscosity of mixture No. 4, the results of Wall No. 1 were not considered in the correlation. Several large air voids attributed to poor consolidation were found on the image analysis for Wall No. 1.

According to Khayat (1997)[D6], a top-bar effect for reinforcing bars of 1.4 can be considered as an upper limit for stable SCC that can develop adequate distribution of bond in deep reinforced concrete elements. Based on the relationship shown in Fig. D.42, SCC with surface settlement of 0.5% and segregation index (Is) of 0.03 can also to secure a modification factor of 1.4 for prestressing strands.

[D6] Khayat, K. H., Manai, K., and Trudel, A., "In-Situ Mechanical Properties of Wall Elements cast Using Self-Consolidating Concrete." *ACI Materials Journal*, Vol. 94 No. 6 (1997) pp. 491-500.

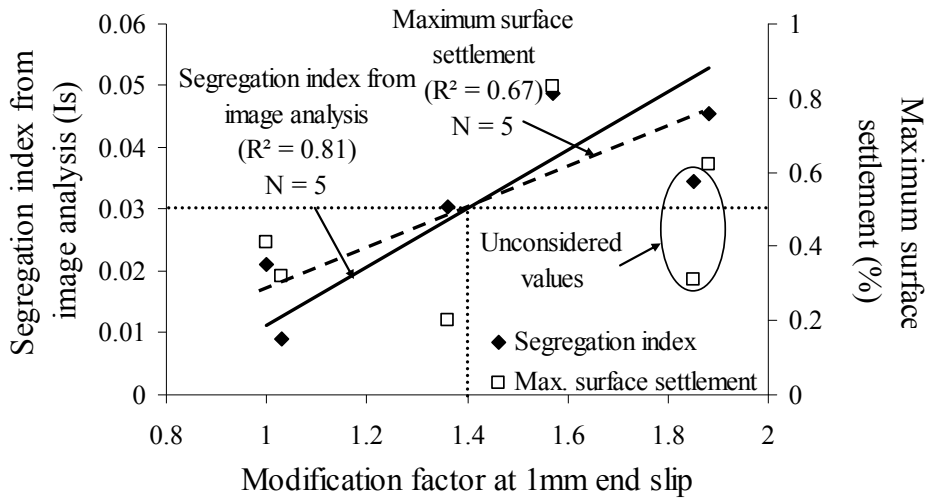

Fig. D.42 − Relationship between modification factor and stability of SCC

D.6.1.4 Recommendations to ensure homogenous in-situ properties

The evaluate SCC mixtures used for casting wall elements had similar workability levels in terms of slump flow consistency of 26 to 27.4 in. (660 to 695 mm), caisson filling capacity higher than 80%, and visual stability index of 0.5 to 1. Despite this, they developed different levels of uniformity of in-situ compressive strength and pull-out bond strength. Differences in behavior can be traced to the static stability of the SCC determined from rigorous testing methods, in particular the surface settlement, segregation of coarse aggregate, and plastic viscosity. Stable SCC can lead to more homogenous in-situ properties than HPC of normal consistency subjected to vibration consolidation. Recommendations to ensure homogenous in-situ properties are summarized in Table D.44. The concrete should have maximum surface settlement, column segregation index, and percent static segregation of 0.5%, 5%, and 15, respectively. These limits can secure a mean core-to-cylinder compressive strength higher than 90% and a modification factor lower or equal to 1.4. Care should be taken in proportioning highly viscous SCC with plastic viscosity greater than 0.073 psi.s (500 Pa.s) (T-50 close to 6 sec) that may lead to inadequate self-consolidation. This can affect bond and in-situ mechanical properties.

Table D.44 – Recommendations to secure homogenous in-situ properties of SCC

Material properties	Recommended values
Static stability	Maximum surface settlement ≤ 0.5% Column segregation index (Iseg) ≤ 5% Percent static segregation (S) ≤ 15
Viscosity	Plastic viscosity ≤ 0.073 psi.s (500 Pa.s) *(Modified Tattersall two-point rheometer with vane device)*
Mechanical properties	Core-to-cylinder compressive strength ≥ 90% (similar curing conditions) Bond strength modification factor ≤ 1.4

D.6.2 Structural Performance of Full-Scale AASHTO-Type Girders

The structural performance of full-scale precast, prestressed bridge girders constructed with selected SCC mixtures was evaluated in order to verify the applicability of existing design provisions (AASHTO and PCI) and recommend necessary modifications to the existing AASHTO LRFD specifications for SCC. The following aspects were studied: constructability, temperature variations, transfer lengths, cambers, flexural cracking, shear cracking, and shear strengths. It is noted that more details on the construction and testing of the full-scale AASHTO girders are given in Appendix P.

D.6.2.1 Testing program and details of AASHTO-Type II girders

Given the results of experimentation on the mix designs, two effective SCC mixtures of different compressive strength levels were used to cast two full-scale AASHTO-Type II girders. Non air-entrained SCC mixtures with target 56-day compressive strengths of 8,000 and 10,000 psi (55 and 69 MPa) and having release strengths of 5,000 psi (34.5 MPa) and 6,250 psi (43 MPa) at 18 hours, respectively, were chosen for the testing. Two additional girders were cast using HPC mixtures with target 56-day compressive strengths of 8,000 and 10,000 psi (55 and 69 MPa). The HRWRA dosages for the HPC and SCC mixtures were adjusted to obtain a slump of 6.3 ± 0.8 in. (160 ± 20 mm) and a slump flow of 26.8 ± 0.8 in. (680 ± 20 mm), respectively.

The AASHTO-Type II girders have overall lengths of 31 ft (9.4 m) with center-to-center spans of 29 ft (8.8m). The girders are prestressed with Grade 270 low-relaxation prestressing strands of 0.6-in. (15.2-mm) diameter, as shown in Fig. D.43. The girders were prestressed with eight strands, six straight strands and two strands harped at double harping points located 4’ – 11” (1.5 m) from mid-span (see Fig. D.43). The pressure in the pre-tensioning jacking system was calibrated to determine accurately the force applied to each strand.

Normal reinforcing bars (No. 5 bars) were added near the top to control cracking at prestress release and in the bottom flange to increase the flexural capacity. The stirrup reinforcement was chosen to satisfy the 2007 AASHTO Clause 5.8.2.5 for minimum transverse reinforcement. In order to choose the size and spacing of the stirrups, the nominal concrete strengths of 8 and 10 ksi (55 and 69 MPa) were assumed along with the nominal yield stress for the reinforcement of 60 ksi (414 MPa). Hence, for the 8 ksi (55 MPa) concrete and using No. 3 double legged stirrups the required spacing is:

$$s \le \frac{A_v f_y}{0.0316\sqrt{f_c'}b_w} = \frac{2 \times 0.11 \times 60}{0.0316\sqrt{8} \times 6} = 24.6 \text{ in. } (625 \text{ mm})$$

In addition, Clause 5.8.2.7 on maximum spacing of transverse reinforcement limits the spacing to 24 in. (610 mm) for low shear stresses. Hence a spacing of 24 in. (610 mm) was chosen for this girder. Similarly, the required spacing for the girders made with 10 ksi (69 MPa) concrete require a spacing for the No. 3 double legged stirrups of 22 in. (560 mm).

As is common practice, additional transverse and longitudinal reinforcement was placed in the end regions of each girder, as shown in Fig. D.44. In order to prevent horizontal shear distress, additional interface shear reinforcement was provided across the interface of the precast girder and the deck slab. This consisted of additional No. 3 U-bars at each full-depth stirrup location (see Fig. D.44).

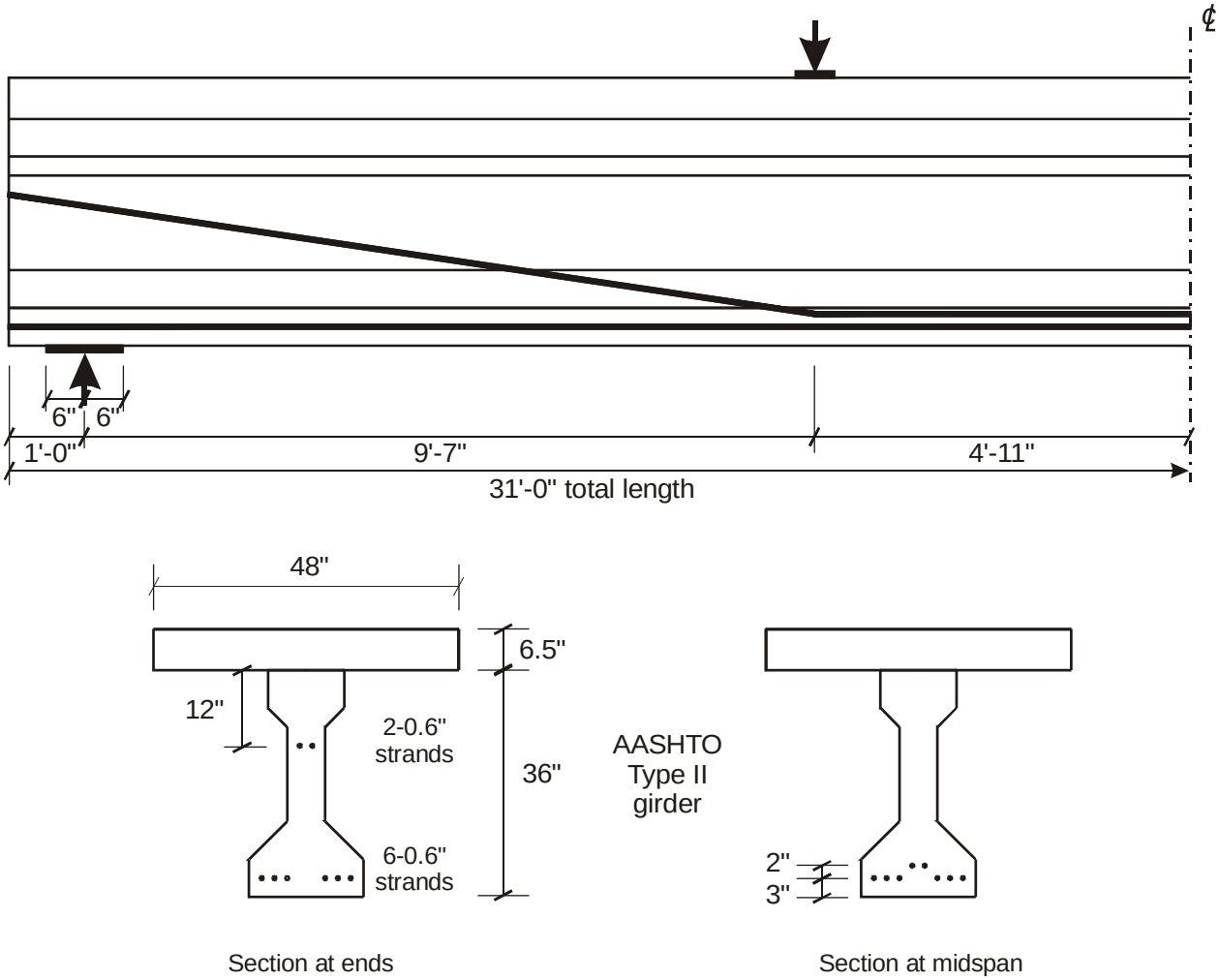

Fig. D.43 – Details of precast, prestressed AASHTO-Type II girders

A 6.5-in. (165-mm) deep and 48-in. (1,219-mm) wide cast-in-place deck slab was cast on top of each girder at least 28 days after the prestress release. The deck slab was cast with a conventional air-entrained concrete with a target compressive strength of 5,000 psi (35 MPa). The deck slab contained four No. 5 reinforcing bars in the longitudinal direction and No. 5 transverse bars at a spacing of 12 in. (305 mm) and 11 in. (280 mm) for the 8,000 and 10,000 psi (55 and 69 MPa) girders, respectively. It is noted that during the casting of the deck slab concrete, the girder was sitting on its end supports. Rather than being supported directly on the precast girder, the formwork for the deck slab was supported on the ground. Following the casting the deck slab was covered with burlap and polyethylene and was moist cured for 5 days.

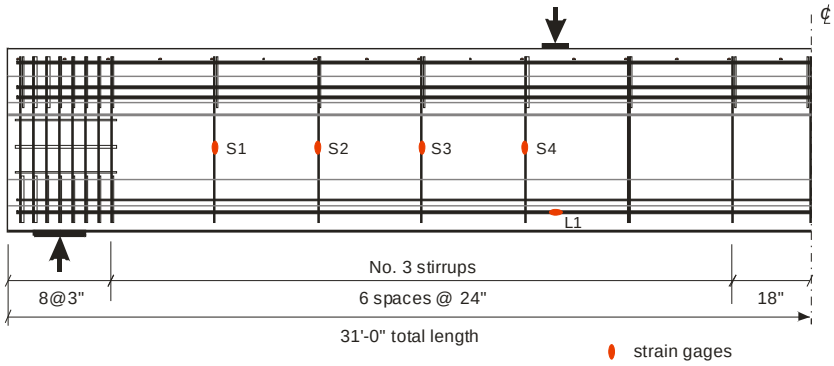

H8 and S8

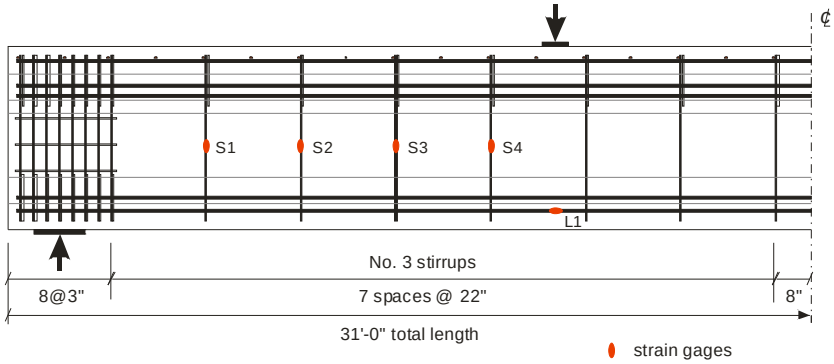

H10 and S10

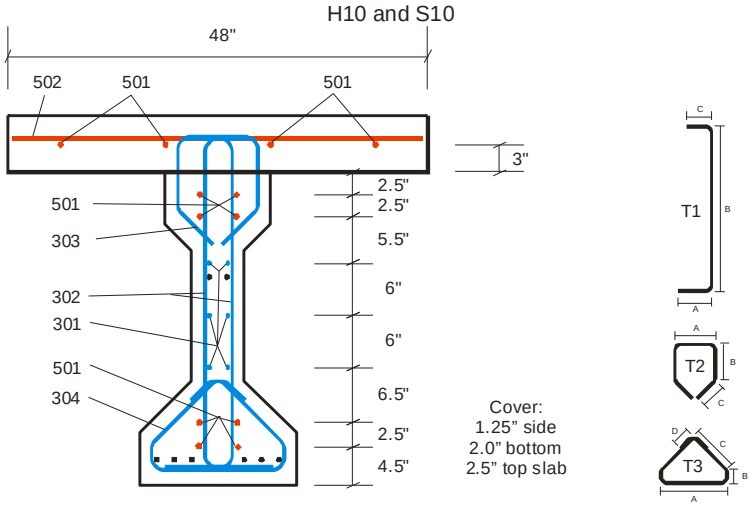

Reinforcing Bar List

Mark	Size	Length	Qty H8 / S8	Qty H10 / S10	Type	A	B	C	D
301	#3	2'-0"	12	12	-				
302	#3	4'-2"	58	60	T1	8"	38"	6"	
303	#3	3'-0"	29	30	T2	9.5"	8.5"	5.75"	
304	#3	4'-1"	16	16	T3	15.5"	3"	11"	4"
501	#5	30'-9"	12	12	-				
502	#5	3'-11"	32	34	-				

Fig. D.44 – Details of non-prestressed reinforcement

D.6.2.2 Instrumentation

A vibrating wire strain gage was installed at mid-span of each girder to measure concrete temperature and concrete strain at the level of the straight prestressing strands for determining prestress losses with time. A second vibrating wire strain gage was installed 4 ft (1.22 m) from mid-span close to one of the harping points (see Fig. D.45). The measured strains from the vibrating wire gages enable a comparison of the measured strains to those predicted for the total deformation determined at the level of the straight prestressing strands due to elastic shortening, creep, and shrinkage of the concrete.

Transfer length devices (Appendix P) were assembled to measure strains at each end of the four girders to determine the transfer lengths upon release of the pretensioning. As presented in Fig. D.44, the No. 3 stirrups and on the No. 5 longitudinal bars in the shear span were instrumented with strain gages.

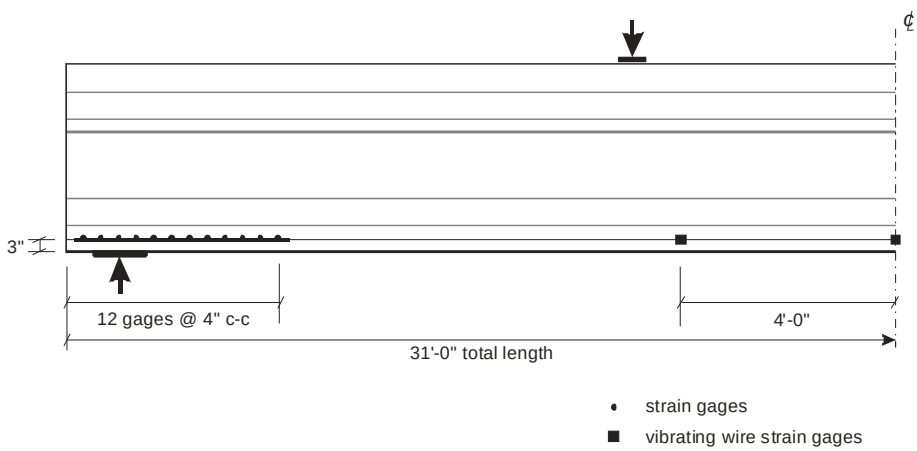

Fig. D.45 – Locations of strain gages and vibrating wire gages

D.6.2.3 Pretensioning operation

The six straight strands were tensioned first, one strand at a time, to a stress level corresponding to 0.7 f_{pu} = 0.7 × 270 = 189 ksi (1.3 GPa), starting with the outermost strands. After the six straight strands were tensioned, the two inclined strands were tensioned to the same level of prestress. In order to minimize losses due to anchorage set in this relatively short stressing bed, the stressing operation involved stressing a strand to the desired level, releasing the jack to set the anchor and then re-stressing each strand and placing steel shims under the anchorage sleeve.

D.6.2.4 Casting and steam curing of AASHTO girders

The two HPC girders, H8 and H10, were cast using ready-mix concrete with a concrete bucket and internal vibration. In contrast, the concrete for the two SCC girders, S8 and S10, was using a chute to deliver the ready-mix concrete to the middle of the girder and the concrete was not vibrated. In order to complete the concreting, a small layer of SCC was added in the top of the end regions of the girders.

After casting, steam curing was started 2.5 and 3 hours after the initial contact of cement and water for the 8,000 and 10,000 psi (55 and 69 MPa) concrete mixtures, respectively.

The temperature history of the concrete was monitored during steam curing, and the results are shown in Fig. D.46. The targeted chamber temperature for the 8,000 psi (55 MPa) SCC and HPC mixtures was set at 131°F (55°C). The target temperature for the 10,000 psi (69 MPa) concrete mixtures was set at 140°F (60°C). During the steam curing operation, an attempt was made to limit the concrete temperature to a maximum value of 150°F (65°C).

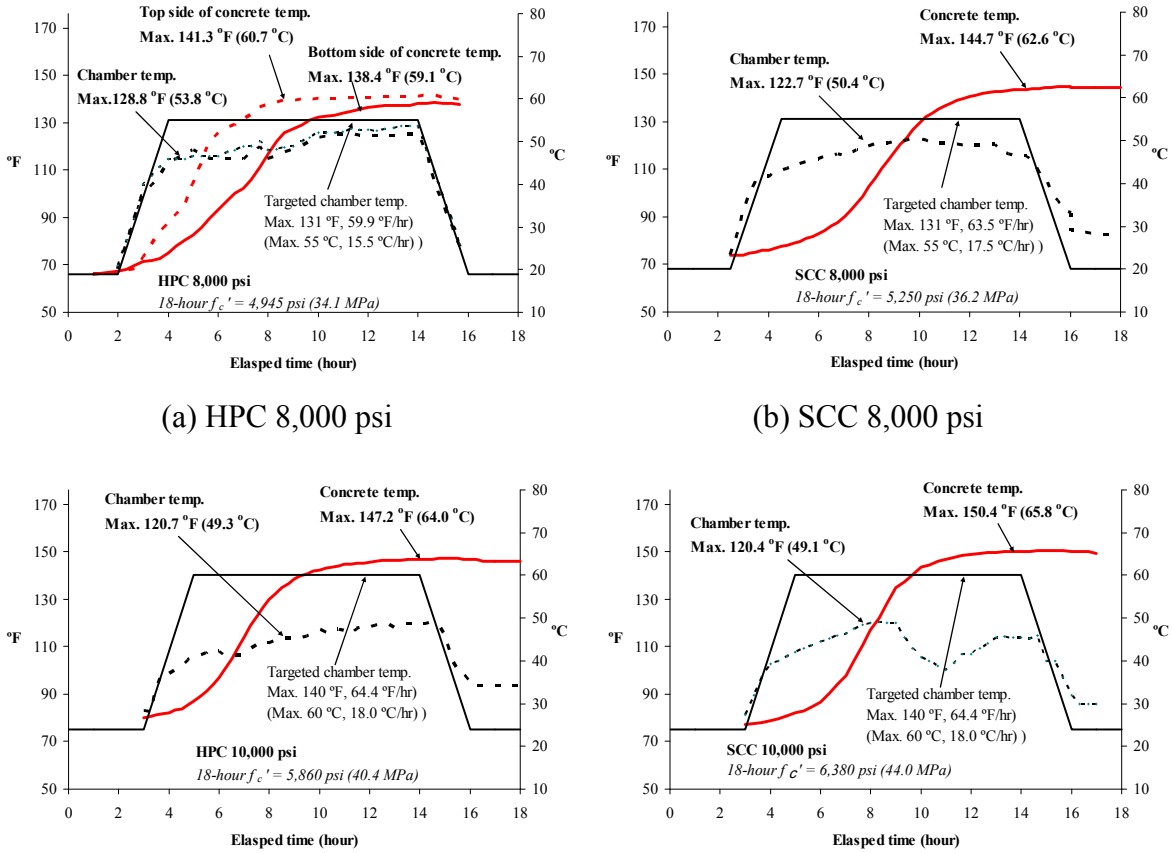

(a) HPC 8,000 psi (b) SCC 8,000 psi

(c) HPC 10,000 psi (d) SCC 10,000 psi

Fig. D.46 – Temperature history of chamber and concrete girder during steam curing

D.6.2.5 Pretensioning release

The release of the prestressing started with the release of the hold-downs for the two harping points. This was followed by the flame cutting of the two central bottom straight strands. The two inclined strands were then flame cut followed by the release of the remainder of the bottom strands, working from the inner strands outwards. The flame cutting was performed first at the jacking end of each girder.

D.6.2.5.1 Strand set measurements

Table D.45 gives the average values of the strand set at each end and the overall average for all the readings. The SCC girders had slightly smaller values of strand set. The average set is 0.036 in. (0.91 mm).

Table D.45 – Average values of strand set

Girder	Flame-cut end in. (mm)	Dead end in. (mm)	Average in. (mm)
H8	0.038 (0.97)	-	0.038 (0.97)
S8	0.031 (0.78)	0.035 (0.88)	0.033 (0.83)
H10	0.033 (0.83)	0.040 (1.01)	0.036 (0.92)
S10	0.032 (0.82)	0.039 (0.98)	0.035 (0.90)

D.6.2.5.2 Transfer length measurements

The results from the strain readings on the transfer length devices that were embedded in each end of the girders at the level of the bottom 6 straight strand are given in Fig. D.47. In order to determine the transfer length from these readings, the procedure described by Russell and Burns[D7] (1997) was used. The procedure involved first determining the average strain in the strain plateau area and then taking 95% of this value to give the "95% AMS".

The transfer length is determined by the intersection of the 95% AMS line with the measured strain profile. The resulting transfer length values are shown in Fig. D.47 and are summarized in Table D.46. It is noted that these transfer lengths are considerably shorter than the transfer length given in the 2007 AASHTO Specifications (5.11.4.1). The average transfer length is 12.8 in. (325 mm). The AASHTO transfer length is 60 strand diameters or 60 × 0.6 = 36 in. (915 mm). This value is very conservative.

For an average l_{tr} of 12.8 in. (325 mm) and a strain in the strand corresponding to a stress level of 0.7 f_{pu}, the estimated strand slip is 0.042 in. (1.1 mm) (see Appendix P). This compares reasonably well with the average measured strand set of 0.036 in. (0.91 mm).

[D7] Russell, B.W., and Burns, N.H., "Measurement of Transfer Lengths on Pretensioned Concrete Elements." *Journal of Structural Engineering*, ASCE, Vol. 123, No. 5 (1997) pp. 541-549.

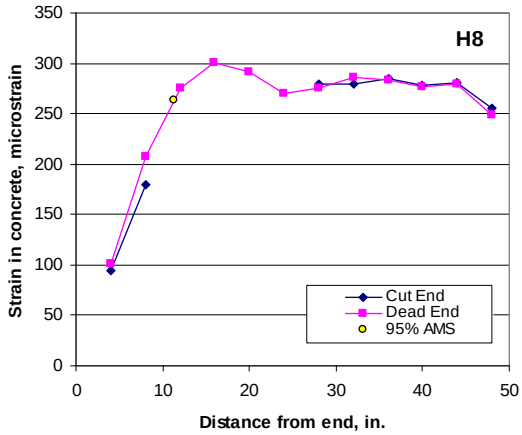

(a) Girder H8

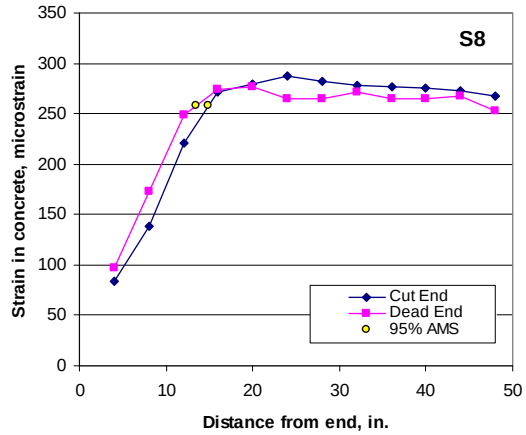

(b) Girder S8

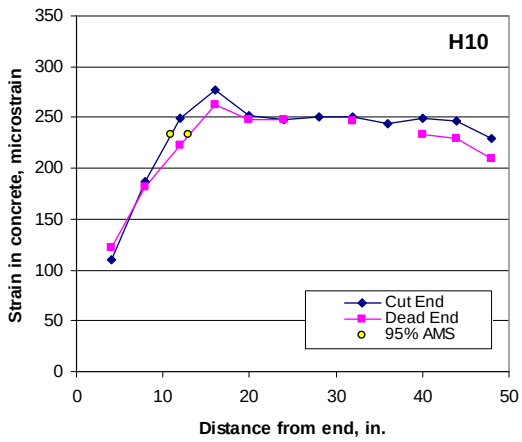

(c) Girder H10

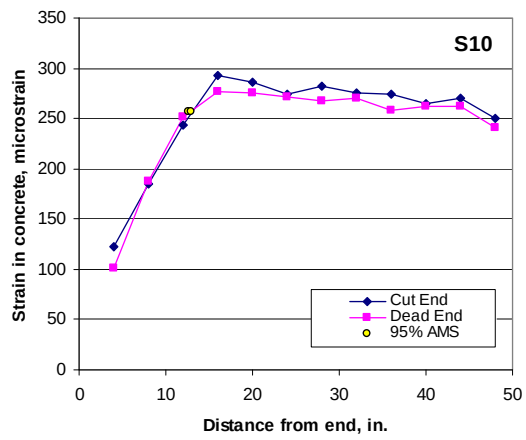

(d) Girder S10

Fig. D.47 – Measurement of transfer length

Table D.46 – Summary of 95% AMS transfer lengths

Girder	Cut end in. (mm)	Dead end in. (mm)
H8	-	11.3 (287)
S8	14.9 (380)	13.5 (343)
H10	11.0 (280)	13.0 (330)
S10	13.0 (330)	12.7 (323)

D.6.2.6 Concrete material properties

The concrete material properties are presented in Appendix P.

D.6.2.6.1 Mixture proportioning and fresh properties of HPC and SCC used for girder casting

The four mixtures were proportioned with Type III cement and 20% Class F fly ash and crushed aggregate with nominal maximum size aggregate (MSA) of ½ in. (12.5 mm), as presented in Table D.47. The HPC mixtures were proportioned with a *w/cm* of 0.38 and 0.33 to attain the two targeted 56-day compressive strengths of 8,000 and 10,000 psi (55 and 69 MPa), respectively. The two SCC mixtures were prepared with *w/cm* of 0.38 and 0.32. During casting, workability characteristics were evaluated. The mixture proportioning and workability characteristics are summarized in Tables D.47 and D.48, respectively.

Table D.47 – Mixture proportioning of SCC and HPC for girders

Mixture	HPC (H8)	SCC (S8)	HPC (H10)	SCC (S10)
	8,000 psi	8,000 psi	10,000 psi	10,000 psi
Cement, lb/yd^3 (kg/m^3)	Type III	Type III	Type III	Type III
	639 (379)	593 (352)	638 (379)	674 (400)
HRWRA demand, fl oz/cwt (L/100 kg CM)	5.7 (0.37)	12.3 (0.80)	13.1 (0.85)	21.9 (1.43)
VMA dosage, fl oz/cwt (L/100 kg CM)	0	0	0	1.54 (0.1)
Class F fly ash, lb/yd^3 (kg/m^3)	158 (94)	148 (88)	155 (92)	169 (100)
Total CM, lb/yd^3 (kg/m^3)	797 (473)	742 (440)	793 (470)	843 (500)
Water, lb/yd^3 (kg/m^3)	299 (177)	285 (169)	258 (153)	270 (160)
w/cm	0.38	0.38	0.33	0.32
Sand, lb/yd^3 (kg/m^3)	1,233 (732)	1,715 (1017)	1,323 (785)	1,391 (825)
Coarse aggregate, lb/yd^3 (kg/m^3)	1,795 (1065)	1,387 (823)	1,803 (1070)	1,627 (965)
Sand/total aggregate, by volume	0.41	0.54	0.42	0.47
Volume of coarse aggregate, %	38.9	30.1	39.2	34.9
Volume of mortar, %	61.1	69.9	60.8	65.1
Volume of paste, %	33.8	31.9	31.4	34.6

Table D.48 – Fresh properties of SCC and HPC mixtures used for girders

Mixture		HPC (H8)	SCC (S8)	HPC (H10)	SCC (S10)
		8,000 psi	8,000 psi	10,000 psi	10,000 psi
Slump flow, in. (mm)	before casting	5.5 (140)*	26.0 (660)	7.5 (190)*	26.0 (660)
	after casting	4.3 (110)*	23.6 (600)	7.1 (180)*	25.2 (640)
T-20 in. (50 cm), sec	before casting	-	3.0	-	3.0
	after casting	-	3.9	-	3.7
Visual stability index	before casting	-	0.5	-	0.5
	after casting	-	0.5	-	0.5
Air content, %	before casting	2.3	2.0	1.9	1.2
	after casting	2.1	1.9	1.9	1.5
Temperature, ^{o}F (^{o}C)	before casting	66.4 (19.1)	69.8 (21.0)	76.1 (24.5)	75.6 (24.2)
	after casting	66.7 (19.3)	70.7 (21.5)	76.6 (24.8)	76.1 (24.5)
J-Ring flow, in. (mm)	before casting	-	23.6 (600)	-	22.8 (580)
	after casting	-	21.7 (550)	-	21.3 (540)
L-box	before casting sec, (h_2/h_1)	-	3.9 (0.73)	-	4.9 (0.70)
	after delivery sec, (h_2/h_1)	-	4.5 (0.68)	-	5.5 (0.62)
Filling capacity, %	before casting	-	82	-	76
	after casting	-	75	-	70
Rheological parameter	τ_o (Pa)	893	3	568	118
	μ_p (Pa.s)**	52	253	233	189
	R^2	0.99	0.99	0.97	0.99
Column segregation index, %		1.58	4.00	-	2.65
Max. surface settlement, %		0.22	0.29	0.21	0.24
Initial setting time, hour		4.20	7.30	5.30	5.4
Final setting time, hour		5.20	8.50	6.10	6.3

* Slump

** 1 Pa = 1.45×10^{-4} psi

D.6.2.6.2 Mechanical properties of HPC and SCC used for girders

The compressive strength, modulus of elasticity, and flexural strength results are presented in Appendix P. The mean 18-hour compressive strength of the 8,000 psi (55 MPa) SCC was 5,250 psi (36.2 MPa); the targeted 18-hour compressive strength was 5,000 psi (34.5 MPa). The release compressive strength of the 10,000 psi SCC (69 MPa) was also greater than the targeted strength of 6,250 psi (43.0 MPa). On the other hand, the 18-hour compressive strengths of the 8,000 and 10,000 psi (55 and 69 MPa) HPC mixtures were 4,945 psi (34.1 MPa) and 5,860 psi (40.4 MPa), which are close to the target compressive strength values of 5,000 psi (34.5 MPa) and 6,250 psi (43.0 MPa), respectively. It is important to note that the temperature (and therefore maturity) of

the concrete in the girder was greater than that of the control cylinders. Therefore, the in-situ compressive strength of the girders should be greater than those determined from the control cylinders.

D.6.2.6.3 Visco-elastic properties of HPC and SCC used for girder casting

Autogenous shrinkage

Autogenous shrinkage of the SCC and HPC mixtures are given in Fig. D.48. The autogenous shrinkage, measured on sealed specimens, ranged from 200 to 285 µstrain after 56 days.

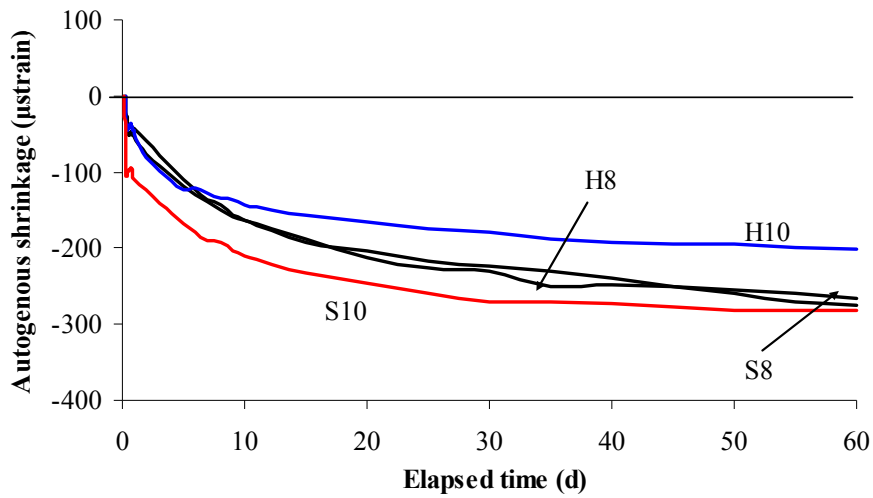

Fig. D.48 – Variations of autogenous shrinkage with time for SCC and HPC

Drying shrinkage

Drying shrinkage was monitored for approximately four months using 6 × 12 in. (150 × 300 mm) cylinders and is summarized in Fig. D.49. At 112 days, the two SCC mixtures exhibited higher drying shrinkage (465 and 495 µstrain) than the two HPC mixtures (390 and 405 µstrain).

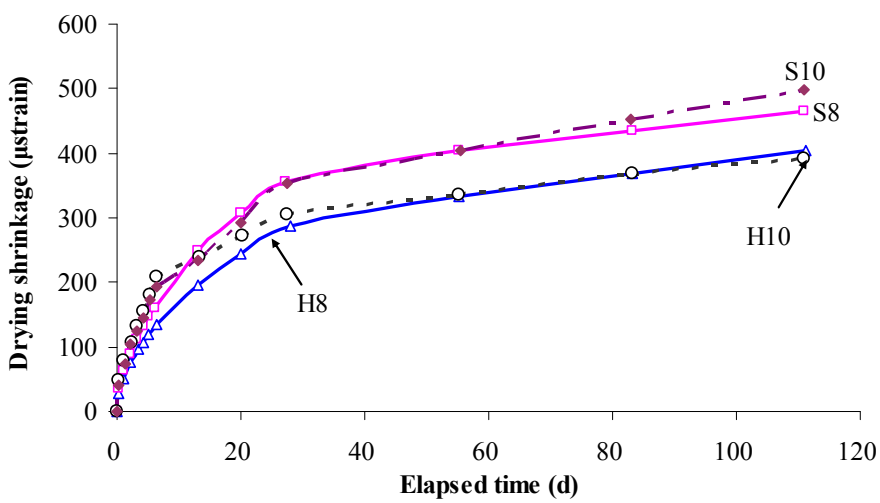

Fig. D.49 – Variations of drying shrinkage with time for SCC and HPC

D.6.2.6.4 Mechanical properties of deck slab concrete

The deck slab concrete had a target 28-day compressive strength of 5,000 psi (35 MPa). Appendix P has details of the mixture proportioning and the measured properties.

D.6.2.7 Reinforcing steel and prestressing steel properties

Appendix P gives the mechanical properties of the #3 and #5 reinforcing bars as well as the properties of the 0.6 in. (15 mm) diameter seven-wire low-relaxation prestressing strand used in the experimental program.

D.6.2.8 Test setup and procedure

Figure D.50 shows the test setup and the locations of the linear voltage differential transducers (LVDTs) used to measure displacements and to determine average strains. A structural steel loading beam was used to provide two equal line loads at the locations shown in Figs. D.50 and D.51. All specimens were loaded using the same procedure. Initially, the total load was applied to the structural loading beam in "load control". After first flexural cracking developed the loading was applied in "deflection control" until failure was reached.

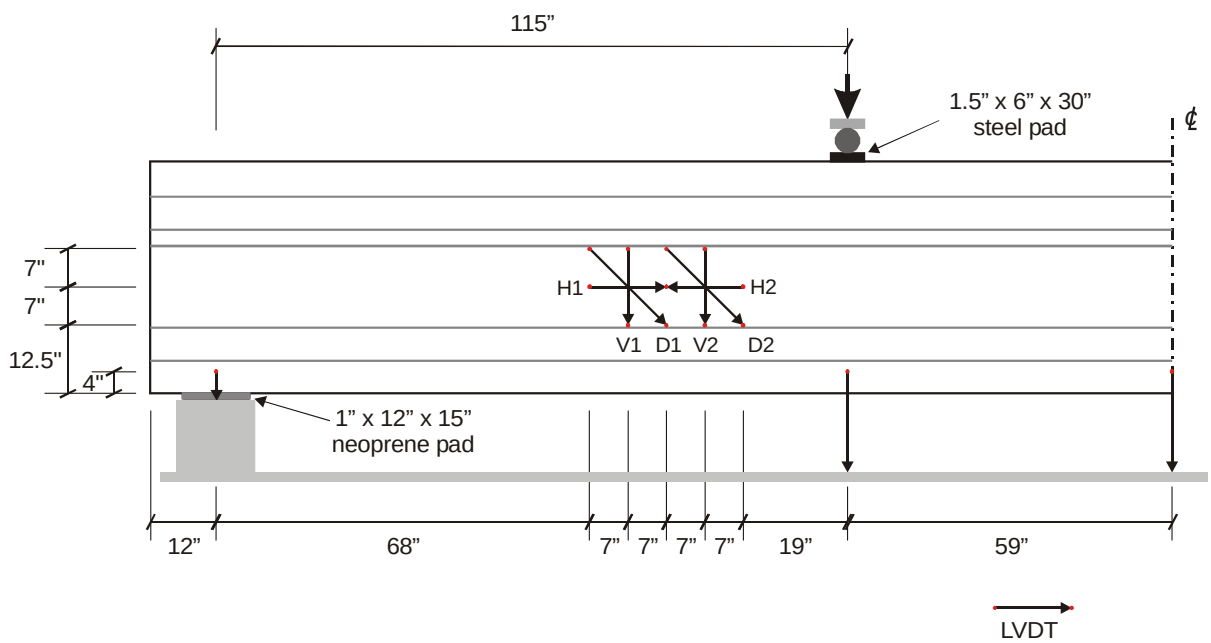

Fig. D.50 – Test setup and locations of LVDTs

Fig. D.51 – Specimen H8 before testing

D.6.3 Flexural Behavior

D.6.3.1 Camber measurements

Figure D.52 shows the variation of the camber with time measured from casting of the concrete, with zero camber just prior to prestress release at an age of about 18 hours. The sudden reduction in camber that occurred is due to the removal of the formwork for the deck slab.

The specimens with target compressive strengths of 8,000 psi (55 MPa) had larger cambers than the companion specimens made with 10,000 psi (69 MPa) concrete.

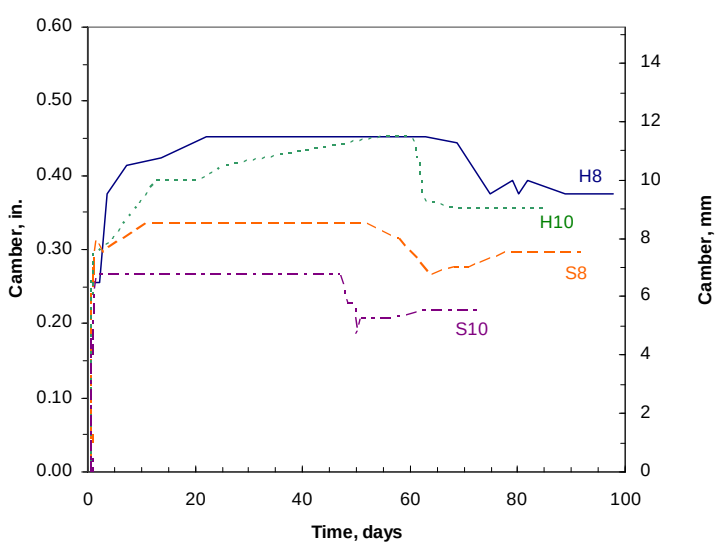

Fig. D.52 – Variation of camber with time

D.6.3.2 Overall response in flexure

Figure D.53 shows the moment versus central deflection responses of Specimens H8, S8, H10, and S10. Table D.49 summarizes the results with the moment at first flexural cracking, M_{cr}, the maximum moment achieved, M_{max}, the predicted flexural capacity, M_n, and the maximum deflection reached before failure, Δ_{max}. The first flexural crack observed in each of the specimens was hairline.

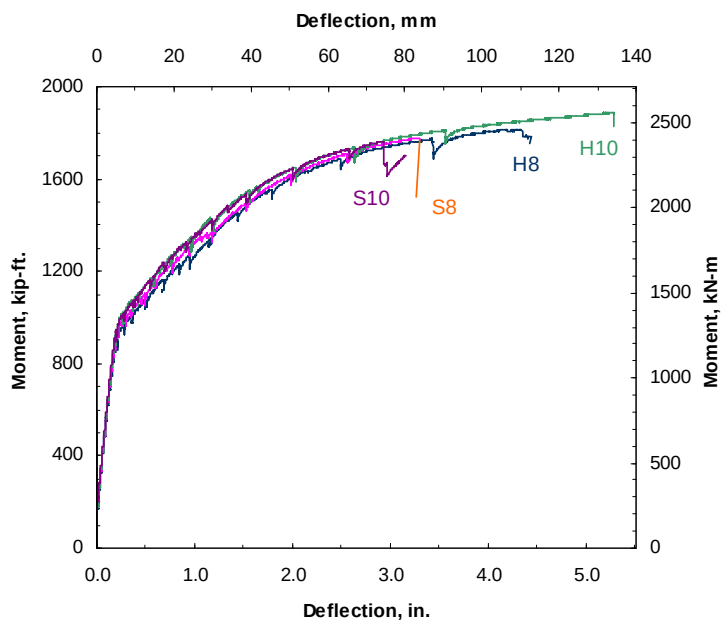

Fig. D.53 – Moment versus central deflection responses of the girders

Table D.49 – Comparison of flexural responses of four specimens

	H8	S8	H10	S10
M_{cr}, ft kips (kN.m)	885 (1,200)	868 (1,177)	937 (1,270)	946 (1,283)
M_{max}, ft kips (kN.m)	1,815 (2,460)	1779 (2,412)	1888 (2,560)	1764 (2,392)
Δ_{max}, in. (mm)	4.43 (113)	3.30 (84)	5.29 (134)	3.15 (80)
$f'_{c\ girder}$, ksi (MPa)	7.38 (50.9)	8.61 (59.4)	9.05 (62.4)	9.56 (65.9)
$f'_{c\ slab}$, ksi (MPa)	5.25 (36.2)	5.25 (36.2)	4.89 (33.7)	4.89 (33.7)
M_n, ft kips (kN.m)	1,800 (2,440)	1800 (2,440)	1791 (2,428)	1791 (2,428)

The two high-performance concrete girders, H8 and H10, both achieved moments greater than the predicted nominal flexural resistances before failing in shear. The two SCC girders, S8 and S10, failed in shear just before reaching their predicted nominal flexural resistances. Specimens H8 and H10 experienced larger deflections at midspan than Specimens S8 and S10. The high strains that were recorded (see Appendix P) indicate that the flexural reinforcement had yielded and had strains beyond strain hardening.

D.6.4 Shear Behavior

Figure D.54 shows the shear versus deflection responses for the four girders. The shear was determined at the inner face of the neoprene bearing pads.

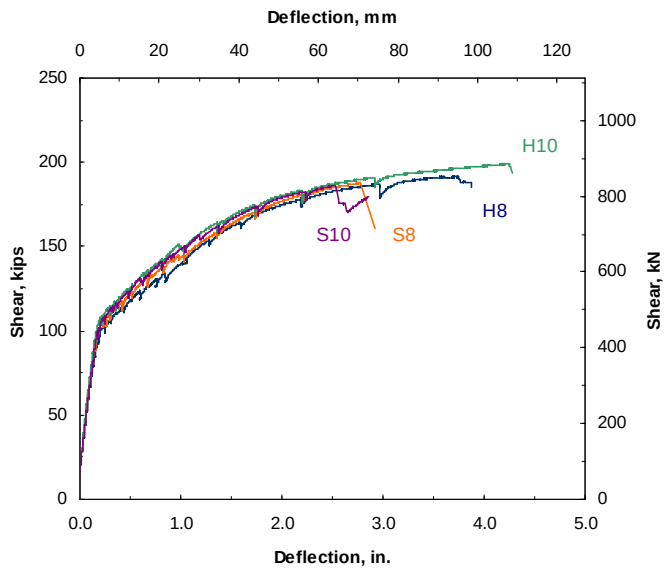

Fig. D.54 – Comparison of shear versus deflection responses for the four specimens (deflection measured at the loading point)

The strains obtained from the vertical LVDT readings (see Fig. D.54) indicated that the stirrups experienced strains well above their yield strain of 2.63 x 10^{-3} (see Appendix P). Figure D.55 shows the four specimens just before and after shear failure on the ends that failed in shear.

Table D.50 compares the shears at first shear cracking, V_{cr}, first stirrup yield, V_y, and the maximum shear, V_{max}. The table also compares the maximum deflection at the loading point attained during testing. Table D.50 also presents the predicted nominal shear resistance using Section 5.8 of the 2007 AASHTO Specifications. For these predictions the measured properties of the reinforcing bars, prestressing steel and concrete mixtures were used. It is noted that the experimentally determined maximum shears are considerably above the predicted nominal shear resistance. There are several reasons for the conservative predictions:

- The tensile strengths obtained from the flexural beam tests (see Appendix P) indicate that the corresponding code values are very conservative for the HPC and SCC mixtures.
- During the testing it was evident that the strength and stiffness of the top and bottom flanges of the specimens considerably increased the shear strengths, with shear cracks of 0.28 in. (7 mm) observed in the webs before shear failure occurred.

(a) Girder H8

(b) Girder S8

(c) Girder H10

(d) Girder S10

Fig. D.55 – Girders just before and just after failure

Table D.50 – Comparison of shear responses of four specimens

	H8	S8	H10	S10
V_{cr}, kips (kN)	115 (511)	109 (485)	117 (520)	116 (516)
V_y, kips (kN)	130 (578)	136 (605)	150 (667)	156 (694)
V_{max}, kips (kN)	192 (854)	188 (836)	199 (885)	186 (827)
Δ_{max}, in. (mm)	3.88 (99)	2.92 (74)	4.28 (109)	2.86 (73)
$f'_{c\ girder}$, ksi (MPa)	7.38 (50.8)	8.61 (59.4)	9.05 (62.4)	9.56 (65.9)
$f'_{c\ slab}$, ksi (MPa)	5.25 (36.2)	5.25 (36.2)	4.89 (33.7)	4.89 (33.7)
V_n, kips (kN)	113 (503)	115 (511)	118 (525)	119 (529)

D.6.5 Conclusions

The following conclusions arise from the construction and testing of the precast, prestressed girders:

- The SCC placement was successful, even with the casting from only one location at midspan of the 31-ft (9.44-m) long girders.
- There was no visible segregation of the concrete in any of the girders.
- During the steam-curing operation the maximum temperatures reached satisfied to maximum temperature limit of 150°F (65°C).
- There were fewer "bug holes" for the SCC concrete than for the HPC.
- The target 18-hour compressive strengths, required at prestress release, were met for the two SCC girders.
- The transfer lengths were similar for the four different concrete mixtures.
- The transfer lengths were considerably shorter than the transfer length given in the 2007 AASHTO Specifications and the ACI 318-05 Code.
- At time of prestress release at 18 hours, the coefficients on the square root of the compressive strength used to determine the modulus of elasticity for the SCC mixtures were about 4% and 11% lower than those for the HPC mixtures.
- The two SCC mixtures experienced about 20% greater drying shrinkage than the comparable HPC mixtures.
- Due to the lower elastic modulus and the higher drying shrinkage, greater elastic shortening losses and greater long-term losses of prestress occurred, resulting in smaller cambers for the SCC girders.
- The cracking moments were similar for the SCC girders and the companion HPC girders.

- The uncracked and cracked stiffnesses for all four girders are very similar.
- The cracking shears were similar for all four girders.
- All four girders failed in shear after developing a significant number of wide shear cracks.
- The shear crack widths just before failure were greater than 0.24 in. (6 mm).
- The stirrups developed significant strains, beyond strain hardening, with the stirrups rupturing at failure.
- The failure shears exceeded the predicted nominal shear resistances of the girders using the approach given in 2007 AASHTO Specifications.
- The increased shear resistance was probably due to the strength and stiffness of the top and bottom flanges of the AASHTO girders.
- The HPC girders experienced flexural resistances which exceeded the predicted nominal resistances using the 2007 AASHTO Specifications.
- The SCC girders experienced flexural resistances which were within 1.5% of the theoretical flexural resistance using the approach in the 2007 AASHTO Specifications.
- The HPC girders exhibited higher ductilities than the corresponding SCC girders.
- The lower shear resistance and lower ductility experienced by the SCC girders is probably due to the lower volume of coarse aggregate, which reduces aggregate interlock and results in a lower energy absorption capability on the sliding shear failure plane.

This research on the structural performance of AASHTO girders has highlighted a number of differences that could affect design. However, it is clear form the testing of only two SCC girders and comparing the responses with two HPC girders that more research is required before any changes be recommended to the design specifications.

D.7 CONCLUSIONS

D.7.1 Test Methods and Material Requirements

The use of proven combinations of test methods is necessary to reduce time and effort required for quality control of SCC used in precast, prestressed bridge elements. These methods include the components required for evaluating simultaneously the deformability, passing ability, and resistance to segregation of the concrete. The most promising SCC test methods that are relevant for these applications are the following:

- Filling ability (slump flow and T-50).
- Passing ability (J-Ring and L-box).
- Filling capacity [Caisson test (filling vessel)].
- Segregation resistance [Visual stability index (VSI), Surface settlement and rate of settlement, and Column segregation].

Recommended acceptance values for SCC tests are summarized in Table D.51. These tests are appropriate for material selection and mix design as well as for quality control (QC) testing.

Table D.51 − Performance-based specifications and workability test methods

Property	Test method	Target value	Design	Q/C
Filling ability	Slump flow T-50 (ASTM C 1611)	23.5 – 29 in. (600 – 735 mm) 1.5 – 6 sec	√	√
Passing Ability	J-Ring flow (ASTM C 1621) Slump flow – J-Ring flow	21.5 – 26 in. (545 – 660 mm) 0 – 3 in. (0 – 75 mm)	√	√
	L-Box blocking ratio (h_2/h_1)	0.5 – 1.0	√	√
Filling Capacity	Filling capacity	70% – 100%	√	
	Slump flow and J-Ring flow			√
	Slump flow and L-Box tests			√
Static stability	Surface settlement	Rate of settlement, 25 – 30 min (value can decrease to 10 – 15 min) - MSA of 3/8 and ½ in. (9.5 and 12.5 mm) ≤ 0.27 %/h (Max. settlement ≤ 0.5%) - MSA of ¾ in. (19 mm) ≤ 0.12 %/h (Max. settlement of 0.3%)	√	
	Column segregation (ASTM C 1610)	Column segregation index (C.O.V.) ≤ 5% Percent static segregation (S) ≤ 15	√	
	VSI (ASTM C 1611)	0 – 1 (0 for deep elements)	√	√
Air volume	AASHTO T 152	4% – 7% depending on exposure conditions, MSA, and type of HRWRA. Ensure stable and uniform distribution of small air voids.	√	√

D.7.2 Material Constituents and Mix Design

Based on the results derived from the factorial design, the relative influence of various mixture parameters on the modeled properties of SCC are summarized in Table D.52. Table D.53 gives recommendations for the mixture proportioning of SCC for the precast prestressed applications.

Table D.52 – Relative significance of modeled SCC parameters

	Binder content			*w/cm*			VMA content			Binder type			S/A		
	Low	Medium	High	Low	Medium	High	Low	Medium	High	Low	Medium	High	Low	Medium	High
HRWRA demand		■				■	■				■		■		
Slump flow retention			■			■	■					■		■	
J-Ring			■			■		■			■			■	
Slump flow – J-Ring flow			■			■	■					■		■	
L-box blocking ratio (h_2/h_1)			■			■	■			■			■		
Caisson filling capacity			■			■	■					■	■		
Maximum surface settlement			■			■	■				■		■		
Column segregation index			■	■					■	■			■		
Plastic viscosity			■			■	■			■				■	
Thixotropy (A_b)			■			■	■			■			■		
Form pressure			■			■	■			■				■	
18-hour f_c'	■					■		■			■		■		
56-day f_c'		■				■	■				■		■		
18-hour MOE		■				■	■				■			■	
56-day MOE	■					■	■				■				■
7-day flexural strength		■			■		■			■					■
56-day flexural strength	■					■	■			■				■	
Autogenous shrinkage at 7 days	■					■	■					■	■		
Autogenous shrinkage at 56 days	■					■	■					■	■		
Drying shrinkage after 28 days of exposure		■				■	■			■			■		
Drying shrinkage after 112 days of exposure			■			■	■				■			■	
Creep after 28 days of loading	■				■		■					■	■		
Creep after 112 days of loading		■		■			■					■	■		

* Darkened areas indicate high degree of influence for the modeled mixture parameter.

Table D.53 – Recommendations for proportioning SCC for precast prestressed applications

	w/cm		Binder type		Binder content		S/A		VMA	
	0.34	0.40	I/II	III + 20% fly ash	742 lb/yd³ (440 kg/m³)	843 lb/yd³ (500 kg/m³)	0.46	0.54	0	Moderate
Filling ability retention	■			■		■	■			
Passing ability		■		■		■	■			
Filling capacity		■		■		■				
Static stability	■			■						■
18-hour f_c'	■		■							
56-day f_c'	■			■		■				
18-hour MOE	■		■		■		■			
56-day MOE	■			■			■			
Flexural strength	■				■			■		
Autogenous shrinkage		■	■							
Drying shrinkage		■	■		■		■			
Creep	■		■		■					

* Darkened areas indicate better performance for each property

Detailed findings and conclusions from this investigation can be made, as follows:

Regarding the fresh properties, the following recommendations and observations are made:

- A *w/cm* should be selected to obtain the targeted stability, mechanical properties, visco-elastic properties, and durability (Typical *w/cm* for precast, prestressed applications can range between 0.34 and 0.40).
- Low S/A values should be used to obtain adequate workability (e. g., 0.46 to 0.50).
- Coarse aggregate with ½ in. (12.5 mm) MSA is recommended to achieve adequate workability and mechanical properties.
- Use of thickening-type VMA is required for SCC made with moderate and relatively high *w/cm* and low binder content to enhance stability and homogenous in-situ properties. The use of thickening-type VMA at low level can enhance static stability (lower column segregation index). VMA can also be used in highly stable SCC (e. g., low *w/cm*) to enhance robustness.
- Use of air entrainment required for frost durability (use of air entraining admixture will help stabilize small air bubbles).

- SCC made with Type III cement and 20% Class F fly ash can exhibit better slump flow retention, higher passing ability, and higher filling capacity than that with Type I/II cement.
- The HRWRA demand decreases with the increase in *w/cm* and binder content. The use of Type III cement and 20% Class F fly ash necessitates higher HRWRA demand than that required for SCC prepared with Type I/II cement (thus resulting in lower early-age compressive strength).
- Better slump flow retention can be obtained with SCC made with low *w/cm* because of the higher HRWRA demand required to achieve 26.0 to 27.5 in. (660 to 700 mm) slump flow.
- Surface settlement of SCC increases with the increase in binder content and *w/cm.*
- Plastic viscosity decreases with the increase in binder content and *w/cm* but increases slightly with the increase in S/A.
- Thixotropy or structural build-up at rest of the SCC decreases with the increase in binder content and *w/cm*. Higher thixotropy can be detrimental to surface finish and advantageous to formwork pressure.
- Initial relative form pressure at 3.3 ft (1 m) in height cast at 13.1 – 16.4 ft/hr (4 – 5 m/hr) varies between 0.80 and 1.00 of hydrostatic pressure; it increases with the increase in binder content and *w/cm* but decreases with the increase in S/A.
- Incorporation of thickening-type VMA in the mixture could delay setting and increase the time to attain peak temperature, thus leading to some delay in early-age strength development. In that case, steam curing could be used to accelerate the strength development.

Regarding the mechanical properties, the following recommendations and observations are made:

- Mechanical properties increase with the decrease in *w/cm*.
- Increase in binder content can lead to higher 56-day compressive strength but lower 18-hour MOE and 7-day flexural strength.
- The increase in S/A results in lower MOE at 18 hours (steam curing) and 56 days (moist curing) and higher flexural strength.
- SCC made with Type III cement and 20% of fly ash exhibits lower early age compressive strength than that made with Type I/II cement (due to higher HRWRA demand).
- SCC made with Type III cement and 20% Class F fly ash can develop higher compressive strength and MOE at 56 days but lower mechanical properties at 18 hours than for concrete made with Type I/II cement (mainly due to delayed setting resulting from greater HRWRA demand).

Regarding the visco-elastic properties, the following recommendations and observations are made:

- The increase in binder content increases drying shrinkage and creep.
- Although for a given binder content, drying shrinkage is expected to increase with increased *w/cm*, for the derived statistical models since the drying shrinkage includes also autogenous shrinkage that decreases with the increase in *w/cm*.
- SCC mixtures made with Type I/II cement develop less creep and shrinkage than those prepared with Type III cement and 20% Class F fly ash. However, the latter concrete has better workability and higher mechanical properties than the former SCC. Therefore, it is recommended to use Type III cement and 20% Class F fly ash with reduction of binder content to assure better overall performance.
- Concrete mixtures containing high binder content and low *w/cm* can exhibit high autogenous shrinkage; the majority (85% to 95%) of which occurs in the first 28 days (values after 56 days can vary between 100 and 350 µstrain, depending on mixture composition).
- Autogenous shrinkage is mostly affected by binder type and paste volume. SCC made with Type III cement and 20% Class F fly ash can develop higher autogenous shrinkage and creep than SCC made with Type I/II cement.
- For a given *w/cm*, increasing binder content can result in higher drying shrinkage (500 and 1000 µstrain after 300 days is possible).
- SCC exhibits up to 30% higher drying shrinkage at 300 days than HPC made with similar *w/cm* but different paste volume. More detailed information on drying shrinkage can be found in Section D.4.5, Statistical Models for Visco-elastic Properties.
- Increase in S/A can lead to higher long-term drying shrinkage.
- The binder type does not have significant effect on drying shrinkage but can significantly affect creep (e.g. SCC made with Type III cement with 20% fly ash exhibited higher creep than similar SCC proportioned with Type I/II cement regardless of the binder content, *w/cm*, S/A, and use of thickening-type VMA).
- The *w/cm* does not have considerable effect on creep because other parameters such as binder content, binder type, and S/A have more predominant influence on creep.
- SCC exhibits up to 20% higher creep after 300 days than HPC made with similar *w/cm* but different paste volume. More detailed information on creep can be found in Section D.4.5, Statistical Models for Visco-elastic Properties.

D.7.3 Validation of Code Provisions to Estimate Mechanical and Visco-elastic Properties

Mechanical properties

Material coefficients of existing prediction models were modified to provide better prediction of mechanical properties of SCC for precast, prestressed concrete bridge elements. Following codes are recommended:

- ACI 209 and CEB-FIP codes with modified coefficients for predicting compressive strength development.
- Current AASHTO 2007 model for predicting elastic modulus.
- Current AASHTO 2007 model for estimating flexural strength.

Visco-elastic properties

Creep and shrinkage strains measured in experimental factorial design were compared to values predicted by the AASHTO 2007, AASHTO 2004, ACI 209, CEB-FIP 1990, and GL 2000 (Gardner and Lockman, 2001) models. Coefficients of the following existing models were modified to provide better prediction of visco-elastic properties for SCC. These modifications are as follows:

- AASHTO 2004 model for estimating drying shrinkage.
- AASHTO 2007 model for estimating creep.

D.7.4 Homogeneity of In-situ Strength and Bond to Reinforcement

- Highly flowable SCC should have adequate static stability with maximum surface settlement of 0.5%, column segregation index of 5%, and percent static segregation of 15. These limits are especially critical in deep elements. Such SCC can develop at least 90% in-situ relative compressive strength (core results) and modification factor of 1.4 for bond to horizontally embedded prestressing strands. More detailed information on bond to prestressing strands is presented in Section D.6.1, Bond Strength of Prestressing Strands.
- Use of highly viscous SCC (plastic viscosity greater than 0.073 psi.s (500 Pa.s) or T-50 nearing 6 seconds obtained from upright cone position) should be avoided to ensure adequate self-consolidation.

D.7.5 Structure Performance of AASHTO-Type II Girders

The following conclusions and observations are based on the construction and testing of the full-scale precast pretensioned girders:

- With the casting from only a single location at midspan of the 31-ft (9.44-m) long girders, no visible segregation was observed and fewer “bug holes” were observed in the SCC concrete than in the HPC.
- The transfer lengths were similar for the four concrete mixtures, and were considerably shorter than the values given in the 2007 AASHTO Specifications and the ACI 318-05 Code.
- At time of prestress release at 18 hours, the coefficients on the square root of the compressive strength used to determine the modulus of elasticity for the SCC concretes were about 4% and 11% lower than those for the HPC concretes.
- Due to the low elastic modulus and greater drying shrinkage, greater elastic shortening losses and greater long-term losses of prestress occurred, resulting in smaller cambers for the SCC girders.

- The cracking moments were similar for the SCC girders and the companion HPC girders, and the uncracked and cracked stiffnesses for all four girders were very similar.
- The cracking shears were similar for all four girders.
- The four girders failed in shear after developing a significant number of wide shear cracks. The failure shears exceeded the nominal shear resistances predicted using the approach given in 2007 AASHTO Specifications. The increased shear resistance was probably due to the strength and stiffness of the top and bottom flanges of the girders.
- The shear crack widths just before failure were greater than 0.24 in. (6 mm).
- The flexural resistances of the HPC girders exceeded the predicted nominal resistances using the 2007 AASHTO Specifications.
- The flexural resistances of the SCC girders were within 1.5% of the flexural resistance calculated using the approach in the 2007 AASHTO Specifications.
- The HPC girders exhibited higher ductilities than the corresponding SCC girders.
- The lower shear resistance and lower ductility experienced by the SCC girders are probably due to the lower volume of coarse aggregate that reduces aggregate interlock and results in lower energy absorption capability on the sliding shear failure plane.

APPENDIX A

Literature Review of Factors Affecting Performance of SCC Used in Precast, Prestressed Applications

CHAPTER 1- FRESH CHARACTERISTICS OF SCC, TEST METHODS, AND ACCEPTANCE CRITERIA

1.1 Workability Requirements

SCC is a new category of high-performance concrete that exhibits a low resistance to undergo deformation and flow into place, even among closely-spaced obstacles, without segregation. The **workability** of concrete refers to the ease of mixing, placement, consolidating, and finishing of concrete. In SCC technology, it also refers to the flowing and filling properties of the concrete during placement. Workability of SCC is described in terms of filling ability, passing ability, and stability; these properties are characterized by specific testing methods. In general, the workability requirements of SCC are complex and depend on several parameters, including the type of construction, selected placement and consolidation methods, the complexity and shape of the formwork, the degree of congestion of the structural member, the intended placement method, labor skills, as well as quality assurance and quality control measures.

Properly designed SCC should have the high workability necessary for ease of placement while maintaining high stability in order to secure homogeneous distribution of in-situ engineering properties and durability [Khayat, 1999]. The basic workability characteristics of SCC that must be balanced to ensure successful casting of SCC include deformability (filling ability), passing ability, and resistance to segregation. These properties are affected by a number of parameters, including raw material properties and concrete proportioning.

The deformability of fresh SCC is closely related to that of the cement paste. An increase in water-to-cementitious materials ratio (*w/cm*), or water-to-binder ratio (*w/b*), can secure high deformability; however, it can also reduce the cohesiveness of the paste and mortar, thus leading to segregation of fine and coarse aggregate particles. Therefore, a balance is needed to enhance deformability without a substantial reduction in cohesiveness. Another major parameter that affects deformability is the interparticle friction between the various solid particles in the concrete matrix. The use of high-range water reducing admixture (HRWRA) can disperse cement grains and reduce interparticle friction among cement particles. It is also essential to reduce the relative volume of coarse aggregate and sand, and increase the paste volume in order to enhance deformability.

Another primary parameter necessary to provide self-consolidating properties is the passing ability of the concrete. The required level of passing ability is a function of the structural detailing and formwork shape of the cast element. Concrete with low cohesiveness can segregate

since it cannot maintain proper suspension of aggregate to ensure uniform deformation around the various obstacles. The lack of stability can weaken the interface between the aggregate and cement paste, and increase the tendency to develop local microcracking that can increase permeability and reduce mechanical properties. The third criterion for producing high-performance SCC is to provide high resistance to segregation following the casting of the concrete to ensure homogenous distribution of the in-place quality of the hardened concrete.

The risk of segregation can decrease by reducing the water-to-cementitious materials ratio (*w/cm*), coarse aggregate content, and maximum size of aggregate (MSA). The increase in viscosity of the cement paste can enhance the suspension of solid particles during flow, hence leading to better dynamic stability. The incorporation of viscosity-modifying admixture (VMA) along with HRWRA can be effective in controlling bleeding, segregation, and surface settlement of highly flowable concrete [Khayat and Guizani, 1997].

1.2 Performance Characteristics of SCC

Concrete can be classified as SCC if the requirements for high filling ability, adequate passing ability, and sufficient segregation resistance are fulfilled. **Filling ability** (also referred to as deformability or unconfined flowability) describes the ability of the concrete to undergo change in shape and flow around obstacles to completely encapsulate the reinforcement and fill the formwork under its own weight without any mechanical consolidation. Concrete with high filling ability can flow into place and completely fill all spaces within the formwork, under its own weight and without any mechanical vibration. This property is of importance to the casting technique, distance between filling points, etc.

Passing ability refers to the ability of the concrete to pass among various obstacles and narrow spacing in the formwork without blockage, in the absence of any mechanical vibration. Such blockage can rise from local aggregate segregation in the vicinity of obstacles. SCC with high filling ability and passing ability can achieve high filling capacity of the formwork.

Filling capacity is the ability of the concrete to completely fill intricate formwork or formwork containing closely spaced obstacles, such as reinforcement. SCC can achieve high ***filling capacity*** if it has high levels of filling ability and passing ability to spread into a predetermined section, fill the form by the action of gravity alone, and achieve complete filling of the section without segregation or blockage.

The resistance to ***segregation*** (stability) describes the ability of the concrete to maintain a homogeneous distribution of its various constituents. There are two types of stability characteristics in SCC technology: dynamic and static stability. **Dynamic stability** refers to the resistance of concrete to the separation of constituents during transport, placement, and spread into the formwork. **Static stability** refers to the resistance to segregation and bleeding after casting while the concrete is still in a plastic state. Inadequate stability can lead to segregation and blockage of the spread of the SCC into place. Bleeding, segregation, and surface settlement can weaken the interface between cement paste and embedded reinforcement, reducing bond

strength. This can also increase the tendency to develop local microcracking at the interface between aggregate and cement paste, which has a direct influence on transport properties. Stability is especially critical in deep structural elements such as prestressed girders and wall elements.

From a rheological point of view, SCC is characterized by low yield stress to ensure high deformability and moderate plastic viscosity to maintain homogeneous suspension of solids, hence reducing inter-particle collision, segregation, flow blockage, and uniform suspension of solid particles during casting and until setting. **Rheology** refers to the science of deformation and is instrumental to understand the flow of fresh SCC. Concrete rheology is evaluated using special rheometers that enable one to relate variations in shear stress to shear rate. The **yield stress** corresponds to the minimum shear stress required to initiate flow. Below such value, the mixture does not undergo any deformation and behaves rather as a solid material. Once under flow, the constant of proportionality between shear stress and shear rate is referred to as the **plastic viscosity**; this refers to the resistance of the plastic material to undergo a given flow. The reduction in viscosity decreases the ability of the mixture to maintain homogeneous dispersion of constituents. The level of plastic viscosity of the concrete has a direct bearing on stability, surface finish, and in-situ properties.

From a workability point of view, the selection of material constituents of SCC intended for use in precast, prestressed beam elements and the mixture proportioning should be tailored to achieve the following performance characteristics necessary for successful casting of structural elements:

- self-consolidation – the SCC must flow into place and encapsulate the reinforcement without segregation or blockage;
- retention of deformability – compatible with duration of transport and provisions for field adjustments. This is especially critical for confined flowability;
- adequate stability during transport and placement (dynamic stability) – resistance to material separation during pumping and spread through restricted spacing;
- proper resistance to segregation, bleeding, and surface settlement during the dormant period of cement hydration (static stability); and
- uniform surface quality and homogeneous distribution of in-situ hardened concrete.

In developing the performance requirement of SCC for mix design purposes, it is necessary to consider both the fresh and hardened properties of the concrete. As shown in Fig. 1.1, the fresh properties of SCC are dictated by the flow characteristics of the concrete, which in turn, are influenced by a number of factors, including the characteristics of locally available materials, the characteristics of the cast element, and concrete production and placement considerations. Therefore, in specifying the plastic properties of SCC, it is important to take into consideration the characteristics of the cast element that can affect flow characteristics, including its shape, dimensions, and density of reinforcement, as will be discussed later in Table 1.4. The type of placement device should also be considered as various placement devices (bucket, tucker, discharge truck, conveyor, or pump) can provide different levels of energy to the cast concrete

and continuity of the placement. The maximum required spread distance in the formwork and initial free-fall drop height must also be considered in selecting the performance characteristics of the fresh concrete. Finally, characteristics of locally available raw materials, including aggregate shape and grading, are also of prime importance for the flow characteristics of SCC.

1.3 Test Methods to Assess Workability of SCC

Various test methods have been used to assess the key workability characteristics of SCC. In general, these methods include the components required for evaluating simultaneously deformability, passing ability, and resistance to segregation, since these properties are rather interrelated. Table 1.1 summarizes some of the main test methods that have been proposed for the evaluation of the workability of SCC. In this Chapter, the following test methods are elaborated: the slump flow and visual assessment, V-funnel, L-box, U-box, J-Ring, filling capacity, rheological parameters, surface settlement test, and column segregation test.

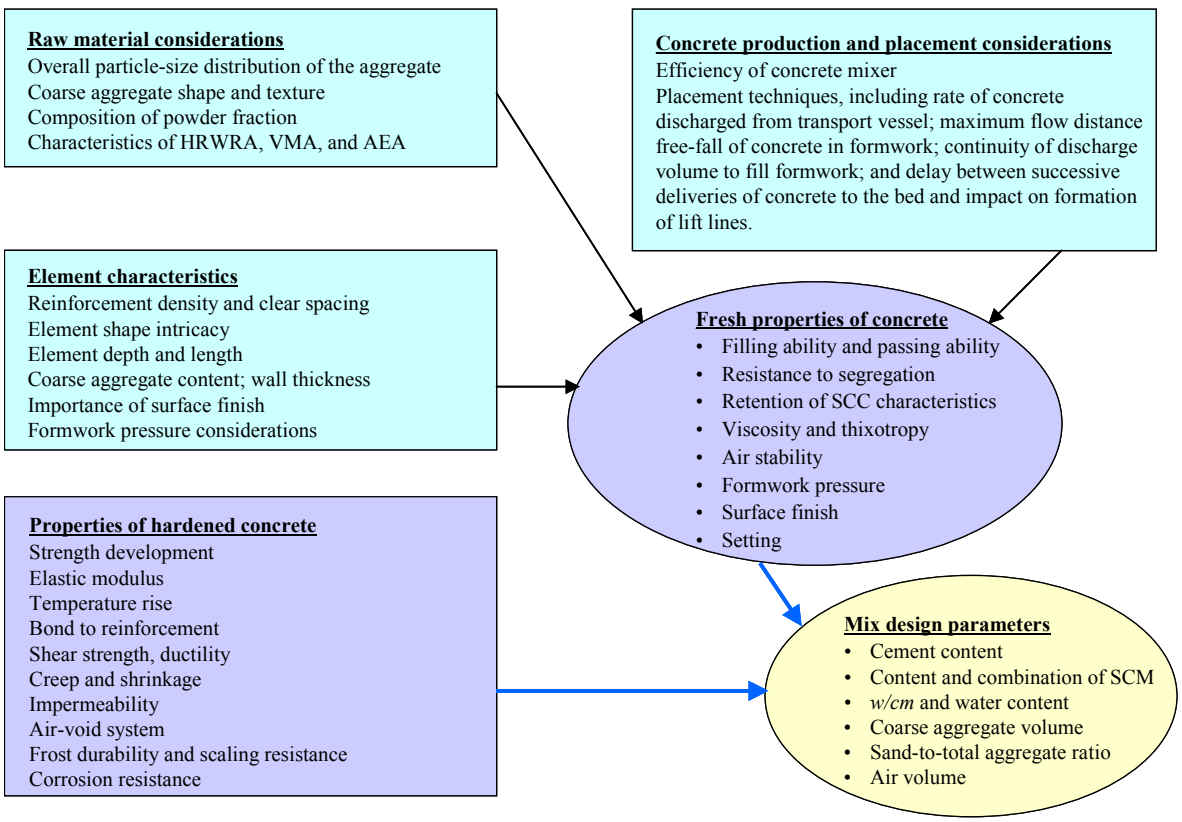

Fig. 1.1 – Parameters affecting requirements for fresh properties and mixture design of SCC

Table 1.1 – Workability properties of SCC and alternative methods

	Test method	Modification of test given maximum-size aggregate
Filling ability	Slump flow T-50_{cm} slump flow	None
Passing ability	L-box U-box J-Ring V-funnel Orimet	Different openings in L-box, U-box and J-Ring
Filling capacity	Filling vessel (caisson)	None
Segregation resistance	GTM screen test Surface settlement Column segregation Visual stability index V-funnel at $T_{5\ min}$ L-box at $T_{5\ min}$ Pressure bleeding Plunger penetration	None

1.3.1 Slump flow and T-50 flow time

The slump flow test consists of determining the mean diameter of concrete spread at the end of a slump test (ASTM C 143). The test evaluates the capability of the concrete to deform under its own weight. The time needed for the concrete to spread 500 mm (T-50) is noted. This is sometimes referred to as T-20, indicating the elapsed time required for the concrete to spread 20 in. in diameter. The slump cone can also be used in the inverted position to perform the slump flow test (Fig. 1.2). Values of slump flow are nearly the same as determined by either the upright or inverted slump cone. In the inverted position, a single operator can carry out the test since it is not necessary to hold down the cone when filling the cone with concrete.

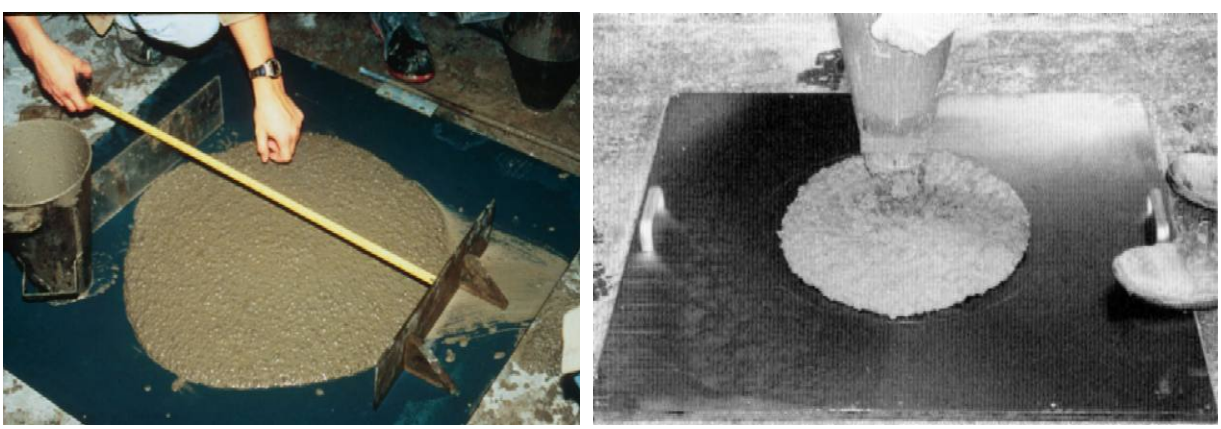

Fig. 1.2 – Slump flow and inverted slump flow tests

1.3.2 V-funnel test

As shown in Fig. 1.3, the V-funnel test consists of a V-shaped recipient with an opening of 2.55 × 3 in. (65 × 75 mm) at the bottom (Fig. 1.3). In some cases, the recipient has a section of 3 × 3 in. (75 × 75 mm). After a given time following the filling of the recipient (usually one minute), the bottom gate is removed, and the time required for the concrete to flow through the tapered outlet is determined. This test is used to evaluate the ability of aggregate particles and mortar to change their flow paths and spread through a restricted section without segregation and blockage. The use of the standard 2.55 × 3 in. (65 × 75 mm) section can enable the evaluation of flow in 3-D, whereas the modified 3 × 3 in. (75 × 75 mm) section corresponds to 2-D flow. The V-funnel can be filled with SCC and left for a given period of time, for example 5 minutes to allow some segregation to take place before determining the V-funnel flow time. Considerable increase in flow time can be indicative of segregation.

1.3.3 L-box test

The L-box test consists of an L-shaped apparatus, as shown in Fig. 1.4 [Petersson et al., 1996]. The vertical part of the box is filled with 12.7 L of concrete and left at rest for one minute. The gate separating the vertical and horizontal compartments is then lifted, and the concrete flows out through closely spaced reinforcing bars at the bottom. A gap of 1.4 in. (35 mm) between the 0.5 in. (12 mm) diameter bars is selected for aggregate top-size of 0.55 in. (14 mm). The time for the leading edge of the concrete to reach the end of the 24 in. (600 mm) long horizontal section is noted. The heights of concrete remaining in the vertical section ($h_1 = 24 - H_1$) and that at the leading edge ($h_2 = 6 - H_2$) are determined. The h_2/h_1 value is calculated to evaluate the self-leveling characteristic of the concrete. The test assesses filling and passing ability of SCC, and serious lack of stability (segregation) can be detected visually. The horizontal section of the box can be marked at 8 and 16 in. (200 and 400 mm) from the gate and the times taken to reach these points measured. These are known as the T20 and T40 times and are an indication of the filling ability. Obvious blocking of coarse aggregate behind the reinforcing bars can be detected visually. The sections of bar can be of different diameters and spaced at different intervals: in accordance with normal reinforcement considerations, 3 times the maximum aggregate size might be appropriate. The bars can principally be set at any spacing to impose a more or less severe test of the passing ability of the concrete.

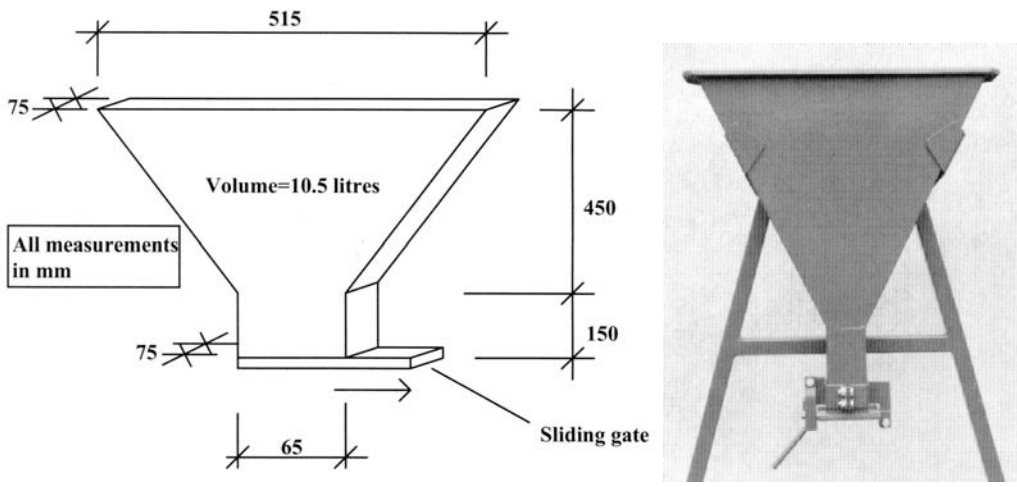

Fig. 1.3 – V-funnel apparatus

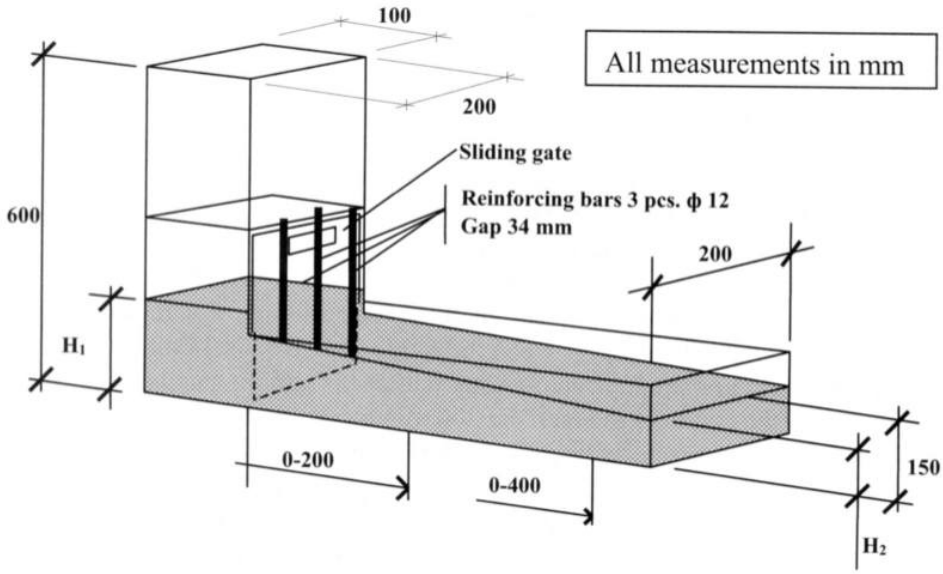

Fig. 1.4 – Schematic of L-box apparatus

1.3.4 U-box test

The test was developed by the Technology Research Center of the Taisei Corporation in Japan Sometimes the apparatus is called a "box-shaped" test. The test is used to evaluate the narrow-opening passing ability of SCC under a particular head of fresh concrete. As shown in Fig. 1.5, the U-box test has two compartments separated by a sliding gate at the bottom that is fitted between the two sections. Reinforcing bars with nominal diameters of 0.5 in. (13 mm) are installed at the gate with center-to-center spacing of 2 in. (50 mm). This creates a clear spacing

of 1.4 in. (35 mm) between the bars. The left-hand section is filled with about 20 liters of concrete, then after one minute, the gate is lifted and concrete flows upwards into the other section. Once the rising level of the concrete is stabilized in the second compartment, the filling height (Bh) is determined; the maximum Bh value is 13.3 in. (338 mm). The time to complete flow into the leading compartment represents the rate of deformability.

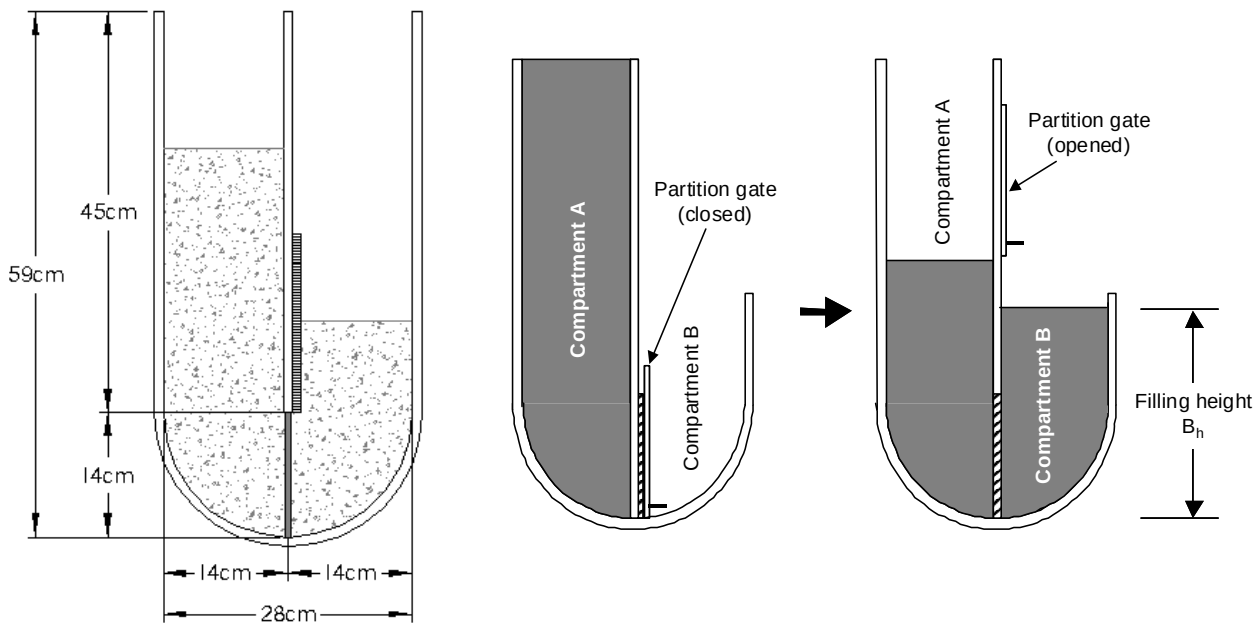

Fig. 1.5 – Schematic of L-box apparatus

1.3.5 J-Ring test

The J-Ring test can be used to assess the restricted deformability of SCC through closely-spaced obstacles [Bartos, 1998]. It consists of an open steel ring, drilled vertically with holes to accept threaded sections of reinforcement bar. These sections of bar can be of different diameters and spaced at different intervals: in accordance with normal reinforcement considerations, 3 times the maximum aggregate size (MSA) might be appropriate. The diameter of the ring of vertical bars is 12 in. (300 mm) and the height 4 in. (100 mm). Two different gaps of 1.4 or 2 in. (35 or 50 mm) between deformed bars can be used. A gap of 1.4 in. (35 mm) is typically used when using 3/8 in. (9.75 mm) MSA.

The ring is positioned around the base of the slump cone, and the mean diameter of the spread concrete at the end of slump flow is determined (Fig. 1.6). The J-Ring can be used in conjunction with the slump flow, the Orimet test, or eventually even the V-funnel. These combinations test the flowing ability and (the contribution of the J-Ring) the passing ability of the concrete.

The German SCC Guidelines propose that the difference between the spread of the slump flow and J-Ring should not exceed 2 in. (50 mm) when the concrete is to spread through reinforcing steel [Brameshuber and Uebachs, 2001]. The difference in height of concrete inside and outside of the J-Ring is also used to assess the passing ability of the SCC and its resistance to blockage and segregation. This is carried out by measuring the value d1 in the center of the J-Ring and at eight points da,i and db,i (i = 1 to 4) just inside and just outside the ring (see Fig.1.6). The value h1 is calculated as 110 - d1 and all values ha,i are calculated as 110 - da,i and hb,i as 110 – db,i, (i = 1 to 4). The four values hmi are calculated as h1 - ha,i; with hm = median (hmi), (i = 1 to 4). Similarly, the four values hri are calculated as ha,i - hb,i with the median value hr = median (hri). The value (2×hr – hm) is finally determined, which should be a maximum of 15 mm.

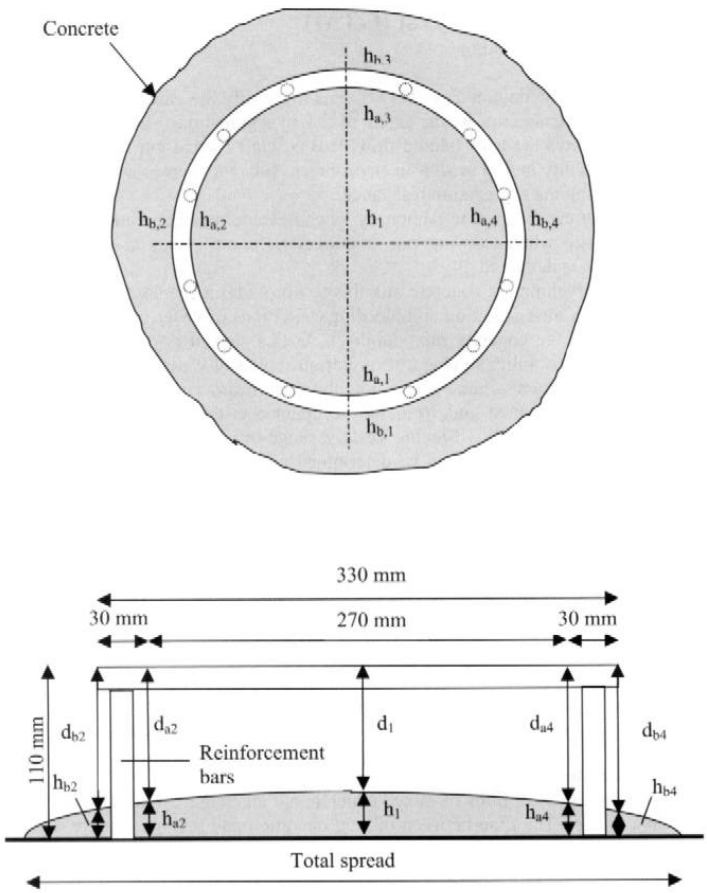

Fig. 1.6 – Photos of J-Ring test

1.3.6 Filling capacity test (caisson box test)

This test is also known as the Kajima test. The test is used to measure the filling ability of self-compacting concrete with a maximum aggregate size of 0.79 in. (20 mm). The filling capacity can be determined by casting the concrete in a transparent box (caisson) measuring 11.9 × 19.7 × 11.8 in. (300 × 500 × 300 mm) containing closely-spaced smooth horizontal tubes of 0.6 in. (16 mm) in diameter (Fig. 1.7) [Yurugi et al., 1993]. The clear spacing among the tubes is 1.3 in. (34 mm) in both the horizontal and vertical directions. The concrete is introduced from a tremie pipe equipped with a hopper at a constant rate of approximately 0.71 ft^3/min (20 L/min) until the concrete reaches 8.9 in. (220 mm) from the bottom part of the box. Once the flow of the SCC among the bars ceases, the area occupied by the concrete in the restricted section is used to calculate the filling capacity. The maximum filling capacity is 100% when determined according to the ratio given in Fig. 1.7. This test is difficult to perform on site due to the complex structure of the apparatus and large weight of the concrete. It gives a good impression of the self-compacting characteristics of the concrete. Even a concrete mix with a high filling ability will perform poorly if the passing ability and segregation resistance are poor.

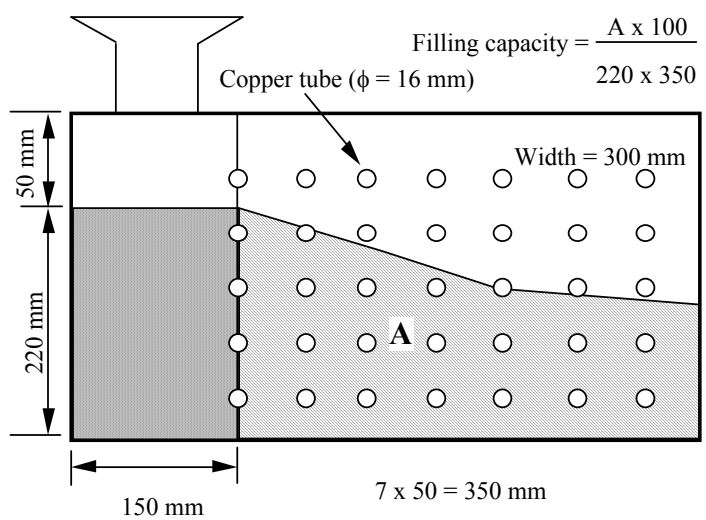

Fig. 1.7 – Caisson filling capacity test

1.3.7 Surface settlement test

This test method can be used to evaluate the surface settlement of SCC from a plastic state until the time of hardening [Manai, 1995]. It enables the quantification of the effect of mixture proportioning on static stability. A PVC column measuring 7.9 in. (200 mm) in diameter and 27.6 in. (700 mm) in height can be used. The settlement is monitored using a dial gauge with a 0.0004 in. (0.01 mm) precision or a linear variable differential transformer (LVDT) with a minimum travel range of 2 in. (50 mm), fixed on top of a thin acrylic plate placed at the upper surface. The plate is anchored into a 23.6 in. (600 mm) high concrete column, and the settlement

is monitored until a steady state condition (Fig. 1.8). The initial reading of the LVDT is taken after 60 sec from the installation of the monitoring set-up. Changes in the readings are monitored at 15-minute intervals for the first three hours and then at 30-minute intervals thereafter. Changes in height are monitored until reaching steady state conditions, which corresponds approximately to the beginning of hardening.

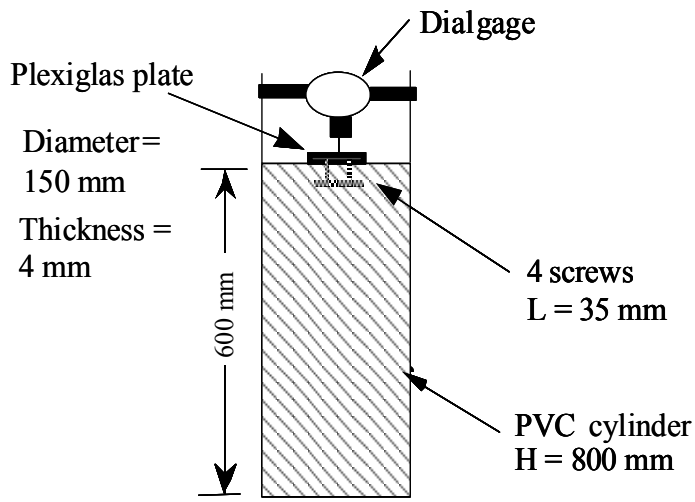

Fig. 1.8 – Surface settlement test

1.3.8 Column segregation test

This test consists in casting concrete in a column measuring 26 in. (660 mm) in height and 7.9 in. (200 mm) in diameter, and then determining the variation in the relative concentration of coarse aggregate at four sections along the concrete sample [Assaad et al., 2004]. The PVC tube is divided into four sections of 6.5 in. (165 mm) in height, as shown in Fig. 1.9. A leak-free joint is provided between the sections so that they can be easily uncoupled. Before conducting the test, the concrete is consolidated vertically five times using a 0.79 in. (20 mm) diameter rodding bar. The concrete is then left to rest for 15 minutes. After removing each section, starting from the top, the concrete is weighed, and the mortar is washed out on a 0.2 in. (5 mm) sieve to retain coarse aggregate. The aggregate is dried to obtain a near surface-saturated dry moisture condition. The coarse aggregate content is then determined for each of the four samples. The coefficient of variation (C.O.V.) of the aggregate distribution along the column is taken as a segregation index (Iseg).

1.3.9 Visual stability index

In order to differentiate the textural properties of the SCC, the appearance of the concrete can be qualitatively ranked according to set criteria given in Table 1.2. The Visual Stability Index (VSI) procedure assigns a numerical rating of 0 to 3, in 0.5 increments, to the texture and homogeneity

of the fresh mixture based on observations made for concrete after conducting the slump flow [Daczko and Kurtz, 2001]. The VSI can be considered as a static stability index when it is observed in a wheelbarrow or mixer following some period of rest time (static condition). This can also be the case during the transport of fresh concrete in a tuckerbilt mixer where some segregation can be induced by the vibration during transport.

Fig. 1.9 – Photo of column segregation test

Table 1.2 – Visual stability index (VSI) rating [Daczko and Kurtz, 2001]

Rating	Criteria
0	No evidence of segregation in slump flow patty, mixer drum, or wheelbarrow
1	No mortar halo in the slump flow patty, but some slight bleeding on the surface of the concrete in the mixer drum and/or wheelbarrow
2	Slight mortar halo, < 0.39 in. (10 mm), in slump flow patty and noticeable layer of mortar on the surface of the testing concrete in the mixer drum and wheelbarrow
3	Clearly segregating by evidence of large mortar halo, > 0.39 in. (10 mm), and thick layer of mortar and/or bleed water on concrete surface in mixer or wheelbarrow

1.3.10 GTM screen stability test

This test was developed by the French contractor, GTM, and consists of taking a sample of 0.88 ft3 (10 L) of concrete, allowing it to stand for a period to allow any internal segregation to occur,

then pouring half of it onto a 0.2 in. (5 mm) sieve of 13.8 in. (350 mm) diameter, which stands on a sieve pan on a weigh scale. After 2 minutes, the mortar that passed through the sieve is weighed, and expressed as a percentage of the weight of the original sample on the sieve. Empirical observations suggest that the percentage of mortar passing through the sieve (segregation ratio) should be 5% to 15% of the weight of the sample for the segregation resistance of SCC to be considered as satisfactory. Strong likelihood of segregation would be obtained for segregation ratios above 15%, and certainly above 30%.

The method may be applied, to some extent, when carrying out suitability or acceptance inspection tests on site. Though simple, the method is not rapid, and requires an accurate weigh-scale, so may not be too suitable for site use. The repeatability of results may be questionable.

1.3.11 Orimet test

The Orimet was developed as a method for assessment of highly workable, flowing, fresh SCC mixes on construction sites. The Orimet consists of a vertical casting pipe fitted with a changeable inverted cone-shaped orifice at its lower, discharge end, with a quick-release trap door to close the orifice (Fig. 1.10). Operation consists simply of filling the Orimet with SCC, then opening the trapdoor and measuring the time taken for light to appear at the bottom of the pipe. The test measures the ease of flow of the SCC; shorter flow times indicate greater flowability. For SCC, a flow time of 5 sec or less is considered appropriate. The inverted cone shape at the orifice restricts flow, and prolonged flow times may give some indication of the susceptibility of the mix to blocking and/or segregation.

Usually, the orifice has an 80 mm internal diameter that is appropriate for assessment of concrete mixes of aggregate size not exceeding 0.79 in. (20 mm). Orifices of other sizes, usually from 2.8 to 3.5 in. (70 to 90 mm) in diameter, can be fitted instead. Operation consists simply of filling the Orimet with concrete then opening the trapdoor and measuring the time taken for light to appear at the bottom of the pipe (when viewed from above). This test is able to simulate the flow of fresh concrete during actual placing on sites. The test has the useful characteristic of being capable of differentiation between highly workable and flowing mixes, and might therefore be useful for compliance testing of successive loads on site. The timing procedure, however, may be subject to error, and ideally requires two people.

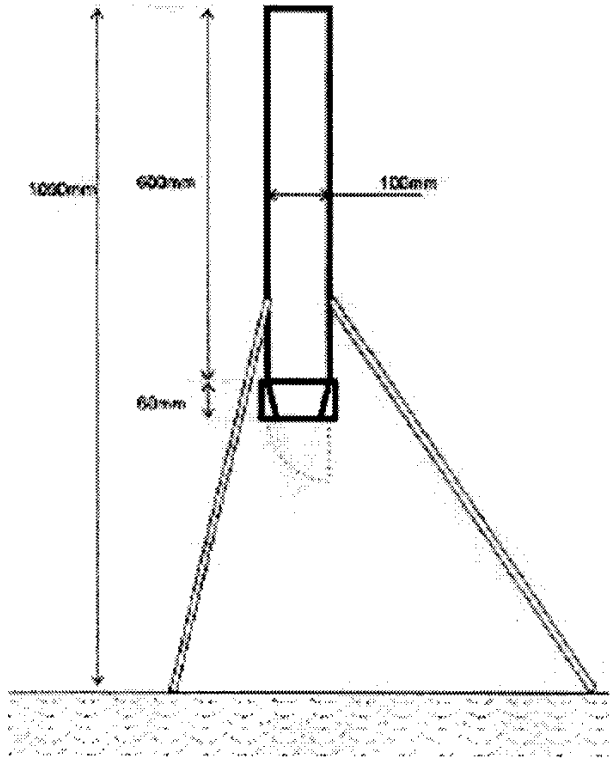

Fig. 1.10 – Schematic of the Orimeter test

1.3.12 Concrete rheometer test

The rheological parameters can be evaluated using a number of concrete rheometers. For example, a modified Tattersall two-point workability rheometer (IBB rheometer, Beaupré, 1994) can be used. The test requires the use of a concrete sample of 0.88 ft^3 (25 L) and involves recording the torque required to maintain a given impeller angular velocity. An H-shaped impeller rotating in a planetary motion is used. The testing protocol consisted of increasing gradually the mixing speed up to a maximum velocity. Subsequently, the speed is reduced in predetermined steps varying from 0.6 to 0.1 rps, and the required torque to shear the material and applied rotation speed is recorded. A total of five measurements are taken at each velocity to determine the mean corresponding torque. The data from the descending part of the curve are used to derive the rheological parameters assuming a Bingham fluid. The slope of the linear regression and the intercept with the torque axis at zero shear rates are determined and related to the torque plastic viscosity (h) and apparent yield stress (g), respectively.

1.4 Combined Test Methods and Performance Specifications

A number of test methods have been used to characterize the properties of SCC, including deformability, passing ability, and segregation resistance. No single method has been found to characterize all the relevant workability aspects of SCC. Furthermore, no combination of test methods has achieved universal approval. Yet, proper selection of combined test methods can facilitate the assessment of workability of SCC and facilitate the testing protocol. For site quality control, two test methods are generally sufficient to monitor production quality.

In the acceptance inspection for workability of SCC, combination tests of slump flow and V-funnel or slump flow and J-Ring [EFNARC, 2002] are generally used. The recommended test methods and performance specifications are normally used in combination to assess the workability of SCC intended for various applications. For example, in Sweden, slump flow and L-box tests have been frequently used for acceptance control at building site with target values of slump flow for outdoor civil engineering concrete structures of 26-29.9 in. (660-760 mm) with a range of approximately $\pm$2 in. (50 mm) [Billberg, 1999; Swedish Concrete Association, 2002]. Such SCC used for civil engineering structures should have a T-50 time of 3 to 7 sec and L-box blocking ratio (h_2/h_1) greater than 0.8. In Japan, slump flow, V-funnel, and U-box tests are popularly adopted, with typical slump flow values of 23.6-26 in. (600-660 mm).

The German SCC Guidelines [2001] recommends the combined use of the J-Ring and slump flow tests to evaluate the passing ability of SCC. This guideline proposes that the difference between flow diameters of the two tests should not exceed 2 in. (50 mm) for the concrete to achieve sufficient flow through the reinforcement. Similarly, the PCI Interim Guidelines [2003] recommend the combined use of the J-Ring and Orimet tests. The extent of blocking is much less affected by the flow characteristics. The greater the difference in height of concrete inside and outside of the J-Ring, the lower the passing ability of the SCC. However, the Guidelines reported that although these combinations of tests measure flow and passing ability at the same time, the results are not independent.

Table 1.3 summarizes various recommendations of combined test methods and performance specifications suggested by the European Federation of National Trade Associations (EFNARC) [2002], Precast, Prestressed Concrete Institute (PCI) Interim Guidelines [2003], RILEM Technical Committee 174 [2001], Swedish Concrete Association (SCA) [2002], and Japan Society of Civil Engineers (JSCE) [1998].

Table 1.3 – Workability characteristics, suitable test methods, and recommended values of SCC mixtures intended for structural applications

Workability characteristic	Test methods	Suggested limits
Deformability and flow rate (filling ability, unrestricted flow)	Slump flow	1. Author, Hwang et al. [2004]: 24.4-28.3 in. (620-720 mm) 2. EFNARC: 25.6-31.5 in. (650-800 mm) MSA up to 0.79 in. (20 mm) 3. JSCE: 23.6-27.6 in. (600-700 mm) 4. PCI: ≥ 26 in. (660 mm) 5. RILEM TC 174: N/A 6. Swedish Concrete Association: 25.6-29.2 in. (650-750 mm)
	T-50	2. 2-5 sec 4. 3-5 sec 6. 3-7 sec
Passing ability (narrow-opening passing ability, confined flow, restricted flow, dynamic stability)	V-funnel [a)]	1. < 8 sec (outlet of 75 × 75 mm) 2. 6-12 sec (outlet of 65 × 75 mm) 4. 6-10 sec (outlet of 65 × 75 mm)
	L-box, h_2/h_1	2. > 0.8 4. > 0.75 6. > 0.8
	U-box, B_h	2. h_2-h_1: 0-1.2 in. (0-30 mm) 3. Rank 1 [b)] for rebar spacing of 1.4-2.4 in. (35-60 mm) Rank 2 [c)] for rebar spacing of 2.4-8 in. (60-200 mm) 4. Rank 1 [b)]
	J-Ring [d)]	2. 0-0.39 in. (0-10 mm) 4. < 0.59 in. (15 mm)
Filling capacity (filling ability + passing ability, restricted deformability)	Filling vessel (caisson)	1. ≥ 80% 2. 90-100%
	L-box, h_2/h_1	Same as passing ability
	U-box, B_h	Same as passing ability
	J-Ring spread	Same as passing ability
Static stability (resistance to segregation, bleeding, and settlement)	Surface settlement	1. ≤ 0.5%
	Visual stability index	4. Rating of 0 or 1
	Penetration depth	5 and 6. ≤ 0.31 in. (8 mm)
	GTM screen stability	2. 0-15%

a) V-funnel opening of 2.6 × 3 in. (65 × 75 mm)
b) Rank 1 refers to B_h of 12 in. (305 mm) through 0.2 to 0.4 in. (5 to 10 mm) diameter bars with 1.4 in. (35 mm) clear spacing
c) Rank 2 refers to B_h of 12 in. (305 mm) through 0.12 to 0.5 in. (3 to 12 mm) diameter bars with internal and external spacing of 1.4 and 1.8 in. (35 and 45 mm), respectively
d) J-Ring value is determined by the difference in height of concrete between the inside and outside in the J-Ring

Values outside the recommended ranges may be acceptable if the producer can demonstrate satisfactory performance for specific conditions, such as large spacing between reinforcement, layer thickness less than 19.7 in. (500 mm), short distance of flow from point of discharge, few obstructions to pass in the formwork, simple design of formwork, etc. The requirements presented in Table 1.3 are to be fulfilled at the time of placing. Likely changes in workability during transport should be taken into account in production. It should be noted that values outside these ranges might be acceptable if the producer can demonstrate satisfactory performance in the specific conditions (e.g., large spaces between reinforcement, layer thickness less than 500 mm, short distance of flow from point of discharge, very few obstructions to pass in the formwork, very simple design of formwork, etc.).

The performance specification of the SCC depends on aggregate characteristics. For example, the University College London [1999] proposed workability recommendations for concrete made with MSA of 0.39 in. (10 mm) and 0.79 in. (20 mm). For mixtures made with 0.39 in. (10 mm) MSA, slump flow consistency of 23.6 to 27.6 in. (600 to 700 mm), V-funnel flow time of 2 to 4 sec, and U-box height of 11.8 to 13.8 in. (300 to 350 mm) are recommended. In the case of SCC prepared with 0.79 in. (20 mm) MSA, these values can be 25.6 to 27.6 in. (650 to 700 mm), 4 to 10 sec, and 11.8 to 13.8 in. (300 to 350 mm), respectively.

In order to ensure adequate filling of restricted structural elements, as in the case of repair applications, filling capacity of 80% is considered as a lower limit according to the performance specifications suggested by the Ministry of Transport of Quebec (MTQ) for use of SCC in structural repair of bridges, as elaborated in Table 1.4 [MTQ, 2000; Hovington, 2000]. Such concrete necessitates the casting of highly flowable concrete to ensure the proper filling of complex structural elements that represent, in some cases, a high degree of restriction by reinforcement and difficult access for consolidation.

Table 1.4 – Specifications of MTQ 3102 Standard [MTQ, 2000; Hovington, 2000]

Characteristics	Target value
Fresh air content	6% - 9%
Slump flow	25.5 ± 2 in. (650 ± 50 mm)
V-funnel flow time	≤ 6 sec (outlet of 75 × 75 mm)
28-day compressive strength	5,075 psi (35 MPa)
Minimum cementitious content	809 lb/yd^3 (480 kg/m^3)
Water-cementitious materials ratio (*w/cm*)	0.35 - 0.40
Maximum coarse aggregate volume, MSA 0.39 in. (10 mm)	33% by volume
Sand-paste ratio, in volume	0.6 - 0.75

The caisson filling capacity test is a severe test and provides good visual assessment of the self-leveling ability of the concrete and its ability to spread into place in 3-D among various obstacles without any mechanical consolidation. This test is, however, difficult to perform on site and necessitates relatively intensive labor and long testing time. Hwang et al. [2004] established statistical correlations between the filling capacity and combinations of the slump flow and either the L-box blocking ratio (h_2/h_1), J-Ring, or V-funnel flow time:

- Combined test methods-1: L-box blocking ratio (h_2/h_1) and slump flow

  Filling capacity (%) = – 49.1 + 0.149 slump flow (mm) + 51.3 h_2/h_1 (1.1)

- Combined test methods-2: Slump flow and J-Ring flow or spread between slump flow and J-Ring flow

  Filling capacity (%) = – 77.5 + 0.162 slump flow (mm) + 0.094 J-Ring (mm) (1.2)

  Filling capacity (%) = – 72.3 + 0.25 slump flow (mm) – 0.09 [Slump flow (mm) – J-Ring flow (mm)] (1.3)

- Combined test methods-3: Slump flow and V-funnel flow time

  Filling capacity (%) = – 23.5 + 0.175 slump flow (mm) – 0.425 flow time (sec) (1.4)

These multiple regression equations are valid for stable mixtures with slump flow values between 20 and 28.3 in. (500 and 720 mm), minimum filling capacity of 40%, and mixtures made with 0.39 in. (10 mm) MSA. Figures 1.11, 1.12, and 1.13 present contour diagrams of the filling capacity related to the slump flow and L-box tests, the slump flow and J-Ring tests, and the slump flow and V-funnel flow tests, respectively. These figures are based on equations 1.1, 1.2, and 1.3, respectively.

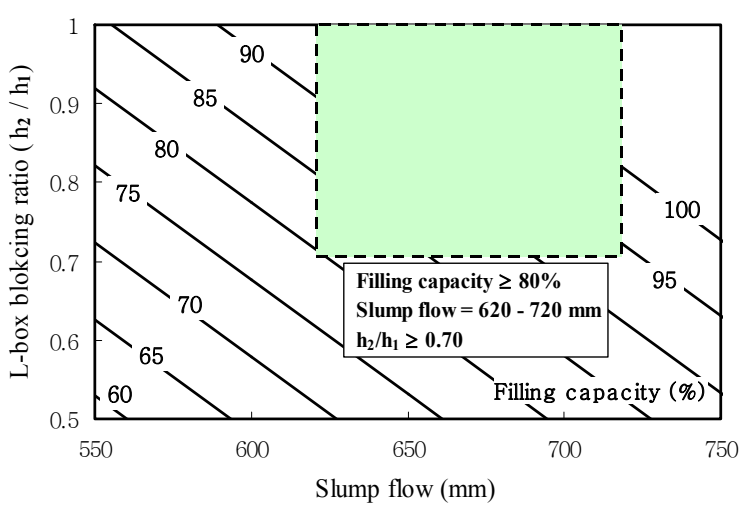

Fig. 1.11 – Contour diagrams of filling capacity, slump flow, and L-box blocking ratio

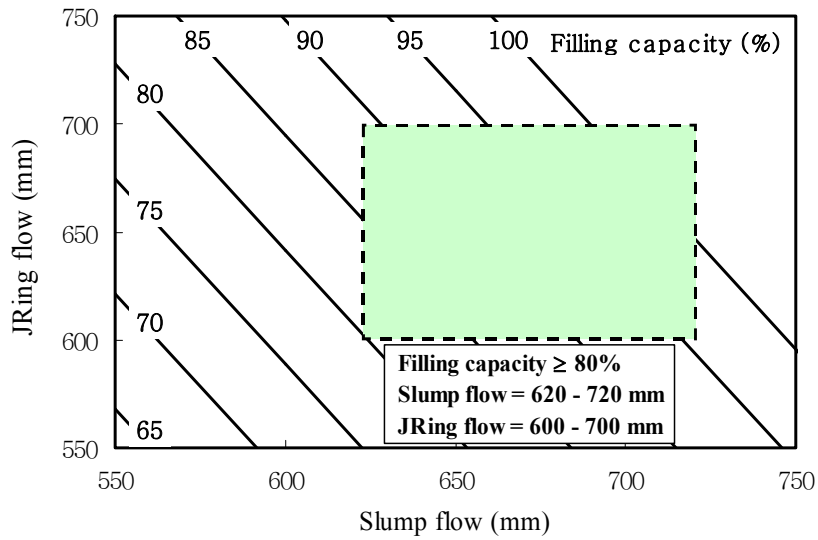

Fig. 1.12 – Contour diagrams between filling capacity, slump flow, and J-Ring flow values

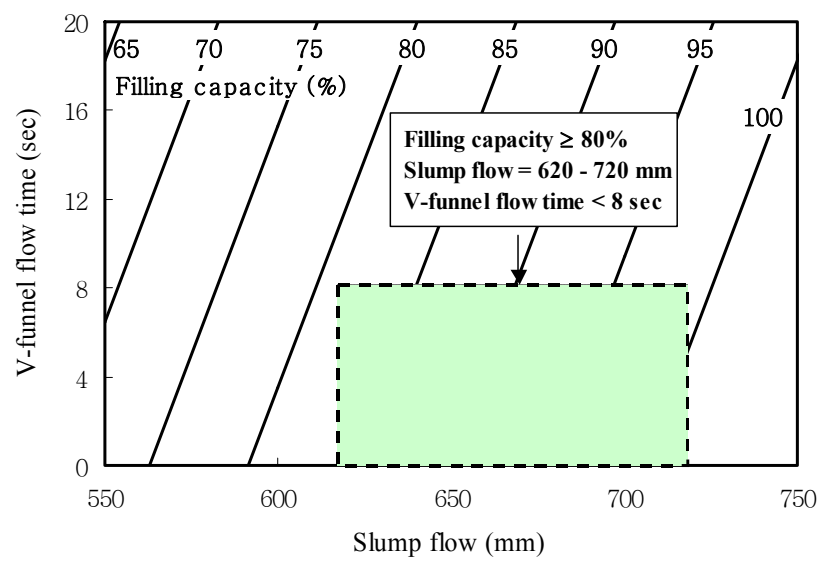

Fig. 1.13 – Contour diagrams between filling capacity, slump flow, and J-Ring flow values

Given the fact that the surface settlement test is rather long for use as a quality control test in the field, the rate of settlement after 15, 30, and 60 minutes from the beginning of the settlement test can be determined. As shown in Fig. 1.14 [Hwang et al., 2004], the rate of settlement after 30 minutes can provide a good correlation to the maximum surface settlement. The settlement rate of 0.16%/h measured at 30 min, corresponding to 0.5% maximum settlement, is also specified to ensure proper static stability of SCC.

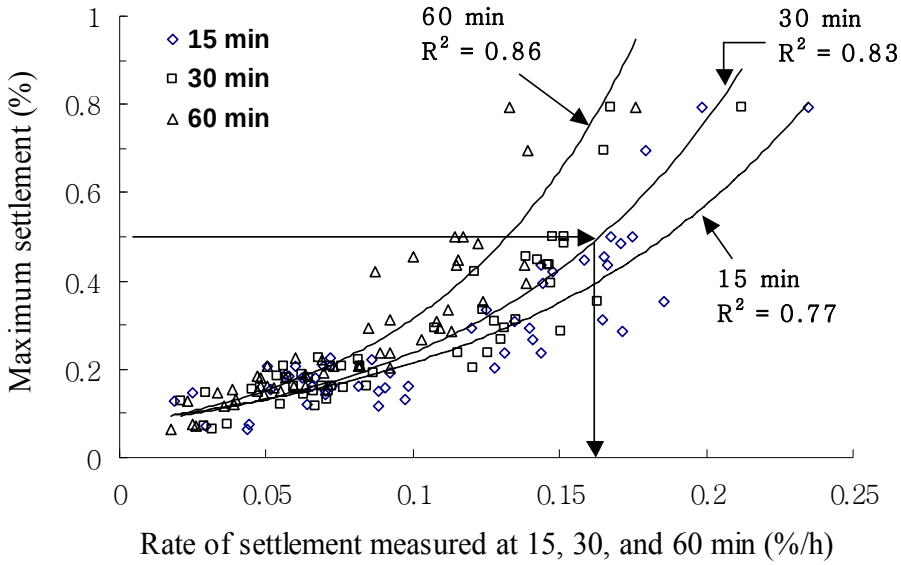

Fig. 1.14 – Relationship between rate of settlement and maximum settlement

Based on the above results, a set of performance specifications of SCC intended for use in structural applications is shown in Table 1.5. Such concrete made with MSA of 0.39 in. (10 mm) should have slump flow of 24.4 to 28.3 in. (620 to 720 mm) and, depending on the passing ability test, L-box blocking ratio (h_2/h_1) greater than 0.70, J-Ring flow of 23.6 to 27.6 in. (600 to 700 mm), slump flow minus J-Ring flow lower than 2 in. (50 mm), or V-funnel flow time smaller than 8 seconds. Such values can lead to SCC with high filling capacity (greater than 80%).

Table 1.5 – Combined test methods and recommended workability values to secure filling capacity ≥ 80% suggested for SCC used in repair applications [Hwang et al., 2004]

<table>
<tr><th></th><th>Combined test methods-1</th><th>Combined test methods-2</th><th>Combined test methods-3</th></tr>
<tr><td>Filling ability</td><td colspan="3">Slump flow: 24.4 - 28.3 in. (620 - 720 mm)</td></tr>
<tr><td rowspan="2">Passing ability</td><td rowspan="2">L-box blocking ratio (h_2/h_1) ≥ 0.7</td><td>J-Ring flow: 23.6 – 27.6 in. (600 - 700 mm)</td><td rowspan="2">V-funnel [1)] flow time ≤ 8 sec</td></tr>
<tr><td>(Slump flow - J-Ring flow) ≤ 2 in. (50 mm)</td></tr>
<tr><td>Static stability</td><td colspan="3">Maximum surface settlement ≤ 0.5%
Settlement rate at 30 minutes ≤ 0.16 (%/h)</td></tr>
</table>

1) V-funnel opening of 3 × 3 in. (75 × 75 mm)

1.5 Most Significant Workability Characteristics Affecting the Performance of Precast, Prestressed Bridge Elements

The most relevant and important workability characteristics that can influence the constructability of precast, prestressed bridge elements are reviewed in this section. Test methods that are most relevant for the fabrication of precast, prestressed concrete bridge elements are suggested, and their limitations are highlighted.

As summarized in Table 1.1, SCC should exhibit high filling ability, proper passing ability, and adequate segregation resistance. In the selection of material constituents and mixture proportioning of SCC for the precasting of prestressed bridge elements, it is essential that the concrete be self-consolidating, i.e. it should flow into place and encapsulate the prestressing strands and reinforcing bars without segregation or blockage. The SCC should exhibit adequate retention of self-consolidation properties for a given period of time (typically 30 minutes for SCC prepared at precast plants) to enable the transport of the concrete and the completion of the placement without the need to readjust the mixture. The concrete should exhibit proper dynamic stability to maintain homogeneous suspension of the mixture constituents during transport and placement. It should also exhibit high resistance to segregation, bleeding, and surface settlement after casting until the onset of hardening, i.e. proper static stability. The latter characteristic is especially important to maintain uniform properties of the hardened concrete. The finished element should also have uniform surface quality and superior surface finish.

In order to secure these workability characteristics, it is important to design a concrete mixture that can represent good balance between the deformability, passing ability, and stability aspects. In selecting the fresh characteristics of the SCC for the casting of prestressed elements, the reinforcement density, the shape and dimensions of the element, the selected placement method used at the precasting plant should be taken into consideration to ensure proper performance. Different placement techniques used in precasting plants, such as truck discharge, pumping, conveyor, buggy, and drop tube, can provide different energy during the initial flow of SCC and hence can affect the level of workability necessary to ensure proper filling of the formwork, encapsulation of the reinforcement, and stability of the mixture. As illustrated in Table 1.6, other characteristics that can affect the required workability level include the following aspects: the cast element reinforcement level, shape, intricacy, depth, wall thickness, and length; the required surface finish; and the content of coarse aggregate. The recommendations given in Table 1.6 are based on work reported by Constantiner and Daczko [2002]. In this analysis, seven different aspects were selected to characterize the cast elements with three levels each (low, medium and high). The ranking of the element characteristics describe a certain level of required workability of the SCC that can be selected to ensure adequate performance. For example, a mixture used for casting highly reinforced elements with intricate shape should have a slump flow greater than 26 in. (660 mm), T-50 time of 3 to 5 sec, L-box blocking ratio (h_2/h_1) higher than 0.75, and V-funnel flow time of 6 to 10 seconds. Shaded areas in Table 1.6 represent potential problem situations that should be avoided.

Table 1.6 – Fresh property limits adequate for member characteristics

Member characteristics		Slump flow			T-50			L-box (h_2/h_1)			J-Ring		
		< 560 mm	560 - 660	> 660	< 3 sec	3 - 5	> 5	< 75%	75 - 90	> 90	< 15 mm	10 - 15	> 10
Reinforce-ment level	Low												
	Medium	■			■			■					■
	High	■			■			■				■	■
Element shape intricacy	Low												
	Medium	■					■						
	High	■	■				■					■	■
Element depth	Low												
	Medium												■
	High				■							■	■
Surface finish importance	Low												
	Medium	■					■						
	High	■	■				■						
Element length	Low												
	Medium	■						■					■
	High	■	■		■			■	■			■	■
Wall thickness	Low	■	■				■	■					
	Medium	■											
	High												
Coarse aggregate content	Low												
	Medium												■
	High									■		■	■
Placement energy	Low	■	■					■				■	■
	Medium	■											■
	High				■								

When optimizing the SCC mixture, it is important to select appropriate test methods to qualify the performance of the concrete in the laboratory and later on to control the quality of the concrete at the plant. Based on the discussion presented earlier, the most promising test methods that are relevant for the fabrication of precast, prestressed concrete bridge elements are given in Table 1.7. It is important to note that the slump flow, T-50, Visual stability index, J-Ring, and column segregation tests are under consideration by ASTM for use in SCC technology. The advantages and limitations of these methods are discussed earlier. These methods are also selected because of their simplicity. Limited published information regarding the repeatability and relative error of the various test methods, and the influence of the operator on testing accuracy. As this information becomes available in the literature (some on-going European studies are underway) and new test methods are developed.

Table 1.7 – Test methods relevant for fabrication of precast, prestressed bridge elements

	Test methods for mix design	Test methods for quality control at plant
Filling ability	Slump flow (ASTM C1611) T-50_{cm} slump flow	Slump flow (ASTM C1611) T-50_{cm} slump flow
Passing ability	L-box J-Ring (ASTM C1621) V-funnel	L-box J-Ring (ASTM C1621)
Filling capacity	Caisson test (filling vessel)	
Segregation resistance	Visual stability index (VSI) Surface settlement and rate of settlement Column segregation (ASTM C1610)	Visual stability index (VSI) Rate of settlement after 30 minutes Column segregation (ASTM C1610)

As mentioned earlier, the caisson filling capacity test provides good visual assessment of the self-leveling ability of SCC and its ability to fill highly congested sections. This test can be used in the design of the mixture whenever such conditions are presented for precast, prestressed bridge elements. Otherwise, simpler methods can be combined to predict the filling capacity of SCC, as presented earlier in Table 1.5 and equations 1.1, 1.2, and 1.3.

The VSI test provides visual assessment of the homogeneity of the SCC. However, a mixture with rating of 0 or 1 determined shortly before casting of a structural element does not guarantee proper resistance to segregation during the plastic state. It is recommended to complement the VSI test with a quantitative test, such as the column segregation or surface settlement test. The former is rather long as it involves the determination of the relative coarse aggregate content at four sections along a concrete column. For field use, this may be substituted by determining the relative coarse aggregate content at the top and bottom sections only, as suggested in ASTM C1610 standard test method. The waiting time of 15 minutes before removing the concrete from various sections for wet sieving may also be reduced providing that the concrete is subjected to some controlled vibration in the form of shock. The surface settlement test is rather long for use as a quality control test in the field. Instead, the rate of settlement after 30 minutes can be determined, as shown in Fig. 1.14. Such value has been shown to correspond well to the maximum surface settlement.

The various deformability and stability test results can be related to the rheological parameters of the concrete, yield stress and plastic viscosity. For example, the slump flow and T-50 values can be related to the yield stress and plastic viscosity, respectively. Similarly, the speed of spread of the concrete through the V-funnel, U-box, and L-box can be related to the plastic viscosity [Khayat et al., 2004]. Assaad et al. [2004] related the segregation index (I_{seg}) of the column segregation test to the apparent yield stress (g) and torque plastic viscosity (h) determined using the IBB rheometer. SCC with apparent g and h of 0.3 to 1.7 N.m and 17 to 30 N.m.s, respectively, were shown to develop adequate resistance to segregation with I_{seg} values of 2% to 4%. Khayat et al. [2004] found that SCC with g values ranging between 0.3 to 1.7 N.m and h

values of 17 to 27 N.m.s can achieve high passing ability determined using the L-box with flow time of 4 to 8 seconds. Better understanding of the rheological parameters that control the workability of SCC is important in developing mix design approaches and interpreting quality control test methods.

Finally, it is important to note that in designing and controlling the workability of SCC, the stability of air should be investigated, even when the concrete is not air-entrained concrete. SCC made with polycarboxylate-based HRWRA can exhibit, in some cases, increase in air volume during mixing and agitation. Such increase in air content does not necessary lead to better air-void system, in the absence of air-entraining admixture. Therefore, the stability of the air must be well determined and controlled in developing the concrete mixture and in quality control during production, especially in regions where air-entrainment is required for frost durability.

CHAPTER 2 - REQUIREMENTS FOR MATERIALS CONSTITUENT AND MIX DESIGN CONSIDERATIONS

2.1 Requirements for Constituent Materials

2.1.1 Introduction

The use of suitable materials, having the required performance specifications, is necessary for producing SCC. The production of SCC requires that the quality of all constituent materials be uniform, and that, to a greater degree than is the case with normal concrete. Specifying the characteristics of the constituent materials thus becomes critical in the case of SCC. A choice of suitable constituent materials is vital to the optimizing of the mix design of SCC adapted to different applications. This applies to all constituents, including chemical admixtures [Swedish Concrete Association, 2002].

This section reviews the main specifications for constituent materials (cements and blended cements, aggregates, mineral admixtures, and chemical admixtures) that are recommended by the AASHTO LRFD Bridge Design [2004] and Construction [1998] Specifications and four State DOTs (Texas, Florida, New York, and Washington). These DOTs are selected from different regions covered by AASHTO for the United States. More details of the various specifications regarding material constituents are given in the Appendix. Specific information regarding the effect of the characteristics of the various constituent materials presented in this section are discussed elsewhere in this report, including workability of SCC in Chapter 1 and mechanical properties of SCC in Chapter 4.

2.1.2 Cements and blended cements

Selection of the type of cement will depend on the overall requirements for the concrete, such as early-age compressive strength, mechanical properties, durability, and color considerations in the case of architectural applications where color and color uniformity are important requirements [PCI Interim Report, 2003]. All standardized cements can be employed in SCC. Differences in cement properties should be taken into account when designing mixtures for specific applications. Type I Portland cement, general-purpose cement, is suitable for all uses where the special properties of other types of cement are not required. Type II and IV cements can be used to reduce the heat of hydration. Type III cement provides high strengths at early age and is particularly appropriate for obtaining high release strengths. Type V cement is used in concrete exposed to severe sulphate attack. Blended hydraulic cements can also be used. These cements are produced by intergrinding and/or blending various combinations of Portland cement, blast-furnace slag, fly ash, and other pozzolans. Unless otherwise specified, Types IS (Portland blast-furnace slag cement) and IP (Portland-pozzolan cement) are used for general concrete construction. Type P Portland-pozzolan cement is used where high early strengths are not required. Type S slag cement is used with Portland cement in concrete or with lime in mortar but

is not used alone in structural concrete. The Standard Specifications generally restrict cement to Portland cement Types I, II, or III; air-entrained Portland cement Types IA, IIA, or IIIA; or blended hydraulic cement Types IP or IS. It should also be noted that not all types of cement are readily available and that the use of some types is not permitted by some states [PCI Bridge Design Manual, 1997].

Table 2.1 reviews some of the main requirements for cement and blended hydraulic cement recommended by AASHTO and Texas, Florida, New York, and Washington State DOTs. According to AASHTO LRFD Bridge Design [2004] and Construction [1998] Specifications, Types I, II, or III cement; Types IA, IIA, or IIIA air-entrained cement; or Types IP or IS blended hydraulic cements shall be used for the construction of precast, prestressed concrete elements, unless otherwise specified. In particular, the pozzolan constituent in Type IP Portland-pozzolan cement shall not exceed 20% of the mass of the binder. Washington DOT specifications [2002] stipulate that the maximum content of fly ash in Type IP (MS) is limited to 25% by mass of the cementitious material, and that the use of blast-furnace slag and pozzolans other than fly ash are not allowed in Type IP (MS) and Type I (PM) (MS) cements.

Florida State DOT specifications [2004] require the use of Types I or III with fly ash or blast-furnace slag, or Type II, Type IP, Type IS, or Type IP (MS) cements for precast superstructure and prestressed elements exposed to moderately aggressive environments. Texas State DOT [2004] sets maximum limits to the fineness of cements used for the production of prestressed concrete members. For example, the mean Blaine fineness of Type I, II, and V cements and Type III cement should be limited to 400 and 560 m^2/kg, respectively (Table A.1, Appendix).

New York State DOT specifications [2002] stipulate that the contents of fly ash, microsilica, and blast-furnace slag should not exceed 22%, 10%, 22% by mass, respectively, of the total binder for Types IP, SF, and SM blended cements. In the case of ternary blend cement consisting of Portland cement, fly ash, and microsilica, the total supplementary cementitious content should not exceed 30%, by mass of binder. The fly ash and microsilica portions in ternary blend cement shall range from 15%-20% and 6%-10% of the total mass of binder, respectively. Other chemical and physical requirements for blended Portland cements required by various New York State DOT specifications are summarized in Table A.2 in Appendix.

The total content of cementitious materials used in prestressed concrete designed to achieve 28-day compressive strength of 4,000 to 8,000 psi (27.6 to 55.2 MPa) can vary from 600 to 1000 lb/yd^3 (356 to 593 kg/m^3) [PCI Bridge Design Manual, 1997]. Such values can vary on a regional basis depending on the concrete constituents. The AASHTO LRFD Bridge Design Specifications [2004] suggest that the sum of Portland cement and other cementitious materials should not exceed 800 lb/yd^3 (475 kg/m^3), except for Class P (HPC) concrete where the sum of Portland cement and other cementitious materials should not exceed 1000 lb/yd^3 (593 kg/m^3).

Table 2.1 – Review of various requirements for cements and blended hydraulic cements

	Cement	Blended cement
AASHTO LRFD Bridge Design and Construction Spec. [2004, 1998]	- AASHTO M 85 (ASTM C 150) - Type I, II, or III cement - Types IA, IIA, or IIIA air-entrained cement	- AASHTO M 240 (ASTM C 595M) - For Type IP cements, pozzolan constituent < 20% - LOI of the pozzolan < 5%
Texas State DOT [2004]	- ASTM C 150 - Limestone < 3% - Max. fineness values for Types I, II, III, and V cements: refer to Table A.1 in Appendix - Max. fineness for Type I, II, and white cements used in prestressed concrete members must not exceed requirements for Type III cement	- ASTM C 595 - For Type IP cements, pozzolan constituent: between 20% and 40% Pozzolan must be a Class F fly ash - Type IS (Portland blast-furnace slag) cements must be the moderate sulfate resistance type IS (MS)
Florida State DOT [2004]	- Types I or III with fly ash or blast-furnace slag, or II for precast superstructure and prestressed elements under moderately aggressive environment - Alkali content of Portland cement ≤ 0.6%	- Types IP, IS, or IP(MS) cements for precast superstructure and prestressed elements under moderately aggressive environment
New York State DOT [2002]	- Types I, II, or I/II cement that meets the requirements of both Type I and II cements	- Chemical and physical requirements: refer to Tables A.2 & A.3 in App. A - Type IP: fly ash < 22% - Type SF: microsilica < 10% - Type SM: blast-furnace slag < 22% - Ternary blend cement: Portland cement + fly ash + microsilica, the total SCM < 30%, by mass. Fly ash and microsilica portion shall range from 15%-20% and 6%-10%, respectively, of the total binder mass
Washington State DOT [2002]	- Types I, II, or III cement conforming to AASHTO M 85 - Alkali content < 0.75% - C_3A content < 8%	- Types IP (MS), I (SM) (MS) or I (PM) (MS) cement conforming to AASHTO M 240 - Use of slag and pozzolans other than fly ash are not allowed in Type IP (MS) and Type I (PM) (MS) cement - Fly ash content in Type IP (MS) < 25%, except when required for mitigation of alkali silica reactivity

Concrete mixtures made with more than 840 lb/yd^3 (500 kg/m^3) of cement can exhibit greater risk of shrinkage. In some cases involving the casting of highly congested sections, the binder content (and filler if any) can be quite high: 930 lb/yd^3 (550 kg/m^3) to increase the paste volume. The use of cement with C_3A content higher than 10% may cause problems of poor workability retention. The typical cement content is 590 to 758 lb/yd^3 (350 to 450 kg/m^3).

For SCC applications where visual appearance is important, to minimize the color variation of the surfaces exposed to view in the finished structure, cement of the same type, brand, and color from the same mill shall be used throughout a given project [PCI Bridge Design Manual, 1997]. Belite-rich Portland cement has been used in Japan for SCC in some cases [JSCE, 1999]. This cement contains a belite content of 40% to 70%, which is higher than moderate-heat Portland cement and can therefore develop lower heat rise.

2.1.3 Aggregates

The workability of SCC and a number of key hardened properties are greatly influenced by the characteristics of the aggregates. Gravel, crushed stone, or combinations can be used as a coarse aggregate. In the case of fine aggregate, natural sand or manufactured sand can be used, and should conform to the grain-size distribution recommendations of the project specifications.

The main requirements of aggregates, coarse and fine aggregate used in the production of normal concrete that are recommended by AASHTO and four State DOTs are summarized in Table 2.2. Examples of gradation requirements for coarse and fine aggregates stipulated in Standard specifications of various State DOTs are summarized in Tables A.4 through A.13 in Appendix.

The nominal maximum size of coarse aggregate (MSA) should be selected based on mix-requirements and the minimum clear spacing between the reinforcing steel, clear cover to reinforcement, and thickness of the member [PCI Bridge Design Manual, 1997]. For prestressed concrete construction of normal consistency, the maximum size of aggregate (MSA) is limited to 3/4 in. (19 mm) [AASHTO LRFD Bridge Design Specifications, 2004]. In the design of SCC, typically the MSA values are smaller than those of conventional vibrated concrete. The reduction in MSA is required to reduce the risk of segregation. Proportioning of SCC with relatively large MSA would necessitate an increase in yield value (lower deformability) to prevent segregation.

According to PCI Interim Guidelines [2003], in general, the MSA of SCC mixtures shall not exceed: one-third of the thickness of panels, three-fourths of the minimum clear depth of cover, and two-thirds of the spacing between individual reinforcing bars or bundles of bars or pretensioning tendons or post-tensioning ducts. Additionally, aggregate particles smaller than 0.005 in. (0.125 mm) contribute to the powder content of the mix [EFNARC, 2002]. Size and volume of coarse aggregate are influential in obtaining the passing ability of the concrete. Therefore, the MSA may accept one stone size smaller than suggested in ACI 302 to improve the passing ability. The MSA depends on the particular applications and is usually limited to 20 mm [EFNARC, 2002; PCI Interim Guidelines, 2003]. Typically, values of MSA in SCC range between 1/2 and 3/4 in. (12.5 and 19 mm) in North America and 0.63 to 0.79 in. (16 to 20 mm)

in Europe. In some repair applications or placement of SCC in highly congested and restricted sections, MSA values of 3/8 in. (9.5 mm) are used. In order to minimize the risk of blocking in SCC placement, the maximum relative volume of coarse aggregate with MSA of 1/2 to 3/4 in. (12.5 to 19 mm) should be in the range of 28% of the total volume for casting sections with a high level of reinforcement and 32% for sections with a low level of reinforcement [ACI, 2004].

Table 2.2 – Review of various requirements of coarse and fine aggregates

	Coarse aggregate	Fine aggregate
AASHTO LRFD Bridge Design and Construction Specifications [2004, 1998]	- AASHTO M 80 - MSA of 19 mm for prestressed concrete	- AASHTO M 6
Texas State DOT [2004]	- Gravel, crushed blast-furnace slag, recycled crushed hydraulic cement concrete, crushed stone, or combinations - Gradation requirements: refer to Table A.4 in Appendix	- Natural or manufactured sand or a combination thereof with or without mineral filler - Gradation requirements: refer to Table A.5 in Appendix
Florida State DOT [2004]	- Natural gravel or resulting from the crushing of parent rock - Physical property requirements, except as noted herein: a) Los Angeles Abrasion: max. loss 45%, b) Soundness: max. loss 12%, and c) Flat or elongated pieces: max. 10% - Gradation requirements: Tables A.6 and A.7 in Appendix	- Natural silica sand, screenings, local materials, or subject to approval, other inert materials with similar characteristics, or combination - Gradation requirements: refer to Table A.8 in Appendix
New York State DOT [2002]	- Crushed stone, crushed gravel, screened gravel or crushed air-cooled blast-furnace slag - All coarse aggregates shall meet the requirements of Table A.9 in Appendix - Gradation requirements: refer to Table A.10 in Appendix	- Natural sand or manufactured sand - Fine aggregates from more than one source or of more than one type of material may be blended. - Fine aggregates meeting the requirements of Table A.11 in Appendix shall be accepted
Washington State DOT [2002]	- Gravel, crushed stone, or other inert material or combinations - Gradation requirements: refer to Table A.12 in Appendix	- Gradation requirements: refer to Table A.13 in Appendix

For normal weight concrete, fine and coarse aggregates should conform to the requirements of AASHTO M 6 and M 80, respectively [PCI Bridge Design Manual, 1997]. Fine aggregate component should be well-graded concrete sand; it may beneficial to blend natural and manufactured sand to improve SCC plastic properties [ACI, 2004]. All normal concreting sands, including crushed or rounded sands, siliceous or calcareous sands, can be used. The amount of fines, including fine sand, that is less than 0.005 in. (0.125 mm) should be considered as powder material in proportioning SCC. Such fine content can have marked effect on the rheology of SCC. A minimum amount of fines (arising from the binders and fine sand) must also be achieved to avoid segregation.

All types of coarse aggregates are suitable for SCC. Rounded aggregate particles improve flow, due to lower internal friction among aggregate particles. Crushed aggregate tends to improve strength (especially tensile and flexural strengths) because of the interlocking of the aggregate particles. It would require greater HRWRA dosage. The volume of coarse aggregate in SCC is usually reduced compared to high-performance concrete of normal consistency. When the volume of coarse aggregate in SCC exceeds a certain limit, the opportunity for collision or contact between coarse aggregate particles increases rapidly and there is an increased risk of blockage when the concrete passes through spaces between steel bars.

Consistency of grading is of vital importance. Slightly gap-graded aggregates can lead to greater deformability than continuously graded aggregate that might experience greater internal friction and decrease flow. Gap-graded aggregate can, however, increase the risk of bleeding, and proper measures should be taken to ensure adequate static stability of the concrete.

Achieving a high degree of packing density of the selected coarse and fine aggregates is essential in reducing the paste content in SCC, and hence cement factor and water content. Khayat et al., [2000b] showed that the increase in packing density of combined sand and coarse aggregate can reduce HRWRA demand and plastic viscosity of SCC made of various binder contents, especially for concrete with low *w/b*. Some concrete manufacturers use several types of aggregate fractions to build up their concrete fine aggregate, which increases the possibility to direct it towards a suitable grading curve. In the absence of fine material in the sand, an increased amount of filler is usually required.

For a given reinforcement density and clear spacing considerations, the optimum coarse aggregate content in SCC depends on the MSA and aggregate shape. The reduction in MSA can enable the use of a higher proportion of coarse aggregate, and the use of rounded aggregates can enable the use of a higher content than in the case of crushed aggregates.

The particle shape of the coarse aggregate has an effect on workability of SCC and water demand. A rounded coarse aggregate will impart greater fluidity for the same water content of a mix compared to a crushed stone of similar size. The blending of No. 7 or No. 8 size stone can often be beneficial to improving the overall characteristics of the mixture.

As in the case of normal concrete, if aggregates susceptible to alkali-aggregate reactivity are used in prestressed concrete members, special precautions must be observed. These include the use of low-alkali cement, blended cements, or pozzolans [PCI bridge design manual, 1997].

2.1.4 Mineral admixtures and fillers

Mineral admixtures here refer to fly ash, blast-furnace slag, silica fume, metakaolin, and other pozzolans that are powdered or pulverized materials that are added to concrete to improve or change the properties of hardened Portland cement concrete. Mineral admixtures are used in concrete to increase early strength development or to reduce the heat of hydration. They may also be used to improve the resistance of concrete to reactive aggregate and to replace cement. They have also been used in high strength concrete to produce higher strengths at later ages. The use of mineral admixtures may affect the workability and finishing characteristics of fresh concrete [PCI Bridge Design Manual, 1997].

In the case of SCC technology, mineral admixtures are often used to increase the content of the binder necessary to produce high-quality SCC. SCC with binder content less than 590 lb/yd^3 (350 kg/m^3) may only be suitable to secure high deformability and stability, and can even lead to more expensive mixtures given the higher demand of HRWRA compared to mixtures with a greater content of mineral admixtures [Khayat, 1999]. In SCC design, the cement content can be limited to relatively low values; however, other fines are required to increase the content of the binder, or fine powder materials. Fine powder materials typically used in SCC include fly ash, pozzolan, blast-furnace slag, and silica fume. In some cases, mostly in Europe and Japan, limestone fillers are also used to increase the powder content.

It is important to note that in this report, the term cementitious materials refers to Portland cement and supplementary cementitious materials, such as fly ash, blast-furnace slag, silica fume, and other pozzolans. On the other hand, the term binder is used for mixtures made with cementitious materials and other filler materials, such as limestone filler.

The requirements for mineral admixtures, including fly ash, blast-furnace slag, and silica fume are summarized in Table 2.3. Fly ash, blast-furnace slag, and silica fume conforming to the requirements of AASHTO or ASTM standards shall be used as supplementary cementitious materials. However, blast-furnace slag shall not be used in conjunction with Type IP or Type IS cements [Florida State DOT, 2004].

For all concrete types, except mass concrete and drilled shaft, the content of cement replaced with fly ash is 18% to 22% by mass and with blast-furnace slag is 25% to 70% for slightly and moderately aggressive environments, and 50% to 70% by mass when used in extremely aggressive environments. When use in combination with silica fume and/or metakaolin, blast-furnace slag content should be limited to 50% to 55% of the total cementitious content, by mass. The quantity of pozzolan in Type IP (MS) is in the range of 15% to 40% by mass. The quantity of cement replaced with silica fume should be 7% to 9% by mass [Florida State DOT, 2004]

For SCC mixtures, due to the special rheological requirements of SCC, both inert and reactive additions are commonly used to improve and maintain the workability, as well as to regulate the cement content and so reduce the heat of hydration [EFNARC, 2002]. Filler materials may well consist of residues from different industrial processes. It will be necessary, from case to case, to ascertain the suitability from both durability and production viewpoints. Even the effect of any variations in grain-size distribution of the filler and its effect on the packing density of the cement matrix must be taken into account [Swedish Concrete Association, 2002].

Other than limestone filler, non-standard fillers have been used in SCC to increase the amount of powder, including crushed dolomite or granite and ground glass filler. In all cases, the fraction less than 0.005 in. (0.125 mm) will be of most benefit to SCC flow properties. It is important to note that dolomite may present a durability risk due to alkali-carbonate reaction. Ground glass filler is usually obtained by finely grinding recycled glass. The particle size should be less than 0.004 in. (0.1 mm) and the specific surface area should be less than 250 m^2/kg. Larger particle sizes may cause alkali-silica reaction [EFNARC, 2002].

2.1.5 Chemical admixtures

Chemical admixtures are used in precast, prestressed concrete to reduce water content, improve deformability and stability, provide air entrainment, accelerate strength development, enhance workability retention, and retard setting time. Since chemical admixtures can produce different results with different binders, and at different temperatures, the selection of the admixtures should be based on the plant materials and conditions that will be utilized in production. Compatibility between admixtures is also important and should be specifically addressed whenever using more than one admixture in producing SCC, even if the same chemical admixture company supplies the admixtures.

The requirements for chemical admixtures, such as air-entraining admixture and high-range water reducing admixture (HRWRA) are summarized in Table 2.4. Unless otherwise specified, only Type A (water-reducing), Type B (retarding), Type D (water-reducing and retarding), Type F (water-reducing, high range), or Type G (water-reducing, high range, and retarding) should be used. According to AASHTO LRFD Bridge Design Specifications, air-entraining and other chemical admixtures shall be used as specified in the contract documents. Otherwise, such admixtures may be used, at the option and expense of the Contractor when permitted by the Engineer, to increase the workability or alter the time of set of the concrete.

Table 2.3 – Review of various requirements for mineral admixtures

	Fly ash	Blast-furnace slag	Silica fume
AASHTO LRFD Bridge Design and Construction Specifications [2004, 1998]	- AASHTO M 295 (ASTM C 618)		
Texas State DOT [2004]	- DMS-4610 - Physical and chemical requirements: both ASTM C 618 and Table A.14 in Appendix - Ultra-fine fly ash: requirements for Class F fly ash with exceptions of additions shown Table A.15 in Appendix	- DMS-4620 - Grade 100 and 120	- DMS-4630
Florida State DOT [2004]	- ASTM C 618 - Quantity of cement replaced with fly ash: 18%-22% - Quantity of pozzolan in Type IP (MS): 15%-40%	- ASTM C 989 - Grade 100 and 120 - Do not use in conjunction with Type IP or Type IS cements - Replacement of 25%-70% for slightly and moderately aggressive environments, 50%-70% for extremely aggressive environments - blast-furnace slag: 50%-55% of total cementitious materials when used with silica fume	- ASTM C 1240 - Quantity of cement replaced with silica fume: 7%-9%
New York State DOT [2002]	- AASHTO M 295 - LOI < 4.0%	- Chemical and physical requirements for Grade 100 blast-furnace slag as described in AASHTO M 302	- AASHTO M 307 - Uniformity of SiO_2 content: Max. ± 7% - Chloride content: max. 0.20% - Fineness: max. 5% retained on a 45-µm sieve (wet method) - Uniformity of percent solids (slurry): max. ± 5%
Washington State DOT [2002]	- AASHTO M 295 - LOI ≤ 1.5%	- AASHTO M 302 - Grade 100 or 120	

In order to avoid corrosion problems, admixtures containing chloride ions shall be limited to a maximum water-soluble chloride-ion content of 0.06% by mass of cement in the case of prestressed concrete or 0.30% in the case of reinforced concrete without prestress when tested in conformance to ASTM C 1218 [PCI Interim Guidelines, 2003]. Similarly, for prestressed concrete, chloride-ion content in chemical admixtures should be limited to 0.1%, by mass of the

admixture [AASHTO LRFD Bridge Design Specifications, 2004]. Washington State DOT [2002] requires that the total water-soluble chloride-ion content (ASTM C 1218) in concrete should be limited to 0.06% of the mass of cementitious materials for prestressed concrete applications.

SCC is often proportioned with polycarboxylate-based or copolymer HRWRA that can develop higher early compressive strength and better fluidity retention than naphthalene- or melamine-based HRWRA. Depending on the synthesis and side chain composition of these polymers, the newer type of sterical dispersing HRWRAs can impart some increase in viscosity compared to conventional naphthalene- or melamine-based HRWRA. Water included in HRWRA, as in the case of other chemical admixtures, should be considered as part of the total allowed mixing water [AASHTO LRFD Bridge Construction Specifications, 1998].

The use of a viscosity-modifying admixture (VMA) gives more possibilities of controlling segregation when the amount of powder material is limited. This is especially true where aggregate quality and gradation are limited, powder content is low, or the production facility has poor moisture control. The use of VMA should not justify that the total content of powder material be reduced to a great extent.

In general, VMAs are classified into two types: those used simply to impart segregation resistance to fresh concrete and those used both for imparting segregation resistance and curbing the effects of fluctuating qualities of the materials. Glycol-type, water-soluble amide-type liquid viscosity agents, as well as conventional powder cellulose-type, acrylic-type, and powder or liquid-based polysaccharide polymers are used as VMA. In general, the use of the VMA at moderate to high concentrations increases the water and/or HRWRA demand. SCC made with VMA can exhibit greater robustness to slight changes in material properties, mixing conditions, and in particular sand surface moisture. Some HRWRAs of different classes are formulated with VMA to provide improved deformability and stability of the mixture.

Air-entraining admixtures are used in concrete primarily to increase the resistance of the concrete to freeze-thaw damage. They may also be used to increase the workability of the concrete and facilitate handling and finishing. Air-entraining admixtures, as in the case of other admixtures, should be incorporated into the concrete mixture in a water solution.

Polycarboxylate-based HRWRA can entrap air, especially after mixing and agitation, and are proportioned with de-foaming agents. In some cases, the high dosage rate of HRWRA, coupled with the high fluidity can make it difficult to ensure the entrainment of a fine air-void system in the concrete. Air-entraining admixture is then needed, often at reduced concentration, to secure a given air-void system in SCC made with polycarboxylate-based HRWRA.

Set accelerating admixtures (Type C) are used to decrease the setting time and increase the early strength development. They are particularly beneficial in precast concrete construction to facilitate early form removal and release of prestressing [PCI Bridge Design Manual, 1997]. In the absence of accelerated radiant heat or steam curing, the use of set accelerating admixture in SCC may be beneficial in precast applications when using naphthalene- or melamine-based

HRWRA. On the other hand, the use of polycarboxylate-based HRWRAs does not typically lead to set retardation, hence reducing the need for use of set accelerating admixtures.

Corrosion-inhibiting admixtures can then be incorporated to protect the reinforcement from corrosion. Corrosion-inhibiting admixtures are more likely to be effective in cast-in-place bridge components that are directly exposed to chloride ions than in precast concrete bridge girders that are already highly impermeable [PCI Bridge Design Manual, 1997]. The use of corrosion-inhibiting admixtures may cause non-uniformity in color of the concrete surface (darkening and mottling) and may disrupt the efficiency of surface retarders.

Table 2.4 – Review of various requirements for chemical admixtures

	Chemical admixtures
AASHTO LRFD Bridge Design and Construction Specifications [2004, 1998]	- Air-entraining admixtures and chemical admixtures conforming to AASHTO M 154 (ASTM C 260) and AASHTO M 194 (ASTM C 494), respectively. - Only Type A (water-reducing), Type B (retarding), Type D (water-reducing and retarding), Type F (water-reducing, high range), or Type G (water-reducing, high range and retarding) shall be used. - Admixtures containing chloride ion in excess of 1%, by mass of the admixture, shall not be used in reinforced concrete. Admixtures in excess of 0.1% shall not be used in prestressed concrete.
Texas State DOT [2004]	- DMS-4640 - Do not use calcium chloride - Air-entraining admixtures conforming to ASTM C 260
Florida State DOT [2004]	- Do not use admixtures or additives containing calcium chloride in reinforced concrete - Type A or Type D conforming to AASHTO M 194, except for the compressive strength at six months and one year, flexural strengths, and relative durability factor requirements are waived - Air-entraining admixture: AASHTO M 154 in all concrete mixtures except counterweight concrete - Use HRWRA, either Type F or Type G, in concrete incorporating silica fume or metakaolin - Use of corrosion-inhibiting admixture only with concrete containing Type II cement, Class F fly ash or blast-furnace slag, and Type D water-reducing retardant admixture or Type G HRWRA to normalize setting time of concrete - All admixtures should be compatible with the corrosion inhibitor admixture (ASTM G 109)
New York State DOT [2002]	- The pH of all admixtures > 8 (total chloride-ion content < 1000 ppm) - Requirement of chemical admixtures: refer to Table A.16 in Appendix
Washington State DOT [2002]	- AASHTO M 194, Type A, B, D, or F - Air-entraining admixture: AASHTO M 154 - Chloride-ion content of chemical admixtures < 1% by weight - Total water-soluble chloride-ion content (ASTM C 1218) of mixed concrete < 0.06%, by mass of cementitious materials for prestressed concrete and < 0.10% for reinforced concrete

2.2 Mix Design Considerations

2.2.1 Introduction

This section reviews some the mix design guidelines for normal vibrated concrete that are given in the AASHTO LRFD Bridge Design [2004] and Construction [1998] Specifications and by Texas, Florida, New York, and Washington State DOTs. General guidelines for mix design of SCC are then discussed to highlight the main principals involved in proportioning such concrete.

2.2.2 Overview of AASHTO LRFD Bridge Design and Construction Specifications

According to AASHTO LRFD Bridge Design and Construction Specifications, the mixture proportion selected for the construction of bridge elements shall be sufficiently workable and finishable for the intended use and shall conform to the mixture requirements summarized in Table 2.5. For prestressed concrete and bridge decks, the specified compressive strength at 28 days shall not be less than 4,000 psi (27.6 MPa). Consideration should be given to limiting the nominal aggregate size to 3/4 in. (19 mm) for prestressed concrete members. Compressive strengths above 5,000 psi (34 MPa) should be used only when the availability of materials for such concrete in the locale is verified.

Table 2.5 – Concrete mixture characteristics by class

Class of concrete	Min. cement content	Max. *w/c*	Air content range	Size of coarse aggregate per AASHTO M 43 (ASTM D 448)	Size number	Specified compressive Strength (28 days)
	lb/yd^3 (kg/m^3)		%	Square opening		psi (MPa)
A	611 (362)	0.49	-	1 in. - No. 4 (25 - 4.75 mm)	57	4000 (28)
A(AE)	611 (362)	0.45	6.0 ± 1.5	Same as above	57	4000 (28)
B	517 (307)	0.58	-	2 in. - No. 3 (50 - 25 mm) and No. 3 - No. 4 (25 - 4.75 mm)	3 57	2400 (17)
B(AE)	517 (307)	0.55	5.0 ± 1.5	Same as above	3 57	2400 (17)
C	658 (390)	0.49	-	1/2 in. - No.4 (12.5 - 4.75 mm)	7	4000 (28)
C(AE)	658 (390)	0.45	7.0 ± 1.5	Same as above	7	4000 (28)
P	564 (334)	0.49	As specified elsewhere	1 in. - No. 4 (25 - 4.75 mm) or 3/4 in. - No. 4 (19 - 4.75 mm)	7 65	As specified elsewhere
S	658 (390)	0.58	-	1 in. - No. 4 (25 - 4.75 mm)	7	-

For conventional concrete, the *w/c* values in Table 2.5 can be reduced to enhance durability of reinforced concrete exposed to saltwater, deicing salt, or sulfates. For calculating the *w/c* of the

mixture, the mass of the water shall be that of the total free water in the mix, which includes the mixing water, the water in any admixture solutions, and any water in the aggregates in excess of that needed to reach a saturated-surface-dry condition.

The maximum cement or cement and mineral admixture content shall not exceed 800 lb/yd^3 (475 kg/m^3) of concrete, except for Class P (HPC) concrete where the sum of Portland cement and other cementitious materials shall be specified not to exceed 1000 lb/yd^3 (593 kg/m^3). The actual cement content used shall be within these limits and shall be sufficient to produce concrete of the required strength and consistency.

The ASSHTO specifications allow the increase in cement and water contents if adequate workability cannot be obtained by the use of the minimum cement allowed. In this case, the cement and water contents shall be increased without exceeding the specified *w/c*, or an approved admixture shall be used. When Type F or G HRWRAs are used, the slump consistency values recommended in Table 2.6 for concrete at the time of casting may be exceeded as permitted by the Engineer. When the consistency of the concrete is found to exceed the nominal slump, the mixture of subsequent batches shall be adjusted to reduce the slump to a value within the nominal range.

Table 2.6 – Normal density concrete slump test limits

Type of work	Normal slump	Maximum slump
Formed elements: - Sections over 300 mm thick - Sections 300 mm thick or less	 1-3 in. (25-75 mm) 3-4 in. (25-100 mm)	 5 in. (125 mm) 5 in. (125 mm)
Cast-in-place piles and drilled shafts not vibrated	5-8 in. (125-200 mm)	9 in. (225 mm)
Concrete placed under water	5-8 in. (127-200 mm)	9 in. (225 mm)
Filling for rip-rap	3-7 in. (75-175 mm)	8 in. (200 mm)

According to AASHTO specifications, mineral admixtures shall be used in the amounts specified in the contract documents. When either Types I, II, IV, or V AASHTO M 85 (ASTM C 150) cements are used and mineral admixtures are neither specified in the contract documents nor prohibited, the Contractor could be permitted to replace up to 20%, by mass, of the required Portland cement with a mineral admixture. In calculating the *w/c*, the mass of the cement shall be considered to be the sum of the mass of the Portland cement and the mineral admixture.

For normal-density concrete, the absolute volume method, such as described in American Concrete Institute Publication 211.1, shall be used in selecting mix proportions. For low-density concrete, and for other classes of concrete when specified in the contract documents or ordered by the Engineer, satisfactory performance of the proposed mix design shall be verified by laboratory tests on trial batches. For mix design approval, a minimum of five test cylinders are

taken from a trial batch and shall average at least 810 psi (5.6 MPa) greater than the specified compressive strength.

2.2.3 Overview of specifications for precast, prestressed concrete structures in various states

Table 2.7 summarizes the main mixture characteristics that are recommended by various State DOTs for conventional concrete used for the construction of precast, prestressed structures.

Table 2.7 – Mixture characteristics for structural concrete

Mixture characteristics	Texas State DOT	Florida State DOT	New York State DOT	Washington State DOT
Structural elements	Precast, prestressed concrete beams, box girders, piling, and traffic barrier	Bridge deck	General purpose structural concrete	Precast, prestressed concrete girder
w/cm	≤ 0.45	≤ 0.44	≤ 0.46	
Cementitious materials content	< 700 lb/yd^3 (415 kg/m^3)	> 611 lb/yd^3 (365 kg/m^3)	607 lb/yd^3 (360 kg/m^3)	> 565 lb/yd^3 (335 kg/m^3)
Type of cementitious materials	Type III cement		Max. 20% replaced with Class F fly ash and blast-furnace slag	Type I or II cements Fly ash < 25%
Air content	Refer to Table 2.8	1% to 6%	6.5% (5% to 8%)	4.5% to 7.5%
Slump, in. (mm)	• 4 in. (100 mm) for design and placement • 6.5 in. (165 mm) for max. acceptable placement • 9 in. (230 mm) when HRWRA is incorporated	• 3 in. (75 mm) • < 7 in. (180 mm) when Type F or G HRWRA is used.	2.5 to 3.5 in. (65 to 90 mm)	
28-day design strength	As indicated on plans or specifications	4,500 psi (31 MPa)		
Min. 28-day compressive strength			3,625 psi (25 MPa)	
MSA				1/2 in. (12.5 mm) for Class 4000P 3/4 in. (19 mm) for Class 4000D

According to Texas State DOT Specifications [2004], the *w/cm* should be limited to 0.45 for the construction of prestressed concrete beams. Other classes of concrete are given in Table A.17 (Appendix). For structural concrete and any other class of concrete designed using more than 520 lb/yd^3 (310 kg/m^3) of cementitious material, Texas State DOT Specifications [2004] stipulate the use one of eight mix design options, of which five pertaining directly to the use of supplementary cementitious materials are shown below.

- **Option 1.** Replace 20% to 35% of the cement with Class F fly ash.
- **Option 2.** Replace 35% to 50% of the cement with blast-furnace slag.
- **Option 3.** Replace 35% to 50% of the cement with a combination of Class F fly ash, blast-furnace slag, or silica fume. However, the fly ash and silica fume substitutions should be limited to 35% and 10%, respectively.
- **Option 4.** Use Type IP or Type IS cement. Up to 10% of the Type IP or Type IS cement may be replaced with Class F fly ash, blast-furnace slag, or silica fume.
- **Option 5.** Replace 35% to 50% of the cement with a combination of Class C fly ash and at least 6% silica fume, ultra-fine fly ash, or metakaolin. However, no more than 35% may be Class C fly ash, and no more than 10% may be silica fume.

Texas DOT Specifications [2004] recommend all concretes, except for Class B concrete (low strength), be air-entrained in accordance with Table 2.8, unless otherwise shown on the plans. The specifications recommend the use of moderate exposure values unless otherwise specified. If the air content is more than 1-1/2% points below or 3% points above the required air, the load of concrete will be rejected. If the air content is more than 1.5% but less than 3% points above the required air, the concrete may be accepted based on strength tests.

Table 2.8 – Requirements for air entrainment (Texas State DOT)

MSA	Air volume (%) 1)	
	Moderate Exposure	Severe Exposure
3/8 in. (9.5 mm) (Grades 7 & 8)	6%	7.5%
1/2 in. (12.5 mm) (Grade 6)	5.5%	7%
3/4 in. (19 mm) (Grade 5)	5%	6%
1 in. (25 mm) (Grade 4)	4.5%	6%
1-1/2 in. (38 mm) (Grades 2 & 3)	4.5%	5.5%
2 in. (50 mm) (Grade 1)	4%	5%

1) For specified concrete compressive strengths above 5,000 psi (35 MPa), a reduction of 1% point is permitted.

Florida State DOT specifications [2004] present separate classifications of concrete designated as Class I, II, III, IV, V, and VI. Compressive strength, slump, and air content of each class of concrete are specified in Table A.18 (Appendix). Table 2.9 summarizes the requirement for minimum cementitious materials content and maximum *w/cm* recommended for each concrete class.

Table 2.9 – Requirement for total cementitious materials content and maximum *w/cm* depending on concrete class (Florida State DOT)

Class of Concrete	Minimum Total Cementitious Materials Content lb/yd^3 (kg/m^3)	Maximum *w/cm* [1)]
I (Pavement)	508 (300)	0.50
I (Special)	508 (300)	0.50
II	564 (335)	0.49
II (Bridge Deck)	611 (365)	0.44
III	611 (365)	0.44
III (Seal)	611 (365)	0.52
IV	658 (390)	0.41
IV (Drilled Shaft)	658 (390)	0.41
V (Special)	752 (445)	0.37[2)]
V	752 (445)	0.37[2)]
VI	752 (445)	0.37

1) The calculation of the *w/cm* is based on the total cementitious material including silica fume, slag, fly ash, or metakaolin.
2) When the use of silica fume or metakaolin is required as a pozzolan, the maximum *w/cm* will be 0.35.

New York State DOT specifications [2002] also offer different recommendations for various concrete classes (Table A.19, Appendix). Such concrete shall have an air content of 5% to 9%. Unless noted otherwise in the contract documents, the minimum compressive strength of concrete used in precast units shall be 3,625 psi (25 MPa) at 28 days. As indicated in Table 2.10, up to 20% of the cement content for Classes A, C, D, E, H, J, and I may be substituted with a pozzolan (fly ash or blast-furnace slag), except where prohibited by the Regional Director. Microsilica may be added as part of a blended cement.

Table 2.10 – Pozzolan substitutions (New York State DOT)

Concrete Class Specified	Substitute With Cement by Mass	Class Substitution Allowed
A, C, E, H	15%-20% Class F Fly Ash	HP[1)]
I, J	15%-20% Class F Fly Ash	-
D	15%-20% Class F Fly Ash	DP[1)]
G[2)] and GG[2)]	20% Class F Fly Ash	-
F	No Substitution Allowed	-

1) Class HP and DP concrete may be substituted to mitigate ASR as listed above. Classes HP and DP require the replacement of Portland cement with 20% pozzolan and 6% microsilica. The pozzolan may be either Class C or F Fly Ash or Ground Granulated Blast-Furnace Slag
2) Classes G and GG require the replacement of Portland cement with 20% pozzolan. The mitigation of ASR in Classes G and GG must be accomplished using Class F Fly Ash. Notify the Regional Materials Engineer prior to using pozzolan substitutions to mitigate ASR when using reactive aggregates in combination with high alkali cement. Approval may be withdrawn when unsatisfactory results occur."

Air-entraining agent is required for all mixtures to produce concrete with air content in the range specified in Table A.19 (Appendix), unless otherwise indicated in the contract documents. The setting time of concrete may be retarded when necessary for proper placement. A water-reducing and retarding admixture (Type D) is required in Class DP for structural slab overlays, Class HP for superstructure slabs and structural approach slabs, Class G and Class GG concrete. It may be used with, or in place of, a water-reducing admixture (Type A) in other applications that allow Class DP or Class HP. Limit the use of the water-reducing and retarding admixture to the minimum amount required to achieve retardation during placing conditions. Unless otherwise specified, Type A is required in Classes DP, HP, I, and J concretes. For all other classes, except G and GG, a water-reducing admixture may be used, subject to advance notification and approval of the Regional Materials Engineer. Type F HRWRA may not be used unless allowed by specification, plans, or the Director, Materials Bureau.

In the case of Washington State DOT Specifications [2002], cementitious materials are considered as the mass of cement plus fly ash, blast-furnace slag, and microsilica. Unless otherwise specified, Type I or II Portland cement shall be used in all concrete. The use of fly ash is required for Class 4000D (for Deck applications) and 4000P (for Piling applications) and is optional for all other classes of concrete, except when required for the mitigation of Alkali Silica Reactivity. As an alternative to the use of cement and fly ash as separate components, blended hydraulic cement that meets the requirements may be used. The concrete for prestressed girders shall have the minimum compressive strengths as specified in the Plans. The proposed mix for Class 4000D shall provide a minimum fly ash content of 75 lb/yd^3 (45 kg/m^3) and a minimum cement content of 660 lb/yd^3 (392 kg/m^3). All other concrete mix designs, except those for lean concrete, shall have a minimum cementitious material content of 565 lb/yd^3 (335 kg/m^3). Class 4000D and 4000P concrete shall include a water-reducing admixture in the amount recommended by the manufacturer. A HRWRA may be used in all mix designs.

2.2.4 Mix design principles of SCC

Mix design of SCC is vital for the performance of the material, both in the plastic and hardened stages. Compared to conventional vibrated concrete, in designing SCC there are a number of factors that should be taken into consideration to a greater degree than conventional concrete, including:

- the properties of locally available raw materials, including mineral, geometric, and physical properties of aggregates and cementitious materials;
- the need for a higher level of quality control, greater awareness of aggregate gradation, and better control of mix water and sand moisture;
- the choice of chemical admixtures and their compatibilities with the selected binder;
- the need to consider the casting technique, the configuration of the cast element, and placement conditions in finalizing the performance specifications of the fresh concrete.

As discussed earlier in Section 1.2, it is necessary to consider both the fresh and hardened properties of the SCC in the development of the mix design that includes specifications for the content of cement and supplementary cementitious materials and fillers, the water content or *w/cm* or *w/b*, the volume of coarse aggregate, the sand-to-aggregate ratio (S/A), as well as the air volume. The selection of the type and combinations of chemical admixtures is part of the mix design process and depends closely on the flow characteristics that are required. As illustrated in Fig. 1.1, the fresh properties of SCC are influenced by the characteristics of locally available materials, the characteristics of the cast element, and concrete production and placement considerations. For the production of SCC for precast, prestressed concrete bridge elements, the most relevant hardened properties that affect material selection and mix design include early and ultimate compressive strengths, flexural strength, elastic modulus, bond to reinforcement, creep, shrinkage, frost durability, impermeability, and resistance to corrosion.

As illustrated in Fig. 2.1, the mix design of SCC is dictated by the required flow characteristics of the fresh concrete in addition to engineering properties and durability requirements [Khayat, 1999]. As discussed in Chapter 1, it is important to ensure both high flowability (low yield value) and high resistance to segregation (moderate viscosity) to secure an SCC that can flow readily around various obstacles and achieve good filling capacity. The deformability of the concrete is closely related to that of the cement paste and can be increased by incorporating a HRWRA. This leads to reduction in the yield value with limited decrease in viscosity. Therefore, a highly flowable concrete can be obtained without significant reduction in cohesiveness. The increase in *w/b* can increase the deformability; however, care must be taken to avoid substantial reduction in cohesiveness resulting from the increase in free water content.

Inter-particle friction between the various solids (coarse aggregate, sand, and powder materials) can limit the rate and extent of deformability of the cast concrete. The extent of inter-particle friction increases when the concrete flows through restricted areas because of the greater collision between various solids that increases viscosity, hence requiring greater shear stresses to maintain a given rate of deformability [Khayat, 1999].

The use of HRWRA can disperse cement grains, reduce inter-particle friction, and enable the reduction in water content while maintaining the required levels of flowability and viscosity. The reduction in coarse aggregate and sand contents can also enhance the deformability and passing ability. For example, Khayat [1999] showed that SCC with a slump flow of 25.6 in. (650 mm) made with 30% to 33% coarse aggregate of 0.79 in. (20 mm) MSA and sand-to-paste volume of 0.60 to 0.66 can be more suitable for casting highly congested structural sections than SCC made with 37.5% to 40% coarse aggregate and a sand-to-paste volume of 0.70 to 0.85.

The incorporation of continuously graded cementitious materials and fillers can also reduce inter-particle friction. Regardless of the mix design approach, properly graded aggregates are required to reduce the risk of bleeding and segregation as well as the inter-particle friction needed to lower water demand. It is important to reduce fluidity loss until the end of casting since such loss can limit the filling capacity and self-compactibility of the concrete.

SCC must exhibit adequate dynamic and static stability. The enhancement of stability involves a reduction in the relative volume of coarse aggregate and a reduction of maximum aggregate size (MSA). It is important to increase the cohesion of the mixture to enhance bond between the mortar and coarse aggregate, hence ensuring uniform flow of both phases in non-restricted and through restricted sections. The increase in the content of ultra-fines (smaller than 80 μm, No. 315) can increase the resistance of SCC to surface settlement [Khayat et al., 2000b].

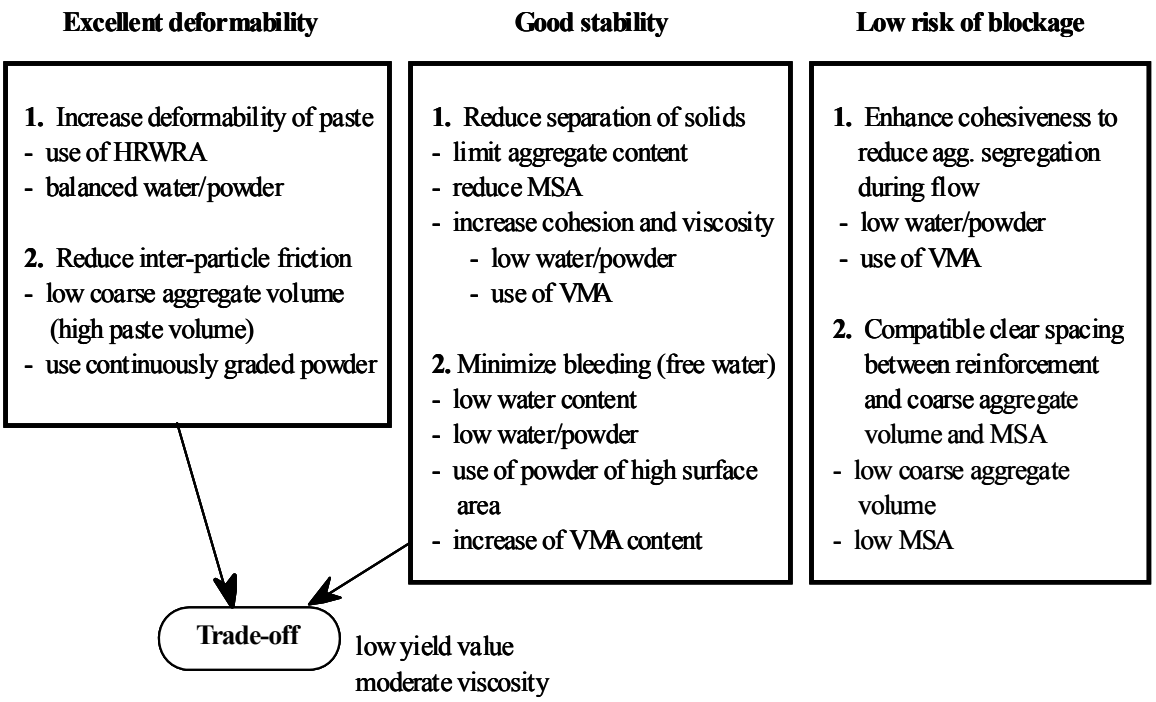

Fig. 2.1 – Principles of SCC mix design [Khayat, 1999]

A low *w/b* can reduce free water content and increase viscosity. The use of VMA can increase viscosity and maintain good suspension of coarse aggregate and reduce inter-particle collision and coagulation of coarse aggregate particles. Another important factor to help ensure good self-compactibility is to minimize bleeding that involves the separation of free water from the concrete. This can be achieved by reducing water content through the incorporation of a HRWRA, decreasing the *w/b*, incorporating a VMA, or using cementitious materials and fillers with high surface areas to adsorb some of the free water.

The third property essential to enhancing self-compactibility properties is a reduction in the risk of blocking resulting from the flow in narrow spaces. Providing adequate viscosity, thus ensuring good suspension of solid particles during deformation of the concrete, reduces the risk of blockage. This can then reduce inter-particle friction that can limit deformability in narrow spaces and hence the ability of the concrete to properly fill the formwork. In order to prevent blockage of concrete flow among closely spaced obstacles, concrete should have adequate

cohesiveness. This can be achieved by reducing the *w/b* and/or incorporating VMA. As the clear spacing between the obstacles in the congested section decreases, the coarse aggregate volume and MSA should be reduced to limit inter-particle collision in the vicinity of reinforcement and hence the risk of blockage.

In general, neither the water nor the cement content of SCC differs substantially from those of normal concrete. The *w/c* remains in the normal range, between 0.40 and 0.50, for the majority of applications. The addition of ultra-fines of high specific surface area significantly increases the mortar volume, but at the same time reduces the relative percentage of water in the cement paste. With such additives, the water-to-binder ratio (*w/b*), or water-to-powder ratio, decreases to typical values of 0.32 to 0.42. It is important to note that in SCC technology, the binder can incorporate Portland cement, supplementary cementitious materials, and in some cases fillers, whereas the term cementitious materials would involve the use of Portland cement and supplementary cementitious materials.

SCC used for structural precast, prestressed applications is typically characterized by relatively low free (or movable) water content, high concentration of ultra-fine particles, and use of polycarboxylate-based HRWRA. These HRWRAs are incorporated to significantly reduce water demand and enhance retention in consistency. A mixture made with such a class of HRWRA can also exhibit short setting times, high early strength, and a reduced tendency to segregation.

In principle, there are three approaches that can be used for the production of SCC:

1. Raising the ultra-fines content by the addition of fine fractions in the form of fly ash, blast-furnace slag or limestone filler (powder type).
2. Use of suitable viscosity-modifying admixtures (VMAs) (viscosity agent type).
3. Combination of above-mentioned measures (combination type).

Minimum free water content - This approach entails the use of a high content of ultra-fine materials and a low water content to enhance fluidity, cohesiveness, and passing ability of the SCC [Okamura, 1997]. Such concrete typically has a *w/b* of 0.30 to 0.35 with a content of ultra-fines ≤ 80 μm (No. 315) of 845 and 1110 lb/yd^3 (500 to 600 kg/m^3). Such a high content of powder increases the paste volume. Ultra-fine materials (Portland cement, blended cement, fly ash, blast-furnace slag, silica fume, metakaolin, natural pozzolans, and fillers) are combined to enhance the packing density and reduce inter-particle friction in the cement paste. The replacement of part of the cement with a less reactive powder is necessary to limit the heat of hydration, and in some cases, gain in mechanical properties [Yurugi et al., 1993]. In general, this approach can result in SCC mixtures with low yield value and moderate-to-high viscosity levels. The low water content requires a relatively high dosage of HRWRA to obtain the required deformability, especially if the powder content is reduced. The resulting reduction in aggregate volume can reduce the risk of segregation and blockage of the flow.

Moderate water content and medium concentration of VMA - In this approach, the *w/b* can be maintained at the level necessary to satisfy economic and technical constraints (for example *w/b*

of 0.40) and moderate dosage of VMA is incorporated to secure the required stability. The majority of VMA affect the aqueous phase of the cement paste whereby chains of the water-soluble polymer can imbibe some of the free water, thus enhancing the yield value and plastic viscosity of the paste. The incorporation of VMA becomes imperative when the powder content is reduced to levels compatible with conventional concrete or high-performance concrete. When incorporated in mixtures with relatively high paste content (sand-to-cement ratio of 0.60 to 0.66, by volume), the use of VMA along with HRWRA can ensure high deformability and adequate stability leading to greater filling capacity and better homogeneity than mixtures made with a low *w/b* and no VMA [Khayat, 1998].

Low water content and low concentration of VMA - This approach involves the combination of a high content of powder materials and low dosage of VMA. Such mixtures are typically more robust than those proportioned with high powder content and low *w/b*. Robust mixtures can react less sensitively to deviations in the mixture composition, characteristics of the raw materials, and water content. Sakata et al. [1996] reported that, compared to SCC made with 0.33 *w/b* with VMA, the incorporation of a low concentration of VMA can reduce slump flow variability of SCC when there are small variations in the Blaine fineness of the cement (320 to 340 m^2/kg), fineness modulus of the sand (2.08 to 3.06), and temperature of the fresh concrete (50 to 86°F, 10 to 30°C). This mix design approach has been used in precasting plants in Germany to produce robust SCC mixtures that can tolerate maximum fluctuations in water content of ± 155 fl oz/yd^3 (± 6 L/m^3) [Gaubner et al., 2001].

2.2.5 Examples of basic mix design approaches for SCC

In North America, mix designs of SCC used in the precast, prestressed concrete industry are often proprietary and in some cases admixture-sensitive as they have been redeveloped initially with assistance from admixture suppliers. As in the case of conventional vibrated concrete, the mix design can vary on a regional basis depending on the availability of concrete constituents and the environmental conditions. This section sheds some lights on the basic principles involved in developing a mix design of SCC without elaborating the various published methods.

The EFNARC [2002] in France offers some basic guidelines for proportioning SCC, as follows:

- *w/b* of 0.80 to 1.10, by volume, typical;
- *w/c* is selected based on strength and durability requirements;
- total binder (powder) content of 674 - 1011 lb/yd^3 (400 - 600 kg/m^3), or 160 - 240 L/m^3
- free water content < 337 lb/yd^3 (200 kg/m^3);
- paste volume > 40% of the volume of the mixture;
- coarse aggregate content normally 28% - 35% by volume of the mixture and < 50% of total solid volume;
- sand content > 40% of the mortar volume, < 50% of paste volume, and 50% by mass of total aggregate;
- further modifications to meet performance criteria of the fresh and hardened concrete.

The mix design principles for these SCC mixes are based on the use of fine materials to enhance stability. It points out that some variations in aggregate moisture content should be allowed for in the mix design stage, and that normally the incorporation of VMA can be useful for compensating for the fluctuations due to any variations of the sand grading and the moisture content of the aggregates.

Okamura [1997] proposed the following sequence for proportioning SCC:

A) Designation of desired air content at 2%, or higher value specified for frost durability.

B) Determination of coarse aggregate volume. Coarse aggregate volume is defined by bulk density. Generally, coarse aggregate content with MSA > 0.16 in. (4 mm) should be 50% to 60% of the total solid volume of the concrete. The reduction in MSA can enable the use of higher proportion of coarse aggregate.

C) Determination of sand content (defined here as all particles larger than 0.125 mm and smaller than 4 mm). The optimal volume content of sand in the mortar varies between 40% and 50%, depending on paste properties.

D) Determination of optimum *water/powder* ratio and HRWRA dosage in mortar. Tests with the flow cone and V-Funnel tests for mortar (Fig. 2.2) are performed at varying *water/powder* ratios, in the range of 0.80 to 0.90. Target values: slump flow = 9.5 to 10.2 in. (240 to 260 mm), V-Funnel time = 7 to 11 sec. At target slump flow, where V-funnel time is lower than 7 sec, the *water/powder* ratio should be decreased to enhance viscosity. For target slump flow and V-funnel time in excess of 11 sec, the *water/powder* ratio should be increased to reduce viscosity.

E) Concrete properties are assessed by standard tests, and the HRWRA dosage is determined. If necessary, adjustments to the mix composition should then be made. Once all requirements are fulfilled, the mix should be tested at full scale at the concrete plant or at site.

Regardless of the mix design approach, the concrete mixture should be robust to exhibit sufficient tolerance to variations in the characteristics of the constituent materials and their quantities. Before delivery, the chosen mix design should be thoroughly tested at the plant, preferably in full-scale trial. The Engineer, the Contractor or the precasting plant shall submit the mix design for approval.

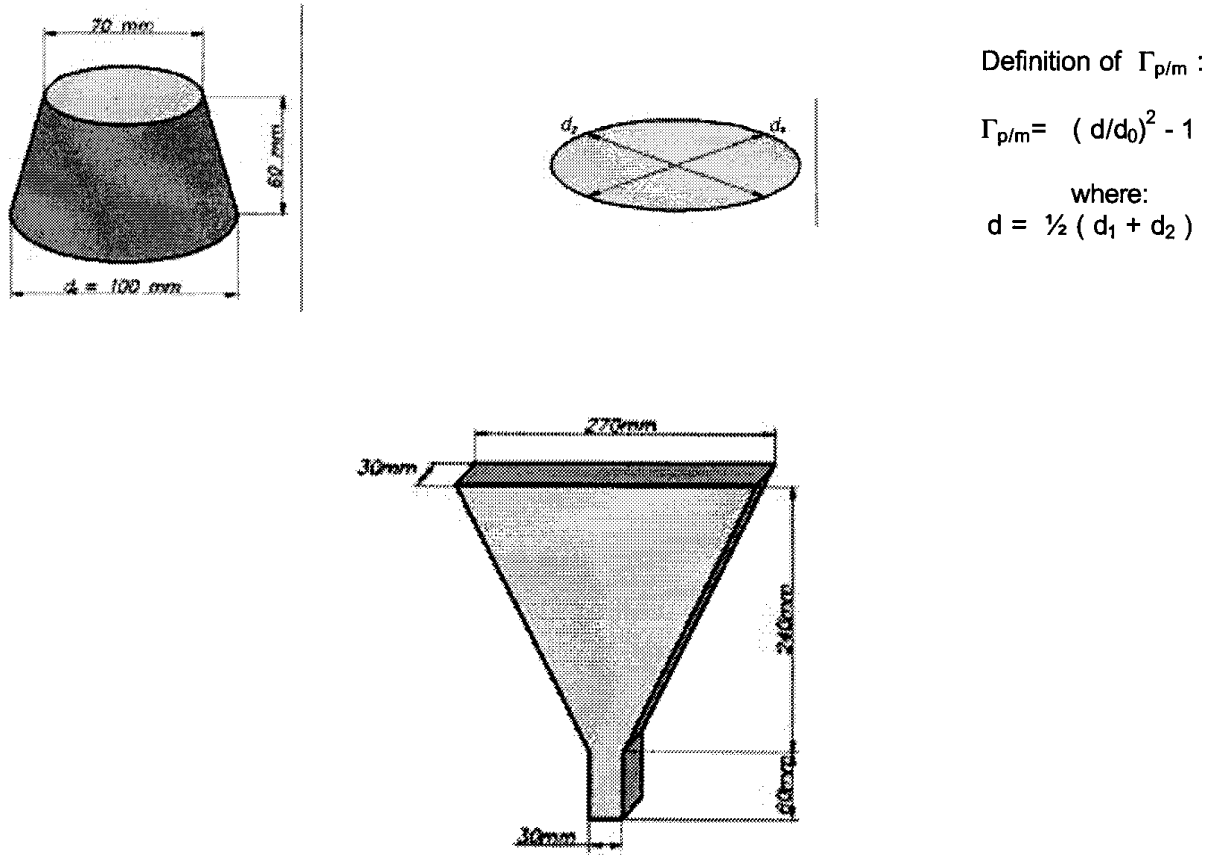

Fig. 2.2 – Flow cone and V-funnel to determine the spread and flow time of mortar

2.3 Most Significant Material Constituents and Mix Design Characteristics Affecting Performance of SCC Used to Produce Precast, Prestressed Bridge Elements

Although mix design of concrete is critical for its workability and performance, adequate selection of material constituents is a key factor in the optimization process of a concrete mixture that can achieve adequate performance and service life. Compared to conventional vibrated concrete, there are a number of factors that should be taken into consideration to a greater degree when designing SCC. This includes the type and shape of coarse aggregate, combined gradation of sand and coarse aggregate, total content of supplementary cementitious materials, and water content in the mixture. Material characteristics and mix design of SCC have marked effect on production, placement, and performance of SCC.

The mixture proportioning selected for the construction of bridge elements shall be sufficiently workable, finishable for the intended use, and achieve the required strength and durability. Therefore, in the selection of material constituents and mixture proportioning for precast, prestressed applications, it is essential that the concrete achieves the targeted properties in terms

of early-strength development to allow the early application of prestress and the re-use of forms, ensure suitable fluidity retention for a sufficient period of time to enable the transport and completion of the placement of concrete without the need for retempering, ensure proper filling, and achieve adequate encapsulation and bond strength to strand. Workability and filling ability of concrete used for casting of prestressed elements is determined based on the shape and dimensions of the element, the level of reinforcement and design details, such as the concrete cover. On the other hand, durability requirements are established based on the exposure conditions of the bridge.

The selection of cement type depends on the required early-age compressive strength. Type I Portland cement is generally used in applications where special properties, such as early-strength or sulphate attack, are not required. Type III cement is used to accelerate strength gain, thus allowing earlier prestressing and demolding to ensure optimal re-use of forms. The use of Type III cement, or finely ground Type I cement, can reduce or eliminate the need for steam curing or radiant heat curing.

Deformability and stability characteristics of the concrete depend on the SCC mix design, which is affected by the type and properties of the cement and supplementary cementitious materials in use. For example, for a given *w/cm*, Type III cement requires higher water and HRWRA demand than Type I/II cement to achieve a given consistency. Furthermore, the loss of fluidity in the case of SCC made with Type III cement than that with Type I/II.

The content of C_3A in the cement and Blaine fineness of the cement and supplementary cementitious materials affect water demand, fluidity retention, as well as setting and hardening characteristics. For a given water content, the increase in cement fineness increases greater water and HRWRA demand. Given the workability, strength, and durability requirements, the fineness of cement should be limited to avoid sharp loss in workability during production of prestressed concrete members.

The use of supplementary cementitious materials is widely accepted in the precast, prestressed industry. For example, Washington State DOT allows the use of fly ash, but limits the replacement of fly ash in Type IP (MS) to 25% by mass of the cementitious materials. New York State DOT specifications [2002] stipulate that the contents of fly ash, silica fume, and blast-furnace slag should not exceed 22%, 10%, 22%, by mass, respectively, of the total binder for Types IP, SF, and SM blended cements.

The total content of cementitious materials used in SCC is relatively high compared to conventional concrete, and can range between 715 to 1000 lb/yd^3 (424 to 593 kg/m^3). The binder content and its composition have direct influence on water and HRWRA demand, fluidity retention, finishing characteristics of fresh concrete, temperature rise, setting, early age strength, and the performance of the hardened concrete.

Properly graded aggregates are required to reduce the risk of bleeding and segregation as well as the inter-particle friction needed to lower water demand. The shape and content of coarse aggregate have marked effect on flow ability, filling capacity, and static stability of SCC.

Rounded aggregates improve flow characteristics of SCC, given the lower internal friction among aggregate particles. Therefore, SCC made with rounded aggregate requires lower HRWRA dosage than that with crushed aggregate. The maximum size of aggregate (MSA) should be selected based on the minimum clear spacing between the reinforcing steel and prestressing stands, clear cover to the reinforcement, and geometry of the elements to be cast. The reduction in MSA is required to enhance deformability and to reduce segregation and blockage during placement. The decrease in coarse aggregate content, reduction of MSA, and increase in the content of powder material can also enhance the resistance to segregation and surface settlement.

Chemical admixtures are used in precast, prestressed concrete to reduce water content, improve deformability and stability, provide air entrainment, accelerate strength development, enhance workability retention, and retard setting time. The performance of these admixtures depends on other mixture parameters, including *w/cm*, binder characteristics, and presence of other admixtures. Of particular interest to precast, prestressed applications is the use of polycarboxylate-based HRWRA; such HRWRA can lead to high reduction water demand without extended set retardation, which could reduce or eliminate heat curing.

SCC used in precast, prestressed applications is typically proportioned with low *w/cm* to secure strength development. The relatively low free water content in such concrete increase the plastic viscosity of the SCC and reduces the need for incorporating a VMA to control segregation. VMA is typically used in SCC proportioned with low to moderate binder content, for example, less than 715 lb/yd^3 (425 kg/m^3), or mixtures with *w/cm* values greater than 0.40. Still, the incorporation of VMA in SCC designated for precast applications can lead to more robust and consistent production of SCC. This is especially true for SCC with relatively low powder content and non-optimum grain-size distribution, especially in the case where the moisture control of aggregate is not adequate. Mixtures made with VMA tend to be more tolerant to small changes in moisture content and fineness modulus of the sand, dosage of HRWRA, and temperature of the fresh concrete.

The use of polycarboxylate-based HRWRA may lead to the entrapment of large volume of coarse air bubbles. This is related to the type and content of the de-foamer in use and the mixing and agitation energy of the concrete after the addition of HRWRA. Concrete subjected to prolonged mixing or agitation after the introduction of HRWRA could exhibit some increase in air content, without necessary refinement in the size of air bubbles. Investigations carried out with naphthalene-based HRWRA indicate that the stability of air volume can be enhanced in SCC mixtures proportioned with a relatively low *w/cm* (i.e. high binder contents) or those made with VMA. However, beyond a certain viscosity level, the stability of fine air bubbles during agitation could be hindered. The use of AEA is required, through at low dosage, to ensure proper air-void system whenever the concrete is designated for frost durability. In order to ensure stable air volume in the fresh concrete, the SCC should be viscous to retain the air bubbles in uniform suspension.

Other relevant material constituents and mix design requirements that can affect the performance of precast, prestressed bridge elements are discussed elsewhere in this report. This includes discussion and recommendations regarding material constituents and mix design characteristics relative to the workability of SCC (Section 1.5), mixing, production, and curing (Section 3.6), mechanical and structural properties (Section 4.12), visco-elastic properties (Section 5.10), and finally, air stability and frost durability (Section 6.6).

CHAPTER 3 - PRODUCTION AND PLACEMENT OF SCC

3.1 Production

3.1.1 General

This chapter offers some review and recommendations regarding concrete mixing and placement practices and quality control testing of SCC. The review is not only limited to precast operations but also involves certain aspects pertaining to the transport and placement of cast in-place SCC.

The production of SCC differs from that of conventional concrete in a number of ways in that the entire manufacturing process demands greater care and precision. The fact that the consistency of the concrete mixture has significant influence on the flow and filling of formwork without mechanical consolidation increases the need for stringent control at the concrete plant and on site. Variations in the characteristics of constituent materials and in their weighed contents affect the workability of SCC (filling ability, passing ability, filling capacity, and segregation resistance) to a greater degree than that of vibrated concrete of normal consistency. Consequently, the need for inspection and quality control increases when producing SCC. It is essential to maintain uniform quality of all constituent materials in the production of SCC. Therefore, the production of SCC pre-supposes greater demands on competence and should be carried out in plants where the equipment and operation are properly controlled.

The production of SCC requires highly-qualified workforce. Production staff involved in the production of SCC must be trained and have experience with SCC. Workers and concrete engineers must be sensitized to the quality demands of the raw materials and the fresh concrete mixture. The concrete plant staff must be trained in handling the changed processes of mixing, placing, and finishing of SCC. A more stringent acceptance inspection of components at the plant is a necessity.

3.1.2 Control of raw materials

The following recommendations are based on a review of various guidelines given by national standards, including ACI Committee 237, 2004; PCI Interim Guidelines, 2003; EFNARC, 2002; and JSCE, 1999. In order to ensure equal quality of the basic materials, the grading curve of the aggregates must be tested frequently (for example every two weeks), and the chemical analysis of chemical admixtures and supplementary cementitious materials and fillers has to be performed weekly. The concrete producer should carry out frequent inspection of the aggregate. The most important factors of aggregate characteristics affecting the performance of SCC are as follows:

- **Moisture content of the sand**: It is important to register the moisture content of the sand since this affects variations in the properties of the concrete to a high degree. It is recommended that a maximum deviation of $\pm$ 0.2% from measured moisture content be maintained to reduce excessive variations in fresh concrete properties. The water content of

the sand should be determined in the storage place at short intervals before the production of SCC. It is highly advantageous if this moisture content is measured continuously.

- **Percentage of fine particles in the sand**: Minor variations in the percentage by mass passing sieve corresponding to ± 2% per 0.01 in. (0.25 mm) sieve are acceptable without adjustment of the mixture.
- **Fineness modulus of sand**: Attention should be paid to particle-size distribution of the coarser particles in the fine material. Variations in the fineness modulus of ± 0.2% can, for similar fine particle content in the fine material, affect the rheological properties of the concrete.
- **Moisture content in the coarse aggregate**: Moisture content in the coarse aggregate must be taken into account. Continuous moisture measurement may not be necessary, but an estimate of the moisture ratio is desirable. It is recommended to prepare a translation table of moisture content as follows: 1) 0% for dry coarse aggregate, 2) 0.5% for moist coarse aggregate, 3) 1.0% for wet coarse aggregate, and 4) 1.5% for very wet coarse aggregate.
- **Particle form**: The rounder a coarse aggregate is, the less risk of blocking it presents. The particle form influences the maximum coarse aggregate volume. Characterization of coarse aggregate form should be carried out at acceptance inspection. Even the form of the fine material is important, though primarily with regard to rheology, and not so much for blocking resistance.

In general, when producing SCC, quality tests on aggregate should be conducted and job site mixture proportions should be adjusted from time to time to adapt to new qualities of aggregate based on test results. In addition, surface moisture of aggregate should be frequently measured to allow prompt correction of the unit content. Changes in coarse aggregate gradations can strongly impact the passing ability of SCC mixtures. Fluctuation in aggregate free-moisture content must be controlled otherwise wide swings in both the fluidity and stability of the mixture can occur. Therefore, strict quality control should be used with respect to aggregate gradations and moisture contents. Aggregates should be covered to minimize the fluctuation of surface moisture content. During production of SCC, tests of aggregate grading and moisture content should be carried out more frequently than usual, since SCC is more sensitive than normal concrete to variations. Where the fluctuation of aggregate grading can have adverse effects on the fluctuation of SCC, aggregates with different grading should be stored separately. Different sizes of aggregate shall be stored in separate stockpiles, sufficiently removed from each other to prevent the material at the edges of the piles from becoming intermixed. The coarse aggregate shall be separated into two or more sizes in order to secure greater uniformity of the concrete mixture [AASHTO, 1998].

Cement that for any reason has become partially set or that contains lumps of caked cement shall be rejected. Cement held in storage for a period of over three months if bagged or six months if bulk, or cement that for any reason the Engineer may suspect is damaged, shall be subjected to a retest before being used in the work [AASHTO, 1998].

3.1.3 Batching

The size of the batch shall not exceed the capacity of the mixer. The measured materials shall be batched and charged into the mixer by means that will prevent loss of any materials due to effects of wind or other causes [AASHTO, 1998]. A batching error should be controlled with lower tolerance where required. It is recommended that the maximum tolerance for batching errors of air-entraining admixtures and HRWRA be 2% [JSCE, 1999]. Equipment must be calibrated so as to limit the potential for fluctuations in the batched proportions. A batching sequence should be established that promotes the optimal production of the mixture [ACI Committee 237, 2004].

3.1.4 Mixer characteristics

Since SCC often contains a high proportion of fine material, greater demands are placed on the mixer and on the order of mixing than in the case of ordinary concrete. There is no requirement for any specific mixer type. Forced action mixers, including paddle mixers, free-fall mixers, and truck mixers can all be used [Swedish Concrete Association, 2002; ACI Committee 237, 2004; EFNARC, 2002; JSCE, 1999; RILEM, 2000; Billberg, 1999].

The type and condition of the mixer have an impact on mixing efficiency, and hence mixing time. Generally, the mixing time for SCC needs to be longer than that for conventional concrete to achieve a homogenous and well-dispersed mass. ACI Committee 237 [2004] stipulates that the mixing time should be twice as long when producing SCC than conventional concrete. The mixing time should be not less than 90 seconds in the case of force action mixers [JSCE, 1999]. The mixing time depends to a great extent on the required *w/c*, fine material quantity, etc. The mixing time necessary should be determined by practical trials for different mix designs at the plant. When mixer performance tests are not made, the required mixing time for stationary mixers shall be not less than 90 seconds or more than 5 minutes [AASHTO, 1998].

The stability of SCC is highly sensitive to changes in total water content. Therefore, accurate determination of the moisture of the aggregates and mix water dosage must be carried out. SCC proportioned with relatively low powder content or without a VMA can be more sensitive to changes in water content. Therefore, in order to keep the consistency of the fresh concrete in the self-compactable range in terms of deformability and stability, determination of the correct water dosage leading to the desired total water content of the mixture is crucial. It is recommended to install a highly sensitive moisture-measuring system to be developed and installed in the concrete mixer to ensure accurate moisture control, especially that of the fine aggregate. With such measuring system, the surface moisture of the aggregates can be determined within the mixer with an accuracy of ± 3 L/m^3. This can lead to sufficiently accurate control of the actual water content of the mixture in everyday production, thus ensuring consistent production of stable SCC.

3.1.5 Mixing process

The mixing method of SCC should be adequately established on the basis of field experience or testing. The batch size should be determined in consideration of the type of SCC, mixing efficiency of the mixer, quantity to be transported, and shipping rate. The batch size should be limited to 80% to 90% of the maximum capacity of the mixer [JSCE, 1999].

Just prior to the mixing, the mixer should be either pre-wetted or 'buttered' with SCC or mortar of similar proportioning as that of the batch concrete [Swedish Concrete Association, 2002; JSCE, 1999]. Alternating production of normal concrete and SCC is possible without cleaning the mixer between batches; however, some precautions should be taken. When the same mixer is used for mixing conventional concrete and SCC without washing between the two, it should be confirmed beforehand by testing or field experience that no adverse effects are produced on the qualities of the SCC. The mixer should be carefully emptied before a new batch of SCC is mixed, and that any admixture from a previous batch must be compatible with HRWRA in SCC. In some cases, it has been observed that different combinations of older and newer HRWRA are incompatible, and make it very difficult to manufacture SCC [Swedish Concrete Association, 2002]. Newer types of HRWRAs are sensitive to limited quantities of air-entraining agents. If an air-entrained conventional concrete precedes the SCC, cleaning between batches becomes essential.

Prior to starting work, it should be confirmed by trial mixtures that the specified mixture proportions attain the required quality using the materials to be used and mixers of the plant to be used for actual construction. In case of nonconformance, the specified mixture proportions should be modified accordingly [JSCE, 1999].

High concrete temperatures should be avoided due to the risk of rapid loss in self-consolidating properties (loss in passing ability is more critical than loss in filling ability). Investigation regarding temperature sensitivity of the selected SCC should be carried out. Low concrete temperatures should also be avoided due to risk of retardation of strength development. If warm water were to be added, the concrete would often require increased mixing time. Excessively high water temperatures should be avoided, particularly in relation with certain air-entraining agents. Heated aggregate should be used as much as possible.

3.1.6 Mixing sequence

Mixing sequence is influenced by several parameters, including the flow of constituent materials into the mixer, the condition of the interior of the mixer, and the selected constituent materials and admixtures. Each plant is unique and should carry out its own experiments to achieve a suitable mixing sequence. Once established, the plant should adhere strictly to the optimized sequence.

In general, cement particles must be wetted before the HRWRA is released into the mixer (i.e. delay addition of HRWRA). Dry mixing of solid constituents before the introduction of water may lead to build-up of fine material in the mixer, resulting in increased wear. The HRWRA

must be carefully stirred before mixing to ensure uniform dispersion of active constituents and any other component (de-foaming agent, VMA, if any). In some cases an improved effect is achieved if the HRWRA is diluted with water, especially if the HRWRA is viscous. The VMA should be introduced towards the end of the mixing sequence, and the air-entraining admixture at the beginning. All water should be added at the same time, if possible. It is important to exercise good control over the moisture content in the aggregate and care in weighing the constituent materials. Intermixing of steel fibers or synthetic fibers can be done in the same way and in the same quantities as for ordinary concrete.

The following are examples of three mixing sequences that can be adopted for SCC.

Mixing sequence A

1. water + coarse aggregate + sand
2. cement + supplementary cementitious materials or filler
3. HRWRA with some delay between stages

Mixing sequence B

1. water + cement + supplementary cementitious materials or filler
2. coarse aggregate + sand
3. HRWRA with 20 sec delay between stages

Mixing sequence C

1. aggregate + water + ½ HRWRA and any other admixture
2. cement + supplementary cementitious materials or filler
3. remaining HRWRA with 5-10 sec between stages 1 and 2 and 30 sec between stages 2 and 3

3.1.7 Inspection of fresh concrete at the plant

The production of SCC requires intensified inspection compared to conventional concrete. Fresh concrete needs to be tested for its self-compacting properties. Since the quality of freshly mixed concrete may fluctuate at the beginning of production, it is recommended that the producer on every load should conduct workability tests, until consistent and compliant results are obtained [ACI Committee 237, 2004; EFNARC, 2002; JSCE, 1999]. When stable values of slump flow and air content have been established in several samples from subsequent deliveries, sampling frequency can be decreased. Given the fact that in a precast concrete plant the manufacturing conditions are rather constant, the first three mixtures of a day can be subjected to more complete inspection and routine testing. Subsequent mixtures of similar composition may be subjected to limited and less frequent testing. Nonetheless, every batch should still be visually checked before transportation and prior to casting.

3.2 Transport and Placement

3.2.1 General

Since SCC is based on concrete placement without vibratory consolidation, adequate construction plan should be formulated in consideration of the properties specific to SCC so that the proportioned concrete can be transported and placed while the required self-compatibility is retained. It is essential to make sure that delivery and placing can be completed within the workability-retention (self-consolidation) time of the concrete. Under normal conditions, SCC has an open time in excess of one hour (time after the end of mixing where the concrete still satisfies stipulated flowability, resistance to segregation, and passing ability requirements). However, for SCC used in precasting plants, this open time may be limited to 30-45 minutes.

3.2.2 Transport of SCC

As is the case of casting with normal concrete, the final result using SCC is influenced by several factors, including the consistency of the fresh concrete, formwork material quality, mould lubricant type and thickness, laying operations, and casting continuity (casting rate, concrete layer heights). However, because SCC does not require vibration for consolidation, the method of transport and discharge becomes an important consideration for placement. For SCC mixtures, the volume placed at a given point in time will affect placement, concrete cost, and ultimate concrete properties. Therefore, it is important to consider the actual placement method being used, as discussed in Chapter 1. Any method of transport can be employed as long as segregation is kept to acceptable levels. Mixer trucks, tuckerbilts, sidewinders, clam buckets, pumping, forklifts, and overhead cranes can be employed for the transport of SCC. SCC can be mixed and delivered to a job site by truck. Truck mixers should have high degree of efficiency with regard to design and condition of the paddles and rotation capacity of the rotator. When loading, the concrete, the container must not be dry, though it must be completely free from any standing water. Because of the fluidity of SCC, the volume of concrete placed into a truck should not exceed the capacity of the drum to avoid spilling of the concrete out the back of a rear discharge truck.

In addition to the placement technique, the required workability of the SCC should be compatible with the rate at which the concrete is discharged, the total volume of concrete being discharged, and whether or not the placement process is continuous or discontinuous. Table 3.1 presents a qualitative comparison between the energy characteristics associated with various standard placement techniques [Bury and Buhler, 2002]. The higher the relative energy delivered, the lower the fluidity level required for the concrete to flow the same distance. In addition, higher energy delivered may require increased awareness regarding the stability of the concrete.

Unexpected production stops can result in consistence variations that adversely affect the end results. It is essential to make sure that delivery and placing can be completed within the workability-retention (self-compactability) time of the concrete. Under normal conditions, SCC

used for ready-mix concrete applications should have a transportation time as short as possible, less than 60 minutes [RILEM, 2000]. During transport, the container is to rotate at low speed to ensure homogeneity of the concrete. The container of truck should rotate at low speed, but not less than one rotation per minute. In heavy rain the truck's feed hopper should be covered to prevent ingress of rain to the rotary container. Once at the site, the container should be rotated at high speed, 10 to 12 rotations per minute, for at least 3 minutes. Similar recommendations are given by JSCE [1999] where the container is required to rotate at high/highest rotation speed for at least 2 minutes before discharge of concrete. In the case of a divided discharge, the container is to rotate slowly while waiting and vigorously before continuing discharge.

Table 3.1 – Energy characteristics associated with different placement techniques

Placement Technique	Discharge Rate	Discharge Type	Single Discharge Volume	Relative Energy Delivered
Truck Discharge	High	Continuous	High	High
Pumping	Medium/High	Continuous	Medium	High/Medium
Conveyor	Medium	Continuous	High	High
Buggy	Medium	Discontinuous	Low	Low
Crane and Bucket	High	Discontinuous	Low	Low/Medium
Auger (Tuckerbilt) Discharge	Medium	Continuous	Medium	Medium
Drop Tube	High	Discontinuous	High	High

3.2.3 Sampling and acceptance on site

It is important that the contractor possesses both competence and mastery of verification methods in order to appraise the concrete in relation to the stipulated criteria. Inspection shall be conducted on produced and placed concrete at an appropriate time to ensure it satisfies the established performance requirements. Inspection of the workability is more important when casting SCC, as the casting will only rely on the inherent properties of the concrete and not on any external input of energy. As discussed earlier, self-compatibility covers not only the filling ability (deformability) and resistance to segregation, but also the passing ability of the concrete. Passing ability depends on the boundary conditions, including the shape, dimension and reinforcement of structures in which the concrete is placed. Therefore, the quality of fresh concrete shall thus also be characterized considering the boundary condition [RILEM, 2000].

All site acceptance testing should be carried out by competent personnel and in suitable environment (area protected against the weather; use of properly maintained and calibrated equipments; stable ground surface, etc.).

The extent of sampling and sampling methods should be dealt with and agreed upon beforehand in consultation with the contractor and concrete supplier. Communication between these parties is important and should be initiated at an early stage and even include pre-investigations of mix

design, transport, and casting methods. Similarly, criteria, and marginal limits for acceptance of SCC must be defined.

Greater slump flow consistency can be obtained from samples taken after the truck has discharged the first cubic meter of load. Differences of up to 4 in. (100 mm) in slump flow have been reported between sampling of the first volume taken from the truck and after two cubic meters have been emptied from a load. In general, samples should be extracted when approximately 0.65 yd^3 (0.5 m^3) has been discharged, and when there is a continuous flow in concrete chute or pump.

In general, a sampling should be made of slump flow and air content of every load until values show that the concrete maintains an even quality, shows resistance to segregation, and lies within the agreed limit values [JSCE, 1999]. Only when stable values of slump flow (and air content) have been established in several samples from subsequent deliveries may sampling frequency be decreased. The inspection for self-compatibility shall be carried out at least once for every 65 yd^3 (50 m^3) or fraction thereof of concrete by flowability tests using a filling tester [JSCE, 1998].

Sampling is to take place both before and after pumping at the outset and early stages of the casting in order to establish how the slump-flow and air content are affected by pumping and to ascertain the relationship between these two properties before and after pumping. As discussed in Chapter 1, several test methods and test combinations can be used for quality control of workability characteristics.

Concrete shall not be retempered with water; however, consistency may be adjusted on site using HRWRA to increase filling ability or air-entraining agent to increase the air volume. It is not recommended to incorporate VMA on site to save a segregating load. Procedures and instructions for such additions must be available on site. For the addition of HRWRA, care must be taken as small quantities can have great effect on the fresh concrete's filling ability and resistance to segregation. Special attention must be paid to the effect of HRWRA on retardation. The concrete manufacturer must guarantee the procedure in a written instruction to be handed, among others, to the truck operator.

An acceptable effect of the HRWRA can only be achieved if the fresh concrete has not stiffened too much during transport and waiting. As a rough estimate, the slump flow should be at least 18.5-19.7 in. (470-500 mm) if the addition of HRWRA to the rotating container is to have the desired effect. Rotation time after the addition of HRWRA should not be less than 5 minutes at highest speed.

3.2.4 Discharge of SCC

SCC mixtures can be transported to forms by sidewinder or hopper-type vehicles and by bucket. When hopper-type vehicles are used, SCC mixtures do not receive any additional mixing and must be stable to resist segregation from vibratory forces encountered during transport from the batch plant to a form. SCC transported by bucket from an overhead lift receives little to no vibration and does not require the same level of stability as SCC transported in a hopper-type

vehicle. Some precast producers have reported bolting rubber strips or pads to the clamshell discharge point of buckets to prevent leakage of fluid, low viscosity SCC mixes during transport to forms. For hopper or bucket placement method, the speed of SCC discharge is slower and discontinuous compared to placement by truck and SCC mixture should have a higher slump flow, such as 24-28 in. (610-710 mm). It is advantageous in precast, prestressed operations to switch to larger volume transport vehicles such as ready-mix trucks rather than hopper or buck transporters. This practice allows an entire piece to be poured with one load of concrete avoiding a situation where batching of the concrete cannot keep up with the placement speed. Although SCC placement by bucket has a high discharge rate, it is discontinuous. SCC transported to the form by bucket should also have a higher slump flow, such as 24-28 in. (610-710 mm), to help facilitate placement and increase flow distance [ACI Committee 237, 2004].

If concrete is placed by skip, attention should be paid to closure of the gate. Discharge of SCC in a receiving bin might be less suitable since the concrete must be kept moving as far as possible, until it rests in the formwork. When the fresh concrete displays pronounced thixotropic characteristics neither receiving bin nor skip should be used [JSCE, 1999].

Whenever practical, a payload with enough SCC to cast a section shall be used. This can help to prevent pour lines, cold joints, and potential segregation [PCI Interim Guidelines, 2003]. In most cases of SCC used in bridge building in Sweden, the time between mixing and casting has been set to 60 minutes but longer open times seem also to be possible to reach [RILEM, 2000].

A frequently recurring problem when casting with a chute is that it is difficult to move the chute over the whole formwork. The result is that the concrete is obliged to flow too far, pass reinforcement, etc., with high risk of segregation. When discharging with a chute, the outlet from the chute should be directed towards the front of the casting, that is, at the farthest reach, and withdrawn as casting proceeds. Attention should be paid to the thixotropy of the concrete when casting with a skip. A prolonged stagnation of the concrete in the skip can cause the concrete to stiffen so that it does not run from the skip spontaneously when opened for discharge.

For placing large quantities of fresh concrete, piston pumps are generally used [PCI Interim Guidelines, 2003]. It is possible to pump SCC using conventional pumping equipment, as long as the mixture is stable. Therefore, special care must be taken to have minimal segregation of the SCC to avoid blockage and overpressure in the pumpline. When pumping stable SCC, the pump pressure can be even lower in relation to the pumping of conventional high-performance concrete used for transportation structures. Measures should be taken to keep the pump pressure as low as possible. Low pressure with high feed speed is preferable to vice-versa. At high pressure, extensive losses in consistency and air content can take place. Pumping should be carried out such that an even rate of rise in the formwork is achieved, with as few breaks as possible. Pumping velocity is to be set so that pump stoppage is avoided as far as possible.

Typically, the pump hose is kept 1.6-2.6 ft (0.5-0.8 m) above earlier concrete layer upper surface. This depends on the rheology of the concrete, design of the formwork, configuration of the reinforcement, etc. [JSCE, 1999]. When casting bigger vertical structures where the concrete

does not drop through reinforcement, after a pause or when the concrete in the formwork has begun to stiffen, the dropping height could be increased to "awaken" the concrete placed earlier and improve bond with the new layer. However, care must be taken to avoid segregation resulting from allowing the concrete to drop through the reinforcement.

Care must be taken to fill the total length of the pump without creating blockage. In order to prevent blockage, a) the pump network must be concrete tight, b) fresh concrete should have minimal segregation, c) a sufficient volume of cement grout has to be pumped before fresh concrete can be pumped, and d) time to initial set needs to be longer than placement time [PCI, 2003].

3.2.5 Placement of SCC

Production coordination is essential on larger placements to ensure adequate and timely supply of SCC. In a placement that will require multiple batches, concrete should be available within a short time frame, because of the ability to discharge SCC fast and over a large area. As a result, surface area exposed to weather conditions is increased and needs to be replenished with additional SCC or protected against premature moisture evaporation that can cause plastic shrinkage cracking. In drier and warmer ambient conditions, pour lines may be a cause of inadequate SCC supply in a timely manner. Pour lines appear as darker thin lines that can distinguish between layers of concrete placed. These pour lines can be merely cosmetic, or can indicate cold joints.

As in the case of conventional concrete, the SCC shall not be placed until the forms and all materials to be embedded in the forms have been inspected and approved by the Engineer.

In casting horizontal elements, the SCC can be cast by starting at one end of the mold, with the discharge as close to the form surfaces as possible. Another method is to start placing in the center of the mold so that the mix flows outward from the center in both directions. It is recommended to discharge the SCC in the direction of desired flow to maximize the travel distance. In the case of structural concrete, the Swedish Concrete Association [2002] recommended that horizontal spread of the concrete should be limited to a maximum of 16 to 20 ft (5 to 6 m), while the permissible distance of horizontal flow from point of discharge is limited to 33 ft (10 m) [EFNARC, 2002; Brite-EuRam Report, 1998]. In most cases, the recommended maximum flowing distance should be between 10 and 33 ft (3 to 10 m) [RILEM, 2000]. In other words, the casting points shall be prepared so that the intervals do not exceed 20 to 66 ft (6 to 20 m). The maximum lateral flow distance suggested by JSCE [1999] is 26 to 49 ft (8 to 15 m). When casting an extensive horizontal area, permanent stop ends of metal lathing may be successfully used [Swedish Concrete Association, 2002]. The flow gradient of SCC can vary typically between 1/10 and 1/100 [RILEM, 2000]. It has also been reported that segregation does not occur if the horizontal flowing distance does not exceed 33 ft (10 m) provided that the mixture proportion is properly designed. The author [Khayat et al., 2000a] reported that SCC developed for building construction with slump flow consistency of 23.6 in. (600 mm) can spread 33 ft (10 m) when cast in an 7.9-in. (200-mm) wide wall section, and maintain more or

less uniform in-situ compressive strength (about 5,800 psi, 40 MPa) throughout that distance. Such concrete can also exhibit excellent uniformity of in-situ air-void system and rapid chloride-ion permeability.

When using relatively non-viscous SCC, too great a casting rate can lead to an increased number of surface pores caused by encapsulated air not having time to rise to the surface and escape when the concrete is supplied too fast. It is recommended that sections with lengths of less than 20 ft (6 m) be filled from one end to give the concrete sufficient time during flow to permit air to rise to the surface, thus reducing the number of surface pores. The exact casting rate should be adequately established according to the mixture proportions, geometry of members, and reinforcement conditions on the basis of test results and field experience [JSCE, 1998].

According to AASHTO LRFD Bridge Construction Specifications [1998], a tube fitted with a hopper head should be employed whenever the placement of concrete would involve dropping the concrete more than 5 ft (1.5 m) in the formwork. Otherwise, the concrete should be placed through other approved devices to prevent segregation of the mix and spattering of mortar on steel and forms above the elevation of the lift being placed. This requirement shall not apply to cast-in-place piling when concrete placement is completed before initial set occurs in the first placed concrete. In the case of SCC, similar practices could apply when casting wall, column, piling, or other deep sections. In addition to higher risk of segregation and splashing of mortar onto upper reinforcement, free-fall of concrete can result in trapping air within the concrete with consequences on in-situ hardened properties and surface quality. Vertical dropping of SCC directly onto existing layers of already placed concrete can produce a vortex of the new concrete influx into the old layer which can cause the creation of a significant amount of entrapped air that will be retained within the concrete. Such entrapped air is not likely to rise completely to the surface in the absence of vibration consolidation of the concrete.

The free-fall distance should be controlled, as with normal concrete, to avoid segregation. Norwegian experience is to limit free-fall height to 6.6 ft (2 m) for casting of wall and beam elements. When casting bigger vertical structures, the concrete does not drop through reinforcement. In special cases this distance can be increased, but it will affect the end result with more surface pores and honeycombs as a result. According to other standards [JSCE, 1998 and 1999; EFNARC, 2002; RILEM, 2000], the dropping height should be limited to 16.5 ft (5 m). Recently, at the Rosenthal Contemporary Arts Center in Cincinnati, 28-ft (8.5-m) tall columns containing acute angles were successfully placed using SCC cast with a tremie pipe of only 8 ft (2.4 m) in length, hence resulting in an initial free-fall of 20 ft (6 m) [Johnston, 2002]. As mentioned earlier, when the concrete in the formwork has begun to stiffen, the dropping height can be increased in order to “awaken” the concrete in earlier concrete layers and improve bond with the new layer [JSCE, 1999].

If the SCC requires some vibration to enhance surface quality or ensure full filling of congested structural elements, pencil vibrators may be used for a short duration for quality assurance purposes and in some critical areas after use. It is difficult to perform vibrating using conventional equipment – frequencies are too high and amplitude too small. Although SCC

bonds well with previously placed concrete, the likelihood of damage resulting from a cold joint cannot be mitigated by vibration, as with normal concrete. Any external vibration to remedy honeycombing or bug holes will do more damage than good and can cause bleeding, sand-streaking, and severe aggregate segregation within the unit.

3.2.6 Specific recommendations for casting different structural elements

For the production of precast, prestressed double Tee beams, it is recommended to cast the stems of each double Tee first, and then proceed with the flange portion. Placement should start from the middle of the bed, allowing the SCC mixtures to flow into place on their own towards the ends of the bed. Slump flow values of 23-26 in. (585-659 mm) can be adequate for such application. Another proven method for placing SCC for casting double Tee sections is to use hopper-type vehicles and to start filling both the stems on one side of the Tee and the flanges at the same time, and moving forward to the end of the section as the concrete fills the stem. The same process is repeated for the other stem and flange side. The final finish should be applied as appropriate. This method does not require a mechanical screed and has only slightly delayed finishing characteristics [Bury and Bühler, 2002].

Many different configurations of precast, prestressed beams are produced in the marketplace. Some of the more difficult to produce beams are quite heavily reinforced with Type V or VI beams often reaching heights of 8 ft (2.4 m) or more. Ideally, the point of SCC filling should be near one end of a beam and remain there until it is filled completely. For more heavily-reinforced, taller beams, a higher slump flow value of 24-28 in. (610-710 mm) has been shown to work best [Bury and Bühler, 2002]. In most cases, no vibration is necessary for consolidation of the SCC mixture.

According to AASHTO LRFD Bridge Construction Specifications [1998], concrete for T-beams or deck girder spans whose depth is less than 4 ft (1.2 m) may be placed in one continuous operation or may be placed in two separate operations: first, to the top of the girder stems, and second, to completion. For T-beams or deck girder spans whose depth is 4 ft (1.2 m) or more, concrete shall be placed in two operations, and at least five days shall elapse after placement of stems before the top deck slab is placed. Concrete for box girders may be placed in two or three separate operations consisting of bottom slag, girder stems, and top slab. In either case, the bottom slab shall be placed first and, unless otherwise permitted by the Engineer, the top slab not be placed until the girder stems have been in place for at least five days.

Caution should be used when SCC is employed for casting slabs. The major challenge is to keep the concrete surface and the front edge of the flow fresh enough to maintain SCC properties at all times. Use of SCC on this kind of slab requires a large supply of concrete and systematic placing and surface finish. SCC should be discharged at one point and allowed to flow as far as practical before moving the point of placement. This will allow the mixture to fill the form and self-level, thereby minimizing the degree of screeding and bull floating typically required when leveling slabs. Reports from some field trials indicate that SCC can be discharged at a rate of 9 yd^3/min (7 m^3/min) from ready-mixed concrete trucks. It has been reported that SCC field trial slabs can

accept virtually any type of finish such as mag swirl, broom, or steel trowel. In Norway, SCC for slabs is generally cast at slump flows of 24.8 to 27.6 in. (630 to 700 mm) and a low T-50 flow time, which means that the concrete flows quickly into place.

In casting slabs, it is normal to have a super elevation at the center of 0.59-0.79 in. (15-20 mm) to compensate for deflection during drying and hardening. Controlled superelevation is however difficult with SCC because of its high flowability which necessitates lowering the slump flow value. Experience shows that a slump flow value in the range 21.6-23.6 in. (550-600 mm) would work well [Bury and Bühler, 2002]. To have full control of the casting, the slabs should be split into areas of 1075 ft^2 (100 m^2).

The potential to achieve an inclined surface depends on the composition of the SCC, choice of casting procedure, and means of surface finishing. It has been possible to cast slopes of up to 4% for bridge decks in Sweden. Experience shows that a 3% to 4% slope is in practice an upper limit. Concreting wet on wet with topping of conventional concrete has been shown to function well for the creation of a sloping, free-top surface. Removal of the top formwork on the wings of bridges and scrubbing of the concrete surface has been successfully carried out after 5 hours.

Modules and walls are more difficult elements to perfect when using SCC, primarily due to the high potential for honeycombing. Some of these structures are very thin in nature and are often less than 4 in. (100 mm) thick. On modules containing a core, SCC should be placed onto the core, and then allowed to run over the edge and into the wall. On walls without cores, specially manufactured deflectors or breaker boards attached to the forms or the discharge container can guide concrete into place to avoid direct free-fall that could entrap air. A high slump flow value of 26-27.6 in. (660-700 mm) seems to work best for modules and walls. The Swedish Concrete Association [2002] recommends that walls with lengths of less than 6 m should be filled from one end to give the concrete sufficient time during flow to permit air to rise to the surface, thereby reducing the number of surface pores. SCC placed in narrow forms can achieve better flowing potential because the discharge is concentrated in one area, creating a head of SCC that facilitates flow in the longer direction.

Column placement necessitates greater care to ensure proper resistance to bleeding, segregation, and surface settlement that the placement of slabs or other elements of limited depth. The deeper the element depth, the higher the required level of dynamic stability during placement and static stability thereafter must be, until the onset of hardening. When casting column sections, a continuous supply of concrete should be provided to maintain a certain head of concrete in the column, and allowed to flow into place. It is also possible to pump SCC mixtures into the bottom of a column form and let the concrete rise up into the form, as was the case for the construction of a new terminal building at Pearson International Airport in Toronto. The fluid nature of SCC makes this placement technique possible with minimal bug holes and no segregation. The volume of the column is normally low, and the casting rate is high. Columns are typically filled with SCC within a few minutes. Concrete has a tendency to settle in the plastic state during the first hours after casting, especially if the casting is very rapid (not much thixotropy). This effect can especially be seen with ordinary concrete in connection with beam-slab interaction as cracks

may appear at the top surface. This is normally solved with a re-vibration 1 to 2 hours after casting. With SCC no vibration is used, and this may be a problem in some cases. As in the case of wall sections and deep beam elements, special attention is required to the static stability of the concrete to minimize surface settlement.

Some columns are precast and produced with the forms positioned horizontally. For this application, SCC can be placed using the same methodology used for beam elements by discharging the concrete at one end of the form and letting it flow into place. It is critical in this application to ensure that the mixture does not bleed where water would collect on the inside top of the mold.

The casting of culvert structures is tough and labor intensive when carried out with ordinary concrete. The outer formworks are put in place during the casting. Only the bottom part is installed when the pouring starts in order to facilitate access with poker vibrators and have a controlled casting. When the concrete has reached the top of the bottom part of the formwork, the casting must pause to install the next section of the formwork. This takes time and involves possible dangerous operations with lifting of formwork systems. With SCC, it is possible to install the formwork before casting, resulting in greater safety. Concrete hose should be placed into the formwork prior to its closure. This ensures a controlled placing of the SCC into the form with reduced probability of segregation during casting. Concrete should be placed by alternating from one side to the other to prevent biased loading on the form. Height difference should be less than 3.3 ft (1 m) on each side of the culvert.

3.3 Formwork and Form Pressure

Some precast, prestressed beams can reach heights of 8 ft (2.4 m) or more necessitating special considerations for lateral pressure to ensure formwork tightness. SCC has high fluidity and will leak trough all openings that are more than a few millimeters in size. All previous holes, mismatched tie rods between different elements, etc., must therefore be sealed before casting. The same also applies to fitting against the ground and end locking of the formwork. The concrete will eventually block small gaps and openings, but not without causing a lot of spills and messing up the formwork and the surroundings. One other important factor is securing the form against the uplift force from the concrete. If this is not done, leakage will occur.

The more intricate the form shape, the more difficult it will be for a concrete mixture to flow into place during the filling process and produce an element without voids or honeycombing. Because of a lack of edges or corners, for example, a round column is easier to produce with few surface voids than a square column. The element intricacy will help determine the required flow level of the SCC mixture. In general, the higher the level of form intricacy and reinforcement congestion, the higher the required slump flow will be.

When a form contains reinforcing steel, there is a minimum clear spacing between different sections of reinforcing steel as well as between the reinforcing steel and the form wall. The more congested the form is however, the higher the potential for aggregate bridging and blocking that

can lead to separation of the SCC mixture. For congested steel reinforced forms, a smaller coarse aggregate top size is required to minimize or eliminate this phenomenon during placement. The SCC mixture must also be stable to reduce the potential of aggregate separation from the paste as the mixture flows between reinforcing bars and prestressing strands.

Formworks can be constructed of several types of materials, including wood, steel, plastic, concrete, fiberglass, or other combinations of material. Wooden formwork often leads to less pores and bubble formation than smooth formwork. The wear on formwork boards is considerably less with SCC than with conventional concrete. SCC does not manage to penetrate the wood fibers, and as it is observed with vibrated concrete, it grips onto them.

Due to the greater surface friction with wooden formwork, the risk of casting ridges and smaller casting faults increases. Smooth formwork has less friction, and the risk of casting ridges diminishes, but encapsulated air and separated water find it difficult to escape and thus lead to greater risk of pores and bubbles [Swedish Concrete Association, 2002]. Fluid form wax has been shown to work well as a mould release agent [Swedish Concrete Association, 2002]. Vegetable oil is also a good release agent as it reduces the amount of pores on the surface of the concrete [Brite-EuRam Report, 1998]. It is important to keep the wood of the formwork dry when the oil is applied.

Formwork shall be rigid enough to maintain proper dimensional tolerances and withstand lateral form pressure exerted by the plastic concrete. Before placing SCC, it should be confirmed that reinforcement and formwork are arranged as planned. The formwork must be in good condition. Contractors may wish to consider possible advantages of pumping from the bottom of formwork.

Formwork pressure is a major concern when SCC is used. The formwork pressure can be affected by the casting rate, formwork height, formwork movements, *w/c*, aggregate content, admixtures in use, temperature conditions, etc. Lateral pressure on formwork is highly dependent on the casting rate and the height of the formwork. Experience shows that the formwork pressure is in the same range as with normal concrete when cast with the same rate of rise. In the case of continuous casting, such as in the case of column and wall panels, the casting rate can be quite high approaching 32.8 ft/hr (10 m/hr), which is considerably greater than when conventional concrete is used. Unless otherwise known, full hydrostatic pressure should be assumed, which is calculated as the multiplication of the unit weight of the concrete by the gravity and the height of placed concrete. RILEM [2000] and JSCE [1998] recommend that the lateral pressure of SCC acting on the formwork should be designed as liquid pressure. EFNARC [2002] recommends that for cast in-place applications, formwork in excess of 9.9 ft (3 m) in depth should be designed for full hydrostatic head.

Depending on the casting rate and the inherent thixotropy of the SCC in use, lower relative pressure can be obtained. This is especially the case when the casting rate does not exceed 9.9 ft /hr (3 m/hr), which is typical in casting structural girders for precast, prestressed applications. For cast in-place SCC used in structural applications, rates of casting of up to 6.6 ft/hr (2 m/hr) have occurred. Measurements show that pressure on formwork of such concrete can be 50% to

80% of the dimensioned pressure one can calculate for conventional vibrated bridge concrete with a slump of 100 mm [RILEM, 2000]. Whenever the cross sections of the structures become smaller, the form pressure tends to decrease, approaching the lateral pressure of the normal concrete.

SCC poured from the top of formwork results in lower form pressure than when the concrete is pumped from the bottom. The reason for the lower form pressure is the inherent thixotropy of the SCC used [RILEM, 2000]. Thixotropy refers to the decrease in viscosity with time of a liquid subjected to a given shear rate. Thixotropy is related to the rate of coagulation and restructuring of the liquid following a given period of rest. Therefore, concrete that exhibits a high level of thixotropy can develop lower lateral pressure and sharper rate of drop in pressure with time [Assaad et al., 2003].

Most formwork systems can manage full hydrostatic pressure if the formwork is not higher than 9 ft (2.7 m). With higher forms and a high casting rate, for extra security, there should be formwork surveillance and possibly measurement of form tie force so that the permitted dimensioning load is not exceeded. Formwork surveillance can check impressions and deformations in clamp ties. When there are signs of pressure on formwork, a break should be made in the casting.

3.4 Finishing

In the case of conventional concrete, AASHTO LRFD Bridge Construction Specifications [1998] allow the use of hand-finishing methods if approved by the Engineer for short bridges 15 meters or less in length or for irregular areas where the use of a machine would be impractical. Otherwise, finishing machines are used and shall go over each area of the surface as many times as required to obtain the required profile and cross-section. After strike-off, the surface shall be finished with a float, roller, or other approved device as necessary to remove any local irregularities and to leave sufficient mortar at the surface of the concrete for later texturing. The addition of water to the surface of the concrete to assist in finishing operations will not be permitted. In the case of SCC, finishing is much easier and faster than for conventional concrete. The reason is the self-leveling effect of SCC that allows skipping one or several operations. The necessity of having a quality surface finish will be dictated by the characteristics of the SCC mixture itself, and by the skill and timing of the finisher during placement. For example, the finish for a residential slab, although affected by mixture properties, is mainly determined by the finishing technique. This is in contrast with an architectural panel or column sections where the surface in question is formed and mainly controlled by the flow properties of the concrete. Improved surface appearance is generally obtained with high levels greater than 24 in. (610 mm) of slump flow with controlled viscosity and minimal to no bleeding.

SCC surfaces should be roughly leveled to the specified dimensions, and the finishing should then be applied at an appropriate time before the concrete stiffens [EFNARC, 2002]. Difficulty may be encountered with the conventional process of final surface hardening of horizontal areas

of concrete by repeated steel troweling. Alternative procedures or different tools may be required.

Due to the greater filler content and/or use of VMA, the concrete can exhibit thixotropic stiffening where its "stickiness" increases rapidly in the period 10-40 minutes after the concrete is in place. Therefore, it is important to begin the completion of the surface with light vibrating screeds, or other manual equipment, as soon as the correct level of the concrete has been reached in the formwork. Vibrating floats proved to be effective in the screeding of bridge decks. If the surface slopes more than 2%, one must be careful in the use of vibrating equipment. It has been possible to cast slopes of up to 4% in the casting of bridge decks. A 4% slope is in practice an upper limit [Swedish Concrete Association, 2002]. It may be difficult to obtain slopes of greater than 2% without using an upper form. If slope is desired, it may even be necessary to reduce slump flow in the mix design phase or use conventional concrete [Brite-EuRam Report, 1998].

As in the case of conventional concrete, a finishing aid/evaporating retardant sprayed upon the surface in a light mist will aid in the finishing and help controls plastic shrinkage cracking. This may be particularly helpful for outside finishing operations. Most surfaces may require only nominal screeding and floating, and other surfaces may require a mild vibratory screeding depending on mix characteristics and ambient conditions [ACI Committee 237, 2004; PCI, 2003]. For the finishing, wood floats, steel trowels, and square timbers have been normally used as well as for conventional concrete. For a better quality of surface, use of air-permeable sheets on the formwork is effective. Moreover, properties of the form release agent, the casting rate and the deformability of the SCC are influential on the surface property of the structure. The incorporation of VMA plays an important role in finishability and outcome of the finished surfaces [RILEM, 2000].

When producing an exposed aggregate finish, high volumes of coarse aggregate are required. This characteristic was created to cover this application. Coarse aggregate content is one of the main issues controlling passing ability, and must be taken into consideration when proportioning the mixture.

After finishing, the entire surface shall be checked with a 9.9 ft (3 m) metal straightedge operated parallel to the centerline of the bridge and shall show no deviation in excess of 0.1 in. (2.5 mm) from the testing edge of the straightedge. For deck surfaces that are to be overlaid with 1 in. (25 mm) or more of another material, such deviation shall not exceed 0.4 in. (10 mm) in 10 ft (3 m). Deviations in excess of these requirements shall be corrected before the concrete sets [AASHTO, 1998]. Exposed surfaces should be covered as soon as possible after the finishing of the surface (leveling, floating, etc.) is completed.

3.5 Curing

Compared to conventional concrete, SCC normally incorporates a greater dosage of HRWRA, which typically results in some retarding effect of setting time. SCC has a prolonged setting time of 1-2 hours when compared to normal concrete of similar type. In winter casting, this

retardation has noticeable effect on stripping time of the formwork and actions necessary to maintain the desired form removal time. Like setting time, heat of hydration and strength development are affected by cement type and use of set accelerator.

SCC tends to dry faster than conventional concrete because there is little or no bleed water at the surface. This is especially the case when casting in hot, sunny or windy conditions. Initial curing should therefore be commenced as soon as practicable after placing and finishing operations are completed in order to minimize the risk of shrinkage cracking [AASHTO, 1998; EFNARC, 2002]. If the surface of the concrete begins to dry before the selected cure method can be applied, the surface of the concrete shall be kept moist by a fog spray applied so as not to damage the surface.

Exposed surfaces should be covered as soon as possible after finishing of the surface (leveling, floating, etc.) is completed. As with vibrated concrete, membrane curing, mating, foils, or similar covering material should be left in place for at least 4 days for cast in-place concrete [Swedish Concrete Association, 2002]. This applies to concrete with low *w/c* and that with high fines content and/or VMA that have little free water content. In very hot, sunny, or windy weather conditions, moisture should be added by watering or by covering the surface with wetted insulation matting. An atomized water curtain, created by spraying the upper surface from a high-pressure nozzle (directed upwards over the concrete surface) has proved effective in counteracting plastic shrinkage cracks at an early stage.

SCC is more sensitive to changes in ambient temperature. In very hot, sunny or windy weather conditions, moisture should be added by watering or by covering the surface with wetted insulation matting [Swedish Concrete Association, 2002].

AASHTO LRFD Bridge Construction Specifications [1998] recommend that for concrete cured other than by steam or radiant heat methods, whenever there is a probability of air temperature below 36°F (2°C) during the cure period, the concrete shall be maintained at a temperature of not less than 7°C for the first 6 days after placement. This period should be extended to 8, 9, and 10 days when pozzolans are used as partial replacement of the cement of 10%, 11%-15%, and 16%-20%, respectively. However, if the compressive strength of 65% of the specified 28-day design strength is achieved in 6 days, an extended period of controlled temperature may be waived [AASHTO LRFD Bridge Construction Specifications, 1998]. For other than top slabs of structures serving as finished pavement, the above curing periods may be reduced and curing terminated when test cylinders cured under the same conditions as the structure indicate that concrete strengths of at least 70% of that specified have been reached [AASHTO, 1998].

In addition to curing temperature, the rate of strength gain depends on the *w/cm*, type and content of cement, use of supplementary cementitious materials, and type and concentration of admixtures. The use of a new generation of polycarboxylate-based HRWRA promotes early strength gain. SCC made with such HRWRA can achieve high-early compressive strength to permit the release of prestressing load without the need for steam curing or radiant heat curing. Consequently, heat curing can potentially be reduced or eliminated in the production of some

precast products that require heat curing for early strength development [ACI Committee 237, 2004].

If necessary, steam curing or radiant heat curing can be used for precast concrete members, According to AASHTO LRFD Bridge Construction Specifications [1998], the initial application of steam or heat shall be from 2 to 4 hrs after the final placement of concrete to allow the initial set of the concrete to take place. If set retarders are used, the waiting period shall be increased to between 4 and 6 hrs after placement. During the waiting period, the temperature within the curing chamber shall not be less than 50oF (10oC), live steam or heat may be used to maintain the curing chamber at the proper minimum temperature and the concrete shall be kept wet. During the initial application of live steam or radiant heat, the ambient temperature within the curing enclosure shall increase at an average rate not exceeding 72oF (22oC) per hour until the curing temperature is reached. The maximum curing temperature shall not exceed 160oF (71oC) and shall be held until the concrete has reached the desired strength. In discontinuing the steam applications, the ambient air temperature shall not decrease at a rate to exceed 72oF (22oC) per hour until a temperature 52oF (11oC) above the temperature of the air to which the concrete will be exposed has been reached. Unless the ambient temperature is maintained above 61oF (16oC), for prestressed members the transfer of the stressing force to the concrete shall be accomplished immediately after the steam curing or the heat curing has been discontinued.

3.6 Most Significant Production and Placement Characteristics Affecting Constructability of Precast, Prestressed Bridge Elements

The constructability of SCC depends on the reliability of quality control of materials, and on mixing process, transportation, casting, finishing, and curing. Relevant factors that need to be considered for the production and placement of precast, prestressed concrete bridge elements produced with SCC have been discussed in detail in this chapter. These factors are briefly summarized here; the reader is urged to refer to the discussion provided in sections 3.1 to 3.5 for further details on the most significant factors affecting the production, discharge, placement, finishing, and curing of SCC.

Production

- Greater care and precision are required for the production of SCC than conventional concrete, thus increasing the need for inspection and quality control.
- Concrete plant staff must be trained in handling the changed processes of mixing, placing, and finishing of SCC.
- Strict quality control should be used with respect to aggregate gradations, moisture contents, fineness modulus of sand, as well as moisture content in coarse aggregate and particle form of the coarse aggregate.

- It is essential to maintain uniform quality of all constituent materials in the production of SCC.
- A lower tolerance for batching errors is required for SCC, necessitating more frequent calibration of batching equipments to limit the potential for fluctuations in the batched proportions.
- A batching sequence should be established that promotes the optimal production of the mixture.
- The type and condition of the mixer have an impact on mixing efficiency. Generally, the mixing time for SCC needs to be longer than that for conventional concrete to achieve a homogenous and well-dispersed mass.
- The mixing method of SCC should be adequately established on the basis of field experience or testing. The batch size should be determined in consideration of the type of SCC, mixing efficiency of the mixer, quantity to be transported, and shipping rate.
- Special considerations are given to mixer condition before mixing SCC to avoid contamination of the SCC by water or admixtures used in previous batches.
- Suitable mixing sequence should be optimized and adhered to strictly to produce uniform quality concrete.
- Acceptance testing should be carried out by competent personnel and in a suitable environment (area protected against the weather; use of properly maintained and calibrated equipments; stable ground surface, etc.).

Transport, discharge, and placement

- Delivery and placement of SCC must be completed within the workability-retention time of the concrete. At the completion of placement, the concrete should still satisfy stipulated deformability, passing ability, and stability requirements.
- In the precasting plant, transportation is much less a problem than for ready-mixed concrete.
- The method of transport and discharge should be taken into consideration in finalizing the workability characteristics of the SCC. The required workability of SCC should be compatible with the rate at which the concrete is discharged, the total volume of concrete being discharged, and whether or not the placement process is continuous or discontinuous.
- Adequate inspection of workability is more important when casting SCC, as the casting will only rely on the inherent properties of the concrete and not on any external input of energy.
- Whenever practical, a payload with enough SCC to cast a section shall be used. This can help to prevent pour lines, cold joints, and potential segregation.
- In casting beam elements, the SCC can be cast by starting at one end of the mold, with the discharge as close to form surfaces as possible. The concrete should be discharged in the

direction of desired flow to maximize the travel distance. Another method is to start placing in the center of the mold so that the mix flows outward from the center in both directions.

- The flow distance of the SCC should be limited to 20 ft (6 m) in densely reinforced beam elements to maintain uniform in-situ properties of the hardened concrete. Other recommendations permitting longer horizontal spread distances of SCC in wall and slab elements are discussed in Section 3.2.5.
- The placing rate of SCC should be established adequately according to the geometry of members, reinforcement conditions, and mixture proportions on the basis of test results and field experience.
- In heavily reinforced precast, prestressed beams, slump flow values of 24-28 in. (610-710 mm) can be adequate (see Chapter 1 for performance specifications). Special care must be taken to provide adequate static stability after the placement, especially when casting deep structural elements.
- It is recommended to cast precast, prestressed beams in one continuous operation to avoid lift lines. The casting rate should be adjusted to reduce the number of surface pores caused by encapsulated air not having time to rise to the surface and escape. This is especially the case when using relatively non-viscous mixtures that flow rapidly into place.
- Free-fall distance of SCC in the formwork should be controlled to avoid segregation, surface pores, and honeycombs and should be limited to 6.6 ft (2 m) for casting of wall and beam elements. Otherwise, the concrete should be placed through other approved devices to prevent segregation of the mix and spattering of mortar on steel and forms above the elevation of the lift being placed.
- Height of vertical dropping of SCC directly onto existing layers of already placed concrete should be reduced to prevent air entrapment.
- If the SCC requires some vibration to enhance surface quality or ensure full filling of congested structural elements, pencil vibrators may be used for a short duration. Great care must be taken to avoid bleeding, sand-streaking, and aggregate segregation that can result from extended vibration.

Formwork and form pressure

- Formwork shall be rigid enough to maintain proper dimensional tolerances, withstand lateral form pressure exerted by the plastic concrete, and prevent grout leakage.
- The formwork pressure is highly dependent on the casting rate and the height of the formwork. Rates of casting of up to 6.6 ft/hour (2 m/hour) can occur in precast applications. Depending on the casting rate and the inherent thixotropy of the SCC in use, lower than hydrostatic pressure can be obtained when the concrete is cast at this rate of rise. However, unless otherwise known, full hydrostatic pressure should be assumed in the design of the formwork.

- Wooden formwork often leads to less pores and bubble formation than smooth formwork systems. Smooth formwork has less friction, and the risk of casting ridges diminishes, but encapsulated air and separated water find it difficult to escape, thus leading to a greater risk of formation of surface voids.
- The use of fluid form wax and mould release agent can work well for SCC.

Finishing and curing

- The necessity of having a quality surface finish will be dictated by the characteristics of the SCC mixture itself, and by the skill and timing of the finisher during placement. Improved surface appearance is generally obtained with high levels of slump flow with controlled viscosity and minimal to no bleeding.
- SCC surfaces should be roughly leveled to the specified dimensions, and the finishing should then be applied at an appropriate time before the concrete stiffens. Care must be exercised in thixotropic mixtures where "stickiness" can increase rapidly after placement.
- If some leveling is necessary, a vibrated screed may be used, at very low setting, to level the SCC.
- Finishing aid/evaporating retardant sprayed upon the surface in a light mist will aid in the finishing and help control plastic shrinkage cracking. Exposed surfaces should be covered as soon as possible after the finishing of the surface is completed.
- The form release agent, casting rate, deformability of the SCC, and content of ultra-fines and incorporation of VMA play an important role in finishability and outcome of the finished surfaces.
- SCC tends to dry faster than conventional concrete because there is little or no bleed water at the surface. This is especially the case when casting in hot, sunny or windy conditions. Initial curing should therefore be commenced as soon as practicable after placing and finishing operations are completed in order to minimize the risk of shrinkage cracking. If the surface of the concrete begins to dry before the selected cure method can be applied, the surface of the concrete shall be kept moist by a fog spray applied so as not to damage the surface.
- SCC is more sensitive to changes in ambient temperature. In very hot, sunny or windy weather conditions, moisture should be added by watering or by covering the surface with wetted insulation matting.
- Depending on the binder composition and content, and on the *w/cm*, SCC mixtures produced with polycarboxylate-based HRWRA can exhibit no significant delay in setting time. SCC made with such HRWRA can achieve high-early compressive strength to permit the release of prestressing load without the need for steam curing or radiant heat curing.

CHAPTER 4 – FACTORS AFFECTING MECHANICAL PROPERTIES AND STRUCTURAL PERFORMANCE OF SCC

4.1 Introduction

Both changes in mixture design and in fluidity of SCC can influence its hardened properties, which can diverge from what is commonly expected from vibrated concrete of normal consistency. If certain key properties are important in a specific application, they need to be considered when designing an SCC mixture. This chapter reviews the most relevant and important mechanical properties that can influence the design and performance of precast, prestressed bridge elements.

4.2 Compressive Strength

In general, compressive strength of SCC should be higher than that of conventional slump concrete since SCC is proportioned with relatively low *w/cm* necessary to enhance resistance to segregation [ACI Committee 237, 2004; RILEM, 2000; Swedish Concrete Association, 2002]. Even at the same *w/cm*, properly designed SCC can exhibit higher compressive strength than conventional slump concrete due to the incorporation of supplementary cementitious materials and fillers that can serve as nucleation sites and refine the porosity of the cement paste.

For precast and structural civil engineering applications, SCC mixtures are typically proportioned with a *w/cm* of 0.32 to 0.36 [ACI Committee 237, 2004]. Mixtures with greater *w/cm* (higher than 0.40) are sometimes employed for cast-in-place and repair applications. For precast, prestressed concrete members exposed to deicing salts or spray from seawater, the maximum *w/cm* is usually limited to 0.40 [PCI, 1997]. According to AASHTO LRFD Bridge Design Specifications [2004], for concrete Classes A (structural elements), A(AE) (air-entrained concrete, $6.0 \pm 1.5\%$), and P (required strength in excess of 4,000 psi (27.6 MPa)) used in or over saltwater, the *w/c* shall not exceed 0.45 for conventional slump concrete.

The minimum specified compressive strength for prestressed concrete bridge elements and decks is 4,000 psi (27.6 MPa) [AASHTO, 1998]. The design of most precast, prestressed concrete members is based on 28-day compressive strength, which is typically 5,000 to 6,000 psi (34.5 to 41.4 MPa) [PCI, 1997]. However, because the mixture proportions are generally dictated by release strengths, actual strengths at 28 days are frequently in excess of specified values. Actual compressive strengths of 8,000 psi (55.2 MPa) or greater are often achieved in the production of precast, prestressed bridge elements. Concrete with a compressive strength above 10,000 psi (69 MPa) shall be used only when physical tests are made to establish the relationships between concrete strength and other properties. In Sweden, in almost all cases where SCC is used in bridge construction, compressive strength is classified as K70 concrete, corresponding to cube compressive strength of 10,150 psi (70 MPa) [Swedish Concrete Association, 2002].

The relationship of the gain in compressive strength with time is established through trial mixtures or previous experience using local producer data. This is particularly important for release strength, which can occur as early as 12 hours. If the relationship is unknown, values recommended by ACI 209 for current practice can be used to estimate strength [PCI, 1997].

$$(f_c')_t = \frac{t}{A + Bt}(f_c')_{28d}$$

where, $(f_c')_t$ = compressive strength of concrete at any time t in psi; $(f_c')_{28d}$ = 28-day compressive strength of concrete; t = time in days from placing concrete; A and B = constants that are functions of both the type of cementitious material in use and the type of curing employed. The use of lightweight sand or lightweight sand and coarse aggregate does not appear to affect these constants significantly. Typical values are given in Table 4.1.

Table 4.1 – Values of concrete A and B [PCI Bridge Design Manual, 1997]

Source	Curing	Cement type	A	B
ACI 209	Moist	I	4.00	0.85
ACI 209	Moist	III	2.30	0.92
ACI 209	Steam	I	1.00	0.95
ACI 209	Steam	III	0.70	0.98
Current Practice	Heat	III	0.28	0.99

Release strength should be achieved within 18 hours after the concrete is cast into place and may be achieved at 12 hours or less. Typically, a release compressive strength determined on control cylinders of 4,000 psi (27.6 MPa) is required. Release strength is selected so that temporary concrete stresses in the prestressed beam do not exceed 60% of the concrete compressive strength at the time of release of pretensioning stresses (before any losses due to creep and shrinkage) [PCI, 1997]. This value is limited to 55% in the case of post-tensioned members [PCI, 1997].

In the design of reinforced or prestressed concrete structures, the combination of normal weight concrete and reinforcement is commonly assumed to weigh 150 lb/ft^3 (2400 kg/m^3). This value may be as high as 160 lb/ft^3 (2560 kg/m^3). Because of the need for early strength gain, Type III cement is often used in precast concrete so that forms may be reused on a daily basis [PCI, 1997]. As mentioned earlier in Chapter 2, the total content of cementitious materials used in prestressed concrete designed to achieve compressive strengths of 4,000 to 8,000 psi (27.6 to 55.2 MPa) can vary from 600 to 1000 lb/yd^3 (356 to 593 kg/m^3) PCI [1997]. Such values can vary on a regional basis depending on the concrete constituents. AASHTO LRFD Bridge Design Specifications [2004] suggest that the sum of Portland cement and other cementitious materials shall not exceed 800 lb/yd^3 (475 kg/m^3), except for Class P (HPC) concrete where the sum of Portland cement and other cementitious materials shall not exceed 1000 lb/yd^3 (593 kg/m^3). For

prestressed concrete, consideration should be given to limiting the nominal aggregate size to 3/4 in. (19 mm).

Holschemacher and Klug [2002] reported that the ratio of cube strength determined on 6-in. (150-mm) cubes to cylinder strength determined using 6×12 in. (150×300 mm) cylinders is about 1.2 for normal concrete, but ranges between 1.0 and 1.1 for SCC. Consequently, the compressive strength of SCC seems to be less related to the slenderness of the specimen.

4.3 Effect of Mix Design and Concrete Constituents on Compressive Strength of SCC

As in the case of conventional slump concrete, the mechanical properties of SCC can vary with material selection and mixture proportioning. Although *w/cm* is a key component in determining the compressive strength of concrete, other changes in mixture design compared to conventional concrete may affect the rate of development and ultimate compressive strength. This can include sand/coarse aggregate ratio, type and content of supplementary cementitious materials and fillers, the combination of various chemical admixtures, the type and dosage of HRWRA, as well as the curing method. This section highlights some of the most relevant factors affecting compressive strength development of SCC.

4.3.1 Effect of chemical admixtures

Concrete proportioned with polycarboxylate-based or copolymer HRWRA can develop higher early compressive strength and ultimate strength and other mechanical properties than similar concrete made with second generation HRWRA (naphthalene- or melamine-based products). The performance of the so-called "third generation" HRWRA depends on the characteristics of the polymer. For example, Attiogbe et al. [2002] reported that the compressive strength of steam-cured SCC made with normal-set polycarboxylate-based HRWRA and VMA and a sand-aggregate ratio of 0.53, by mass, to be similar to that of steam-cured conventional slump concrete prepared with the same HRWRA and a sand-aggregate ratio of 0.44. Both mixtures were proportioned with 0.37 *w/cm* and 800 lb/yd^3 (475 kg/m^3) of Type III cement with 20% replacement with Class F fly ash. However, the use of high early-strength polycarboxylate-based HRWRA led to a slightly greater compressive strength of the air-cured SCC than the air-cured concrete of conventional slump.

The use of VMA increases the HRWRA demand and could lead to set retardation and reduction in early strength development. Nehdi et al. [2004] compared the strength development of SCC mixtures made with various types and combinations of supplementary cementitious materials. As indicated in Fig. 4.1, the binary blend of cement and fly ash (OPC:FA=50:50) developed the lowest early-age compressive strength. Slightly lower strength was obtained when a polysaccharide VMA (welan gum) was used, which necessitated a greater dosage of naphthalene-based HRWRA. The mixtures in Fig. 4.1 were proportioned with 0.38 *w/cm*, a binder content of 715 lb/yd^3 (425 kg/m^3), and a relative coarse aggregate volume of 34%. When

ternary cement (OPC:FA:Slag=50:25:25) was used, the early-age strength was improved; the incorporation of VMA did not have significant detrimental effect on compressive strength.

Bosiljkov [2003] found that the incorporation of polysaccharide-based VMA could be effective in replacing fine quartzite sand traditionally used to compensate for the lack of fine materials in crushed sand. However, the use of the VMA increases water demand, or HRWRA demand.

4.3.2 Effect of cement type and supplementary cementitious materials

Supplementary cementitious materials, including silica fume and fly ash as well as blast-furnace slag are often used in SCC to enhance the performance of the concrete, including reduction in materials cost, heat rise, shrinkage and creep, and enhancement in mechanical properties and durability. The level of benefit depends on a number of factors, including mixture composition, *w/cm*, type and combination of cement and supplementary cementitious materials, and curing conditions. Examples of the effects of these parameters are elaborated herein.

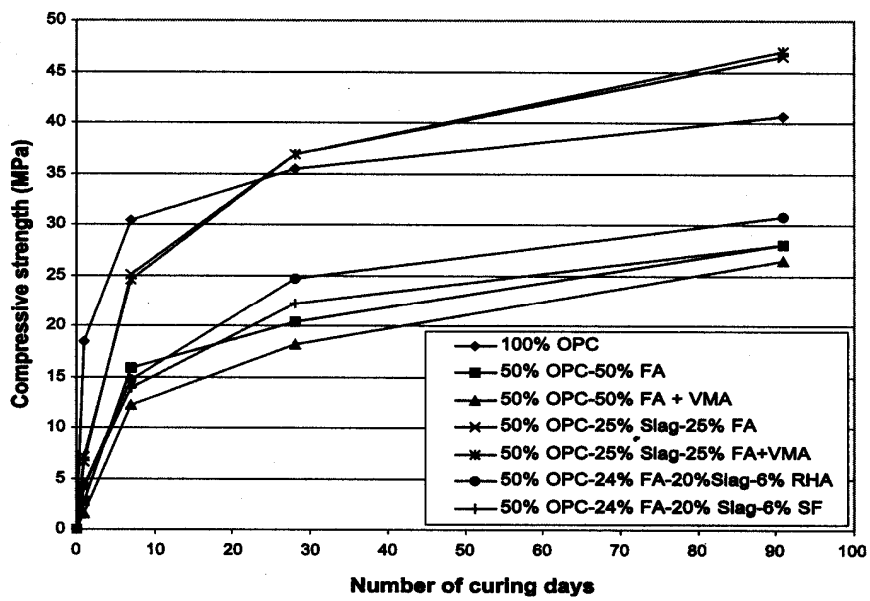

Fig. 4.1 – Compressive strength versus time for various SCC mixtures [Nehdi et al., 2004]

Mokhtarzadeh and French [2000] reported that compressive strength of high-strength concrete of conventional slump consistency, with slump values in the range of 4 to 6 in. (100 to 150 mm) developed at early ages, is higher for moist-cured concrete made with Type III cement than that for Type I cement. However, heat-cured specimens made with the two types of cement had basically the same rate of compressive strength development. In the absence of adequate moist-curing, any benefit from inclusion of fly ash and/or silica fume was limited to grain refinement of the cement matrix (filler effect).

As shown in Fig. 4.1, the level of substitution of Portland cement by supplementary cementitious materials and the type of cementitious materials can affect strength development. Shadle and Somerville [2002] reported that for lab-cured specimens made with 0.34 *w/cm* and Type III

cement, a decrease in early-age strength was observed with the increase in Class F fly ash from 0 to 20%. Depending on the fly ash replacement level, the reduction in early-age strength can be offset by using a non-chloride accelerator. The 12-hour compressive strength of concrete made with 10% fly ash and set accelerator was essentially equivalent to that of the control SCC made without any fly ash. On the other hand, the authors found that heat-cured specimens had higher 12-hour compressive strength than those of lab-cured specimens. It was also observed that SCC mixtures containing fly ash had similar or higher 28-day compressive strengths compared to the straight cement SCC control mixture, irrespective of the fly ash replacement level (up to 20%). Therefore, for lab-cured concrete, the replacement level of cement with Class F fly ash can be optimized, along with a given dosage of set accelerator if necessary, to provide the desired benefits in terms of mechanical properties and durability that can be obtained from the use of supplementary cementitious materials.

Sonebi et al. [2000] showed that SCC made with 0.36 *w/b*, a binder content of 890 lb/yd^3 (530 kg/m^3) containing 38% blast-furnace slag replacement, and a copolymer-based HRWRA can develop lower compressive strengths at 1 and 7 days than a reference mixture made with 0.43 *w/c*, a cement factor of 870 lb/yd^3 (515 kg/m^3), and normal HRWRA. However, significantly higher compressive strength was obtained with the SCC at 28 days, 11,530 vs. 8,920 psi (79.5 vs. 61.5 MPa), and beyond. This is due to the slower, but prolonged hydraulic and pozzolanic reaction of the blast-furnace slag.

The Blaine fineness of the supplementary cementitious materials used to replace part of the cement can affect its performance. Song et al. [2001] reported that for SCC mixtures made with 0.34 *w/cm*, a total binder content of 810 lb/yd^3 (479 kg/m^3) with 40% blast-furnace slag replacement, three different fineness of slag 400, 600, and 800 m^2/kg, a gypsum content of 6 lb/yd^3 (9.8 kg/m^3), MSA of 0.79 in. (20 mm), the SCC mixture with the highest fineness showed a slightly higher compressive strength at 5 days of age. At 28 days, all SCCs made with blast-furnace slag exhibited higher compressive strengths than that of ordinary Portland cement concrete.

4.3.3 Effect of limestone filler

The use of limestone filler in SCC is fairly common in Japan and some European countries, such as Sweden, the Netherlands, and France where these materials are fairly controlled. The use of finely ground limestone filler can enhance compressive strength development at early age. This may be due to the fact that the inclusion of fine limestone powder may accelerate the hydration of C_3S and hence early strength development. Furthermore, finely ground fillers and supplementary cementitious materials can lead to a denser hardened cement matrix and a denser interfacial transition zone with aggregate and embedded reinforcement. This can lead to greater strength and durability.

Petersson [2002] compared the development of compressive strength of normal consistency concrete with a SCC mixture made with fine sand of 0-0.08 in. (0-2 mm) and another SCC made with finely ground limestone filler. For structural concrete proportioned with 0.40 *w/c* intended

for civil engineering applications (Fig. 4.2), compressive strength increased when using limestone filler. The normal concrete and SCC made with fine sand had similar compressive strengths when considering the spreads in air contents (6% vs. 4.8%). Figure 4.3 compares the effect of the Blaine fineness of the filler (330 and 555 m^2/kg) used in 0.65 *w/c* SCC intended for housing construction. The increase in fineness was beneficial at early age but had insignificant effect after 28 days of age.

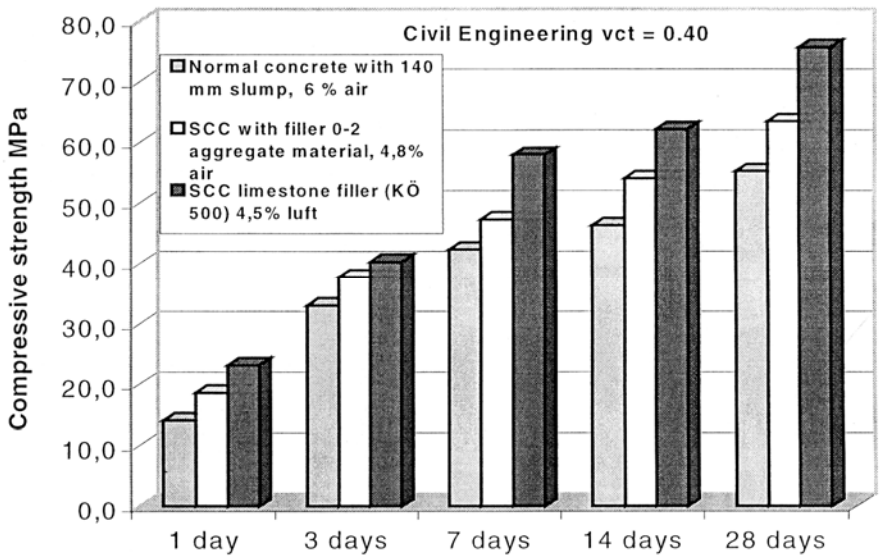

Fig. 4.2 – Compressive strength development of conventional concrete and SCC made with fine sand and limestone filler [Petersson, 2002]

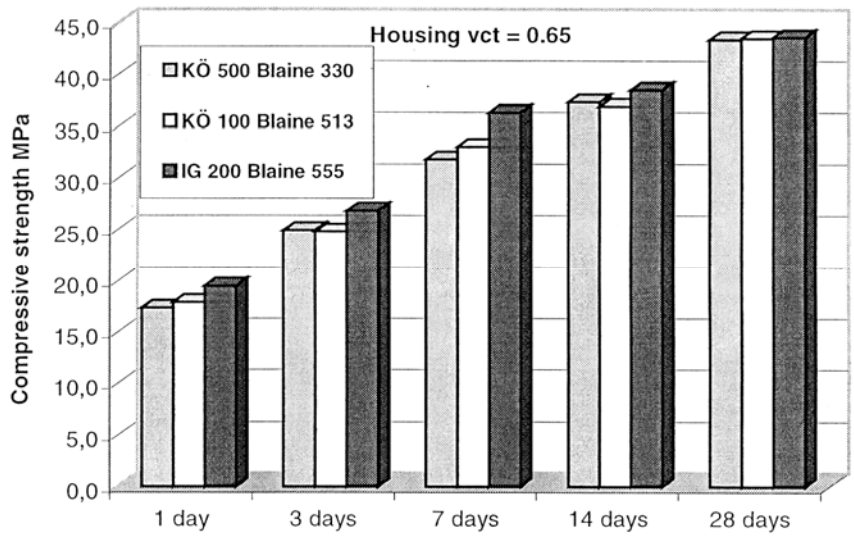

Fig. 4.3 – Compressive strength for SCC with limestone fillers of different Blaine fineness [Petersson, 2002]

Holschemacher and Klug [2002] compared the compressive strength development of various SCC mixtures to strength development values described in the CEB-FIP MC 90 model for mixtures made with various fillers and cementitious materials (Fig. 4.4). The authors concluded that compressive strength of SCC and vibrated concrete of normal consistency having similar compositions does not differ significantly after 28 days for the majority of the test results. Mixtures made with limestone powder developed particularly higher compressive strength at early ages. Up to 7 days of age, there is a relatively larger spread in compressive strength of SCC compared to values predicted by the CEB-FIP MC 90 model. Such spread seems to decrease thereafter.

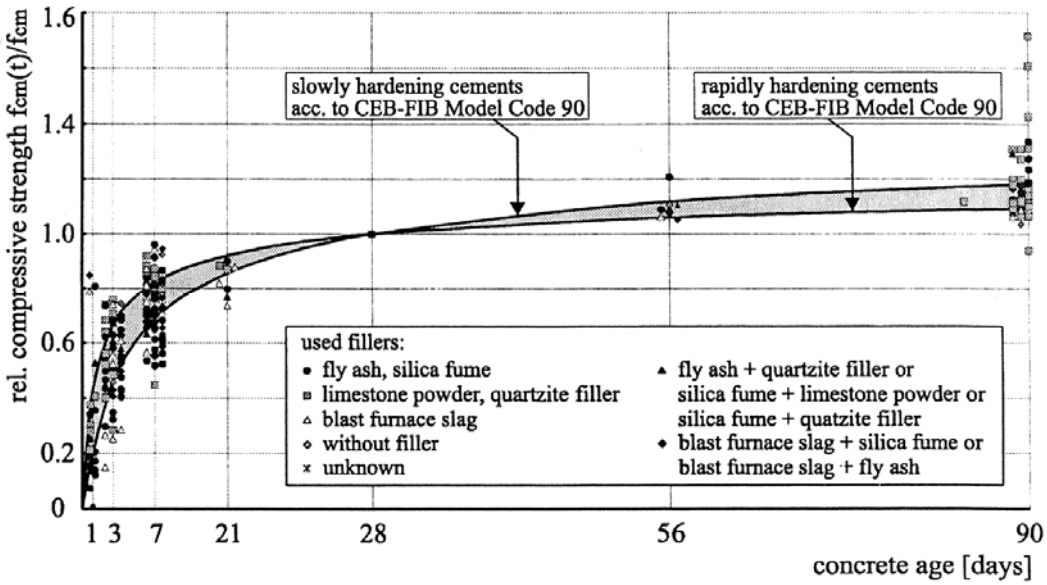

Fig. 4.4 – Compressive strength development with time relative to 28-day results of various SCC mixtures compared to strength development as per CEB-FIP MC 90 model; mixtures made with various fillers and cementitious materials [Holschemacher and Klug, 2002]

4.4 Elastic Modulus and Poisson's Ratio

Elastic modulus is the ratio of uniaxial normal stress to corresponding strain up to the proportional limit for both tensile and compressive stresses. The level of elastic modulus affects the amount of deformation that the material can undergo under a given load. The elastic modulus can be used to calculate camber of prestressed members at the release of the prestressing load, elastic deflections caused by dead and live loads, axial shortening and elongation, and prestress losses.

Elastic modulus is related to the compressive strength of the concrete, type and amount of aggregate, and unit weight of the concrete. The moduli of elasticity of the aggregate in use and its relative volume have the largest influence on the modulus of elasticity of concrete. In addition to the total aggregate volume, adjustments of the sand to coarse aggregate ratio can influence the elastic modulus of the SCC.

As in the case of other mechanical properties, the modulus of elasticity of concrete is affected by testing parameters, including loading rate, moisture and temperature conditions of the test specimens, specimen size and shape. For example, Mokhtarzadeh and French [2000] investigated the effect of the moisture condition of test specimens on the elastic modulus of concrete, as part of an extensive testing carried out to correlate the elastic modulus to compressive strength of high-performance and high-strength concrete. In total, 98 mixtures of normal consistency were evaluated and were made with 0.30 *w/cm* and both Types I and III cements (Fig. 4.5). The

compressive strengths ranged between 6,000 and 19,600 psi (41 and 135 MPa). Seventeen of the mixtures contained no supplementary cementitious materials, 23 mixtures were made with 10%, 20%, and 30% fly ash replacements, another 23 mixtures incorporated silica fume substitutions at 7.5%, 10%, and 15%, and the rest of the mixtures contained both fly ash and silica fume. Six different types of coarse aggregates were investigated: high-absorption limestone, low-absorption limestone, round river gravel, partially crushed river gravel, and two types of granite. In general, for a given compressive strength, wet specimens that were moist-cured until the time of testing resulted in greater elastic modulus than dry specimens. Dry specimens that were initially heat-cured or moist-cured then stored in the laboratory until the time of testing had higher compressive strength, with correspondingly lower elastic modulus.

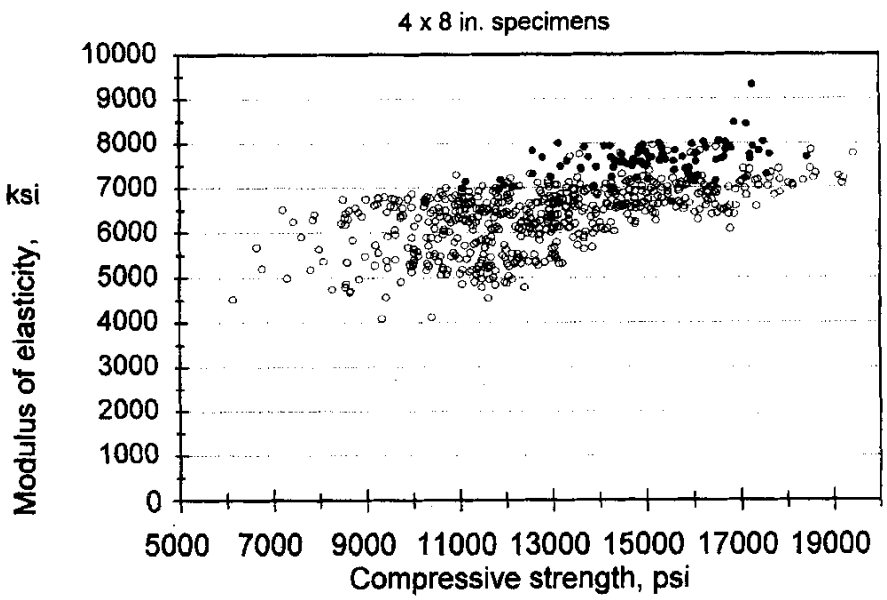

Fig. 4.5 – Variations in modulus of elasticity with compressive strength of high-performance and high-strength concrete of normal consistency [Mokhtarzadeh and French, 2000]

Mokhtarzadeh and French [2000] also reported that the elastic modulus values measured using 4×8 in. (100×200 mm) cylinders were on average 624 ksi (4.3 GPa) higher than those determined using 6×12 in. (150×300 mm) cylinders, as indicated in Fig. 4.6. Figure 4.7 shows that for similar compressive strength, the limestone aggregate concrete was less stiff than the round river gravel concrete. Fig. 4.7 also shows that the current ACI model overestimated high-strength concrete stiffness and that the ACI 363 relationship provided a reasonable lower bound to the data. At equivalent strength, high-strength concretes made with different cement types and brands resulted in practically identical modulus of elasticity values when cured and tested under identical conditions. Moreover, the cementitious material composition did not have a significant effect on the elastic modulus of high-strength concretes made with each of the six coarse

aggregates used. By comparing the measured modulus of elasticity values for 4×8 in. (100×200 mm) specimens (Fig. 4.8) and for 6×12 in. (150×300 mm) specimens with prediction of six widely used equations, it is shown that current design equations may overpredict the elastic modulus based on the compressive strength of concrete, and should be used with caution. Equations proposed by ACI 363 and CEB-FIP resulted in the most reasonable predictions [Mokhtarzadeh and French, 2000].

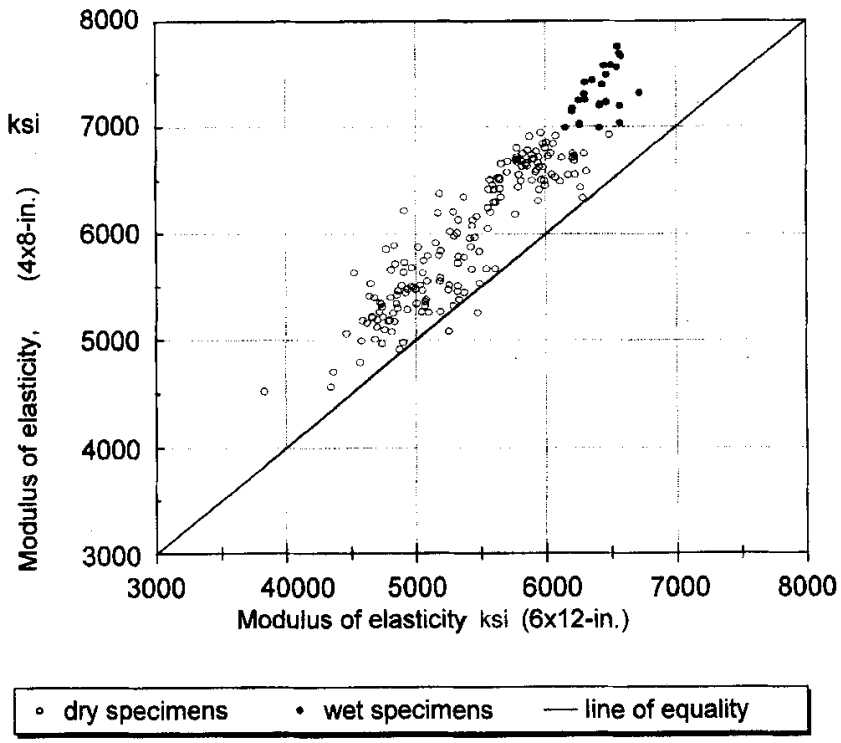

Fig. 4.6 – Effect of specimen size on measured elastic modulus of concrete [Mokhtarzadeh and French, 2000]

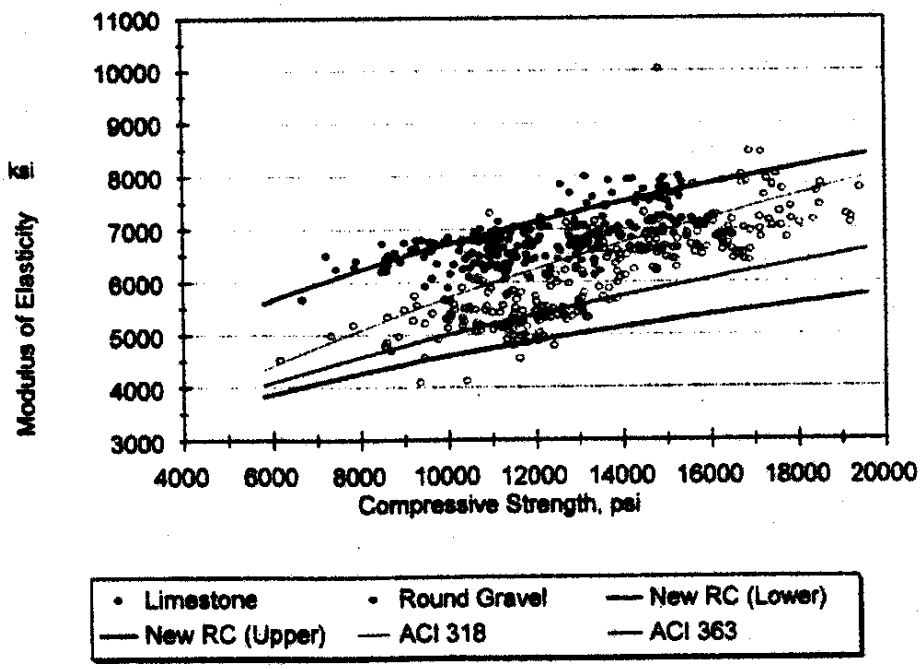

Fig. 4.7 – Effect of aggregate type on modulus of elasticity [Mokhtarzadeh and French, 2000]

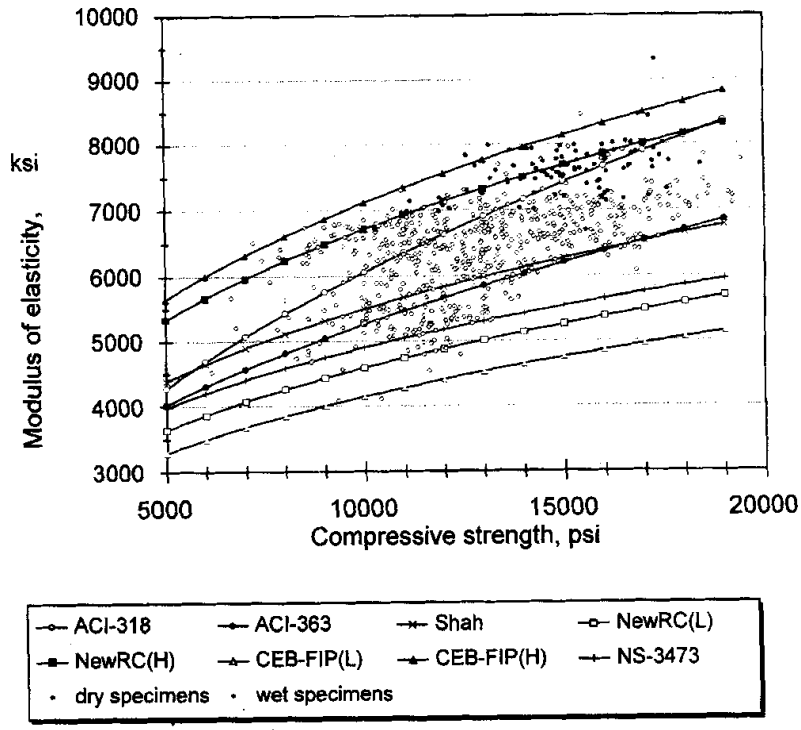

Fig. 4.8 – Comparison of measured elastic modulus values for 4×8 in. (100×200 mm) specimens [Mokhtarzadeh and French, 2000]

The variation of elastic modulus with time can be estimated using the ACI 318 equation for mixtures with compressive strength lower than 8,000 psi (55 MPa) [ACI Committee 237, 2004; PCI, 1997 and 2003; AASHTO, 2004]. The model given by ACI 363 equation can be used for higher strength mixtures of normal consistency [PCI, 1997]. Again, deviations from predicted values are highly dependent on the properties and content of the coarse aggregate in use.

Current information indicates that the elastic modulus of SCC can be comparable to that of conventional concrete. However, it is reported that for some SCC mixtures, the modulus of elasticity may be 80% of that typically found in high-performance concrete of normal consistency. In applications where elastic modulus is an important design parameter, these values should be determined and considered in the design of the prestressed concrete member. Holschemacher and Klug [2002] showed that the elastic modulus of SCC could be up to 20% lower compared with normal consistency concrete of the same compressive strength made with the same aggregate type. This is mainly due to the reduced coarse aggregate volume in SCC and the increase in paste content and relative content of ultra-fine materials. Nevertheless, the relationship between the elastic modulus and compressive strength can still be within the range of predicted modulus of values given compressive strength values that are calculated from the CEB-FIB Model Code 90. As shown in Fig. 4.9, the actual modulus of elasticity values of SCC mixtures made with various types of fillers lie in the lower end of predicted values. Indeed, Ma and Dietz [2002] reported that the measured elastic modulus values of SCC at 28 days correspond to approximately 80% of values estimated by the CEB-FIB Model Code 90.

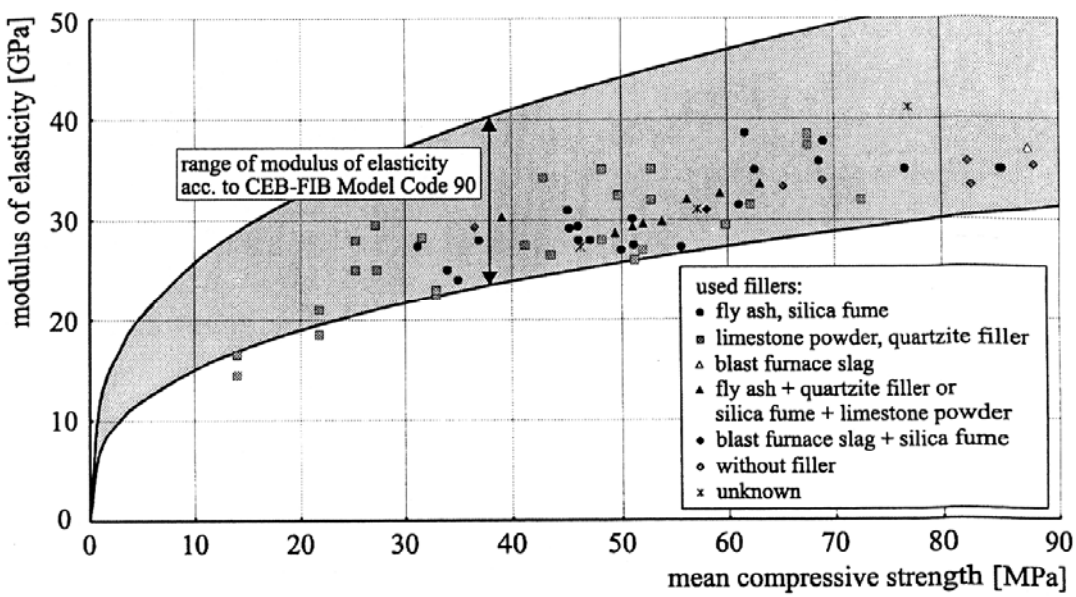

Fig. 4.9 – Modulus of elasticity of SCC in comparison to CEB-FIP MC 90 [Holschemacher and Klug, 2002]

Sonebi et al. [2000] reported the relationship between elastic modulus and compressive strength of SCC to be the same as that of reference mixtures of concrete with normal consistency. The

$E/\sqrt{f_c'}$ ratio was close to the value of 4.73 recommended by ACI 318 that is applicable to normal weight concrete. Turcry et al. [2002] found the ratio of elastic modulus to compressive strength at 28 days to be lower in the case of SCC (0.6) than for ordinary concrete of normal consistency (0.7). This difference was associated with the higher paste volume of the SCC.

Shi et al. [2002] compared the stress-strain curves of two SCC mixtures made with the same *w/cm* of 0.40 and binder composition that uses 28% replacement of the Portland cement by blast-furnace slag. The concrete made with higher sand content (sand to total aggregate ratio of 0.54 vs. 0.48) had greater slope in the stress-strain curve than the mixture made with lower sand content. The former mixture necessitated a higher dosage of polycarboxylate-based HRWRA and incorporated both a cellulose-based VMA and a de-foaming agent. For the SCC mixture made with the higher sand content, the elastic modulus from stress-strain relationship was significantly higher than that estimated by the ACI 318 equation. On the other hand, the other mixture had an elastic modulus close to the estimated value.

Deformability-related properties in the hardened state of SCC and normal concrete were investigated by Vieira and Bettencourt [2003]. The SCC and normal concrete mixtures were prepared with 161 and 168 L/m^3 of water, respectively. SCC mixtures incorporated fly ash as replacement. Test results showed that for a similar compressive strength, SCC developed a lower elastic modulus than normal concrete. However, under air-drying conditions, the elastic modulus of SCC can be higher than normal concrete in the long term. They attributed these results to the lower loss of water that may occur in the case of SCC.

Limited data are available on Poisson's ratio of SCC. For components expected to be subject to cracking, the effect of Poisson's ratio may be neglected [AASHTO, 1998].

4.5 Tensile Strength

In the design of bridge elements, AASHTO [2004] stipulates that for tension areas with no bonded reinforcement, the strength should be selected so that the tensile stress does not exceed 200 psi (1.38 MPa) or $3\sqrt{f_{ci}'}$, where f_{ci}' is the compressive strength in psi of concrete at the time of initial prestress. In an area with a given amount of bonded reinforcement, the maximum tensile stress should exceed $7.5\sqrt{f_{ci}'}$ [PCI, 1997]. For most regular concretes of conventional consistency, the direct tensile strength may be estimated using the following equation: $f_r = 0.23\sqrt{f_c'}\ (ksi)$ where f_r is the direct tensile strength.

Mokhtarzadeh and French [2000] measured the splitting tensile strength of 314 concrete cylinders measuring 6×12 in. (150×300 mm) made with five different types of coarse aggregate and a variety of cementitious materials and fillers. The 28-day compressive strength of the conventional slump concrete ranged from 7,500 to 15,400 psi (52 to 106 MPa) for heat-cured

specimens and 8,700 to 14,650 psi (60 to 101 MPa) for moist-cured specimens. Splitting tensile strengths were 5% to 8% of compressive strength results. The mean value was 6.27%, which is lower than conventional concrete and is indicative of the brittle nature of high-strength concrete. For the tested concrete, the splitting tensile to compressive strength ratio was not significantly affected by the type of curing condition: 6.4% for heat-cured concrete vs. 6.12% for moist-cured concrete. Figure 4.10 compares the data to results of ACI recommendations. ACI 363 equation ($f_{sp} = 7.4\sqrt{f_c}$) is shown to overestimate the splitting tensile strength of concrete with compressive strengths up to approximately 12,000 psi (83 MPa). The splitting tensile strength of both heat- and moist-cured cylinders can be more closely predicted by ACI 318 equation ($f_{sp} = 6.7\sqrt{f_c}$).

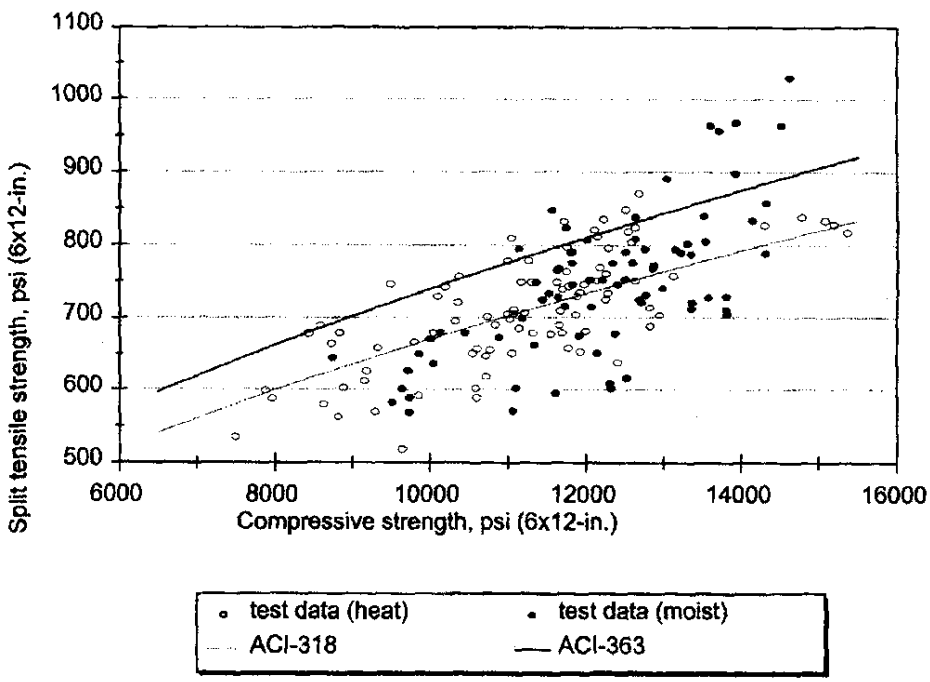

Fig. 4.10 – Scatter plot of 28-day splitting tensile strength versus compressive strength for high-strength concrete [Mokhtarzadeh and French, 2000]

Providing that the SCC is designed with adequate resistance to bleeding, segregation, and surface settlement, it develops relatively high tensile to compressive strength ratio given the improved microstructural characteristics of the concrete. The common use of supplementary cementitious materials (and in some cases fillers) and high content of ultra-fine materials can contribute to the densification of the cement matrix and the reduction of the extent of interfacial transition zone with the aggregate. These parameters are of decisive importance with respect of the tensile load bearing behavior. Indeed, Klaug et al. (2003) conducted literature review of tensile strength of

SCC and reported that higher tensile strength values are obtained with SCC compared to those with conventional concrete.

Turcry et al. [2002] showed the 28-day tensile to compressive strength ratio to be higher for SCC mixtures; between 0.087 and 0.1 compared to 0.075 in the case of ordinary concrete. Sonebi et al. [2000] reported the ratios of splitting tensile strength to compressive strength of SCC made with 0.36 *w/b* containing 38% blast-furnace slag replacement to be 0.059 at 28 days and 0.062 at 180 days. Similar values were obtained by Bosiljkov [2003] for SCC made with limestone filler. The authors reported that the splitting tensile strength to compressive strength ratio of SCC could range between 0.08 and 0.09 for mixtures made with limestone filler and low *w/b* of 0.22 to 0.25. The tested mixtures were prepared with crushed limestone coarse aggregate with MSA of 0.6 in. (16 mm) and polycarboxylate-based HRWRA and polysaccharide-type VMA. The tested mixtures developed compressive strength values ranging between 3,190 and 3,625 psi (22 and 25 MPa) after 1 day, determined on 6-in. (150-mm) cubes, and 28-day compressive strength of 9,280 and 9,860 psi (64 to 68 MPa).

As shown in Fig. 4.11, Holschemacher and Klug [2002] illustrated that for SCC made with various types of supplementary cementitious materials and fillers, the majority of measured splitting tensile strength data lie within the range of valid regulations (CEB-FIB Model Code 90) that can be expected for normal vibrated concrete of the same compressive strength. In about 30% of the data, a higher splitting tensile strength was obtained.

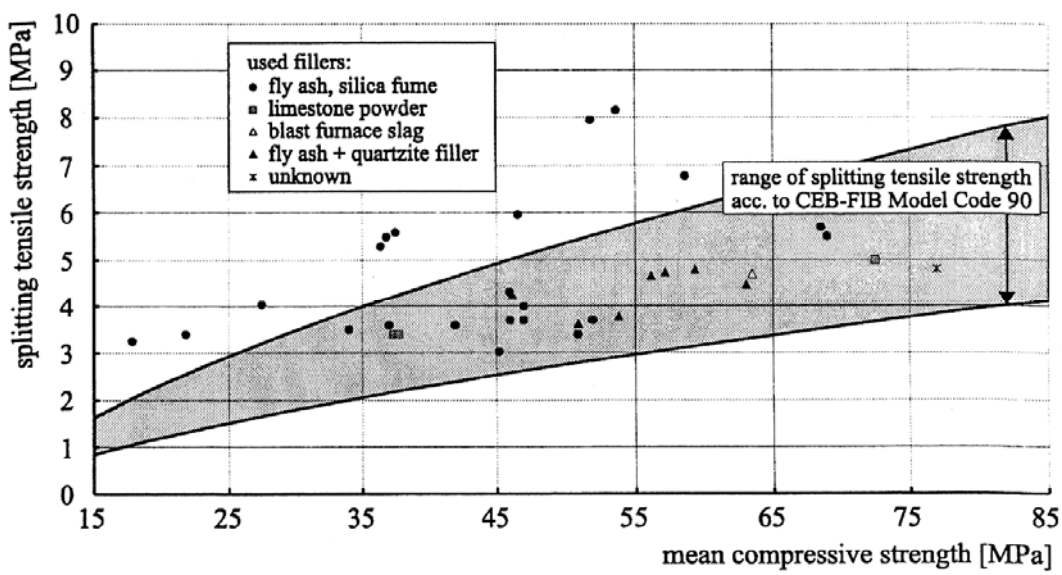

Fig. 4.11 – Comparison of splitting tensile strength of SCC to CEB-FIP MC 90 model developed for normal consistency concrete [Holschemacher and Klug, 2002]

4.6 Modulus of Rupture

The modulus of rupture (MOR) is a measure of the flexural tensile strength of the concrete. As in the case of normal consistency concrete, the MOR of SCC depends on the *w/cm*, coarse aggregate volume, and quality of the interface between the aggregate and cement paste. As in the case of tensile strength, the lower *w/cm* typically used in proportioning SCC and the use of supplementary cementitious materials and fillers is expected to lead to higher flexural strength and flexural-to-compressive ratio than conventional slump concrete [ACI Committee 237, 2004].

The MOR can be determined by testing or can be estimated from the compressive strength. For normal weight concrete of conventional slump, the MOR can be estimated as: $f_r = 7.5\sqrt{f_c'}\ (psi)$ [PCI, 1997] or $f_r = 0.24\sqrt{f_c'}\ (ksi)$ [AASHTO, 2004].

Mokhtarzadeh and French [2000] reported that the curing mode of concrete can significantly influence the MOR. Moist-cured specimens can exhibit higher MOR, as shown in Fig. 4.12. This is because the moist-cured samples do not undergo drying shrinkage strains at the outer surfaces that can lead to premature cracking. Figure 4.12 also indicates that the MOR of moist-cured high-performance concrete specimens of normal consistency can be closely predicted by ACI 363 equation ($f_r = 11.7\sqrt{f_c'}$).

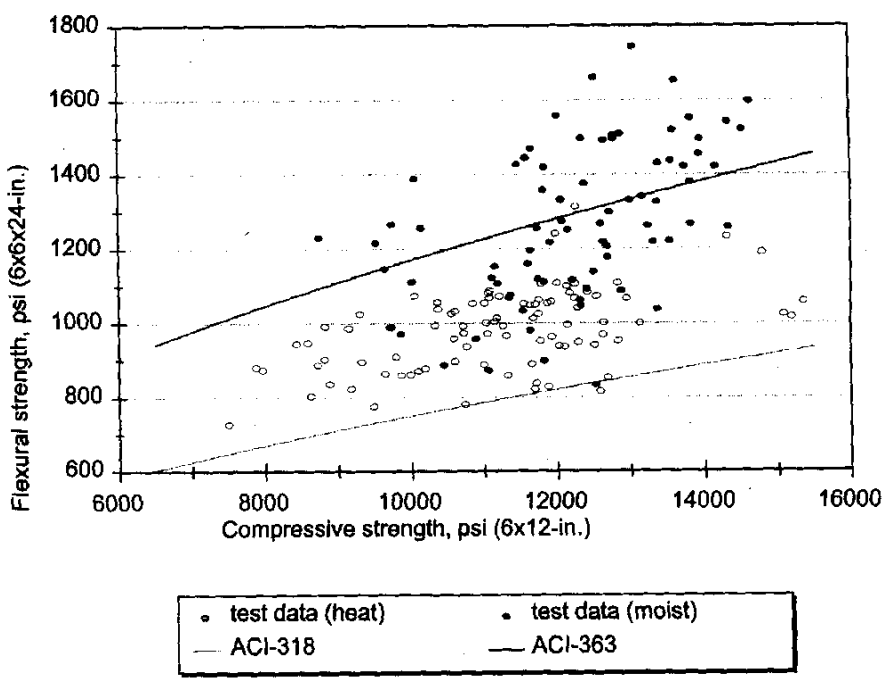

Fig. 4.12 – Scatter plot of 28-day flexural strength versus compressive strength for high-strength concrete [Mokhtarzadeh and French, 2000]

4.7 Uniformity of In-Situ Properties

Ensuring adequate consolidation of concrete is essential to obtain proper mechanical properties. With the increasing use of highly flowable concrete and SCC, it is important to ensure that such concrete can secure uniform in-situ mechanical properties that are similar to those obtained with properly consolidated concrete of conventional fluidity.

Khayat et al. [1997] investigated the uniformity of compressive strength, elastic modulus, and bond strength to embedded reinforcing bars along the height of experimental wall elements measuring 3.1 ft (0.95 m) in length, 5 ft (1.5 m) in height, and 0.66 ft (0.2 m) in width. Eight optimized SCC mixtures with slump flow values greater than 24.8 in. (630 mm) and a control concrete with a slump of 6.5 in. (165 mm) were investigated. The SCC mixtures were prepared with various types of supplementary cementitious materials, *w/cm* of 0.37 to 0.42, MSA of 0.39 and 0.79 in. (10 and 20 mm), and welan gum VMA. In general, the highly stable mixtures exhibited uniform distribution of compressive strength along the wall elements that was comparable to values obtained with the vibrated concrete. Statistically insignificant differences were obtained between the variations in in-situ compressive strength values along the height of wall elements made with SCC and conventional concrete. In general, variations in compressive strength of cores tested from the top and bottom sections were limited to 8%, as indicated in Fig. 4.13. Compared to SCC made with 0.39 in. (10 mm) MSA, mixtures prepared with 0.79 in. (20 mm) MSA exhibited a slight reduction in compressive strength with height compared to strength values obtained near the bottom of the walls. This is probably due to the entrapment of bleed water underneath coarse aggregate particles. As in the case of compressive strength, the modulus of elasticity was slightly weaker near the top of each wall. Slight reductions in in-situ MOE were observed between core samples obtained near the top and bottom portions of the walls. The maximum reduction in MOE between the top and bottom sections varied between 0 and 8% for SCC mixtures and was 7% for the Control concrete, again indicating uniform mechanical properties of the optimized SCC mixtures. Compared to control cylinders measuring 4×8 in. (100×200 mm), core samples obtained, on average, 10% and 20% lower compressive strengths in SCC mixtures made with 0.39 and 0.79 in. (10 and 20 mm) MSA, respectively, compared to 10% to 15% in the case of the vibrated reference concrete made with the latter coarse aggregate size. A spread of 10% is typical for compressive strength of core samples perpendicular to the direction of casting vs. control samples tested parallel to the direction of casting.

Similar findings were observed by Sonebi et al. [2002] who evaluate the distribution of compressive strength along the height of wall elements measuring 6.4 ft (1.95 m) in length, 6.6 ft (2 m) in height, and 0.82 ft (0.25 m) in width. The SCC was prepared with limestone powder and a w/b of 0.29. The mean in-situ 28-day compressive strengths at the top, middle, and bottom sections of the wall were 8,120 psi (56 MPa), 8,555 psi (59 MPa), and 8,050 psi (55.5 MPa), respectively. The spread in compressive strength between cores and reference cubes was 22%.

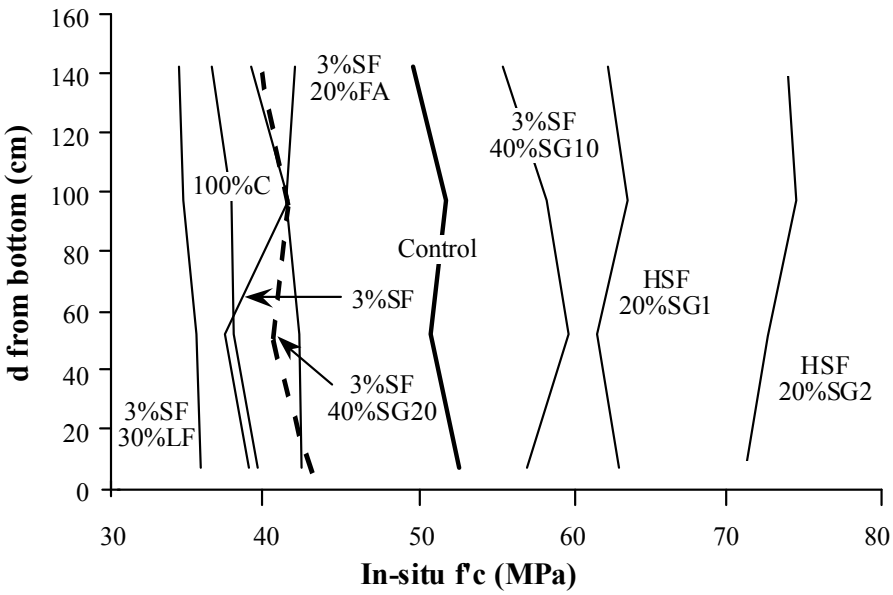

Fig. 4.13 – Variations of in-situ compressive strength with depth [Khayat et al., 1997]

Zhu et al. [2001] cast full-scale reinforced columns measuring 9.8 ft (3 m) in height and 1×1 ft (0.3×0.3 m) in section, and reinforced beams measuring 12.5 ft (3.8 m) in length and 0.66×1 ft (0.2×0.3 m) in section. The in-situ compressive strengths of the bottom part of the columns were found to be higher than near the top part. Compressive strength of core samples in the columns varied between 80% and 100% of standard 28-day compressive strength value for the SCC mixtures. The compressive strength variation along the length of the beams was much smaller than along the height of the columns.

Khayat et al. [2000a] evaluated the in-situ properties of two wall elements cast with SCC of relatively low slump flow consistency of 23.6 in. (600 mm). The concrete was cast in L-shaped sections measuring 49 ft (15 m) in length, 8 in. (200 mm) in width, and 3.9 ft (1.2 m) in height. The in-situ compressive strength after 56 days varied between 30 and 40 MPa for the SCC made with 20% fly ash and 3% silica fume replacements (*w/cm* of 0.45) and 42 and 50 MPa for the mixture with 40% blast-furnace slag and 3% silica fume replacements (*w/cm* of 0.42). The strength decreased slightly near the top of the walls compared to the bottom and away from the casting position, as shown in Fig. 4.14. The concrete exhibited excellent uniformity of in-situ air-void system and rapid chloride-ion permeability. The mean spacing factor and rapid chloride-ion permeability were determined along the walls and were shown to vary between 0.005 and 0.007 in. (120 and 175 μm) and 575 and 900 coulombs at 56 days, respectively.

4.8 Bond Strength

Literature review conducted by Holschemacher and Klug [2002] showed that bond to reinforcing bars and prestressed tendons can be influenced by the flow properties of the SCC, grading of the

aggregate, and content of fines in the matrix. The survey showed that, in general, the bond stress is improved when using SCC.

Measurement of bond strength conducted by Gibbs and Zhu [1999] showed that the bonds to reinforcing bars developed using SCC are equal to those obtained with a normal vibrated concrete. Similar results were reported by Sonebi and Bartos [1999]. This enhancement of bond strength is mainly due to the high stability of SCC that can secure a denser microstructure with the reinforcement. Dehn et al. [2000] reported that SCC proportioned with 0.41 *w/cm* can develop higher bond strength values compared to those obtained with normal vibrated concrete. Pull-out tests were conducted using 4×4 in. (100×100 mm) cylindrical specimens in which 0.39-in. (10-mm) reinforcing bars were anchored. The tested SCC mixtures had 28-day compressive strength and elastic modulus of 7,540 psi (52 MPa) and 4,366 ksi (30.1 GPa), respectively.

Chan et al. [2003] conducted an experimental study to evaluate and compare bond strength of deformed reinforcing bar anchored in SCC and in normal concrete incorporating blast-furnace slag and fly ash. The SCC mixtures were proportioned with a *w/b* of 0.40, 725 lb/yd^3 (430 kg/m^3) of total binder, and coarse aggregate having a maximum size of 0.51 in. (13 mm). The SCC incorporated a polycarboxylate-based HRWRA and VMA. In the case of normal concrete, a *w/b* of 0.42, 792 lb/yd^3 (470 kg/m^3) of binder and a 0.79-in. (20-mm) size coarse aggregate were used. Normal concrete mixtures incorporated an ordinary water reducer. The pull-out specimens consisted of wall elements measuring 47.2 in. (1200 mm) in height, 11.8 in. (300 mm) in width, and 55.1 in. (1400 mm) in length. Immediately after casting, pull-out specimens were sealed with plastic during 4 days before being subjected to air-drying. At 28 days, the SCC mixture developed a higher compressive strength of 6,960 psi (48 MPa) compared to 4,790 psi (33 MPa) in the case of the normal concrete. Bond stresses were determined at different heights of the wall. The authors defined the Critical bond strength as the bond stress corresponding to a slip of 0.10 in. (0.25 mm). On the other hand, the Modified critical bond strength was used to take into account the elastic elongation. In case of the D32, No. 19 bars, the estimated elastic elongation was 0.006 in. (0.15 mm). Therefore, the bond stress corresponding to a total displacement of 0.016 in. (0.40 mm), instead of 0.10 in. (0.25 mm), was regarded as the critical bond strength. Test results revealed that at early age, the development of bond strength and compressive strength using SCC was significantly lower than conventional concrete. This is probably due to the retarding effect in the presence of HRWRA-VMA on early age mechanical properties. For the conventional concrete, the magnitudes of bond strength $/\sqrt{f_c'}$ were nearly constant at various ages, indicating that the development of bond strength is closely related to that of compressive strength. On the other hand, there is obviously an ascending portion at early ages (before 7 days) in the case of SCC. Test results revealed that at a given compressive strength, reinforced concrete members made with SCC could develop significantly higher bond strength than when normal concrete is used. Lower variations in bond strength at different elevations were also obtained when using SCC compared to normal concrete, indicating the more consistent nature of SCC [Chan et al., 2003].

Other researchers, however, have found that the bond strength of the reinforcement to SCC can be lower than that of normal concrete. For example, Koning et al. [2001] found that SCC developed lower bond strength than conventional concrete but higher bond stiffness at low displacement. The authors observed ductile post-peak bond behavior in the case of SCC that is characterized by the nearly linear slope of the load-displacement curve. Therefore, after reaching the maximum bond stress, the slip increases gradually, while the bond stress decreases slowly. The German Committee for Reinforced Concrete reported that pull-out test results revealed that slightly lower bond strength can be obtained with SCC compared to normal vibrated concrete [Hegger et al., 2003]. When measuring transfer length on beam elements, tests revealed that the transfer length obtained on SCC beams is similar to that observed with vibrated concrete beams. The transfer length was calculated based on the compressive strength determined during prestressing using cylinder specimens.

4.9 Top-Bar Effect

Ensuring proper stability of SCC is essential to enhance the uniformity of in-situ mechanical properties, including bond to embedded reinforcement, which is critical for structural engineers considering the specification of SCC for precast, prestressed applications [Moustafa, 1974 and Logan, 1997]. Despite its high fluidity, SCC can develop similar top-bar effect as that of conventional concrete when it is designed with sufficient static stability. Decrease in top-bar effect results in reducing the difference between the bond stresses determined at the top and bottom of the element. Figure 4.14 shows a relationship between the surface settlement determined on top of column samples measuring 1.6 to 3.6 ft (0.5 to 1.1 m) in height and the spread between the bond strength determined with reinforcing bars embedded near the two extremities of the columns. The samples were cast with conventional concrete with slumps of 220 and 190 mm and SCC with slump flow values of 23.6 to 27.2 in. (600 to 690 mm). The improvement of cohesiveness, determined from surface settlement measurements, can reduce the structural defects resulting from accumulation of bleed water, rising air bubbles, and settlement of the plastic concrete around the top reinforcement. Therefore, SCC with a high level of static stability can exhibit lower top-bar effect compared to that obtained with conventional vibrated concrete [Khayat et al., 1997; Sonebi and Bartos 1999, Gibbs and Zhu, 1999; Attiogbe et al., 2002; and Holschemacher and Klug, 2002].

Khayat et al. [1997] evaluated the uniformity of bond strength of embedded reinforcing bars along the height of experimental wall elements measuring 3.1 ft (0.95 m) in length, 5 ft (1.5 m) in height, and 0.66 ft (0.2 m) in width. Eight optimized SCC mixtures with slump flow values greater than 24.8 in. (630 mm) and a control concrete with a slump of 6.5 in. (165 mm) were investigated. SCC mixtures were prepared with various types of supplementary cementitious materials, *w/cm* of 0.37 to 0.42, MSA of 0.39 and 0.79 in. (10 and 20 mm), and welan gum VMA. The top-bar factor for reinforcing bars positioned at 4.6 ft (1.4 m) from the bottom of the experimental walls was 1.4 $\pm$ 0.2 for seven of the SCC mixtures and approximately 2.0 for the

Control concrete and one of the SCC mixtures. In the case of highly stable concrete made with 0.39 in. (10 mm) MSA, a lower top-bar effect of 1.0 to 1.2 was obtained.

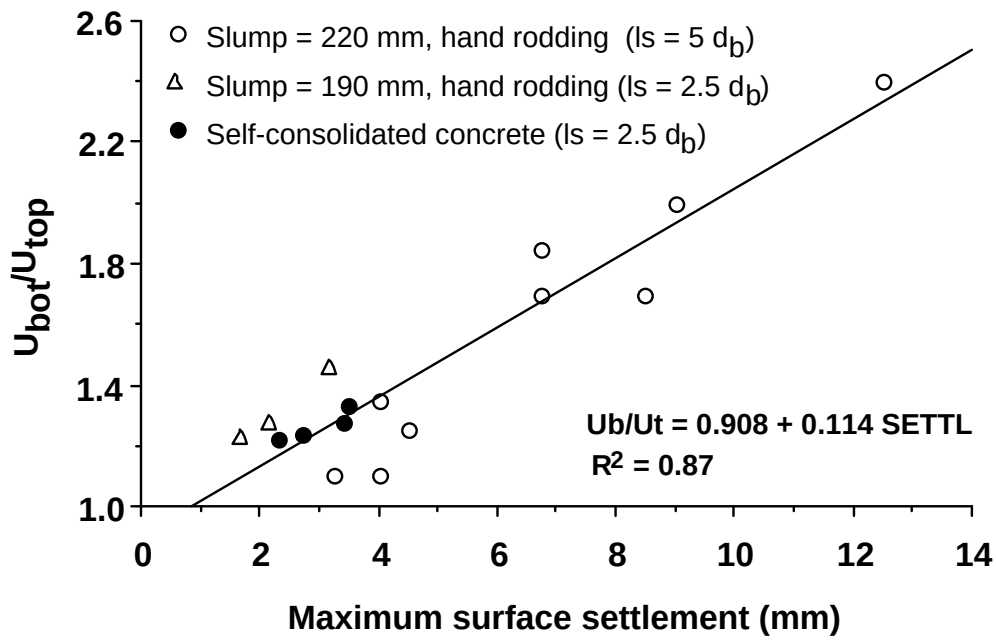

Fig. 4.14 – Relationship between surface settlement and top-bar factor [Khayat et al., 1997]

Khayat et al. [2003] also investigated the uniformity of bond strength to prestressing strands along the height of experimental wall elements (Fig. 4.15). Four SCC mixtures and two conventional flowable mixtures made with Type III cement and 20% Class C fly ash and *w/cm* of 0.37 were used for casting experimental wall elements measuring 5.1 ft (1.54 m) in height, 3.6 ft (1.1 m) in length, and 0.66 ft (0.2 m) in width. Two concrete walls were steam-cured, while the remaining elements were air-cured. Each wall had 16 prestressing strands, four per row positioned at four levels, that were subjected to pull-out tests at 1 and 28 days of age. All mixtures developed 1-day compressive strength greater than 40 MPa. Uniform distribution of in-place compressive strength and adequate bond to prestressing strands were obtained. The 1- and 28-day top-bar effect ratios varied between 0.9 and 1.9. These values were lower for the air-cured mixtures compared to the steam-cured mixture. For steam curing, the top-bar effect was larger in the case of the SCC than in the case of the conventional flowable concrete at 1 day, but lower at 28 days. The top-bar effect was shown to be sensitive to the type of VMA in use.

The long-term prestress losses associated with the combined effects of shrinkage and creep would be expected to be similar for SCC and conventional concrete. The use of VMA facilitates the development of SCC mixtures for normal sand-to-aggregate ratio with the additional benefit that may result from using low sand-to-aggregate ratio in reducing shrinkage of SCC.

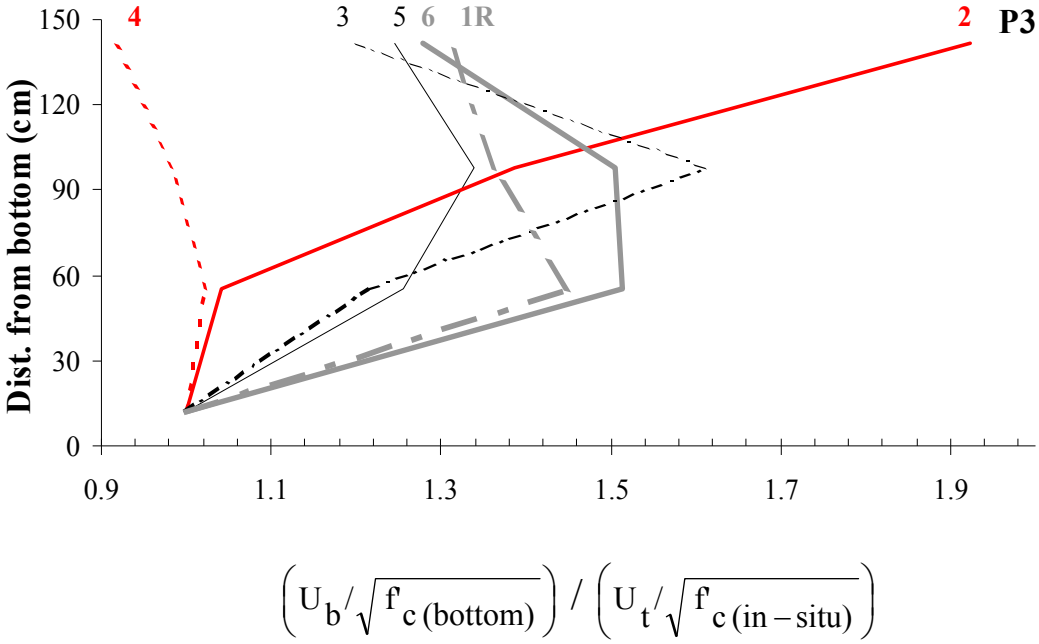

Fig. 4.15 – Variations of top-bar ratio of prestressing strands at 28 days (1 and 2: conventional concrete; 3-6: SCC with different HRWRA-VMA) [Khayat et al., 2003]

Schiessl and Zilch [2001] investigated the bond behavior of SCC and conventional concrete made with 317 lb/yd^3 (188 kg/m^3) of water content and 995 lb/yd^3 (590 kg/m^3) of binder. The materials included ordinary Portland cement, fly ash, and limestone filler. Pull-out tests were conducted in accordance to RILEM recommendations using specimens measuring 300 mm in height. Each specimen had two bars, the first anchored at the top and the second at the bottom of the specimen. As expected, higher bond stress was obtained when the pull-out test is carried out for vertically-positioned bars than for horizontal bars when carried out in the opposite direction as the casting direction. In terms of bond-slip relationship, specimens cast with SCC and conventional concrete showed similar behavior. Specimens cast with SCC had uniform coarse aggregate distribution and lower top-bar effect compared to the performance of conventional concrete. Significant top-bar effect was observed in the case of conventional concrete specimens due to the settlement that can occur under the effect of vibration during the casting process. On the other hand, the bond behavior of SCC was almost independent of the bar position.

4.10 Shear Force Capacity

Limited studies on crack surface structure have been conducted using SCC. The fact that SCC is typically proportioned with relatively small nominal size aggregate and lower content of coarse aggregate compared to conventional concrete may limit the contribution of aggregate interlock to shear strength of concrete. Furthermore, given the fact that SCC often develops higher than required compressive strength and that the interfacial transition zone with the aggregate is often

intact, cracked surfaces can involve a greater degree of intergranular crack propagation that again reduce aggregate interlock. The applicability of codes calculation used with normal strength, vibrated concrete and prestressed concrete needs to be verified when using SCC.

Schiessl and Zilch [2001] investigated the shear behavior of SCC and conventional concrete made with the same materials. The SCC was proportioned with a water content of 317 lb/yd^3 (188 kg/m^3) and a binder content of 995 lb/yd^3 (590 kg/m^3). The binder materials included ordinary Portland cement, fly ash, and limestone filler. Concrete prisms measuring 1.57 in. (40 mm) in length, 1.02 in. (26 mm) in height, and 0.79 in. (20 mm) in depth were used to evaluate the shear capacity (aggregate interlock). Each prism was split in the center along the longitudinal direction and loaded by shear force. In addition, two normal forces were applied to generate a normal stress perpendicular to the crack plain. In total, 20 experiments were conducted, 10 for each type of concrete. Test results revealed that the maximum shear stress obtained with SCC is indeed lower than that obtained with conventional concrete. This is explained by the smoother crack surface observed with SCC mixtures. The smoother crack surface observed with SCC mixtures is probably due to the relatively lower coarse aggregate content and the higher paste volume in SCC compared to conventional concrete. As with the case of conventional concrete, the shear stress of SCC increases with the normal applied stress.

4.11 Structural Response

Zia et al. [2005] evaluated the performance of SCC in prestressed concrete bridge girders. Three standard AASHTO Type III girders measuring 54.8 ft (16.7 m) in length were selected for experimentation. Two girders were cast using SCC and the third one was cast using normal concrete with a compressive strength of 5,800 psi (40 MPa). Both the SCC and normal concrete mixtures were proportioned with w/c of 0.42, Type III cement, and granite coarse aggregate. The SCC mixture had a water content of 261 lb/yd^3 (155 kg/m^3), a cement content of 809 lb/yd^3 (480 kg/m^3), and a maximum-size aggregate of 1/2 in. (12.5 mm). These values were 219 lb/yd^3 (130 kg/m^3), 674 lb/yd^3 (400 kg/m^3), and 3/4 in. (19 mm), respectively for the normal concrete. Air-entraining agent and corrosion inhibitor were incorporated in both the SCC and normal concrete mixtures. The SCC mixtures achieved a slump flow of 24 in. (610 mm) and developed compressive strengths of 5,510, 8,700, and 10,440 psi (38, 60, and 72 MPa) at 18 hours, 7, and 28 days, respectively. In the case of normal concrete, these values were 4,640, 6,530, and 7,250 psi (32, 45, and 50 MPa), respectively. SCC and normal concrete mixtures developed 28-day modulus of elasticity values of 2,900 and 3,480 ksi (20 and 24 GPa), respectively. Based on the experimental observations drawn during the casting, the authors recommended the use of SCC with a slump flow of 26 to 28 in. (660 to 710 mm) to ensure proper casting of the girders. Analysis of end slips of strands showed that there is no significant difference in bond behavior between the top and bottom strands. Furthermore, the comparison between the end slips of strands embedded 0.13 in. (3.4 mm) in SCC and those embedded 0.15 in. (3.8 mm) in normal concrete suggest that there is no difference in performance between the SCC and control girders. The strand transfer length of the three experimental girders was in the range of 30 to 40 in. (760

to 1010 mm), which is about 30% longer than the limit recommended by AASHTO [Zia et al., 2005]. Test results showed that immediately after prestress release (18 hours), the three experimental girders exhibited similar initial camber and comparable strand slip-end. However, test results showed that the creep of the SCC could be about twice that of the normal concrete. The creep coefficient was estimated by dividing the camber growth by the initial camber. Similarly, the growth of the camber for the SCC girders was almost twice that of the normal concrete girder. The study reported that under load test, the three experimented girders behaved elastically and exhibited virtually identical load-deflection relationships up to the design service load, with no cracks observed.

Ozyildirim [2004] reported that the Virginia Department of Transportation employed SCC in an arch bridge of 25 arches placed side by side to span 30 ft (9.1 m) across a small creek. Each segment was an ellipsoidal arch measuring 7.5 ft (2.5 m) in width and 10 in. (25 mm) in thickness with two mats of reinforcement. SCC mixtures were designed to achieve a specified 28-day compressive strength of 5,000 psi (34.5 MPa). SCC mixtures were proportioned with Type II cement and 35% blast-furnace slag with a total binder content of 750 lb/yd^3 (445 kg/m^3). The SCC was proportioned with *w/cm* of 0.37 and polycarboxylate-based HRWRA and had a sand-to-total aggregate ratio of 0.50, by mass. The mean compressive strengths of various batches tested at 1, 7, and 28 days of age were 3,050, 6,120, and 7,500 psi (21.0, 42.2, and 51.7 MPa), respectively. The rapid chloride-ion permeability of the SCC at 28 days was lower than 1800 coulombs. Test conducted on one beam indicated that the beam developed a flexural and shear capacity similar to those evaluated from theoretical calculations. The use of SCC was reported to result in minimal slip and good bond strength between the concrete and prestressing strand. Ozyildirim [2004] reported that the use of a high dosage of HRWRA affected the stability of the air system, and large bubbles were observed during petrographic examination. Such air-void system could lead to poor freeze thaw resistance even though the air content was within the specification. The reduction in HRWRA content or use of a different type of HRWRA resulted in more durable SCC and adequate air-void system.

Labonte et al. [2004] constructed and tested full-scale AASHTO Type II beams. The beam testing was conducted to compare transfer length, camber growth, and structural properties of the beams, specifically shear and flexural characteristics. The beam tendon size and configuration were designed to meet the requirements of AASHTO LRFD Bridge Design Specifications for a fictitious bridge in which the beams were spaced 6 ft (1.8 m) apart with a 40-ft (12.2-m) span and a deck thickness of 10 in. (25 mm). The SCC beams were poured in 40% less time and required approximately 50% fewer workers than the control beam due to the increase in flow rate of the concrete and elimination of vibration. Floridal State DOT Class VI mixture with targeted compressive strength of 8,500 psi (60 MPa) was used as template for the development of two pairs of "standard" and SCC mixtures. Cement, fly ash, and water contents were kept the same for each pair of mix designs. All mixtures were proportioned with a Type I/II cement and Class F fly ash. Pair A mixtures were made with total binder content of 825 lbs/yd^3 (500 kg/m^3) and 425 lbs/yd^3 (252 kg/m^3) of water. Pair B mixtures were made with 927 lbs/yd^3 (550 kg/m^3) of binder

(920 lbs/yd^3) and 435 lbs/yd^3 (258 kg/m^3) of water. SCC mixture in Pair A achieved a slump flow of 26.8 in. (680 mm), while that of Pair B achieved a slump flow of 27.5 in. (700 mm). The standard concrete achieved a slump of 5.1 in. (130 mm). Test results revealed that the hardened properties of the SCC mixtures were comparable with those of the standard concrete. Difference between the SCC and control beams in terms of prestress transfer length was insignificant. The camber of the SCC beams and standard beams was monitored for approximately 200 days after casting. The mean camber measured on SCC beams matched that for the standard beams, although there was slightly more variation with the camber of the SCC beams.

Hegger et al. [2003] conducted an experimental study to evaluate the performance of prestressed beams made with SCC, including flexural and shear strength, bond, crack behavior, and ductility. Four prestressed T beams were cast with different SCC mixtures. One of the four beams was cast with a conventional vibrated concrete of equal strength. The SCC was made with cement, fly ash, and polycarboxylate-based HRWRA. All test specimens were prestressed at the age of 5 days. The failure of beams subjected to bending occurred when exceeding the yield strain in the longitudinal reinforcement. A secondary cause of failure was due to spalling of the concrete cover in the compression zone. Shear strength tests conducted on small specimens revealed a reduction in crack-friction capacity of members made with SCC.

Khayat et al. [1999] evaluated the structural response of densely reinforced concrete columns with closely spaced stirrups. A total of eight columns with a standard compressive strength of 5,800 and 7,250 psi (40 to 50 MPa) were tested. Two pairs of columns were cast using normal concrete and SCC in reinforced sections, and four companion columns were cast without any reinforcement. The reinforced columns were made with the same percentage of longitudinal reinforcement (ρ_g=3.6%) and approximately the same amount of lateral reinforcement (ρ_g=4.9%). A stirrup spacing of 50 mm on centers was used for all specimens. One column from each pair of unreinforced columns was tested in uniaxial compression to determine the load-carrying capacity; the other provided core samples to determine the homogeneity of the distribution of compressive strength and modulus of elasticity along the height. The core results were compared to strengths obtained from control cylinders cured under similar conditions. The SCC mixtures were proportioned with 978 lb/yd^3 (580 kg/m^3) of ternary blended cement (Type I cement and silica fume combined with either blast-furnace slag or limestone filler) and crushed coarse aggregate with 0.39 in. (10 mm) nominal size. The SCC mixtures had slump flow values of 24.8 to 26.0 in. (630 to 660 mm). Test results showed that the SCC columns developed similar stiffness, but approximately 7% lower load-carrying capacity than the normal concrete. This spread in strength is partly due to the 10% lower cylinder compressive strength of the SCC. Depending on the stirrup configuration, the SCC columns exhibited 62% and 23% greater ductility than similar normal concrete columns. The distribution of in-situ properties along the height of non-reinforced columns was found to be more homogeneous in the SCC than the normal concrete. However, the SCC yielded approximately 10% greater compressive-strength

spread between core samples and standard cylinders, reflecting better consolidation of the conventionally vibrated concrete.

Sonebi et al. [2003] tested full-scale beams measuring 7.9×11.8 in. (200×300 mm) in section and 12.5 ft (3.5 m) in length cast with conventional concrete and SCC to evaluate cracking behavior, load-carrying capacity, mode of failure, and load deflection response. A four-point flexural test was carried out. The SCC and conventional concrete mixtures had 28-day compressive cube strengths of 11,530 psi (79.5 MPa) and 8,920 psi (61.5 MPa), respectively. The SCC was proportioned with a *w/cm* of 0.36, and 38% slag, with total binder content of 893 lb/yd^3 (530 kg/m^3), crushed granite with MSA of 0.39 in. (10 mm), and sand-to-total aggregate ratio of 54%. The conventional mixture had a *w/c* of 0.43, 868 lb/yd^3 (515 kg/m^3) of Portland cement without any slag, MSA of 0.79 in. (20 mm), and sand-to-total aggregate ratio of 41%. The SCC had slump flow of 27 in. (690 mm), and the conventional concrete had a slump value of 2.7 in. (70 mm). Test results showed that the average crack spacing of SCC and conventional concrete beams at 90% of the ultimate load was approximately 3.2 and 6.3 in. (82 and 160 mm). The SCC beam experienced a maximum deflection slightly higher than the reference beam at ultimate load. Both concrete beams exhibited similar initial stiffness, maximum moment-carrying capacity, and deflection. The yielding in the reinforcement led to an increase in deflection with little change in load for both beams; the SCC beam exhibited a slightly higher deflection compared with the reference concrete. The ultimate moment capacity of the SCC beam was comparable to the reference beam, given the lower compressive strength at the time of testing which was 10,150 psi (70 MPa) at 4.5 months for reference concrete and 13,340 psi (92 MPa) at 6 months for the SCC specimen.

4.12 Most Significant Mechanical Properties of SCC Affecting Structural Design and Performance of Precast, Prestressed Bridge Elements

Changes in mix design and workability of SCC can influence hardened properties and performance that can diverge from what is commonly expected from conventional concrete. The most important mechanical properties affecting the performance of precast, prestressed concrete bridge elements cast with SCC have been addressed in detail in this chapter. Factors that can influence the mechanical properties and structural performance of precast, prestressed bridge elements are briefly highlighted in this section.

For precast and structural civil engineering applications, SCC mixtures are typically proportioned with a *w/cm* of 0.32 to 0.36. The design of most precast, prestressed concrete members is based on 28-day compressive strength, which is typically 5000 to 6000 psi (34.5 to 41.4 MPa). However, mixtures for precast, prestressed girder elements should be proportioned to achieve the specified release strength of 4000 psi (27.6 MPa) within 18 hours after casting, as specified in AASHTO LRFD Bridge Design Specifications 1998. However, the high early-strength requirement and the typically low *w/cm* used in some SCC to enhance stability of SCC could lead to 28-day compressive strength greater than 8000 psi (55.2 MPa).

It is important to establish the relationship of gain in compressive strength for a given SCC mixture using local producer data. This is particularly important in estimating the release compressive strength. Testing of compressive strengths of core samples taken from experimental wall elements shows that the in-situ strength can be 20% and 15% lower than standard compressive strength determined from control cylinders when SCC and conventional vibrated concrete are used, respectively; the lower spread of 15% is observed for SCC made with smaller aggregate of 0.39 in. (10 mm) MSA. Testing carried out on full-scale reinforced columns and beams revealed that compressive strength of core samples in the columns varied between 80% and 100% of standard 28-day cylinder strength for SCC. The compressive strength variation along the length of the beams was much smaller than along the height of the columns.

Knowledge of the elastic modulus of concrete is important to estimate camber of prestressed members at the release of the prestressing load, as well as to determine elastic deflections caused by dead and live loads, axial shortening and elongation, and prestress losses. The modulus of elasticity of the parent rock and the relative volume of the aggregate in the concrete mixture has significant influence on the modulus of elasticity of the concrete. In addition to the total aggregate volume, adjustments of the sand-to-aggregate ratio (S/A) can influence the elastic modulus of the SCC. Spread of up to 20% could be obtained compared to the modulus of elasticity of high-performance concrete of normal consistency given the lower coarse aggregate volume of SCC. However, under air-drying conditions, the elastic modulus of SCC can be higher than that of conventional concrete in long term. These results can be attributed to the lower loss of water that may occur in the case of SCC.

In the case of concrete with normal consistency, the variation of elastic modulus with time can be estimated using the ACI 318 equation for mixtures with compressive strengths lower than 8,000 psi (55 MPa) [PCI, 1997 and 2003; AASHTO, 2004]. Similar recommendations are for SCC mixture [ACI Committee 237, 2004], which need to be validated in Phase II.

Because of the relatively low *w/cm* typically used in proportioning SCC and the incorporation of supplementary cementitious materials, SCC could develop higher flexural strength and flexural-to-compressive ratio than conventional slump concrete. For normal weight concrete of conventional slump, the modulus of rupture can be estimated from compressive strength results using standard equations recommended by PCI, 1997, AASHTO, 2004, or ACI 363. Limited published data are available on relationships between flexural strength and compressive strength of SCC, and the various code models need to be validated for SCC.

The stability of SCC is a key property in ensuring uniform mechanical properties and adequate performance of precast, prestressed bridge girders. Properly designed SCC mixtures can exhibit uniform distribution of in-situ compressive strength. Stability of SCC can be enhanced by using low *w/cm*, reducing the MSA, or incorporating a VMA.

Ensuring adequate bond to reinforcing bars and prestressed strands is essential for the structural performance of precast, prestressed bridge girders. Bond strength and its uniformity along the height of cast girders can be influenced by flow properties of the SCC, grading of the aggregate,

and content of fines. There is a controversy regarding bond strength of prestressing strands embedded in SCC. Some studies have found that bond strength of the reinforcement to SCC can be lower than that of normal concrete. Other studies, however, have shown that for a given compressive strength, reinforced concrete members made with SCC can develop higher bond strength than in the case of normal concrete. Tests carried out using full-scale girders revealed that the strand transfer length obtained on experimental girders cast with SCC is about 30% longer than the limit recommended by AASHTO. Full-scale tests revealed that immediately after prestress release (18 hours), girders cast with SCC are shown to exhibit similar initial camber and comparable strand slip-end as those of girders cast with normal concrete. SCC can develop similar top-bar effect as that of conventional concrete when it is proportioned with sufficient static stability.

The shear strength of the concrete affects the structural performance of precast, prestressed girders. Given the relatively high compressive strength of SCC used in precast structural applications and the fact that the interfacial transition zone with the aggregate is intact, cracked surfaces can involve a greater degree of intergranular crack propagation. This can then reduce aggregate interlock crack-friction capacity of members made with SCC.

CHAPTER 5 – FACTORS AFFECTING VISCO-ELASTIC PROPERTIES OF STRUCTURAL SCC

5.1 Introduction

Because of the length changes of prestressed members due to time-dependent deformations, creep and shrinkage play a crucial role in the design process of concrete structures and on the structural performance after construction, especially in the long term. Incorrect or inaccurate design for creep and shrinkage may have important undesirable consequences on stability and performance of the structure. For example, in segmental construction bridges, inaccurate creep analysis may cause excessive deflection, difficulties with closure, or un-aesthetic permanent deflections [Ulm et al., 1999a]. Furthermore, among other factors such as the modulus of elasticity and maturity of concrete, an accurate creep coefficient is necessary to camber calculation in segmented constructed bridges [AASHTO, 1994; ACI, 1997; PCI Interim Guidelines, 2003].

Creep may have detrimental effects in statically undetermined prestressed structures, built by successive steps. Indeed, some problems were highlighted 30 years ago, especially in bridges built using the cantilever method. Most of these bridges had to be strengthened, generally by external prestressing. Indeed, in prestressed elements, the prestress may be lower than expected and cracks may appear in critical areas, leading to shortening the service life of the structure. In general, the appearance of cracks in prestressed structures denotes the imperfect assessment of creep effects. L'Hermite noted that the value of shrinkage strain that is necessary to produce the first cracks is much larger for small specimens than for large ones [L'Hermite and Grieu, 1952].

The literature review presented in this chapter compares the visco-elastic properties of SCC to those of normal concrete, also referred to here as conventional vibrated concrete. This section reviews the different mechanisms of creep and shrinkage, the importance of creep and shrinkage in the design of prestress members, the factors affecting creep and shrinkage and provides a comparative analysis of visco-elastic properties of SCC versus those of normal concrete. This is intended to furnish guidelines and show the tendency of visco-elastic properties of SCC compared to those of normal concrete rather than an exhaustive comparison between creep and shrinkage coefficient values of different mixtures.

5.2 Types of Creep and Shrinkage

Basic creep refers to time-dependent deformation that occurs when concrete is loaded in a sealed condition so that the moisture cannot escape [Neville, 1981]. Drying creep (also called Pickett effect) is defined as the additional creep strain in excess of basic creep that is observed when the same concrete is allowed to dry while the concrete is under load. Therefore, the total observed creep could be considered as the sum of basic creep and drying creep. In practice, however, these distinctions are not always made, the total creep strain being included in the creep compliance function [Ulm et al., 1999b]. Furthermore, there is arbitrariness in separating creep strain from

so-called "elastic" (i.e. instantaneous) strain. Creep occurs from the immediate onset of loading, whereas it takes a finite time to measure the elastic strain.

The creep coefficient refers to the creep strain as a fraction of the elastic strain. For normal concrete, this value typically ranges between 2.0 and 6.0 for ultimate creep, i.e. the maximum creep attainable by the system [Ulm et al., 1999a]. Specific creep (or creep compliance) refers the amount of creep per unit-applied stress.

Unless specifically designed, shrinkage is generally taken as drying shrinkage, which is the strain associated with loss of moisture from the concrete under drying conditions. Autogenous (hydration or chemical) shrinkage refers to shrinkage of concrete that occurs as water is removed internally by chemical combination during the hydration of cement in a moisture-sealed state. It is related to hydration shrinkage and capillary shrinkage [Wittman, 1976].

5.3 Mechanisms of Creep and Shrinkage

In the absence of drying, two mechanisms of creep may be distinguished: short-term creep and long-term creep. Short-term creep is a consequence of redistribution of capillary water within the structure of the hardened cement matrix, and long-term creep is a consequence of the displacement of gel particles under loading and, to a lesser extent, of the neat creep of the gel particles themselves [Neville and Meyers, 1964; Neville, 1981; Ulm et al., 1999a; Acker, 1988; Acker and Bazant, 1998]. However, simultaneous drying further complicates the process because the sum of instantaneous plus creep deformations is larger than the sum of the creep and shrinkage measured separately. It is reported that the additional deformation is associated with drying creep. In structural analysis and design, creep is usually accounted for by using a creep factor calculated as the ratio between creep strain and instantaneous strain at any time [AASHTO, 1994; ACI 209, 1997; PCI, 2003].

Three mechanism of concrete shrinkage may be distinguished: 1) capillary, 2) chemical, and 3) drying [Neville, 1981; Wittman 1976; Acker, 1988]. Capillary shrinkage is the result of capillary pressure due to surface tension of water in fresh concrete during the early age of drying. Chemical shrinkage (or swelling) is caused by a number of chemical processes, such as hydration shrinkage, thermal shrinkage, and dehydration shrinkage. Drying shrinkage, is probably the most significant contributor to macroscopic dilation and is mainly caused by the migration of water from pores and capillaries [Ojdrovic and Zarghamee, 1976; Ulm et al., 1999a]. However, for relatively low *w/cm*, autogenous shrinkage can significantly contribute to the total deformation due to shrinkage.

5.4 Main Factors Affecting Creep and Shrinkage

Extensive research on creep and shrinkage of concrete showed that, aside from the mechanical behavior itself, the main governing phenomena for concrete creep and shrinkage is the diffusion of free water through the pore system and water exchange with the surrounding environment [Neville and Meyers, 1964; Ojdrovic and Zarghamee, 1996; Acker, 1998; Acker and Bazant,

1998; Ulm et al., 1999a]. It is reported that this diffusion process is highly non-linear since the diffusivity coefficient depends on the moisture content itself [Bazant, 1988]. For example, a saturated pore system allows water to move much more easily than a partially empty pore system.

Among the factors that increase creep and shrinkage deformations are the increase in water content in the mixture, the reduction in element size, the decrease in ambient relative humidity, and increase in ambient temperature [Neville and Meyers, 1964; Acker, 1998; Ulm et al., 1999a; ACI subcommittee 209]. Other factors affecting creep and shrinkage in real structures include the type and chemical composition of the cement in use, the type and content of cement replacement by supplementary cementitious materials, the content of ultra-fine particles in the cement paste, the volume fraction and rigidity of the aggregate, the particle-distribution of aggregate, the type of chemical admixtures, the oscillation of ambient conditions, the irregular shape and sizes of structural elements, as well as the location of these element in the structure (loading level).

It is important to distinguish real and apparent mechanisms that affect creep and shrinkage (Wittman, 1982). The former type is associated with the hydrated cement paste and can be considered as material properties determined by physical and chemical phenomena taking place during the hydration of cement, and should be independent of the specimen size and shape. On the other hand, apparent mechanisms are caused by other factors that modify the anticipated strains, such as the composite nature of the matrix. Indeed, due to the composite nature of concrete, differential strains between the hydrated cement paste and aggregate can cause high localized stresses and hence, microcracking at the transition zone. The use of SCC may result in reducing these effects since the coarse aggregate content is reduced.

5.5 Designing for Creep and Shrinkage

For structural applications, engineers are concerned with length changes of members due to time-dependent deformations. Creep and shrinkage are important in the design and analysis of prestressed concrete structures. Creep and shrinkage coefficients should be accurately evaluated and taken into consideration in the design of prestressed concrete elements in order to determine their effect on loss of prestressing force and to control deflections. For example, creep and shrinkage coefficients in conjunction with the moment of inertia may be used to determine the effects of creep and shrinkage on the deflection of structural elements [AASHTO, 1994; ACI 209, 1997; PCI, 2003]. Based on AASHTO specifications, for normal concrete and in the absence of accurate data, the shrinkage coefficient may be assumed to be 0.0002 after 28 days of drying and 0.0005 after one year of drying. The creep and shrinkage coefficients can also be estimated using:

- Collin and Mitchell model
- CEB-FIB model code
- ACI Committee 209 (Creep and shrinkage of concrete).

5.5.1 Creep

The creep coefficient may be estimated as:

$$\psi(t,t_i) = 3.5 k_c k_f (1.58 - \frac{H}{120}) t_i^{-0.118} \frac{(t-t_i)^{0.6}}{10.0 + (t-t_i)^{0.6}} \tag{5.1}$$

for which: $$k_f = \frac{1}{0.67 + \left(\frac{f_c'}{9}\right)} \tag{5.2}$$

where:

- H = relative humidity (%)
- k_c = factor for the effect of volume to surface ratio (V/S)
- k_f = factor for the effect of concrete strength
- t = maturity of concrete (day)
- t_i = age of concrete when load is initially applied (day)
- f'_c = specified compressive strength at 28 days (ksi)

Remarks:

1) The coefficient k_c can be determined using Fig. 5.4.2.3.2-1 in AASHTO specifications [1998]. This figure is based on the following equation [PCI, 1997]:

$$k_c = \left[\frac{\frac{t}{26e^{0.36(V/S)}+t}}{\frac{t}{45+t}}\right]\left[\frac{1.80 + 1.77e^{-0.54(V/S)}}{2.587}\right] \tag{5.3}$$

2) The maximum volume to surface ratio (V/S) considered in the development of the above equation is 6 in.^{3}/in.^{2} (150 mm^3/mm^2).

3) In determining the maturity of concrete at the time of loading, t_i, one day of accelerated curing by steam or radiant heat may be taken as equal to 7 days of normal curing.

4) The surface area used in determining the volume-to-area ratio should include only the area exposed to drying.

5.5.2 Shrinkage

For moist-cured concrete mixtures made with shrinkage-prone aggregate, the strain due to shrinkage, ε_{sh}, at time t, may be estimated using the following equation:

$$\varepsilon_{sh} = -k_s\, k_h \left(\frac{t}{35.0+t} \right) 0.51\times10^{-3} \tag{5.4}$$

where:

t = drying time (day)

k_s = size factor as specified by Eq. 6.7 or Fig. 5.4.2.3.3-2 of AASHTO specifications [2004]

k_h = humidity factor as specified in Table 5.1 below.

Table 5.1 – Values of k_h as a function of ambient relative humidity [AASHTO, 2004]

Average ambient relative humidity, H (%)	k_h
40	1.43
50	1.29
60	1.14
70	1.00
80	0.86
90	0.43
100	0.00

The k_h coefficients in Table 5.1 may be approximated by the following equations:

For H < 80% $$k_h = \frac{140-H}{70} \tag{5.5}$$

For H ≥ 80% $$k_h = \frac{3(100-H)}{70} \tag{5.6}$$

5.5.3 Loss of prestress

Prestress losses in members constructed and prestressed in a single stage can be estimated relative to the stress existing immediately before the transfer of the prestressing as:

1) Pretensioned members: $\Delta f_{pT} = \Delta f_{pES} + \Delta f_{pSR} + \Delta f_{pCR} + \Delta f_{pR2}$

2) Posttensioned members: $\Delta f_{pT} = \Delta f_{pF} + \Delta f_{pA} + \Delta f_{pES} + \Delta f_{pSR} + \Delta f_{pCR} + \Delta f_{pR2}$

where:

Δf_{pT} = total loss (ksi)

Δf_{pF} = loss due to friction (ksi)

Δf_{pA} = loss due to anchorage set (ksi)

Δf_{pES} = loss due to elastic shortening (ksi)

Δf_{pSR} = loss due to shrinkage (ksi)

Δf_{pSR} = loss due to creep of concrete (ksi)

Δf_{pR2} = loss due to relaxation of steel after transfer (ksi)

Remark:

1) The coefficient k_s can be determined using Fig. 5.4.2.3.3-2 in AASHTO specifications. This figure is based on the following equation [PCI, 1997]:

$$k_s = \left[\frac{\dfrac{t}{26e^{0.36(V/S)} + t}}{\dfrac{t}{45+t}} \right] \left[\frac{1064 - 94V/S}{923} \right] \tag{5.7}$$

The maximum volume to surface ratio (V/S) considered in the development of the above equation is 6 in.^{3}/in.^{2} (150 mm^3/mm^2).

5.6 Plastic Shrinkage

Shrinkage of concrete occurs in two distinct stages: at early and later ages. The early-age stage includes the first 24 hours after the first contact between cement and water, and the long-term period refers here to concrete with an age beyond 24 hours. Plastic shrinkage is the contraction that occurs when the concrete is at fresh state before and after setting. Plastic shrinkage can take place when the evaporation rate of water from the top exposed surface of the concrete is greater than the rate of bleeding water at that surface.

The mechanism of plastic shrinkage can be explained by the presence of water menisci at the concrete surface [Neville, 1964, 1981; Acker, 1988; Aïtcin, 1998]. It is well established that the plastic shrinkage increases with the binder content and decreases with the *w/cm* or *w/b*. The latter term is used to reflect the fact that the binder may contain materials other than supplementary cementitious materials, for example limestone filler.

Plastic shrinkage can increase in mixtures that are not prone to bleeding. SCC mixtures are typically proportioned with a relatively high content of binder, or binder with high specific surface area, and in some cases with Type III cement to ensure high early-strength development. Furthermore, SCC can incorporate VMA and is prepared with relatively low *w/cm*. These combined conditions increase the risk of plastic shrinkage. Turcry et al. [2002] compared the plastic shrinkage of SCC and normal concrete mixtures with various 28-day compressive strength values of 4,350, 5,800, 7,250, and 10,150 psi (30, 40, 50, and 70 MPa). The SCC mixtures were proportioned with a *w/b* ranging between 0.23 and 0.41, while the normal concrete

mixtures had a *w/b* of 0.50 to 0.60. Some of the investigated SCC mixtures even contained limestone filler and VMAs. Two types of HRWRAs corresponding to lignosulfonate and polycarboxylate were used. The test results showed that plastic shrinkage of SCC can be two times higher than that of normal concrete. The maximum plastic shrinkage amplitude of the SCC was 1000 to 1300 μm/m, while that of the normal concrete was between 100 and 500 μm/m.

The relatively low *w/b* of SCC mixtures may be one of the most important factors to explain the difference in shrinkage observed between SCC and normal concrete. Indeed, in the case of SCC made with a low *w/b*, no apparent external bleeding was observed. Therefore, the use of SCC necessitates extra care to protect exposed surfaces against evaporation during the plastic state of hydration, especially around the setting time. Proper curing immediately after casting to prevent moisture loss can eliminate early-age drying shrinkage of the concrete.

Holt and Schodet [2002] evaluated the early-age vertical shrinkage (settlement) and horizontal shrinkage (plastic and autogenous shrinkage) of SCC containing different types of cementitious materials and fillers (fly ash, limestone filler, and natural filler). Tests specimens consisted of square samples measuring 10.6 × 10.6 in. (270 × 270 mm) and 4 in. (100 mm) in height. For each concrete mixture, the quantity of evaporated water was determined on smaller samples measuring $4\times4\times4$ in. ($100\times100\times100$ mm). The internal capillary pressure was measured at the middle of the concrete specimens using a pore pressure transducer. In total, three SCC mixtures and a normal concrete were considered. The plastic shrinkage tests were performed under a constant wind speed of 2.5 m/sec. The mixtures were proportioned with a *w/b* ranging from 0.21 to 0.30 and a *w/c* ranging between 0.39 and 0.62, with the lowest values corresponding to the reference concrete. Test results revealed that SCC mixtures containing fly ash or limestone filler had a lower plastic shrinkage than that of normal concrete. This could be due to the relatively higher stiffness of the matrix, which results in reducing the shrinkage period before setting. It is also reported that the three SCC containing limestone and fly ash presented linear evaporation for the first 12 hours of measurement.

5.7 Drying Shrinkage

Although SCC technology is in its infancy, considerable research has been carried out to investigate the visco-elastic properties of SCC [Persson 1999, 2001a, 2001b, 2003a, 2003b; Vieira and Bettencourt 2003; Pons et al., 2003; Assié et al., 2003; Heirman and Vanderwalle, 2003; Song et al., 2001a, 2001b; Hu and Barcelo, 1998; Hammer, 2003; Trucry and Loukili, 2003; Klug and Holschemacher, 2003; Holt and Schodet, 2002; Turcry et al., 2002; Bui and Montgomery, 1998; Holschemacher and Klug, 2002; Attiogbe et al., 2002; Byun et al., 1998; Koning et al., 2001; Bouzoubaa and Lachemi, 2001]. As in the case of creep, drying shrinkage (referred to here simply as shrinkage) of SCC depend on the mix design of the concrete and can be higher than in the case of conventional vibrated concrete given the fact that the concrete is often proportioned with relatively high binder content and low coarse aggregate volume. Furthermore, SCC contains a higher content of ultra-fines and is often made with some

replacement of the cement with fly ash, blast-furnace slag, or limestone powder (sometimes in combination with silica fume). It can then be expected to have some differences in visco-elastic properties of SCC and conventional vibrated concrete. However, assuming the fact that shrinkage of concrete depends mainly on the water content, it may be fair to assume that no significant change in shrinkage occurs in SCC since it is proportioned with equal water content as conventional concrete (although the *w/cm* is lower).

A detailed analysis of data reported in literature and gathered through personal contacts reveals the existence of a controversy regarding the shrinkage of SCC compared to conventional vibrated concrete. On one hand, it is reported that shrinkage of SCC is higher than that of conventional vibrated concrete, or normal concrete. For a given compressive strength, shrinkage of SCC was reported to be similar to that observed with normal concrete [Persson 1999, 2001a, 2001b, 2003a, 2003b; Vieira and Bettencourt 2003; Pons et al., 2003; Assié et al., 2003; Attiogbe et al., 2002; Bouzoubaa and Lachemi, 2001]. On the other hand, shrinkage of SCC is reported in other studies to be higher than that of normal concrete [Heirman and Vanderwalle, 2003; Song et al., 2001a, 2001b; Hu et Barcelo, 1998; Hammer, 2003; Trucry et Loukili, 2003; Klug and Holschemacher, 2003; Turcry et al., 2002] and in some cases lower than that of normal concrete [Holt and Schodet, 2002].

According to Persson [1999, 2001a, 2001b, 2003a, 2003b], shrinkage and elastic modulus of SCC mixtures proportioned with a *w/b* ranging between 0.27 and 0.80 are similar to those of normal concrete made with the same materials and the same mixture proportioning. Both creep and shrinkage tests were performed in both air-drying and sealed conditions. The compressive strength of the tested mixtures ranged from 3,625 to 20,300 psi (25 to 140 MPa). Persson [2001a, 2001b] also conducted an experimental study to compare compressive strength, elastic modulus, creep, and shrinkage of SCC to normal concrete mixtures. The mixtures were proportioned with a *w/b* of 0.24 and 0.80. Test specimens considered in this investigation were 4 in. (100 mm) in diameter and 20 in. (500 mm) in length. The study was carried out using both sealed and air-cured specimens and involved the application of loading at ages of 2 to 90 days. Four different stress-to-compressive strength ratios were investigated. The ambient temperature during the creep testing was held constant, and the relative humidity was set at 60%. According to this study, creep and shrinkage of SCC did not differ significantly from the corresponding properties of normal concrete.

According to Pons et al. [2003], shrinkage testing conducted on two-classes SCC of 28-day compressive strengths of 5,800 psi (40 MPa) and 10,150 psi (70 MPa) revealed that for the same constituent materials, SCC and normal concrete mixtures exhibited similar shrinkage performance. The SCC mixtures were proportioned with a *w/b* ranging between 0.41 and 0.59, while the normal concrete mixtures were prepared with a *w/b* between 0.37 and 0.45. The similar shrinkage results were obtained on specimens exposed to air-drying [Assié et al., 2003]. However, in the case of sealed specimens, the SCC mixtures exhibited higher shrinkage than normal concrete after 100 days of testing. A comparative study conducted by Vieira and Bettencourt [2003] on SCC proportioned with 0.30 *w/b* and normal concrete made with 0.50 *w/b*

showed that for similar 28-day compressive strength, both concrete types developed similar shrinkage, regardless of the exposure conditions (air-dried vs. sealed specimens). The investigated SCC mixtures contained fly ash and limestone filler, while the normal concrete was prepared with fly ash only.

Bouzoubaa and Lachemi [2001] evaluated the performance of four SCC mixtures prepared with various *w/cm* of 0.35, 0.40, and 0.45 made with 40%, 50%, and 60% fly ash replacements. SCC mixtures contained 32% coarse aggregate volume and 674 lb/yd^3 (400 kg/m^3) of binder. A control mixture with *w/cm* of 0.50 and 28-day compressive strength of 5,075 psi (35 MPa) was considered for comparison. Drying shrinkage of SCC and that of the control concrete were similar after 224 days of standard drying (600 microstrain). The authors noted, however, slightly higher shrinkage values in SCC mixtures made with fly ash.

Byun et al. [1998] evaluated the drying shrinkage of SCC mixtures made with *w/b* varying between 0.35 and 0.38 and unit water contents of 124, 132, 143, and 147 lb/yd^3 (165, 175, 190, and 195 kg/m^3). The SCC mixtures contained 27% to 39% coarse aggregate volume and 30% to 40% fly ash replacement. The authors reported that SCC could develop 30% to 50% higher drying shrinkage than normal concrete. The authors attributed this difference to the pore refinement of SCC containing fly ash. SCC mixtures made with the lowest water content and moderate coarse aggregate relative volume of 33% developed the lowest degree of drying shrinkage. On the other hand, the SCC mixture proportioned with the highest water content of 147 lb/yd^3 (195 L/m^3) and high volume of coarse aggregate of 39% showed the highest level of drying shrinkage. The authors compared experimental drying shrinkage strains to existing prediction models and concluded that, in general, the scatter between measured and predicted shrinkage was greater in the case of SCC than that of normal concrete when using the ACI model. The experimental shrinkage strains were found to be larger than those estimated by the model. This was attributed to the fact that the empirical model does not consider the effect of fly ash and water-reducing admixtures.

The use of limestone powder with Blaine fineness greater than that of Portland cement can reduce drying shrinkage of SCC [Holschemacher and Klug, 2002]. This may be due to the denser matrix obtained when using especially fine limestone powder. The authors found that shrinkage of SCC can decrease when using mixtures of low *w/b* and low paste volume, provided that the paste volume is enough to ensure good deformability of the SCC. Mixtures made with MSA of 0.55 in. (14 mm) showed higher drying shrinkage than those with 0.79 (20 mm) MSA. This may be due to the increase in paste volume of the former mixture that is necessary to achieve a given deformability.

Assié et al. [2003] investigated on shrinkage of several SCC mixtures proportioned with a *w/b* of 0.38, gravel/sand ratio of 0.89, and calcareous filler. The vibrated concrete of normal consistency was similar to the SCC mixture and had the same cement factor, aggregate proportion, and *w/c* of 0.50. Test results showed that under similar testing conditions, SCC and vibrated concrete had similar total shrinkage values. However, under autogenous conditions, both concretes presented

similar shrinkage performance up to 90 days of testing. Beyond 100 days, the SCC exhibited higher shrinkage values than the vibrated concrete.

Shrinkage measurements carried out on 12 SCC mixtures made with various filler types and constant cement content of 590 lb/yd^3 (350 kg/m^3) showed that SCC can develop greater shrinkage than normal concrete, especially in the case of finely ground fillers [Heirman and Vanderwalle, 2003]. Drying shrinkage values after 90 days of testing were 325 microstrain for the reference concrete and varied between approximately 350 and 600 microstrain for the SCC mixtures with fillers. Seven limestone fillers, one dolomite filler, two fly ashes, and two quartzite fillers were tested. All mixtures were proportioned with 0.50 *w/c*, constant coarse aggregate volume, and filler/cement ratio of 0.90, by volume. Shrinkage measurements started after 24 hours of age and were carried out on cylinders measuring 4.5 × 11.8 in. (113 × 300 mm) that were kept at 60% relative humidity.

The effect of HRWRA and VMA on shrinkage of SCC is reported to be beneficial. Indeed, the use of HRWRA reduces the surface tension of the water, thus decreasing the capillary tension of pore water [Ulm et al., 1999a; Acker, 1988; Acker and Bazant, 1998; Neville, 1981; Wittman, 1976; Neville and Meyers, 1964]. However, the air content may increase when using polycarboxylate-based HRWRA, which could lead to greater shrinkage.

Turcry and Loukili [2004] compared the shrinkage cracking potential of SCC mixtures with 28-day compressive strengths of 3,625 to 7,250 psi (25 to 50 MPa) to those of normal concrete. Both types of concrete were prepared using the same raw materials and tested under similar drying conditions. Test results revealed that for a constant compressive strength, the total shrinkage, and specific creep of SCC are almost equivalent to those of normal concrete. Although the differences were small, it was observed that SCC mixtures developed lower modulus of elasticity values and in some cases higher shrinkage values than normal concrete. In terms of restrained shrinkage cracking, the testing revealed that under windy conditions (high evaporation rate), SCC tends to develop less cracking than normal concrete. Moreover, the SCC mixtures were shown to have a tendency to crack at a later elapsed testing time than in the case of normal concrete. Restrained shrinkage testing showed that crack openings developed in SCC tend to be less wide than those observed with normal concrete.

5.8 Autogeneous Shrinkage

Song et al. [2001b] investigated the autogenous shrinkage of SCC containing 40% cement replacement by blast-furnace slag of different Blaine finesses levels of 400, 600, and 800 m^2/kg (S4, S6, and S8, respectively, in Fig. 5.1). The mixtures were proportioned with 0.34 *w/cm* and developed a 28-day compressive strength of 9,570 psi (66 MPa). The autogenous shrinkage was shown to increase with the Blaine finenesses of the blast-furnace slag, as illustrated in Fig. 5.1. The use of finely ground blast-furnace slag with Blaine finenesses of 600 and 800 m^2/kg resulted in significantly greater autogenous shrinkage than SCC with blast-furnace slag of Blaine finenesses of 400 m^2/kg and that of the reference mixture made with ordinary Portland cement

(OPC). This result may be due to the higher surface area of the blast-furnace slag that can activate the reactivity of the binder, hence increasing the degree of autogenous shrinkage.

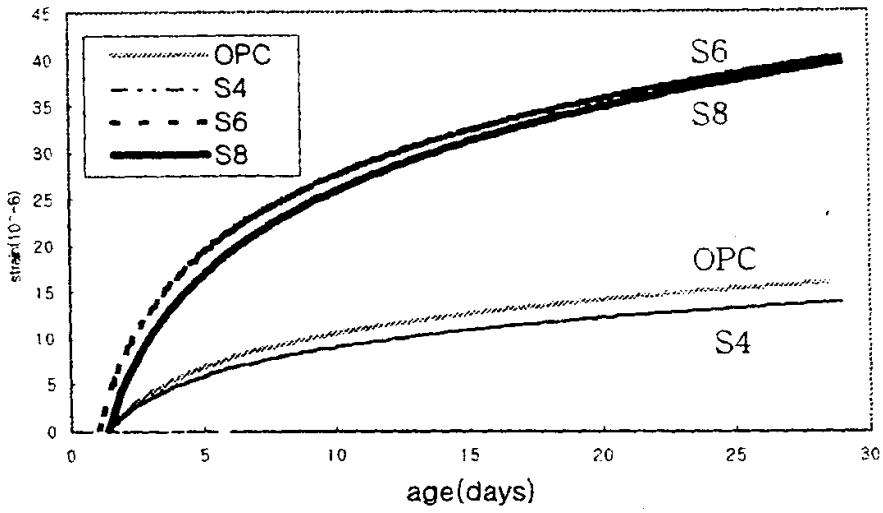

Fig. 5.1 – Effect of Blaine fineness of blast-furnace slag on autogenous shrinkage of SCC [Song et al., 2001b]

Hu and Barcelo [1998] evaluated the autogenous and drying shrinkage of SCC proportioned with *w/b* ranging between 0.73 and 0.80, and the shrinkage of conventional vibrated concrete. In general, the SCC mixtures exhibited 100 to 150 μm/m higher ultimate drying shrinkage than conventional concrete. However, the autogenous shrinkage of SCC mixtures was lower than or equal to that of the conventional vibrated concrete. At early age (during the first 2 days), the autogenous shrinkage of SCC was still negligible. These results are probably due to the relatively high *w/b* used to prepare the SCC mixtures. In cement paste made high *w/b*, the capillary porosity pressure is low and results in a low level of autogenous shrinkage [Ulm et al., 1999a]. Test results showed that the use of blast-furnace slag could increase the autogenous shrinkage of SCC; however, no effect was observed for the partial replacement of cement by fly ash. This result is in agreement with the results reported by Song et al. [2001b]. The effect of slag on drying shrinkage was shown to depend on the curing method. The authors reported that the ACI 209 model could be suitable to estimate drying shrinkage of SCC.

5.9 Creep of SCC

Creep behavior is related to the compressive strength of the matrix, coarse aggregate type, and relative content of the aggregate. Literature review of creep evaluations of SCC indicate that the creep potential of SCC appears to be slightly higher than that of conventional concrete made with the same raw materials and having the same 28-day design strength [Attiogbe et al., 2002; Pons et al., 2003; Byun et al., 1998]. Person [1999] found that for a given compressive strength, creep of SCC could be similar to that of normal concrete. In applications where creep characteristics

are an important design parameter, this aspect of the SCC mixture should be considered in design and confirmed for the mixture used in the production of precast members.

Byun et al. [1998] reported that for similar constant compressive strength and elastic modulus values, the creep rate of SCC can be greater than that of normal concrete at early ages, up to 20 days of testing. The authors attributed this difference mainly to the higher paste and lower coarse aggregate volume of the SCC. However, after 20 days of testing, both the SCC and normal concrete showed similar creep rates. The SCC mixtures were proportioned with various water contents ranging between 124 and 147 lb/yd^3 (165 and 195 L/m^3) and relative coarse aggregate volumes of 27% to 39%.

Experimental creep measurements conducted starting at loading times of 1, 3, 7, and 28 days by Song et al. [2001a] on SCC mixtures incorporating 40% blast-furnace slag replacements of different Blaine fineness levels of 400, 600, and 800 m^2/kg (S4, S6, and S8, respectively) showed that the effect of fineness of blast-furnace slag on creep is significant at early-age (1-3 days) of loading, but the effect becomes quite small for loading at later ages [Song et al., 2001a]. The mixtures were proportioned with a *w/cm* of 0.34. The authors evaluated the applicability of major creep-prediction models (AASHTO, JSCE, ACI-209, CEB-FIP MC 90, and BP models) to early-age creep of SCC incorporating blast-furnace slag (Figs. 5.2 to 5.5). The parameters considered for creep prediction, such as structural shapes, concrete internal properties and external environmental conditions are summarized in Table 5.2. From these figures, it can be concluded that in the case of early-age loading of 1 day, the creep prediction did not result in accurate results, regardless of the model in use. For example, it was observed that the BP model underestimates early-age creep strain, and the AASHTO model resulted in a large discrepancy. When the loading is carried out after 3 days of age, the BP model overestimates creep strain, while the AASHTO-94 underestimates it. At later loading ages of 7 and 28 days, the ACI-209, JSCE-95, and AASHTO-94 models are shown to underestimate the specific creep of SCC.

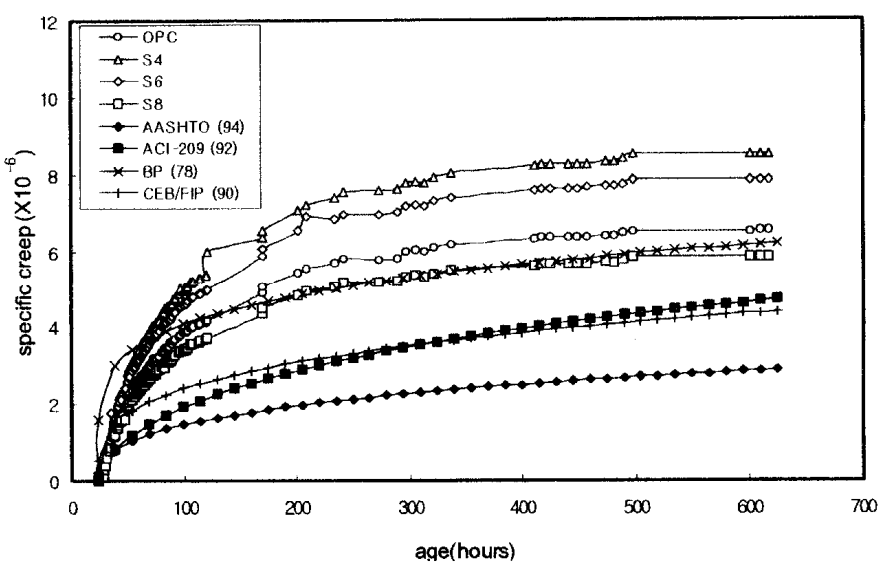

Fig. 5.2 – Specific creep obtained on specimens loaded after 1 day of age [Song et al., 2001b]

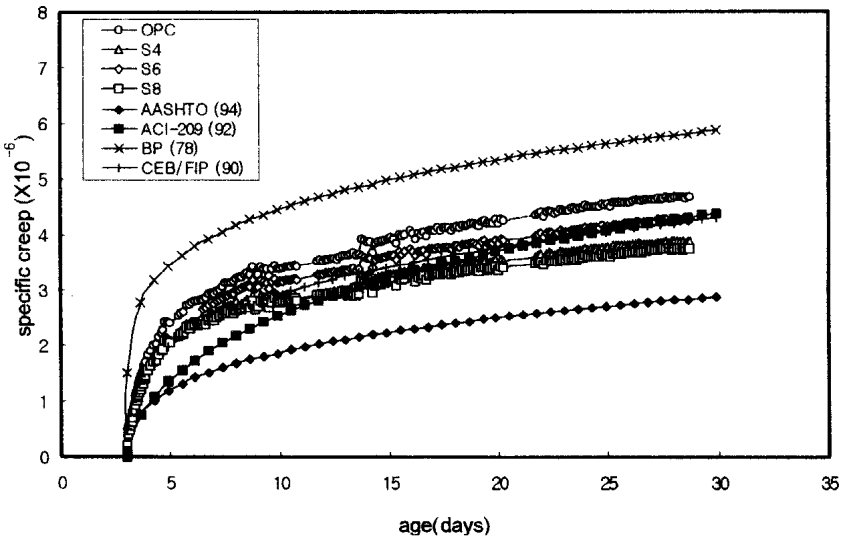

Fig. 5.3 – Specific creep obtained on specimens loaded after 3 days of age [Song et al., 2001b]

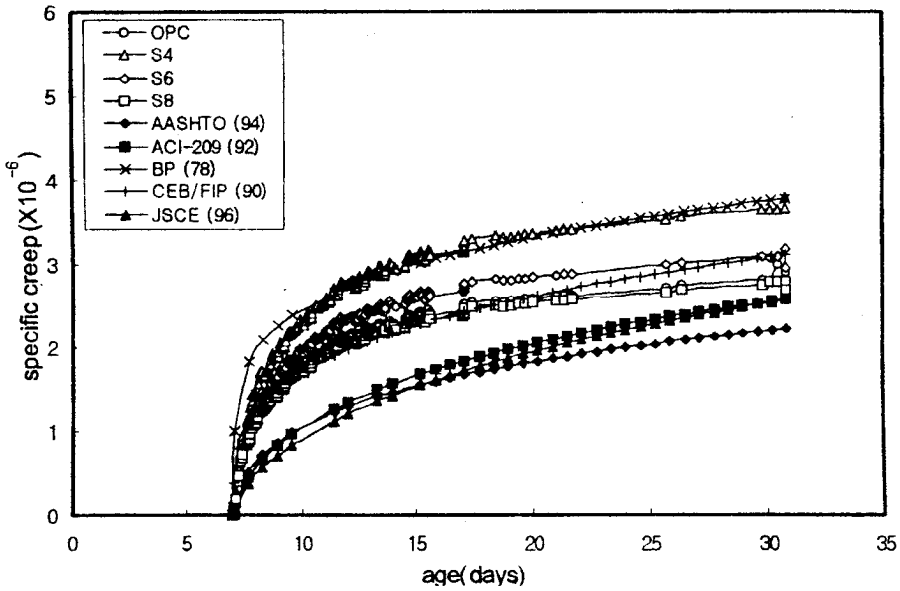

Fig. 5.4 – Specific creep obtained on specimens loaded after 7 days of age [Song et al., 2001b]

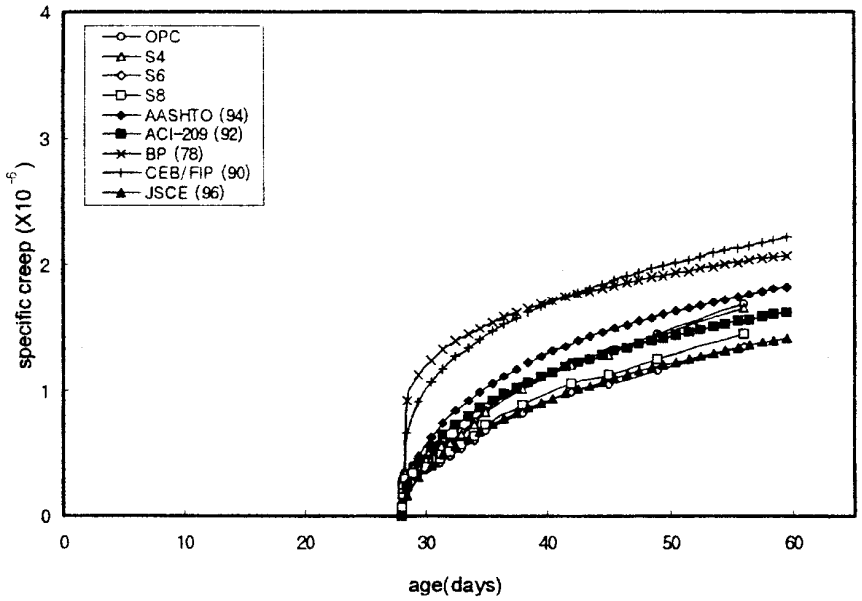

Fig. 5.5 – Specific creep obtained on specimens loaded after 28 days of age [Song et al., 2001]

Table 5.2 – Creep prediction parameters [Song et al., 2001b]

Major parameter	Detailed parameter	AASHTO -94	ACI-209 -92	BP-78	CEB/FIP -90	JSCE -96
Materials	Binder content		*	*		*
	Water content			*		*
	w/cm			*		*
	Sand content			*		
	Coarse aggregate			*		
	Sand/aggregate		*	*		
	Comp. strength	*		*	*	
	Slump level		*			
	Air volume		*			
	Type of cement				*	
Structure	Volume/surface	*	*	*	*	*
	Avg. thickness		*			
	Element shape			*		
External	Curing time	*		*		
	Curing method		*		*	
	Temperature			*	*	
	Relative humidity	*	*	*	*	*
	Initial loading age	*	*	*	*	*

According to Pons et al. [2003], creep of SCC and conventional vibrated concrete made with the same coarse aggregate are comparable. Hauke [2001] evaluated the creep of SCC specimen cylinders 5.9×11.8 in. (150×300 mm) that were cured in water for 7 days and loaded at 28 days at a constant load of σ = 20 N/mm^2. SCC mixtures were proportioned with a *w/b* of 0.54 and contained fly ash. The binder content of SCC was kept constant at 758 lb/yd^3 (450 kg/m^3). Creep tests were performed on SCC specimens at 28 days. Test results showed that for the same binder content of 758 lb/yd^3 (450 kg/m^3) and coarse aggregate composition, SCC mixtures presented 35% lower creep values than the normal concrete. After 135 days of loading, the creep strain obtained with SCC was 400 μm/m while the strain of normal concrete was 610 μm/m. Results reported by Kim et al. [1996] showed that SCC mixtures presented 15-25% higher creep than normal concrete. However, it should be noted that these results were obtained on mixtures made with different binder contents, 895 lb/yd^3 (530 kg/m^3) and 675 lb/yd^3 (400 kg/m^3) for the SCC and normal concrete mixtures.

5.10 Most Significant Visco-Elastic Properties of SCC Affecting Structural Design and Performance of Precast, Prestressed Bridge Elements

Creep and shrinkage play a crucial role in the design process of concrete structures and on the structural behavior, especially at long term. Therefore, creep and drying shrinkage characteristics of concrete need to be considered in the design of precast, prestressed bridge elements to account for losses in prestress and avoid cracking of the concrete that can shorten the service life of the structure. Aside from the mechanical behavior itself, the main phenomena governing creep and shrinkage is the diffusion of free water through the pore system and the water exchange with the surrounding environment.

The most relevant material characteristics that can affect creep and shrinkage of concrete are: volume fraction and rigidity of the aggregate, cement type, the type and content of supplementary cementitious materials, paste volume, water content, type of chemical admixtures, and compressive strength of the matrix, which is related to air content. Decrease in relative humidity, increase in ambient temperature, oscillation of ambient conditions, early exposure to drying and loading, reduction in element size, use of irregular shape and sizes of structural elements, as well as the location of these elements in the structure (loading level) are also important factors that affect creep and shrinkage.

According to the literature review, there seems to be some discrepancy regarding the visco-elastic properties of SCC. Several factors can explain this discrepancy, in particular the mix design (*w/cm* or *w/b*), type and content of coarse aggregates, type of chemical admixture, and testing exposure. The discrepancy also lies in the type of comparison used in the experimental program. Some studies have compared the visco-elastic properties of SCC proportioned differently from normal vibrated concrete, while others have compared the performance of SCC and conventional concrete of similar mix design and compressive strength levels.

On one hand, SCC proportioned with the same water content as normal concrete can develop similar visco-elastic characteristics because of the refinement of capillary pores and the reduction in microcracking at the interfacial transition zone that can result from the reduction in *w/cm*, use of supplementary cementitious materials, and reduction in aggregate size and volume. These factors could contribute to reducing shrinkage and creep. On the other hand, SCC mixtures have a relatively high paste volume; creep and shrinkage of some types of SCC made with relatively high water content can be greater than normal high-performance concrete.

Creep appears to be slightly higher than conventional concrete made with the same raw materials and having the same 28-day design strength. Creep behavior is related to the compressive strength of the matrix, coarse aggregate type, and relative content of the aggregate. It is reported that the creep potential of SCC appears to be slightly higher than that of conventional concrete made with the same raw materials and having the same 28-day compressive strength. For a given compressive strength, creep of SCC could be almost similar to that of normal concrete. In precast applications involving the use of SCC, the concrete is usually proportioned with polycarboxylate-based HRWRA, which increases early-age strength gain. Depending on the selected binder, *w/cm*, and ambient temperature at the precasting plant, the use of such HRWRA can eliminate the need to use radiant heat or steam curing. Such practice could then affect the visco-elastic properties of the SCC compared to normal concrete.

SCC used in precast, prestressed applications is typically proportioned with a low *w/cm* of 0.32 to 0.36 to enhance stability of the plastic concrete. Relatively low *w/cm* values, coupled with high content of binder can lead to greater degree of autogenous shrinkage than conventional concrete. Autogenous shrinkage can also increase with the fineness of the binder and fillers in use. Therefore, in addition to drying shrinkage, the increased volume of ultra-fines in SCC can lead to higher autogenous shrinkage and thermal contraction that have to be managed in the mix design process and in the structural detaining of the prestressed element.

Compared to existing prediction models, studies have shown that the scatter between measured and predicted shrinkage values is greater in the case of SCC than that for conventional concrete. Experimental shrinkage strains for SCC were reported to be larger than those estimated by various prediction models for drying shrinkage. Similarly, comparison of experimental creep data to major creep-prediction models did not result in accurate results, thus justifying the need for investigating creep and shrinkage of SCC designated for precast, prestressed applications.

CHAPTER 6 - DURABILITY CHARACTERISTICS OF SCC

6.1 Introduction

Concrete structures should be designed to provide protection of the reinforcing and prestressing steel against corrosion throughout the life of the structure. Design considerations for durability include concrete quality, protective coatings, minimum cover, distribution and size of reinforcement, details, and crack widths. According to AASHTO LRFD Bridge Design Specifications [1998], the critical factors contributing to the durability of concrete structure are:

- Adequate cover over reinforcement,
- Non reactive aggregate-cement combinations,
- Thorough consolidation of concrete,
- Adequate cement content,
- Low *w/c*, and
- Thorough curing, preferably with water.

Durability is a concern when bridges are exposed to aggressive environment. This generally occurs where deicing salts are used on highways during winter or in coastal regions where structures are exposed to salt from seawater. The ideal approach is to make the concrete as impermeable as possible. Precast, prestressed concrete has inherent advantages over cast-in-place concrete since it is produced in a controlled environment that results in high quality concrete.

It is important to note that the initial aim for developing SCC was to produce high-performance concrete that can be placed without mechanical vibration to prevent some durability problems that could arise from badly vibrated concrete. However, the majority of SCC research has dealt with workability issues with limited information regarding durability aspects of such concrete. The incorporation of high amounts of ultra-fine particles in SCC and HRWRA can lead to changes in the pore structure of the cement paste of SCC mixtures compared to conventional concrete. On the other hand, the high fluidity of such concrete can result in greater potential of bleeding and segregation and lead to more porous interfacial zone between the cement paste and the aggregate. However, when properly designed, the low bleeding tendency of SCC coupled with the lack of mechanical vibration and use of ultra-fines can indeed secure a denser microstructure.

Limited studies on the microstructure of SCC appear to confirm that the interfacial zones around reinforcement and large aggregate particles are denser and their properties more homogeneous in SCC mixtures than those in traditional vibrated normal concrete mixtures [Petersson et al., 1998]. Tragardh [1999] also found that compared to conventional concrete, SCC can develop a denser interfacial zone around the aggregate and denser bulk paste. A denser microstructure can lead to improved durability and increase concrete's resistance to corrosion of the reinforcement induced by chloride ions or carbonation.

Bridge structures constructed in environments prone to freezing and thawing necessitate air-entrainment for frost durability. According to AASHTO LRFD Bridge Design Specifications

[1998], the use of air-entrainment is generally recommended when 20 or more cycles of freezing and thawing per year are expected at the location and exposure. Under these conditions, prestressed bridge beams are air-entrained to resist internal damage caused by repetitive cycles of freezing and thawing. Table 6.1, based on ACI 211.1, provides the required air content for severe and moderate exposure conditions. Severe exposure is defined as a climate where the concrete may be in almost continuous contact with moisture prior to freezing, or where deicing salts come in contact with the concrete. This includes bridge decks. Salt laden air found in coastal areas is also considered a severe exposure. A moderate exposure is one where deicing salts are not used or where concrete will only occasionally be exposed to moisture prior to freezing. This is generally the case for bridge beams. It should be noted that some state highway departments specify air contents that are slightly different from those shown below. Other states do not require air entrainment in prestressed concrete beams given the fact that the bridge deck shelters the beams, or because air entrainment is not required for good performance.

Table 6.1 – Requirement for air content of concrete to secure proper frost durability

Nominal Maximum Aggregate Size, in. (mm)	Minimum Air Content (%)[1)]	
	Severe Exposure	Moderate Exposure
3/8 (10)	7-1/2	6
1/2 (13)	7	5-1/2
3/4 (19)	6	5
1.0 (25)	6	4-1/2
1-1/2 (38)	5-1/2	4-1/2

1) The usual tolerance on air content as delivered is ± 1.5%.

The durability of SCC should be well understood to facilitate its successful use in transportation structures. This chapter reviews research findings regarding the air-void system, frost durability, permeability to chloride ions, carbonation, and corrosion resistance of SCC.

6.2 Transport Properties of SCC

Permeation properties include permeability, absorption, and diffusivity, and are often used to quantify the durability characteristics of concrete. Theoretically, the main factors that control the permeation properties of concrete are the relative volume of the paste, the pore structure of the bulk matrix, and the interfacial zone around the aggregate particles. As mentioned earlier, given the enhanced stability of the fresh mixture and use of additional ultra-fines, together with the elimination of vibration, SCC mixtures should have a more homogeneous microstructure and denser interfacial zones may be expected.

Care must be taken to ensure that the powder materials and chemical admixtures used in proportioning SCC do not have an adverse effect on permeability and electrical resistance of the matrix. Audenaert [2003] carried out an experimental program to compare the transport properties of six SCC mixtures and one traditional concrete shown in Table 6.2. The CTH

method (method described below) was used to determine in a short period of time, the diffusion coefficient of chloride ions of the concrete at 28, 60, and 90 days of age. Based on these tests, illustrated in Fig. 6.1, it was suggested that the penetration depth in real conditions could not be predicted based on chloride-ion diffusion coefficient results without taking into account the capillary absorption coefficient. Compared to mixtures made with limestone filler and fixed w/c, the replacement of 40% of the binder by fly ash (SCC 6) and use of finely ground slag cement with limestone filler (SCC 2) can lead to considerably lower chloride-ion diffusion coefficient.

Table 6.2 – Mixture composition [Audenaert, 2003]

	SCC						TC
	1	2	3	4	5	6	1
CEM I 42.5 R (kg/m^3)	360		300	450	360	360	360
CEM III A 42.5 LA (kg/m^3)		360					
Fly ash (kg/m^3)						240	
Limestone filler S (kg/m^3)					240		
Limestone filler P2 (kg/m^3)	240	240	300	150			
Water (kg/m^3)	165	165	165	165	165	165	165
Sand 0/5 (kg/m^3)	853	853	853	853	853	853	640
Gravel 4/14 (kg/m^3)	698	698	698	698	698	698	1225
Glenium 51 (kg/m^3)	2.3	2.3	2.2	3.0	2.8	2.8	
w/c	0.46	0.46	0.55	0.37	0.46	0.46	0.46
Cement/(cement + filler)	0.60	0.60	0.50	0.75	0.60	0.60	1
Slump flow (mm)	665	845	628	741	751	810	
Compressive strength (MPa)	59	69	49	67	59	66	52

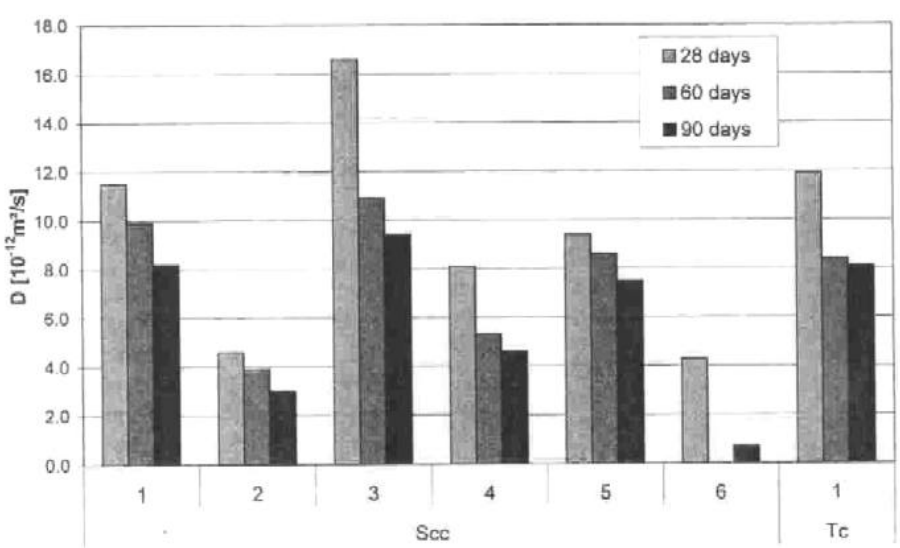

Fig. 6.1 – Chloride-ion diffusion coefficients of results [Audenaert, 2003]

The CTH Rapid Test used by Audenaert [2003] to determine chloride diffusivity of SCC was developed by Tang et al. [1999] to provide rapid measurement of diffusivity (coefficient of migration, D) of chloride ions in concrete. As illustrated in Fig. 6.2, the test involves placing a concrete cylinder measuring 4 in. (100 mm) in diameter and 2 in. (50 mm) in length into a test cell with the face of the sample in contact with a chloride solution. The specimen is preconditioned by vacuum treatment and saturation in a limewater solution. An external potential of 10-60 V is applied across the specimen to force chloride-ion migration into the specimen. After 24 h, the fresh specimen is axially split in two, and the mean depth of penetration of chloride is measured, after the application of 0.1-N silver nitrate solution. The mean depth of two test samples is used to calculate the coefficient of chloride migration.

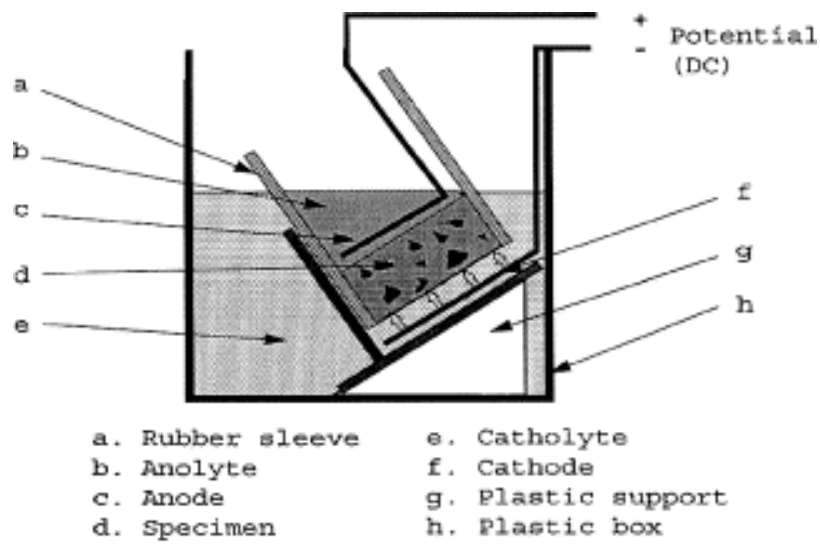

Fig. 6.2 – Experimental arrangement of the CTH Rapid Test [Tang et al., 1999]

Zhu and Bartos [2003] studied the permeation properties of various SCC mixtures, including oxygen permeability, capillary water absorption, and chloride diffusivity. The results were compared to those of selected reference concrete mixtures made of the same compressive strength grades, 5,800 and 8,700 psi (C40 and C60 MPa). The authors reported that SCC mixtures showed significantly lower permeability coefficient, water sorptivity, and water absorption values compared to vibrated normal concrete of the same compressive strength level. The authors reported that the chloride diffusivity of the tested concrete was much dependent on the type of powder in use for the binder. Both SCC and reference concrete made with pulverized fuel ash (PFA) showed much lower chloride migration coefficient than the other tested mixtures. SCC made without any powder addition but with a VMA to maintain proper stability of the fresh mixture developed the lowest impermeability and the highest sorptivity and chloride diffusivity.

Persson [2001a] investigated the chloride migration coefficient of SCC and reference conventional concrete made with the same *w/c* of 0.39 and air content of 6%. The chloride

migration coefficient was found to be 60% larger in the case of SCC made with limestone filler than that of conventional concrete. In the case of SCC made with 5% silica fume and 12% fly ash replacements, the chloride migration coefficient corresponded to 60% of the value obtained with the reference concrete. After 90 days of age, the chloride migration coefficient was 60% of that obtained at 28 days. Mixtures made with a low *w/c* (0.30) developed higher chloride migration coefficients than similar concretes made with higher a *w/c* (0.35-0.38). This performance could be due to self-desiccation that could occur at low *w/c*. Persson [2001a] recommended that for SCC mixtures containing limestone filler, the same amount of Portland cement be used as in the case of normal concrete to maintain the same chloride migration coefficient level. The incorporation of 5% silica fume in SCC is shown to lower significantly the chloride migration coefficient.

Boel and Audenaert [2003] found that using blast-furnace slag cement instead of pozzolan cement could enhance water impermeability of SCC compared to vibrated conventional concrete made of the same *w/c*. The gas impermeability of the SCC seemed to be much higher than that of the normal concrete.

6.3 Corrosion Resistance

Corrosion resistance affects the structural performance and service life of the reinforced concrete structures. The corrosion product resides at the interface between reinforcement and concrete, degrading the bond between rebar and concrete and thus reducing the service life of the structure. Corrosion is an electrochemical reaction between the steel and its surrounding environment. Reinforcing steel in concrete is in a passive state due to the highly alkaline environment allowing the formation of a thin oxide film on the surface. This oxide layer generally provides reliable protection against corrosion as long as it is intact. However, any disruption of this film, such as a significant concentration of chloride ions on the steel surface or reduction of the pH of the pore solution around the reinforcement due to carbonation, in the presence of oxygen and moisture, can initiate the corrosion process. In concrete bridge decks, chloride ions are derived mainly from deicing salts used during winter maintenance operations and from exposure to seawater. The chlorides in the salt penetrate the concrete and, when they reach a critical concentration, they break the passive film surrounding the reinforcing steel, and corrosion is initiated.

According to AASHTO LRFD Bridge Design Specifications [1998], a minimum cover over the main reinforcing bars, including bars protected by epoxy coating, shall be 1.0 in. (25 mm). The increase in concrete cover in well-cured and uncracked concrete reduces the risk of corrosion due to carbonation and the ingress of chloride ions, along with moisture and oxygen. Audenaert and Boel [2002] reported that the degree of carbonation in SCC decreases with the reduction in *w/c* and *w/b*.

Limited information is available regarding the influence of SCC on in-situ corrosion performance. The corrosion of reinforcing bars and changes in corrosion current depend largely on the impermeability of the concrete and the cover thickness over the reinforcement. The lack

of static stability of plastic SCC can lead to bleeding and segregation and weaken the quality of the interface between cement paste and embedded reinforcement with direct influence on corrosion resistance. Petrov et al. [2001] evaluated the effect of stability of the SCC on the potential corrosion characteristics of reinforcing steel using an accelerated corrosion test approach. Experimental wall elements measuring 4.9 ft (1.5 m) in height were cast with concrete. For each wall element, 12 steel rebars of 0.39 in. (10 mm) in diameter were embedded at four heights. The rebars were staggered resulting in cover thickness of 0.79, 1.38, and 2 in. (20, 35, and 50 mm) once the walls were saw-cut. Each wall was cut in four sections that were then used to construct a watertight basin for the accelerated corrosion testing. A galvanized steel mesh was provided at the outer surface of the concrete in contact with 5% NaCl solution. A potential of 5 V was provided between reinforcing bars and the cathodic steel mesh. The reduction in current passing through a known resistance of 1 Ω was used to monitor corrosion current. Three wall elements were cast with SCC of different stability levels. The SCC mixtures differed in their stability levels, adjusted by varying the dosage of VMA (0 to 0.075% welan gum, by mass of binder). The HRWRA concentrations were adjusted to maintain a slump flow of 24.6-25.6 in. (625-650 mm). A control concrete of similar composition was also tested and was prepared with lower HRWRA dosage in order to limit the slump consistency to 8 in. (200 mm). The values of surface settlement (test described in section 1.3.7) ranged between 0.20% and 0.81%. The decrease in settlement resulted in more uniform distribution of bond to embedded reinforcing bars along the height of the wall elements and a denser interfacial zone between the paste and reinforcement. As shown in Fig. 6.3, for a cover thickness of 1.38 in. (35 mm), the more stable SCC mixtures proportioned with 0.03% and 0.075% VMA exhibited greater corrosion resistance than for SCC made without any VMA or that of the control concrete. This is reflected by the longer elapsed time before the onset of corrosion.

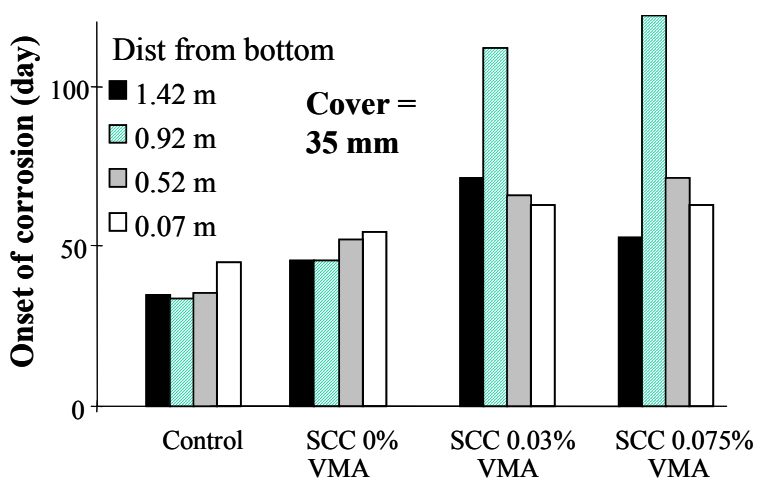

Fig. 6.3 – Effect of mixture composition and cover thickness on the elapsed time needed for the onset of corrosion [after Petrov et al., 2001]

In the same study, Petrov et al. [2001] found that SCC incorporating 0.075% welan gum VMA had greater rapid chloride-ion permeability (RCP) value than similar mixtures with 0 or 0.03% VMA. This, however, was not accompanied by an increase in capillary porosity or by difference in corrosion performance. The incorporation of HRWRA, or HRWRA and VMA was found to have no effect on the content of bound chloride-ions determined on cement paste made with fixed *w/c*. Therefore, the higher RCP value in the SCC mixture containing the highest concentration of welan gum VMA and naphthalene-based HRWRA can well be due to the ionic nature of the polymer employed at relatively high contents.

6.4 Air-Void System

In order to ensure proper resistance to freezing and thawing and de-icing salt scaling, an artificial air-void system with a defined geometric structure is needed in concrete, giving space for expansion in the pore structure. Thus, the concrete is enabled to take up the volume extension of the freezing water without suffering any damage. The stabilization of micro air voids is ensured by the use of effective air-entraining agent (AEA) in the mixture. In general, the use of a high dosage of HRWRA and the highly fluid nature of SCC can lead to reduced stability of entrained air bubbles in the plastic concrete. It is critical to select AEAs that can stabilize small air bubbles in highly flowable concrete. Such admixtures used to achieve an adequate air network and enhance frost durability of the concrete shall conform to the requirements of ASTM C260 and AASHTO M154.

Despite the highly flowable nature of SCC, proper air volume can still be produced in a stable manner, especially when the concrete has a relatively low *w/cm* or when it is proportioned with VMA. In general, the spacing factor of the entrained air bubbles in SCC can decrease with the increase in binder content or reduction in *w/cm* [Khayat and Assaad, 2002]. As is the case with normal-slump concrete, the authors found that air content in the hardened concrete can be within 1% of that determined at the fresh state in SCC. The mixtures were proportioned with naphthalene-sulfonic acid formaldehyde condensate HRWRA. A direct relationship exists between the air-void system parameters (spacing factor and specific volume), which is similar to that obtained for conventional concrete of normal slump.

The use of polycarboxylate-based HRWRA could cause entrapment of a large volume of air given the type and content of the de-foamer used in the formulation of these polymers. Concrete subjected to prolonged mixing or agitation after the introduction of HRWRA could exhibit some increase in air content, without necessary refinement in the size of air bubbles.

In general, greater air-void stability can be obtained when the SCC is proportioned with a higher content of cementitious materials and lower *w/cm*. For mixtures with a relatively low content of cementitious materials and a high *w/cm*, the air-void stability increases when a VMA is incorporated [Khayat, 2000]. In order to prevent coalescence of small air bubbles during agitation, the torque plastic viscosity (h) and apparent yield stress (g) should be limited to values ranging between 3 and 10 N.m.s and 0.5 and 2 N.m, respectively [Khayat and Assaad, 2002].

Such rheological characteristics are necessary to maintain a stable air-void system with respect to agitation. A maximum variation of ± 0.05 mm in spacing factor between non-agitated concrete and that subjected to occasional agitation over 95 minutes can be obtained when the concrete has these rheological characteristics.

6.5 Frost Durability and Salt Scaling of SCC

Concrete can be damaged by exposure to freeze-thaw conditions due to the expansion of water in the capillaries upon freezing. This can lead to micro-cracking with a consequential loss of strength and modulus of elasticity. Saturated concrete exposed to severe environment requires a satisfactory air-void system, sufficient maturity, and proper aggregate. When proper air-void system is provided, SCC can exhibit excellent resistance to freezing and thawing and to de-icing salt scaling [Persson, 2003a; Khayat, 2000]. Khayat [2000] reported that SCC mixtures with 0.45 and 0.5 *w/cm* made with 710 to 885 lb/yd^3 (420 to 525 kg/m^3) of ternary binder containing combinations of silica fume and fly ash or blast-furnace slag can develop favorable air-void systems with spacing factors less than 220 µm. Such SCC can develop excellent durability to freezing and drawing with longitudinal elongation limited to 250 µm/m after 300 frost cycles of freezing and thawing.

Audenaert and Boel [2002] investigated the different key parameters that could affect the transport properties of SCC, such as *w/c*, *w/b* (with the binder here referring to Portland cement and filler), and type of filler. Compared to vibrated conventional concrete, the chloride penetration by frost action with de-icing salts was found to be lower in the case of SCC than that of normal concrete. As in the case of normal concrete, the chloride penetration of SCC increases as the *w/c* and *w/b* increase.

Persson [2003b] studied the internal frost resistance and salt scaling of SCC that contains increased amount of limestone filler and the performance of normal concrete made with the same *w/c* of 0.39 and air content of 6% (Table 6.3). The author evaluated the chloride migration coefficient of SCC and normal concrete subjected to freezing and thawing cycles in the presence of de-icing salt. In general, as can be observed in Fig. 6.4, no significant difference in salt frost resistance can be observed between the two normal concrete mixtures (RO and ROII) and the six tested SCC mixtures. The amount of filler and the mixing sequence of the concrete did not seem to have an effect on salt frost scaling of SCC. Less scaling damage was observed for SCC with limestone powder having a higher Blaine fineness.

Table 6.3 – Mixture composition and properties [Persson, 2003b]

Material/mix composition	KN	KOB	KN8	KO	KOT	SO	RO	ROII
Crushed aggregate Bålsta 8–16	363	371	355	367	363	402	862	876
Natural sand Bålsta 0–8	853	872	836	864	855	786	715	727
Natural sand SÄRÖ 0–2	316	135	309	320	316	422	146	149
Limestone filler	183	375	180	186	184	94	0	
Cement Degerhamn	418	427	409	423	419	416	431	438
Air entrainment (g, 10% dry)	585	213	1203	106	117	125	474	482
Superplasticiser (35% dry)	2.97	4.13	3.2	3.39	3.69	2.99	7.32	5.92
Water	163	167	160	165	163	162	168	171
Water-to-cement ratio	0.39	0.39	0.39	0.39	0.39	0.39	0.39	0.39
Air content (%)	5.6	4.9	8	5.5	6.3	5.6	5.8	6.1
28-Day cube strength (MPa)	63	84	50	75	75	61	68	63
Slump flow (mm)	720	780	735	620	640	710	110	150
Density	2297	2348	2250	2323	2300	2285	2325	2368
Aggregate with filler (vol.%)	0.643	0.654	0.630	0.652	0.645	0.641	0.650	0.661

B=increased amount of filler; K=Limus 40 limestone filler; N=new way of mixing (filler at last); O=ordinary way of mixing (filler first); R=normal; S=Limus 15 limestone filler; T=5.5 m hydrostatic pouring pressure instead of 0.23 m; II=second; 8=8% air content.

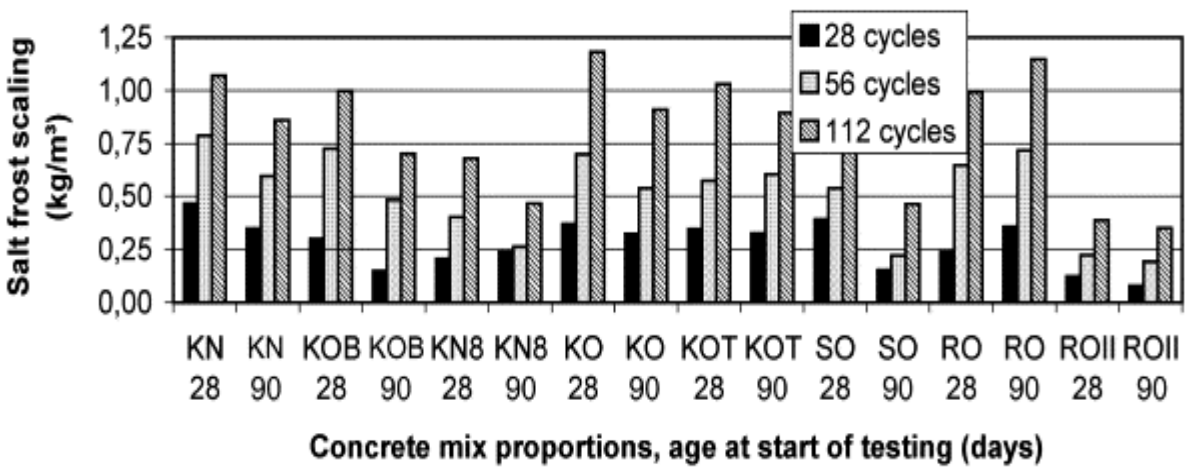

Fig. 6.4 – Salt frost scaling of normal concrete and SCC (Note: mix proportions and notations are given in Table 6.3) [Persson, 2003b]

Boel and Audenaert [2003] evaluated the resistance to de-icing salt scaling of 12 SCC mixtures and one conventional concrete. The test parameters included cement type and content, powder content, filler type (limestone filler and fly ash), and water content. The authors found that SCC and conventional concrete made with the same cement type showed little difference regarding the de-icing salt scaling mass loss. As in the case of conventional concrete, the reduction in *w/c*

decreases the quantity of capillary pores and enhances the impermeability and tensile strength of the matrix, thus leading to better scaling resistance. The replacement of part of the cement with blast-furnace slag cement can enhance these properties of the matrix and improve the resistance to salt scaling. However, salt scaling can increase in SCC if large substitutions of cement are made using blast-furnace slag [Persson, 2003b].

6.6 Most Significant Durability Characteristics Affecting Performance of SCC Used to Produce Precast, Prestressed Bridge Elements

Precast, prestressed concrete used for the production of bridge elements must be durable to ensure adequate service life. The most significant durability characteristics affecting the performance of SCC used in precast, prestressed elements production were reviewed in this chapter. Critical factors contributing to the durability of concrete structures include: w/cm, cement content, consolidation of fresh concrete, curing, cover over the reinforcement, and reactivity of aggregate-cement combinations. Similarly, the main factors that control the permeation properties of concrete are the relative volume of the paste, the pore structure of the bulk matrix, and the interfacial zone between the cement paste and aggregate particles. Precast, prestressed concrete bridge beams produced with conventional, vibrated concrete usually have good performance in aggressive environments.

The incorporation of high amounts of ultra-fine particles and HRWRA in SCC can lead to changes in the pore structure of the cement paste of SCC mixtures compared to conventional concrete. On the other hand, the high fluidity of such concrete can result in greater potential of bleeding and segregation and lead to weak interfacial zone between the cement paste and the aggregate. However, when properly designed and cast, SCC can lead to more homogeneous microstructure and denser interfacial zone with reinforcement and coarse aggregate particles. This is especially the case in mixtures made with relatively low w/cm that are typical of SCC used in precast applications.

A denser microstructure can decrease diffusion of chloride ions and other harmful substances, increase frost resistance, and improve service life of the structure. Densification of the cement matrix and increase in concrete cover in well-cured and uncracked concrete can reduce the risk of corrosion. At similar compressive strength, SCC can develop significantly lower permeability coefficient, water sorptivity, and water absorption compared to conventional vibrated concrete.

In concrete bridge decks, chloride ions are derived mainly from deicing salts used during winter maintenance operations and from exposure to seawater in coastal regions. Limited information is available regarding the influence of SCC mixture composition and the effect of high fluidity on in-situ corrosion performance. The mix design of SCC must ensure that the concrete can develop adequate stability during the dormant period of cement hydration. Lack of stability can lead to bleeding and segregation and weaken the quality of the interface between the cement paste and embedded reinforcement. The type of supplementary cementitious materials and fillers and their levels of substitutions, as well as the type of chemical admixture in use in SCC must be selected

to avoid any adverse effect on permeability and electrical resistance of the concrete. The electrical resistivity can be estimated from the rapid chloride-ion test (AASHTO T 277, Standard Specification for Electrical Indication to Resist Chloride Ion Penetration).

Bridge structures constructed in environments prone to freezing and thawing necessitate air-entrainment when 20 or more cycles of freezing and thawing per year are expected at the project location. Despite these conditions, some states do not require air entrainment in prestressed concrete beams. One of the reasons lies in the fact that the bridge deck shelters the beams, thus reducing the rate of saturation of the concrete and exposure to any deicing salt applied on the bridge deck.

In most cases, bridge girders can be considered to be subjected to moderate exposure conditions that correspond to situations where deicing salts are not used or where the concrete is only occasionally exposed to moisture prior to freezing. Under these conditions, prestressed bridge beams required sufficient air content for moderate exposure conditions. SCC proportioned with ½ in. (12.5 mm) nominal MSA would then require 4% to 7% fresh air volume to provide adequate frost durability.

Stable and closely spaced air voids can be obtained when the SCC is proportioned with an effective air-entraining agent that is compatible with the HRWRA and other chemical admixtures in use. The dosage of air-entraining agent in SCC prepared with polycarboxylate-based HRWRA is quite low compared to values recommended for conventional concrete of normal consistency. Yet, it is critical to incorporate an air-entraining agent in concrete subjected to moderate frost exposure conditions to secure stable and closely spaced air bubbles. When proper air-void system is provided, SCC can exhibit excellent resistance to freezing and thawing and to de-icing salt scaling.

The use of polycarboxylate-based HRWRA may lead to the entrapment of a large volume of coarse air bubbles given the type and content of the de-foamer used in the formulation of these polymers. Concrete subjected to prolonged mixing or agitation that occurs during transport could exhibit some increase in air content, without necessary refinement in the size of the bubbles. Investigations carried out with naphthalene-based HRWRA indicate that the stability of air volume can be enhanced in SCC mixtures proportioned with a relatively low *w/cm* (i.e. high binder contents) or those made with VMA. However, beyond a certain viscosity level, the stability of fine air bubbles during agitation could be hindered. Similar investigation is required for SCC mixtures made with polycarboxylate-based HRWRA.

REFERENCES

American Association of State Highway Transportation Officials (AASHTO), *Standard Specification for Electrical Indication to Resist Chloride Ion Penetration*, AASHTO T 277.

AASHTO, (1998). *AASHTO LRFD Bridge Construction Specifications.*

AASHTO, (1994). *AASHTO LRFD Bridge Design Specifications*, 1st edition.

AASHTO, (1998). *AASHTO LRFD Bridge Design Specifications*, 2nd edition.

AASHTO, (2004). *AASHTO LRFD Bridge Design Specifications*, 3rd edition.

ACI 209 Sub-Committee I, (1971). *Effects of Concrete Constituents, Environment, and Stress on the Creep and Shrinkage of Concrete*, Symposium on Creep, Shrinkage, and Temperature Effects, SP-27-1, ACI, Detroit, pp. 1-42.

ACI Committee 209, (1997). *Prediction of Creep, Shrinkage, and Temperature Effects in Concrete Structure,* ACI-209R-13.

ACI Committee 237, (2004). *Provisional Guidelines on Self-Consolidating Concrete*.

Acker, P., and Bazant, Z.P., (1998). *Measurement of Time-Dependent Strains of Concrete*, RILEM Draft Recommendations, Material and Structures, RILEM.

Acker, P., (1988). *Mechanical Behavior of Concrete: Physico-Chemical Approach,* Etudes et Recherches des LPC, 152, Laboratoire Central des Ponts et Chaussées. (In French)

Aïtcin, P.-C. (1998). *High-Performance Concrete*, E & FN Spon, London, 591 p.

Assaad, J., Khayat, K.H., and Daczko, J., (2004). *Evaluation of Static Stability of Self-Consolidating Concrete*, ACI Materials Journal, **101** (3), pp. 207-215.

Assaad, J., Khayat, K.H., and Mesbah, H., (2003). *Influence of Thixotropy on Formwork Pressure of Flowable and Self-Consolidating Concrete – Laboratory Tests*, ACI Materials Journal, **100** (1), pp. 29-37.

Assié, S., Escadeillas, G., and Marchese, G., (2003). *Durability of Self-Compacting Concrete*, Proc., 3rd International RILEM Symposium on Self-Compacting Concrete, August 17-20, Reykjavik, Iceland, pp. 655-662.

Attiogbe, E.K., See, H.T., and Daczko, J.A., (2002). *Engineering Properties of Self-Consolidating Concrete,* Proc., 1st North American Conference on the Design and Use of SCC, Chicago, Illinois, USA, pp. 371-376.

Audenaert, K., and Boel, V., (2002). *Durability of Self-Compacting Concrete*, Proc., 1st North American Conference on the Design and Use of SCC, Chicago, Illinois, USA, pp. 377-383.

Audenaert, K., (2003). *Chloride Penetration in SCC*, Proc., 3rd International RILEM Symposium on Self-Compacting Concrete, August 17-20, Reykjavik, Iceland, pp. 818-825.

Bazant, Z.P., (1988). Mathematical Modeling of Creep and Shrinkage of Concrete, Edited by Bazant, Z. P., John Wiley & Sons Ltd., (1988), 456 p.

Bartos, P.J.M., (1998). *An Appraisal of the Orimet Test as a Method for On-Site Assessment of Fresh SCC Concrete*, International Workshop on Self-Compacting Concrete, Japan, pp. 121-135.

Beaupré, D., (1994). *The Rheology of High-Performance Shotcrete*, Doctoral Thesis, University of British Columbia, February, 250 p.

Billberg, P., (1999). *Self-Compacting Concrete for Civil Engineering Structures – The Swedish Experience*, CBI report 2:99, Swedish Cement and Concrete Research Institute, 80 p.

Boel, V., and Audenaert, K., (2003). *Behaviour of SCC Concerning Frost Action with Deicing Salts*, Proc., 3rd International RILEM Symposium on Self-Compacting Concrete, August 17-20, Reykjavik, Iceland, pp. 837-843.

Bosiljkov, V.B., (2003). *SCC Mixes with Poorly Graded Aggregate and High Volume of Limestone Filler*, Cement and Concrete Research, **33**, pp. 1279-1286.

Bouzoubaâ, N., and Lachemi, M., (2001). *Self-Compacting Concrete Incorporating High Volumes of Class F Fly Ash: Preliminary Results*, Cement and Concrete Research, **31**, pp. 413-420.

Brameshuber, W., and Uebachs, S., (2001). *Practical Experience with the Application of Self-Compacting Concrete in Germany*, Proc., 2nd International Symposium on Self-Compacting Concrete, Tokyo, Japan, pp. 687-696.

Brite-EuRam Project on SCC-BRPR-CT96-0366, (1998). *Rational Production and Improved Working Environmental Through Using Self-Compacting Concrete.*

Bui, V.K., and Montgomery, D., (1998). *Drying Shrinkage of Self-Consolidating Concrete Containing Milled Limestone*, Proc., 1st RILEM International Symposium on Self-Compacting Concrete, Stockholm, Sweden, September 13-14, pp. 227-238.

Bury, M.A., and Bühler, E., (2002). *Methods and Techniques for Placing Self-Consolidating Concrete – An Overview of Field Experiences in North American Applications*, Proc., 1st North American Conference on the Design and Use of Self-Consolidating Concrete, ACBM, Chicago, Illinois, Nov. 12-13, pp. 281-286.

Byun, K.J., Kim, J.K., and Song, H.W., (1998). *Self-Compacting Concrete in Korea*, Proc., International Workshop on Self-Compacting Concrete, Kochi, Japan, pp. 23-33.

CEP/FIP (1990). Model Code 1990, Comité Euro-International du Béton.

Chan, Y.-W., Chen Y.-S., and Liu, Y.-S., (2003). *Development of Bond Strength of Reinforcement Steel in Self-Consolidating Concrete*, ACI Materials Journal, **100** (4), pp. 490-498.

Constantiner, D., and Daczko, J., (2002). *Not All Applications are Created Equal; Selecting the Appropriate SCC Performance Targets*, Proc., 1st North American Conference on the Design and Use of Self-Consolidating Concrete, Chicago, USA, pp. 179-184.

Daczko, J., and Kurtz, M., (2001). *Development of High Volume Coarse Aggregate Self-Compacting Concrete*, Proc., 2nd International Symposium on Self-Compacting Concrete, Tokyo, Japan, pp. 403-412.

Dehn, F., Holschemacher, K., and Weibe, D., (2000). *Self-Compacting Concrete (SCC) Time Development of the Material Properties and the Bond Behavior*, Leipzig Annual Civil Engineering Report No. 5, Universität Leipzig, pp. 115-124.

Domone, P., and Chai, H., (1999). *Optimum Mix Proportioning of Self-Compacting Concrete*, Proc., International Conference on Innovation in Concrete Structures: Design and Construction, Dundee, pp. 277-285.

European Federation of National Trade Associations (EFNARC), (2002). *Specification and Guidelines for Self-Compacting Concrete*, UK, 32 p.

Florida DOT, (2004). *Standard Specifications for Road and Bridge Construction*, Florida State.

Gaubner, C.-A., Muller-Falcke, G., Kleen, E., Lieberum, K.-H., and Rieger, T., (2001). *New Self-Compacting Concrete for Precast Elements*, Betonwerk + Fertigteil-Technik (Concrete Plant + Precast Technology), **3**, pp. 100-108.

Gibbs, J.C., and Zhu, W., (1999). *Strength of Hardened Self-Compacting Concrete*, Proc., 1st RILEM International Symposium on SCC, Stockholm, Sweden, September 13-14, pp. 199-209.

Hammer, T.A., (2003). *Cracking Susceptibility Due to Volume Change of Self-Compacting Concrete*, Proc., 3rd International RILEM Symposium on Self-Compacting Concrete, August 17-20, Reykjavik, Iceland, pp. 553-557.

Hauke, B., (2001). Self-Compacting Concrete for Precast Concrete Products in Germany*, Proc., 2nd International Symposium on Self-Compacting Concrete, October 23-25, Tokyo, pp. 633-642.*

Hegger, J., Gortz, S.G., Kommer, B., Tiggs, C., and Dross, C., (2003). Prestressed Precast Beams Made of Self-Compacting Concrete*, Betonwerk + Fertigteil-Technik (Concrete Plant + Precast Technology), **8**, pp. 40-46.*

Heirman, G., and Vanderwalle, L., (2003). *The Influence of Fillers on the Properties of Self-Compacting Concrete in Fresh and Hardened State*, Proc., 3rd International RILEM Symposium on Self-Compacting Concrete, August 17-20, Reykjavik, Iceland, pp. 606-618.

Holschemacher, K., and Klug. Y., (2002). *A Database for the Evaluation of Hardened Properties of SCC*, Leipzig Annual Civil Engineering Report No. 7, Universität Leipzig, pp. 123-134.

Holt, E., and Schodet. O., (2002). *Self-Consolidating Concrete: Early-Age Shrinkage*, Technical Research Center of Finland, VTT Building and Transport, Internal Report (RTE40-IR-21/2002), 26 p.

Hovington, A., (2000). *Experience of the Ministry of Transport of Quebec with SCC (1997-2000)*, in French, Proc., Annual Meeting of ACI Quebec and Eastern Ontario Chapter, Quebec, Canada, 8 p.

Hu, C., and Barcelo, L., (1998). *Investigation on the Shrinkage of Self-Compacting Concrete for Building Construction*, Proc., 1st Symposium International Conference on Self-Compacting Concrete, Kochi, Japan, pp. 228-242.

Hwang, S.-D., Khayat, K.H., and Bonneau, O., (2004). *Performance-Based Specifications of Self-Consolidating Concrete Used for Repair Applications*, ACI Materials Journal, (submitted).

Japan Society of Civil Engineers, (1998). *Recommendation for Construction of Self-Compacting Concrete*, Technical Session: Recommendations and Materials, pp. 417-437.

Japan Society of Civil Engineers, (1999). *Recommendations for Self-Compacting Concrete,* Tokyo, 77 p.

Johnston, J., (2002). *Making A Vision Concrete*, The Cincinnati Enquirer, August 11, p. A1.

Khayat, K.H., (1998). *Use of Viscosity-Modifying Admixture to Reduce Top-Bar Effect of Anchored Bars Cast with Fluid Concrete*, ACI Materials Journal, **95** (2), pp. 158-167.

Khayat, K.H., (1999). *Workability, Testing, and Performance of Self-Consolidating Concrete*, ACI Materials Journal, **96** (3), pp. 346-353.

Khayat, K.H., (2000). *Optimization and Performance of Air-Entrained SCC*, ACI Materials Journal, **97** (5), pp. 526-535.

Khayat, K.H., Hu, C., and Laye, J.-M. (2000b). *Influence of Aggregate Grain-Size Distribution on Workability of Self-Consolidating Concrete (SCC),* Proc., International Conference on High-Performance Concrete, December 10-15, Hong Kong, pp. 1001-1024.

Khayat, K.H., and Assaad, J., (2002). *Air-Void Stability in SCC*, ACI Materials Journal**, 99**, pp. 408-416.

Khayat, K.H., Assaad, J., and Daczko, J., (2004). *Comparison of Field-Oriented Test Methods to Assess Dynamic Stability of Self-Consolidating Concrete*, ACI Materials Journal**, 101** (2), pp. 168-176.

Khayat, K.H., Bickley, J., and Lessard, M,. (2000a). *Performance of Self-Consolidating Concrete for Casting Basement and Foundation Walls*, ACI Materials Journal**, 97** (3), pp. 374-380.

Khayat, K.H., Ghezal, A., and Hadriche, M. (2000b). *Utility of Statistical Models in Proportioning Self-Consolidating Concrete*, RILEM Materials and Structures, **33**, June, pp. 338-344.

Khayat, K.H., and Guizani, Z., (1997). *Use of Viscosity-Modifying Admixtures to Enhance Stability of Fluid Concrete*, ACI Materials Journal, **94** (4), pp. 332-340.

Khayat, K.H., Manai, K., and Trudel, A., (1997). *In-Situ Mechanical Properties of Wall Elements Cast Using Self-Consolidating Concrete,* ACI Materials Journal, **94** (6), pp. 491-500.

Khayat, K.H., Petrov, N., Attiogbe, E., and See, H., (2003). *Uniformity of Bond Strength of Prestressing Strands in Conventional Flowable and Self-Consolidating Concrete Mixtures*, Proc., 3rd International Symposium on Self-Compacting Concrete, August 17-20, Reykjavik, Iceland, pp. 703-712.

Kim, J.K., Han, S.H., Park, Y.D., Noh, J.H., Park, C.L., Kwon, Y.H., and Lee, S.G., (1996). *Experimental Research on the Material Properties of Super Flowing Concrete*, Proc., International RILEM Conference on Production Methods and Workability of Concrete, Paisely, Scotland, June 3-5, London, E&FN Spon, pp. 271-284.

Klug, Y., and Holschemacher, K., (2003). *Comparison of the Hardened Properties of Self-Compacting and Normal Vibrated Concrete*, Proc., 3rd International RILEM Symposium on Self-Compacting Concrete, August 17-20, Reykjavik, Iceland, pp. 596-605.

Koning, G., Holschemacher, K., Dehn, F., and Weiβe, D., (2001). *Self-Compacting Concrete-Time Development of Materials Properties and Bond Behaviour*, Proc., 2nd International Symposium on Self-Compacting Concrete, October 23-25*,* Tokyo, pp. 507-516.

Labonte, T., Hamilton, H.R., Ansley, M.H., and Ishee, C.A., (2004). *Construction and Testing of Type II AASHTO Girders Using Self-Consolidating Concrete*, Proc., 2004 PCI Annual Convention, Atlanta, October 17-20, 16 p.

L'Hermite, R., and Grieu, J.J., (1952). *Recent Experimental Studies on Shrinkage of Cement Pastes and Concretes*, (In French), Annales ITBTP, **5** (52-3), pp. 494-514.

Logan, D., (1997). *Acceptance Criteria for Bond Quality of Strand for Pretensioned Prestressed Concrete Applications*, PCI Journal, March-April, pp. 58-90.

Ma, J., and Dietz, J., (2002). *Ultra High Performance Self Compacting Concrete*, Leipzig Annual Civil Engineering Report No. 7, Universität Leipzig, pp. 33-42.

Manai, K., (1995). *Evaluation of the Effect of Chemical and Mineral Admixtures on the Workability, Stability, and Performance of Self-Compacting Concrete*, Master's Thesis, Université de Sherbrooke, Québec, Canada, 182 p. (in French)

Ministère des Transports du Québec, (2000). *Spécifications de la norme MTQ 3102*, Bulletin d'information technique, **5** (10), 2 p.

Mokhtarzadeh, A., and French, C., (2000). *Mechanical Properties of High-Strength Concrete with Consideration for Precast Applications*, ACI Materials Journal, **97** (2), pp. 136-146.

Moustafa, S., (1974). *Pull-out Strength of Strand and Lifting Loops,* Concrete Technology Associates Technical Bulletin, 74-B5, May.

Nehdi, M., Pardhan, M., and Koshowski, S., (2004). *Durability of Self-Consolidating Concrete Incorporating High-Volume Replacement Composite Cements*, Cement and Concrete Research, **34** (11), pp. 2103-2112.

Neville, A.M., and Meyers, B.L., (1964). *Creep of Concrete: Influencing Factors and Prediction*, Symposium on Creep of Concrete, SP-9 ACI, Detroit, 1964, pp. 1-33.

Neville, A.M., (1981). Properties of Concrete*, 3rd Edition*, Pittman, London, 779 p.

New York DOT, (2002). *Standard Specifications – Construction and Materials*, New York State.

Ojdrovic, R.O., and Zarghamee M., (1996). *Concrete Creep and Shrinkage Prediction from Short-Term Tests*, ACI Materials Journal, **93** (2), pp. 169-177.

Okamura, H., (1997). *Self-Compacting High-Performance Concrete*, Concrete International, **19** (7), pp. 50-54.

Ozyildirim, C., (2004). *VDOT Applications of HPC with Lightweight or SCC*, Proc., 2004 PCI Annual Convention, Atlanta, October 17-20, 8 p.

Persson, B., (1999). *Creep, Shrinkage and Elastic Modulus of Self-Compacting Concrete*, Proc., 1st International RILEM Symposium on Self-Compacting Concrete, Stockholm, Sweden, September 13-14, pp. 239-250.

Persson, B., (2001a). *A Comparison Between Mechanical Properties of Self-Compacting Concrete and the Corresponding Properties of Normal Concrete*, Cement and Concrete Research, **31**, pp. 193-198.

Persson, B., (2001b). *Assessment of the Chloride Migration Coefficient, Internal Frost Resistance, Salt Frost Scaling and Sulphate Resistance of SCC*, Division of Building Materials, Lund University, TVBM-3100, 86 p.

Persson, B., (2003a). *Creep and Shrinkage of High-Performance SCC*, Personal communication, ACI Journal, in press, 17 p.

Persson, B., (2003b). *Internal Frost Resistance and Salt Frost Scaling of SCC*, Cement and Concrete Research, **33**, pp. 373-379.

Petersson, Ö., (2002). *Limestone Powder as Filler in Self-Compacting Concrete – Frost Resistance, Compressive Strength and Chloride Diffusivity*, Proc., 1st North American Conference on the Design and Use of Self-Consolidating Concrete, Chicago, Illinois, Nov. 12-13, pp. 391-396.

Petersson, Ö., Billberg, P., and Osterberg, T., (1998). *Application of SCC for Bridge Casting*, Proc., International Workshop on SCC, Kochi, Japan, pp. 318-327.

Petersson, Ö., Billberg, P., and Van, B.K., (1996). *A Model for Self-Compacting Concrete*, Proc., International RILEM Conference on Production Methods and Workability of Concrete, Ed. By P.J.M. Bartos, et al. (Chapman & Hall), Paisley, Scotland, June 3-5, pp. 483-490.

Petrov, N., Khayat, K.H., and Tagnit-Hamou, A., (2001). *Effect of Stability of Self-Consolidating Concrete on the Distribution of Steel Corrosion Characteristics Along Experimental Wall Elements*, Proc., 2nd International Symposium on Self-Compacting Concrete, Tokyo, Japan, pp. 441-450.

Pons, G., Proust, E., and Assié, S., (2003). *Creep and Shrinkage of Self-Compacting Concrete: A Different Behaviour Compared with Vibrated Concrete?*, Proc., 3rd International RILEM Symposium on Self-Compacting Concrete, August 17-20, Reykjavik, Iceland, pp. 645-654.

Precast/Prestressed Concrete Institute, (1997). *Precast Prestressed Concrete Bridge Design Manual*, 1st Edition.

Precast/Prestressed Concrete Institute, (2003). *Interim Guidelines for the Use of Self-Consolidating Concrete in Precast/Prestressed Concrete Institute Member Plants*, April, 148 p.

Sakata, N., Marruyama, K., and Minami, M., (1996). *Basic Properties and Effects of Welan Gum on Self-Consolidating Concrete*, Proc., International RILEM Conference on Production Methods and Workability of Concrete, Ed. Bartos et al., (Chapman & Hall), Paisley, Scotland, pp. 237-253.

Schiessl, A., and Zilch, K., (2001). *The Effect of the Modified Composition of SCC on Shear and Bond Behaviour*, Proc., 2nd International Symposium on Self-Compacting Concrete, 23-25 October, Tokyo, pp. 501-506.

Shadle, R., and Somerville, S., (2002). *The Benefits of Utilizing Fly Ash in Producing Self-Consolidating Concrete*, Proc., 1st North American Conference on the Design and Use of Self-Consolidating Concrete, Chicago, Illinois, Nov. 12-13, pp. 235-241.

Shi C., Wu, Y., Shao, Y., and Riefler, M., (2002). *Comparison of Two Design Approaches For Self-Consolidating Concrete*, Proc., 1st North American Conference on the Design and Use of Self-Consolidating Concrete, Chicago, Illinois, Nov. 12-13, pp. 349-354.

Sonebi, M., and Bartos, P.J.M., (1999). *Hardened SCC and Its Bond with Reinforcement*, Proc., 1st RILEM International Symposium on Self-Compacting Concrete, Stockholm, Sweden, September 13-14, pp. 275-289.

Sonebi, M., Bartos, P.J.M., Zhu, W., Gibbs, J., and Tamimi, A., (2000). *Task 4 – Properties of Hardened Concrete*, Final report of Brite EuRam Project No. BE96-3801/Contract BRPR-CT96-0366.

Sonebi, M., Rooney, M., and Bartos, P., (2002). *In-Situ Compressive Strength of Self-Compacting Concrete*, Concrete, **36** (3), pp. 48-49.

Sonebi, M., Tamimi, A.K., and Bartos, P.J.M., (2003). *Performance and Cracking Behavior of Reinforced Beams Cast with Self-Consolidating Concrete*, ACI Materials Journal, **100** (6), pp. 492-500.

Song, H.-W., Cho, H.-J., Park, S.-S., Byun, K.-I, and Maekawa, K., (2001a). *Early-Age Cracking*

Resistance Evaluation of Concrete Structures, Concrete Science and Engineering, **3**, pp. 62-72.

Song, H.W., Byun, K.J., Kim, S.H., and Choi, D.H., (2001b). *Early-Age Creep and Shrinkage in Self-Compacting Concrete Incorporating GGBFS*, Proc., 2nd International Symposium on Self-Compacting Concrete, Tokyo, Japan, October 23-25, 413-422.

State-of-the-Art Report of RILEM Technical Committee 174-SCC, (2000). *Self-Compacting Concrete*, Report 23, Ed. A. Skarendahl, O. Petersson, 154 p.

Subcommittee I, ACI 209, (1971). *Effects of Concrete Constituents, Environment, and Stress on the Creep and Shrinkage of Concrete*, Symposium on Creep, Shrinkage, and Temperature Effects, SP-27-1, ACI, Detroit, pp. 1-42.

Swedish Concrete Association, (2002). *Self-Compacting Concrete, Recommendations for Use*, Concrete report No. 10(E), 84 p.

Tang, L., Andalen, A., Johansson, J.O., and Hjelm, S., (1999). *Chloride Diffusivity of SCC*, Proc. 1st International RILEM Symposium on Self-Compacting Concrete, Ed. by Skarendahl, A. and Petersson, O., RILEM Publications s.a.r.l., France, pp. 187-198.

Texas DOT, (2004). *Standard Specifications for Construction and Maintenance of Highway, Streets, and Bridge*, Texas State.

Tragardh, J., (1999). *Microstructural Features and Related Properties of SCC*, Proc., 1st International RILEM Symposium on Self-Compacting Concrete, Sweden, September, RILEM, Paris, pp. 175-186.

Trucry, P., and Loukili, A., (2003). *A Study of Plastic Shrinkage of Self-Compacting Concrete*, Proc., 3rd International RILEM Symposium on Self-Compacting Concrete, August 17-20, Reykjavik, Iceland, pp. 576-585.

Turcry P., Loukili, A., and Haidar, K., (2002). *Mechanical Properties, Plastic Shrinkage and Free Deformations of Self-Consolidating Concrete*, Proc., 1st North American Conference on the Design and Use of Self-Consolidating Concrete, Chicago, Illinois, Nov. 12-13, pp. 335-340.

Turcry, P., and Loukili, A., (2004). *Plastic Shrinkage Cracking of Self-Compacting Concrete*, Personal communication.

Ulm, F.-J., Le Maou, F., and Boulay, C., (1999a). *Creep and Shrinkage Coupling: New Review of Some Evidence*, Creep and Shrinkage of Concrete, Edited by Ulm, F.-J., Prat M., Calgaro, J.-A., Carol, I., Special issue of Revue Française de Génie Civil, HERMES Science Publications, pp. 21-37.

Ulm, F.-J., Prat, M., Calgaro, J.-A., and Carol, I.. (1999b). Creep and Shrinkage of Concrete, Special issue of revue Francaise de genie civil, HERMES Science Publications, Paris, 243 p.

Vieira, M., and Bettencourt, A., (2003). *Deformability of Hardened SCC*, Proc., 3rd International RILEM Symposium on Self-Compacting Concrete, August 17-20, Reykjavik, Iceland, pp. 637-644.

Washington DOT, (2002). *Standard Specifications,* Washington State.

Wittman, F.H., (1976). *On the Action of Capillary Pressure in Fresh Concrete*, Cement and Concrete Research, **6**, pp. 49-56.

Wittman, F.H., (1982). *Creep and Shrinkage Mechanisms*, Creep and Shrinkage in Concrete Structures, Edited by Bazant and Wittman, John Wiley & Sons, Chichester, pp. 129-161.

Yurugi, M., Sakata, N., Iwai, M., and Sakai, G., (1993). *Mix Proportion of Highly Workable Concrete*, Proc., Concrete 2000, Dundee, September 7-9, pp. 579-589.

Zhu, W., Gibbs, J.C., and Bartos, P.J.M., (2001). *Uniformity of In Situ Properties of Self-Compacting Concrete in Full-Scale Structural Elements*, Cement and Concrete Composites, **23**, pp. 57-64.

Zhu, W.Z., and Bartos, P.J.M., (2003). *Permeation Properties of SCC*, Cement and Concrete Research, **33**, pp. 921-926.

Zia, P., Nunez, R.A., Mata, L.A., and Dairi, H.M., (2005). *Implementation of Self-Consolidating Concrete (SCC) for Prestressed Concrete Girder*, Paper to be presented in 7th International Symposium of High-Strength/High Performance Concrete, Washington, D.C., June 2004, 24 p.

APPENDIX

Summary of Specifications for Constituent Materials and Mixture Characteristics of Prestressed Concrete Structures Recommended by Texas, Florida, New York, and Washington State DOTs

Table A.1 – Maximum fineness value (Texas State DOT)

Test Method	Maximum Average Value (m^2/kg)		Maximum Single Sample (m^2/kg)	
	Type I, II, and V	Type III	Type I, II, and V	Type III
Air permeability (ASTM C 204)	400	560	420	580
Turbidimeter (ASTM C 115)	220	310	230	320

Table A.2 – Chemical requirements for blended Portland cements (New York State DOT)

	Portland/fly ash (IP)	Portland/microsilica (SF)	Ternary Blend	Portland /slag (SM)
Loss on Ignition	5.0% max. 1	3.4% max.	3.6% max.	3.0% max. 2
SiO_2	---1	22.0% min.	31.5% min.	---
MgO	6.0% max. 1	6.0% max.	6.0% max.	---
SO_3	4.0% max. 1,3	3.1% max. 3	3.5% max. 3	3.0%
Total Alkalinity	0.85% max. 4	0.80% max. 4	0.95% max. 4	0.75% max. 4

Note 1- As per chemical requirements of AASHTO M 240 for Type IP blended cement.
Note 2- As per chemical requirements of AASHTO M 240 for Type I(SM) blended cement.
Note 3- There are cases where the optimum SO_3 (using ASTM test method C563) for particular cement is close to or in excess of the limit in this specification. In such cases where the properties of cement can be improved by exceeding the SO_3 limits stated in this table, it is permissible to exceed the values in the table, provided it has been demonstrated by ASTM test method C1038 that the cement with the increased SO_3 will not develop expansion under water exceeding 0.020% at 14 days. When the manufacturer supplies cement under this provision, the supporting data will be supplied, on request, to the Materials Bureau.
Note 4- Any blended cement where the Portland cement portion contains alkali content in excess of 0.70% may be either rejected, accepted, or have use limitations imposed as directed by the Materials Bureau.

Table A.3 – Physical requirements for blended Portland cements (New York State DOT)

Passing 45µm (ASTM C430)	70% min.
Time of setting, Vicat test (ASTM C191) (minute)	45 min., 420 max.
Autoclave contraction (ASTM C151)	0.2% max.
Autoclave expansion	0.8% max.
Compressive strength (ASTM C109 "AASHTO T 106" EI03004) 3 days 7 days 28 days	 10 MPa min. 20 MPa min. 25 MPa min.

Table A.4 – Gradation requirements for coarse aggregate (Texas State DOT)

Aggregate grade No.[1)]	Nominal size	Percent passing on each sieve								
		2-1/2"	2"	1-1/2"	1"	3/4"	1/2"	3/8"	No. 4	No. 8
1	2"	100	80 - 100	50 - 85		20-40			0-5	
2 (467)	1-1/2"		100	95-100		35-70		10-30	0-5	
3	1-1/2"		100	95-100		60-90	25-60		0-5	
4 (57)	1"			100	95-100		25-60		0-10	0-5
5 (67)	3/4"				100	90-100		20-55	0-10	0-5
6 (7)	1/2"					100	90-100	40-70	0-15	0-5
7	3/8"						100	70-95	0-25	
8	3/8"						100	95-100	20-65	0-10

1) Corresponding ASTM C 33 gradation shown in parentheses

Table A.5 – Fine aggregate gradation (Grade 1) (Texas State DOT)

Sieve Size	3/8 in.	No. 4	No. 8	No. 16	No. 30	No. 50	No. 100	No. 200
Percent Passing	100	95-100	80-100	50-85	25-65	10-35[1)]	0-10	0-3[2)]

1) 6-35 when sand equivalent value is greater than 85.
2) 0-6 for manufactured sand.

Table A.6 – Standard sizes of coarse aggregate (Florida State DOT)

Amounts Finer than Each Laboratory Sieve (Square Openings), weight %								
Size No.	Nominal Size Square Openings	4 in. (100 mm)	3 1/2 in. (90 mm)	3 in. (75 mm)	2 1/2 in. (63 mm)	2 in. (50 mm)	1 1/2 in. (37.5 mm)	1 in. (25 mm)
1	3 1/2 - 1 1/2 in. (90 - 37.5 mm)	100	90 - 100	-	25 - 60	-	0 - 15	-
2	2 1/2 - 1 1/2 in. (63 - 37.5 mm)	-	-	100	90 - 100	35 - 70	0 - 15	-
Size No.	Nominal Size Square Openings	4 in. (100 mm)	3 1/2 in. (90 mm)	3 in. (75 mm)	2 1/2 in. (63 mm)	2 in. (50 mm)	1 1/2 in. (37.5 mm)	1 in. (25 mm)
24	2 1/2 - 3/4 in. (63 - 19 mm)	-	-	100	90 - 100	-	25 - 60	-
3	2 - 1 in. (50 - 25 mm)	-	-	-	100	90 - 100	35 - 70	0 - 15
357	2 in. - No. 4 (50 - 4.75 mm)	-	-	-	100	95 - 100	-	35 - 70
4	1 1/2 - 3/4 in. (37.5 - 19 mm)	-	-	-	-	100	90 - 100	20 - 55
467	1 1/2 in. - No. 4 (37.5 - 4.75 mm)	-	-	-	-	100	95 - 100	-
5	1 - 1/2 in. (25 - 12.5 mm)	-	-	-	-	-	100	90 - 100
56	1 - 3/8 in. (25 12.5 mm)	-	-	-	-	-	100	90 - 100
57	1 in. - No. 4 (25 - 4.75 mm)	-	-	-	-	-	100	95 - 100
6	3/4 - in. (19 - 9.5 mm)	-	-	-	-	-	-	100
67	3/4 - 3/8 in. (19 - 9.5 mm)	-	-	-	-	-	-	100
68	3/4 in. - No. 8 (19 - 2.36 mm)	-	-	-	-	-	-	-
7	1/2 in. - No. 4 (12.5 - 4.75 mm)	-	-	-	-	-	-	-
78	1/2 in. - No. 8 (12.5 - 2.36 mm)	-	-	-	-	-	-	-
8	3/8 in. - No. 16 (9.5 - 1.18 mm)	-	-	-	-	-	-	-
89	3/8 in. - No. 16 (9.5 - 1.18 mm)	-	-	-	-	-	-	-
9	No. 4 - No. 16 (4.75 - 1.18 mm)	-	-	-	-	-	-	-
10	No. 4 - 0 (4.75 mm)	-	-	-	-	-	-	-

Table A.7 – Standard sizes of coarse aggregate (Florida State DOT)

Size No.	Nominal Size Square Openings	3/4 in. (19 mm)	1/2 in. (12.5 mm)	3/8 in. (9.5 mm)	No. 4 (4.75 mm)	No. 8 (2.36 mm)	No. 16 (1.18 mm)	No.50 (0.30 mm)
1	3 1/2 - 1 ½ in. (90 - 37.5 mm)	0 - 5	-	-	-	-	-	-
2	2 1/2 - 1 ½ in. (63 - 37.5 mm)	0 - 5	-	-	-	-	-	-
24	2 1/2 - ¾ in. (63 - 19 mm)	0 - 10	0 - 5	-	-	-	-	-
3	2 - 1 in. (50 - 25 mm)	-	0 - 5	-	-	-	-	-
357	2 in. - No. 4 (50 - 4.75 mm)	-	10 - 30	-	0 - 5	-	-	-
4	1 1/2 - ¾ in. (37.5 - 19 mm)	0 - 15	-	0 - 5	-	-	-	-
467	1 1/2 in. - No.4 (37.5 - 4.75 mm)	35 - 70	-	10 - 30	0 - 5	-	-	-
5	1 - 1/2 in. (25 - 12.5 mm)	20 - 55	0 - 10	0 - 5	-	-	-	-
56	1 - 3/8 in. (25 - 9.5 mm)	40 - 85	10 - 40	0 - 15	0 - 5	-	-	
57	1 in. - No. 4 (25 - 4.75 mm)	-	25 - 60	-	0 - 10	0 - 5	-	-
6	3/4 - 3/8 in. (19 - 9.5 mm)	90 - 100	20 - 55	0 - 15	0 - 5	-	-	-
67	3/4 in. - No. 4 (19 - 4.75 mm)	90 - 100	-	20 - 55	0 - 10	0 - 5	-	-
68	3/4 in. - No. 8 (19 - 2.36 mm)	90 - 100	-	30 - 65	5 - 25	0 - 10	0 - 5	-
7	1/2 in. - No. 4 (12.5 - 4.75 mm)	100	90 - 100	40 - 70	0 - 15	0 - 5	-	-
78	1/2 in. - No. 8 (12.5 - 2.36 mm)	100	90 - 100	40 - 75	5 - 25	0 - 10	0 - 5	-
8	3/8 in. - No. 8 (9.5 - 4.75 mm)	-	100	85 - 100	10 - 30	0 - 10	0 - 5	-
89	3/8 in. - No. 16 (9.5 - 1.18 mm)	-	100	90 - 100	20 - 55	5 - 30	0 - 10	0 - 5
9	No. 4 - No. 16 (4.75 - 1.18 mm)	-	-	100	85 - 100	10 - 40	0 - 10	0 - 5
10	No. 4 - 0 (4.75 mm)	-	-	100	85 - 100	-	-	-

NOTE: The gradations in Table A.7 represent the extreme limits for the various sizes indicated, which will be used in determining the suitability for use of coarse aggregate from all sources of supply. For any grade from any one source, the gradation shall be held reasonably uniform and not subject to the extreme percentages of gradation specified above.

Table A.8 – Silica sand gradation (Florida State DOT)

Sieve Opening Size	Percent Retained	Percent Passing
No. 4 (4.75 mm)	0 - 5	95 - 100
No. 8 (2.36 mm)	0 - 15	85 - 100
No. 16 (1.18 mm)	3 - 35	65 - 97
No. 30 (600 µm)	30 - 75	25 - 70
No. 50 (300 µm)	65 - 95	5 - 35
No. 100 (150 µm)	93 - 100	0 - 7
No. 200 (75 µm)	Min. 96	Max. 4

Table A.9 – Physical requirements (Testing) (1) (New York State DOT)

Material Designation	Crushed Stone	Crushed Gravel	Screened Gravel	Crushed Slag
Magnesium Sulfate Test (703-07 P,G)(2) Max. percent loss by weight at 10 cycles	18	18	18	6
Freezing and Thawing Test (703-08 P,G)(3) Max. percent loss by weight at 25 cycles	20	20	20	_
Los Angeles Abrasion Test (703-11 P,G) Max. percent loss by weight (Grading A or B)	35(4) 45(5)	35	35	40
Flat and Elongated to the Degree of 5:1	10(6)	10(6)	-	-
Larger than 12.5 mm (1 fractured face)	-	75(7)	-	-
Smaller than 12.5 mm (2 fractured faces)	-	85(7)	-	-
Minimum unit weight (703-10 P,G) kg/m^3	-	-	-	7-

(1) To determine its conformance to specification limits, processed coarse aggregate may be tested at any point after completion of processing. The manufactured material shall be separated into the primary sizes indicated in Table 703-5, "Primary Size." Each size fraction shall conform to the requirements of §703-02 Coarse Aggregate.

(2) Loss applies to No. 2 size fraction.

(3) The freeze-thaw requirement applies only to aggregate used in Portland cement concrete. The loss applies to the No. 2 size fraction.

(4) Loss applies to all materials excepting marble, granite, and other similar materials. (5) Loss applies to marble, granite, and other similar materials.

(6) Requirement applies to coarse aggregate for use in hot mix asphalt with design ESALs of 0.3 million or greater.

(7) Gravel which has not been processed through a crusher shall not be combined with crushed gravel. EI03042.

Table A.10 – Size of stone, gravel and slag (New York State DOT)

Size Designation	Screen Sizes										
	100	75	63	50	37.5	25	12.5	6.3	3.2	180	75
Screenings (2)	-	-	-	-	-	-	100	90-100	-	-	0-1.0
1B	-	-	-	-	-	-	-	100	90-100	0-15	0-1.0
1A	-	-	-	-	-	-	100	90-100	0-15	-	0-1.0
1ST	-	-	-	-	-	-	100	0-15	-	-	0-1.0
1	-	-	-	-	-	100	90-100	0-15	-	-	0-1.0
2	-	-	-	-	100	90-100	0-15	-	-	-	0-1.0
3A	-	-	-	100	90-100	0-15	-	-	-	-	0-0.7
3	-	-	100	90-100	35-70	0-15	-	-	-	-	0-0.7
4A	-	100	90-100	-	0-20	-	-	-	-	-	0-0.7
4	100	90-100	-	0.15	-	-	-	-	-	-	0-0.7
5	90-100	0-15	-	-	-	-	-	-	-	-	0-0.7

(1) Percentage by weight passing the following square openings.
(2) Screenings shall include all of the fine material passing a 6.3 mm screen.
(3) The minus 75 μm material requirements apply only to aggregate for use in Portland cement concrete, surface treatment, cold mix bituminous pavements and underdrain filter material. The test (NYSDOT 201) will be performed on the entire sample of the designated size aggregate. Primary size does not apply in the determination of the minus 75 μm material.

Table A.11 – Fine aggregate requirements (Testing) (New York State DOT)

Test Method	Portland Cement Concrete	Bituminous Concrete
Magnesium Sulfates (NYSDOT 207) Max. percent loss by weight at 5 cycles	30	45
Organic Impurities (NYSDOT 202, AASHTO T-21) Organic Plate, Lighter Than	3	-
Gardner Color, Lighter Than	11	-

Table A.12 – Requirement for coarse aggregate grading (Washington State DOT)

Passing	AASHTO Grading No. 467		AASHTO Grading No. 57		AASHTO Grading No. 67		AASHTO Grading No. 7		AASHTO Grading No. 8	
Sieve Size	Min.	Max.	Min.	Max.	Min.	Max.	Min.	Max.	Min.	Max.
2″ square	100	—	—	—	—	—	—	—	—	—
11/2″square	95	100	100	—	—	—	—	—	—	—
1″ square	—	—	95	100	100	—	—	—	—	—
3/4″ square	35	70	—	—	90	100	100	—	—	—
1/2″ square	—	—	25	60	—	—	90	100	100	—
3/8″ square	10	30	—	—	20	55	40	70	85	100
U.S. No. 4	0	5	0	10	0	10	0	15	10	30
U.S. No. 8	—	—	0	5	0	5	0	5	0	10
U.S. No. 16	—	—	—	—	—	—	—	—	0	5

Table A.13 – Fine aggregate gradation (Washington State DOT)

	Class 1		Class 2[1)]	
	Percent passing		Percent passing	
Sieve Size	Min.	Max.	Min.	Max.
3/8″ square	100		100	
U.S. No. 4	95	100	95	100
U.S. No. 8	68	86	-	-
U.S. No. 16	47	65	45	80
U.S. No. 30	27	42	-	-
U.S. No. 50	9	20	10	30
U.S. No. 100	0	7	2	10
U.S. No. 200	0	2.5	0	2.5

1) Within the gradation limits for Class 2, uniformity of gradation is limited to a range of plus or minus 0.20 of the reference fineness modulus.

Table A.14 – Supplementary specification requirements (Texas State DOT)

Item	Limit
Calcium oxide (CaO) variation in percentage points of CaO from the average of the last 10 samples (or less, provided 10 have not been tested) must not exceed ±	4.0
Moisture content, max., %	2.0
Loss on ignition, max., %	3.0
Increase of drying shrinkage of mortar bars at 28 days, max., %	0.03

Table A.15 – Additional ultra-fine specification requirements (Texas State DOT)

Item	Limit
Pozzolanic activity index 7-day, min., % of control 28-day, min., % of control	 85 95
Particle size distribution, as measured by laser particle size analyzer particles less than 3.25 microns, min., % particles less than 8.50 microns, min., %	 50 90
Fineness, amount retained when wet-sieved on 45- mm sieve, max., %	6.0
Moisture content, max., %	1.0
Loss on ignition, max., %	2.0

Table A.16 – Requirements for chemical admixtures (New York State DOT)

Requirement	Admixture			
	Air-entraining	Water-Reducing and Retarding Admixtures (ASTM TYPE D)	Water-Reducing Admixtures (ASTM TYPE A)	Water-Reducing (High Range) Admixtures (ASTM TYPE F)
Time of setting	Not deviate from that of concrete made with the reference admixture by more than ±1 hour and 15 minutes.	Be increased by at least 50% when compared to that of the reference concrete without the admixture.	Not deviate from that of similar concrete without the admixture used as a reference by more than ±1 hour and 15 minutes.	Not be more than 1 hour earlier nor 1 hour, 30 minutes later.
Compressive strength	Not less than 90% of the control concrete, at the same air content, containing the reference admixture at 48 hours, 7 days and 28 days.	When compared to concrete without the admixture under test, shall be equal or greater at 48 hours, 7 days and 28 days.	When compared to concrete without the admixture under test, shall be equal or greater at 48 hours, 7 days and 28 days.	Minimum percent of control: 140%, 125%, 115%, and 110% at 1, 3, 7, and 28 days, respectively. At any test age, not less than 100% of that attained at any previous age.
Resistance to freezing and thawing	Not exceed a weight loss of 4.0% in 25 cycles in a 10% NaCl solution.	Not exceed a weight loss of 4.0% in 25 cycles in a 10% NaC1 solution.	Not exceed a weight loss of 4.0% in 25 cycles in a 10% NaC1 solution.	Not exceed a weight loss of 4.0% in 25 cycles in a 10% NaC1 solution.
Length change	Not be greater than ± 20%	Not be greater than ± 35%	Not be greater than ± 35%	Not be greater than ± 35%
Water reduction		Mixing water shall be reduced at least 5% when compared to that of reference mix without the admixture.	Same as ASTM TYPE D	Mixing water shall be reduced at least 12% when compared to that of reference concrete without the admixture.
Bleeding	Not exceed that of concrete made with the reference admixture by more than 2%.			

Table A.17 – Concrete classes (Texas State DOT)

Class of Concrete	28-day minimum design strength, psi	Max. *W/C* (1)	Coarse Aggregate Grades (2,3)	General Usage (4)
A	3,000	0.60	1-4, 8	Inlets, manholes, curb, gutter, curb & gutter, conc. retards, sidewalks, driveways, backup walls, anchors
B	2,000	0.60	2-7	Riprap, small roadside signs, and anchors
C(5)	3,600	0.45	1-6	Drilled shafts, bridge substructure, bridge railing, culverts except top slab of direct traffic culverts, headwalls, wing walls, approach slabs, concrete traffic barrier (cast-in-place)
D	1,500	0.60	2-7	Riprap
E	3,000	0.50	2-5	Seal concrete
F(5)	Note (6)	0.45	2-5	Railroad structures; occasionally for bridge piers, columns, or bents
H(5)	**Note (6)**	**0.45**	**3-6**	**Prestressed concrete beams, boxes, piling, and concrete traffic barrier (precast)**
S(5)	4,000	0.45	2-5	Bridge slabs, top slabs of direct traffic culverts
P	See Item 360	0.45	2-3	Concrete pavement
DC(5)	5,500	0.40	6	Dense conc. overlay
CO(5)	4,600	0.40	6	Concrete overlay
LMC(5)	4,000	0.40	6-8	Latex-modified concrete overlay
SS(5)	Note (7)	0.45	4-6	Slurry displacement shafts, underwater drilled shafts
K(5)	Note (6)	0.45	Note (6)	Note (6)
HES	Note (6)	0.45	Note (6)	Note (6)

(1) Maximum *w/c* or *w/cm* by weight.
(2) Unless otherwise permitted, do not use Grade 1 coarse aggregate except in massive foundations with 4-in. minimum clear spacing between reinforcing steel bars. Do not use Grade 1 aggregate in drilled shafts.
(3) Unless otherwise approved, use Grade 8 aggregate in extruded curbs.
(4) For information only.
(5) Structural concrete classes.
(6) As shown on the plans or specified.
(7) Cementitious material content shall be minimum 658 lb/yd^3 of concrete.

Table A.18 – Concrete classes (Florida State DOT)

Class of Concrete	28-day specified minimum strength, psi (MPa)	Target slump, in. (mm) (c)	Air content range (%)
I (Pavement)	3,000 (21)	2 (50)	1 - 6
I (Special) (a)	3,000 (21)	3 (75) (b)	1 - 6
II (a)	3,400 (23)	3 (75) (b)	1 - 6
II (Bridge Deck)	4,500 (31)	3 (75) (b)	1 - 6
III	5,000 (35)	3 (75) (b)	1 - 6
III (Seal)	3,000 (21)	8 (200)	1 - 6
IV	5,500 (38)	3 (75) (b)	1 - 6
IV (Drilled Shaft)	4,000 (28)	8 (200)	0 - 6
V (Special)	6,000 (41)	3 (75) (b) (d)	1 - 5
V	6,500 (45)	3 (75) (b)	1 - 5
VI	8,500 (59)	3 (75) (b)	1 - 5

(a) For precast drainage products that are manufactured at the precast plant the Contractor is permitted to use concrete meeting the requirements of ASTM C 478 (ASTM C 478M) 4,000 psi (30 MPa) in lieu of Class I or Class II concrete. Apply the chloride content limits specified in 346-4.2 to all box culverts.

(b) The Engineer may allow higher target slump, not to exceed 7 in. (180 mm), when a Type F or Type G admixtures is used.

(c) The Engineer may approve a reduction in the target slump for slip-form operations.

(d) When the use of silica fume or metakaolin is required as a pozzolan in Class V (Special) concrete, ensure that the concrete does not exceed a permeability of 1,000 coulombs at 28-days when tested per AASHTO T 277. Submit 2, 4 × 8 in. (100 × 200 mm) cylindrical test specimens to the Engineer for permeability testing before mix design approval. Submit the test specimens within 7 days prior to the 28-day test. The permeability of the concrete will be taken as the average of two tests, one test per cylinder.

Table A.19 – Concrete classes (New York State DOT)

Con-crete Class	Design Mix Guidelines (where sand fineness modulus = 2.80)[1]						Primary Use
	T.C.M.[5] Content (kg/m^3)	Sand % Total Agg. (solid volume)	Water/ Cementitious Materials (by mass)	Air Content % desired (Range)	Slump Range (mm)	Type of Coarse Aggregate Gradation	
A	360	56.2	0.46	6.5 (5.0-8.0)	65-90	CA 2	General purpose structural
C[6]	359	35.8	0.44	6.5 (5.0-8.0)	25-75	CA 2	Pavement: slipform paving, form paving
D	430	45.8	0.44	7.5 (6.0 - 9.0)	65-90	CA 1	Thin structural applications
DP[2]	430	45.8	0.40	7.5 (6.0-9.0)	75-125	CA 1	Thin structural applications,overlays
E	384	35.8	0.44	6.5 (5.0-8.0)	75-100	CA 2	Structural slabs and structural approach slabs
F	425	34.6	0.38	6.5 (5.0-8.0)	50-75	CA 2	High early strength for pavement or structural applications
G[3]	431	45.0	0.45	6.0 (4.0-8.0)	150-180	CA 2	Underwater
GG[3]	475	45.0	0.45	6.0 (4.0-8.0)	150-180	CA 1	Underwater (special)
H	400	40.0	0.44	6.5 (5.0-8.0)	75-100	CA 2	Pumping applications
HP[2]	405	40.0	0.40	6.5 (5.0-8.0)	75-125	CA 2	Pumping, structural slabs, approach slabs, substructures exposed to chlorides
I[4]	380	41.0	0.44	6.0 (4.0-8.0)	15-40	CA 2	Slipforming highway median barriers
J[4]	430	45.8	0.44	6.0 (4.0-8.0)	15-40	CA 1	Slipforming structural median barriers, parapet walls and curbs

1. Mixture proportions will be computed by the Regional Materials Engineer using the fineness modulus and bulk specific gravities (saturated surface dry) of the aggregates proposed for use.
2. Class DP and HP require the replacement of Portland cement with 20% pozzolan and 6% microsilica and the addition of a water reducing admixture and / or water- reducing and retarding admixture. Refer to §501-3.01 B, Admixtures.
3. Class G and GG require the replacement of Portland cement with 20% pozzolan, and the addition of a water-reducing and retarding admixture. Refer to §501-3.01 B, Admixtures.
4. These mixes require the use of a water reducing admixture. Refer to §501-3.01 B, Admixtures.
5. T.C.M. = Total Cementitious Material.
6. Slump range for slipform paving is 25 – 65 mm and for fixed form paving is 40 – 75 mm. EI04021.

APPENDIX B

Test Methods to Assess Workability of SCC

B.1 Slump flow and T-50 flow test

ASTM C 1611/C 1611M-05 (Standard Test Method for Slump Flow of Self-Consolidating Concrete (http://www.astm.com).

B.2 J-Ring test

ASTM C1621/C1621M-06 Standard Test Method for Passing Ability of Self-Consolidating Concrete by J-Ring (http://www.astm.com).

B.3 L-Box test

B.3.1 Introduction

The L-box test is used to assess the passing ability of SCC to flow through tight openings including spaces between reinforcing bars and other obstructions without segregation or blocking. The equipment consists of a rectangular-section box in the shape of an "L", with a vertical and horizontal section, separated by a moveable gate, in front of which three vertical lengths of reinforcement bar are fitted, as presented in Fig. B.3. The vertical section is filled with SCC, then the gate lifted to let the concrete flow into the horizontal section. When the flow has stopped, the height of the SCC at the end of the horizontal section is expressed as a proportion of that remaining in the vertical section. This is an indication of the passing ability of SCC.

B.3.2 Normative reference

No references are available for this testing

B.3.3 Precision statement

Table B.1 – Precision of L-box test

Slump flow level	Precision of measurement	Single-operator relative error	Multi-operator relative error
24.8 ± 0.4 in. (630 ± 10 mm)	± 0.1	12.1%	10.5%
27.6 ± 0.4 in. (700 ± 10 mm)	± 0.1	12.6%	16.0%

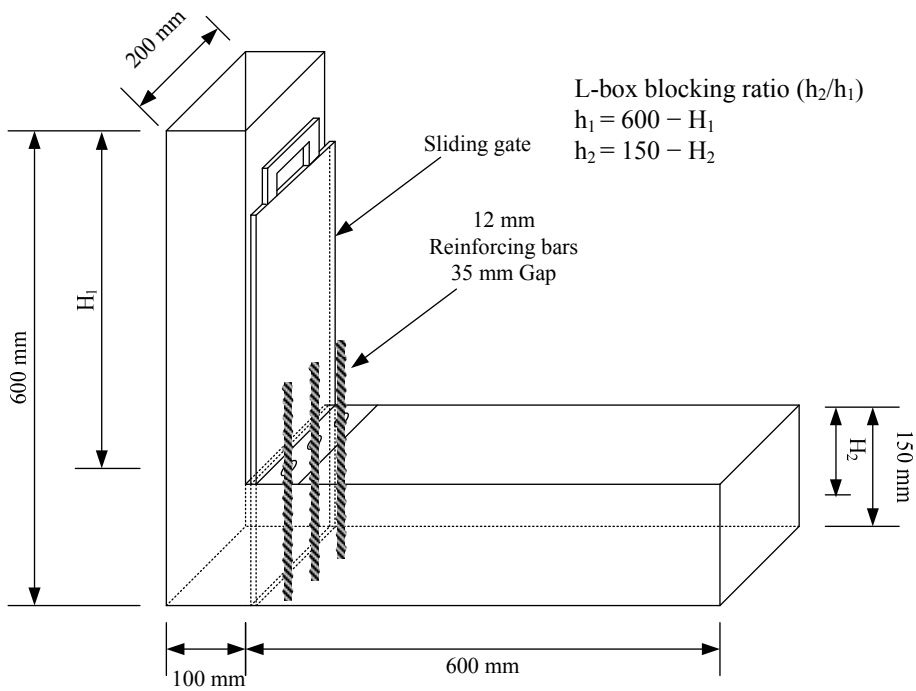

Fig. B.1 – Schematic of L-box apparatus (100 mm = 3.94 in.)

B.3.4 Equipment

I. L-box of a stiff non-absorbing material
II. Trowel
III. Scoop
IV. Ruler
V. Measuring tape
VI. Stopwatch

B.3.5 Procedure

I. About 0.5 ft³ (14 L) of SCC is needed to perform the test, sample normally.
II. Moisten the apparatus and remove any surplus water.
III. Place L-box apparatus on level stable ground.
IV. Fill the vertical section of the apparatus without any agitation or rodding.
V. Leave it to stand during one minute.
VI. Lift the sliding gate and allow the SCC to flow out into horizontal section.
VII. Simultaneously to VI, start the stopwatch and record the time taken for the SCC to reach the end of the horizontal section.
VIII. When the SCC stops flowing, the dimensions "H_1" and "H_2" are measured.
IX. The blocking ratio (h_2/h_1) is calculated.

B.4 Caisson filling capacity test

B.4.1 Introduction

The Caisson filling capacity test is used to assess the filling capacity ability of the SCC. The equipment consists of a container with a flat and smooth surface. In the container are 35 obstacles made of copper with a diameter of 5/8 in. (16 mm) and a distance center to center of 2 in. (50 mm), as shown in Fig B.4. The concrete is introduced from a tremie pipe equipped with a hopper at a constant rate of approximately 0.70 ft^3/min (20 L/min) until the concrete rises in the caisson to a height of 8.9 in. (220 mm). The area occupied by the concrete in the restricted section is used to calculate the filing capacity.

B.4.2 Normative reference

No references are available for this testing

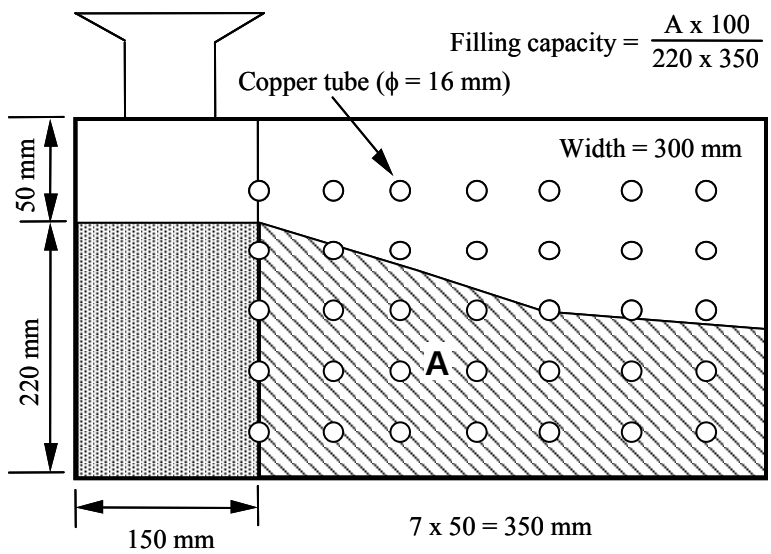

Fig. B.2 – Caisson filling capacity test (100 mm = 3.94 in.)

B.4.3 Precision statement of the test

Table B.2 – Precision of Caisson filling capacity test

Slump flow level	Precision of measurement	Single-operator relative error	Multi-operator relative error
24.8 ± 0.4 in. (630 ± 10 mm)	± 0.8%	2.6%	1.8%
27.6 ± 0.4 in. (700 ± 10 mm)	± 1.1 %	1.1%	2.5%

B.4.4 Equipment

I. Fill box of a stiff, transparent, non-absorbing material
II. 5-gallon (19 L) bucket
III. Scoop
IV. Ruler
V. Measuring tape
VI. Stopwatch

B.4.5 Procedure

I. About 1.5 ft^3 (45 L) of SCC is needed to perform the test, sampled normally.
II. Moisten the apparatus and remove any surplus water.
III. Place the apparatus on level stable ground.
IV. Fill the apparatus without any agitation or rodding.
V. Pour the concrete through the tremie pipe at a constant rate of 0.7 ft^3/min (20 L/min).
VI. Stop pouring when the concrete reaches a level of 8.9 in. (220 mm) from the bottom part of the box.
VII. Measure the surface occupied by the SCC.
VIII. Calculate the filling capacity.

B.5 Surface settlement test

B.5.1 Introduction

The Surface settlement test is used to assess the static stability of SCC after casting until the time of hardening. A rigid PVC column measuring 8 in. (200 mm) in diameter and 28 in. (700 mm) in height can be used. The column is filled with 24 in. (610 mm) of concrete, as shown in Fig B.5. The settlement is monitored using a dial gage with a 0.0004 in. (0.01 mm) precision or a Linear voltage differential transducer (LVDT) with a minimum travel range of 2 in. (50 mm). The gage or LVDT is fixed on top of a thin acrylic plate placed at the upper surface of the concrete; the plate has four holes to enable the evacuation of surface bleed water. The initial reading of the LVDT is taken after 60 sec from the installation of the monitoring set-up. Settlement values are monitored at 5-minute intervals. Changes in height are monitored until the beginning of hardening.

B.5.2 Normative reference

No references are available for this testing.

B.5.3 Equipment

I. 8 in. (200 mm) in diameter and 28 in. (700 mm) height PVC column
II. Linear voltage differential transducer (LVDT) with a minimum travel range of 2 in. (50 mm)

III. Thin acrylic plate
IV. Data acquisition system
V. 5-gallon (19 L) bucket

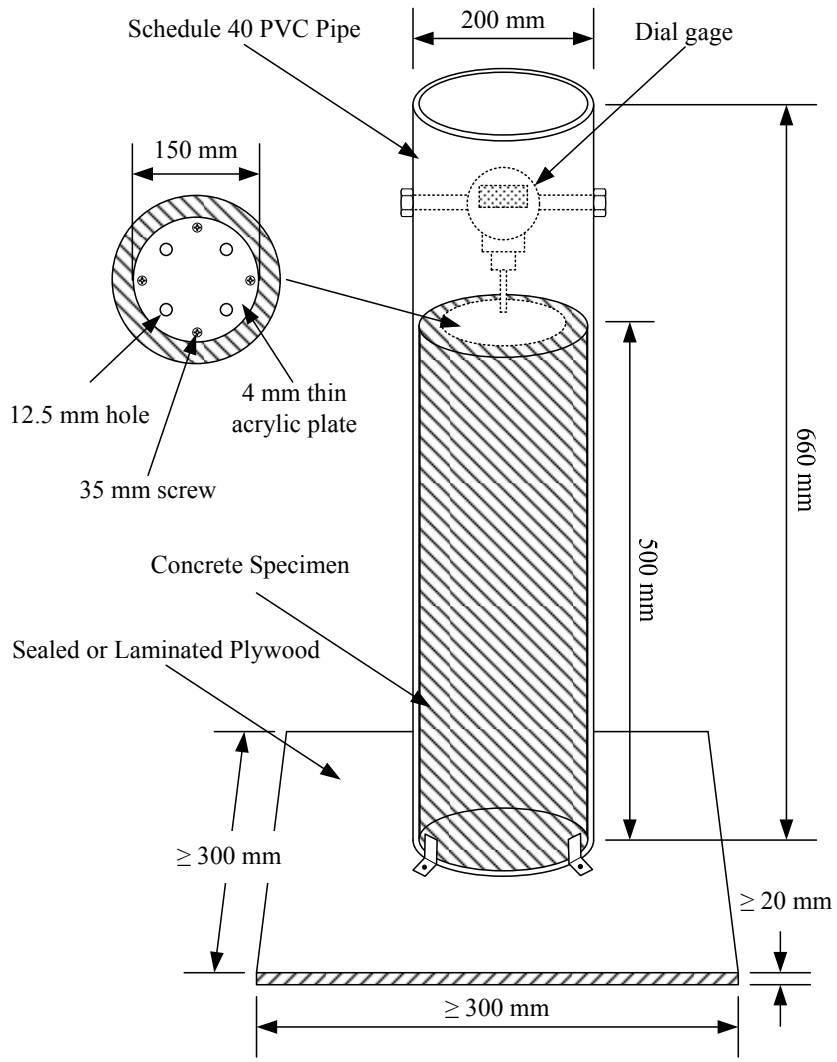

Fig. B.3 – Surface settlement test (100 mm = 3.94 in.)

B.5.4 Procedure

I. About 0.8 ft³ (21 L) of concrete is needed to perform the test, sampled normally
II. Oil the apparatus and remove any surplus
III. Place the apparatus on level stable ground
IV. Fill the apparatus without any agitation or rodding
V. Stop pouring when the concrete reaches a level of 24 in. (610 mm) from the bottom part of the cylinder
VI. Place the thin acrylic plate on the top ton the SCC
VII. Install the LVDT at mid-range on the top of the column

VIII. Start the data acquisition system
IX. Stop the test when the concrete is hardened
X. Collect data from acquisition system
XI. Surface settlement can be expressed as the maximum settlement divided by the height of the concrete column, in percent. The rate of settlement between 15 and 10 minutes as well as between 25 and 30 minutes can also be determined to determine the rate of surface settlement.

B.6 Column segregation test

B.6.1 Introduction

The column segregation test[D8] is used to assess static stability of SCC and its ability to ensure proper suspension of aggregate. The segregation test consists of casting concrete in a column measuring 26 in. (660 mm) in height and 8 in. (200 mm) in diameter, and then determining the variation in the relative concentration of coarse aggregate at four sections along the concrete sample, as presented in Fig. B.6.

The PVC tube is divided into four sections of 6.5 in. (165 mm) in height. A leak-free joint is provided between the sections so that they can be easily uncoupled. Before conducting the test, the concrete is consolidated vertically five times using a ¾ in. (20 mm) diameter rod. The concrete is left to rest for 15 minutes. After removing each section, starting from the top, the concrete is weighed, and the mortar is washed out on a No. 4 (4.75 mm) sieve to retain the coarse aggregate. Surface water is removed to attain surface-saturated dry moisture condition. The mass of the coarse aggregate is then determined for each of the sections. The coefficient of variation (C.O.V.) of the aggregate distribution along the column is taken as a segregation index (I_{seg}) and is expressed as follows:

$$I_{seg}\,(\%) = \frac{std.dev.\sum_{n=4}^{4}\left(\frac{Ma}{Mt}\right)_i}{mean\sum_{n=4}^{4}\left(\frac{Ma}{Mt}\right)_i} \times 100$$

where, *Ma* and *Mt* refer to the mass of aggregate and the total mass of concrete in each section, respectively.

This method is simplified and adopted by ASTM C 1610 where only the aggregate mass at the top and bottom sections of the column are determined. The percent static segregation (S) is expressed as follows:

[D8] Assaad, J., Khayat, K.H., and Daczko, J., "Evaluation of Static Stability of Self-Consolidating Concrete." *ACI Materials Journal*, Vol. 101, No. 3 (2004) pp. 207-215.

$$S(\%) = 2 \times \left(\frac{CA_B - CA_T}{CA_B + CA_T} \right) \times 100, if\ CA_B \rangle CA_T$$

$$S(\%) = 0, \quad if \quad CA_B \leq CA_T$$

where, CA_T and CA_B refer to the mass of coarse aggregate at the top and bottom of the column.

B.6.2 Normative reference

ASTM C 1610/C 1610M-06a Standard Test Method for Static Segregation of Self-Consolidating Concrete Using Column Technique (http://www.astm.com).

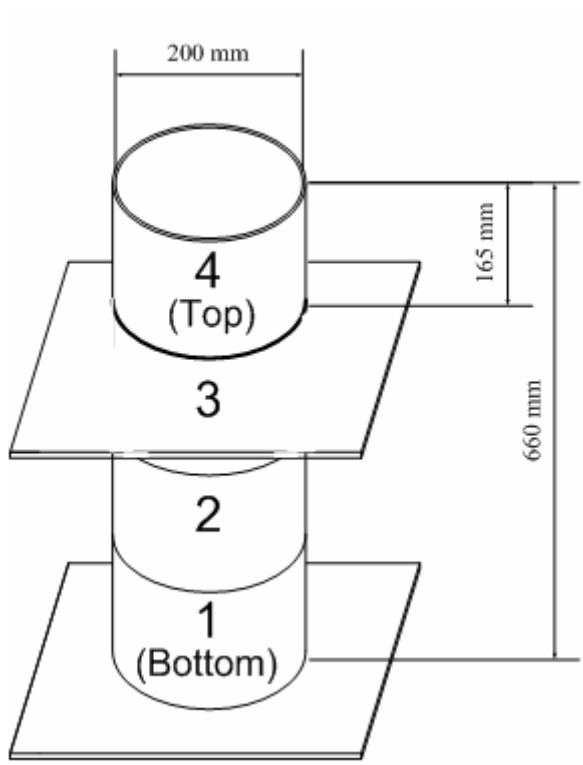

Fig. B.4 – Schematic of column segregation test apparatus (100 mm = 3.94 in.)

B.6.3 Equipment

I. Balance
II. Base plate of a stiff non-absorbing material used to easily move the column
III. Collector plate o a stiff non-absorbing material used to obtain the concrete measuring at least 20 in. (550 mm) × 20 in. (550 mm) square.
IV. Column mold with couplers, brackets, clamps or other equivalent fastening system
V. Trowel
VI. Scoop

VII. A steel rod with diameter 0.79 in. (20 mm)
VIII. Sample receptacle
IX. No. 4 (4.75 mm) sieve with minimum dimension of 13 in. (330 mm) × 25 in. (630 mm)

B.6.4 Procedure

I. About 0.8 ft³ (21 L) of SCC is needed to perform the test, sampled normally.
II. Moisten the four PVC tubes and base plate.
III. Place the base plate on level and stable ground and the four PVC tubes vertically on the base plate
IV. Fill the apparatus with a constant speed without any agitation.
V. Consolidate the concrete vertically five times using steel rod.
VI. Allow to rest for 15 ± 1 minutes.
VII. Collect the concrete from each section by carefully removing the tubes starting from the top section.
VIII. Weigh the concrete in each column section.
IX. Wash the concrete on the No. 4 (4.75 mm) sieve to get coarse aggregate only.
X. Remove with towel excess water from coarse aggregate surface.
XI. Measure the weigh of coarse aggregate for each section.
XII. Calculate the coefficient of variation and the Percent of Static Segregation.

B.7 Visual stability test

B.7.1 Introduction

In order to differentiate the textural properties of SCC, the appearance of the concrete can be qualitatively ranked according to a set of criteria given in Table B.5. The Visual Stability Index (VSI) procedure assigns a numerical rating of 0 to 3, in 0.5 increments, to the texture and homogeneity of the fresh mixture [Daczko and Kurtz, 2001]. The VSI can be considered as a static stability index when it is observed in a wheelbarrow or mixer following some period of rest time (static condition). This can also be the case during the transport of fresh concrete in a tuckerbilt mixer where some segregation can be induced by the vibration during transport.

Table B.5 – Visual stability index (VSI) rating [Daczko and Kurtz, 2001]

Rating	Criteria
0	No evidence of segregation in slump flow patty, in the mixer drum, or in the sampling wheelbarrow
0.5	No mortar halo or aggregate pile in the slump flow patty, but very slight evidence of bleed or air popping on the surface of the SCC in the mixer drum or sampling wheelbarrow
1	No mortar halo in the slump flow patty, but some slight bleeding on the surface of the concrete in the mixer drum and/or wheelbarrow
1.5	Just noticeable mortar halo and/or a just noticeable aggregate pile in the slump flow patty and noticeable bleeding in the mixer drum and sampling wheelbarrow
2	Slight mortar halo, < 0.4 in. (10 mm), in slump flow patty and noticeable layer of mortar on the surface of the testing concrete in the mixer drum and wheelbarrow
3	Clearly segregating by evidence of large mortar halo, > 0.4 in. (10 mm), and thick layer of mortar and/or bleed water on concrete surface in mixer or wheelbarrow

B.8 Concrete rheometer

B.8.1 Introduction

The rheological parameters can be evaluated using a number of concrete rheometers. A modified Tattersall MK-III two-point workability rheometer was employed in the NCHRP investigation (Fig. B.7). This rheometer uses an H-shaped impeller rotating in a planetary motion; the impeller was replaced by a four-blade vane impeller rotating in a coaxial manner in order to enable the evaluation of rheological parameters in terms of shear stress and shear rate, instead of torque and angular velocity[D9]. With the modified impeller geometry rotating in a co-axial motion, the yield stress can take place within the material itself along the localized surface circumscribed by the vane, thus eliminating an

y wall slip that may be obtained with the H-shaped impeller. The use of the cross-shaped vane causes less disruption to a sample than introducing the concrete into a conventional geometry, such as coaxial cylinders. Given the axial rotation and the geometry of the vane, the shear stress and shear rate can be calculated by considering a cylinder of equal dimension of the vane and assuming that the force due to shearing is distributed uniformly over the entire surface of the cylinder.

B.8.2 Normative reference

No references are available for this testing

[D9] Assaad, J., Khayat, K.H., and Mesbah, H., "Assessment of Thixotropy of Flowable and Self-Consolidating Concrete." *ACI Materials Journal*, Vol. 100, No. 2 (2003) pp. 111-120.

B.8.3 Equipment

I. Tattersall two-point workability rheometer
II. Cross-shaped vane

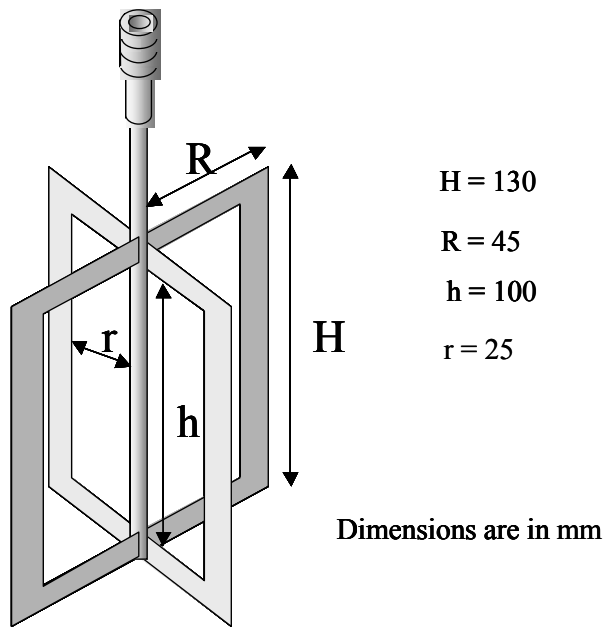

Fig. B.5 – Geometry of vane used to determine the rheological flow curves of SCC (100 mm = 3.94 in.)

B.8.4 Procedure

I. About 0.9 ft³ (25 L) of SCC is needed to perform the test, sampled normally.
II. Moisten the bowl.
III. Fill the bowl with a constant speed without any agitation.
IV. Gently immersing the vane of the rheometer into its bowl.
V. Rotational speed is increased gradually from 0.3 rev/sec to a maximum speed of 0.9 rev/sec for 15 second.
VI. The highest speed is maintained during 15 seconds to ensure the breakdown of the structure of the concrete before starting the downward portion of the flow curve.
VII. The rotational speed is reduced in predetermined steps varying from 0.9 to 0.3 rev/sec
VIII. Each speed is maintained during 15 seconds, and the torque required to shear the material at each rotational speed is recorded and used to derive the rheological parameters using the Bingham model.
IX. The slope of the linear regression and the intercept with the torque axis at zero shear rates are determined and related to the torque plastic viscosity (h) and apparent yield stress (g), respectively.

B.8.5 Analysis of data

The apparent yield stress (g) and torque plastic viscosity (h) values determined typically with the modified Tattersall two-point workability rheometer using the H-impeller cannot be expressed in terms of fundamental units of yield stress (Pa) and plastic viscosity (Pa.s). However, given the shape of the newly designed vane shown in Fig. B.7 and the geometry of the test apparatus, the g and h parameters can be converted into fundamental units, as elaborated below[D10].

The use of the vane device rotating in a coaxial movement aims to simulate conditions of the coaxial rheometer. Indeed, when the vane is rotating, a localized surface circumscribed by the vane is formed, and this cylindrical surface simulates the rotor cylinder in a coaxial viscometer (Fig. B.8).

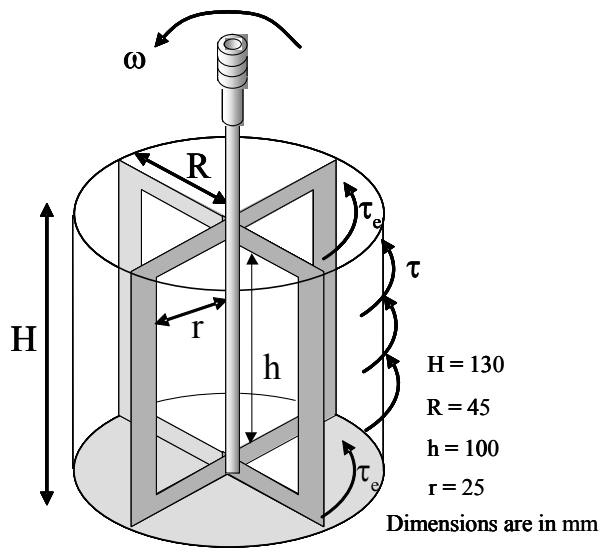

Fig. B.6 – Shear flow induced during the vane rotation

Given the torque values as well as the geometry of the vane, the torque measured at the central axis of the vane can be converted to shear stress at the sheared surface circumscribed by the vane, as follows:

$$T = 2\pi R^2 H\tau + 2\int_0^{2\pi}\int_0^{R} \tau_e r^2 dr d\theta \qquad \text{(B.1)}$$

where T is the torque measured at the central axe of the vane, ($2\pi R^2 H$) is the lateral area of the sheared surface, τ is the lateral shear stress, and the second term in the equation is due to the shear stress at the upper and bottom surface (τ_e) of the sheared cylinder. The force to shearing action is assumed to be distributed uniformly over the entire surface of the sheared cylinder.

[D10] Yahia, D., and Khayat, K.H., "Modification of the Concrete Rheometer to Determine Rheological Parameters of Self-Consolidating Concrete – Vane Device" Proceedings of the 2nd International RILEM Symposium on Advances in Concrete through Science and Engineering, Quebec City (2006) pp. 375-380.

The shear stress (τ_e) acting on both ends of the sheared surface is estimated using the following equation:

$$\tau_e = (\frac{r}{R})^m \tau \quad \text{(for r = R, } \tau_e = \tau) \tag{B.2}$$

The approach adopted in this study assumes that the distributions of τ_e across the end surfaces is linear, and therefore $\tau_e = (\frac{r}{R})\ \tau$ (i.e. m = 1).

Replacing $\tau_e = (\frac{r}{R})\ \tau$ in Eq. B.1 can lead to the following expression of shear stress:

$$\tau = \frac{T}{2\pi R^2 H + \pi R^3} \tag{B.3}$$

where T is in N.m, R and H in m, the shear stress is in Pa.

In the case of shear rate, the calculation approach is more complicated, especially in the case of rheometer with large gap (i.e. distance between the sheared surface and the edge of container is too large). For small gaps where the ratio between the radius of the vane (Ri) and the container (Re) is greater than 0.99, the shear rate can be considered as almost constant across the gap. However, in the case of coaxial viscometer used for concrete, many instruments have $\frac{Ri}{\text{Re}}$ less than 0.99, and therefore the shear rate would change across the gap. For large gap sizes used to accommodate the presence of coarse aggregate in concrete, the shear rate (γ) could be estimated as follows:

$$\gamma = r\frac{d\omega}{dr} \tag{B.4}$$

$$\tau = \frac{T}{2\pi R^2 H} \tag{B.5}$$

$$\text{then :} \quad r\frac{d\omega}{dr} = r\frac{d\omega}{d\tau}\frac{d\tau}{dr} = -r\frac{d\omega}{d\tau}\frac{T}{\pi H r^3} = \frac{d\omega}{d\tau}\frac{T}{\pi H r^2}$$

Therefore, the shear rate is given as a function of the shear stress, as follows:

$$\gamma = -2\tau\frac{d\omega}{d\tau} \tag{B.6}$$

This equation is expanded into a Maclaurin series by Krigger and Elrod[D11] [1953] to derive an estimated shear rate expression, as follows:

$$\gamma(\tau_i) = \frac{\omega_i}{Ln(s)}\left[1 + mLn(s) + \frac{(mLn(s))^2}{3} - \frac{(mLn(s))^4}{45}\right] \tag{B.7}$$

where $m = \frac{dLn(\omega_i)}{d\ln(\tau_i)}$, i.e. the slope of the curve $Ln(\omega_i)$ vs. $Ln(\tau_i)$, and $s = \frac{\mathrm{Re}}{Ri}$

The torque and rotational velocity values are then converted to shear stress and shear rate values using Eqs. B.3 and B.7, respectively. The converted shear stress and shear rate data are then employed to estimate the rheological parameters assuming a given flow model.

[D11] Krieger, I.M., and Elrod, H. "Direct Determination of the Flow Curves of Non-Newtonian Fluids: II. Shearing Rate in the Concentric Cylindrical Viscometer."*Journal of Applied Physics*, Vol. 24 No. 2 (1953) pp. 134-136.

APPENDIX C

Variations of Temperatures of Chamber and Concrete during Steam Curing

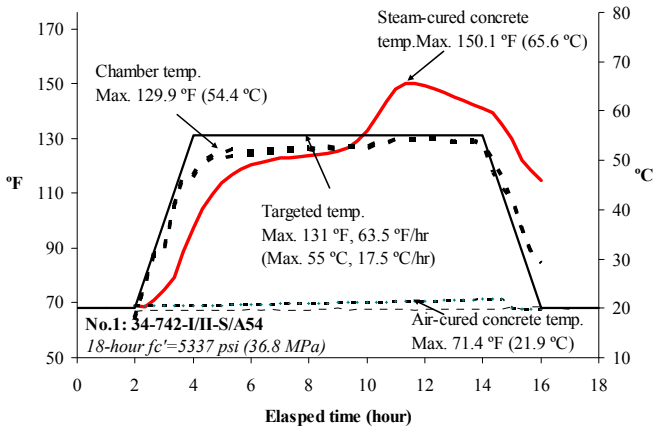

(1) SCC No. 1

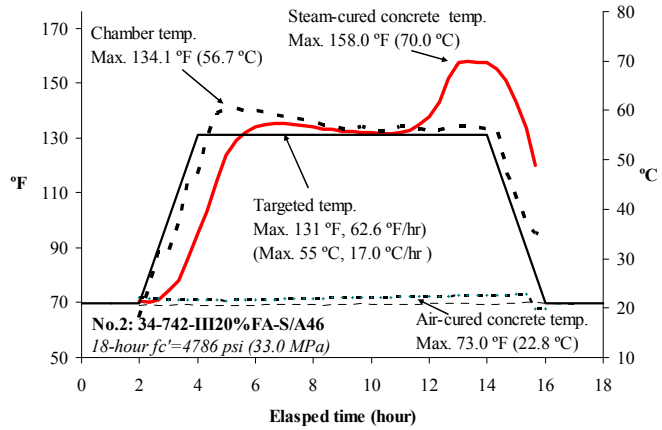

(2) SCC No. 2

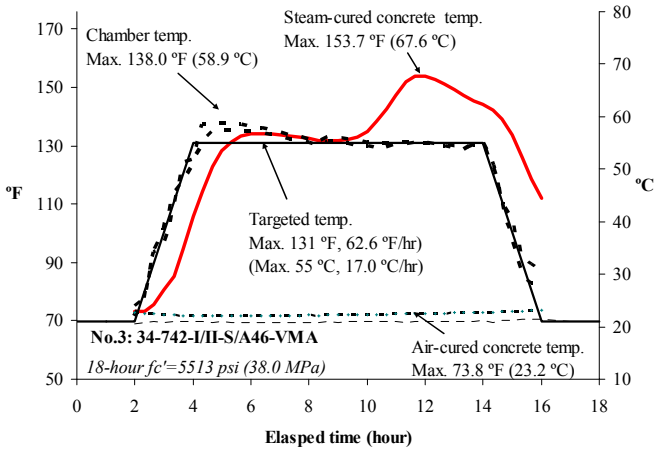

(3) SCC No. 3

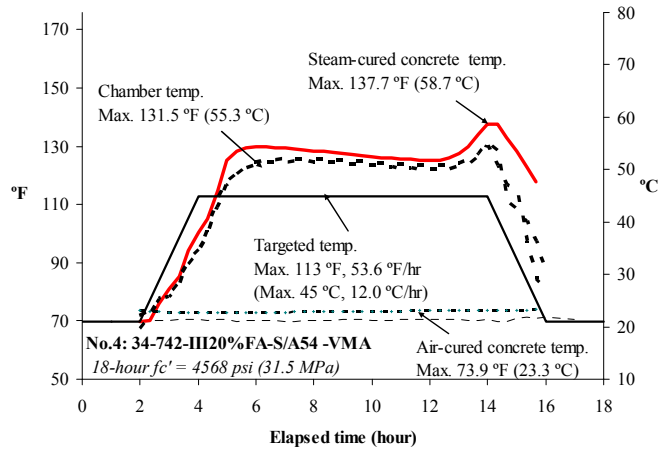

(4) SCC No. 4

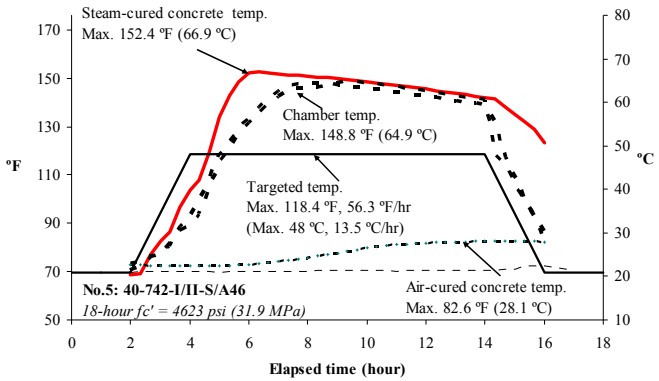

(5) SCC No. 5

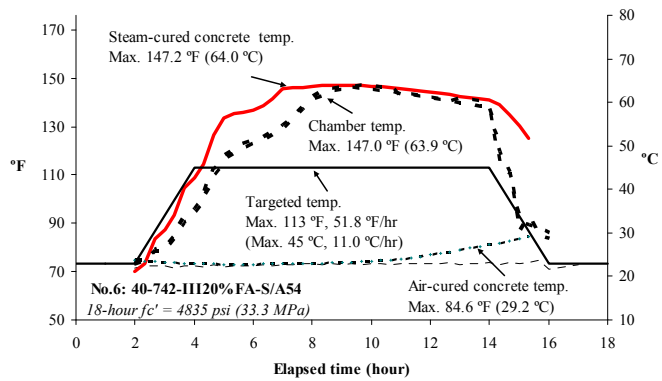

(6) SCC No. 6

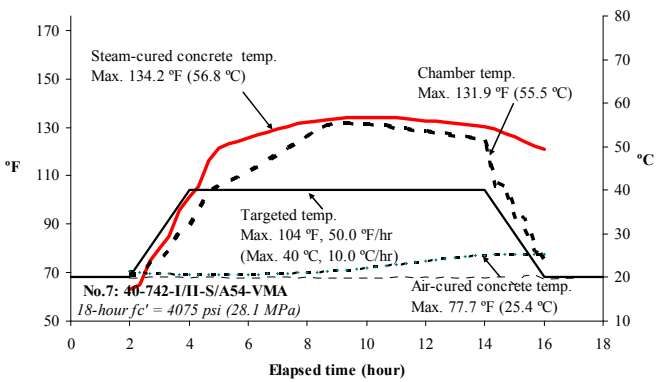

(7) SCC No. 7

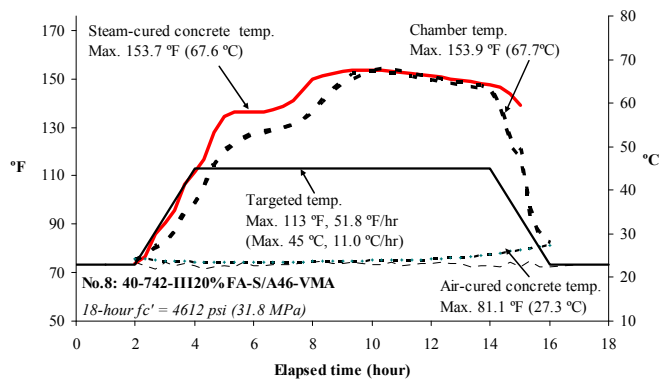

(8) SCC No. 8

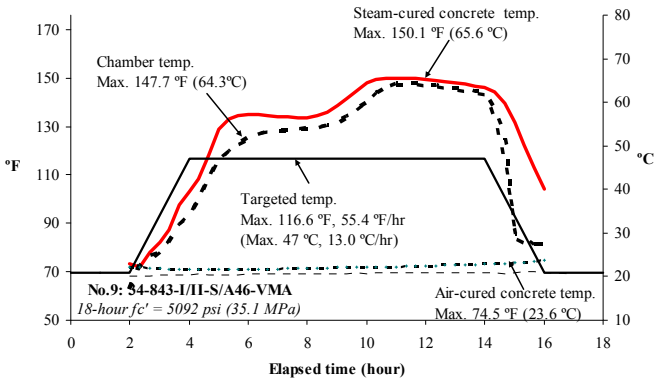

(9) SCC No. 9

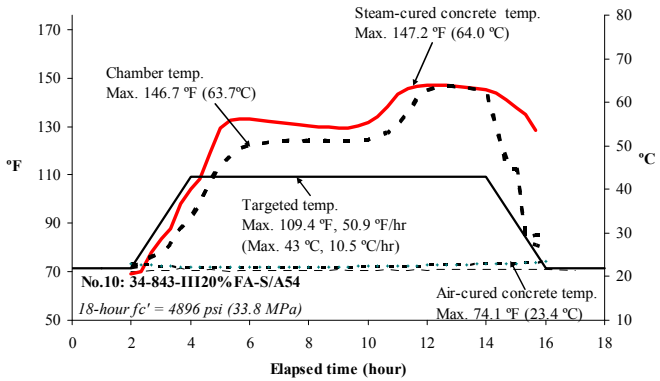

(10) SCC No. 10

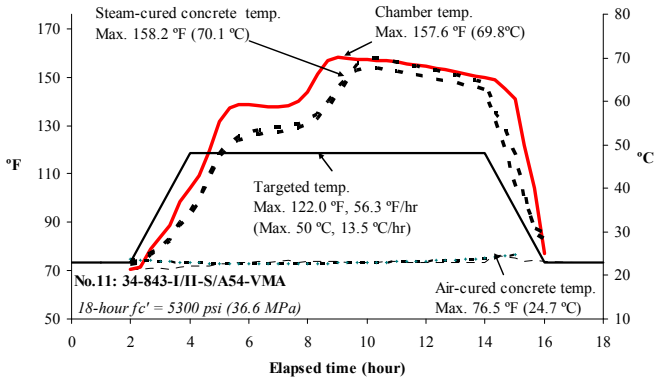

(11) SCC No. 11

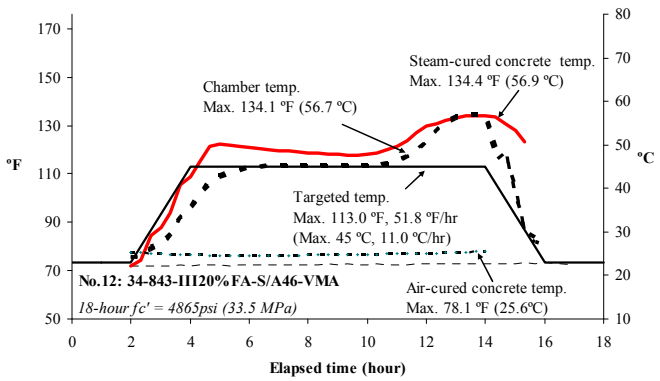

(12) SCC No. 12

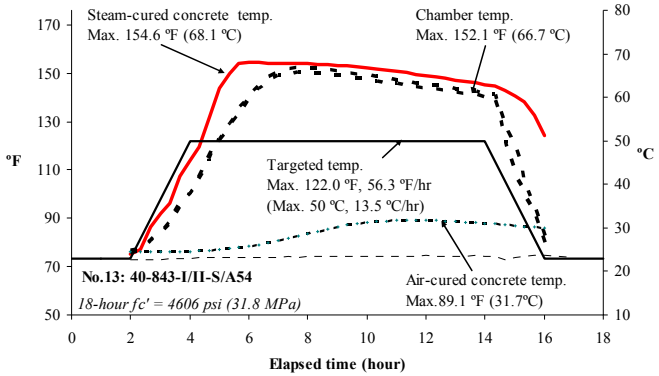

(13) SCC No. 13

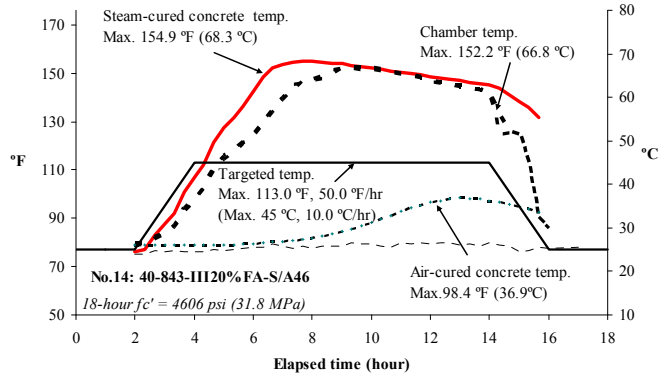

(14) SCC No.14

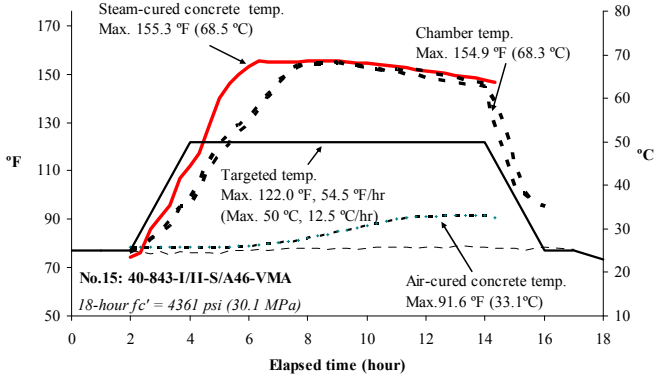

(15) SCC No. 15

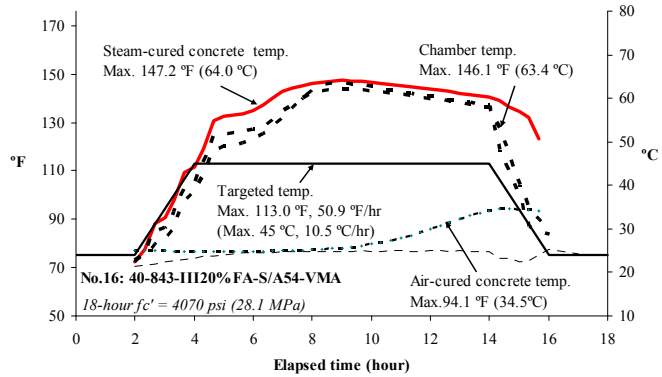

(16) SCC No. 16

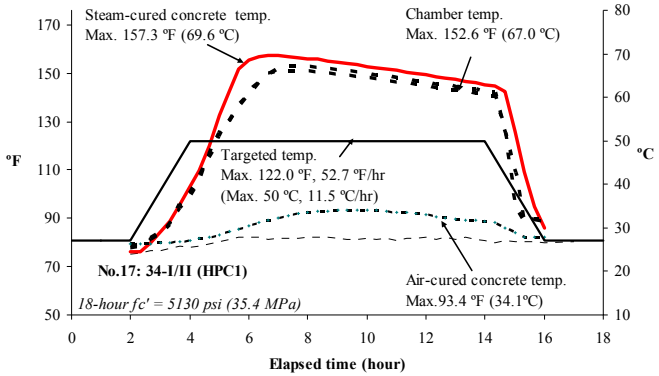

(17) HPC No. 17

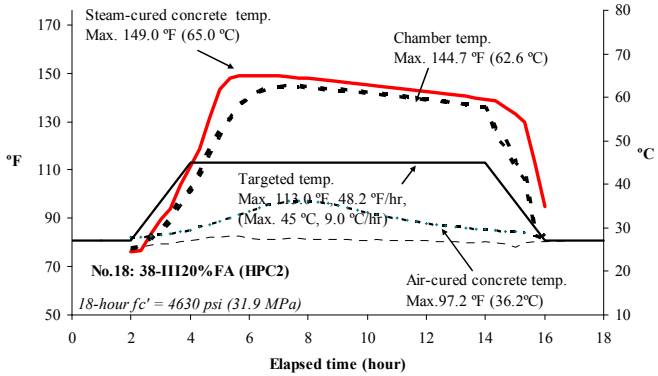

(18) HPC No. 18

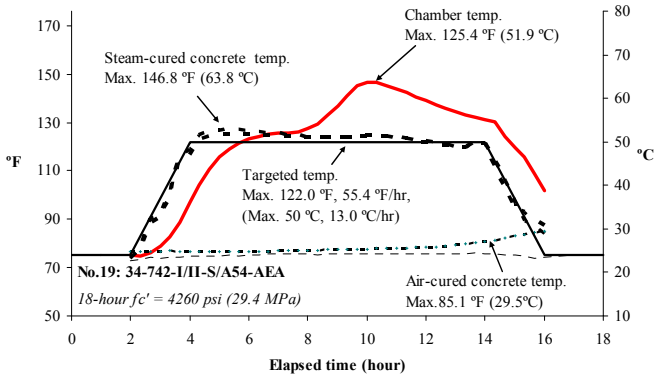

(19) SCC No. 19

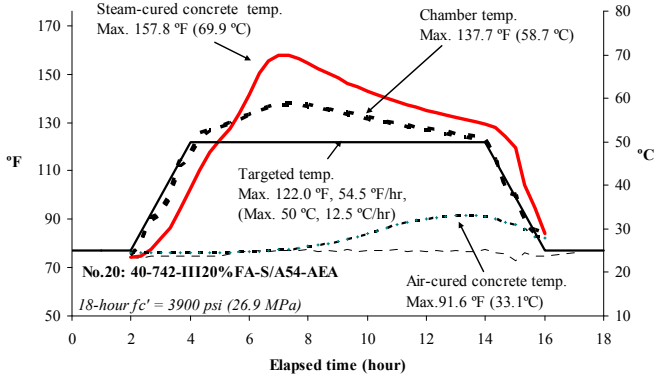

(20) SCC No. 20

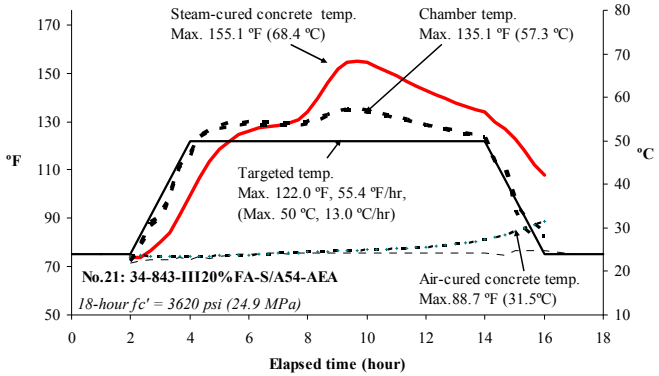

(21) SCC No. 21

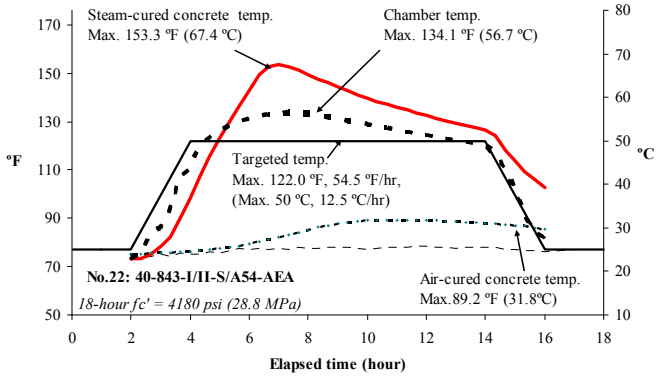

(22) SCC No. 22

APPENDIX D

Decay in Formwork Pressure Determined on 3.6-ft (1.1-m) High Columns (casting rate 4 – 5 m/hr)

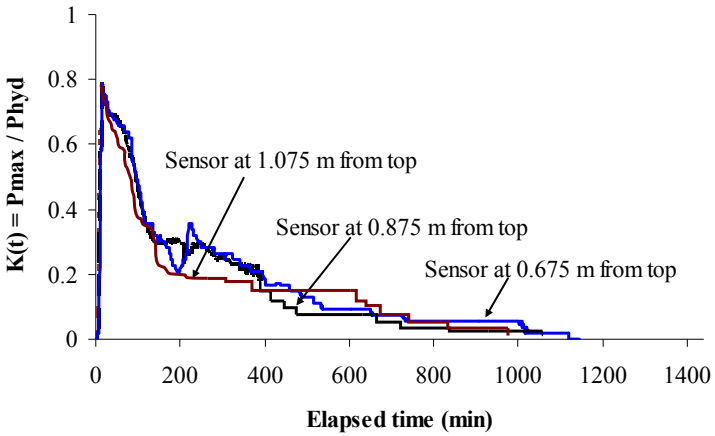

(1) SCC No. 1

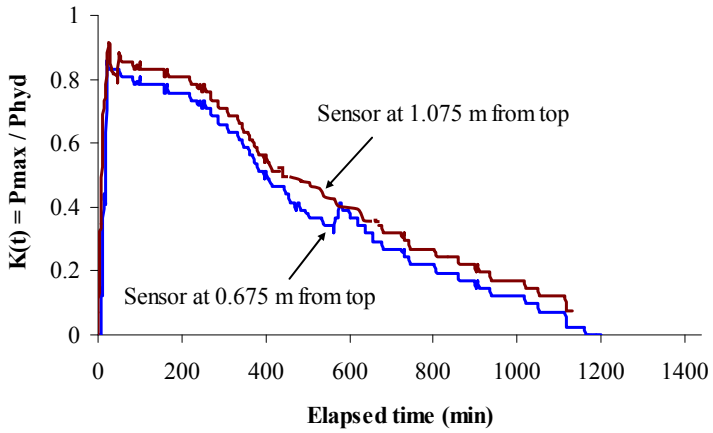

(2) SCC No. 2

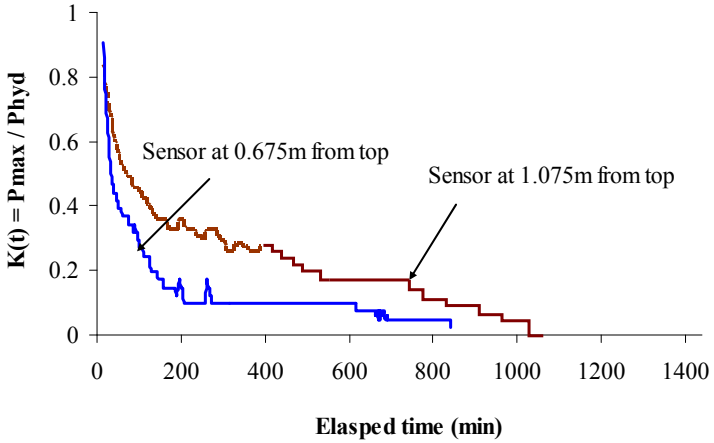

(3) SCC No. 3

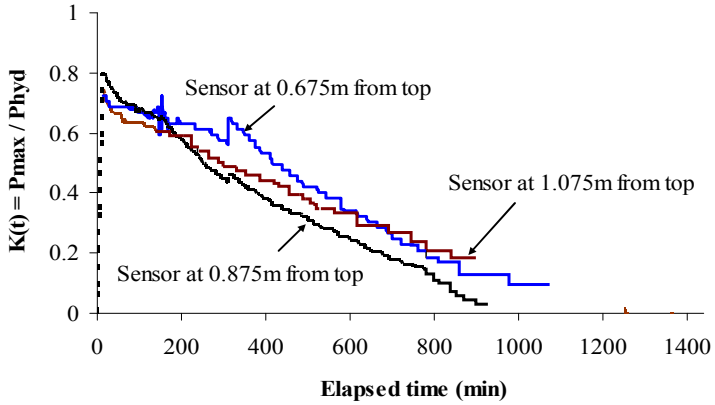

(4) SCC No. 4

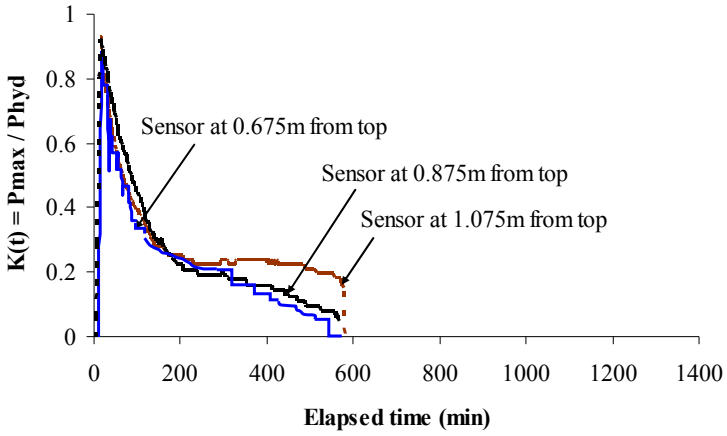

(5) SCC No. 5

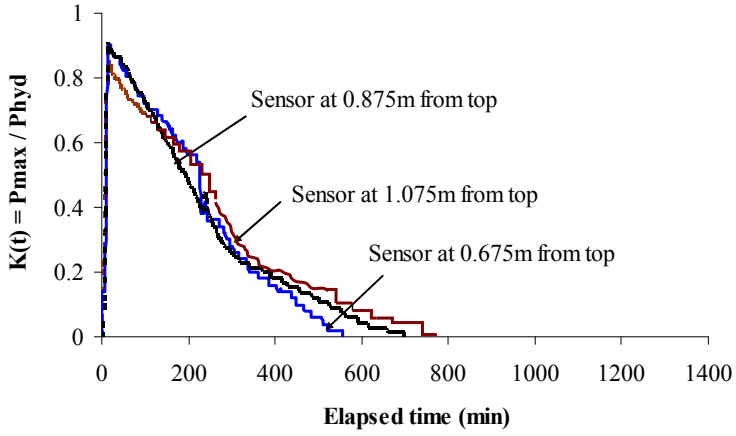

(6) SCC No. 6

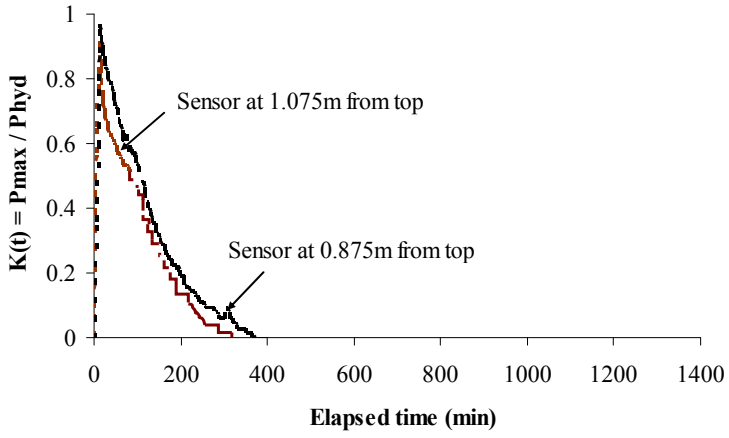

(7) SCC No. 7

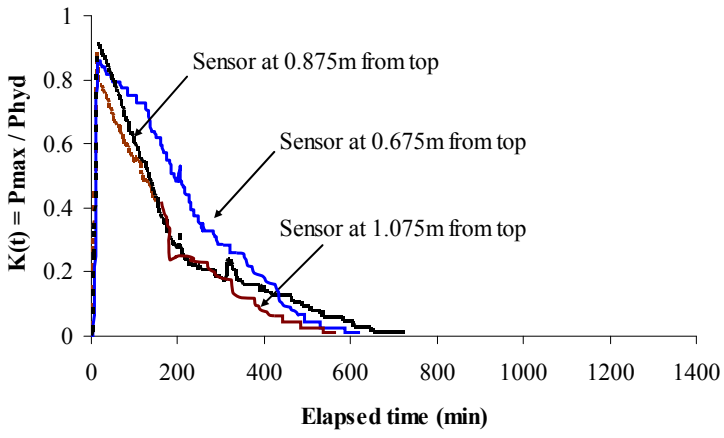

(8) SCC No. 8

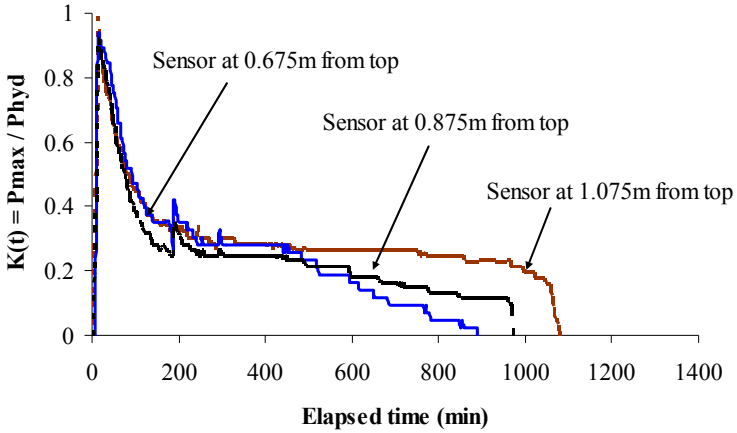

(9) SCC No. 9

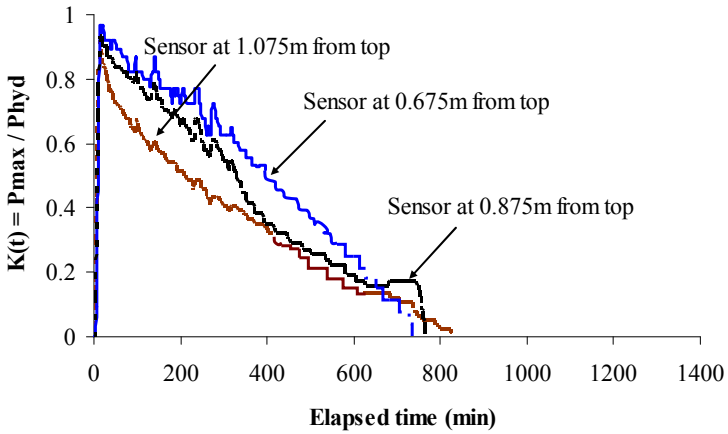

(10) SCC No. 10

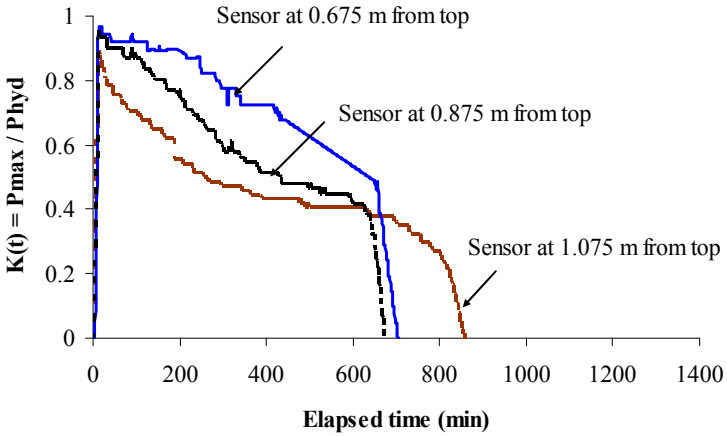

(11) SCC No. 11

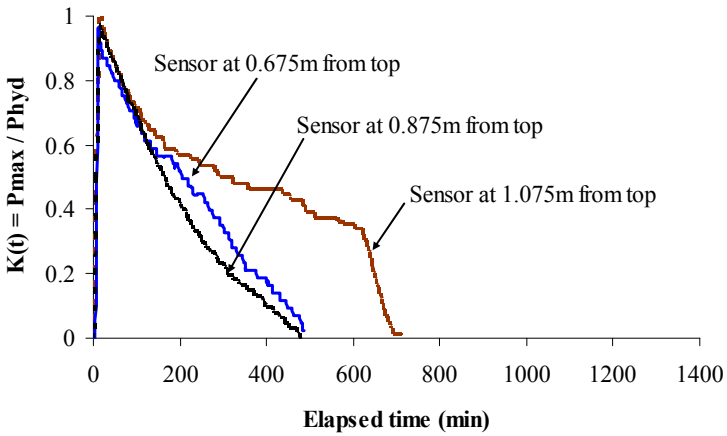

(12) SCC No. 12

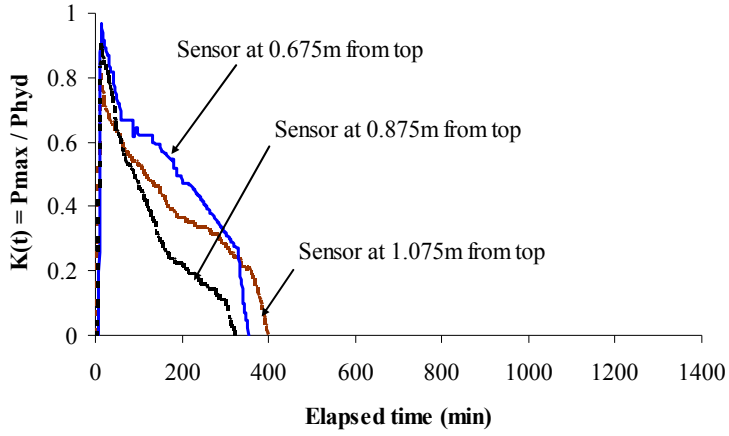

(13) SCC No. 13

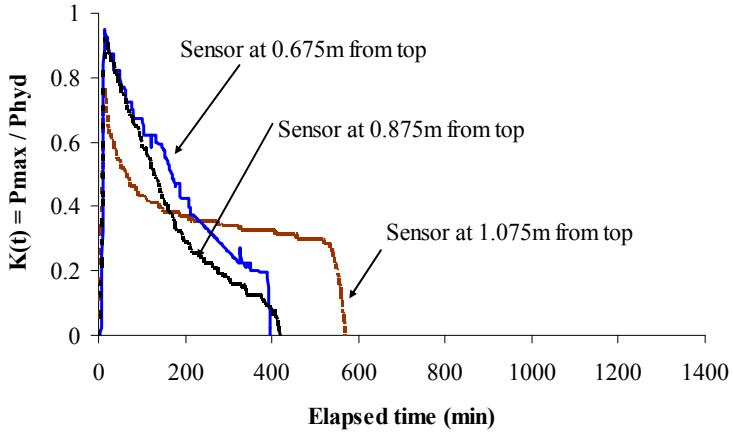

(14) SCC No. 14

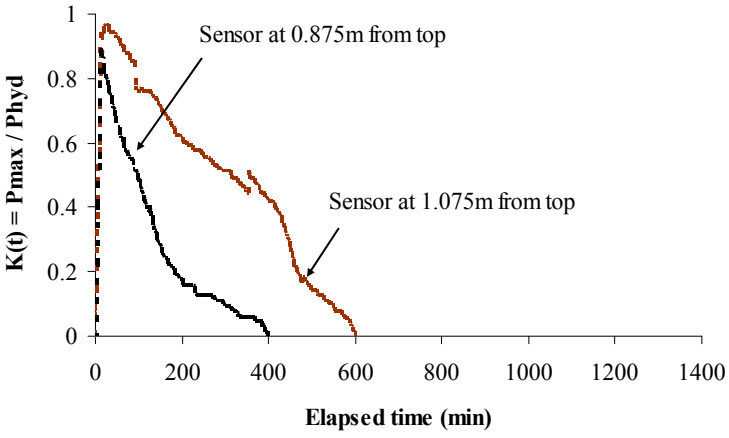

(15) SCC No. 15

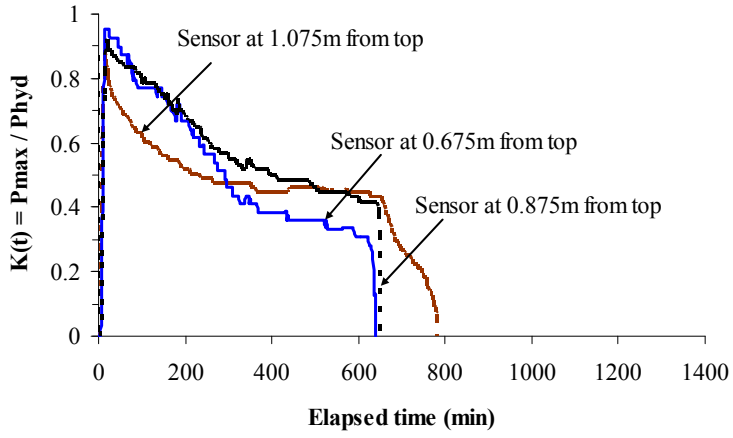

(16) SCC No. 16

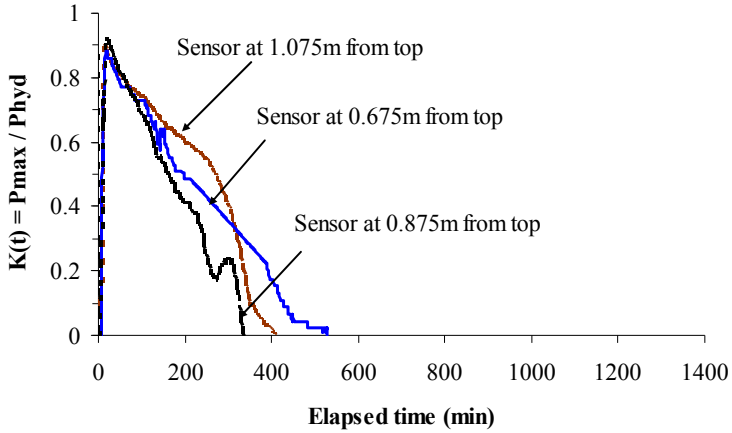

(17) HPC No. 17

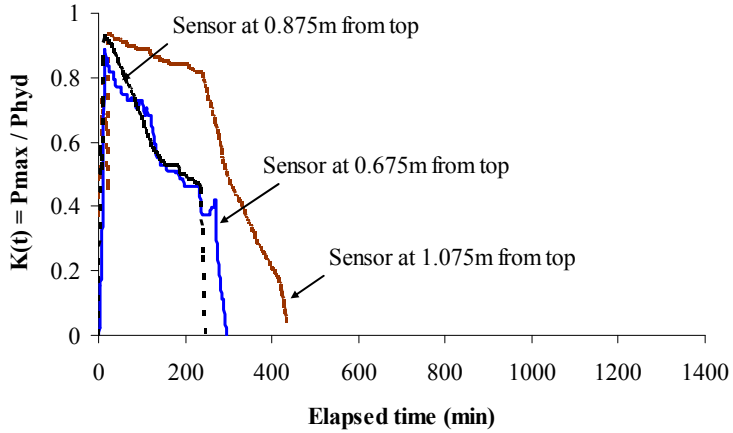

(18) HPC No. 18

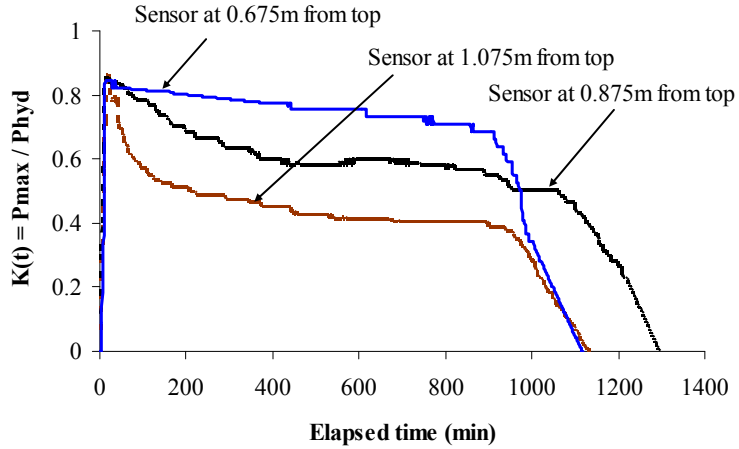

(19) SCC No. 19

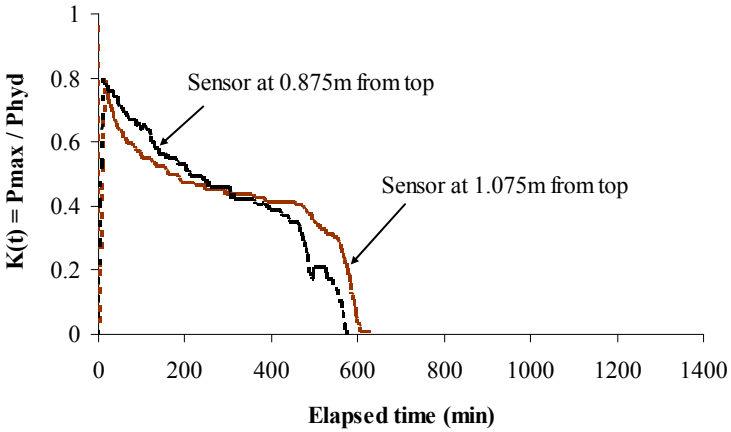

(20) SCC No. 20

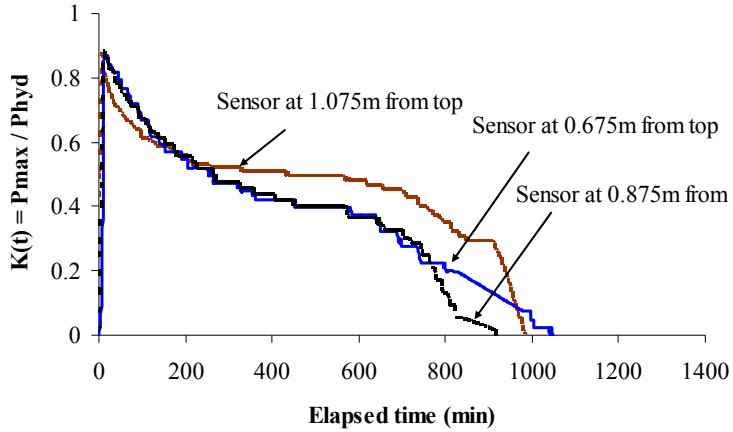

(21) SCC No. 21

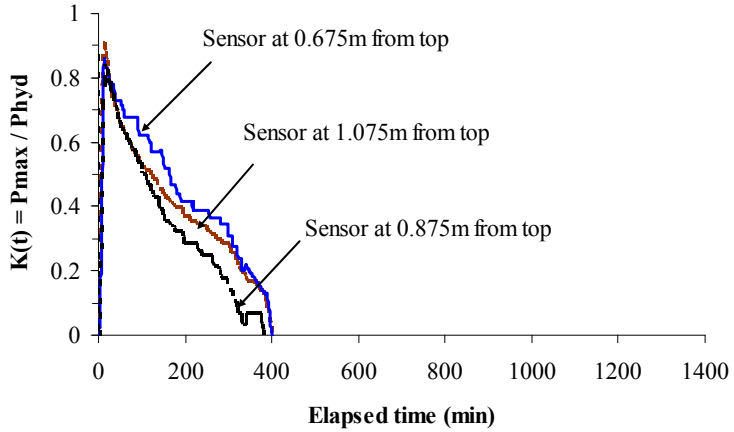

(22) SCC No. 22

APPENDIX E

Materials Characteristics of Cement, Supplementary Cementitious Materials, Sand, and Coarse Aggregate

Table E.1 – Physical and chemical analyses of cement and supplementary cementitious materials

Cement and supplementary cementitious materials	Type I/II cement	Type III cement	Class F fly ash	Blast-furnace slag
Physical properties				
Specific gravity	3.14	3.15	2.53	2.95
Blaine specific surface area, m^2/kg	390	530	410	400
Passing No. 325 (45 µm), %	91	99	90	92
Chemical composition, %				
SiO_2	21.4	20.0	52.4	36.0
Al_2O_3	4.6	5.4	27.2	10.4
Fe_2O_3	2.9	2.3	8.3	1.5
CaO	63.3	63.5	4.5	42.9
MgO	2.0	1.4	0.96	6.7
SO_3	3.4	4.4	0.05	0.48
K_2O	0.94	1.1	2.33	0.37
Na_2O	0.07	0.15	0.20	0.17
Na_2O eq*	0.69	0.88	1.74	0.41
LOI	0.98	0.80	2.73	0.41
Bogue composition, %				
C_3S	50.0	54.9	-	-
C_2S	23.7	15.8	-	-
C_3A	7.4	10.5	-	-
C_4AF	8.8	6.9	-	-

* Na_2O eq = Na_2O + 0.64 K_2O

Table E.2 – Grading and properties of coarse aggregate and sand

Sieve opening	Siliceous sand	Crushed coarse aggregate			Gravel
	0 - No. 4 (0 - 4.75 mm)	¾ in. - No. 4 (19 - 4.75 mm)	½ in. - No. 4 (12.5 - 4.75 mm)	3/8 in. - No. 8 (9.5 - 2.36 mm)	½ in. - No. 4 (12.5 - 4.75 mm)
1 in. (25 mm)	100	100	100	100	100
¾ in. (19 mm)	100	99	100	100	100
½ in. (12.5 mm)	100	68	95	100	99
3/8 in. (9.5 mm)	100	40	69	100	94
No. 4 (4.75 mm)	98	7	18	13	32
No. 8 (2.36 mm)	85	1	4	2	1
No.16 (1.18 mm)	72	1	3	2	-
No. 30 (600 µm)	55	-	-	-	-
No. 50 (300 µm)	32	-	-	-	-
No.100 (150 µm)	9	-	-	-	-
Pan	2	0	0	0	0
Specific gravity	2.66	2.72	2.71	2.73	2.66
Absorption, %	1.1	0.3	0.5	0.4	1.3

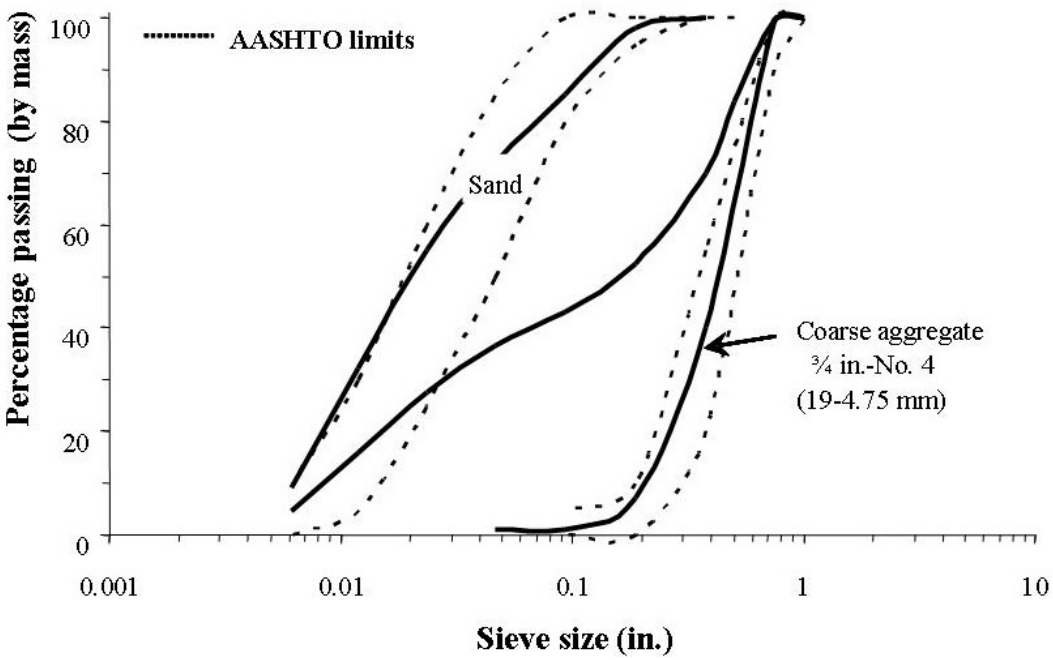

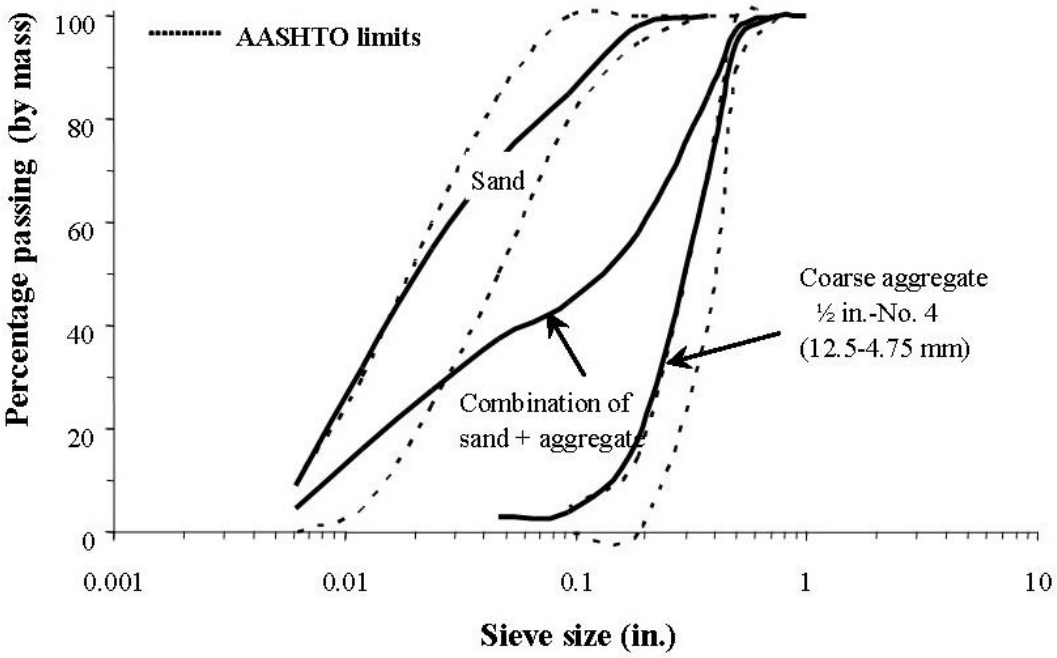

Fig. E.1 – Grading of sand and coarse aggregate

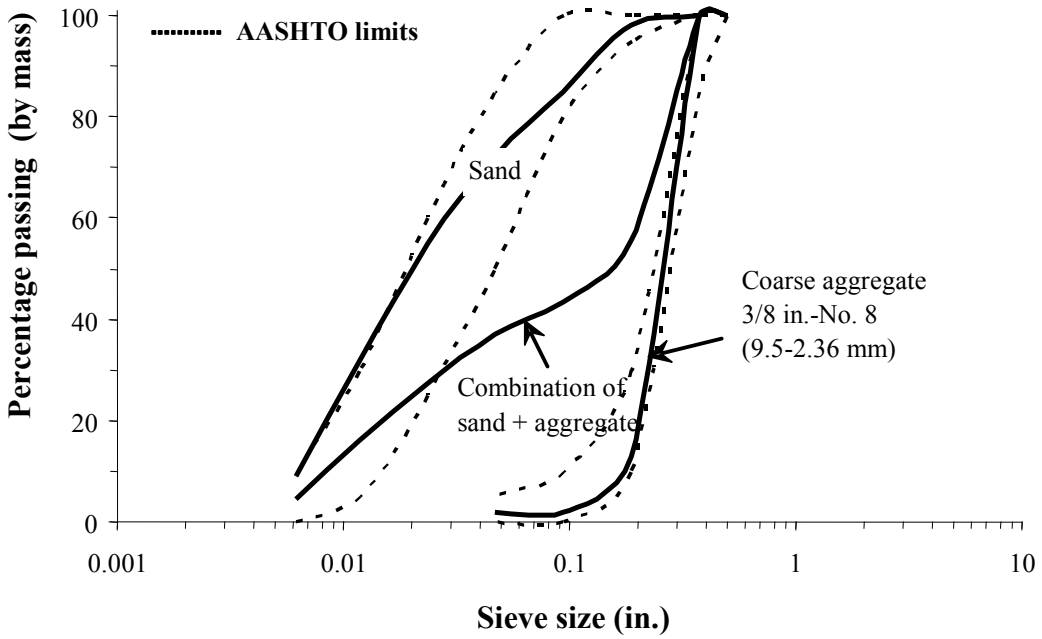

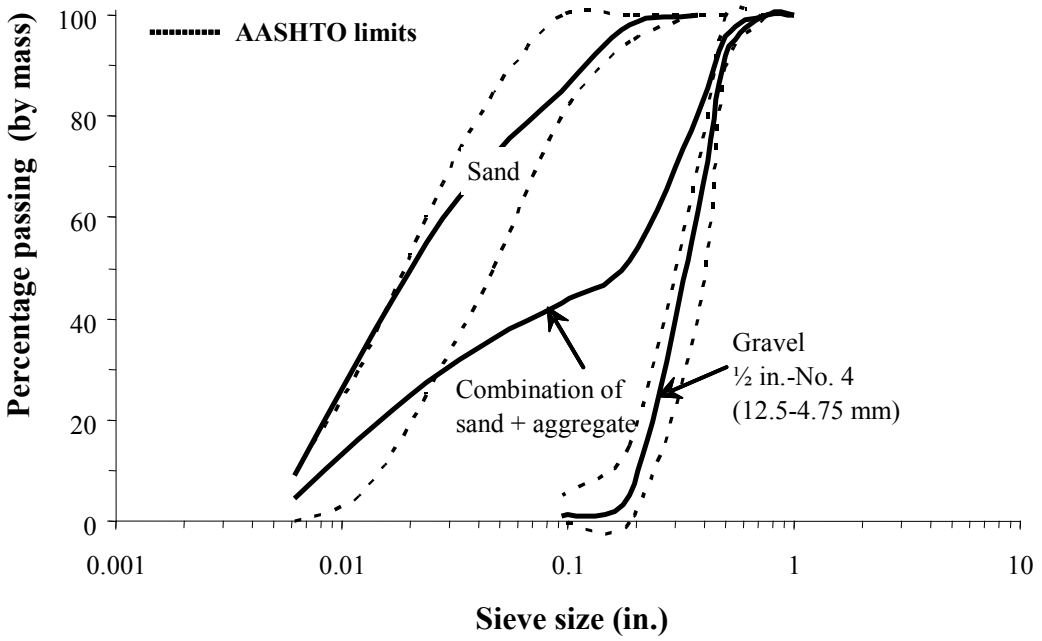

Fig. E.1 (cont'd) – Grading of sand and coarse aggregate

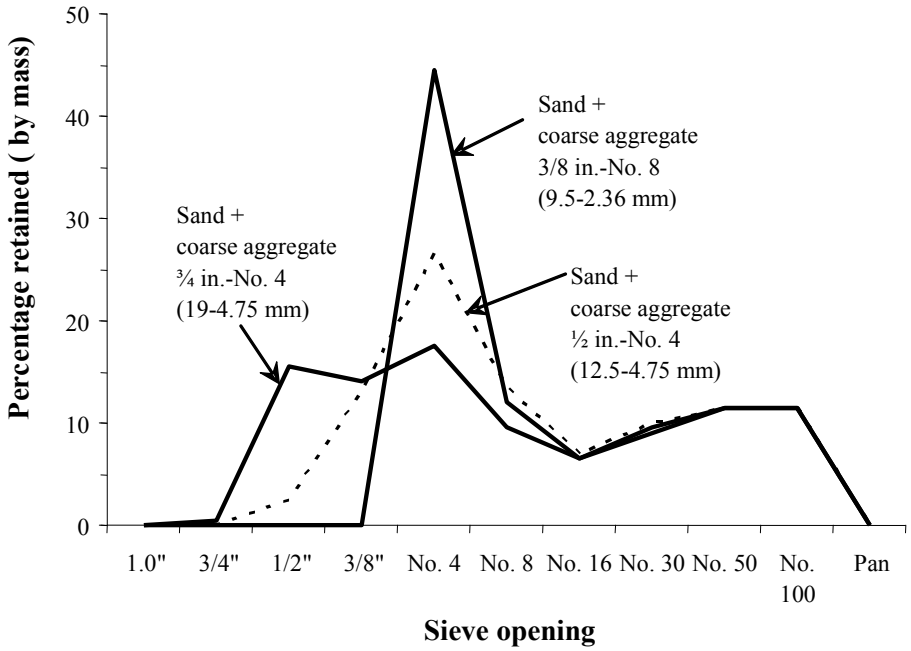

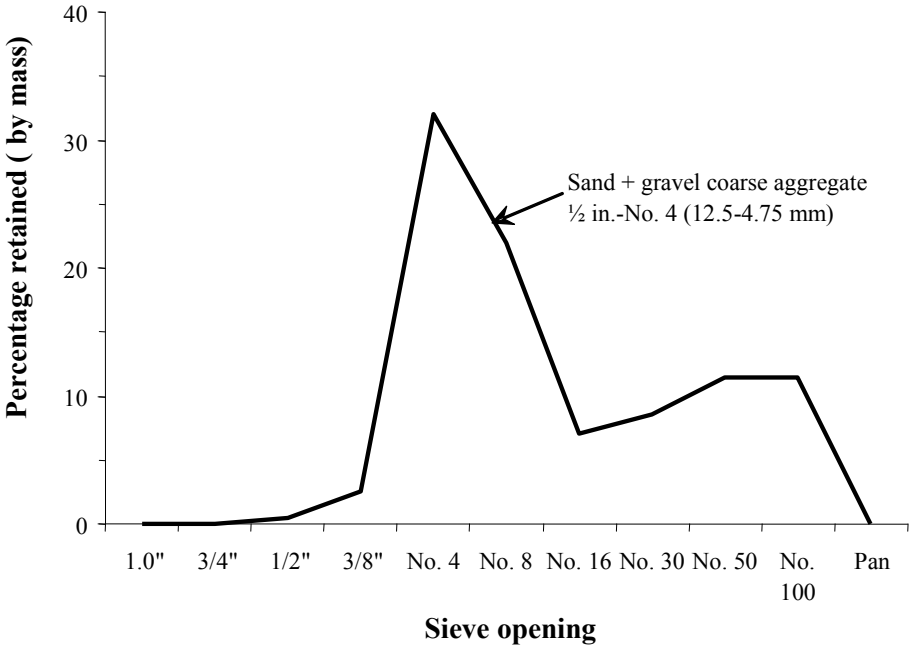

Fig. E.2 – Grading of combined aggregate retained on various sieve openings

APPENDIX F

Mixture Proportioning of Mixtures No. 1 to 22 Evaluated in Factorial Design

Table F.1 – Mixture proportioning of SCC mixtures No. 1 to 5

Mixture No.	1	2	3	4	5
Codification	34-742-I/II -S/A54	34-742-III 20%FA -S/A46	34-742-I/II-S/A46 -VMA	34-742 -III20%FA -S/A54 -VMA	40-742-I/II -S/A46
Cement, lb/yd^3 (kg/m^3)	Type I/II	Type III	Type I/II	Type III	Type I/II
	742 (440)	594 (352)	742 (440)	594 (352)	742 (440)
HRWRA demand*, fl oz/cwt (L/100 kg CM**)	34.2 (2.23)	41.8 (2.73)	36.7 (2.39)	45.4 (2.95)	11.9 (0.77)
VMA dosage, fl oz/cwt (L/100 kg CM)	0	0	1.55 (0.1)	1.55 (0.1)	0
Class F fly ash, lb/yd^3 (kg/m^3)	0	148 (88)	0	148 (88)	0
Total CM, lb/yd^3 (kg/m^3)	742 (440)	742 (440)	742 (440)	742(440)	742 (440)
Water, lb/yd^3 (kg/m^3)	243 (144)	235 (139)	240 (142)	235(139)	294 (174)
w/cm	0.34	0.34	0.34	0.34	0.40
Sand, lb/yd^3 (kg/m^3)	1674 (993)	1415 (839)	1428 (848)	1658 (984)	1374 (815)
Coarse aggregate, lb/yd^3 (kg/m^3)	1428 (847)	1661 (985)	1677 (995)	1412 (838)	1612 (957)
Sand/total aggregate, by volume	0.54	0.46	0.46	0.54	0.46
Volume of coarse aggregate, %	32.2	37.7	37.9	32.0	36.3
Volume of mortar, %	67.8	62.3	62.1	68.0	63.7
Volume of paste, %	29.3	29.6	29.2	29.6	32.2

* Polycarboxylate-based AASHTO M 194, Type F HRWRA

** CM = Cementitious materials

Table F.2 – Mixture proportioning of SCC mixtures No. 6 to 10

Mixture No.	6	7	8	9	10
Codification	40-742 -III20%FA -S/A54	40-742-I/II-S/A54 -VMA	40-742 -III20%FA -S/A46 -VMA	34-843-I/II -S/A46	34-843 -III20%FA -S/A54
Cement, lb/yd^3 (kg/m^3)	Type III	Type I/II	Type III	Type I/II	Type III
	594 (352)	742 (440)	594 (352)	843 (500)	675 (400)
HRWRA demand*, fl oz/cwt (L/100 kg CM**)	18.5 (1.20)	13.3 (0.86)	21.8 (1.41)	27.8 (1.8)	31.0 (2.0)
VMA dosage, fl oz/cwt (L/100 kg CM)	0	1.55 (0.1)	1.55 (0.1)	0	0
Class F fly ash, lb/yd^3 (kg/m^3)	148 (88)	0	148 (88)	0	168 (100)
Total CM, lb/yd^3 (kg/m^3)	742 (440)	742 (440)	742 (440)	843 (500)	843 (500)
Water, lb/yd^3 (kg/m^3)	289 (171)	292 (172)	300 (176)	286 (170)	286 (170)
w/cm	0.40	0.40	0.40	0.34	0.34
Sand, lb/yd^3 (kg/m^3)	1593 (945)	1609 (955)	1361 (807)	1347 (798)	1561 (925)
Coarse aggregate, lb/yd^3 (kg/m^3)	1358 (805)	1372 (814)	1596 (947)	1612 (955)	1331 (788)
Sand/total aggregate, by volume	0.54	0.54	0.46	0.46	0.54
Volume of coarse aggregate, %	30.6	30.9	36.0	35.8	30.1
Volume of mortar, %	69.4	69.1	64.0	64.2	69.9
Volume of paste, %	32.8	32.2	32.7	33.1	33.9

* Polycarboxylate-based AASHTO M 194, Type F HRWRA

** CM = Cementitious materials

Table F.3 – Mixture proportioning of SCC mixtures No. 11 to 14

Mixture No.	11	12	13	14
Codification	34-843-I/II -S/A54-VMA	34-843-III20%FA-S/A46-VMA	40-843-I/II - S/A54	40-843-III20%FA -S/A46
Cement, lb/yd^3 (kg/m^3)	Type I/II	Type III	Type I/II	Type III
	843 (500)	674 (400)	843 (500)	674 (400)
HRWRA demand*, fl oz/cwt (L/100 kg CM**)	30.7 (2.00)	30.7 (2.00)	7.7 (0.50)	15.6 (1.02)
VMA dosage, fl oz/cwt (L/100 kg CM)	1.55 (0.1)	1.55 (0.1)	0	0
Class F fly ash, lb/yd^3 (kg/m^3)	0	168 (100)	0	168 (100)
Total CM, lb/yd^3 (kg/m^3)	843 (500)	843 (500)	843 (500)	843 (500)
Water, lb/yd^3 (kg/m^3)	275 (163)	272 (161)	332 (197)	329 (195)
w/cm	0.34	0.34	0.40	0.40
Sand, lb/yd^3 (kg/m^3)	1578 (936)	1330 (789)	1505 (893)	1268 (752)
Coarse aggregate, lb/yd^3 (kg/m^3)	1345 (798)	1563 (927)	1283 (761)	1489 (883)
Sand/total aggregate, by volume	0.54	0.46	0.54	0.46
Volume of coarse aggregate, %	30.4	35.4	28.9	33.6
Volume of mortar, %	69.6	64.6	71.1	66.4
Volume of paste, %	33.2	33.9	36.6	37.3

* Polycarboxylate-based AASHTO M 194, Type F HRWRA

** CM = Cementitious materials

Table F.4 – Mixture proportioning of mixtures No. 15 to 18

Mixture No.	SCC		HPC	
	15	16	17	18
Codification	40-843-I/II-S/A46-VMA	40-843-III20%FA-S/A54-VMA	34-I/II	38-III20%FA
Cement, lb/yd^3 (kg/m^3)	Type I/II	Type III	Type I/II	Type III
	843 (500)	674 (400)	792 (470)	634 (376)
HRWRA demand*, fl oz/cwt (L/100 kg CM**)	10.7 (0.70)	15.5 (1.00)	6.7 (0.43)	4.2 (0.27)
VMA dosage, fl oz/cwt (L/100 kg CM)	1.55 (0.1)	1.55 (0.1)	0	0
Class F fly ash, lb/yd^3 (kg/m^3)	0	168 (100)	0	158 (94)
Total CM*, lb/yd^3 (kg/m^3)	843 (500)	843 (500)	792 (470)	792 (470)
Water, lb/yd^3 (kg/m^3)	331 (196)	329 (195)	270 (160)	302 (179)
w/cm	0.40	0.40	0.34	0.38
Sand, lb/yd^3 (kg/m^3)	1285 (762)	1487 (882)	1249 (741)	1131 (671)
Coarse aggregate, lb/yd^3 (kg/m^3)	1507 (894)	1266 (751)	1770 (1050)	1770 (1050)
Sand/total aggregate, by volume	0.46	0.54	0.41	0.39
Volume of coarse aggregate, %	34.0	28.6	39.7	39.7
Volume of mortar, %	66.0	71.4	60.3	60.3
Volume of paste, %	36.6	37.3	31.7	34.4

* Polycarboxylate-based AASHTO M 194, Type F HRWRA

** CM = Cementitious materials

Table F.5 – Mixture proportioning of SCC mixtures No. 19 to 22

Mixture No.	AEA SCC			
	19	20	21	22
Codification	34-742-I/II -S/A54	40-742-III20%FA -S/A54	34-843-III20%FA - S/A54	40-843-I/II -S/A54
Cement, lb/yd^3 (kg/m^3)	Type I/II	Type III	Type III	Type I/II
	742 (440)	594 (352)	675 (400)	843 (500)
HRWRA demand*, fl oz/cwt (L/100 kg CM**)	32.4 (2.09)	19.1 (1.23)	26.5 (1.70)	7.4 (0.48)
VMA dosage, fl oz/cwt (L/100 kg CM)	0	0	0	0
AEA, fl oz/cwt (mL/100 kg CM)	28.0 (1.8)	28.0 (1.8)	6.2 (0.4)	24.8 (1.6)
Class F fly ash, lb/yd^3 (kg/m^3)	0	148 (88)	168 (100)	0
Total CM, lb/yd^3 (kg/m^3)	742 (440)	843 (500)	843 (500)	843 (500)
Water, lb/yd^3 (kg/m^3)	240 (142)	290 (172)	273 (162)	334 (198)
w/cm	0.34	0.40	0.34	0.40
Sand, lb/yd^3 (kg/m^3)	1565 (928)	1484 (880)	1450 (860)	1395 (827)
Coarse aggregate, lb/yd^3 (kg/m^3)	1356 (804)	1285 (762)	1256 (745)	1211 (718)
Sand/total aggregate, by volume	0.54	0.54	0.54	0.54
Volume of coarse aggregate, %	32.0	30.2	29.7	28.4
Volume of mortar, %	68.0	69.8	70.3	71.6
Volume of paste, %	30.4	34.2	35.5	38.3

* Polycarboxylate-based AASHTO M 194, Type F HRWRA

** CM = Cementitious materials

APPENDIX G

Fresh Properties of Mixtures No. 1 to 22 Evaluated in Factorial Design

Table G.1 – Fresh properties and rheological parameters of SCC mixtures No. 1 to 5

Mixture No.		1	2	3	4	5
Codification		34-742-I/II -S/A54	34-742-III20%FA -S/A46	34-742-I/II-S/A46 -VMA	34-742-III20%FA -S/A54 -VMA	40-742-I/II -S/A46
HRWRA demand, fl oz/cwt (L/100 kg CM)		34.2 (2.23)	41.8 (2.73)	36.7 (2.39)	45.4 (2.95)	11.9 (0.77)
Slump flow, in. (mm)	10 min	26.0 (660)	26.4 (670)	26.4 (670)	26.6 (675)	27.0 (685)
	40 min*	23.6 (600)	26.2 (665)	26.0 (660)	26.4 (670)	26.8 (680)
T-20 in. (500 mm), sec	10 min	9.8	8.8	8.2	6.19	1.4
	40 min	9.6	8.6	6.9	6.12	1.6
Visual stability index	10 min	0.5	0.5	0.5	0.5	1
	40 min	0.5	0.5	0.5	0.5	1
Air content, %	10 min	1.3	0.7	1.0	1.8	2.5
	40 min	1.4	0.6	0.9	1.9	2.4
Unit weight, lb/ft^3 (kg/m^3)	10 min	152.5 (2441)	152.0 (2433)	154.1 (2466)	147.3 (2385)	148.5 (2377)
	40 min	151.9 (2432)	151.8 (2430)	153.3 (2454)	147.0 (2380)	148.4 (2375)
Temperature, ^{o}F (^{o}C)	10 min	71 (21.4)	76.5 (24.7)	76.6 (24.8)	74.5 (23.6)	75.2 (24.0)
	40 min	71 (21.8)	76.1 (24.5)	75.7 (24.3)	73.4 (23.0)	73.4 (23.0)
J-Ring, in. (mm)	10 min	20.9 (530)	(24.6) 625	21.5 (545)	25.2 (640)	26.6 (675)
	40 min	16.9 (430)	(23.8) 605	21.5 (545)	24.6 (625)	24.8 (630)
L-box	10 min, sec (h_2/h_1)	14.8 (0.47)	25.7 (0.17)	**	13.4 (0.73)	1.5 (0.95)
	40 min, sec (h_2/h_1)	13.9 (0.32)	31.1 (0.20)	**	10.3 (0.69)	2.1 (0.73)
Filling capacity, %	10 min	73	88	64	96	96
	40 min	67	82	62	85	89
Rheological parameter***	τ_o (Pa)	21	12	18	5	5
	μ_p (Pa.s)	840	480	550	930	221
	R^2	0.97	0.97	0.98	0.99	0.99
Column segregation index, %		2.87	3.10	3.77	4.23	2.42
Percent static segregation		4.4	14.0	15.1	0.0	10.7
Max. surface settlement, %		0.40	0.27	0.35	0.44	0.44
Initial setting time, hour		9.8	14.0	11.6	13.2	7.4
Final setting time, hour		14.2	17.6	14.7	17.2	8.8

* Agitation of concrete between 10 and 40 minutes at 6 rpm

** L-box blocking ratio smaller than 0.10

*** 1 Pa = 1.45×10^{-4} psi

Table G.2 – Fresh properties and rheological parameters of SCC mixtures No. 6 to 10

Mixture No.		6	7	8	9	10
Codification		40-742-III20%FA-S/A54	40-742-I/II-S/A54-VMA	40-742-III20%FA-S/A46-VMA	34-843-I/II-S/A46	34-843-III20%FA-S/A54
HRWRA demand, fl oz/cwt (L/100 kg CM)		18.5 (1.20)	13.3 (0.86)	21.8 (1.41)	27.8 (1.8)	31.0 (2.0)
Slump flow, in. (mm)	10 min	26.8 (680)	26.8 (680)	26.8 (680)	27.4 (695)	26.4 (670)
	40 min*	26.4 (670)	25.2 (640)	26.4 (670)	27.2 (690)	30.3 (700)
T-20 in. (500 mm), sec	10 min	2.59	1.87	3.15	3.59	4.10
	40 min	3.07	2.31	2.44	3.13	2.81
Visual stability index	10 min	1	1	1	1	0.5
	40 min	1	1	1	1	0.5
Air content, %	10 min	1.8	1.9	0.8	0.4	1.3
	40 min	1.7	2.0	0.5	0.3	0.6
Unit weight, lb/ft^3 (kg/m^3)	10 min	145.8 (2334)	147.3 (2358)	150.6 (2409)	149.9 (2399)	146.7 (2374)
	40 min	146.6 (2346)	147.3 (2357)	150.0 (2400)	152.3 (2436)	149.7 (2395)
Temperature, ^oF (^oC)	10 min	75.2 (24.0)	74.7 (23.7)	76.1 (24.5)	76.5 (24.7)	75.2 (24.0)
	40 min	73.8 (23.2)	72.1 (22.3)	75.7 (24.3)	74.8 (23.8)	75.2 (24.0)
J-Ring, in. (mm)	10 min	26.6 (675)	24.2 (615)	26.2 (665)	26.8 (680)	26.2 (665)
	40 min	25.4 (645)	22.0 (560)	26.2 (665)	26.8 (680)	30.3 (700)
L-box	10 min, sec (h_2/h_1)	3.0 (0.85)	2.9 (0.80)	1.8 (0.82)	5.7 (0.94)	3.09 (0.83)
	40 min, sec (h_2/h_1)	3.0 (0.73)	2.8 (0.69)	3.5 (0.68)	3.9 (0.94)	2.81 (0.90)
Filling capacity, %	10 min	96	93	95	97	99
	40 min	90	84	93	92	99
Rheological Parameter**	τ_o (Pa)	4	37	21	19	3
	μ_p (Pa.s)	258	217	144	151	441
	R^2	0.99	0.99	0.99	0.97	0.99
Column segregation index, %		6.07	2.42	4.30	5.82	3.19
Percent static segregation		16.2	8.0	11.7	23.2	10.5
Max. surface settlement, %		0.26	0.62	0.50	0.50	0.45
Initial setting time, hour		10.2	7.1	11.9	12.8	12.4
Final setting time, hour		11.9	8.5	14.0	15.4	14.9

* Agitation of concrete between 10 and 40 minutes at 6 rpm

** 1 Pa = 1.45×10^{-4} psi

Table G.3 – Fresh properties and rheological parameters of SCC mixtures No. 11 to 14

ure No.		11	12	13	14
Codification		34-843-I/II -S/A54-VMA	34-843 -III20%FA -S/A46-VMA	40-843-I/II -S/A54	40-843- III20%FA -S/A46
HRWRA demand, fl oz/cwt (L/100 kg CM)		30.7 (2.00)	30.7 (2.00)	7.7 (0.50)	15.6 (1.02)
Slump flow, in. (mm)	10 min	26.4 (670)	26.0 (660)	26.8 (680)	26.8 (680)
	40 min*	26.8 (680)	27.2 (690)	23.6 (600)	27.4 (695)
T-20 in. (500 mm), sec	10 min	3.0	3.7	1.9	3.3
	40 min	3.9	2.9	1.6	3.3
Visual stability index	10 min	0.5	0.5	1	1
	40 min	0.5	0.5	1	1
Air content, %	10 min	2.6	1.6	1.8	2.0
	40 min	2.7	1.2	1.7	1.4
Unit weight, lb/ft^3 (kg/m^3)	10 min	149.8 (2398)	150.1 (2402)	147.5 (2362)	147.3 (2357)
	40 min	150.4 (2408)	150.3 (2405)	148.3 (2373)	148.2 (2372)
Temperature, ^{o}F (^{o}C)	10 min	76.5 (24.7)	77.4 (25.2)	77.4 (25.2)	79.2 (26.2)
	40 min	75.7 (24.3)	76.6 (24.8)	76.5 (24.7)	78.4 (25.8)
J-Ring, in. (mm)	10 min	25.0 (635)	25.6 (650)	25.6 (650)	26.4 (670)
	40 min	25.6 (650)	26.8 (680)	20.9 (530)	27.2 (690)
L-box	10 min, sec (h_2/h_1)	4.9 (0.81)	5.4 (0.75)	0.6 (0.77)	1.5 (0.83)
	40 min, sec (h_2/h_1)	6.5 (0.75)	4.8 (0.80)	1.2 (0.60)	1.3 (0.90)
Filling capacity, %	10 min	94	95	92	98
	40 min	94	97	75	98
Rheological Parameter**	τ_o (Pa)	52	25	67	89
	μ_p (Pa.s)	420	256	145	123
	R^2	0.99	0.99	0.99	0.99
Column segregation index, %		2.24	2.16	3.50	2.66
Percent static segregation		10.6	4.1	12.9	12.0
Max. surface settlement, %		0.39	0.43	0.60	0.60
Initial setting time, hour		10.7	12.4	5.7	8.2
Final setting time, hour		12.6	15.1	7.5	9.7

* Agitation of concrete between 10 and 40 minutes at 6 rpm

** 1 Pa = 1.45×10^{-4} psi

Table G.4 – Fresh properties and rheological parameters of SCC mixtures No. 15 to 18

ixture No.		SCC		HPC	
		15	16	17	18
Codification		40-843-I/II -S/A46-VMA	40-843-III20%FA -S/A54-VMA	34-I/II (HPC1)	38-III20%FA (HPC2)
HRWRA demand, fl oz/cwt (L/100 kg CM)		10.7 (0.70)	15.5 (1.00)	6.7 (0.43)	4.2 (0.27)
Slump flow, in. (mm)	10 min	27.4 (695)	26.6 (675)	6.3 (160) **	5.5 (140) **
	40 min*	27.0 (685)	27.6 (700)	2.0 (50) **	2.4 (60) **
T-20 in. (50 cm), sec	10 min	1.7	1.8	-	-
	40 min	2.0	1.1	-	-
Visual stability index	10 min	1	0.5	0	0
	40 min	1	0.5	0	0
Air content, %	10 min	2.9	3.8	3.2	2
	40 min	2.4	3.6	2.0	1.8
Unit weight, lb/ft^3 (kg/m^3)	10 min	144.9 (2319)	137.5 (2200)	150.3 (2405)	149.9 (2399)
	40 min	147.6 (2363)	143.2 (2291)	151.9 (2430)	150.1 (2401)
Temperature, ^{o}F (^{o}C)	10 min	77.5 (25.3)	76.6 (24.8)	77.4 (25.2)	78.4 (25.8)
	40 min	77.0 (25.0)	75.9 (24.4)	76.6 (24.8)	77.4 (25.2)
J-Ring, in. (mm)	10 min	27.2 (690)	25.2 (640)	-	-
	40 min	25.4 (645)	27.2 (690)	-	-
L-box	10 min, sec (h_2/h_1)	0.9 (0.94)	0.8 (0.80)	-	-
	40 min, sec (h_2/h_1)	0.9 (0.90)	0.8 (0.84)	-	-
Filling capacity, %	10 min	98	98	-	-
	40 min	97	98	-	-
Rheological Parameter***	τ_o (Pa)	32	65	575	890
	μ_p (Pa.s)	68	80	351	198
	R^2	0.99	0.99	0.99	0.99
Column segregation index, %		2.43	2.37	0.20	1.83
Percent static segregation		11.8	9.5	1.0	4.9
Max. surface settlement, %		0.59	0.45	0.29	0.33
Initial setting time, hour		8.6	11.6	4.6	4.0
Final setting time, hour		9.9	13.3	5.7	4.9

* Agitation of concrete between 10 and 40 minutes at 6 rpm
** Slump
*** 1 Pa = 1.45×10^{-4} psi

Table G.5 – Fresh properties and rheological parameters of SCC mixtures No. 19 to 22

Mixture No.		AEA SCC			
		19	20	21	22
Codification		34-742-I/II -S/A54	40-742-III20%FA-S/A54	34-843-III20%FA-S/A54	40-843-I/II -S/A54
HRWRA demand, fl oz/cwt (L/100 kg CM)		32.4 (2.09)	19.1 (1.23)	26.5 (1.70)	7.4 (0.48)
AEA, fl oz/cwt (mL/100 kg CM)		28.0 (1.8)	28.0 (1.8)	6.2 (0.4)	24.8 (1.6)
Slump flow, in. (mm)	10 min	26.4 (670)	26.4 (670)	27.2 (690)	26.4 (670)
	40 min*	26.6 (675)	26.2 (665)	27.6 (700)	26.0 (660)
T-20 in. (50 cm), sec	10 min	4.1	1.1	2.3	1.6
	40 min	3.3	1.4	1.9	3.6
Visual stability index	10 min	0	0.5	0	0.5
	40 min	0	0.5	0	0.5
Air content, %	10 min	6.9	7.0	6.4	6.8
	40 min	7.4	7.5	6.5	6.2
Unit weight, lb/ft^3 (kg/m^3)	10 min	142.8 (2285)	141.7 (2267)	141.8 (2269)	140.8 (2252)
	40 min	137.5 (2200)	137.8 (2205)	140.6 (2250)	142.4 (2279)
Temperature, ^{o}F (^{o}C)	10 min	77.7 (25.4)	78.6 (25.9)	78.1 (25.6)	75.6 (24.2)
	40 min	77.0 (25.0)	78.4 (25.8)	77.5 (25.3)	75.0 (24.0)
J-Ring, in. (mm)	10 min	24.4 (620)	25.6 (650)	26.4 (670)	24.6 (625)
	40 min	24.4 (620)	25.4 (645)	27.2 (690)	19.7 (500)
L-box	10 min, sec (h_2/h_1)	3.2 (0.83)	1.2 (0.76)	2.3 (0.80)	1.6 (0.70)
	40 min, sec (h_2/h_1)	2.5 (0.77)	0.7 (0.75)	2.4 (0.82)	1.8 (0.60)
Filling capacity, %	10 min	96	91	89	89
	40 min	94	94	74	74
Rheological Parameter**	τ_o (Pa)	64	130	94	135
	μ_p (Pa.s)	258	69	178	60
	R^2	0.99	0.99	0.99	0.99
Column segregation index, %		2.94	3.95	5.94	1.41
Percent static segregation		13.9	12.9	2.4	1.30
Max. surface settlement, %		0.25	0.28	0.26	0.34
Initial setting time, hour		14.7	8.5	13.0	5.9
Final setting time, hour		17.6	9.9	15.2	7.4

* Agitation of concrete between 10 and 40 minutes at 6 rpm

** 1 Pa = 1.45×10^{-4} psi

APPENDIX H

Bingham Flow Curves and Rheological Parameters of 22 SCC Mixtures Investigated in Factorial Design

(1 Pa = 1.45 × 10^{-4} psi)

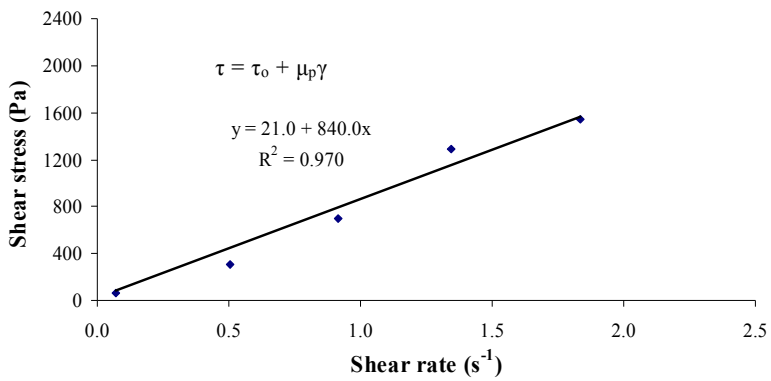

(1) SCC No. 1

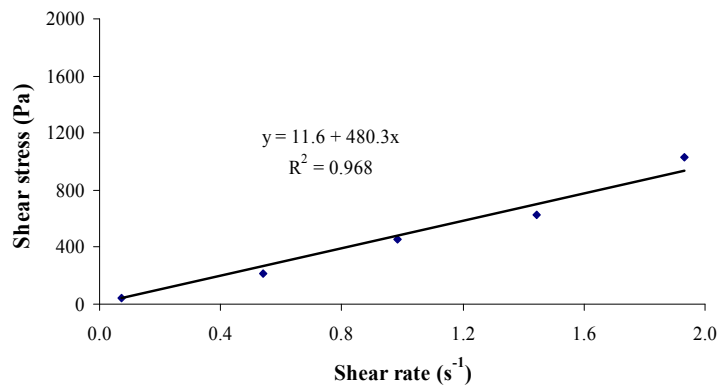

(2) SCC No. 2

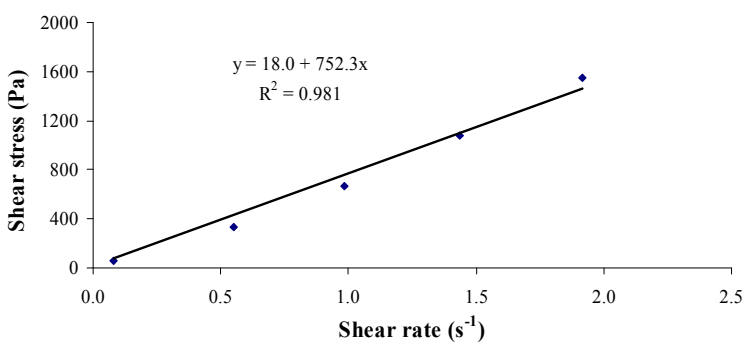

(3) SCC No. 3

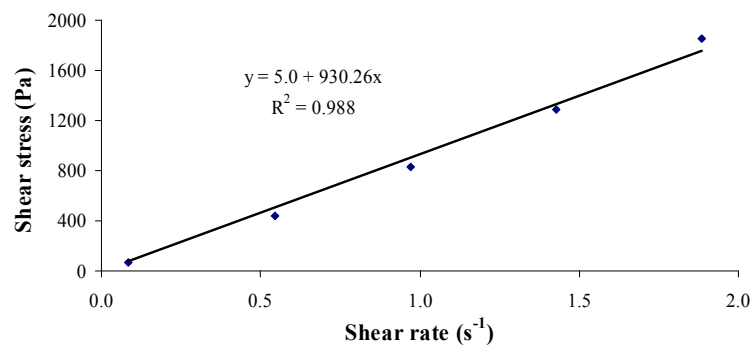

(4) SCC No. 4

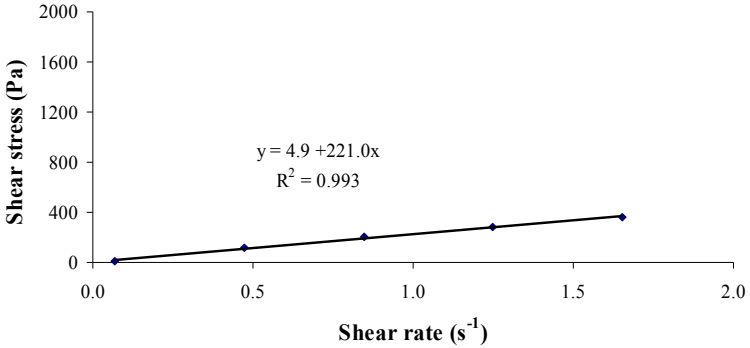

(5) SCC No. 5

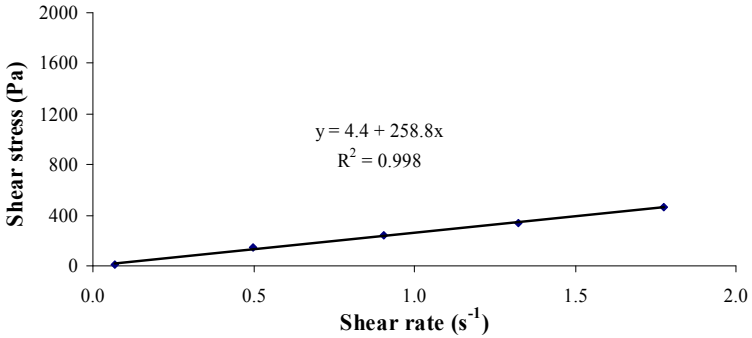

(6) SCC No. 6

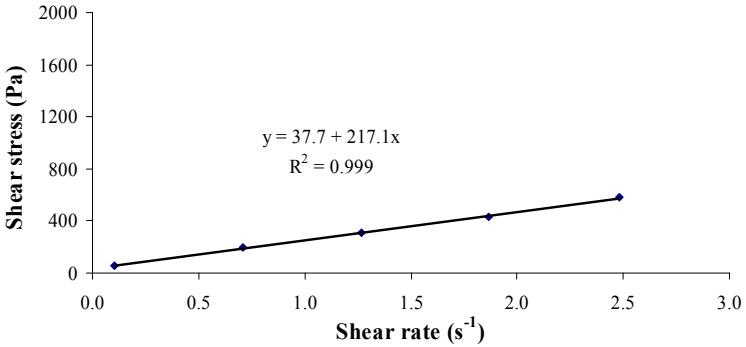

(7) SCC No. 7

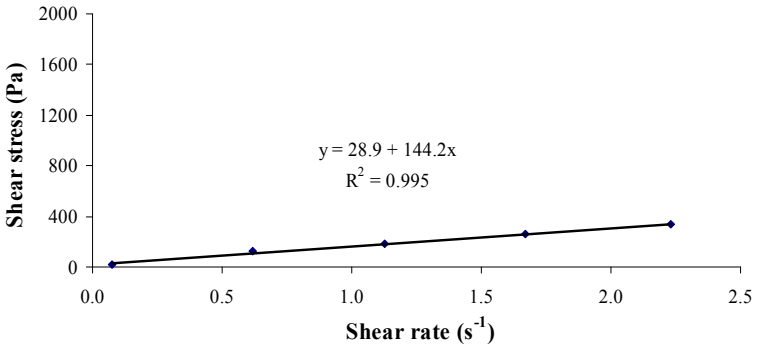

(8) SCC No. 8

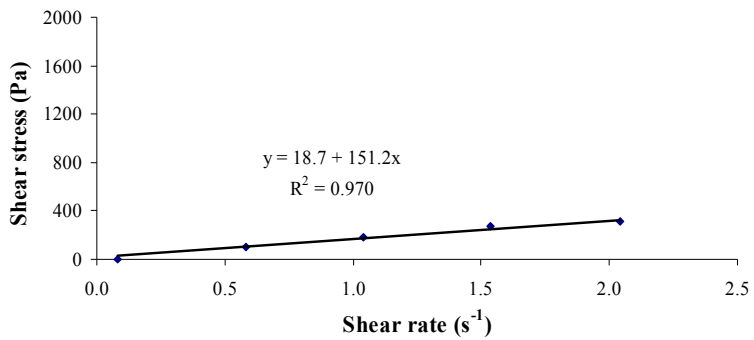

(9) SCC No. 9

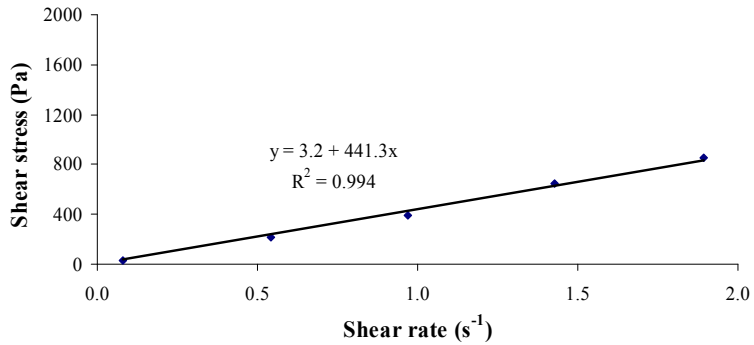

(10) SCC No. 10

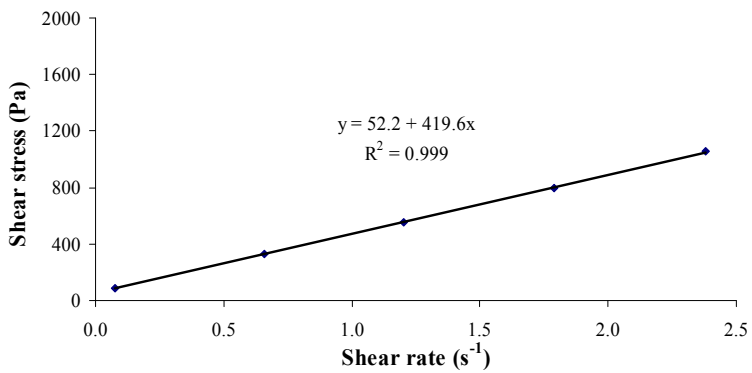

(11) SCC No. 11

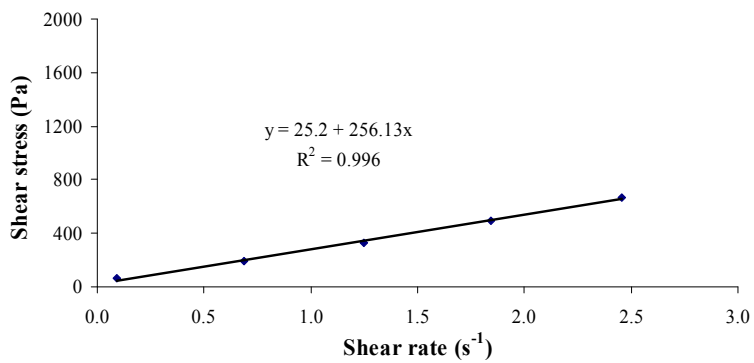

(12) SCC No. 12

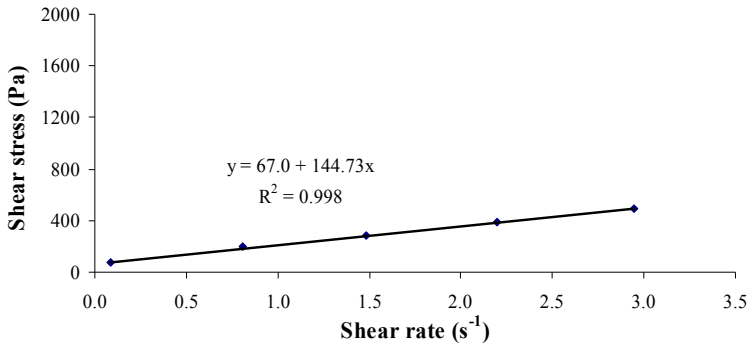

(13) SCC No. 13

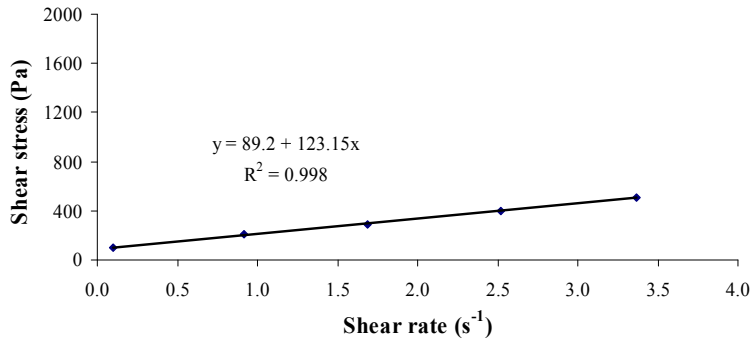

(14) SCC No. 14

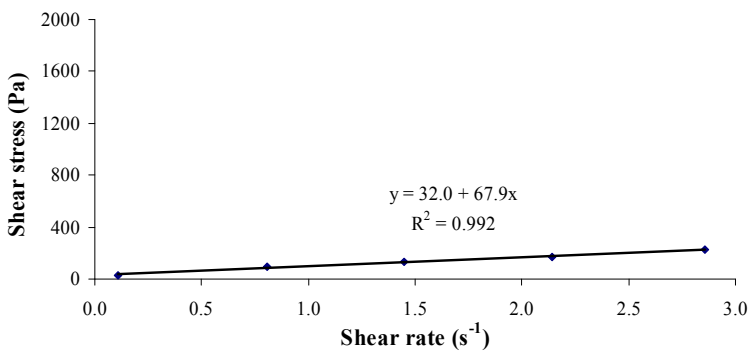

(15) SCC No. 15

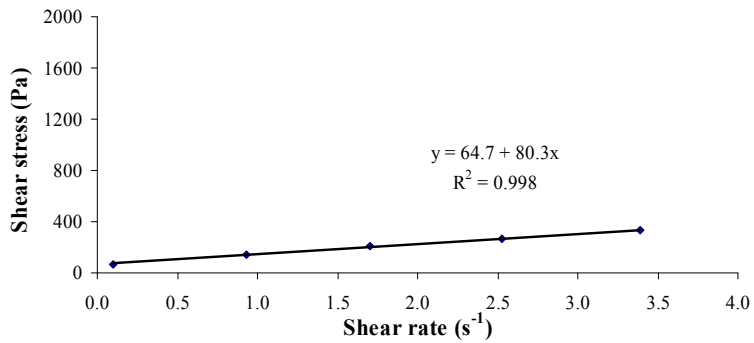

(16) SCC No. 16

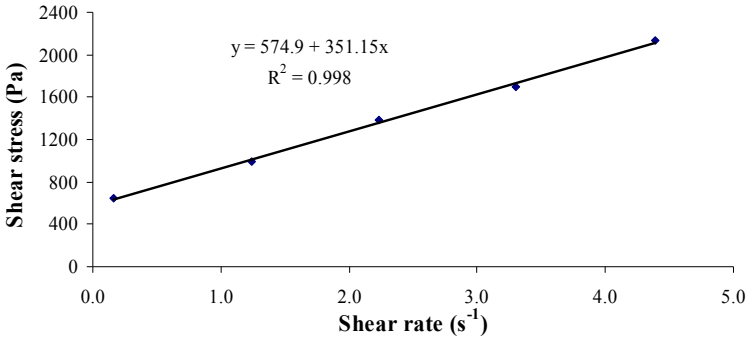

(17) HPC No. 17

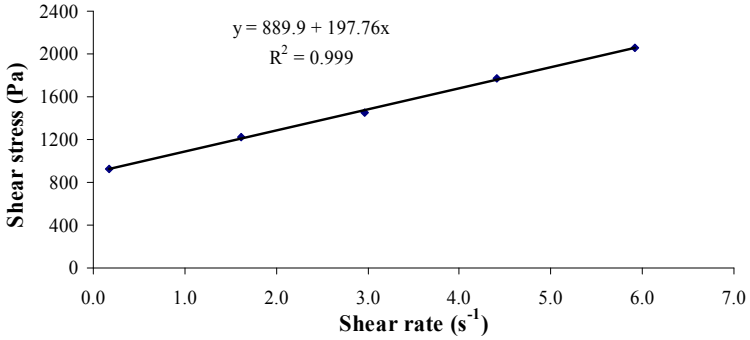

(18) HPC No. 18

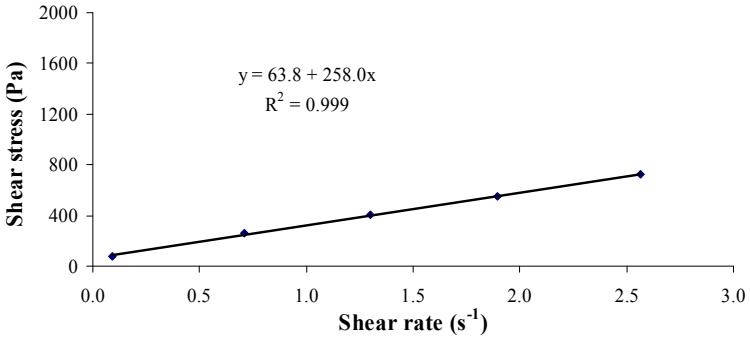

(19) SCC No. 19

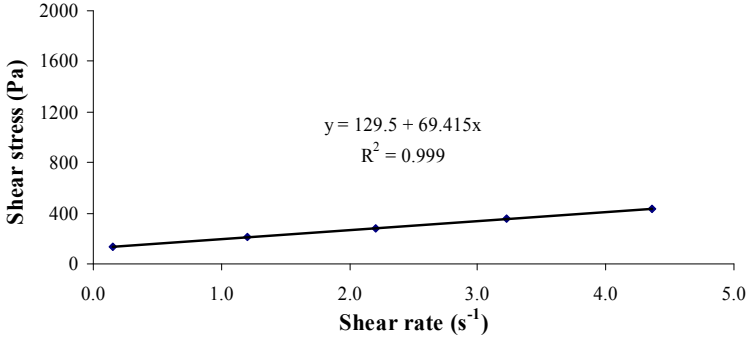

(20) SCC No. 20

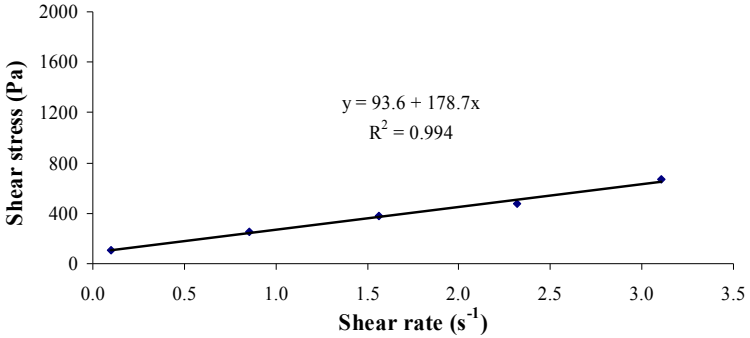

(21) SCC No. 21

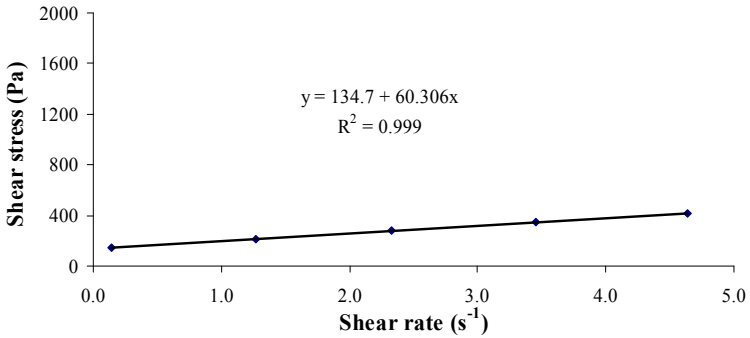

(22) SCC No. 22

APPENDIX I

Breakdown Area Curves of 22 SCC Mixtures Investigated in Factorial Design

(1 Pa = 1.45 × 10^{-4} psi)

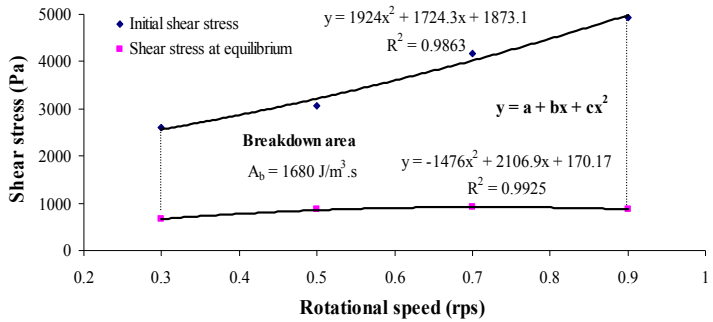

(1) SCC No. 1

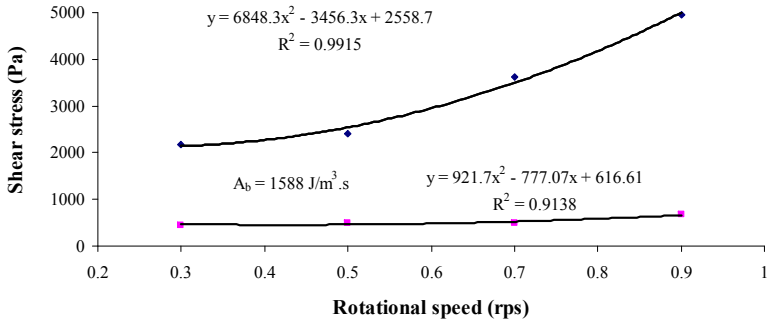

(2) SCC No. 2

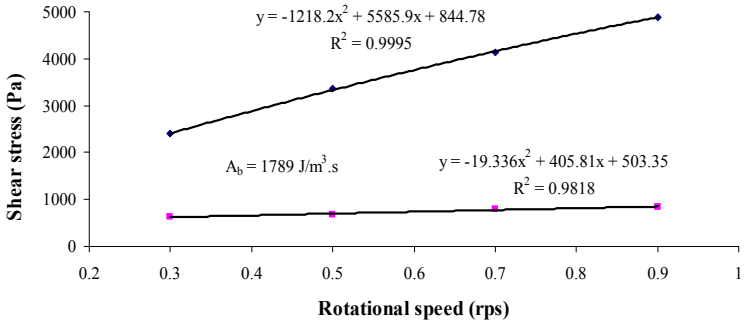

(3) SCC No. 3

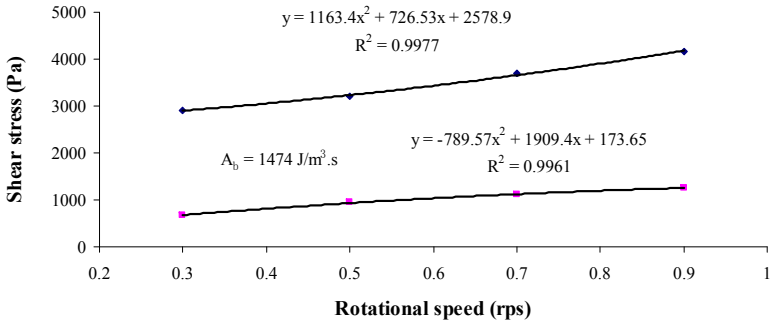

(4) SCC No. 4

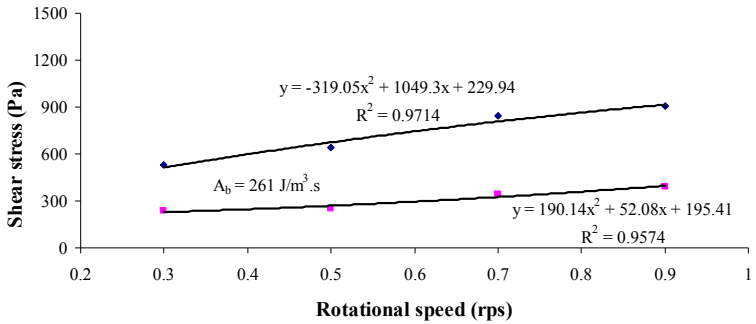

(5) SCC No. 5

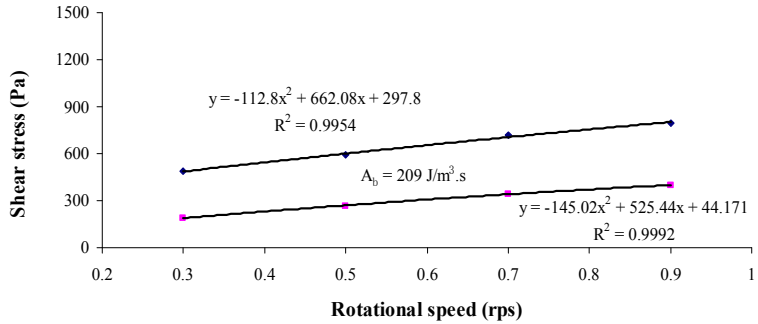

(6) SCC No. 6

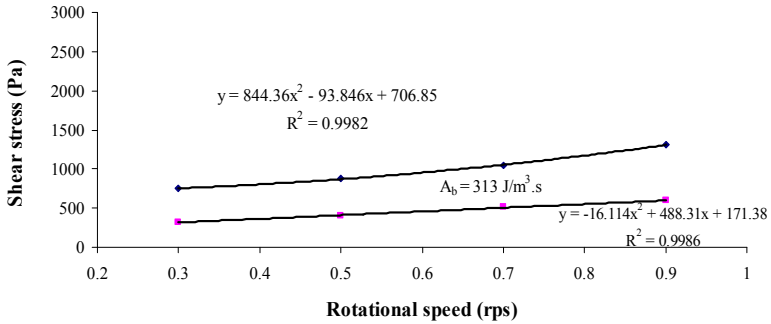

(7) SCC No. 7

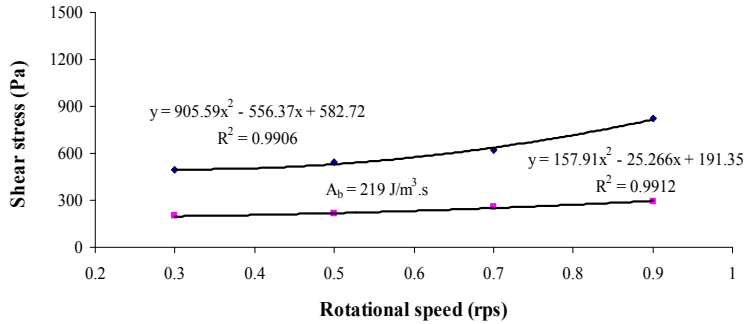

(8) SCC No. 8

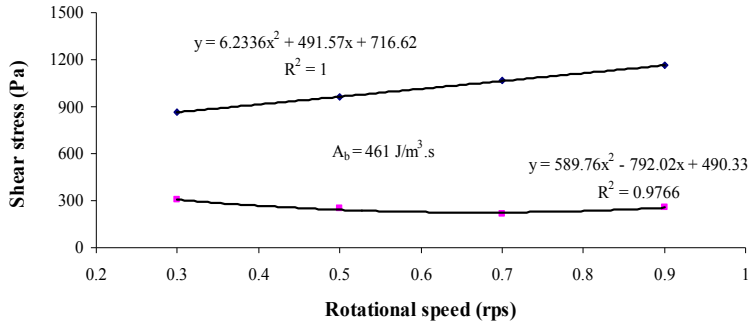

(9) SCC No. 9

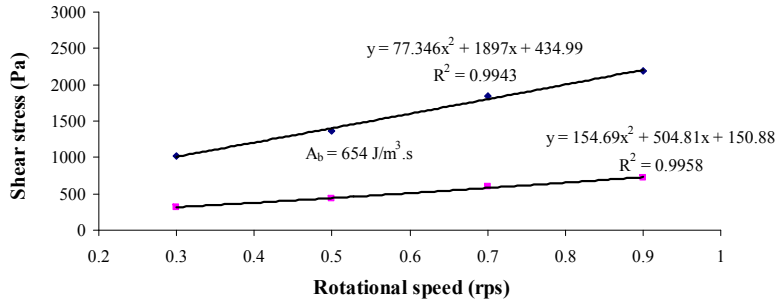

(10) SCC No. 10

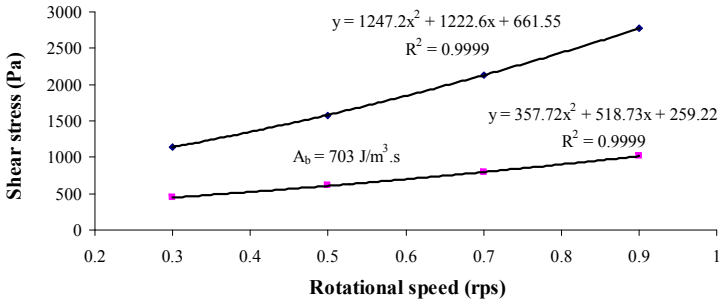

(11) SCC No. 11

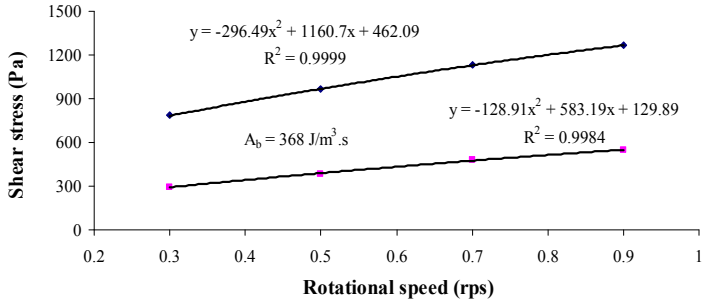

(12) SCC No. 12

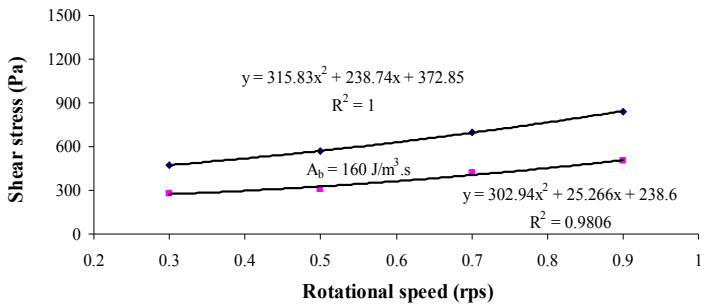

(13) SCC No. 13

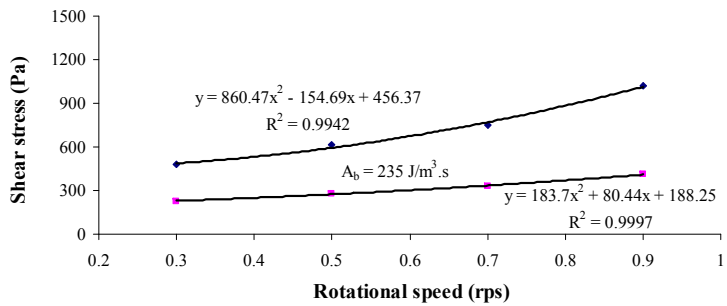

(14) SCC No. 14

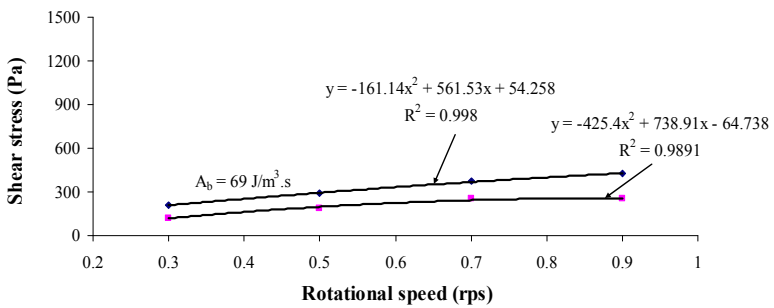

(15) SCC No. 15

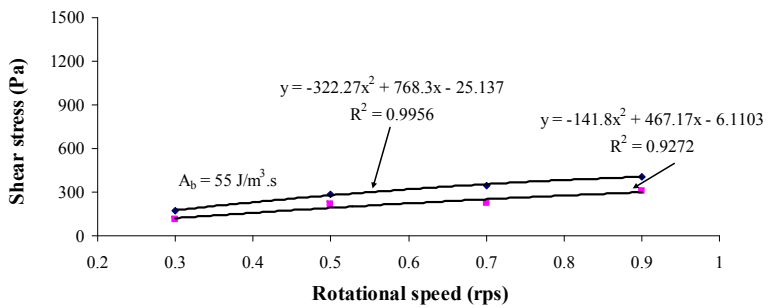

(16) SCC No. 16

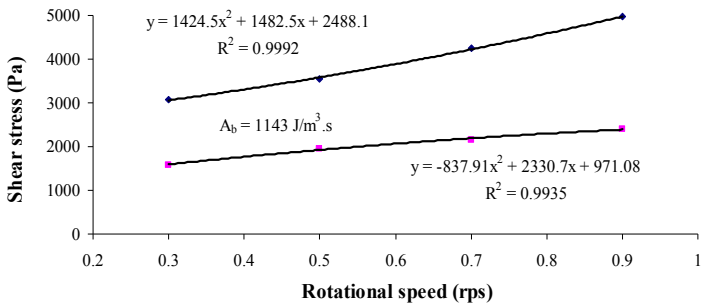

(17) HPC No. 17

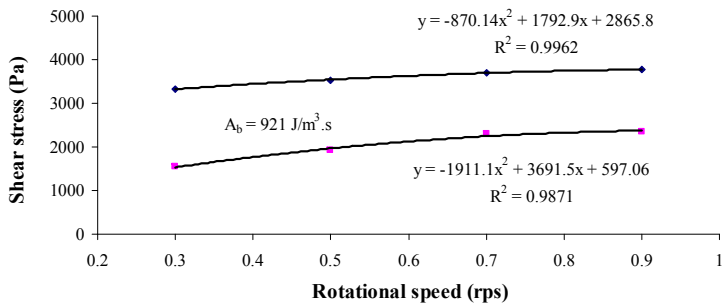

(18) HPC No. 18

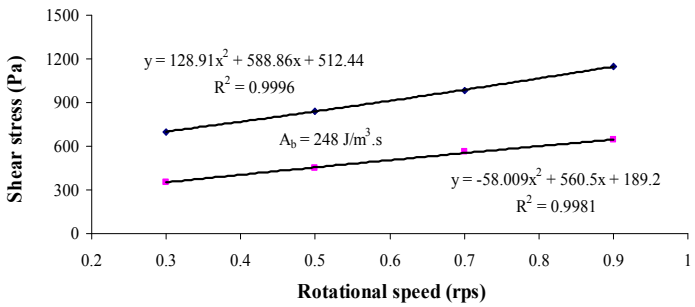

(19) SCC No. 19

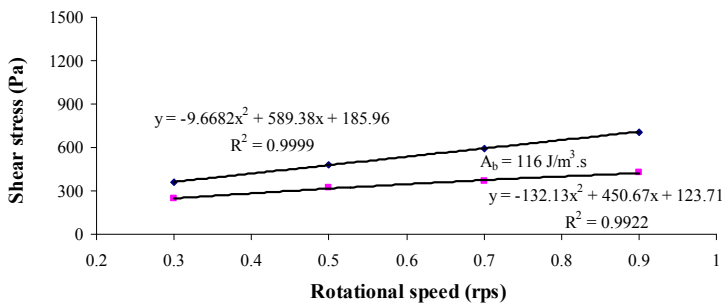

(20) SCC No. 20

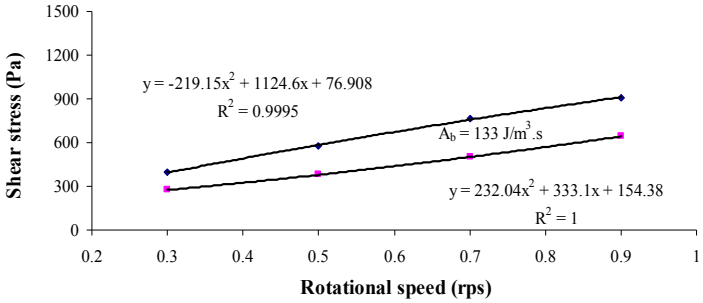

(19) SCC No. 21

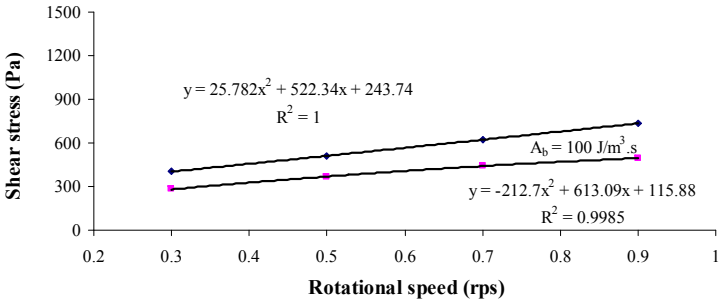

(20) SCC No. 22

APPENDIX J

Mechanical Properties of Mixtures No. 1 to 22 Evaluated in Factorial Design

Table J.1 – Mechanical properties of SCC mixtures No. 1 to 5 at 18 hours and 7 days

Mixture No.				1	2	3	4	5
Codification				34-742-I/II -S/A54	34-742 -III20%FA -S/A46	34-742-I/II-S/A46 -VMA	34-742 -III20%FA -S/A5-VMA	40-742-I/II - S/A46
Compressive strength, psi (MPa)	18 hours	Air-cured**	1	2800 (19.3)*	3170 (21.8)*	2740 (18.9)	1300 (8.9)*	2470 (17.0)
			2	2790 (19.3)*	3220 (22.2)*	2600 (18.0)	1260 (8.7)*	2470 (17.0)
			3	2870 (19.7)*	3300 (22.8)*	2670 (18.4)	1350 (9.3)*	2450 (16.9)
			Mean	2820 (19.4)	3230 (22.3)	2670 (18.4)	1300 (8.9)	2460 (17.0)
			C.O.V. (%)	1.4	2.1	2.4	1.9	0.6
		Steam-cured	1	5370 (37.0)	4830 (33.3)	5440 (37.5)	4500 (31.0)	4640(32.0)
			2	5270 (36.3)	4760 (32.8)	5630 (38.8)	4640 (32.0)	4610 (31.8)
			3	5370 (37.0)	4770 (32.9)	5470 (37.7)	4590 (31.6)	4630 (31.9)
			Mean	5340 (36.8)	4790 (33.0)	5510 (38.0)	4570 (31.5)	4620 (31.9)
			C.O.V. (%)	1.1	0.8	1.8	1.7	0.3
			Max. chamber temperature °F (°C)***	130 (54.4)	134.1 (56.8)	153.7 (67.6)	173.7 (78.6)	159.3 (75.1)
		f_c', $_{steam}$ / f_c', $_{air}$		-	-	2.07	-	1.88
	7 days	Moist-cured	1	7860 (54.2)	6960 (48.0)	8120 (56.0)	7540 (52.0)	6470 (44.6)
			2	7940 (54.8)	6800 (46.9)	7710 (53.1)	7470 (51.5)	6390 (44.1)
			3	7790 (53.7)	7320 (50.5)	7950 (54.8)	7460 (51.4)	6560 (45.2)
			Mean	7860 (54.2)	6970 (48.0)	7920 (54.6)	7490 (51.6)	6470 (44.6)
			C.O.V. (%)	1.0	3.8	2.6	0.5	1.3
Modulus of elasticity, ksi (GPa)	18 hours	Air-cured	1	3050 (21.0)*	3190 (22.0)*	2900 (20.0)	2610 (18.0)*	3190 (22.0)
			2	3050 (21.0)*	3340 (23.0)*	3050 (21.0)	2750 (19.0)*	3050 (21.0)
			Mean	3050 (21.0)	3270 (22.5)	2970 (20.5)	2680 (19.0)	3120 (22.0)
		Steam -cured	1	4930 (34.0)	4500 (31.0)	4930 (34.0)	4210 (29.0)	4210 (29.0)
			2	4640 (32.0)	4500 (31.0)	4930 (34.0)	4210 (29.0)	4500 (31.0)
			Mean	4790 (33.0)	4500 (31.0)	4930 (34.0)	4210 (29.0)	4350 (30.0)
Flexural strength psi (MPa)	7 days	Moist-cured	1	1020 (7.1)	1120 (7.7)	1020 (7.1)	1080 (7.4)	870 (6.0)
			2	970 (6.7)	1030 (7.1)	1080 (7.4)	1080 (7.4)	930(6.4)
			3	1040 (7.2)	1080 (7.4)	1090 (7.5)	1080 (7.4)	810 (5.6)
			Mean	1010 (7.0)	1080 (7.4)	1060 (7.3)	1080 (7.4)	870 (6.0)
			C.O.V. (%)	3.4	4.1	3.3	0.1	7.3

* Values determined at 24 hours since concrete was not fully hardened at 18 hours (air-cured).

** 18 hours in molds covered with wet burlap

*** Chamber temperature refers to ambient temperature inside steam curing chamber determined during steam curing.

Table J.2 – Long-term mechanical properties of SCC mixtures No. 1 to 5 at 28 and 56 days

Mixture No.				1	2	3	4	5
Codification				34-742-I/II -S/A54	34-742 -III20%FA - S/A46	34-742-I/II- S/A46 -VMA	34-742 -III20%FA- S/A54-VMA	40-742-I/II - S/A46
Compressive strength, psi (MPa)	28 days	Moist-cured	1	8560 (59.0)	8250 (56.9)	8730 (60.2)	8670 (59.8)	7860 (54.2)
			2	8230 (56.8)	8600 (59.3)	8460 (58.4)	8660 (59.7)	7380 (50.9)
			3	8780 (60.5)	8900 (61.4)	9070 (62.6)	8840 (60.9)	7470 (51.5)
			Mean	8520 (58.8)	8580 (59.2)	8760 (60.4)	8720 (60.2)	7420 (51.2)
			C.O.V. (%)	3.2	3.8	3.5	1.1	3.5
	56 days		1	8890 (61.3)	9520 (65.6)	10070 (69.4)	9380 (64.7)	7720 (53.2)
			2	8930 (61.6)	8980 (61.9)	10160 (70.1)	9560 (65.9)	7670 (52.9)
			3	8580 (59.2)	8720 (60.2)	10060 (69.3)	9470 (65.3)	7760 (53.5)
			Mean	8800 (60.7)	9070 (62.5)	10100 (69.6)	9470 (65.3)	7720 (53.2)
			C.O.V. (%)	2.2	4.5	0.6	0.9	0.6
Modulus of elasticity, ksi (GPa)	28 days	Moist-cured	1	5370 (37.0)	5800 (40.0)	5800 (40.0)	5510 (38.0)	5080 (35.0)
			2	5370 (37.0)	5500 (38.0)	6090 (42.0)	5370 (37.0)	4930 (34.0)
			Mean	5370 (37.0)	5660 (39.0)	5950 (41.0)	5440 (37.5)	5000 (34.5)
	56 days		1	5800 (40.0)	5950 (41.0)	6240 (43.0)	5510 (38.0)	5220 (36.0)
			2	5660 (39.0)	6090 (42.0)	6090 (42.0)	5510 (38.0)	5370 (37.0)
			Mean	5730 (39.5)	6020 (41.5)	6160 (42.5)	5510 (38.0)	5290 (36.5)
Flexural strength psi (MPa)	28 days	Moist-cured	1	1080 (7.5)	1240 (8.6)	1170 (8.1)	1100 (7.6)	910 (6.3)
			2	1150 (8.0)	1160 (8.0)	1150 (7.9)	1110 (7.7)	890 (6.1)
			3	1150 (8.0)	1320 (9.1)	1190 (8.2)	1230 (8.5)	860 (5.9)
			Mean	1130 (7.8)	1240 (8.6)	1170 (8.1)	1150 (7.9)	880 (6.1)
			C.O.V. (%)	3.6	6.8	2.0	6.0	2.9
	56 days	Moist-cured	1	1290 (8.9)	1220 (8.4)	1270 (8.8)	1150 (7.9)	970 (6.7)
			2	1360 (9.4)	1320 (9.1)	1220 (8.4)	1250 (8.6)	950 (6.6)
			3	1340 (9.2)	1290 (8.9)	1240 (8.6)	1190 (8.2)	920 (6.4)
			Mean	1330 (9.2)	1270 (8.8)	1240 (8.6)	1200 (8.3)	950 (6.5)
			C.O.V. (%)	2.6	4.1	2.0	4.0	2.4

Table J.3 – Mechanical properties of SCC mixtures No. 6 to 10 at 18 hours and 7 days

Mixture No.				6	7	8	9	10
Codification				40-742 -III20%FA -S/A54	40-742-I/II -S/A54 -VMA	40-742 -III20%FA -S/A46 -VMA	34-843-I/II -S/A46	34-843 -III20%FA -S/A54
Compressive strength, psi (MPa)	18 hours	Air-cured**	1	1220 (8.4)	1620 (11.2)	1330 (9.2)	3710 (25.6)*	3350 (23.1)*
			2	1090 (7.5)	1620 (11.2)	1330 (9.1)	3610 (24.9)*	3280 (22.6)*
			3	1220 (8.4)	1710 (11.8)	1570 (9.7)	3990 (27.5)*	3490 (24.1)*
			Mean	1180 (8.1)	1650 (11.4)	1410 (9.3)	3770 (26)	3380 (23.3)
			C.O.V. (%)	6.6	3.0	3.3	5.3	3.2
		Steam-cured	1	4870 (33.6)	4050 (27.9)	4540 (31.3)	5170 (35.7)	4880 (33.6)
			2	4790 (33.0)	4030 (27.8)	4770 (32.9)	5010 (34.5)	4790 (33.0)
			3	4840 (33.4)	4150 (28.6)	4540 (31.3)	5090 (35.1)	5030 (34.7)
			Mean	4840 (33.3)	4080 (28.1)	4620 (31.8)	5090 (35.1)	4900 (33.8)
			C.O.V. (%)	0.8	1.5	2.9	1.6	2.5
			Max. chamber temperature °F (°C)***	169.7 (76.5)	134.2 (56.8)	153.9 (67.7)	150.1 (65.6)	147.2 (64.0)
	$f_c'_{,steam} / f_c'_{,air}$			4.11	2.46	3.42	-	-
	7 days	Moist-cured	1	6830 (47.1)	5860 (40.4)	7140 (49.2)	7470 (51.5)	8070 (55.6)
			2	6680 (46.1)	6030 (41.6)	7070 (48.8)	7480 (51.6)	8190 (56.5)
			3	6590 (45.5)	6170 (42.6)	7370 (50.8)	7550 (52.1)	7980 (55.0)
			Mean	6700 (46.2)	6020 (41.5)	7200 (49.6)	7500 (51.7)	8080 (55.7)
			C.O.V. (%)	1.8	2.6	2.2	0.6	1.3
Modulus of elasticity, ksi (GPa)	18 hours	Air-cured	1	2610 (18.0)	3190 (22.0)	3190 (22.0)	3480 (24.0)*	3340 (23.0)*
			2	2760 (19.0)	3190 (22.0)	3190 (22.0)	3480 (24.0)*	3050 (21.0)*
			Mean	2680 (19.0)	3190 (22.0)	3190 (22.0)	3480 (24.0)	3190 (22.0)*
		Steam-cured	1	4350 (30.0)	4500 (31.0)	4500 (31.0)	4790 (33.0)	4640 (32.0)
			2	4030 (29.0)	4350 (30.0)	4500 (31.0)	4640 (32.0)	4500 (31.0)
			Mean	4280 (29.5)	4420 (30.5)	4500 (31.0)	4710 (32.5)	4570 (31.5)
Flexural strength psi (MPa)	7 days	Moist-cured	1	1460 (10.0)	1310 (9.0)	990 (6.8)	960 (6.6)	1540 (10.6)
			2	1650 (11.4)	1490 (10.3)	1030 (7.1)	990 (6.8)	1560 (10.7)
			3	1500 (10.3)	1290 (8.9)	1030 (7.1)	1010 (7.0)	1540 (10.6)
			Mean	1540 (10.6)	1360 (9.4)	1010 (7.0)	990 (6.8)	1550 (10.7)
			C.O.V. (%)	6.8	8.2	2.4	2.7	0.6

* Values determined at 24 hours since concrete was not fully hardened at 18 hours (air-cured).

** 18 hours in molds covered with wet burlap

*** Chamber temperature refers to ambient temperature inside steam curing chamber determined during steam curing.

Table J.4 – Long-term mechanical properties of SCC mixtures No. 6 to 10 at 28 and 56 days

Mixture No.				6	7	8	9	10
Codification				40-742-III20%FA -S/A54	40-742-I/II - S/A54 -VMA	40-742-III20%FA -S/A46-VMA	34-843-I/II -S/A46	34-843-III20%FA -S/A54
Compressive strength, psi (MPa)	28 days	Moist-cured	1	8040 (55.4)	7470 (51.5)	8040 (55.4)	8900 (61.5)	9490 (65.4)
			2	7650 (52.8)	7020 (48.4)	8530 (58.8)	9070 (62.5)	9270 (63.9)
			3	7880 (54.4)	7180 (49.5)	7940 (54.8)	9090 (62.6)	9440 (64.8)
			Mean	7860 (54.2)	7230 (49.8)	8170 (56.3)	9030 (62.2)	9400 (64.8)
			C.O.V. (%)	2.4	3.1	3.9	1.0	1.2
	56 days		1	8650 (59.6)	7840 (54.1)	9410 (64.9)	9920 (68.4)	11360 (78.4)
			2	8860 (61.1)	8420 (58.0)	9940 (68.5)	9790 (67.5)	11120 (76.7)
			3	9040 (62.3)	7990 (55.1)	9340 (64.4)	9970 (68.7)	11440 (78.9)
			Mean	8850 (61.0)	8080 (55.7)	9560 (66.9)	9890 (68.2)	11310 (78.0)
			C.O.V. (%)	2.2	3.7	3.4	0.9	1.5
Modulus of elasticity, ksi (GPa)	28 days	Moist-cured	1	5080 (35.0)	4930 (34.0)	5370 (37.0)	5660 (39.0)	5660 (39.0)
			2	5220 (36.0)	4930 (34.0)	5510 (38.0)	5800 (40.0)	5660 (39.0)
			Mean	5150 (35.5)	4930 (34.0)	5440 (37.5)	5730 (39.5)	5660 (39.0)
	56 days		1	5370 (37.0)	4930 (34.0)	5660 (39.0)	5950 (41.0)	5950 (41.0)
			2	5510 (38.0)	4930 (34.0)	5660 (39.0)	5950 (41.0)	5800 (40.0)
			Mean	5440 (38.0)	4930 (34.0)	5660 (39.0)	5950 (41.0)	5870 (40.5)
Flexural strength psi (MPa)	28 days	Moist-cured	1	1030 (7.1)	980 (6.8)	810 (5.6)	820 (5.6)	1220 (8.4)
			2	1050 (7.2)	940 (6.5)	820 (5.7)	860 (5.9)	1260 (8.7)
			3	1120 (7.8)	990 (6.8)	800 (5.5)	850 (5.8)	1220 (8.4)
			Mean	1070 (7.3)	970 (6.7)	810 (5.6)	840 (5.8)	1240 (8.5)
			C.O.V. (%)	4.9	3.1	1.4	2.6	1.6
	56 days		1	1100 (7.6)	1060 (7.3)	910 (6.3)	940 (6.5)	1510 (10.4)
			2	1110 (7.7)	950 (6.6)	860 (6.0)	1080 (7.5)	1430 (9.8)
			3	1030 (7.1)	1000 (6.9)	920 (6.3)	1110 (7.6)	1550 (10.7)
			Mean	1080 (7.4)	1000 (6.9)	900 (6.2)	1040 (7.2)	1500 (10.3)
			C.O.V. (%)	4.5	5.3	3.4	8.8	4.2

Table J.5 – Mechanical properties of SCC mixtures No. 11 to 15 at 18 hours and 7 days

Mixture No.				11	12	13	14	15
Codification				34-843-I/II -S/A54 -VMA	34-843-III20%FA -S/A46-VMA	40-843-I/II -S/A54	40-843-III20%FA -S/A46	40-843-I/II -S/A46 -VMA
Compressive strength, psi (MPa)	18 hours	Air-cured**	1	2970 (20.5)*	3110 (21.4)*	3140 (21.6)	4060 (27.8)	2420 (16.7)
			2	2870 (19.8)*	3270 (22.5)*	3000 (20.7)	3790 (26.1)	2410 (16.6)
			3	2870 (19.8)*	3480 (24.0)*	3160 (21.8)	4100 (28.2)	2570 (17.7)
			Mean	2910 (20.0)	3290 (22.6)	3098 (21.4)	3980 (27.5)	2470 (17.0)
			C.O.V. (%)	2.1	5.7	2.9	4.2	3.4
		Steam-cured	1	5360 (36.9)	4830 (33.3)	4530 (31.3)	4380 (30.2)	4300 (29.7)
			2	5180 (35.7)	4770 (32.9)	4780 (33.0)	4530 (31.2)	4460 (30.8)
			3	5380 (37.1)	5000 (34.4)	4500 (31.1)	4540 (31.3)	4320 (29.8)
			Mean	5300 (36.6)	4870 (33.5)	4610 (31.8)	4480 (30.9)	4360 (30.1)
			C.O.V. (%)	2.0	2.4	3.3	2.0	2.0
			Max. chamber temperature °F (°C)***	157.6 (69.8)	134.1 (56.7)	152.1 (66.7)	152.2 (66.8)	154.9 (68.3)
		f_c', steam / f_c', air		-	-	-	1.13	1.77
	7 days	Moist-cured	1	8290 (57.2)	8400 (57.9)	6470 (44.6)	5630 (38.9)	5370 (37.0)
			2	8410 (58.0)	8250 (56.9)	6540 (45.1)	6060 (41.8)	5690 (39.3)
			3	8310 (57.3)	8460 (58.3)	6540 (45.1)	5880 (40.6)	5300 (36.6)
			Mean	8340 (57.5)	8370 (57.7)	6520 (44.9)	5860 (40.4)	5460 (37.6)
			C.O.V. (%)	0.8	1.3	0.7	3.6	3.8
Modulus of elasticity, ksi (GPa)	18 hours	Air-cured	1	3050 (21.0)*	3770 (26.0)*	3920 (27.0)	3920 (27.0)	3190 (22.0)
			2	3050 (21.0)*	3630 (25.0)*	3770 (26.0)	3920 (27.0)	3190 (22.0)
			Mean	3050 (21.0)	3700 (25.5)	3840 (26.5)	3920 (27.0)	3190 (22.0)
		Steam-cured	1	4790 (33.0)	4930 (34.0)	4060 (28.0)	3920 (27.0)	4060 (28.0)
			2	4790 (33.0)	5080 (35.0)	4210 (29.0)	4060 (28.0)	4060 (28.0)
			Mean	4790 (33.0)	5000 (34.5)	4130 (28.5)	3990 (27.5)	4060 (28.0)
Flexural strength psi (MPa)	7 days	Moist-cured	1	1030 (7.1)	1000 (6.9)	920 (6.3)	620 (4.2)	700 (4.8)
			2	1040 (7.2)	940 (6.5)	970 (6.7)	700 (4.8)	700 (4.9)
			3	1050 (7.2)	880 (6.1)	960 (6.6)	690 (4.8)	640 (4.4)
			Mean	1040 (7.2)	940 (6.5)	950 (6.5)	670 (4.6)	680 (4.7)
			C.O.V. (%)	0.9	6.4	3.1	7.1	5.3

* Values determined at 24 hours since concrete was not fully hardened at 18 hours (air-cured).

** 18 hours in molds covered with wet burlap

*** Chamber temperature refers to ambient temperature inside steam curing chamber determined during steam curing.

Table J.6 – Long-term mechanical properties of SCC mixtures No. 11 to 15 at 28 and 56 days

Mixture No.				11	12	13	14	15
Codification				34-843-I/II -S/A54 -VMA	34-843-III20%FA -S/A46-VMA	40-843-I/II -S/A54	40-843-III20%FA -S/A46	40-843-I/II -S/A46 -VMA
Compressive strength, psi (MPa)	28 days	Moist-cured	1	9280 (64.0)	10190 (70.3)	7130 (49.2)	7730 (53.3)	6500 (44.8)
			2	9500 (65.5)	10410 (71.8)	7540 (52.0)	8010 (55.2)	7210 (49.7)
			3	9270 (64.5)	9960 (68.7)	7620 (52.5)	8260 (56.9)	6980 (48.1)
			Mean	9350 (64.5)	10190 (70.2)	7430 (51.2)	8000 (55.2)	6900 (47.5)
			C.O.V. (%)	1.4	2.2	3.5	3.3	5.3
	56 days		1	10190 (70.3)	10880 (75.0)	8420 (58.0)	8570 (59.1)	7860 (54.2)
			2	9930 (68.5)	11030 (76.0)	8210 (56.6)	8830 (60.9)	8000 (55.2)
			3	9950 (68.6)	10890 (75.1)	8700 (6000)	9090 (62.7)	8250 (56.9)
			Mean	10020 (69.1)	10930 (75.4)	8440 (58.2)	8830 (60.9)	8040 (55.4)
			C.O.V. (%)	1.5	0.8	2.9	3.0	2.5
Modulus of elasticity, ksi (GPa)	28 days	Moist-cured	1	5510 (38.0)	5950 (41.0)	4930 (34.0)	5370 (37.0)	4930 (34.0)
			2	5510 (38.0)	5950 (41.0)	4930 (34.0)	5370 (37.0)	4930 (34.0)
			Mean	5510 (38.0)	5950 (41.0)	4930 (34.0)	5370 (37.0)	4930 (34.0)
	56 days		1	5660 (39.0)	6090 (42.0)	5080 (35.0)	5510 (38.0)	4930 (34.0)
			2	5660 (39.0)	5950 (41.0)	5080 (35.0)	5660 (39.0)	5220 (36.0)
			Mean	5660 (39.0)	6020 (41.5)	5080 (35.0)	5580 (38.5)	5080 (35.0)
Flexural strength psi (MPa)	28 days	Moist-cured	1	1120 (7.7)	1160 (8.0)	1120 (7.7)	670 (4.6)	700 (4.8)
			2	1090 (7.5)	1180 (8.0)	890 (6.1)	740 (5.1)	730 (5.1)
			3	1050 (7.3)	1080 (7.5)	1040 (7.2)	680 (4.7)	730 (5.0)
			Mean	1090 (7.5)	1140 (7.9)	1020 (7.0)	700 (4.8)	730 (5.0)
			C.O.V. (%)	3.1	4.5	11.7	5.7	2.4
	56 days		1	1160 (8.0)	1150 (8.0)	1100 (7.6)	1080 (7.5)	1070 (7.4)
			2	1160 (8.0)	1180 (8.2)	1030 (7.1)	1010 (7.0)	1070 (7.4)
			3	1100 (7.6)	1200 (8.3)	1110 (7.7)	1010 (7.0)	960 (6.6)
			Mean	1140 (7.9)	1180 (8.1)	1080 (7.5)	1030 (7.1)	1030 (7.1)
			C.O.V. (%)	3.1	2.2	4.1	3.9	6.0

Table J.7 – Mechanical properties of SCC mixtures No. 16 to 18 at 18 hours and 7 days

Mixture No.				SCC	HPC	
				16	17	18
Codification				40-843-III -S/A54-VMA	34-I/II (HPC1)	38-III20%FA (HPC2)
Compressive strength, psi (MPa)	18 hours	Air-cured*	1	2430 (16.7)	4110 (28.4)	4510 (31.1)
			2	2600 (17.9)	4320 (29.8)	4570 (31.5)
			3	2450 (16.9)	4230 (29.2)	4550 (31.4)
			Mean	2490 (17.2)	4220 (29.1)	4540 (31.3)
			C.O.V. (%)	3.7	2.5	0.7
		Steam-cured	1	4060 (28.0)	5180 (35.7)	4500 (31.0)
			2	3990 (27.5)	5070 (35.0)	4610 (31.8)
			3	4170 (28.8)	5140 (35.4)	4790 (33.0)
			Mean	4070 (28.1)	5130 (35.4)	4630 (31.9)
			C.O.V. (%)	2.2	1.1	3.2
			Max. chamber temperature °F (°C)**	146.1 (63.4)	152.6 (67.0)	144.7 (62.6)
		f_c', steam / f_c', air		1.64	1.22	1.02
	7 days	Moist-cured	1	5580 (38.5)	6890 (47.5)	6740 (46.5)
			2	5720 (39.5)	6960 (48.0)	6680 (46.0)
			3	5680 (39.2)	6900 (47.6)	6590 (45.4)
			Mean	5660 (39.0)	6920 (47.7)	6670 (46.0)
			C.O.V. (%)	1.3	0.6	1.1
Modulus of elasticity, ksi (GPa)	18 hours	Air-cured	1	3050 (21.0)	4060 (28.0)	4640 (32.0)
			2	2900 (20.0)	4060 (28.0)	4640 (32.0)
			Mean	2970 (20.5)	4060 (28.0)	4640 (32.0)
		Steam-cured	1	3340 (23.0)	4930 (34.0)	4640 (32.0)
			2	3630 (25.0)	4640 (32.0)	4790 (33.0)
			Mean	3480 (24.0)	4790 (33.0)	4710 (32.5)
Flexural strength psi (MPa)	7 days	Moist-cured	1	750 (5.2)	850 (5.8)	770 (5.3)
			2	730 (5.1)	800 (5.5)	730 (5.1)
			3	740 (5.1)	780 (5.4)	730 (5.0)
			Mean	740 (5.1)	810 (5.6)	750 (5.1)
			C.O.V. (%)	1.4	4.3	3.3

* 18 hours in molds covered with wet burlap

* Chamber temperature refers to ambient temperature inside steam curing chamber determined during steam curing.

Table J.8 – Long-term mechanical properties of SCC mixtures No. 16 to 18 at 28 and 56 days

Mixture No.				SCC	HPC	
				16	17	18
Codification				40-843-III -S/A54 -VMA	34-I/II (HPC1)	38-III20%FA (HPC2)
Compressive strength, psi (MPa)	28 days	Moist-cured	1	7060 (48.7)	7790 (53.7)	7860 (54.2)
			2	6660 (45.9)	8210 (56.6)	7710 (53.2)
			3	6980 (48.2)	8190 (56.5)	7720 (53.3)
			Mean	6900 (47.6)	8070 (55.6)	7770 (53.5)
			C.O.V. (%)	3.1	2.9	1.1
	56 days		1	7760 (53.5)	9280 (64.0)	7850 (57.5)
			2	7880 (54.3)	8410 (58.0)	8010 (55.6)
			3	7510 (51.8)	8900 (61.3)	7850 (59.1)
			Mean	7720 (53.2)	8860 (61.1)	8320 (57.4)
			C.O.V. (%)	2.4	5.0	3.0
Modulus of elasticity, ksi (GPa)	28 days	Moist-cured	1	4790 (33.0)	5660 (39.0)	5220 (36.0)
			2	4640 (32.0)	5660 (39.0)	5370 (37.0)
			Mean	4710 (32.5)	5660 (39.0)	5290 (36.5)
	56 days		1	4790 (33.0)	5800 (40.0)	5800 (40.0)
			2	4930 (34.0)	5800 (40.0)	5800 (40.0)
			Mean	4890 (33.5)	5800 (40.0)	5800 (40.0)
Flexural strength psi (MPa)	28 days	Moist-cured	1	740 (5.1)	730 (5.0)	1080 (7.5)
			2	720 (5.0)	680 (4.7)	990 (6.8)
			3	790 (5.5)	770 (5.3)	1070 (7.4)
			Mean	750 (5.2)	720 (5.0)	1050 (7.2)
			C.O.V.(%)	4.9	6.4	5.1
	56 days		1	1160 (8.0)	1060 (7.3)	1170 (8.1)
			2	1020 (7.0)	990 (6.8)	1160 (8.0)
			3	1030 (7.1)	940 (6.5)	1170 (8.1)
			Mean	1070 (7.4)	1000 (6.9)	1170 (8.0)
			C.O.V.(%)	7.1	5.9	0.5

Table J.9 – Mechanical properties of SCC mixtures No. 19 to 22 at 18 hours and 7 days

Mixture No.				AEA SCC			
				19	20	21	22
Codification				34-742-I/II -S/A54	40-742-III20%FA -S/A54	34-843-III20%FA -S/A54	40-843-I/II -S/A54
Compressive strength, psi (MPa)	18 hours	Air-cured*	1	2120 (14.6)	3090 (21.3)	2670 (18.4)	2920 (20.1)
			2	2170 (15.0)	3130 (21.6)	2680 (18.5)	2990 (20.6)
			3	1960 (14.4)	2790 (19.3)	2670 (18.4)	2900 (20.0)
			Mean	2080 (14.4)	3000 (20.7)	2670 (18.4)	2930 (20.2)
			C.O.V. (%)	5.4	6.1	0.2	1.6
		Steam cured	1	4240 (29.3)	3920 (27.0)	3640 (25.1)	4090 (28.2)
			2	4220 (29.1)	3820 (26.3)	3600 (24.9)	4180 (28.8)
			3	4320 (29.8)	3970 (27.4)	3600 (24.9)	4280 (29.5)
			Mean	4260 (29.4)	3900 (26.9)	3620 (24.9)	4180 (28.8)
			C.O.V. (%)	1.2	2.0	0.5	2.3
			Max. chamber temperature °F (°C)**	125.4 (51.9)	137.7 (58.7)	135.1 (57.3)	134.1 (56.7)
		f_c', steam / f_c', air		2.05	1.30	1.35	1.43
	7 days	Moist-cured	1	5740 (39.6)	5560 (38.3)	6060 (41.8)	5450 (37.6)
			2	5790 (39.9)	5430 (37.5)	6040 (41.7)	5570 (38.4)
			3	5610 (38.7)	5460 (37.7)	5700 (39.3)	5210 (35.9)
			Mean	5720 (39.4)	5490 (37.8)	5940 (40.9)	5410 (37.3)
			C.O.V. (%)	1.7	1.2	3.5	3.3
Modulus of elasticity, ksi (Gpa)	18 hours	Air-cured	1	2760 (19.0)	3050 (21.0)	3050 (21.0)	2760 (19.0)
			2	2900 (20.0)	2900 (20.0)	3050 (21.0)	2900 (20.0)
			Mean	2830 (19.5)	2970 (20.5)	3050 (21.0)	2830 (19.5)
		Steam-cured	1	4210 (29.0)	3050 (21.0)	3190 (22.0)	3480 (24.0)
			2	4210 (29.0)	3050 (21.0)	3340 (23.0)	3480 (24.0)
			Mean	4210 (29.0)	3050 (21.0)	3260 (22.5)	3480 (24.0)
Flexural strength psi (MPa)	7 days	Moist-cured	1	590 (4.1)	590 (4.1)	660 (4.6)	610 (4.2)
			2	610 (4.2)	590 (4.1)	630 (4.3)	630 (4.4)
			3	600 (4.1)	610 (4.2)	670 (4.6)	620 (4.3)
			Mean	600 (4.1)	590 (4.1)	650 (4.5)	620 (4.3)
			C.O.V. (%)	1.4	1.6	3.4	1.7

* 18 hours in molds covered with wet burlap

* Chamber temperature refers to ambient temperature inside steam curing chamber determined during steam curing.

Table J.10 – Mechanical properties of SCC mixtures No. 19 to 22 at 28 and 56 days

Mixture No.				19	20	21	22
Codification				34-742-I/II -S/A54	40-742-III20%FA -S/A54	34-843-III20%FA -S/A54	40-843-I/II -S/A54
Compressive strength, psi (MPa)	28 days	Moist-cured	1	6970 (48.1)	6780 (46.8)	7000 (48.3)	6540 (45.1)
			2	6690 (46.1)	6590 (45.4)	6840 (47.2)	6580 (45.4)
			3	6660 (45.9)	6690 (46.2)	7060 (48.7)	6490 (45.1)
			Mean	6770 (46.7)	6690 (46.1)	6970 (48.1)	6540 (45.1)
			C.O.V. (%)	2.6	1.5	1.6	0.7
	56 days		1	7680 (53.0)	7140 (49.2)	8220 (56.7)	7100 (49.0)
			2	7610 (52.4)	7080 (48.8)	7880 (54.3)	7260 (50.1)
			3	7920 (54.6)	7310 (50.4)	8300 (57.2)	6990 (48.2)
			Mean	7740 (53.3)	7180 (49.5)	8130 (56.1)	7120 (49.1)
			C.O.V. (%)	2.1	1.7	2.7	2.0
Modulus of elasticity, ksi (GPa)	28 days	Moist-cured	1	5080 (35.0)	4640 (32.0)	4500 (31.0)	4210 (29.0)
			2	5080 (35.0)	4500 (31.0)	4640 (32.0)	4060 (28.0)
			Mean	5080 (35.0)	4750 (31.5)	4570 (31.5)	4130 (28.5)
	56 days		1	5080 (35.0)	4350 (30.0)	4790 (33.0)	4350 (30.0)
			2	5080 (35.0)	4350 (30.0)	4640 (32.0)	4500 (31.0)
			Mean	5080 (35.0)	4350 (30.0)	4710 (32.5)	4420 (30.5)
Flexural strength psi (MPa)	28 days	Moist-cured	1	1110 (7.6)	920 (6.4)	1090 (7.5)	740 (5.1)
			2	940 (6.5)	1010 (7.0)	1030 (7.1)	720 (5.0)
			3	1000 (6.9)	900 (6.2)	1040 (7.1)	790 (5.5)
			Mean	1020 (7.0)	940 (6.5)	1050 (7.2)	750 (5.2)
			C.O.V. (%)	8.3	6.5	3.2	4.9
	56 days		1	1070 (7.4)	905 (6.2)	1200 (8.3)	1020 (7.1)
			2	1050 (7.2)	960 (6.6)	1190 (8.2)	900 (6.2)
			3	1080 (7.5)	960 (6.6)	1110 (7.7)	950 (6.5)
			Mean	1070 (7.4)	940 (6.5)	1170 (8.0)	960 (6.6)
			C.O.V. (%)	1.5	3.5	3.9	6.5

APPENDIX K

Statistical Models for Fresh and Mechanical Properties

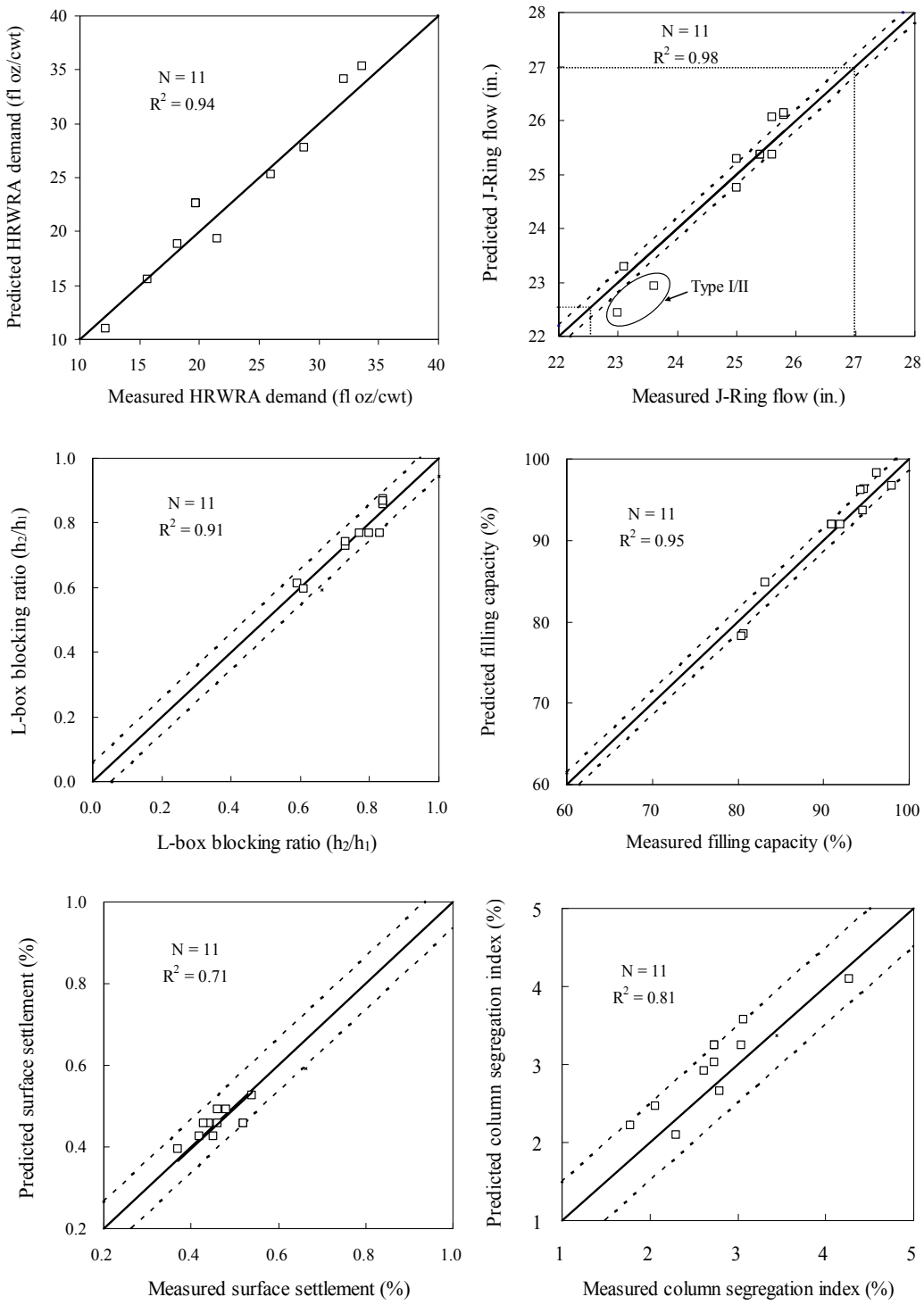

Fig. K.1 − Comparison between predicted and measured workability responses

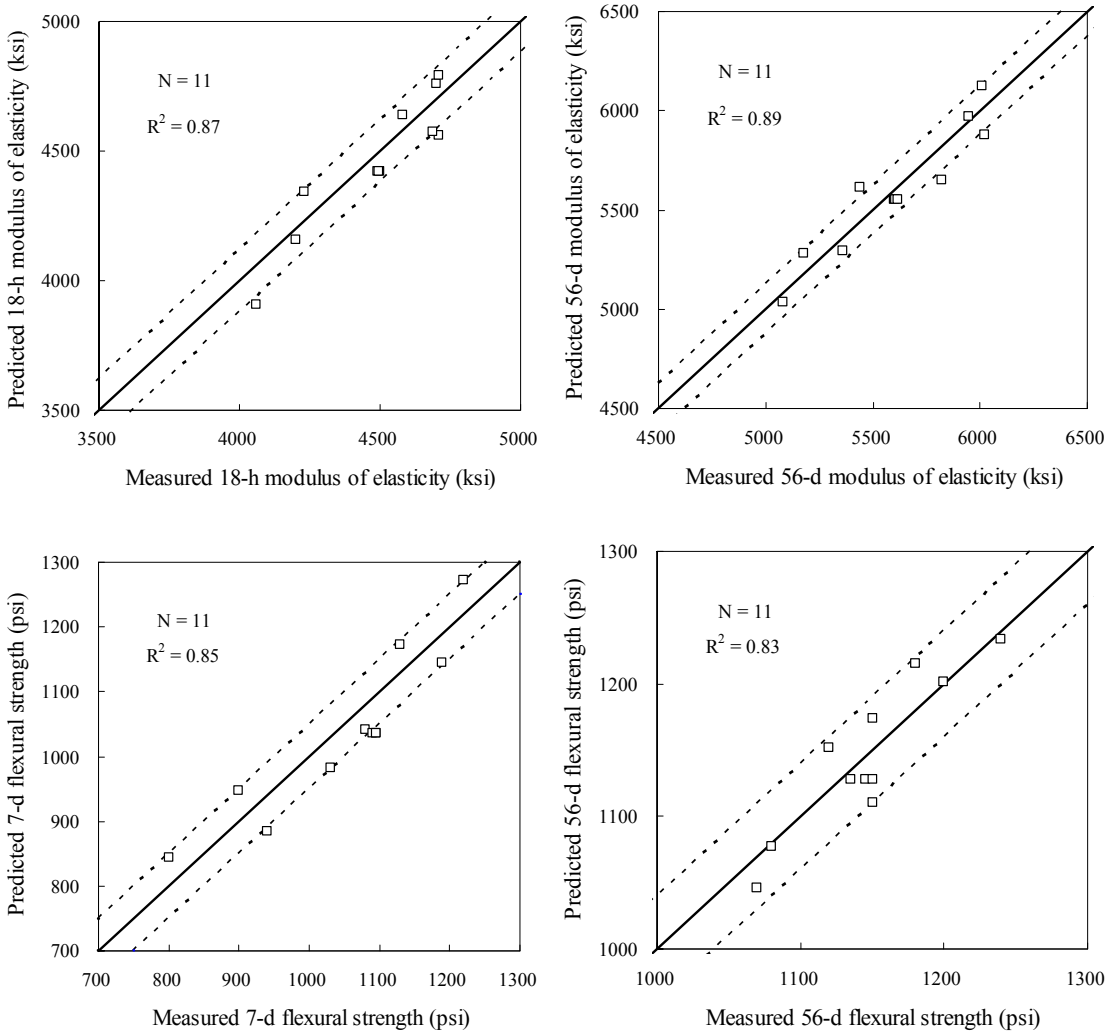

Fig. K.2 – Comparison between predicted and measured mechanical properties

APPENDIX L

Comparisons of Measured and Predicted Drying Shrinkage Strains

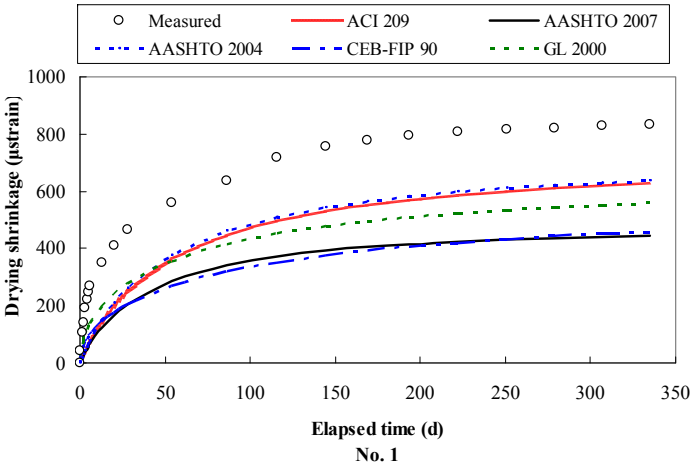

No. 1

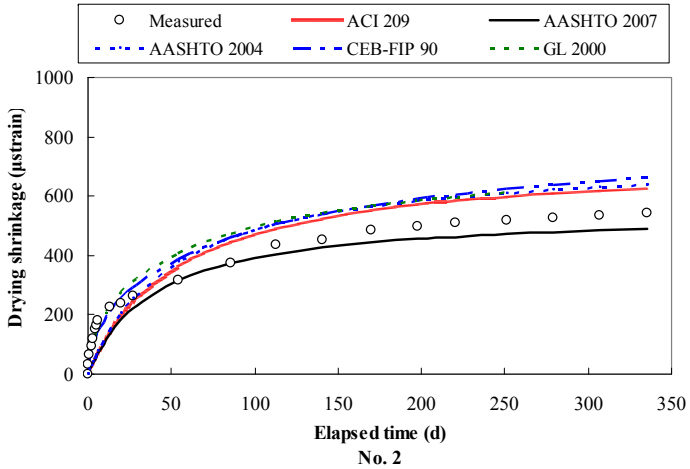

No. 2

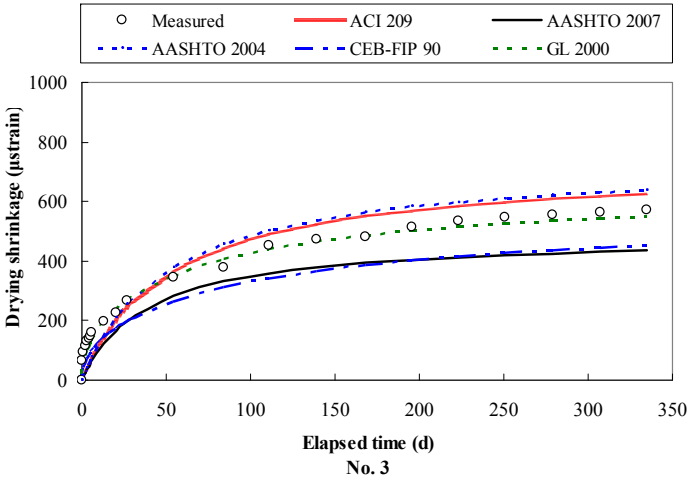

No. 3

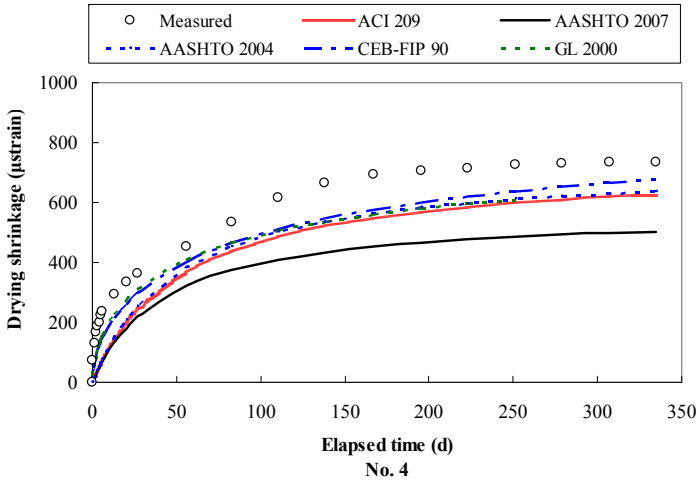

No. 4

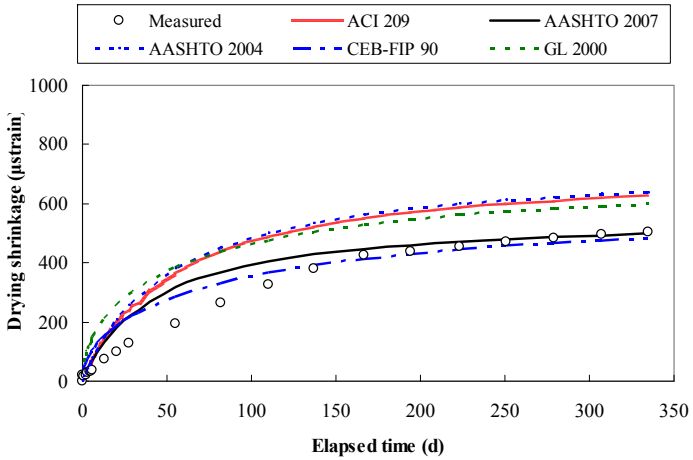

No. 5

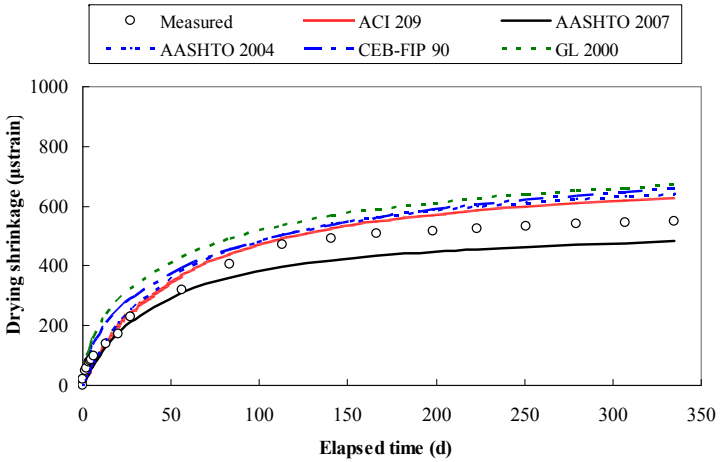

No. 6

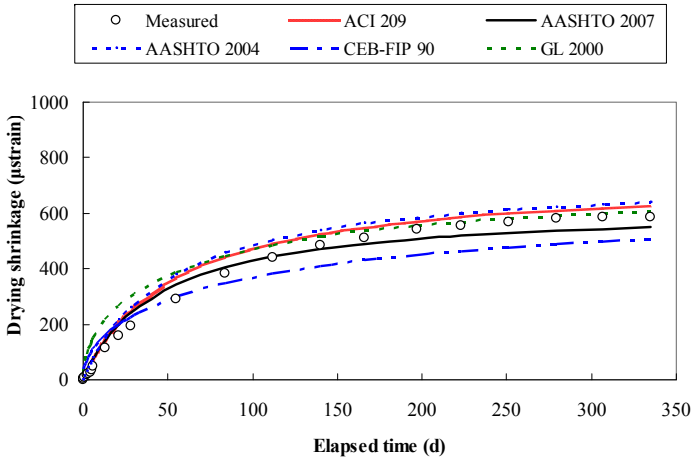

No. 7

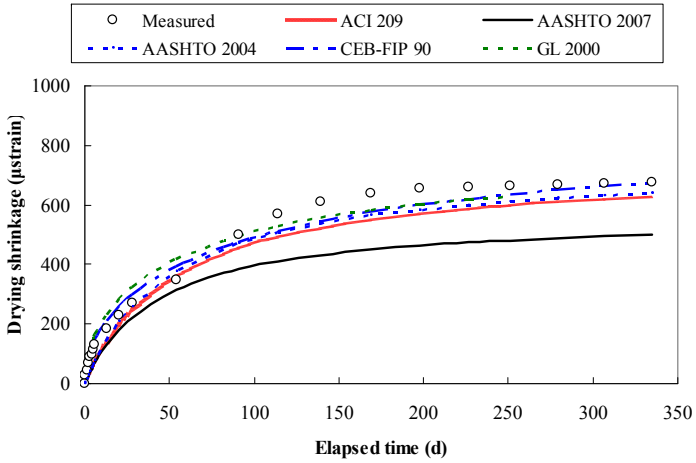

No. 8

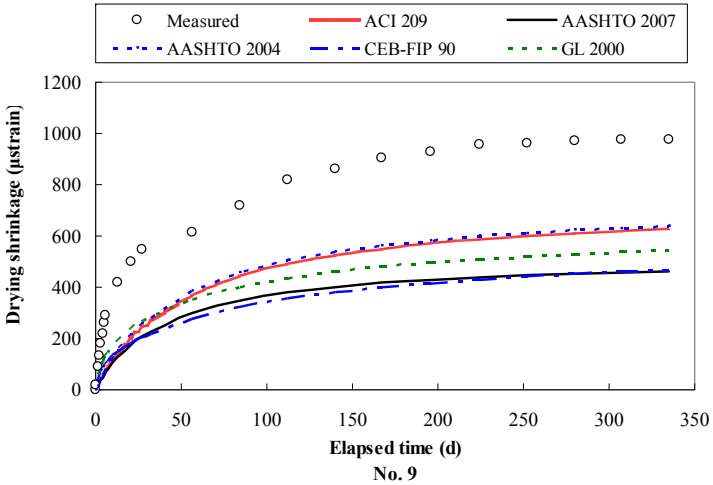

No. 9

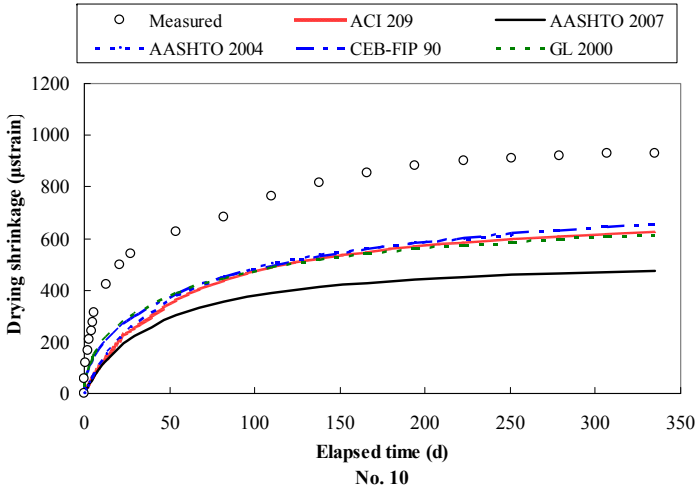

No. 10

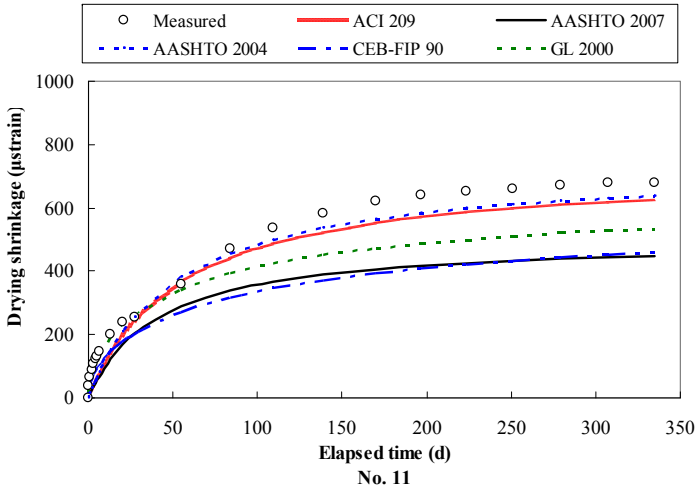

No. 11

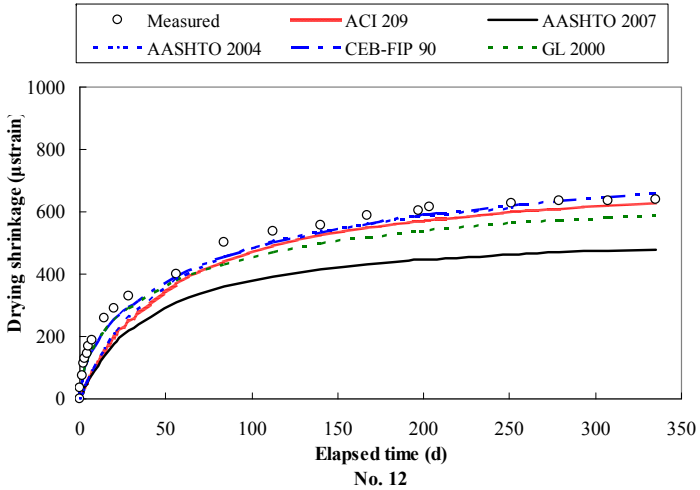

No. 12

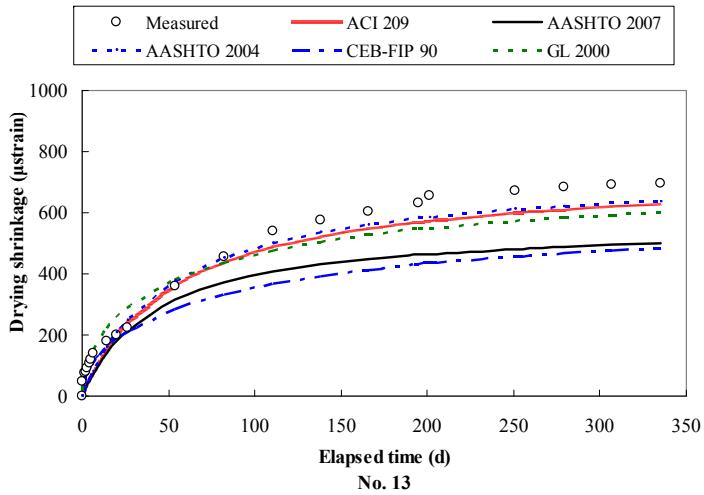

No. 13

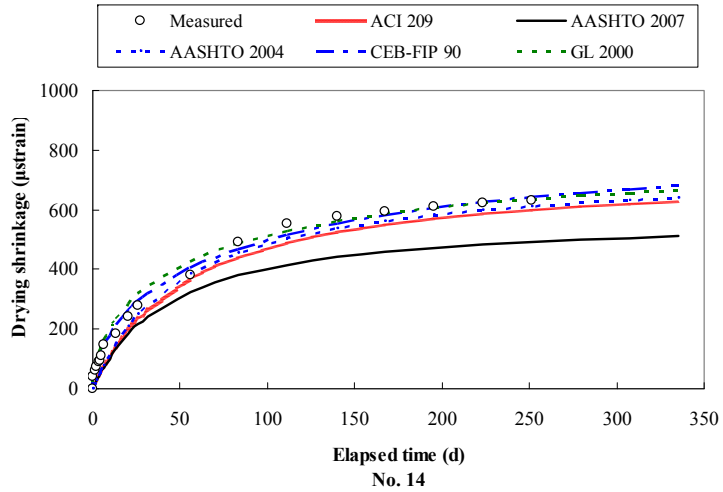

No. 14

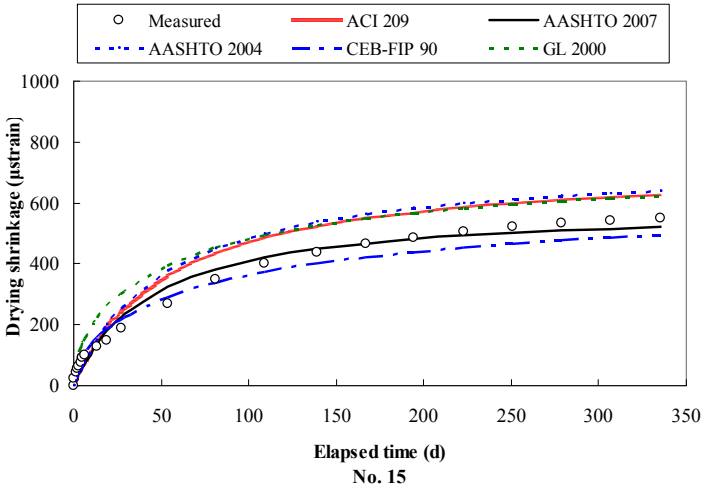

No. 15

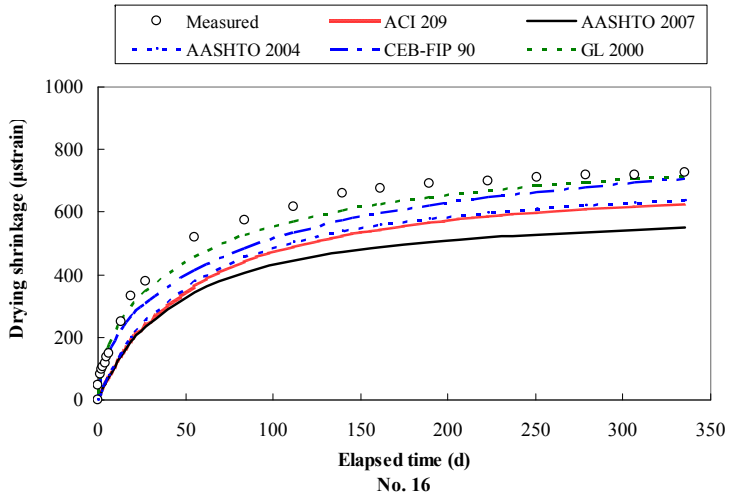

No. 16

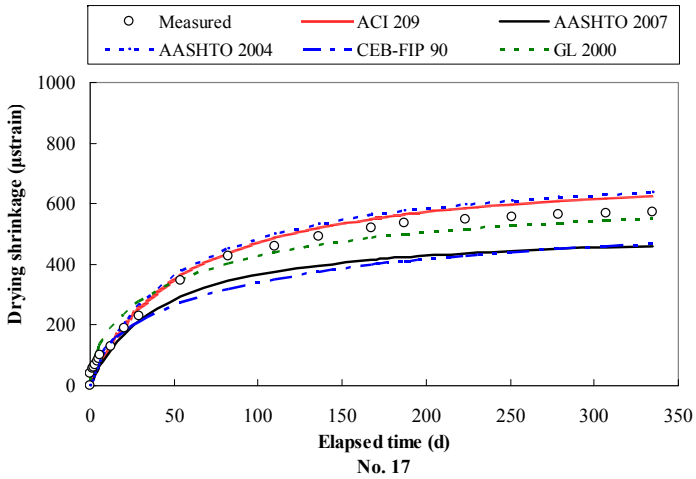
Measured
ACI 209
AASHTO 2007
AASHTO 2004
CEB-FIP 90
GL 2000
Drying shrinkage (µstrain)
1000
800
600
400
200
0
0
50
100
150
200
250
300
350
Elapsed time (d)

No. 17

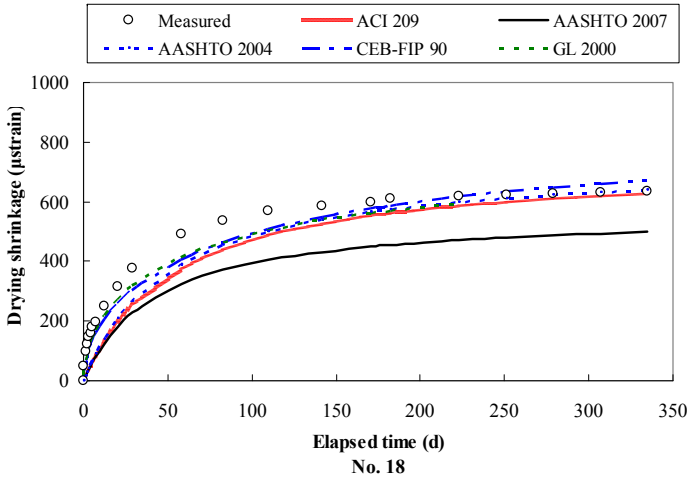
Measured
ACI 209
AASHTO 2007
AASHTO 2004
CEB-FIP 90
GL 2000
Drying shrinkage (µstrain)
1000
800
600
400
200
0
0
50
100
150
200
250
300
350
Elapsed time (d)

No. 18

APPENDIX M

Comparisons of Measured and Predicted Creep Strains

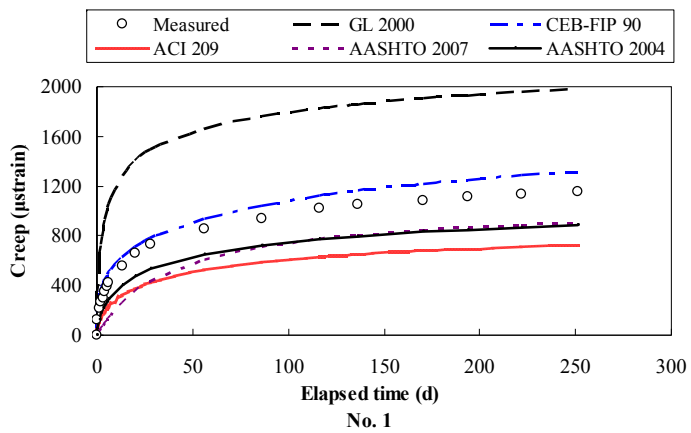

No. 1

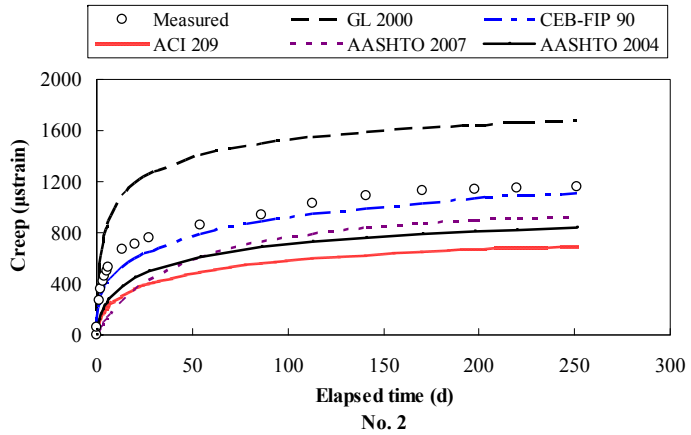

No. 2

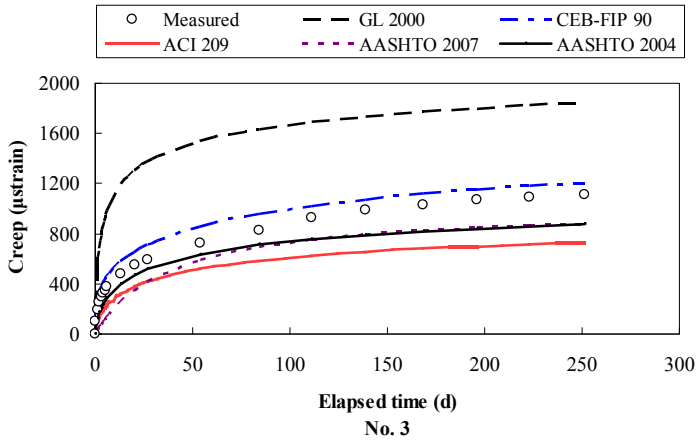

No. 3

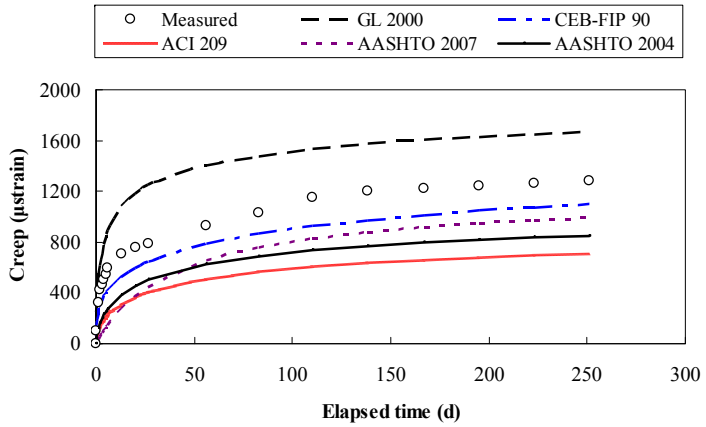

No. 4

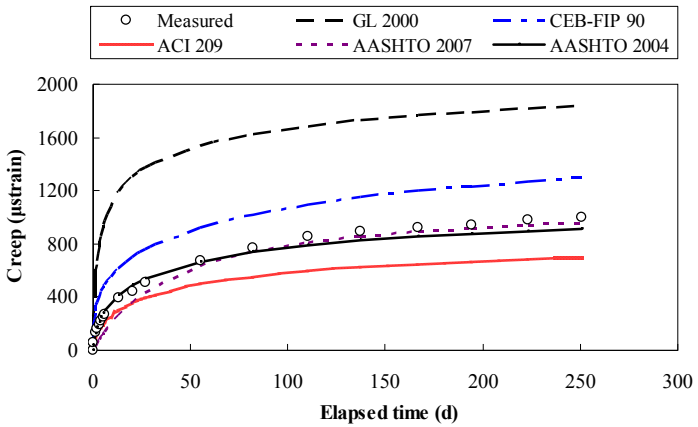

No. 5

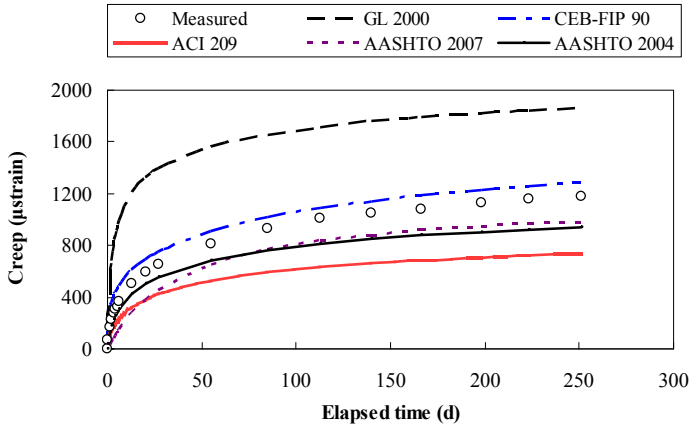

No. 6

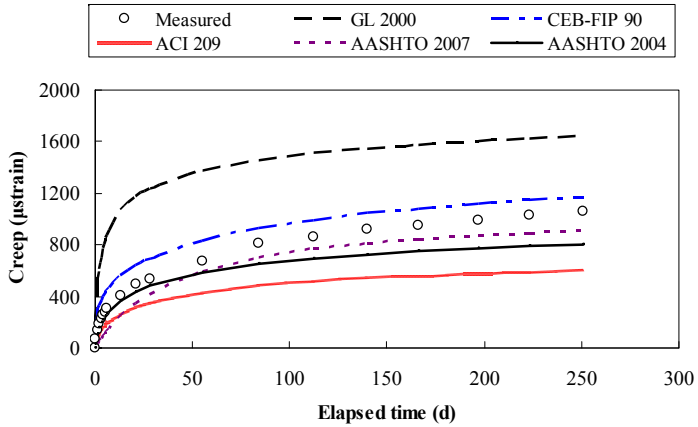

No. 7

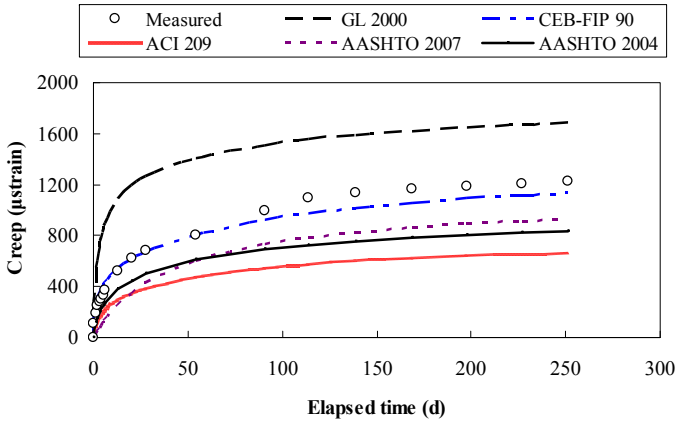

No. 8

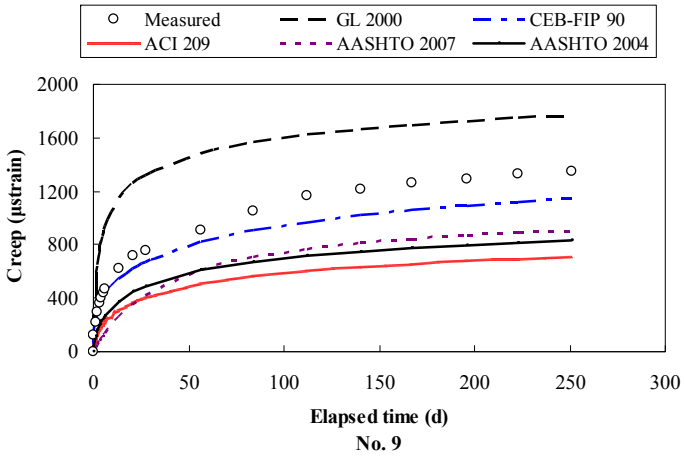

No. 9

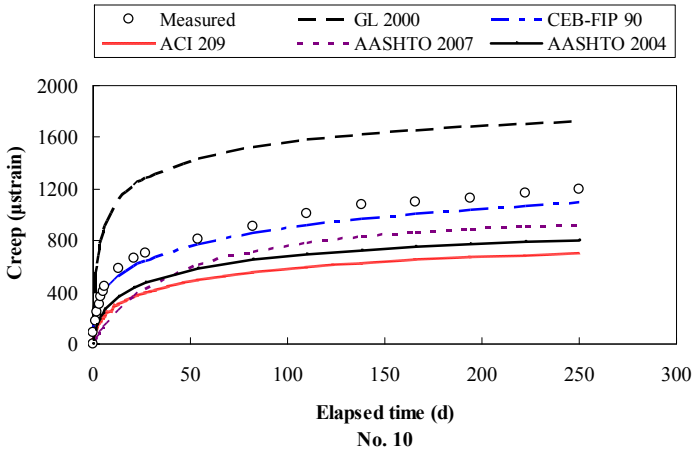

No. 10

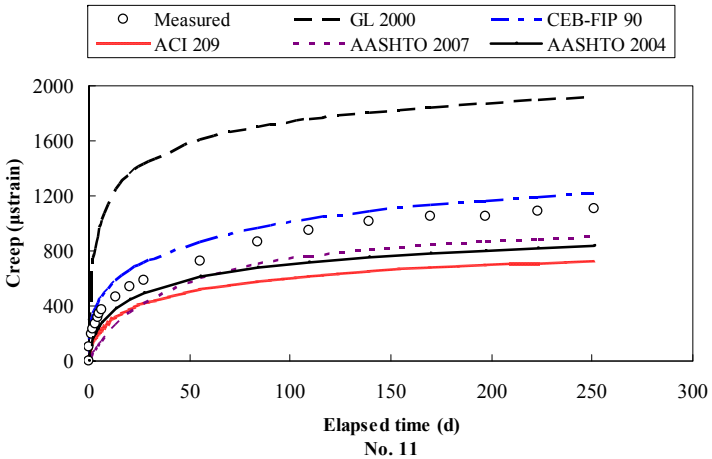

No. 11

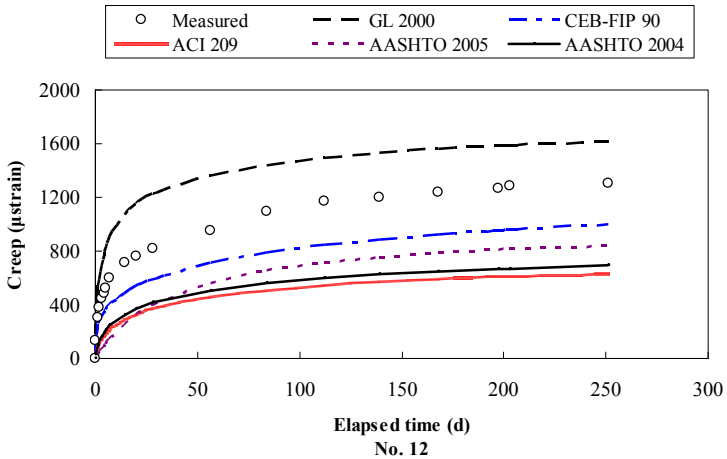

No. 12

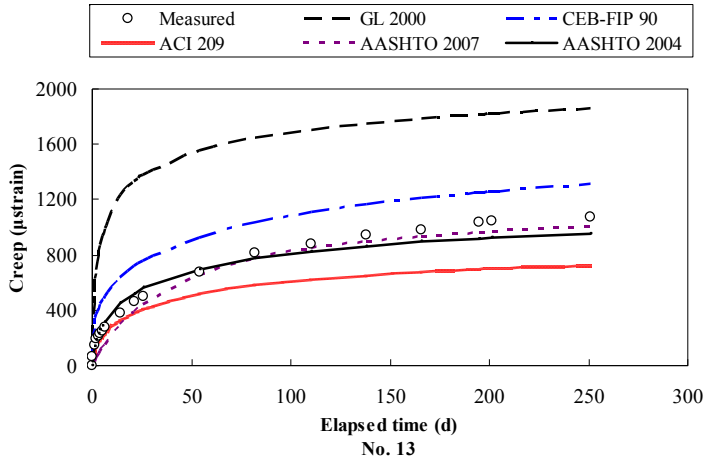

No. 13

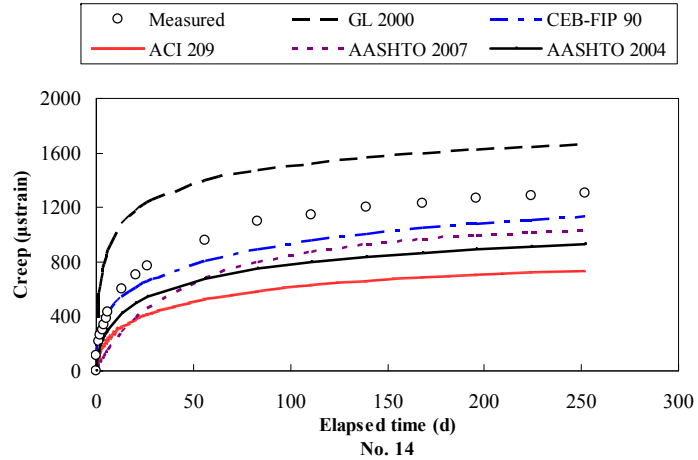

No. 14

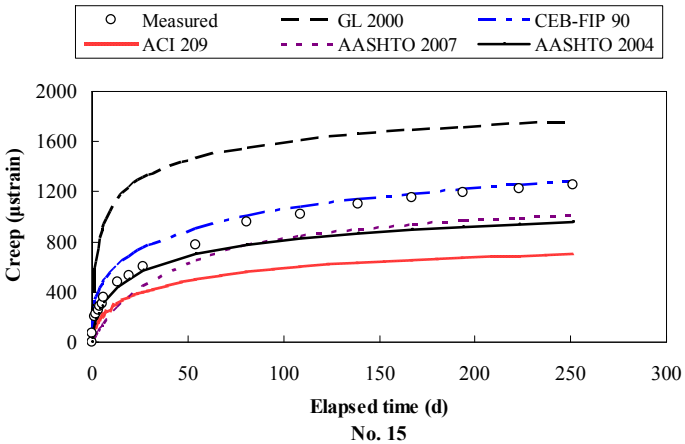

No. 15

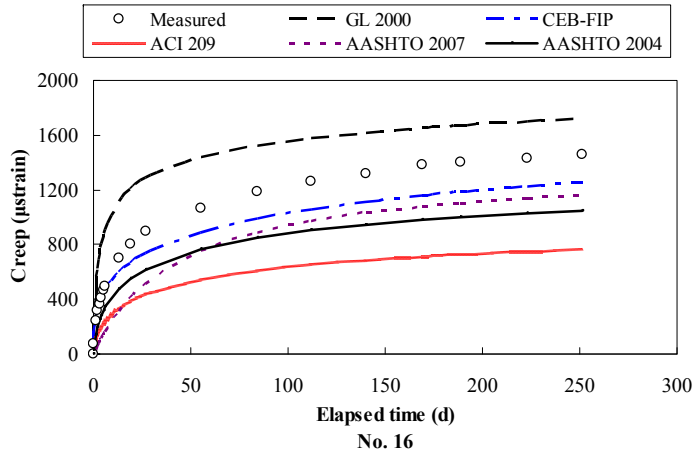

No. 16

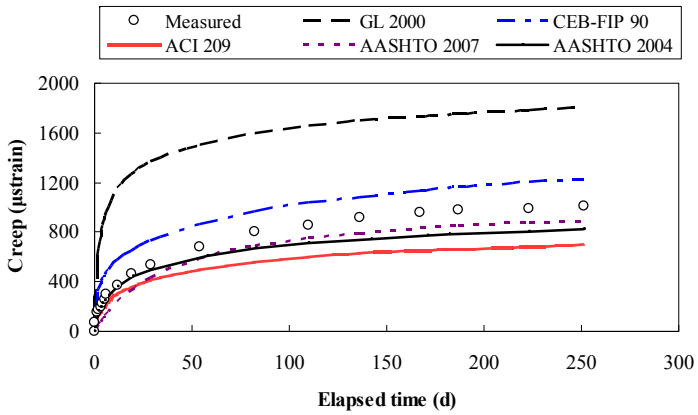
Measured
GL 2000
CEB-FIP 90
ACI 209
AASHTO 2007
AASHTO 2004
Creep (µstrain)
2000
1600
1200
800
400
0
0
50
100
150
200
250
300
Elapsed time (d)

No. 17

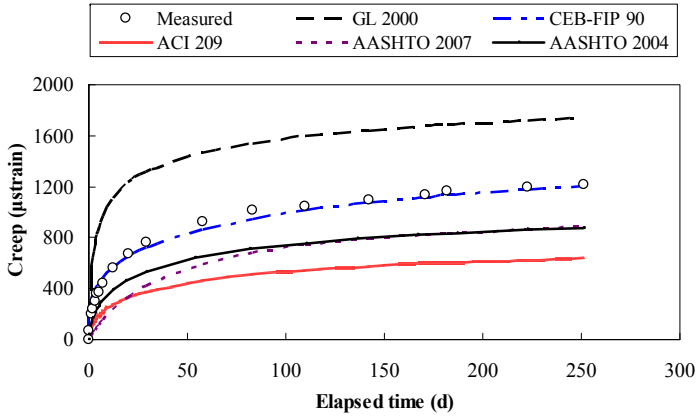
Measured
GL 2000
CEB-FIP 90
ACI 209
AASHTO 2007
AASHTO 2004
Creep (µstrain)
2000
1600
1200
800
400
0
0
50
100
150
200
250
300
Elapsed time (d)

No. 18

APPENDIX N

Pull-Out Load versus Free-End Slip Responses Determined on Wall Elements No. 1 to 6

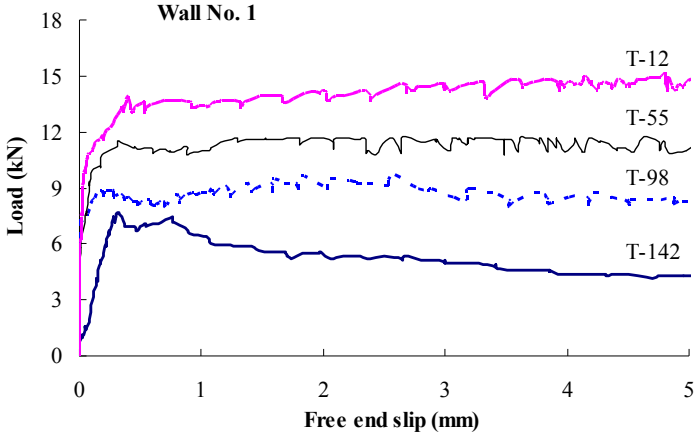

(1) Wall No. 1

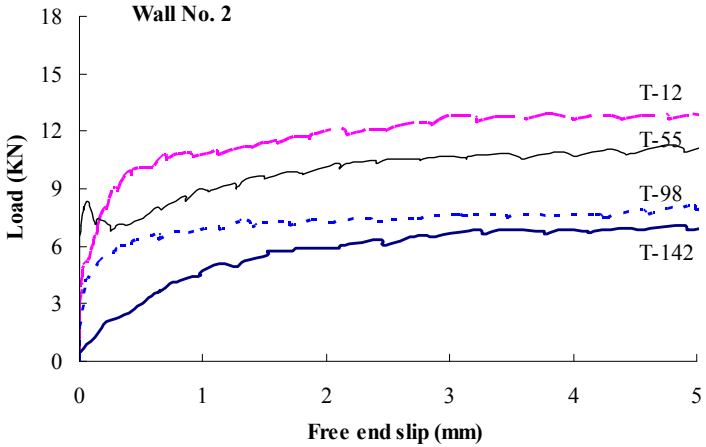

(2) Wall No. 2

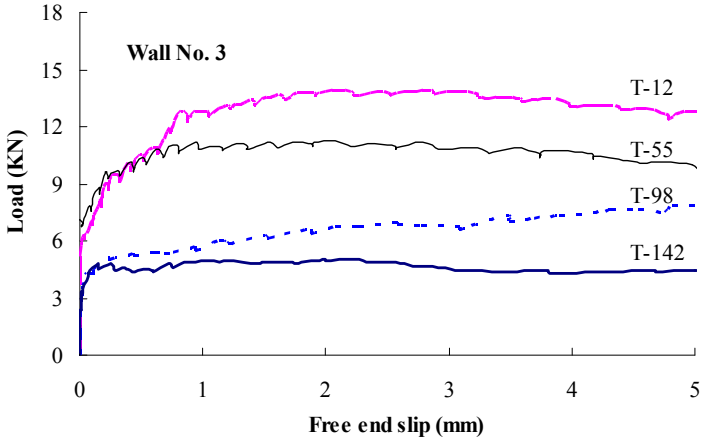

(3) Wall No. 3

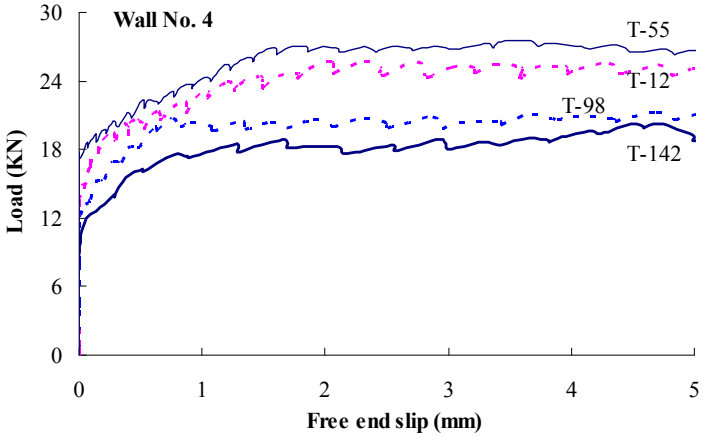

(4) Wall No. 4

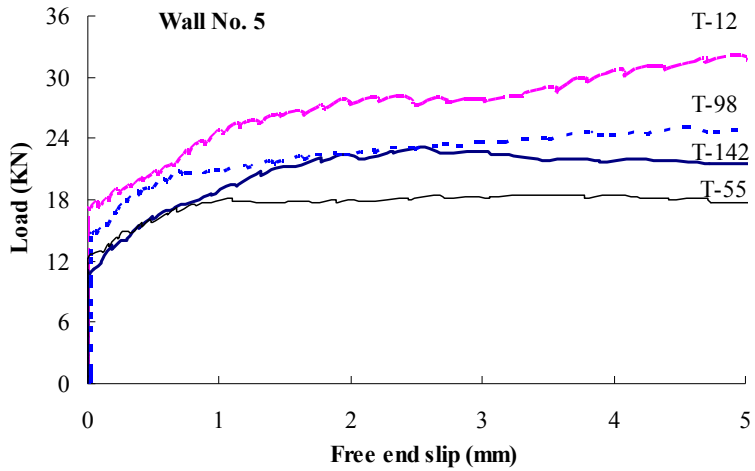

(5) Wall No. 5

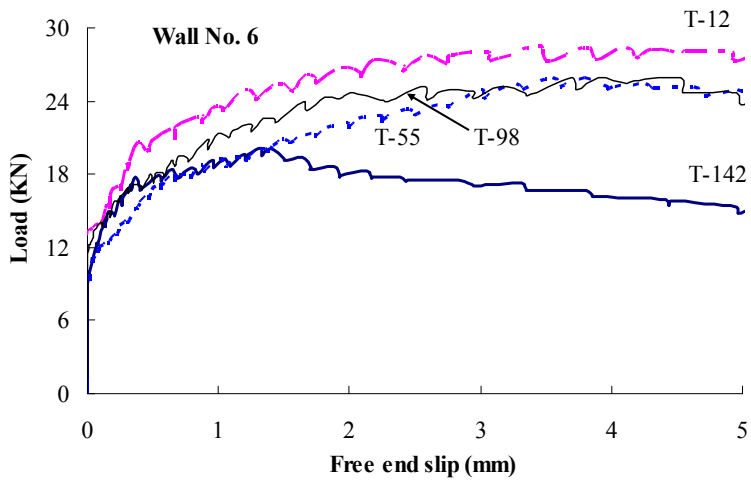

(6) Wall No. 6

APPENDIX O

In-place Compressive Strength of Wall Elements Cast with Different SCC with Different Stability Levels

Table O.1 – In-place compressive strength of wall elements No.1 to 3 cast with SCC with different stability levels

	Dist. from bottom, in. (mm)	Compressive strength, psi (MPa)					f'c core / f'c cylinder (%)
		1	2	3	Mean	C.O.V. (%)	
Wall No. 1	4.7 (120)	11880 (81.9)	11300 (77.9)	11360 (78.3)	11520 (79.4)	2.79	98
	21.7 (550)	10300 (71.0)	11180 (77.1)	10890 (75.1)	10790 (74.4)	4.16	92
	38.6 (980)	10700 (73.8)	10790 (74.4)	10790 (74.4)	10760 (74.2)	0.49	92
	55.9 (1420)	10900 (75.1)	9150 (63.1)	11100 (76.5)	10370 (71.5)	10.27	88
	Cylinder	11790 (81.3)	11700 (80.7)	11690 (80.6)	11730 (80.9)	0.48	100
Wall No. 2	4.7 (120)	8110 (55.9)	7980 (55.0)	7350 (50.7)	7810 (53.9)	5.21	99
	21.7 (550)	6970 (48.1)	6590 (45.4)	6860 (47.3)	6810 (46.9)	2.87	86
	38.6 (980)	6470 (44.6)	6660 (45.9)	6930 (47.8)	6690 (46.1)	3.40	84
	55.9 (1420)	6270 (43.3)	6660 (45.9)	6600 (45.5)	6510 (44.9)	3.23	82
	Cylinder	7850 (54.1)	7810 (53.8)	8080 (55.7)	7912 (54.6)	1.86	100
Wall No. 3	4.7 (120)	8750 (60.4)	9560 (59.0)	8530 (58.8)	8610 (59.4)	1.44	98
	21.7 (550)	8080 (55.7)	7890 (54.4)	7890 (55.1)	7890 (55.1)	1.19	91
	38.6 (980)	7670 (52.9)	7840 (54.0)	8210 (56.6)	7910 (54.5)	3.54	90
	55.9 (1420)	7460 (51.4)	7460 (51.4)	7490 (51.7)	7470 (51.5)	0.25	85
	Cylinder	8820 (60.8)	8660 (59.7)	8770 (60.5)	8750 (60.3)	0.90	100

Table O.2 – In-place compressive strength of wall elements No. 4 to 6 cast with SCC with different stability levels

	Dist. from bottom, in. (mm)	Compressive strength, psi (MPa)					f'c core / f'c cylinder (%)
		1	2	3	Mean	C.O.V. (%)	
Wall No. 4	4.7 (120)	10290 (71.0)	10150 (70.0)	10700 (73.8)	10380 (71.6)	2.76	95
	21.7 (550)	10290 (70.9)	9990 (68.9)	10290 (71.0)	10190 (70.3)	1.71	93
	38.6 (980)	10780 (74.4)	9620 (66.4)	10520 (72.6)	10310 (71.1)	5.90	94
	55.9 (1420)	10470 (72.2)	10130 (69.8)	10110 (69.7)	10230 (70.6)	1.97	94
	Cylinder	11140 (76.8)	11350 (78.3)	10340 (71.3)	10940 (75.5)	4.86	100
Wall No. 5	4.7 (120)	10910 (75.2)	10090 (69.6)	9870 (68.1)	10290 (71.0)	5.34	91
	21.7 (550)	10760 (74.2)	10450 (72.1)	10020 (69.1)	10410 (71.8)	3.60	92
	38.6 (980)	11290 (77.8)	11730 (80.9)	10460 (72.1)	11160 (77.0)	5.75	99
	55.9 (1420)	10770 (74.3)	10850 (74.8)	11050 (76.2)	10890 (75.1)	1.33	96
	Cylinder	11440 (78.9)	11310 (78.0)	11140 (76.8)	11300 (77.9)	1.37	100
Wall No. 6	4.7 (120)	9390 (64.8)	9270 (63.9)	9580 (66.0)	9410 (64.9)	1.66	99
	21.7 (550)	9380 (64.7)	8950 (61.7)	8550 (59.0)	8960 (61.8)	4.59	94
	38.6 (980)	8990 (62.0)	8880 (61.2)	8880 (61.2)	8910 (61.5)	0.70	94
	55.9 (1420)	8990 (62.0)	8450 (58.3)	9060 (62.5)	8830 (60.9)	3.79	93
	Cylinder	9340 (64.4)	9350 (64.5)	9900 (68.3)	9530 (65.7)	3.36	100

APPENDIX P

Structural Performance of Full-Scale AASHTO-Type Girders

P.1 INTRODUCTION

This appendix presents the results of construction and structural testing of full-scale precast, prestressed bridge girders constructed with selected SCC mixtures and companion HPC specimens, to verify the applicability of existing design provisions (AASHTO and PCI). The following aspects were studied: constructability, temperature variations, transfer lengths, cambers, flexural cracking, shear cracking, and shear strengths.

P.2 TESTING PROGRAM AND DETAILS OF AASHTO-TYPE II GIRDERS

Given the results of experimentation on the mix designs, two effective SCC mixtures of different compressive strength levels were used to cast two full-scale AASHTO Type II girders. Non air-entrained SCC concretes with target 56-day compressive strength of 8,000 and 10,000 psi (55 and 69 MPa) and having release strengths of 5,000 psi (34.5 MPa) and 6,250 psi (43 MPa) at 18 hours, respectively, were chosen for the testing. Two additional girders were cast using two high-performance concretes with target 56-day compressive strengths of 8,000 and 10,000 psi (55 and 69 MPa). The HRWRA dosages for the HPC and SCC mixtures were adjusted to obtain a slump of 6.3 ± 0.8 in. (160 ± 20 mm) and a slump flow of 26.8 ± 0.8 in. (680 ± 20 mm), respectively. The test program for casting the concrete girders is summarized in Table P.1.

The AASHTO II girders have overall lengths of 31 ft (9.4 m) with center-to-center spans of 29 ft (8.8m). The girders are prestressed with Grade 270 low-relaxation prestressing strands of 0.6 in. (15.2 mm) diameter, as shown in Fig. P.1. The girders were prestressed with eight strands, six straight strands and two strands harped at double harping points located 4’ – 11” (1.5 m) from mid-span (see Fig. P.1). The pressure in the pre-tensioning jacking system was calibrated to determine accurately the force applied to each strand.

Table P.1 – Test program for concrete girders

Structural Element	Concrete type	Mixture characteristics
AASHTO-Type II Girder	SCC	Girders cast with two SCC mixtures with compressive strengths of 8,000 and 10,000 psi (55 and 69 MPa) at 56 days
	HPC	Girders cast with two HPC mixtures of normal consistency having compressive strengths of 8,000 and 10,000 psi (55 and 69 MPa) at 56 days
Deck slab	Normal concrete	Air-entrained concrete of normal consistency with 5,000 psi (35 MPa); 5% to 8% of air entrainment, 0.42 *w/cm*, Type I cement

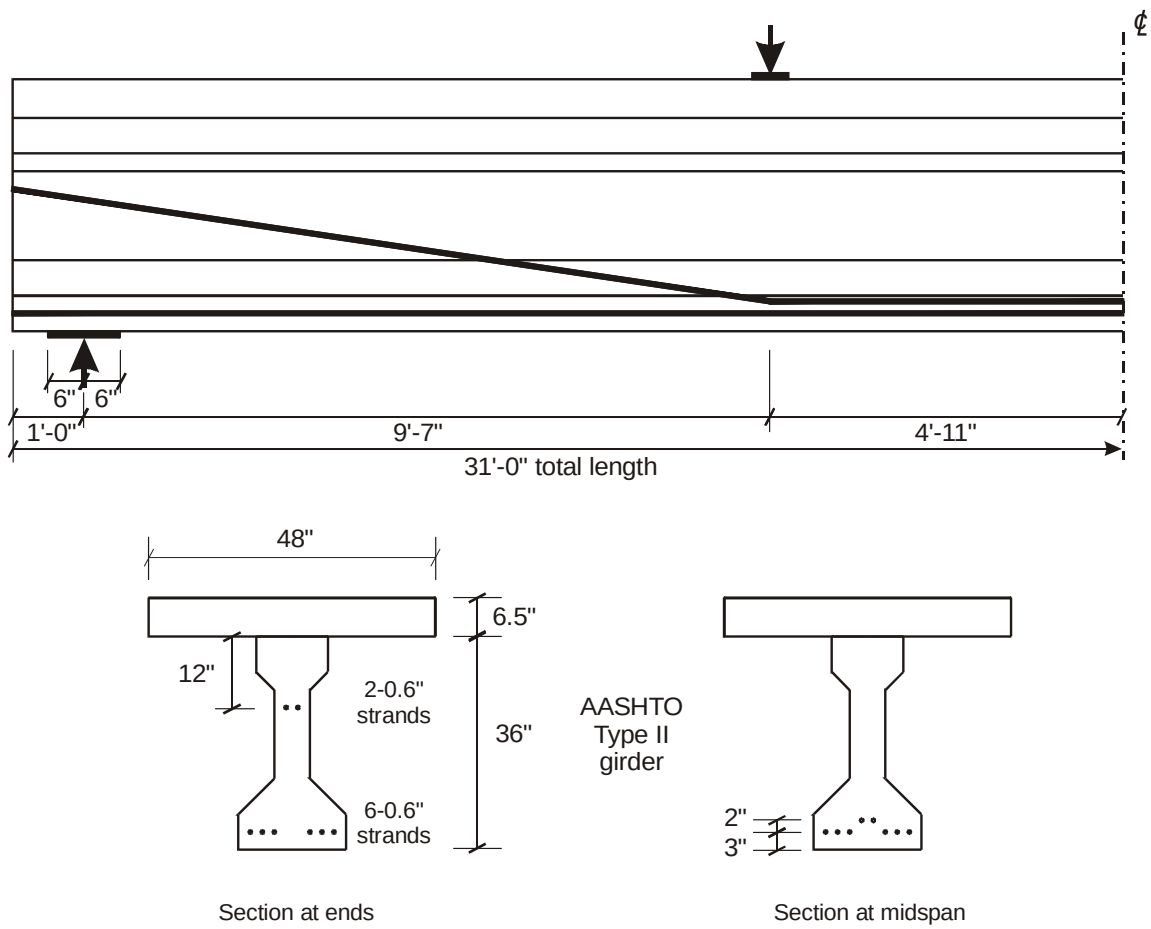

Fig. P.1 – Details of precast, prestressed AASHTO-Type II girders

Normal reinforcing bars (No. 5 bars) were added near the top to control cracking at prestress release and in the bottom flange to increase the flexural capacity. The stirrup reinforcement was chosen to satisfy the 2007 AASHTO Clause 5.8.2.5 for minimum transverse reinforcement. In order to choose the size and spacing of the stirrups the nominal concrete strengths of 8 and 10 ksi (55 and 69 MPa) were assumed along with the nominal yield stress for the reinforcement of 60 ksi (414 MPa). Hence, for the 8 ksi (55 MPa) concrete and using No. 3 double legged stirrups the required spacing is:

$$s \le \frac{A_v f_y}{0.0316\sqrt{f_c'}b_w} = \frac{2 \times 0.11 \times 60}{0.0316\sqrt{8} \times 6} = 24.6 \text{ in. } (625 \text{ mm})$$

In addition, Clause 5.8.2.7 on maximum spacing of transverse reinforcement limits the spacing to 24 in. (610 mm) for low shear stresses. Hence a spacing of 24 in. (610 mm) was chosen for this girder. Similarly, the required spacing for the girders made with 10 ksi (69 MPa) concrete require a spacing for the No. 3 double legged stirrups of 22 in. (560 mm).

As is common practice additional transverse and longitudinal reinforcement was placed in the end regions of each girder, as shown in Figs. P.2, P.3, and P.4. In order to prevent horizontal shear distress, additional interface shear reinforcement was provided across the interface of the

precast girder and the deck slab. This consisted of additional No. 3 U-bars at each full-depth stirrup location as shown in Figs. P.3 and P.5.

A 6.5 in. (165 mm) deep and 48 in. (1219 mm) wide cast-in-place deck slab was cast on top of each girder at least 28 days after the prestress release. The deck slab was cast with a conventional air-entrained concrete with a target compressive strength of 5,000 psi (35 MPa). The deck slab contained four No. 5 reinforcing bars in the longitudinal direction and No. 5 transverse bars at a spacing 12 in. (305 mm) and 11 in. (280 mm) for the 8,000 and 10,000 psi (55 and 69 MPa) girders, respectively. It is noted that during the casting of the deck slab concrete, the girder was sitting on its end supports. Rather than being supported directly on the precast girder, the formwork for the deck slab was supported on the ground. Following the casting the deck slab was covered with burlap and polyethylene and was moist cured for 5 days.

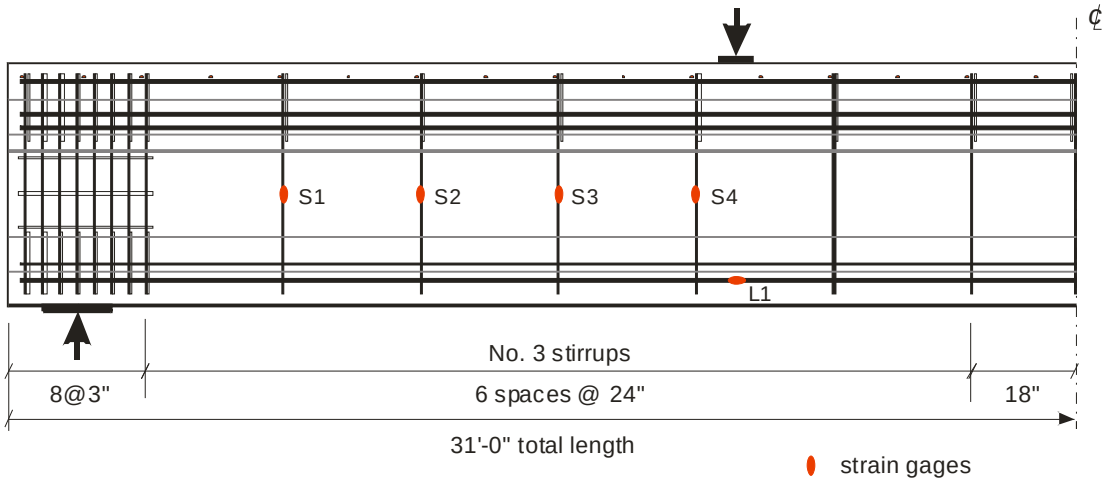

H8 and S8

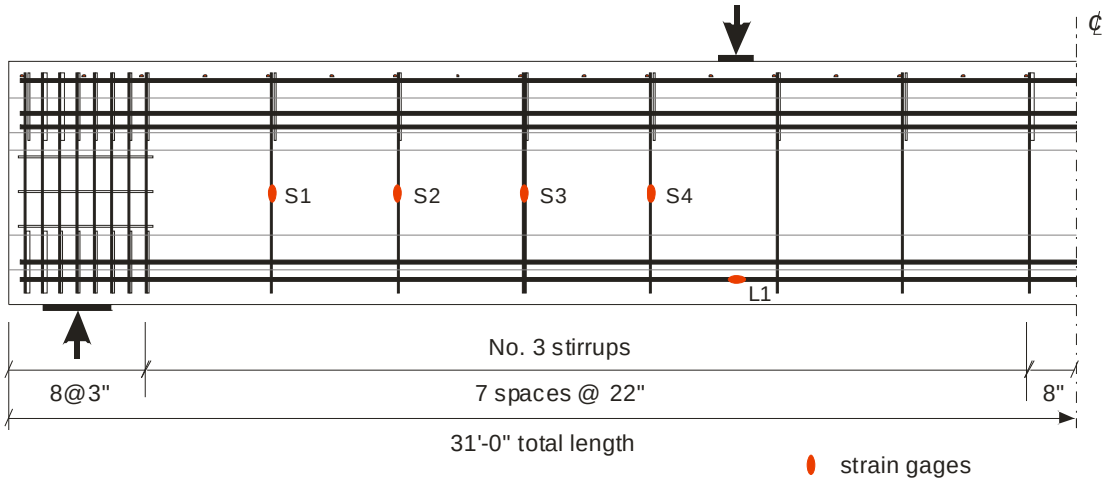

H10 and S10

Fig. P.2 – Details of non-prestressed reinforcement

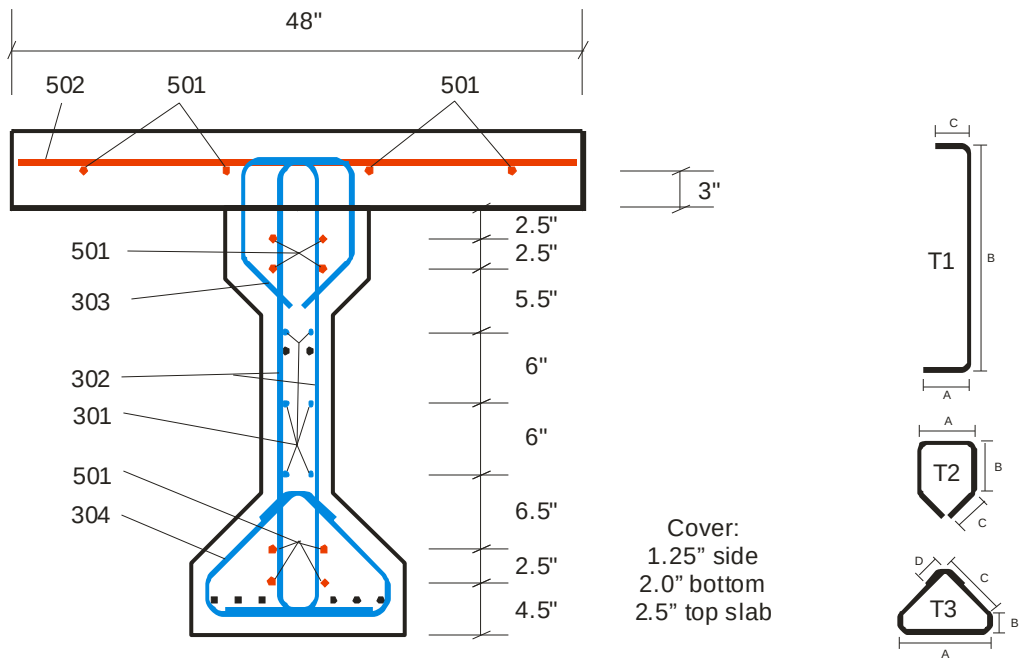

Reinforcing Bar List

Mark	Size	Length	Qty H8 S8	Qty H10 S10	Type	A	B	C	D
301	#3	2'-0"	12	12	-				
302	#3	4'-2"	58	60	T1	8"	38"	6"	
303	#3	3'-0"	29	30	T2	9.5"	8.5"	5.75"	
304	#3	4'-1"	16	16	T3	15.5"	3"	11"	4"
501	#5	30'-9"	12	12	-				
502	#5	3'-11"	32	34	-				

Fig. P.3 – Cross section details

Fig. P.4 – Details of reinforcement in end region

Fig. P.5 – Details of stirrups and interface shear reinforcement

P.2.1 Instrumentation

A vibrating wire strain gage was installed at mid-span of each girder to measure concrete temperature and concrete strain at the level of the straight prestressing strands for determining prestress losses with time. A second vibrating wire strain gage was installed 4 ft (1.22 m) from mid-span close to one of the harping points (see Fig. P.6). The measured strains from the vibrating wire gages enable a comparison of the measured strains to those predicted for the total deformation determined at the level of the straight prestressing strands due to elastic shortening, creep, and shrinkage of the concrete.

Transfer length devices were assembled to measure strains at each end of the four girders to determine the transfer lengths upon release of the pretensioning. The transfer length device consisted of a metal rod with steel disks welded to the rod to create bond between the device and the surrounding concrete. Strain gages glued to the rod permitted strains to be determined at a number of locations (see Fig. P.6). Figure P.7 shows a close-up of one of the transfer length devices. As presented in Fig. P.2, the No. 3 stirrups and on the No. 5 longitudinal bars in the shear span were instrumented with strain gages.

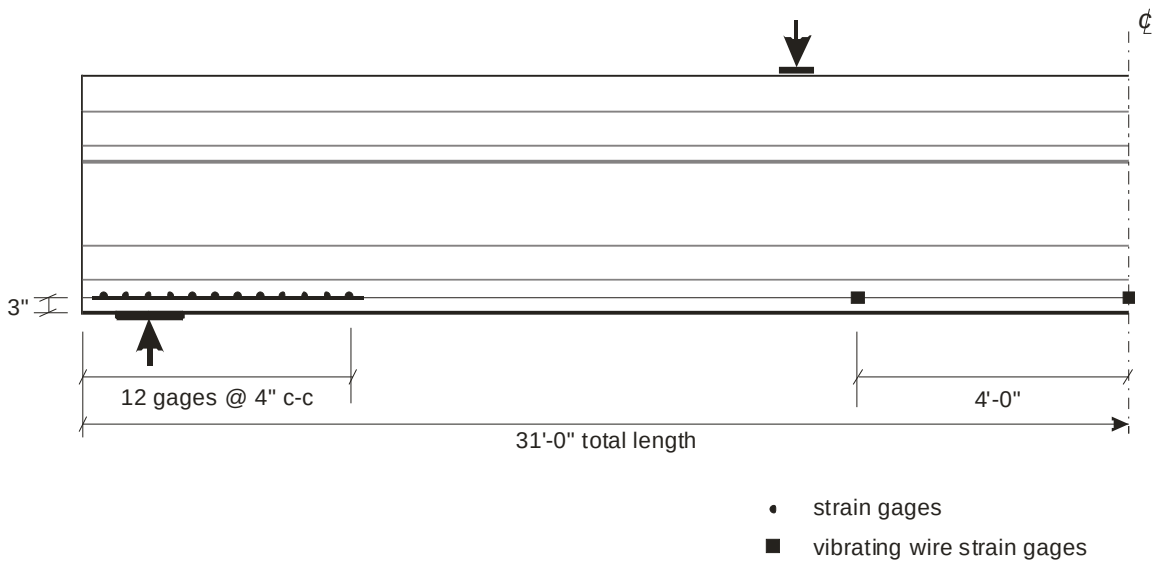

Fig. P.6 – Locations of strain gages and vibrating wire gages

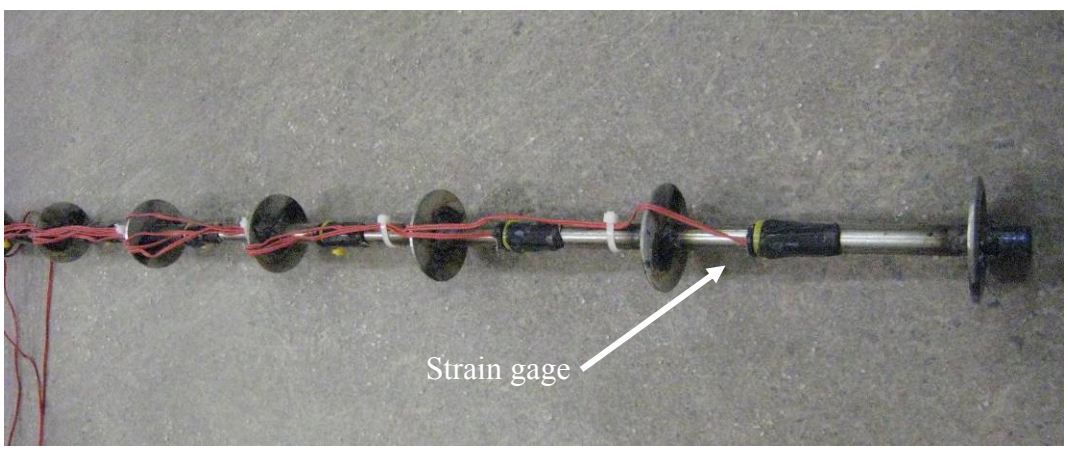

Fig. P.7 – Transfer length measuring device

P.2.2 Pretensioning Operation

Figure P.8 shows the jacking operation in the pretensioning bed which was carried out at one end of the girders. The six straight strands were tensioned first, one strand at a time, to a stress level corresponding to $0.7f_{pu} = 0.7 \times 270 = 189$ ksi (1.3 GPa), starting with the outermost strands. After the six straight strands were tensioned, the two inclined strands were tensioned to same level of prestress. In order to minimize losses due to anchorage set in this relatively short stressing bed, the stressing operation involved stressing a strand to the desired level, releasing the jack to set the anchor and then re-stressing each strand and placing steel shims under the anchorage sleeve.

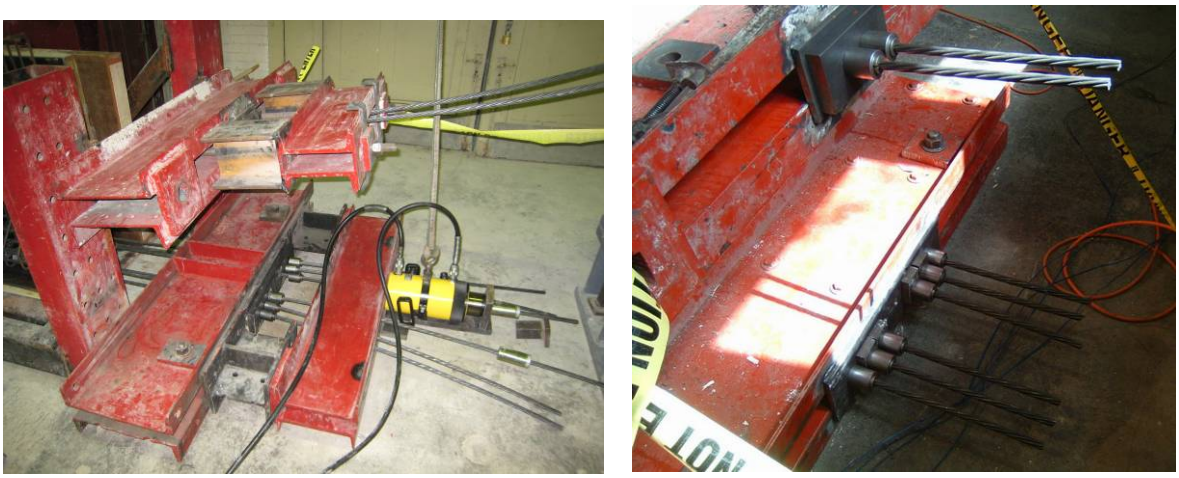

(a) Stressing of straight strand (b) Anchorage at "dead end"

Fig. P.8 – Jacking of 0.6 in. (15 mm) diameter strands

P.2.3 Casting and Steam Curing of AASHTO Girders

Figure P.9 shows the reinforcing cage in the formwork after stressing and before casting the concrete.

Fig. P.9 – Reinforcing cage in formwork prior to casting

The concrete was mixed at the central ready-mix plant of Unibéton in Laval and delivered to the structural laboratory at McGill University. The two HPC girders, H8 and H10, were cast using a concrete bucket and internal vibration. In contrast, the concrete for the two SCC girders, S8 and S10, was using a chute to deliver the concrete to the middle of the girder (see Fig. P.10) and the concrete was not vibrated. In order to complete the concreting, a small layer of SCC was added in the top of the end regions of the girders.

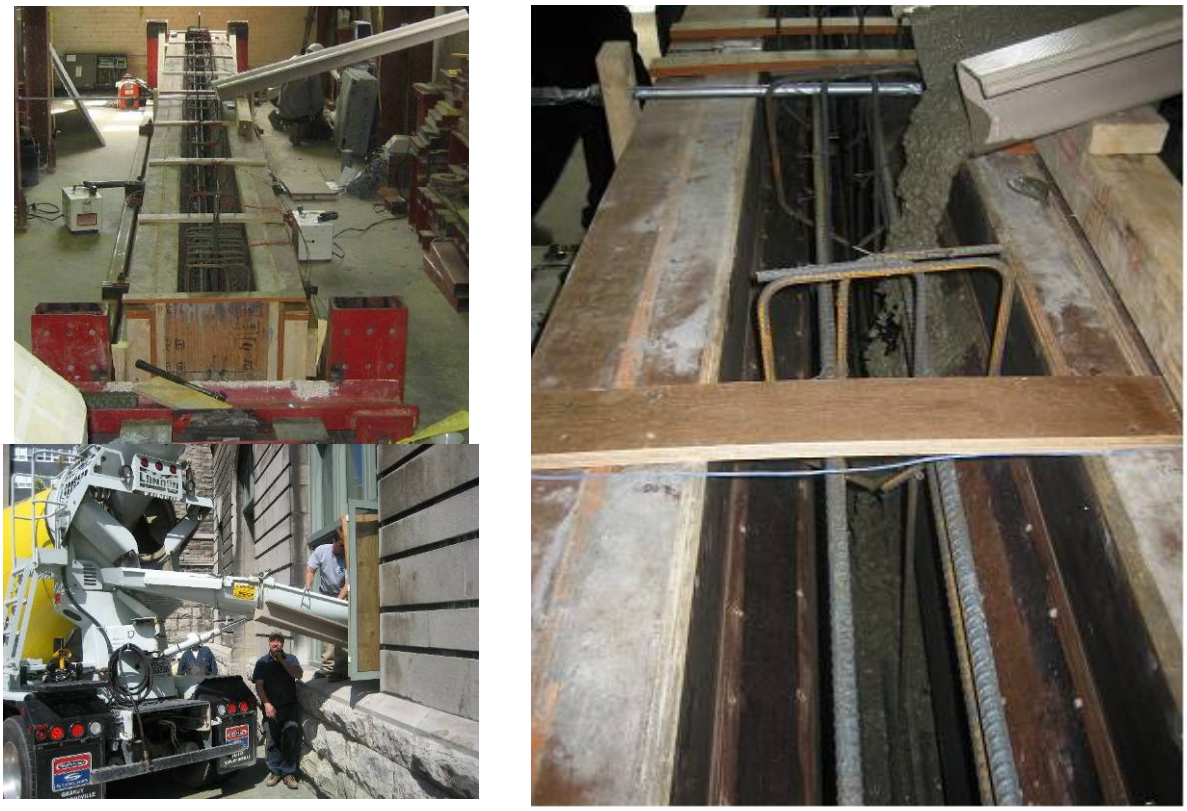

Fig. P.10 – SCC girder casting operation

After casting, the stressing bed and formwork were enclosed by sheets of 1.5 in. (38 mm) thick Styrofoam, which in turn were covered by 6 mil polyethylene sheets for the steam-curing operation (see Fig. P.11). Four steamers, two on each side of the girder, provided the steam required. An electric fan was also installed inside of the steam curing chamber to allow uniform circulation of the steam. The steam curing was started 2.5 and 3 hours after the initial contact of cement and water for the 8,000 and 10,000 psi (55 and 69 MPa) concrete mixtures, respectively.

In total, eight thermo-couples were used to monitor the temperature variations of each girder and that of the steam curing chamber. Four thermo-couples were installed inside each girder, two near the bottom and two near the top of the girder. Four thermo-couples were also used to determine chamber temperature. The temperature history of the concrete was monitored during steam curing and the results are shown in Fig. P.12. The targeted chamber temperature for 8,000 psi (55 MPa) SCC and HPC mixtures was set at 131°F (55°C). The target temperature for the 10,000 psi (69 MPa) concrete mixtures was set at 140°F (60°C). During the steam curing operation an attempt was made to limit the concrete temperature to a maximum value of 150°F (65°C). It is noted that the volume of steam was reduced when the concrete temperature reached 122°F (50°C) and 131°F (55°C) for the 8,000 and 10,000 psi (55 and 69 MPa) concrete, respectively.

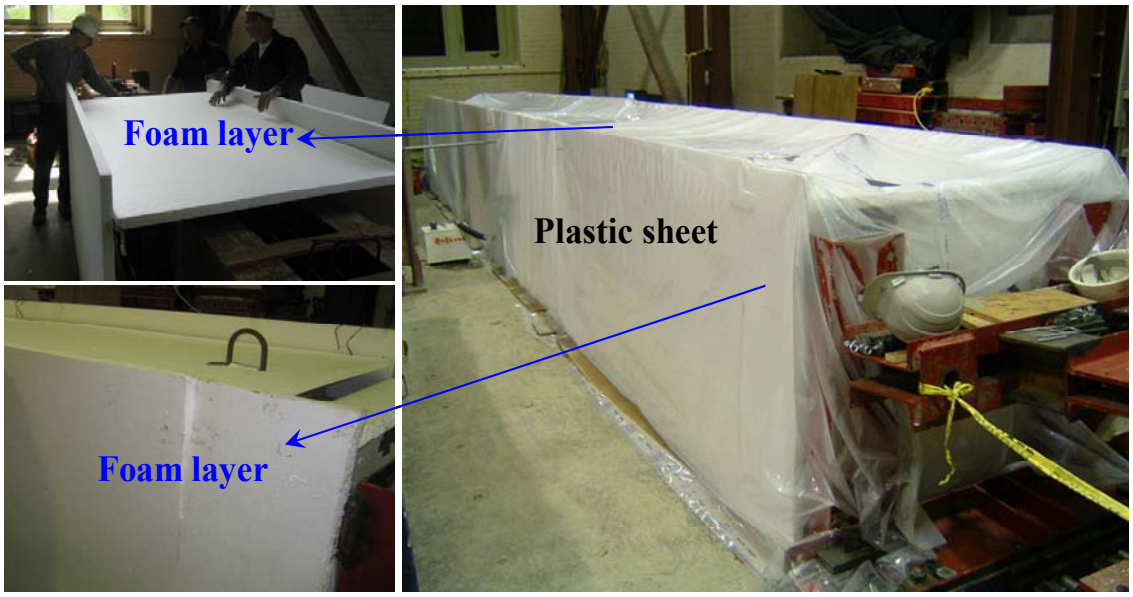

Fig. P.11 – Steam curing facility used for AASHTO Type II girders

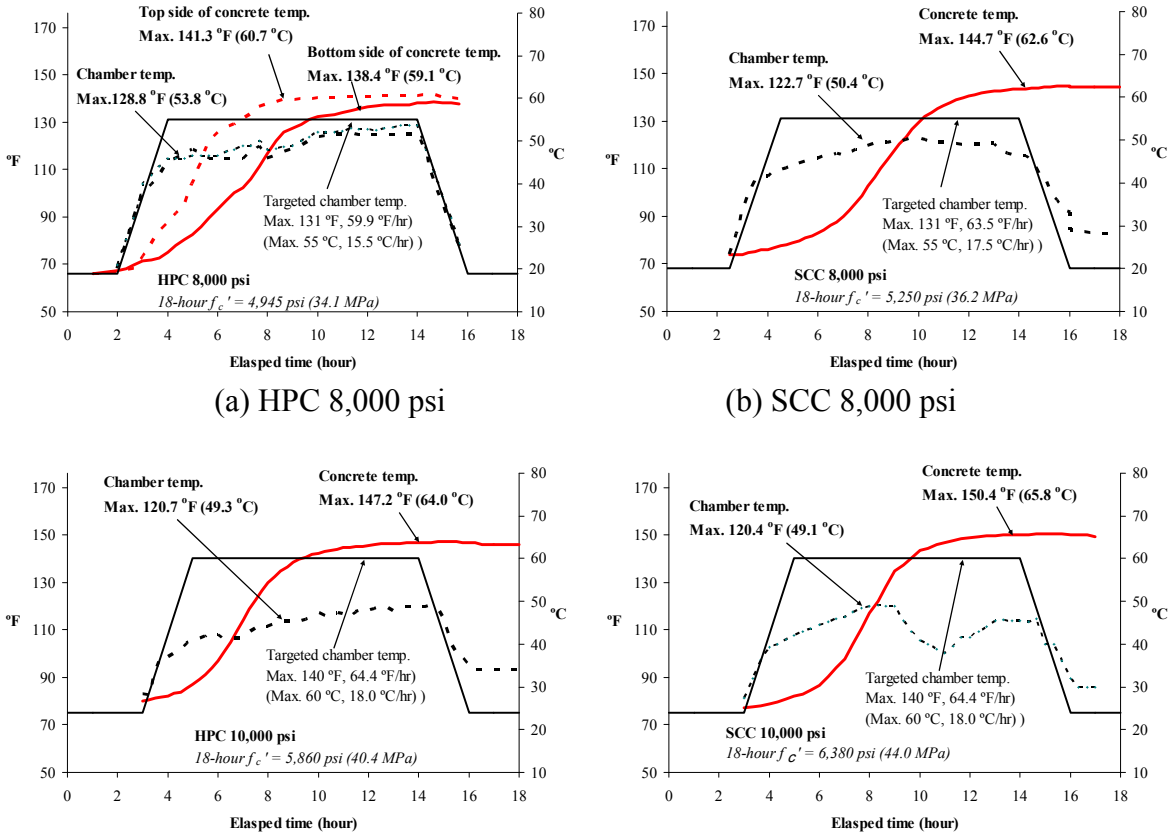

Fig. P.12 – Temperature history of chamber and concrete girder during steam curing

P.2.4 Pretensioning Release

The release of the prestressing started with the release of the hold-downs for the two harping points. This was followed by the flame cutting of the two central bottom straight strands. The two inclined strands were then flame cut followed by the release of the remainder of the bottom strands, working from the inner strands outwards. The flame cutting was performed first at the jacking end of each girder (see Fig. P.13).

(a) Release of bottom strand

(b) Release of inclined strand

Fig. P.13 – Flame cutting of strands during prestress release

P.2.4.1 Strand set measurements

Figure P.14 shows the measuring technique to determine the strand set after pretensioning release. A digital caliper was used to measure the distance between a steel clamp and a mark on the concrete next to the strand. The measurements taken before and after release enabled the strand set to be estimated for each strand at the jacking end (flame-cut release end) and the dead end (gradual release). In determining the strand set an adjustment was made from the caliper readings to account for the strain in the strand between the concrete face and the end of the clamp (see Fig. P.14). Table P.2 gives the average values of the strand set at each end and the overall average for all the readings. The SCC girders had slightly smaller values of strand set. The average set is 0.036 in. (0.91 mm).

Table P.2 – Average values of strand set

Girder	Flame-cut end in. (mm)	Dead end in. (mm)	Average in. (mm)
H8	0.038 (0.97)	-	0.038 (0.97)
S8	0.031 (0.78)	0.035 (0.88)	0.033 (0.83)
H10	0.033 (0.83)	0.040 (1.01)	0.036 (0.92)
S10	0.032 (0.82)	0.039 (0.98)	0.035 (0.90)

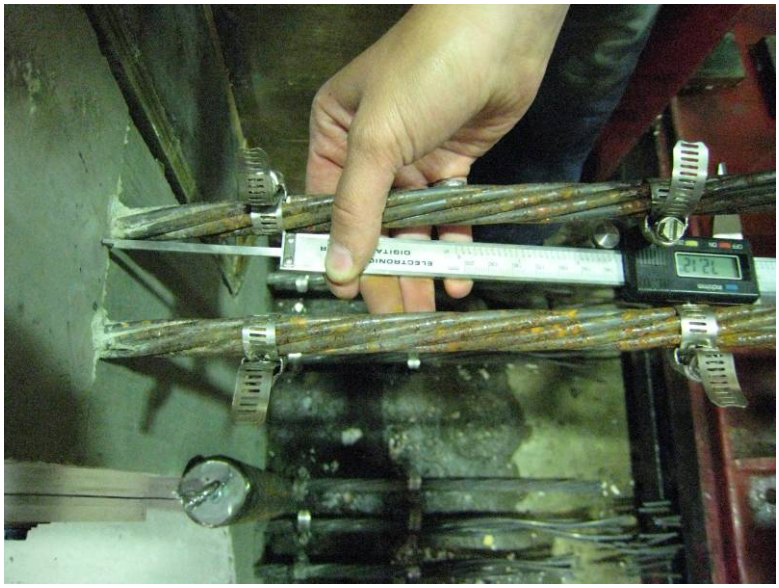

Fig. P.14 – Measurement of strand set

P.2.4.2 Transfer length measurements

The results from the strain readings on the transfer length devices (see Figs. P.6 and P.7) that were embedded in each end of the girders at the level of the bottom 6 straight strand are given in Fig. P.15.

In order to determine the transfer length from these readings, the procedure described by Russell and Burns[D12] (1997) was used. The procedure involved first determining the average strain in the strain plateau area and then taking 95% of this value to give the "95% AMS". The transfer length is determined by the intersection of the 95% AMS line with the measured strain profile. The resulting transfer length values are shown in Fig. P.15 and are summarized in Table P.3.

It is noted that these transfer lengths are considerably shorter than the transfer length given in the 2007 AASHTO Specifications (5.11.4.1). The average transfer length is 12.8 in. (325 mm). The AASHTO transfer length is 60 strand diameters or 60 × 0.6 = 36 in. (915 mm). This value is very conservative.

If it is assumed that the strand stress varies linearly over the transfer length, l_{tr}, then the theoretical strand set, Δ_{set} can be approximated as:

$$\Delta_{set} = 0.5 \times \varepsilon_{pi} \times l_{tr}$$

For an average l_{tr} of 12.8 in. (325 mm) and a strain in the strand corresponding to a stress level of $0.7f_{pu}$, the estimated strand slip is 0.042 in. (1.1 mm). This compares reasonably well with the average measured strand set of 0.036 in. (0.91 mm).

[D12] Russell, B.W. and Burns, N.H., "Measurement of Transfer Lengths on Pretensioned Concrete Elements." *Journal of Structural Engineering*, ASCE, Vol. 123, No. 5 (1997) pp. 541-549.

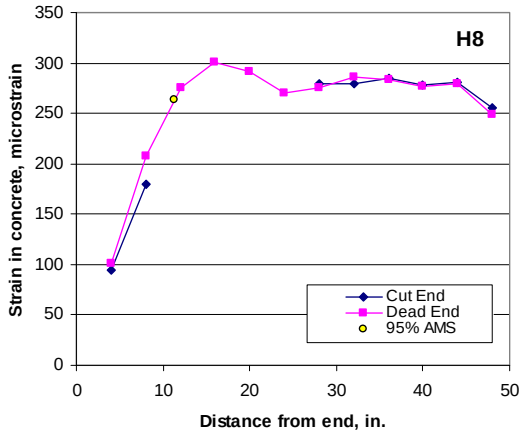

(a) Girder H8

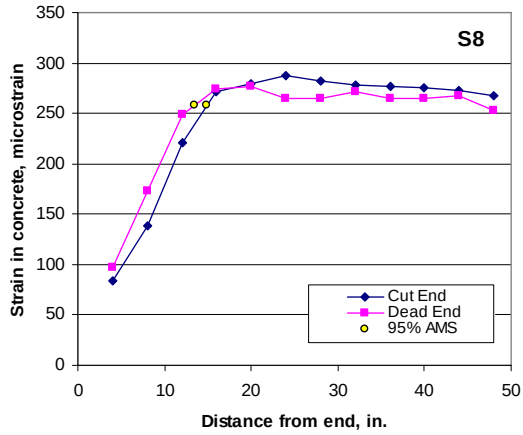

(b) Girder S8

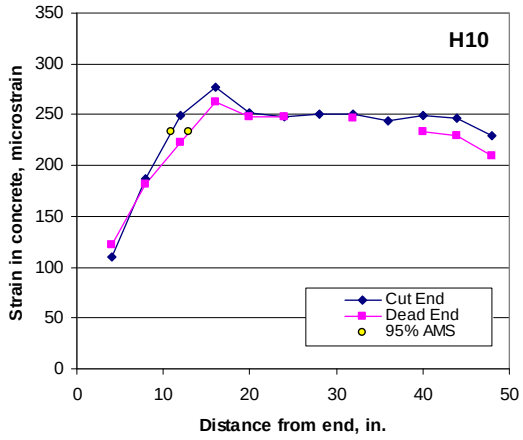

(c) Girder H10

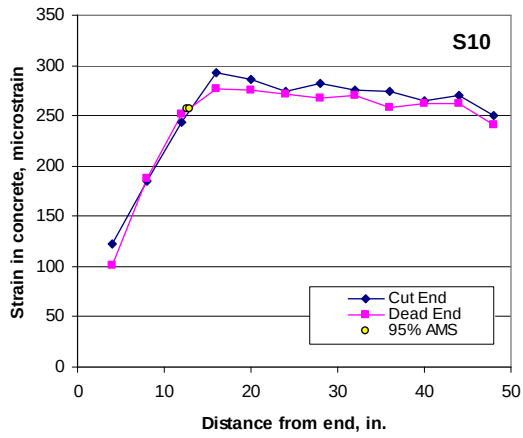

(d) Girder S10

Fig. P.15 – Measurement of transfer length

Table P.3 – Summary of 95% AMS transfer lengths

Girder	Cut end in. (mm)	Dead end in. (mm)
H8	-	11.3 (287)
S8	14.9 (380)	13.5 (343)
H10	11.0 (280)	13.0 (330)
S10	13.0 (330)	12.7 (323)

P.2.5 Concrete Material Properties

P.2.5.1 Semi-adiabatic temperature measurements

Variations of concrete temperature under semi-adiabatic conditions are presented in Fig. P.16. As expected, the 10,000 psi (69 MPa) SCC and HPC mixtures (S10 and H10) developed higher peak temperatures of 139°F (59.4°C) compared to 130.1°F (54.5°C) and 127.4°F (53°C) for 8,000 psi (55 MPa) SCC and HPC mixtures (S8 and H8), respectively. In addition, the S10 and H10 mixtures had shorter times to reach peak temperatures than the S8 and H8 mixtures. The elapsed times to reach peak temperature for H8, S8, H10, and S10 mixtures are 17.7, 18.3, 12.7, and 14.3 hours, respectively. For a given compressive strength level, the SCC and HPC mixtures developed similar peak temperatures; the SCC exhibited slightly longer elapsed time to reach the peak temperature, which can be due to the higher HRWRA dosage.

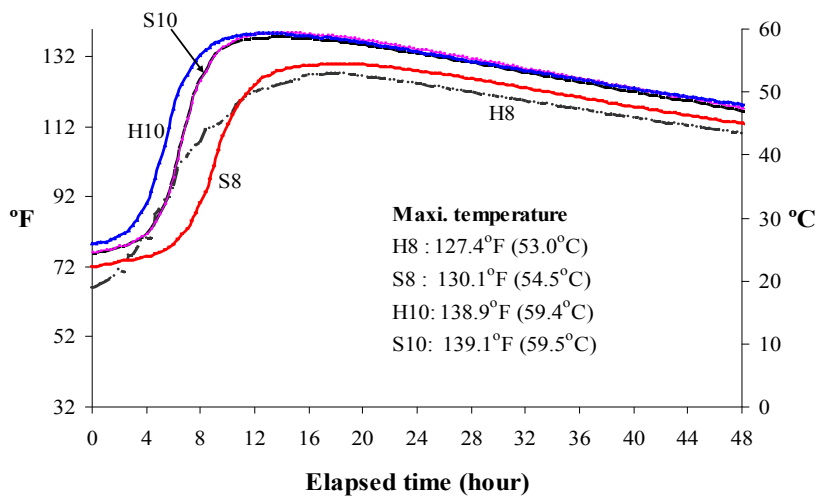

Fig. P.16 – Temperature rise of concrete girder under semi-adiabatic conditions

P.2.5.2 Concrete field testing program

The program for the field testing of the concrete in the girders is presented in Table P.4. For each girder, a minimum of 50 - 4 × 8 in. (100 × 200 mm) cylinders and 18 - 3.9 × 3.9 × 15.7 in. (100 × 100 × 400 mm) flexural beams were prepared. In total, 28 cylinders and nine flexural beams were match-cured with the concrete girders. The rest of the cylinders and flexural beam specimens were demolded after 18 hours of air curing, then moist-cured at 100% RH and 73.4°F (23°C) in a chamber until testing. At the time of prestress release, three steam-cured and three air-cured cylinders were tested to determine the compressive strength.

Four cylinders, two for each curing method, were used to determine the modulus of elasticity. The remaining steam-cured cylinders were stored near the girders and tested to determine the compressive strength and modulus of elasticity at 7, 28, and 56 days, as well as at the age corresponding to the time of testing the girders. Similarly, the flexural beam specimens provide data on the modulus of rupture at the time of prestress release and at 28 and 56 days.

Table P.4 – Concrete field testing program for the girders

SCC behavior	Property	Test Method	Test age	Number of samples per mixture	Size/volume of specimens
Rheology	Yield stress, plastic viscosity	Modified Tattersall MK III rheometer	at delivery & after casting*	N.A.	0.89 ft^3 (25 *l*)
Filling ability	Slump flow**, T-50	ASTM C 1611		N.A.	0.11 ft^3 (3.14 *l*)
Passing ability, filling capacity	J-Ring	ASTM C 1621		N.A.	2.54 ft^3 (72 *l*)
	L-box, Caisson filling capacity	-			
Stability	Surface settlement	-	Over 24 hours	1	7.9×23.6 in. (200×600 mm) cylinders
	Column segregation	ASTM C 1610		1	7.9×26 in. (200×660 mm) cylinders
	Visual stability index	ASTM C 1621		N.A.	0.11 ft^3 (3.14 *l*)
	Stability of air	AASHTO T 152	at delivery & after casting	N.A.	0.25 ft^3 (7 *l*)
Visco-elastic properties	Autogenous shrinkage***	Embedded vibrating wire gages	Over 1 months	2	3×3×11.2 in. (75×75×285 mm) prisms
	Drying shrinkage****	AASHTO T160	Over 6 months	3	6×12 in. (150×300 mm) cylinders

* At arrival of the concrete and just after casting of the girder
** Slump for HPC mixtures
*** Prisms for autogenous shrinkage were sealed after demolding at release time
**** Same curing regime used for release strength was applied to prisms for drying shrinkage

Table P.4 (cont'd) – Concrete field testing program for the girders

SCC behavior	Property	Test Method	Test age	Number of samples per mixture	Size/volume of specimen
Mechanical properties	Compressive strength	AASHTO T 22	At release	3 steam-cured 3 air-cured[A]	4×8 in. (100×200 mm) cylinders
			7 days	3 moist-cured[B] 3 match-cured[C]	
			28 days	3 moist-cured[B] 3 match-cured[C]	
			56 days	3 moist-cured[B] 3 match-cured[C]	
			At shear testing	3 moist-cured[B] 3 match-cured[C]	
	Modulus of elasticity	ASTM C 469	At release	2 steam-cured 2 air-cured[A]	4×8 in. (100×200 mm) cylinders
			7 days	2 moist-cured[B] 2 match-cured[C]	
			28 days	2 moist-cured[B] 2 match-cured[C]	
			56 days	2 moist-cured[B] 2 match-cured[C]	
			At shear testing	2 moist-cured[B] 2 match-cured[C]	
	Flexural strength	AASHTO T 97	At release	3 steam-cured 3 air-cured[A]	3.9×3.9× 15.7 in. (100×100×400 mm) prisms
			28 days	3 moist-cured[B] 3 match-cured[C]	
			56 days	3 moist-cured[B] 3 match-cured[C]	
Hydration kinetics	Temperature rise (semi-adiabatic conditions)			1	6×12 in. (150×300 mm) cylinders
	Setting time	AASHTO T 197		1	Sieved mortar
Structural performance	Transfer length, flexural cracking, and shear capacity	3-point flexural & shear testing		4 girders (2 SCC & 2 HPC)	Full-scale AASHTO Type II girder with 31 ft (9.4 m) in length
	Camber growth			2 SCC girders 2 HPC girders	

[A] Air curing at 50 ± 4% RH and 73 ± 4°F (23 ± 2°C)

[B] 18 hours of air curing followed by moist curing at 100% RH and 73°F (23°C)

[C] 18 hours of steam curing followed by air curing near the corresponding girder

P.2.5.3 Mix proportioning and fresh properties of HPC and SCC used for girder casting

The four mixtures were proportioned with Type III cement and 20% Class F fly ash and crushed aggregate with nominal maximum size aggregate (MSA) of ½ in. (12.5 mm), as presented in Table P.5. The HPC mixtures were proportioned with a *w/cm* of 0.38 and 0.33 to attain the two targeted 56-day compressive strengths of 8,000 and 10,000 psi (55 and 69 MPa), respectively. The two SCC mixtures were prepared with *w/cm* of 0.38 and 0.32. During casting, workability characteristics were evaluated. The mixture proportioning and workability characteristics are summarized in Tables P.6 and P.7, respectively.

Table P.5 – SCC and HPC mixtures used for girder casting

	Targeted 56-day compressive strength	Codification (*w/cm*-binder content-binder type-S/A-VMA)
HPC	8,000 psi (55 MPa)	38-797-III20%FA (*w/cm* = 0.38, Type III cement + 20% Class F fly ash)
	10,000 psi (69 MPa)	33-793-III20%FA (*w/cm* = 0.33, Type III cement + 20% Class F fly ash)
SCC	8,000 psi (55 MPa)	38-742-III20%FA-S/A54 (*w/cm* = 0.38, Type III cement + 20% Class F fly ash, S/A = 0.54)
	10,000 psi (69 MPa)	32-843-III20%FA-S/A46-VMA (*w/cm* = 0.32, Type III cement + 20% Class F fly ash, S/A = 0.46, VMA)

***** MSA = ½ in. (12.5 mm) crushed aggregate

Table P.6 – Mixture proportioning of SCC and HPC for girders

Mixture	HPC (H8)	SCC (S8)	HPC (H10)	SCC (S10)
	8,000 psi	8,000 psi	10,000 psi	10,000 psi
Cement, lb/yd^3 (kg/m^3)	Type III	Type III	Type III	Type III
	639 (379)	593 (352)	638 (379)	674 (400)
HRWRA demand, fl oz/cwt (L/100 kg CM)	5.7 (0.37)	12.3 (0.80)	13.1 (0.85)	21.9 (1.43)
VMA dosage, fl oz/cwt (L/100 kg CM)	0	0	0	1.54 (0.1)
Class F fly ash, lb/yd^3 (kg/m^3)	158 (94)	148 (88)	155 (92)	169 (100)
Total CM, lb/yd^3 (kg/m^3)	797 (473)	742 (440)	793 (470)	843 (500)
Water, lb/yd^3 (kg/m^3)	299 (177)	285 (169)	258 (153)	270 (160)
w/cm	0.38	0.38	0.33	0.32
Sand, lb/yd^3 (kg/m^3)	1,233 (732)	1,715 (1017)	1,323 (785)	1,391 (825)
Coarse aggregate, lb/yd^3 (kg/m^3)	1,795 (1065)	1,387 (823)	1,803 (1070)	1,627 (965)
Sand/total aggregate, by volume	0.41	0.54	0.42	0.47
Volume of coarse aggregate, %	38.9	30.1	39.2	34.9
Volume of mortar, %	61.1	69.9	60.8	65.1
Volume of paste, %	33.8	31.9	31.4	34.6

Table P.7 – Fresh properties of SCC and HPC mixtures used for girders

Mixture		HPC (H8)	SCC (S8)	HPC (H10)	SCC (S10)
		8,000 psi	8,000 psi	10,000 psi	10,000 psi
Slump flow, in. (mm)	at delivery	5.5 (140)*	26.0 (660)	7.5 (190)*	26.0 (660)
	after casting	4.3 (110)*	23.6 (600)	7.1 (180)*	25.2 (640)
T-20 in. (50 cm), sec	at delivery	-	3.0	-	3.0
	after casting	-	3.9	-	3.7
Visual stability index	at delivery	-	0.5	-	0.5
	after casting	-	0.5	-	0.5
Air content, %	at delivery	2.3	2.0	1.9	1.2
	after casting	2.1	1.9	1.9	1.5
Temperature, ^{o}F (^{o}C)	at delivery	66.4 (19.1)	69.8 (21.0)	76.1 (24.5)	75.6 (24.2)
	after casting	66.7 (19.3)	70.7 (21.5)	76.6 (24.8)	76.1 (24.5)
J-Ring flow, in. (mm)	at delivery	-	23.6 (600)	-	22.8 (580)
	after casting	-	21.7 (550)	-	21.3 (540)
L-box	at delivery sec, (h_2/h_1)	-	3.9 (0.73)	-	4.9 (0.70)
	after delivery sec, (h_2/h_1)	-	4.5 (0.68)	-	5.5 (0.62)
Filling capacity, %	at delivery	-	82	-	76
	after casting	-	75	-	70
Rheological parameter	τ_o (Pa)	893	3	568	118
	μ_p (Pa.s)	52	253	233	189
	R^2	0.99	0.99	0.97	0.99
Column segregation index, %		1.58	4.00	-	2.65
Max. surface settlement, %		0.22	0.29	0.21	0.24
Initial setting time, hour		4.20	7.30	5.30	5.4
Final setting time, hour		5.20	8.50	6.10	6.3

* Slump

** 1 Pa = 1.45×10^{-4} psi

P.2.5.4 Mechanical properties of HPC and SCC used for girders

The compressive strength, modulus of elasticity, and flexural strength results are summarized in Tables P.8, P.9 and P.10. The mean 18-hour compressive strength of the 8,000 psi (55 MPa) SCC was 5,250 psi (36.2 MPa); the targeted 18-hour compressive strength was 5,000 psi (34.5 MPa). The release compressive strength of the 10,000 psi SCC (69 MPa) was also greater than the targeted strength of 6,250 psi (43.0 MPa). On the other hand, the 18-hour compressive strengths of the 8,000 and 10,000 psi (55 and 69 MPa) HPC mixtures were 4,945 psi (34.1 MPa) and 5,860 psi (40.4 MPa), which are close to the target compressive strength values of 5,000 psi (34.5 MPa) and 6,250 psi (43.0 MPa), respectively. It is important to note that the temperature

(and therefore maturity) of the concrete in the girder was greater than that of the control cylinders. Therefore, the in-situ compressive strength of the girders should be greater than those determined from the control cylinders.

Table P.8 – Concrete Compressive Strengths of SCC and HPC mixtures used for girders

Age	Curing		H8		S8		H10		S10	
			psi	(MPa)	psi	(MPa)	psi	(MPa)	psi	(MPa)
18 hour	SA	1	4945	(34.1)	5235	(36.1)	5725	(39.5)	6855	(47.2)
		2	4990	(34.4)	5270	(36.3)	6005	(41.4)	6970	(48.1)
		3	5030	(34.7)	5300	(36.5)	5845	(40.3)	6950	(47.9)
		Mean	4988	(34.4)	5268	(36.3)	5858	(40.4)	6925	(47.8)
		COV %	0.9		0.6		2.4		0.9	
		Max. chamber temp. °F (°C)*	126.3	(52.4)	120.7	(49.3)	122.7	(50.4)	120.4	(49.1)
	AM	1	5160	(35.6)	5085	(35.1)	5775	(39.8)	6830	(47.1)
		2	4700	(32.4)	4920	(33.9)	5705	(39.3)	6910	(47.7)
		3	4975	(34.3)	5115	(35.3)	5830	(40.2)	6855	(47.3)
		Mean	4945	(34.1)	5040	(34.7)	5770	(39.8)	6865	(47.3)
		COV %	4.7		2.1		1.1		0.6	
	$f'_{c,SA}/f'_{c,AM}$		1.01		1.05		1.02		1.01	
7 days	SA	1	6355	(43.8)	7095	(48.9)	7690	(53.0)	8600	(59.3)
		2	6220	(42.9)	7200	(49.7)	7580	(52.3)	8710	(60.1)
		3	6180	(42.6)	7265	(50.1)	7775	(53.6)	8440	(58.2)
		Mean	6252	(43.1)	7187	(49.6)	7682	(53.0)	8583	(59.2)
		COV %	1.5		1.2		1.3		1.6	
	AM	1	6295	(43.4)	7130	(49.1)	6980	(48.1)	8045	(55.5)
		2	6185	(42.7)	7120	(49.1)	6955	(48.0)	7995	(55.1)
		3	6325	(43.6)	6990	(48.2)	7145	(49.3)	7780	(53.6)
		Mean	6268	(43.2)	7080	(48.8)	7027	(48.5)	7940	(54.7)
		COV %	1.2		1.1		1.5		1.8	

Curing: SA: 18 hours steam curing followed by air curing near the corresponding girder
Curing: AM: 18 hours of air curing followed by moist curing at 100% RH and 73°F (23°C)

* Chamber temperature refers to the maximum ambient temperature inside the steam-curing chamber determined during steam curing

Table P.8 (cont'd) – Concrete Compressive Strengths of SCC and HPC mixtures used for girders

Age	Curing		H8		S8		H10		S10	
			psi	(MPa)	psi	(MPa)	psi	(MPa)	psi	(MPa)
28 days	SA	1	7125	(49.1)	7980	(55.0)	8175	(56.4)	10210	(62.4)
		2	7200	(49.7)	7585	(52.3)	8305	(57.3)	9795	(59.5)
		3	7130	(49.2)	7900	(54.5)	8600	(59.3)	10190	(60.7)
		Mean	7152	(49.3)	7822	(53.9)	8360	(57.6)	10065	(60.9)
		COV %	0.6		2.7		2.6		2.3	
	AM	1	7990	(55.1)	8450	(58.3)	8235	(56.8)	9045	(70.4)
		2	7620	(52.5)	8295	(57.2)	8760	(60.4)	8630	(67.5)
		3	7855	(54.2)	8600	(59.3)	8330	(57.4)	8805	(70.2)
		Mean	7822	(53.9)	8448	(58.3)	8442	(58.2)	8827	(69.4)
		COV %	2.4		1.8		3.3		2.4	
56 days	SA	1	7760	(53.5)	8630	(59.5)	8875	(61.2)	9500	(65.5)
		2	7225	(49.8)	8715	(60.1)	9325	(64.3)	9660	(66.6)
		3	7150	(49.3)	8470	(58.4)	8950	(61.7)	9515	(65.6)
		Mean	7378	(50.9)	8605	(59.3)	9050	(62.4)	9558	(65.9)
		COV %	4.5		1.4		2.7		0.9	
	AM	1	8370	(57.7)	9660	(66.6)	9355	(64.5)	11095	(76.5)
		2	8410	(58.0)	9805	(67.6)	9180	(63.3)	11255	(77.6)
		3	8105	(55.9)	9730	(67.1)	9500	(65.5)	11705	(80.7)
		Mean	8295	(57.2)	9732	(67.1)	9345	(64.4)	11352	(78.3)
		COV %	2.0		0.7		1.7		2.8	
Test day	SA	1	7225	(49.8)	8105	(55.9)	9045	(62.4)	10235	(70.6)
		2	6920	(47.7)	8095	(55.8)	9015	(62.2)	9835	(67.8)
		3			7770	(53.6)	8710	(60.0)	9810	(67.6)
		Mean	7073	(48.8)	7990	(55.1)	8923	(61.5)	9960	(68.7)
		COV %	3.0		2.4		2.1		2.4	
	AM	1	8610	(59.4)	10885	(75.1)	10610	(73.2)	12265	(84.6)
		2	9220	(63.6)	10745	(74.1)	10875	(75.0)	11920	(82.2)
		3	9295	(64.1)	10775	(74.3)	10600	(73.1)	12195	(84.1)
		Mean	9042	(62.3)	10802	(74.5)	10695	(73.7)	12127	(83.6)
		COV %	4.2		0.7		1.5		1.5	

Curing: SA: 18 hours steam curing followed by air curing near the corresponding girder
Curing: AM: 18 hours of air curing followed by moist curing at 100% RH and 73°F (23°C)

Table P.9 – Elastic modulus of SCC and HPC mixtures used for girders

Age	Curing		H8		S8		H10		S10	
			ksi	(GPa)	ksi	(GPa)	ksi	(GPa)	ksi	(GPa)
18 hour	SA	1	5280	(36.4)	5040	(34.7)	5485	(37.8)	5335	(36.8)
		2	4875	(33.6)	4970	(34.3)	5605	(38.6)	5365	(37.0)
		Mean	5078	(35.0)	5005	(34.5)	5545	(38.2)	5350	(36.9)
	AM	1	4975	(34.3)	4330	(29.9)	5265	(36.3)	5345	(36.8)
		2	4530	(31.2)	4905	(33.8)	5580	(38.5)	5075	(35.0)
		Mean	4753	(32.8)	4618	(31.8)	5423	(37.4)	5210	(35.9)
7 days	SA	1	4900	(33.8)	4700	(32.4)	6070	(41.9)	5245	(36.2)
		2	5090	(35.1)	4900	(33.8)	5455	(37.6)	5120	(35.3)
		Mean	4995	(34.4)	4800	(33.1)	5763	(39.7)	5183	(35.7)
	AM	1	4760	(32.8)	5170	(35.6)	5235	(36.1)	5510	(38.0)
		2	4975	(34.3)	5150	(35.5)	5490	(37.9)	5720	(39.4)
		Mean	4868	(33.6)	5160	(35.6)	5363	(37.0)	5615	(38.7)
28 days	SA	1	5425	(37.4)	5795	(40.0)	5890	(40.6)	6250	(43.1)
		2	5520	(38.0)	5670	(39.1)	6270	(43.2)	5955	(41.0)
		Mean	5473	(37.7)	5733	(39.5)	6080	(41.9)	6103	(42.1)
	AM	1	6115	(42.2)	5800	(40.0)	6480	(44.7)	6565	(45.3)
		2	6015	(41.5)	6020	(41.5)	6480	(44.7)	6805	(46.9)
		Mean	6065	(41.8)	5910	(40.8)	6480	(44.7)	6685	(46.1)
56 days	SA	1	5365	(37.0)	5800	(40.0)	5945	(41.0)	6090	(42.0)
		2	5510	(38.0)	5655	(39.0)	6235	(43.0)	6090	(42.0)
		Mean	5438	(37.5)	5728	(39.5)	6090	(42.0)	6090	(42.0)
	AM	1	6235	(43.0)	6235	(43.0)	6525	(45.0)	6670	(46.0)
		2	6235	(43.0)	6380	(44.0)	6525	(45.0)	6670	(46.0)
		Mean	6235	(43.0)	6308	(43.5)	6525	(45.0)	6670	(46.0)
Test day	SA	1	-	-	4715	(32.5)	5905	(40.7)	5580	(38.5)
		2	-	-	5145	(35.5)	5805	(40.0)	6030	(41.6)
		Mean	-	-	4930	(34.0)	5855	(40.4)	5805	(40.0)
	AM	1	5285	(36.5)	6340	(43.7)	6600	(45.5)	6645	(45.8)
		2	5915	(40.8)	6235	(43.0)	6470	(44.6)	6830	(47.1)
		Mean	5600	(38.6)	6288	(43.4)	6535	(45.1)	6738	(46.5)

Curing: SA: 18 hours steam curing followed by air curing near the corresponding girder
Curing: AM: 18 hours of air curing followed by moist curing at 100% RH and 73°F (23°C)

Table P.10 – Flexural Strength of SCC and HPC mixtures used for girders

Age	Curing		H8		S8		H10		S10	
			psi	(MPa)	psi	(MPa)	psi	(MPa)	psi	(MPa)
18 hour	SA	1	685	(4.7)	660	(4.5)	745	(5.1)	815	(5.6)
		2	665	(4.6)	730	(5.0)	640	(4.4)	770	(5.3)
		3	660	(4.6)	720	(5.0)	730	(5.0)	825	(5.7)
		Mean	670	(4.6)	703	(4.8)	705	(4.9)	803	(5.5)
		COV %	2.0		5.4		8.1		3.6	
	AM	1	585	(4.0)	680	(4.7)	685	(4.7)	730	(5.0)
		2	590	(4.1)	635	(4.4)	745	(5.2)	775	(5.3)
		3	590	(4.1)	620	(4.3)	685	(4.7)	755	(5.2)
		Mean	588	(4.1)	645	(4.4)	705	(4.9)	753	(5.2)
		COV %	0.5		4.8		4.9		3.0	
28 days	SA	1	815	(5.6)	795	(5.5)	740	(5.1)	815	(5.6)
		2	740	(5.1)	795	(5.5)	950	(6.5)	865	(6.0)
		3	970	(6.7)	790	(5.4)	820	(5.6)	765	(5.3)
		Mean	842	(5.8)	793	(5.5)	837	(5.8)	815	(5.6)
		COV %	13.9		0.4		12.7		6.1	
	AM	1	1055	(7.3)	1140	(7.9)	1255	(8.6)	1450	(10.0)
		2	1155	(8.0)	1100	(7.6)	1235	(8.5)	1430	(9.9)
		3	1115	(7.7)	1115	(7.7)	1335	(9.2)	1405	(9.7)
		Mean	1108	(7.6)	1118	(7.7)	1275	(8.8)	1428	(9.8)
		COV %	4.5		1.8		4.2		1.6	
56 days	SA	1	970	(6.7)	885	(6.1)	855	(5.9)	855	(5.9)
		2	985	(6.8)	900	(6.2)	855	(5.9)	855	(5.9)
		3	930	(6.4)	985	(6.8)	825	(5.7)	840	(5.8)
		Mean	962	(6.6)	923	(6.4)	845	(5.8)	850	(5.9)
		COV %	3.0		5.8		2.0		1.0	
	AM	1	1100	(7.6)	1220	(8.4)	1260	(8.7)	1480	(10.2)
		2	1115	(7.7)	1245	(8.6)	1245	(8.6)	1550	(10.7)
		3	1115	(7.7)	1260	(8.7)	1305	(9.0)	1525	(10.5)
		Mean	1110	(7.7)	1242	(8.6)	1270	(8.8)	1518	(10.5)
		COV %	0.8		1.6		2.5		2.3	

Curing: SA: 18 hours steam curing followed by air curing near the corresponding girder
Curing: AM: 18 hours of air curing followed by moist curing at 100% RH and 73°F (23°C)

P.2.5.5 Visco-elastic properties of HPC and SCC used for girder casting

Autogenous shrinkage

Autogenous shrinkage strains of two SCC and two HPC mixtures summarized in Table P.11. The autogenous shrinkage, measured on sealed specimens, ranged from 200 to 285 µstrain, after 56 days.

Table P.10 – Autogenous shrinkage strains at various ages (µstrain)

Time (d)	H8	S8	H10	S10
1	-45	-55	-50	-110
3	-80	-90	-100	-140
7	-135	-140	-125	-190
14	-185	-190	-155	-230
28	-225	-230	-180	-265
56	-260	-265	-200	-285

Figure P.17 presents the autogenous shrinkage results of two SCC and two HPC mixtures. In general, SCC mixtures exhibited higher autogenous shrinkage of 265 and 285 µstrain compared to HPC mixtures made with same Type III cement with 20% of fly ash ranged from 200 and 260 µstrain, at the age of 56 days. S10 proportioned with *w/cm* of 0.32 given the highest autogenous shrinkage compared to remaining mixtures. H8 and S8 mixtures made with the same *w/cm* of 0.38 exhibited similar autogenous shrinkage at various ages.

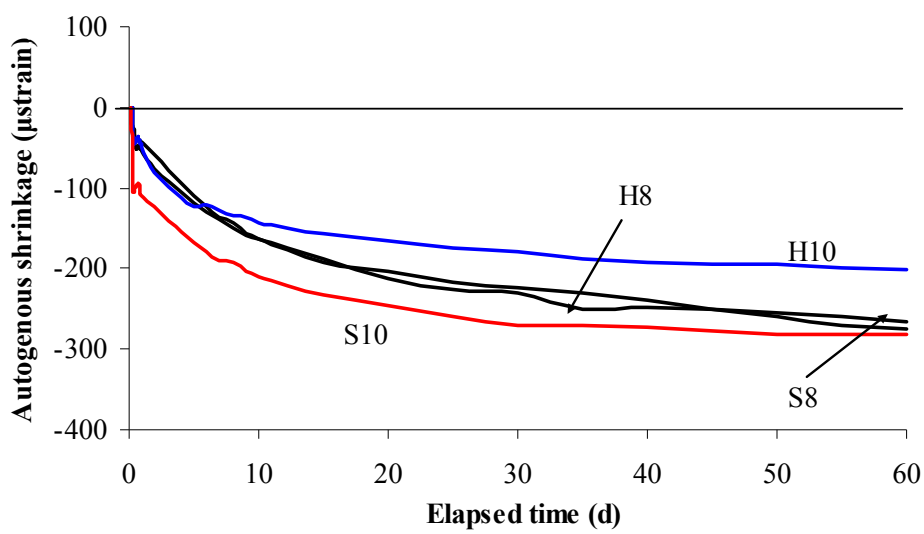

Fig. P.17 – Variations of autogenous shrinkage with time for SCC and HPC

Drying shrinkage

To data, drying shrinkage was monitored for approximately four months using 6 × 12 in. (150 × 300 mm) cylinders. Three samples were prepared for each concrete to monitor drying shrinkage and were steam-cured with the girder in the same conditions employed for compressive strength specimens. The specimens were then transferred to a curing chamber with 50% ± 4% relatively humidity and temperature of 73 ± 4ºF (23 ± 2 ºC). Initial length measurements were taken at the age of 18 hours. The results of drying shrinkage of the two SCC and two HPC are summarized in Table P.12. For the two SCC and two HPC mixtures, the drying shrinkage values ranged from 390 and 495 µstrain after 112 days of drying.

Table P.12 – Drying shrinkage strains after various periods of drying (µstrain)

Time (d)	H8	S8	H10	S10
1	50	65	80	75
7	135	160	210	195
28	290	355	305	355
56	330	405	335	405
84	370	435	370	455
112	405	465	390	495

Figure P.18 compares the results of drying shrinkage of two SCC and two HPC mixtures. For a given binder content and Type III cement with 20% of fly ash, H8 proportioned with *w/cm* of 0.38 exhibited higher drying shrinkage of 405 µstrain compared to H10 made with 0.33 *w/cm* of 390 µstrain at the age of 112 days. On the other hand, S10 prepared with higher binder content of 843 lb/yd^3 (500 kg/m^3) exhibited higher drying shrinkage of 495 µstrain compared to S8 made with 742 lb/yd^3 (440 kg/m^3) at the age of 112 days, regardless of *w/cm*. Two SCC mixtures exhibited also higher drying shrinkage ranged between 465 and 495 µstrain than two HPC mixtures of 390 to 405 µstrain, respectively.

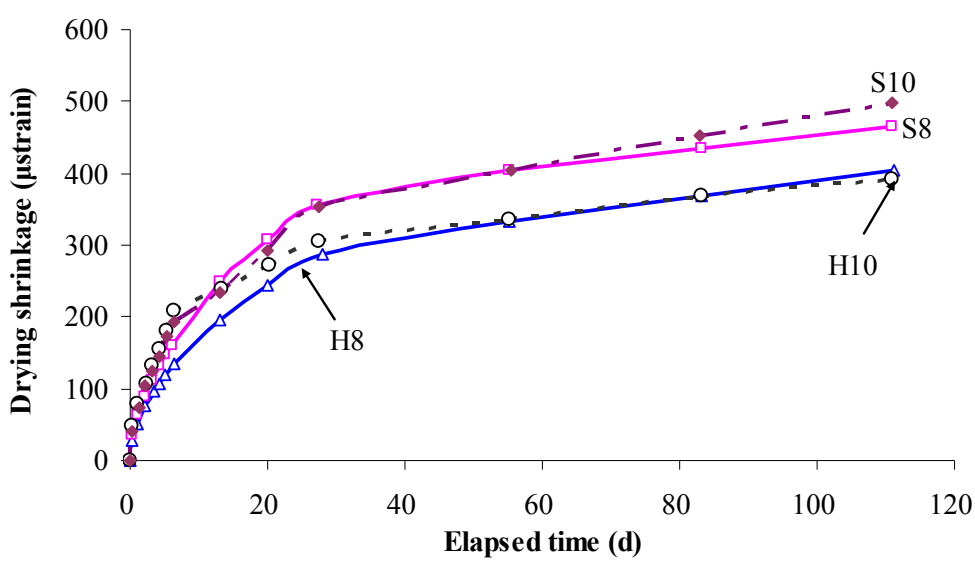

Fig. P.18 – Variations of drying shrinkage with time for SCC and HPC

P.2.5.6 Mechanical properties of deck slab concrete

Table P.13 gives the mixture proportioning used in the production of the ready-mix concrete for the deck slabs. Table P.14 indicates the concrete properties used for the deck slabs. Two different casts were used as shown in the table.

Table P.13 – Mix proportions for deck slab concrete

Mixture	Deck Slab Concrete
	5,000 psi
Cement, lb/yd^3 (kg/m^3)	Type I
	639 (380)
Water, lb/yd^3 (kg/m^3)	269 (160)
w/cm	0.42
Sand, lb/yd^3 (kg/m^3)	1,189 (707)
Coarse aggregate, lb/yd^3 (kg/m^3)	1,822 (1083)
Retarder, oz/yd^3 (ml/m^3)	17.7 (684)
Air entraining agent, oz/yd^3 (ml/m^3)	8.8 (342)

Table P.14 – Properties of deck slab concrete

	Specimens H8 and S8	Specimens H10 and S10
Slump	3.75 in. (95 mm)	3.75 in. (95 mm)
Air content, %	6.1	7.6
Initial concrete temperature	77.9 ^{o}F (25.5^{o}C)	80.6 ^{o}F (27.0^{o}C)
Average compressive strength at 28 days	5030 psi (34.7 MPa)	4690 psi (32.4 MPa)
Modulus at 28 days	4590 ksi (31.6 GPa)	4280 ksi (29.5 GPa)
Average compressive strength at 38 days	5250 psi (36.2 MPa)	5090 psi (35.1 MPa)

P.2.6 Reinforcing Steel and Prestressing Steel Properties

P.2.6.1 Reinforcing steel

Figure P.19 shows typical stress strain relationships for the No. 3 and No. 5 reinforcing bars. Table P.15 summarizes the mechanical properties of the reinforcing bars, with average values of the yield stress, f_y, the ultimate stress, f_u, the strain at strain hardening, ε_{sh} and the ultimate strain, ε_u.

P.2.6.2 Prestressing steel

Figure P.20 shows the stress-strain relationship for the 7-wire 0.6 in. (15 mm) diameter low-relaxation prestressing strand used in the experimental program. Table P.16 summarizes the mechanical properties.

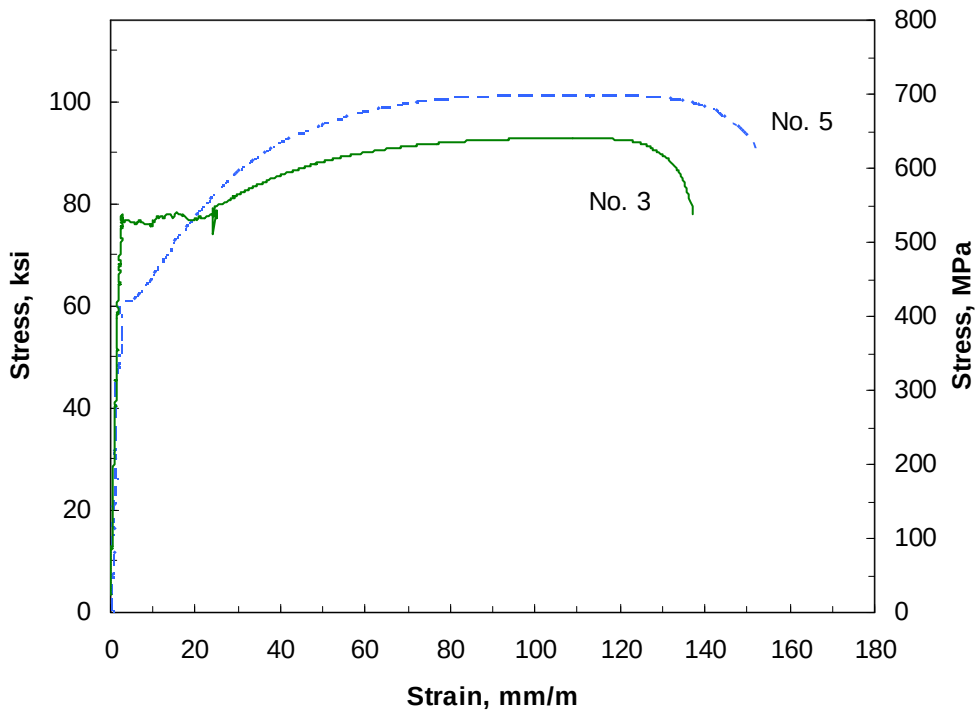

Fig. P.19 – Typical stress-strain relationships for No. 3 and No. 5 bars

Table P.15 – Average mechanical properties of reinforcing bars

	A_s in^2 (mm^2)	E_s ksi (GPa)	f_y ksi (MPa)	ε_y	f_u ksi (GPa)	ε_{sh}	ε_u
No. 3	0.11 (71)	29,000 (200)	76.3 (526)	0.00263	92.5 (638)	0.0240	0.127
No. 5	0.31 (200)	29,000 (200)	60.9 (42)	0.00210	101.1 (697)	0.0057	0.152

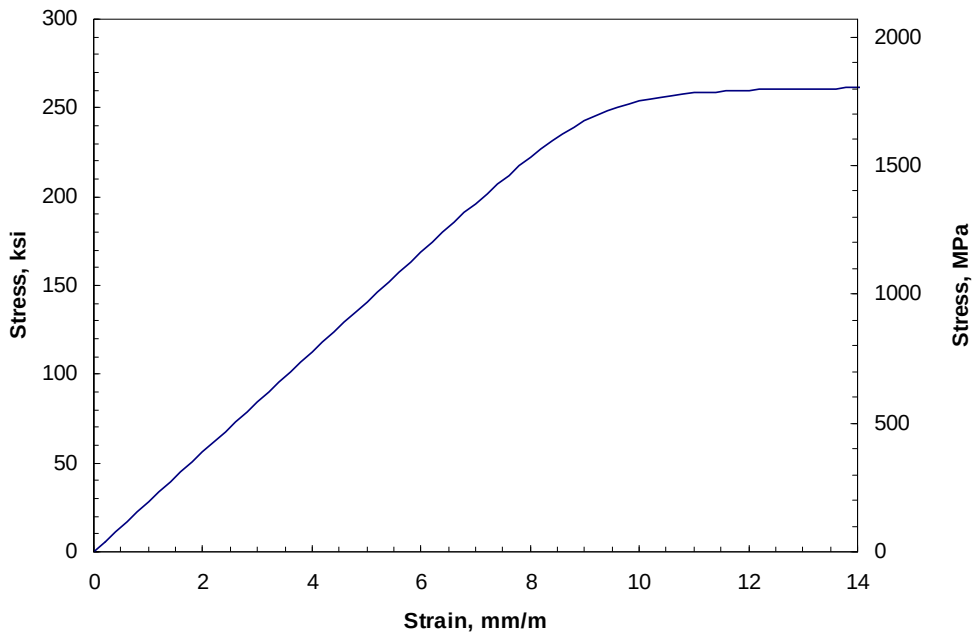

Fig. P.20 – Typical stress-strain relationship for 0.6 in. (15 mm) diameter strand

Table P.16 – Typical mechanical properties of prestressing strand

	A_{ps} in^2 (mm^2)	E_{ps} ksi (GPa)	0.2% offset stress ksi (GPa)	Stress at 1% strain ksi (GPa)	f_{pu} ksi (GPa)	ε_{pu}
0.6 in. (15 mm) diameter	0.217 (140)	28,100 (194)	259 (1.78)	254 (1.75)	278.1 (1.92)	0.072

P.2.7 Test Setup and Procedure

The composite precast pretensioned girder and deck slab specimens were tested using the 2,600 kip capacity computer-controlled MTS testing machine. Figure P.21 shows the test setup and the locations of the Linear voltage differential transducer (LVDTs) used to measure displacements and to determine average strains. The LVDTs were attached to pins anchored into the concrete on the back face of the specimen. As is typical for this type of construction the specimens were supported on neoprene bearing pads at their ends. A structural steel loading beam was used to provide two equal line loads at the locations shown in Figs. P.21 and P.22.

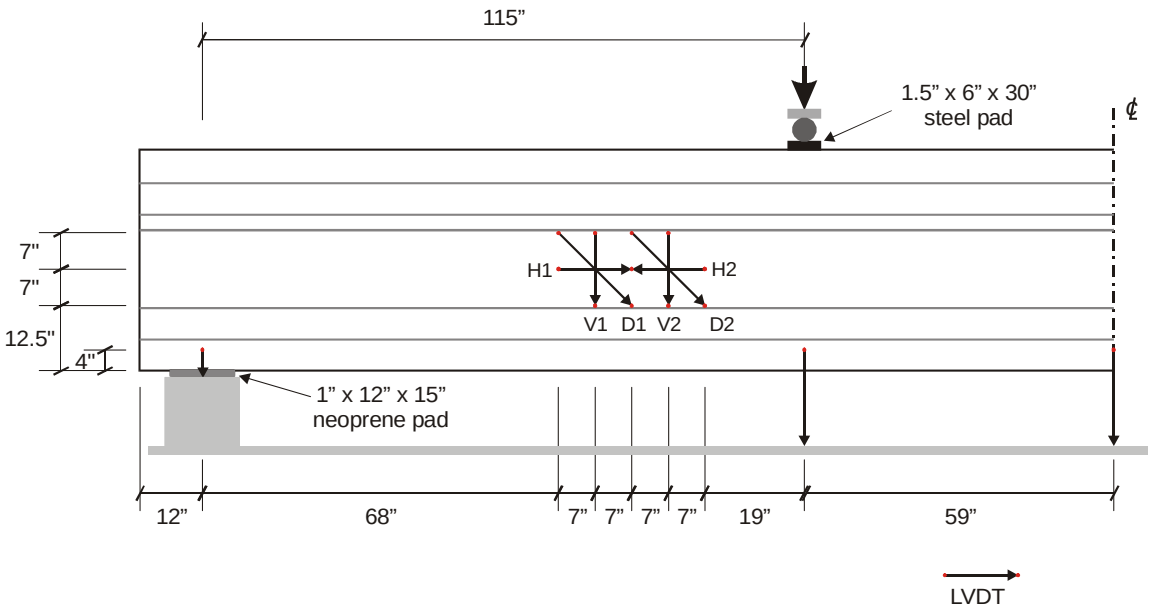

Fig. P.21 – Test setup and locations of LVDTs

Fig. P.22 – Specimen H8 before testing

All specimens were loaded using the same procedure. Initially, the total load was applied to the structural loading beam in "load control" at a rate of 11 kips/min (50 kN/min). After first flexural cracking developed the loading was applied in "deflection control" at a rate of 0.06 in./min (1.5 mm/min) until failure was reached. The loading was stopped at key load stages to enable detailed measurements of the crack widths and to take photographs. During the testing the LVDT and strain gage readings were taken every 0.5 second.

P.3 FLEXURAL BEHAVIOR

P.3.1 Camber Measurements

Figure P.23 shows the variation of the camber with time measured from casting of the concrete, with zero camber just prior to release. The camber was measured at midspan using a piano wire subjected to constant tension that was attached to the ends of the specimen and with the reading at midspan taken by sighting against a mirrored scale to minimize parallax. The prestress release occurred at an age of about 18 hours. The sudden reduction in camber that occurred is due to the removal of the formwork for the deck slab.

The specimens with target compressive strengths of 8,000 psi (55 MPa) had larger cambers than the companion specimens made with 10,000 psi (69 MPa) concrete.

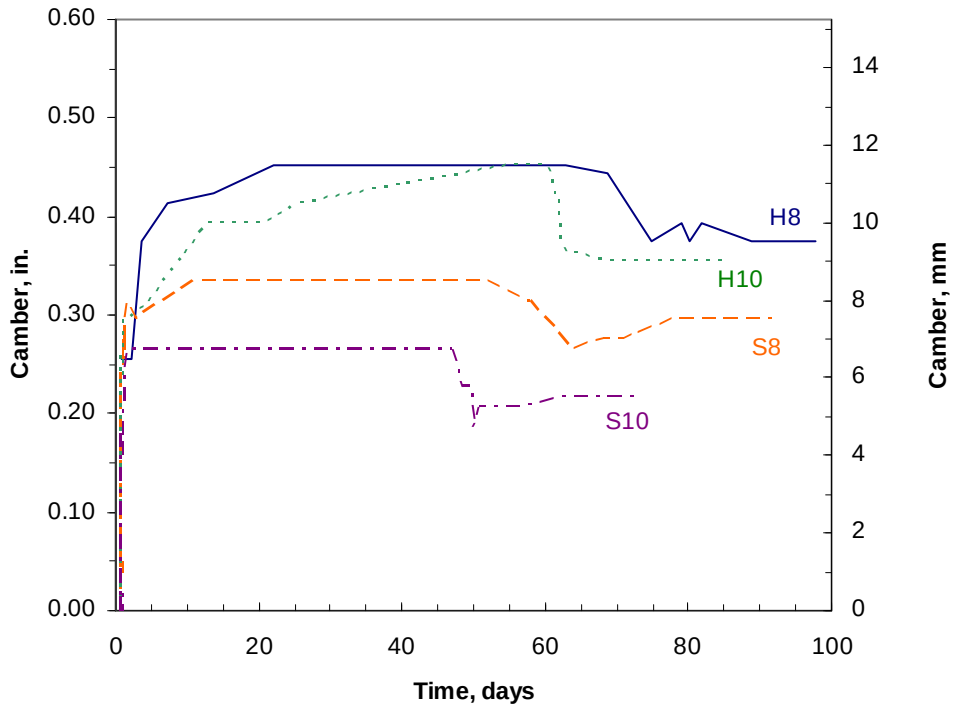

Fig. P.23 – Variation of camber with time

P.3.2 Overall Response in Flexure

Figures P.24 to P.27 Show the moment versus central deflection responses of Specimens H8, S8, H10 and S10, respectively. Table P.17 summarizes the results with the moment at first flexural cracking, M_{cr}, the maximum moment achieved, M_{max}, the predicted flexural capacity, M_n, and the maximum deflection reached before failure, Δ_{max}. The first flexural crack observed in each of the specimens was hairline.

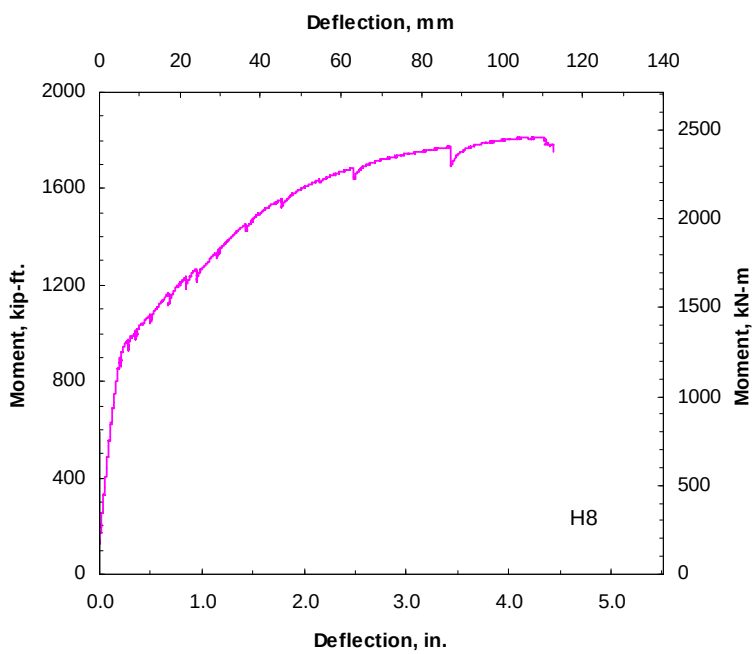

Fig. P.24 – Moment versus central deflection – Specimen H8

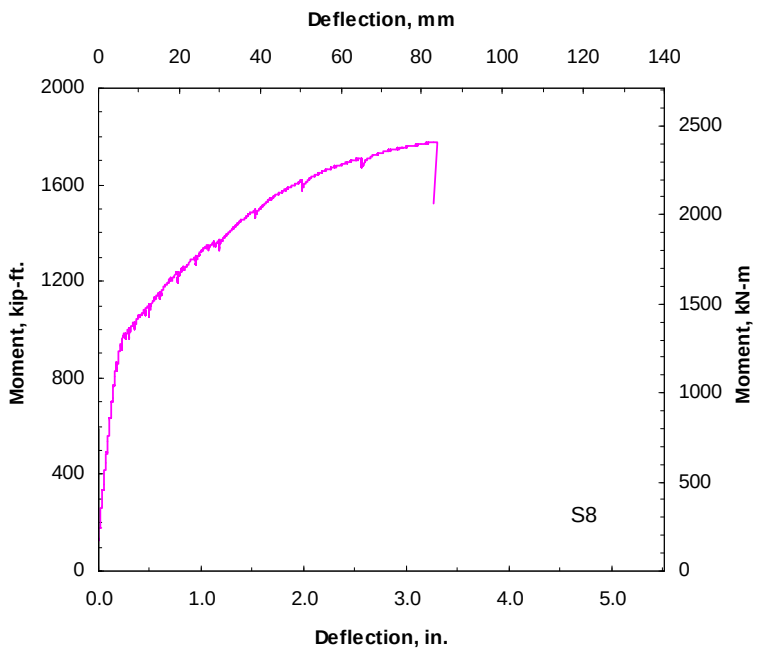

Fig. P.25 – Moment versus central deflection – Specimen S8

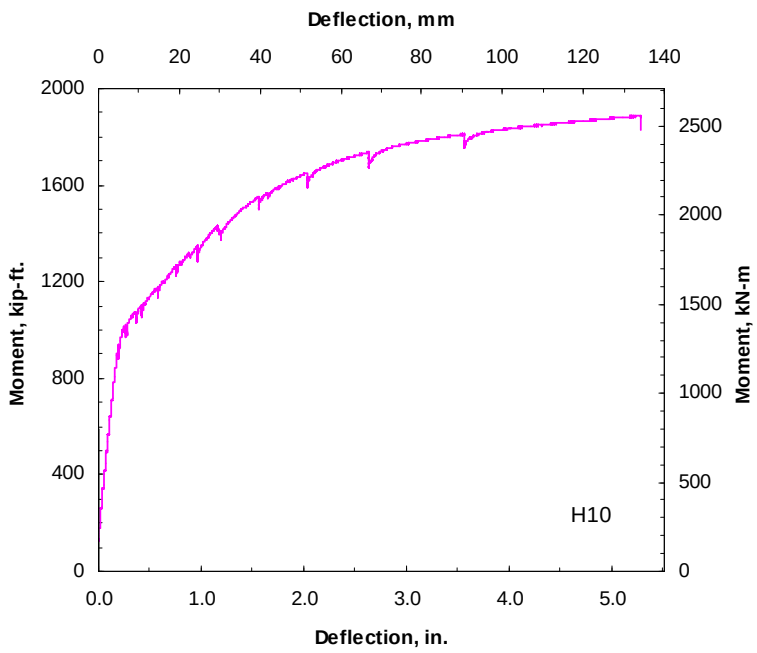

Fig. P.26 – Moment versus central deflection – Specimen H10

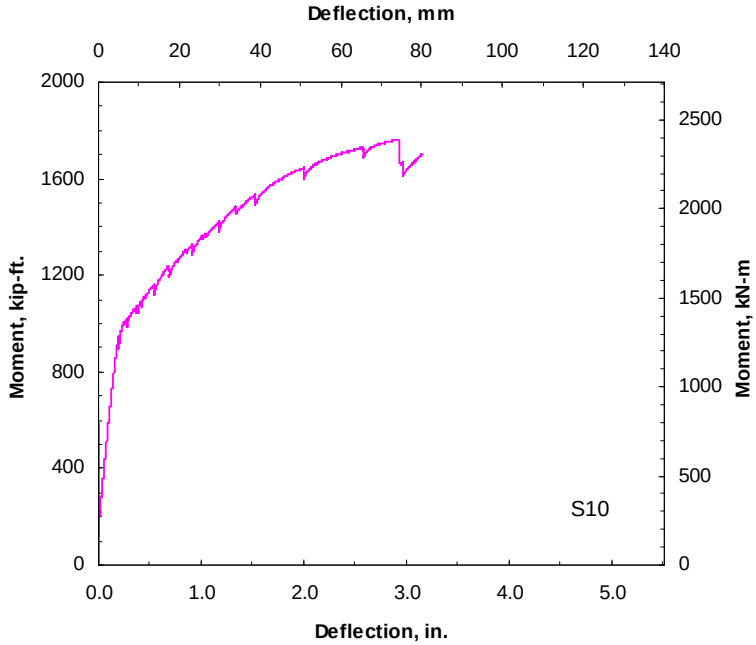

Fig. P.27 – Moment versus central deflection – Specimen S10

Table P.17 – Comparison of flexural responses of four specimens

	H8	S8	H10	S10
M_{cr}, ft kips (kN.m)	885 (1200)	868 (1177)	937 (1270)	946 (1283)
M_{max}, ft kips (kN.m)	1,815 (2460)	1,779 (2412)	1,888 (2560)	1,764 (2392)
Δ_{max}, in. (mm)	4.43 (113)	3.30 (84)	5.29 (134)	3.15 (80)
$f'_{c\ girder}$, ksi (MPa)	7.38 (50.9)	8.61 (59.4)	9.05 (62.4)	9.56 (65.9)
$f'_{c\ slab}$, ksi (MPa)	5.25 (36.2)	5.25 (36.2)	4.89 (33.7)	4.89 (33.7)
M_n, ft kips (kN.m)	1,800 (2440)	1,800 (2440)	1,791 (2428)	1,791 (2428)

Table P.17 also shows the predicted nominal flexural resistances for each of the beams. Also shown are the concrete strengths for the girders and the deck slab used to make these predictions. It is noted that the two high-performance concrete girders, H8 and H10, both achieved moments greater than the predicted nominal flexural resistances before failing in shear. The two SCC girders, S8 and S10, failed in shear just before reaching their predicted nominal flexural resistances. Specimens H8 and H10 experienced larger deflections at midspan than Specimens S8 and S10.

Figure P.28 shows the moment versus strain responses for each of the specimens with the strains obtained from the vibrating wire gages, one located at the center of the span and the other located 4 ft (1.22 m) from the center of the span, near one of the loading points. The high strains that were recorded indicate that the flexural reinforcement had yielded and had strains beyond strain hardening.

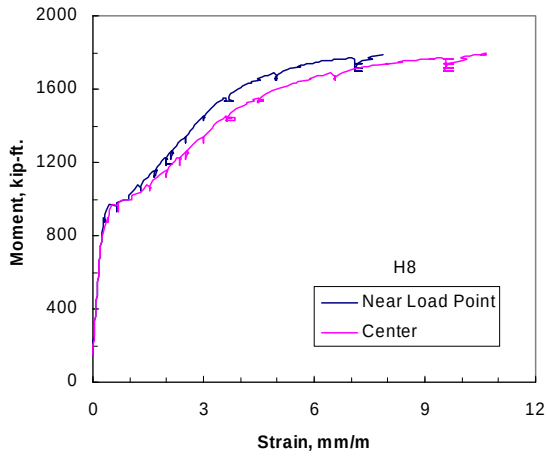

(a) Specimen H8

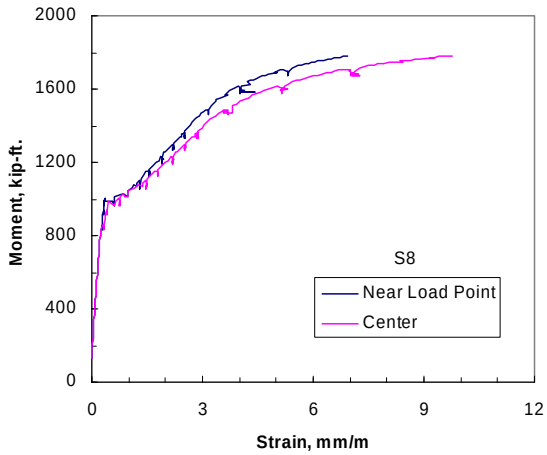

(b) Specimen S8

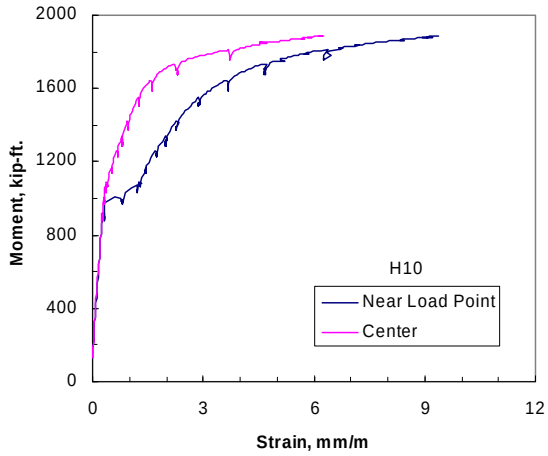

(c) Specimen H10

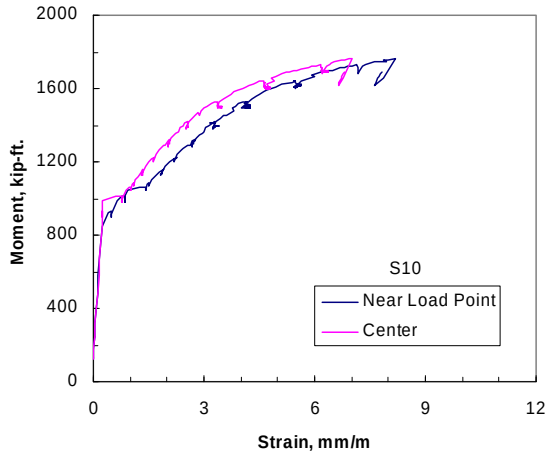

(d) Specimen S10

Fig. P.28 – Moment versus longitudinal strain response at the level of the straight strands

P.4 SHEAR BEHAVIOR

Figures P.29 to P.32 show the shear versus deflection response for the side of each specimen that experienced shear failure. The deflection that is plotted is the deflection measured at the location of the loading point. The shear was determined at the inner face of the neoprene bearing pads.

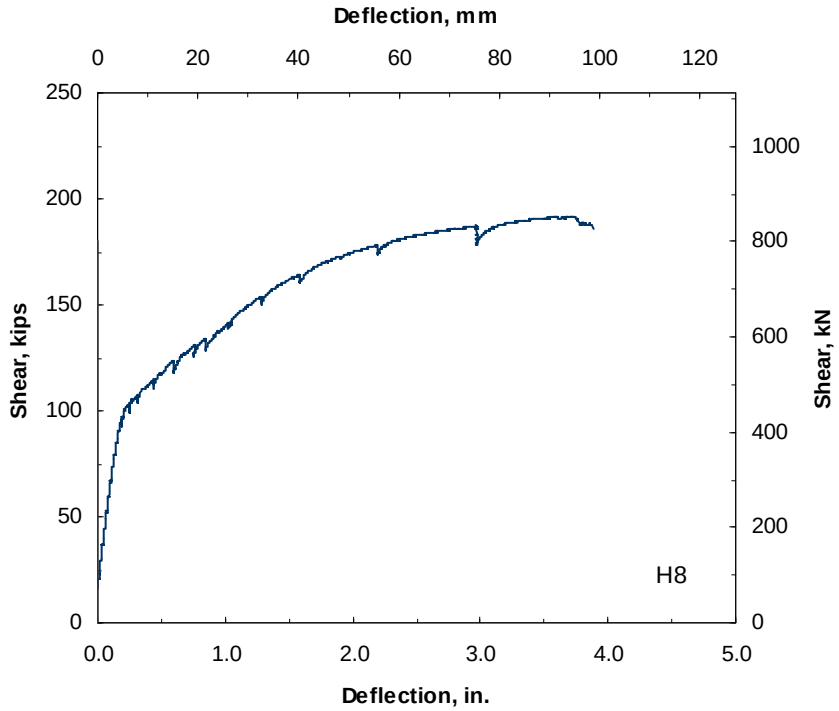

Fig. P.29 – Shear versus deflection at load point – Specimen H8

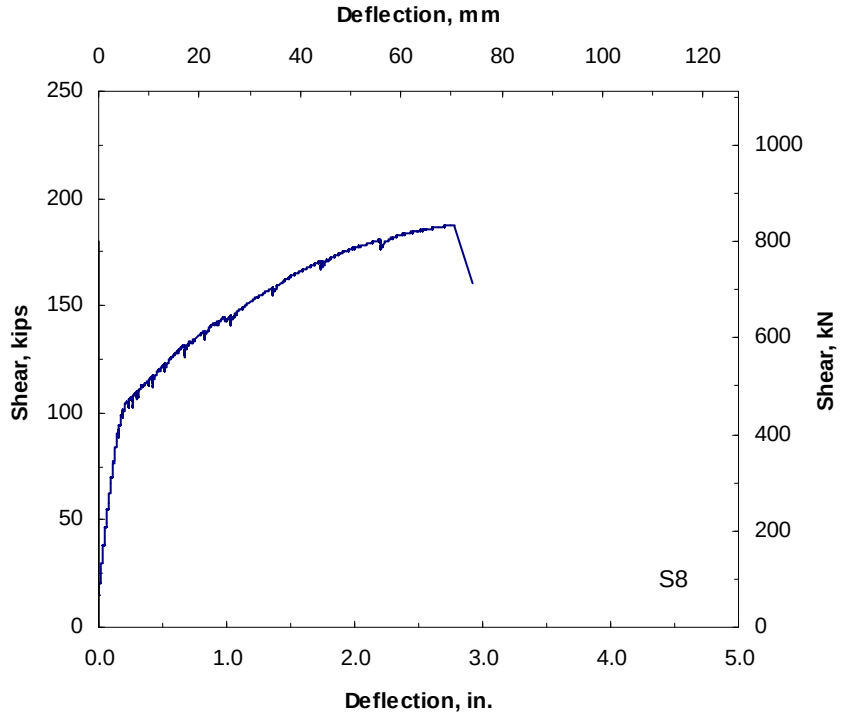

Fig. P.30 – Shear versus deflection at load point – Specimen S8

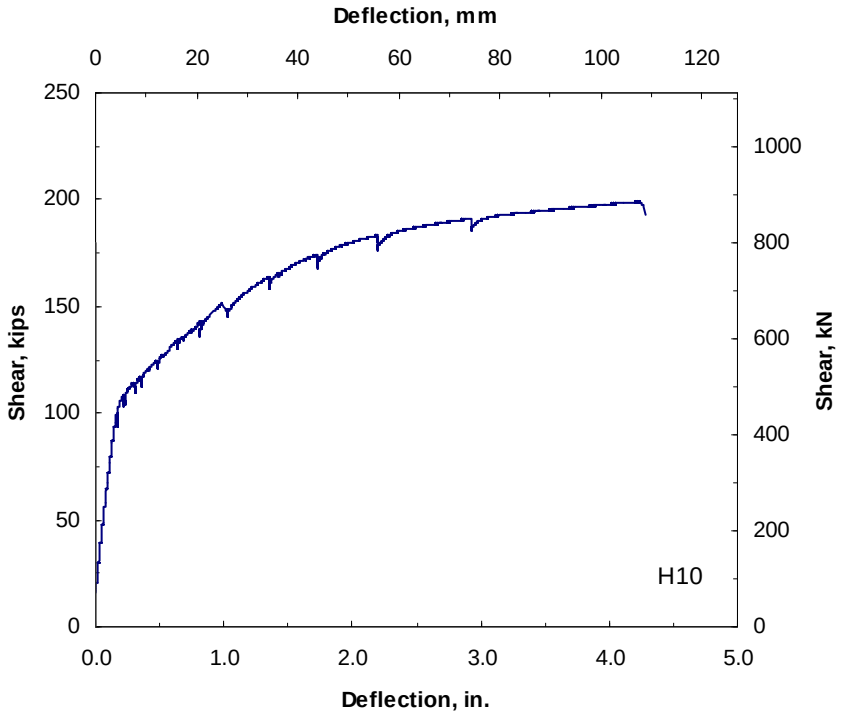

Fig. P.31 – Shear versus deflection at load point – Specimen H10

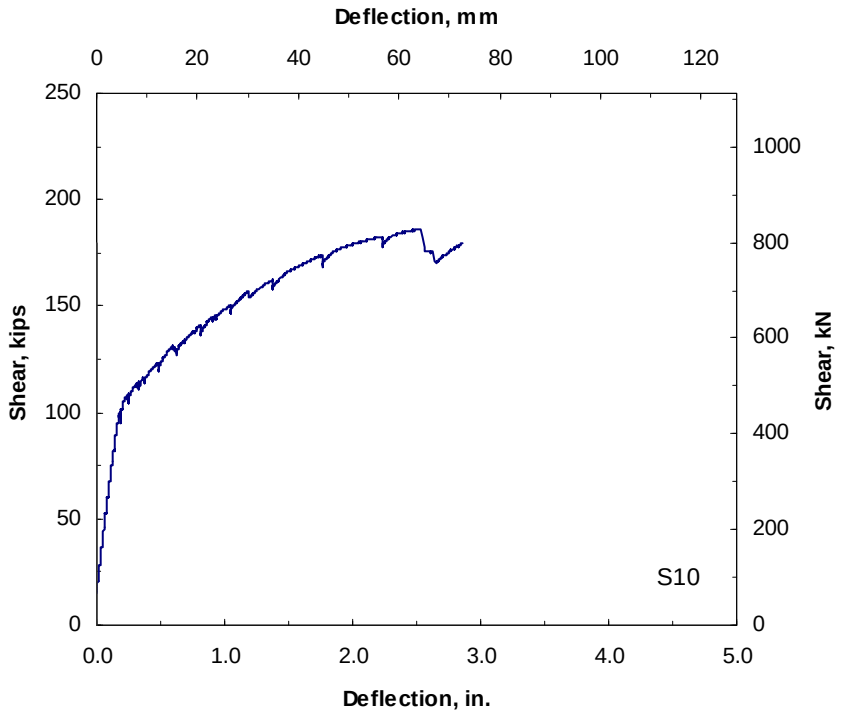

Fig. P.32 – Shear versus deflection at load point – Specimen S10

Figure P.33 shows the variations in the average vertical strains obtained from the LVDT rosette readings for all of the specimens on the end that failed in shear. The strains obtained from the vertical LVDT readings are average strains determined over the 14 in. (356 mm) gage length. It was found that these strains were more representative of the stirrup strains than the reading obtained from the stirrup strain gages. LVDTs V1 and V2 are located at distances of 40 and 26 in. (1016 and 660 mm), respectively from the loading point. As can be seen from this figure the stirrups experienced strains well above their yield strain of 2.63 x 10^{-3}.

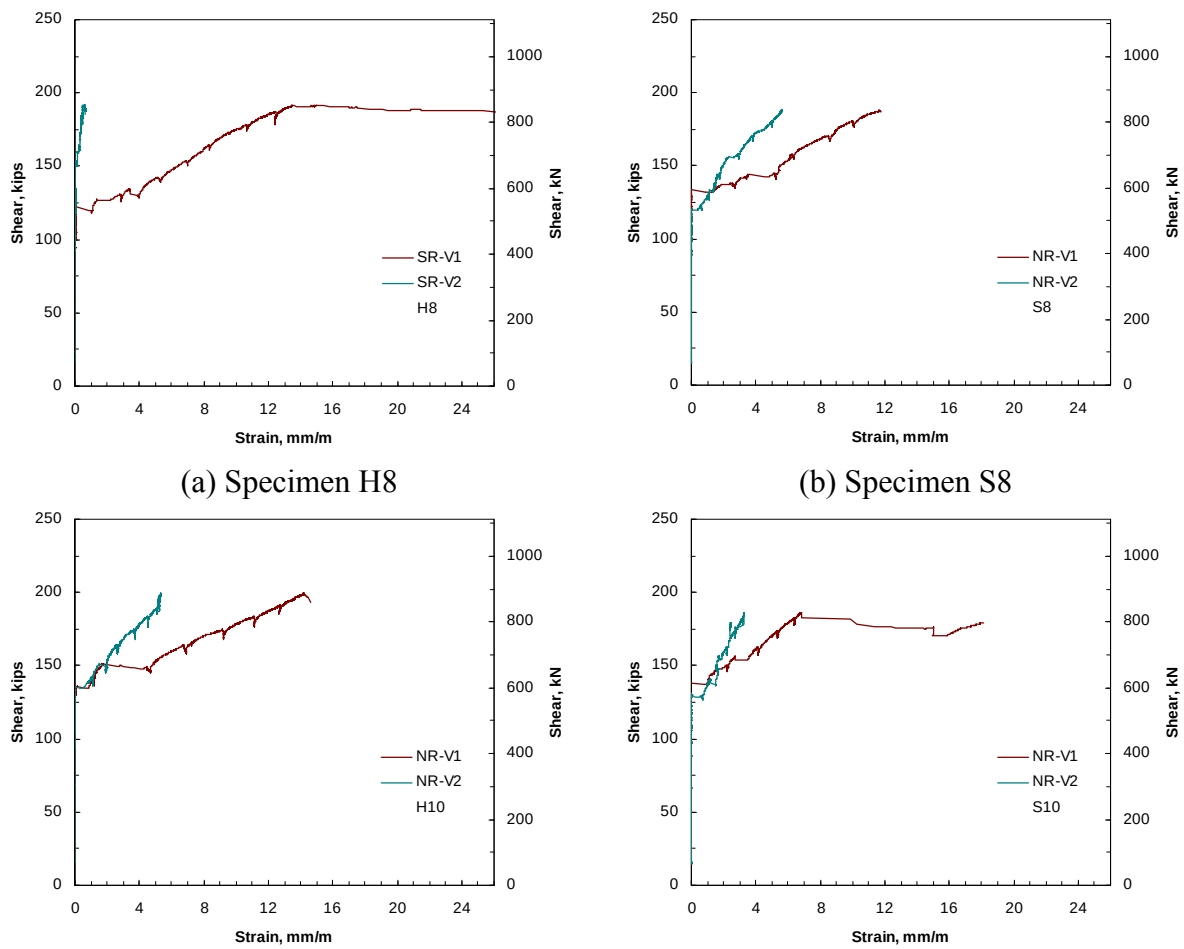

(a) Specimen H8 (b) Specimen S8

(c) Specimen H10 (d) Specimen S10

Fig. P.33 – Variations in the average vertical strains obtained from the LVDT rosette readings for all of the specimens on the end that failed in shear.

Figures P.34 to P.37 show the four specimens just before and after shear failure on the ends that failed in shear.

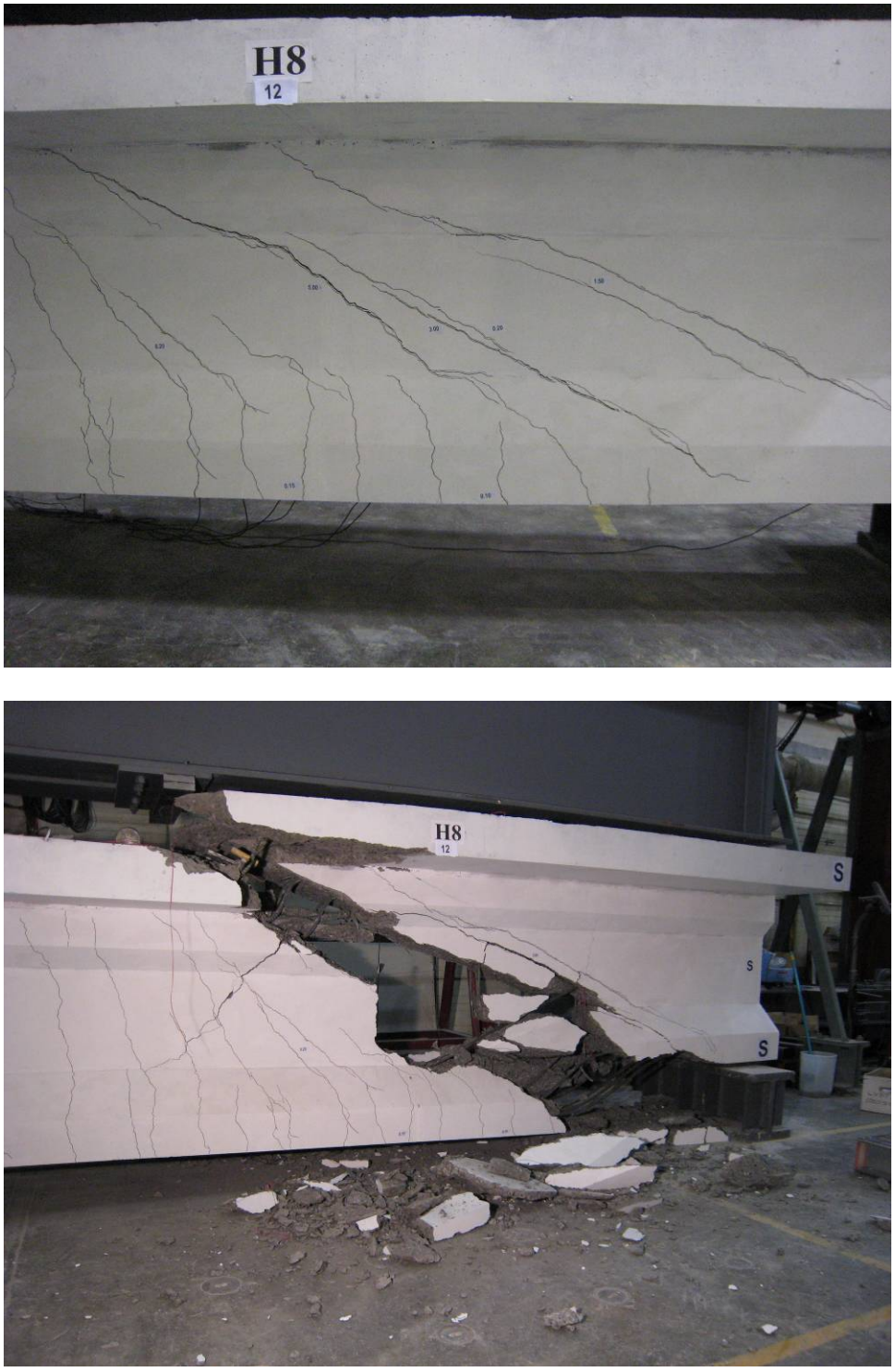

Fig. P.34 – Specimen H8 just before and just after failure

Fig. P.35 – Specimen S8 just before and just after failure

Fig. P.36 – Specimen H10 just before and just after failure

Fig. P.37 – Specimen S10 just before and just after failure

Table P.18 compares the shears at first shear cracking, V_{cr}, first stirrup yield, V_y, and the maximum shear, V_{max}. The table also compares the maximum deflection at the loading point attained during testing. Table P.18 also presents the predicted nominal shear resistance using Section 5.8 of the 2007 AASHTO Specifications. For these predictions the measured properties

of the reinforcing bars, prestressing steel and concrete mixtures were used. It is noted that the experimentally determined maximum shears are considerably above the predicted nominal shear resistance. There are several reasons for the conservative predictions:

- The tensile strengths obtained from the flexural beam tests indicate that the corresponding code values are very conservative for the HPC and SCC mixtures.
- During the testing it was evident that the strength and stiffness of the top and bottom flanges of the specimens considerably increased the shear strengths, with shear cracks of 7 mm (0.28 in.) observed in the webs before shear failure occurred.

Table P.18 – Comparison of shear responses of four specimens

	H8	S8	H10	S10
V_{cr}, kips (kN)	115 (511)	109 (485)	117 (520)	116 (516)
V_y, kips (kN)	130 (578)	136 (605)	150 (667)	156 (694)
V_{max}, kips (kN)	192 (854)	188 (836)	199 (885)	186 (827)
Δ_{max}, in. (mm)	3.88 (99)	2.92 (74)	4.28 (109)	2.86 (73)
$f'_{c\ girder}$, ksi (MPa)	7.38 (50.8)	8.61 (59.4)	9.05 (62.4)	9.56 (65.9)
$f'_{c\ slab}$, ksi (MPa)	5.25 (36.2)	5.25 (36.2)	4.89 (33.7)	4.89 (33.7)
V_n, kips (kN)	113 (503)	115 (511)	118 (525)	119 (529)

P.5 COMPARISON BETWEEN STRUCTURAL PERFORMANCES OF SCC AND VIBRATED HPC

Figures P.38 and P.39 show the moment versus central deflection responses and the shear versus loading point deflection responses, respectively, for the four specimens.

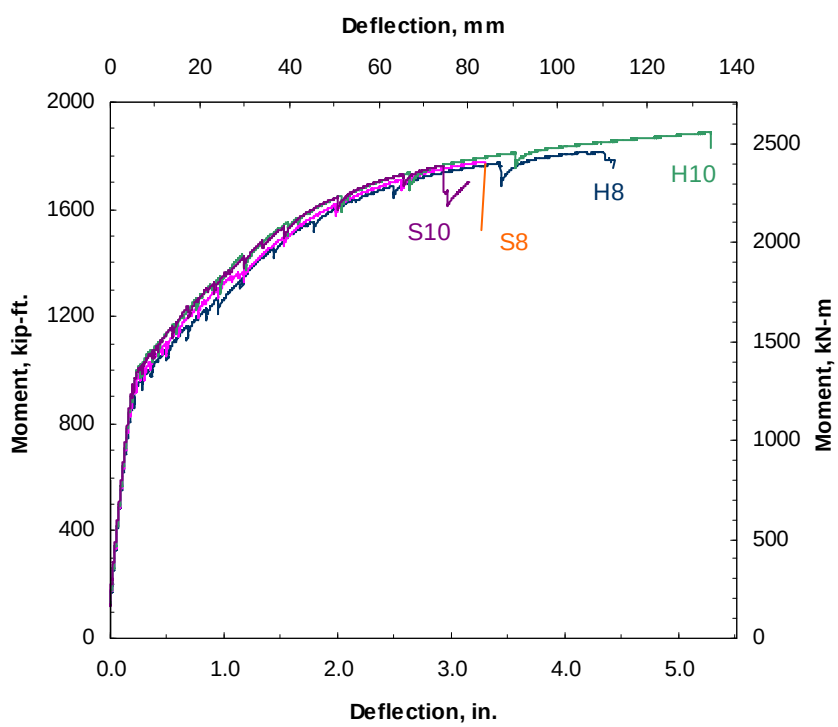

Fig. P.38 – Comparison of moment versus loading point deflection responses for the four specimens

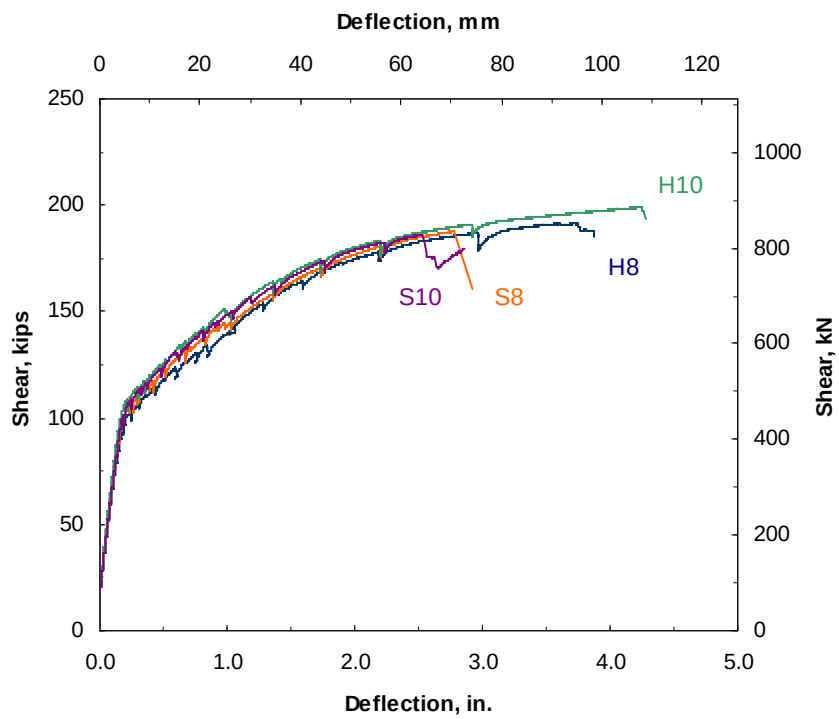

Fig. P.39 – Comparison of shear versus deflection responses for the four specimens

P.6 CONCLUSIONS

The following conclusions arise from the construction and testing of the precast, prestressed girders:

- The SCC placement was successful, even with the casting from only one location at midspan of the 31-ft (9.44-m) long girders.
- There was no visible segregation of the concrete in any of the girders.
- During the steam-curing operation the maximum temperatures reached satisfied to maximum temperature limit of 150°F (65°C).
- There were fewer "bug holes" for the SCC concrete than for the HPC.
- The target 18-hour compressive strengths, required at prestress release, were met for the two SCC girders.
- The transfer lengths were similar for the four different concrete mixtures.
- The transfer lengths were considerably shorter than the transfer length given in the 2007 AASHTO Specifications and the ACI 318-05 Code.
- At time of prestress release at 18 hours, the coefficients on the square root of the compressive strength used to determine the modulus of elasticity for the SCC mixtures were about 4% and 11% lower than those for the HPC mixtures.

- The two SCC mixtures developed about 20% greater drying shrinkage than the comparable HPC mixtures.
- Due to the lower elastic modulus and the greater drying shrinkage, greater elastic shortening losses and greater long-term losses of prestress occurred, resulting in smaller cambers for the SCC girders.
- The cracking moments were similar for the SCC girders and the companion HPC girders.
- The uncracked and cracked stiffnesses for all four girders are very similar.
- The cracking shears were similar for all four girders.
- All four girders failed in shear after developing a significant number of wide shear cracks.
- The shear crack widths just before failure were greater than 0.24 in. (6 mm).
- The stirrups developed significant strains, beyond strain hardening, with the stirrups rupturing at failure.
- The failure shears exceeded the predicted nominal shear resistances of the girders using the approach given in 2007 AASHTO Specifications.
- The increased shear resistance was probably due to the strength and stiffness of the top and bottom flanges of the AASHTO girders.
- The HPC girders experienced flexural resistances which exceeded the predicted nominal resistances using the 2007 AASHTO Specifications.
- The SCC girders experienced flexural resistances which were within 1.5% of the theoretical flexural resistance using the approach in the 2007 AASHTO Specifications.
- The HPC girders exhibited higher ductilities than the corresponding SCC girders.
- The lower shear resistance and lower ductility experienced by the SCC girders is probably due to the lower volume of coarse aggregate, which reduces aggregate interlock and results in a lower energy absorption capability on the sliding shear failure plane.

This research on the structural performance of AASHTO girders has highlighted a number of differences that could affect design. However, it is clear form the testing of only two SCC girders and comparing the responses with two HPC girders that more research is required before any changes be recommended to the design specifications.